Analysis of solid state calorimetric data using non-iterative strategies

L. Almeida e Sousa[1], A. Beezer[1], N. Alem[1], D. Clapham[2], S. Gaisford[1]

[1]Department of Pharmaceutics, The School of Pharmacy, University of London, London, UK.
[2]GlaxoSmithKline R&D, Ware, UK.

INTRODUCTION

The analysis of solid state calorimetric data is critical in a pharmaceutical context since most dosage forms are available in the solid state. However, most of the existing strategies of analysis rely on the prior knowledge of the total heat output which can only be determined if the reaction goes to completion.

This paper presents some new non-iterative strategies that allow the determination of all solid state reaction parameters using partial calorimetric data.

MATERIALS AND METHODS

The strategies used for the analysis of solid state calorimetric data involve mathematical deductions and rearrangements of the Ng equation which describes single solid state reactions [1]. The equations presented here allow the determination of all reaction parameters even if only partial solid state data is available.

Three methods are proposed. One of them uses the last portion of calorimetric data and does not require the first part of data to be known (method 1). The second method uses the first part of data and does not require the reaction to go to completion (method 2). The third method only allows the determination of the total reaction heat output and uses the time point at which the reaction rate is at a maximum (method 3).

Two methods for simulating solid state thermal power/time data are also proposed and the previous methodologies were tested with simulated data ($Q = 1 \times 10^9$, $k = 3 \times 10^{-7}$ s^{-1}, $m = 0.75$ and $n = 0.625$) and real data. The experimental data was collected for the degradation of 300 mg of indomethacin in an isothermal calorimeter at 35^{0}C.

RESULTS AND DISCUSSION

All parameters were successfully returned when the different strategies were applied to simulated data using specific data points.

Using the data obtained for the degradation of indomethacin and fitting it to the Ng equation using iterative methods, the parameters obtained were: $Q = 16.526$ J, $k = 4.314\text{x}10^{-6}$ s^{-1}, $m = 0.602$ and $n = 0.816$.

Using method 1 to determine the reaction parameters, the following values were obtained: $Q = 16.351$ J, $k = 4.128\text{x}10^{-6}$ s^{-1}, $m = 0.589$ and $n = 0.767$. Using method 2 the parameters returned were $Q = 16.833$ J, $k = 3{,}978 \times 10^{-6}$ s^{-1},
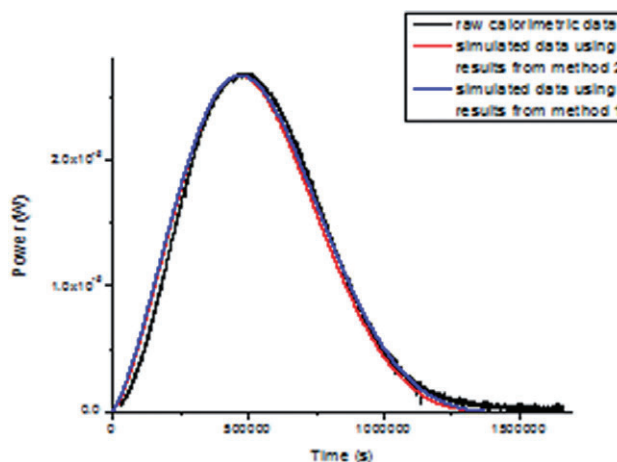

Figure 1. Comparison of the raw calorimetric data with data simulated using the parameters obtained with the different methods

$m = 0.580$ and $n = 0.766$. The total heat output (Q) was also calculated using method 3 and a value of 16.314 J was obtained.

Figure 1 compares the raw calorimetric data with simulated data obtained using the parameters returned from methods 1 and 2.

CONCLUSIONS

Three methods were developed in order to determine all parameters involved in solid state reactions. They do not require all data points to be known and they are based in mathematical non-iterative strategies.

The parameters obtained with all methods are similar to the ones obtained with iterative methods, which proves the accuracy of the mathematical strategies.

ACKNOWLEDGMENTS

REFERENCES

[1] W.-L. Ng, "Thermal decomposition in the solid state" *Aust. J. Chem.*, **28** (1975) 1169–1178.

Assessment of drug photostability using a photocalorimeter

L. Almeida e Sousa[1], A. Beezer[1], D. Clapham[2], S. Gaisford[1]

[1]Department of Pharmaceutics, The School of Pharmacy, University of London, London, UK.
[2]GlaxoSmithKline R&D, Ware, UK.

INTRODUCTION

Although the International Conference on Harmonisation (ICH) guideline on photostability testing of new drug substances and products is very clear in many aspects it directs the decision towards a simple pass/fail test which provides no quantitative data [1].

The purpose of this work is to develop a photocalorimeter that is capable of discriminating small heats of reaction allowing quantitative characterisation of the photostability of pharmaceuticals.

The photocalorimeter (Figure 1) consists of an isothermal heat conduction calorimeter (TAM) adapted with a light source consisting of an array of light-emitting diodes (LEDs) of different wavelengths (from 360 nm to visible) that is placed on top of a calorimetric ampoule with a quartz disc in the lid.

The LED-array is not in contact with the ampoule, providing a necessary thermal break. The LEDs can be switched individually allowing different combinations of wavelengths to be tested and the determination of the causative wavelength.

MATERIALS AND METHODS

In order to test the instrument's capacity to discriminate small reaction heat changes due to photoreactions, two separate experiments were performed.

In both experiments, the baseline signal with the lights on was first assessed using 500 mg of talc in the reference and in the sample ampoules. Then the content of the sample side was replaced by 500 mg of talc in one case and 500 mg of nifedipine in the other. The lights were turned on again and the deflection from the initial baseline was determined. The Isothermal microcalorimeter was set to run at 25^{0}C. Both experiments were performed in triplicate.

RESULTS AND DISCUSSION

When the talc in the sample ampoule was replaced by a new sample of talc, no considerable change was observed in the calorimetric signal. Differences of approximately 3 µW were observed which is very close to the baseline noise and stability limits of ±2 µW specified by the TAM's manufacturer [2]. After replacing the talc sample with nifedipine, a significant deflection from baseline was observed. The average deflec-
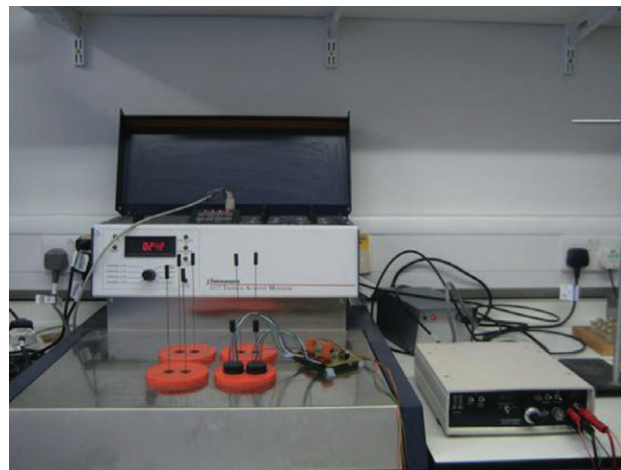

Figure 1. The TAM-based photocalorimeter

tion from baseline for the three experiments was 26.3 µW with a standard deviation of 3.9 µW. The signal was constant for approximately 22 hours of exposure but then started to decay. This decay is assumed to be due to a decrease in the photoreaction rate.

CONCLUSIONS

A new photocalorimeter was developed for photostability testing of pharmaceuticals. The instrument allows the discrimination of small heats of reaction and this was proved using the degradation of nifedipine powder as a reference photoreaction.

ACKNOWLEDGMENTS

REFERENCES

[1] ICH Q1B guideline, "Stability testing: photostability testing of new drug substances and products" (1996).
[2] Technical Specification, Thermometric AB, Note 22016.

Chemometrics analysis of solid herbal products and development of spectral databases

Mazlina M. Said*, Simon Gibbons and Mire Zloh

The School of Pharmacy, 29-39 Brunswick Square, London WC1N 1AX

INTRODUCTION

The quality and composition of herbal products are of paramount importance for their safety and efficacy. Product consistency and variation between manufacturers affecting the product fingerprints were observed using a combination of spectroscopic methods and chemometrics. A spectral database of herbal products is being developed and will enable direct comparison of the products' fingerprints. Such a database is a potential tool for quick analysis and product identification, screening and classification without having to use a standard.

MATERIALS AND METHODS

Three types of solid herbal products with a different number of batches and from different manufacturers were purchased in Malaysia using convenient sampling. The sample sets having (1) *Ginkgo biloba* (2) *Eurycoma longifolia* and (3) mixed Chinese herbal medicines as their declared ingredients were initially analysed by NIR to obtain the products' spectral fingerprints. Principal Component Analysis (PCA) was employed to show inter- and intra- batch variability between samples. Representative samples from each set were later analysed by NMR and ESI-MS to understand the reason for observed clustering and correlate differences in compositions of samples from different manufacturers. A spectral database was created using commercial software (GRAMS Suite 9.0). A cut-off point was determined and set for a quick search of unknown products.

RESULTS AND DISCUSSION

PCA of the second derivative spectra showed each batch of herbal products was nicely clustered according to the manufacturers. However, as herbs contained a complex mixture of components, the score plot analysis showed overlapping score points between the samples of different origins (Fig.1A). Classifications by soft independent modelling of class analogy (SIMCA) confirmed these findings whereby approximately 75% of the samples were classified correctly. A degree of difference between two samples of the same type (e.g. samples GBX and GBY) from two manufacturers can be measured relatively by observing the distance of the coordinate in the score plot, which most likely was due to the variation of compound composition. The NMR spectra (Fig. 1B) showed an additional peak in the GBY sample between 1.5–4.0 ppm and some dissimilarity of the peaks in other regions while the ESI-MS spectra (Fig.1C) confirmed the presence of different
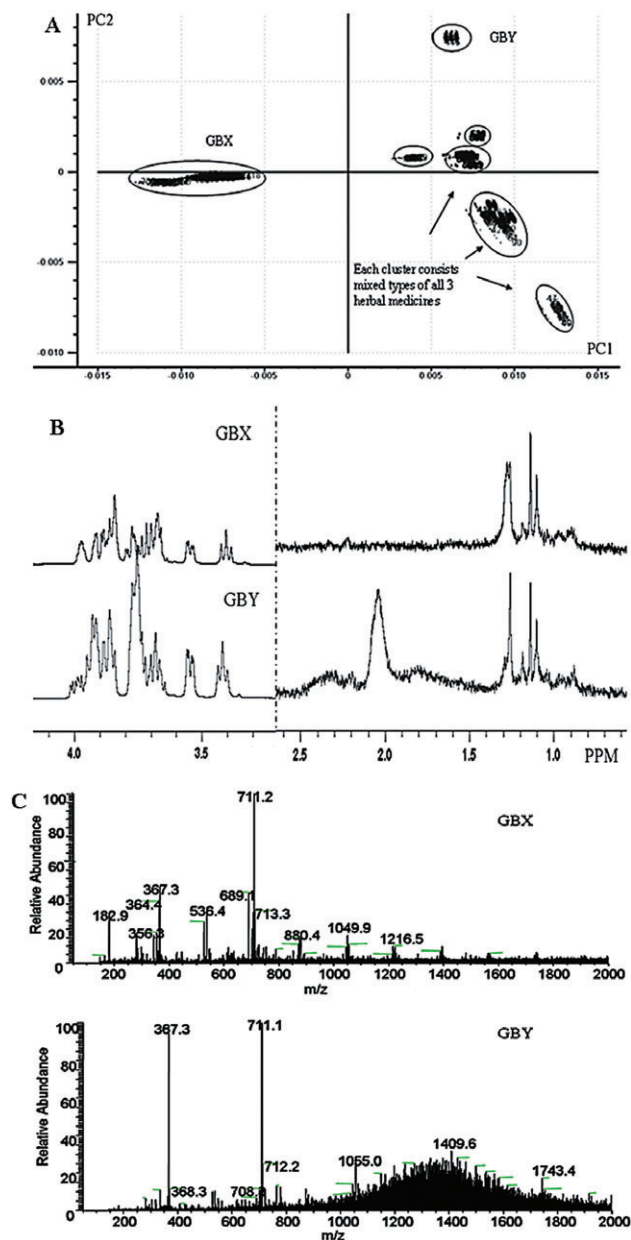

Figure 1. Analysis of herbal medicines available on the Malaysian market using spectroscopic methods (A) Score plot distribution of second derivative NIR spectra (B) NMR spectra of *Ginkgo biloba* (GBX and GBY) samples (C) ESI-MS spectra of GBX and GBY samples showing the presence of other small molecule compounds in different formulations

molecules available in lower concentration for both samples. The NIR data of several different herbal products was used to build a spectral database. Although some spectra were correctly classified by the type of a product and manufacturer, in some cases a search using NIR spectrum of an unknown sample gave ambiguous answers. In those cases the NMR and ESI-MS spectra were acquired and compared to the spectra in the databases created from NMR and ESI-MS data. The accuracy, robustness, and advantages of these databases will be compared and discussed further.

CONCLUSIONS

Chemometric analysis allowed observation of differences in intra-batch and inter-batch variability for different products. Further analysis by NMR and ESI-MS were able to pin-point the actual differences of the compositions between the products. The creation of a spectral database has allowed a quick product screening procedure. However, using NIR spectra as the source of search may lead to doubtful answers which have to be clarified using other analytical methods.

Correlation between ranitidine quantification measured in Dried Blood Spots and Plasma paediatric samples using different detection techniques

S. Yakkundi, J.S. Millership, P.C. Collier, J. McElnay

School of Pharmacy, Clinical Practice and Research Group, Belfast, UK

INTRODUCTION

Children are sometimes prescribed medicines that have not been properly researched and licensed for use within their age group. As a result, a significant proportion of the medicines used to treat children are used off-label or as an unlicensed preparation. Ranitidine is one such drug. Such unlicensed and off label use of drugs in paediatric patients is of concern [1]. In order to get proper dosing guidelines, pharmacokinetic profile of the drug has to be determined in the relevant paediatric population. Traditionally blood plasma is used to measure the drug levels, for which you need a minimum amount of blood (0.5 ml) taken from an individual. However in infants and neonates it is difficult to get sufficient volumes. The use of Dried Blood Spots (DBS) Fig. 1 provides an alternate sampling method in the paediatric population which not only has significant advantages at the sampling point but also in the transportation and storage. The primary aim of this study is to compare and investigate the correlation between the ranitidine concentrations in these two matrices.

METHOD

Paediatric patient blood samples were collected opportunistically at different time points from children who were administered ranitidine. The blood sample (30 µl) was spotted on to a Guthrie (Whatman 903) card. Fig. 1 and the remainder was spun down to give plasma. The plasma samples were extracted and analysed using a validated HPLC-UV method, where as the matched DBS samples were analysed using a validated HPLC-MS/MS method [2].

RESULTS

Eighty-one matched samples (plasma and DBS) were collected from 36 paediatric patients. The validated methods were demonstrated to be accurate, precise and complied with
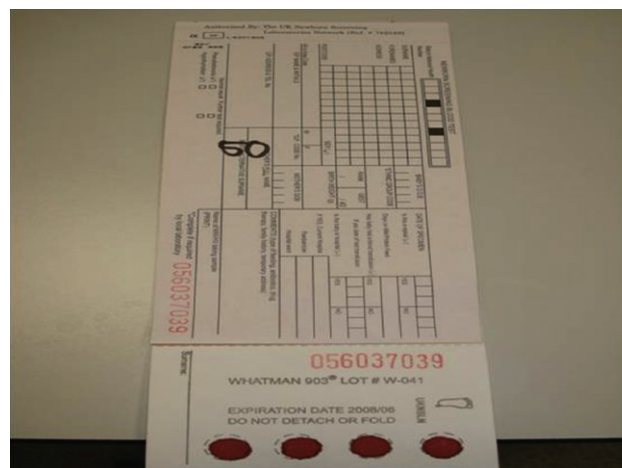

Fig. 1 Dried Blood Spots (DBS) on a Guthrie card

the regulatory guidelines [3]. Intra and inter-day accuracy (% RE) for plasma over four QC concentrations ranged from 0.5 to 2.8 and −0.9 to 3.4 respectively, while intra and inter-day precision (% CV) ranged from 0.2 to 6.2 and 1.3 to 1.9 respectively. For DBS, intra and inter-day accuracy over three QC concentrations ranged from −3.0 to 0.2 and −5.8 to 4.0 respectively, while intra and inter-day precision ranged from 2.6 to 5.9 and 0.8 to 6.02 respectively.

CONCLUSION

From the clinical perspective, the results obtained from DBS sample analysis, which represent the concentration of an analyte in whole blood, may not be directly comparable with those obtained from plasma. This relationship has been studied by means of linear regression analysis. The Bland Altman plots [4] have demonstrated good agreement between the two methods.

REFERENCES

[1] S. Turner, A. J. Nunn, K. Fielding, I. Choonara, "Adverse drug reactions to unlicensed and off-label drugs on paediatric wards: a prospective study,"Acta Paediatr. 88 (1999) 965–968.

[2] S. Yakkundi, J. S. Millership, J. McElnay, "Development and validation of a dried blood spot LC-MS/MS and plasma HPLC assay to quantify ranitidine in paediatric samples," unpublished.

[3] US Department of Health and Humans Services, Food and Drug Administration, Centre for Drug Evaluation and Research (CDER), "Guidance for Industry, Bioanalytical Method Validation," 2001.

[4] J. Martin Bland, D. G. Altman, "Statistical methods for assessing agreement between two methods of clinical measurements," The Lancet, 327, 8476 (1986) 307–310.

Detection of Testoterone in Human Hair Using Liquid Chromtography – Tandem Mass Spectrometry

Nawed Deshmukh[1], Iltaf Hussain[1], James Barker[1], Andrea Petroczi[2] and Declan P. Naughton[2]

[1]School of Pharmacy and Chemistry, Kingston University, London, UK
[2]School of Life Sciences, Kingston University, London, UK

BACKGROUND AND AIMS

Doping with endogenous anabolic androgenic steroids (AASs) is an increasing problem for the World-Anti Doping Agency's (WADA) anti-doping effort. Over the past 5 years, WADA Laboratory reports showed a marked increase in the proportion of testosterone abuse among adverse analytical findings for AAS, rising from 33% in 2004 to 68% in 2008 [1]. According to the WADA, external administration of Testosterone is suspected if the ratio of concentrations of Testosterone glucuronide to Epitestosterone glucuronide in urine exceeds 4. Owing to numerous limitations and inconveniences associated with urinalysis, there is an ever increasing need to develop new methods to detect drug doping. Hair specimens can be collected easily and provide a retrospective history of chronic drug use. Hence, following the successful detection of synthetic AASs such as Stanozolol and Nandrolone in human hair [2], the project was extended to detect the most used endogenous AAS: Testosterone. The primary aim was to develop highly sensitive, specific, reliable, reproducible and robust LC-MS/MS methods to detect Testosterone in human hair. A secondary aim of the project was to detect Epitestosterone and to facilitate the estimation of physiological ratio of Testosterone to Epitestosterone concentrations in human hair.

METHODOLOGY

Hair samples from 180 participants (108 males, 72 females, 62% athletes) were initially screened using competitive enzyme-linked immunosorbent assay (ELISA) and all the positive samples were confirmed on LC-MS/MS. Basic hydrolysis was employed for hair digestion. For LC-MS/MS analysis, the neutralised hair digest was extracted with pentane. The dried residue of the extract was reconstituted in acetonitrile prior to LC-MS/MS analysis. An Agilent ZORBAX SB-C18 column was used for analysis. The mass spectrometer was operated in selective reaction monitoring
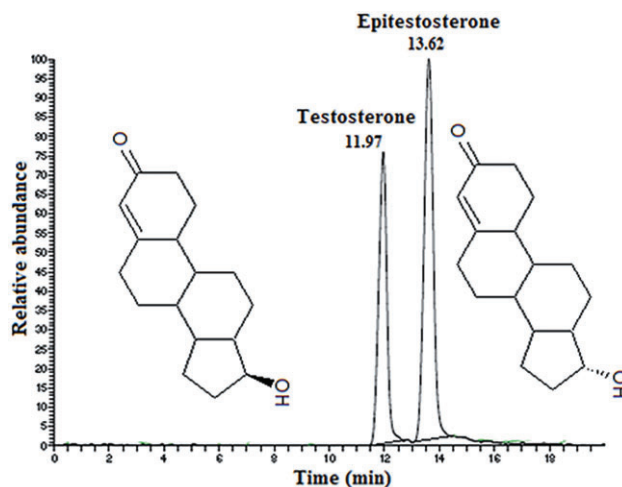

Fig 1. LC-MS/MS chromatogram of Testosterone and Epitestosterone.

mode using positive electrospray ionisation. The one precursor ion/two product ions for each analyte were monitored.

RESULTS

The assay showed good linearity in the range 0.5 to 400 pg/mg. The method was validated for LLOD, interday precision, intraday precision, specificity, extraction recovery and accuracy. The assay was capable of detecting 0.25 pg testosterone per mg hair when approximately 20 mg of hair were processed. ELISA screening revealed 3 athletes tested positive for Testosterone. LC-MS/MS analysis confirmed only one athlete was positive for Testosterone (0.75 pg/mg), thus avoiding false results from ELISA screening. Under the given chromatographic conditions it was possible to detect Testosterone and Epitestosterone in a single injection without any interference (Fig 1).

CONCLUSIONS

The results obtained demonstrate the first time ever application of a method for hair analysis to detect testosterone at low concentrations using LC-MS/MS. The new method facilitates improved doping testing regimes by complementing urinalysis or blood testing, and affords significant reduction in the amount of hair required. Hair analysis benefits from non invasiveness, negligible risk of infection and facile sample storage and collection, whilst reducing risks of tampering and cross contamination. Owing to the wide detection window, this approach may also offer an alternative approach for out-of-competition testing.

REFERENCES

[1] WADA laboratory statistics http://www.wada-ama.org/Documents/Science_Medicine/Laboratories/WADA_LaboStatistics_2008.pdf [accessed 17 May 2010].

[2] Deshmukh N, Hussain I, Barker J, Petroczi A, Naughton DP, "Analysis of anabolic steroids in human hair using LC-MS/MS" *Steroids*, in press, doi:10.1016/j.steroids.2010.04.007.

Elemental Profile of *Hypericum perforatum* (St John's Wort) Preparations Using Icp-Oes

Jade D. Owen, Sara J. Evans and Jacqueline L. Stair

Department of Pharmacy, University of Hertfordshire, Hatfield, UK

Abstract – **The elemental profile of St John's Wort was collected for a raw plant (SJW herb) and 6 processed forms (SJW A – F). A total of 27 elements were monitored including the toxic elements As, Cd, Hg and Pb as well as essential elements Ca, Mg, Cu and Zn. The level of As, Hg or Pb for all 7 samples were below detection limits. The raw plant and SJW sample C contained 0.86 ± 0.01 μg/g and 0.22 ± 0.02 μg/g of Cd. All samples showed > 20 μg/g of Al, Ca, Fe, Mg and Zn; in addition, the herb also had 103.1 ± 0.4 μg/g of Mn.**

Figure 1. Elements in *Hypericum perforatum* herb
[a]Elements greater than 60 μg/g included Ca, Mg and Mn.

INTRODUCTION

Hypericum Perforatum, otherwise known by its common name 'St John's Wort' (SJW), is a medicinal herb mainly used in the treatment of mild to moderate depression [1]. Herbal remedies, such as SJW, are often complex substances due to their natural origin. This makes them difficult to characterise and regulate compared to mainstream synthetic pharmaceuticals.

From collecting the elemental "fingerprint" of SJW, it is possible to see the differences between the raw plant material and the processed form. Moreover, fingerprinting may differentiate which elements are inherent to the plant itself as well as those added or removed during manufacturing processes.

Previous studies [2, 3] on SJW have looked only at a small group of metals and samples. In this study 27 elements were monitored to compare the profile of SJW raw plant material and available processed forms.

MATERIALS AND METHODS

Acid digestion was carried out in a Teflon digestion vessel with 0.6 g of herbal sample and 5 ml of nitric acid. Once digested the 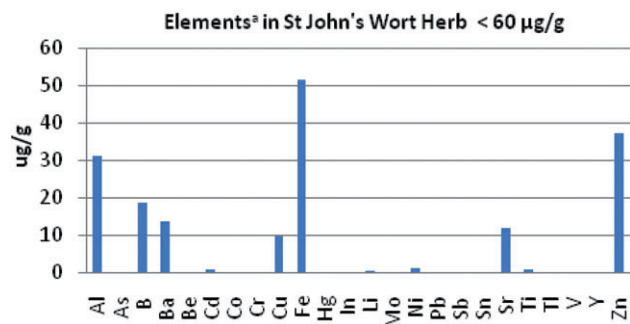sample was diluted (1 : 10) with deionised water, centrifuged (9000 rpm for 45 minutes) and syringe filtered (0.22 μm). Samples were analysed by Inductively Coupled Plasma-Optical Emission Spectroscopy.

Sample preparation was carried out once per herb sample. The average and standard deviation were calculated from four sequential readings.

RESULTS AND DISCUSSION

The unprocessed SJW herb showed >20 μg/g of elements Al, Ca, Fe, Mg, Mn and Zn; 1–20 μg/g of elements B, Ba, Cu, Ni and Sr; and <1 μg/g of Cd, Li and Ti. The remaining elements were below detection limits (see Figure 1).

The processed samples contained >20 μg/g of elements Al, Ca, Fe, Mg and Zn; 1–20 μg/g of elements B, Cu, Mn, Ni and Sr; and <1 μg/g (for most samples) of Ba, Cd, Co, Cr, Li, Mo, Ti, V and Y. The remaining elements were below detection limits.

All samples are composed of the same species of plant and thus show many elemental similarities. Elements common to all samples include: Al, B, Ba, Cu, Fe, Mg, Mn, Ni, Sr, Ti

and Zn. Elements Co, Cr, Mo, V and Y appear in the processed samples only. Cd levels in the raw plant and SJW sample C were 0.86 ± 0.02 µg/g and 0.22 ± 0.02 µg/g, respectively. Levels of Cd in these samples do not exceed the TDI for Cd [4].

CONCLUSIONS

In this study, both the raw plant and processed forms of SJW contained several metallic elements inherent to all samples. Other elements such as Co, Cr, Mo, V and Y are only seen in processed forms and thus could be due to growth conditions, cleaning, preparation, manufacturing processes or unsatisfactory storage.

REFERENCES

[1] Axel Brattström, 'Long-term effects of St. John's Wort (Hypericum perforatum) treatment: A 1-year safety study in mild to moderate depression', Phytomedicine 16 (2009) 277–283.

[2] Maria R Gomez, Soledad Cerutti, Roberto A. Olsina, Maria F. Silva, Luis D. Martinez, 'Metal content monitoring in *Hypericum perforatum* pharmaceutical derivatives by atomic absorption and emission spectroscopy', Journal of pharmaceutical and biomedical analysis 34 (2004) 569–576.

[3] Maria R Gomez, Soledad Cerutti, Roberto A. Olsina, Maria F. Silva, Luis D. Martinez, 'Determination of heavy metals for the quality control in Argentinean herbal medicines by ETAAS and ICP-OES', Food and Chemical Toxicology, 45 (2007) 1060–1064.

[4] Committee of Toxicology, Statement on the 2006 UK Total Diet Study of Metals and Other Elements.

Evaluation of the physico-chemical and biological properties of the proteasomal inhibitor PSI

Abderrezzaq Soltani[1], Sarah Rose[2], Sukhivinder Bansal[1], Peter Jenner[2] and Robert C. Hider[1].

[1]Pharmaceutical Sciences Research Division, King's College London, 150 Stamford Street, Waterloo, London SE1 9NH.
[2]Neurodegenerative Diseases Research Group, Pharmaceutical Sciences Division, Hodgkin Building, Guy's Campus, King's College London, London SE1 1UL.

BACKGROUND

Recent findings of ubiquitin-proteasomal system (UPS) dysfunction and its implication in Parkinson's disease (PD) pathogenesis have triggered interest on the use of proteasomal inhibitors to model PD [1]. A key observation was that the systemic administration of a synthetic UPS inhibitor, the peptidyl aldehyde PSI induced progressive neuronal loss in the substantia nigra (SN), development of motor abnormalities and the formation of intracellular inclusions resembling Lewy bodies (LBs) [2]. However, several laboratories failed to reproduce the original findings which raised questions over the reproducibility of the model. Hence, key to the establishment of the paradigm is to assess the chemical properties, pharmacological effects and the pharmacokinetic profile of the neurotoxin in an attempt to optimise the model, which is the aim of our study.

METHODS

The peptidyl aldehyde, PSI, was synthesised using a novel synthetic pathway. A reverse-phase high-performance liquid chromatographic method for the analysis of PSI was developed and validated and used to determine the stability of PSI in 70% ethanol and 100% dimethyl sulfoxide (DMSO) at $-20°C$, $-80°C$ and $37°C$. The inhibitory effects of PSI (0.25–500 nM) on the trypsin-like, chymotrypsin-like and peptidylglutamyl-peptide hydrolysing activities were also evaluated. Concurrently, the effect of PSI (0.1–100 µM) was studied *in-vitro*. using the neuroblastoma SH-SY5Y cell line, where cell death was analysed by lactate dehydrogenase (LDH) release. A rapid and sensitive analytical method based on liquid-chromatography – tandem mass spectrometry (LC-MS/MS) has been developed for the determination of PSI in rat plasma.

RESULTS

The newly synthesised PSI was successfully prepared, structure confirmed and characterised. Purity of 97% was confirmed by HPLC. The stability tests indicated that there was no significant degradation when PSI was kept at low temperatures. However, storage in ambient conditions resulted in 50% degradation over 75 hrs. The neurotoxin selectively blocked the chymotrypsin-like activity with an IC_{50} of 2.3 nM, which was significantly low compared to the commercially available PSI ($IC_{50} = 15.2$ nM). PSI caused a concentration-dependent cell death with an EC_{50} of 42.3 µM. The LC-MS/MS bioassay was validated, and good recovery of PSI was obtained (92–109 %). The calibration curve was linear over the concentration range of 10–5000 ng/ml with a limit of quantification of 10 ng/ml.

The assay was also accurate (relative error RE 7.5–9.4 %) and precise (coefficient of variation CV 3.4–10.4 %).

CONCLUSION

We have demonstrated that the new synthetic scheme allows the production of PSI batches with physical consistency and higher chemical purity compared to the commercially available compound. The proteasomal activity assays showed that

the synthesised inhibitor was significantly more potent than the commercial material. The rapid degradation of PSI in ambient conditions might explain the unpredictable and inconsistent results reported by other groups. A highly sensitive and validated LC-MS/MS method has been developed for the quantitation of PSI in rat plasma samples.

ACKNOWLEDGMENTS

REFERENCES:

[1] T. M. Dawson and V. L. Dawson. "Molecular Pathways of Neurodegeneration in Parkinson's Disease". *Science* **302** (2003) 819–822.

[2] K. P. McNaught, D. P. Perl, A. L. Brownell and C. W. Olanow (2004). "Systemic Exposure to Proteasome Inhibitors Causes a Progressive Model of Parkinson's Disease". *Annals of Neurology,* **56**(2004) 149–162.
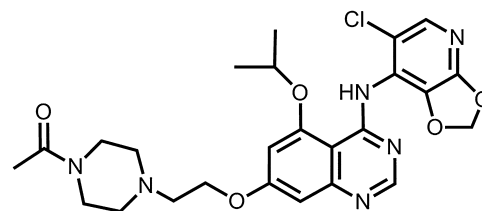
Experimental scrutiny and project timelines: an example

N. Dooley, S.J. Ford, E. Schmidt, M. Elliott, G.W. Halbert

Cancer Research UK Formulation Unit, Strathclyde Institute for Pharmacy and Biomedical Sciences, University of Strathclyde, Glasgow, G4 0NR

INTRODUCTION

AZD0424 (Fig. 1) is a dual selective inhibitor of Src and Abl non-receptor tyrosine kinases being developed for clinical trial through a partnership between AstraZeneca and Cancer Research UK. Formulation, pre-formulation and development studies were performed at the Cancer Research UK Formulation Unit at the University of Strathclyde. Here the authors report an example where the proper use and interpretation of 'forced degradation' experiments (performed during the early development stages of a drug project) allowed analysts to quickly identify problems occurring at subsequent stages.

MATERIALS AND METHODS

AZD0424 analysis was performed on Thermo Surveyor and Accela HPLC systems with PDA and/or Thermo LCQ Deca XP Max MS (ion trap) detection. HPLC analysis was performed using a Synergi Polar RP80 column with 0.3% formic acid: methanol gradient elution.

AZD0424 oxidative stress samples were by incubation of the drug in a 0.2% solution of H_2O_2 at $25°C$ overnight. Formulated AZD0424 samples were generated using 1% AZD0424 in PEG heated to $55°C$.

RESULTS AND DISCUSSION

Upon closer inspection of the HPLC traces from AZD0424/ PEG capsules incubated in an ICH compliant stability study [1], the retention time of the main degradant was found to coincide with the main degradant observed during the earlier oxidative stress degradation experiments. The main degradant increased with time and storage temperature (see Table 1). Armed with this information, degraded samples of AZD0424 were assayed by LCMS leading to a proposed degradant structure (Fig. 2). In addition, a review of the literature affirmed the presence of peroxide contaminants in PEGs [2].
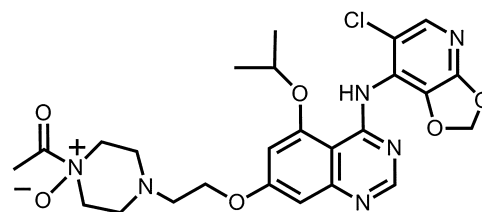

Fig. 1. AZD0424.

Fig. 2. AZD0424 degradant.

Table 1. Effect of time and temperature on main degradant concentration (%relative standard deviation in parenthesis)

Time (months)	5°C storage	25°C storage	40°C storage
	%pa/pa of main degradant		
0.0	2.2(0.7%)	N/A	N/A
1.4	2.6(0.4%)	4.9(0.4%)	9.4(13.7%)
3.3	3.3(0.3%)	5.8(2.0%)	11.5(7.4%)
6.5	3.9(0.6%)	6.8(2.5%)	13.9(4.5%)
9.8	4.5(1.6%)	7.7(11.2%)	13.9(4.5%)

CONCLUSIONS

Establishing and understanding degradation mechanisms via forced degradation studies was, in this case, a key part of establishing the chemical mechanisms for a deleterious degradation of AZD0424 found at a later stage of drug develop-

ment. The authors believe that a firm foundation of chemical and physico-chemical knowledge is key to effective progression of a clinical drug project. In this case, the work allowed the development team to move rapidly onto other formulations that would mitigate the degradation thus allowing the project to proceed in a timeous manner.

REFERENCES

[1] ICH Harmonised Tripartite Guideline Q1A, "Stability testing of new drug substances and products", http://www.ich.org/MediaServer.jser?@_ID = 419&@_MODE = GLB.

[2] V. Kumar and D.S. Kalonia, "Removal of Peroxides in Polyethylene Glycols by Vacuum Drying: Implications in the Stability of Biotech and Pharmaceutical Formulations" *AAPS PharmSciTech*, **7** (2006) Article 62.

LC Purity and Related Substances Screening for Mephedrone

N. Singh, P. Day, V.R. Katta, G.P. Mohammed, W.J. Lough

Department of Pharmacy, Health and Well-Being, University of Sunderland, Sunderland, UK.

Abstract – **LC methodology was developed for determining the purity and related substances of the drug of abuse, mephedrone. While batches of mephedrone purchased from the Internet proved, with one exception, to be relatively free from structurally-related impurities, they varied widely in their mephedrone content.**

INTRODUCTION

Mephedrone is a drug of abuse which has recently received much press attention [1], leading to it being declared illegal following reports of severe adverse effects [2]. This is unsurprising as it will not have been subjected to many years of scrutiny that are required to assure the quality, safety and efficacy of a pharmaceutical product. However, while major studies would be required to, for example, investigate the possibility of the drug *per se* being unsafe or drug-drug or drug-alcohol interactions being a problem, it was felt that the drug quality with its obvious links to drug safety could more readily be studied. Accordingly the aim of this study was to develop and validate LC methodology suitable for determining the purity and related substances of mephedrone and to apply it to the analysis of samples of mephedrone that had been available legally on the Internet.

MATERIALS AND METHODS

The LC system used consisted of a Shimadzu LC-6A, Rheodyne 7125 injector and a Shimadzu SPD-6A UV-vis detector with Dionex AI-450 based data handling. The analyses were carried out on a ACE-5- C18 (250 × 4.6 mm id, 5 μm) column with mobile phase [methanol – 0.02 M aq. ammonium formate (28:72, v/v)] containing 2 ml formic acid per litre of mobile phase. Samples of mephedrone were donated by BBC Radio North East (Cumbria) (M1) or purchased from websites www.flowerpowerfeeder.co.uk (M2),
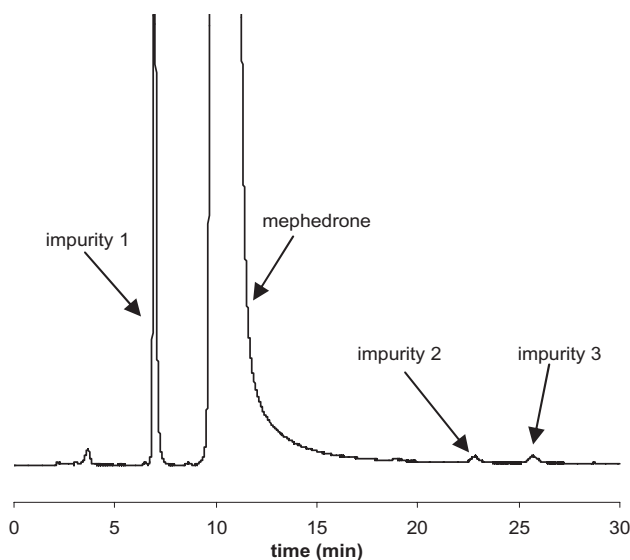

Fig. 1. 20 μl M2 (1.0 mg ml^{-1} in mobile phase); flow 1 ml min^{-1}; $\lambda = 260$ nm; ambient temperature – robust for 28 °C ± 3 °C.

www.ordermephedrone.co.uk (M3), www.mrmeph.com (M4), www.mephedrone2u.com (M5) and www.fastmephedrone.co.uk (M6).

RESULTS AND DISCUSSION

The approach to developing an LC method suitable for determining the purity and related substances of mephedrone involved the use of ACE-5-C18 and a low pH, formate – formic acid buffer based mobile phase. The ratio of organic to aqueous mobile phase component was adjusted to give *k* ~2 for the main mephedrone peak and specificity checks were

made by using alternative analyses to look for any undetected/unresolved impurities. Mephedrone at 0.1 mg ml^{-1} was used for a purity assay (repeatability (n = 10) 0.41%; linearity $r^2 = 0.999$) with M1 assigned as 100% pure. A 2000 × dilution of a 1.0 mg ml^{-1} test solution was used as an external standard to determine related substances (for the 0.0005 mg ml^{-1} solution, repeatability (n = 10) 1.20%; linearity $r^2 = 0.989$). All six samples contained impurities 2 and 3 (Fig. 1) at levels <0.02% w/w. Only M2 (Fig. 1) contained another impurity (impurity 1 at 0.31% w/w). However, when the purity assays were carried out it was found that the levels of mephedrone present were much lower than had been anticipated (M2 94.6 ± 1.04, M3 42.3 ± 0.71, M4 98.2 ± 1.51, M5 84.4 ± 0.91, M6 82.2 ± 1.78 % w/w).

Further TLC, ^{1}H NMR and microscopy investigations revealed that the low potencies determined arose from the samples being different salts of mephedrone rather than there being other materials such as non-UV absorbing excipients being added.

CONCLUSIONS

As can be seen from the data obtained, while batches of mephedrone purchased from the Internet proved, with one exception, to be relatively free from structurally-related impurities, they varied widely in their mephedrone content. While this is not likely to be the reason for some of severe adverse effects that have been reported, it certainly suggests that the 'effect' of mephedrone will be batch variable and the variability will depend on the route of administration.

REFERENCES

[1] P Bracci. "Mephedrone menace: The deadly drug that's cheap, easy to order as pizza . . . and totally legal'. Daily Mail Online. 12.12.2009. accessed *via*: http://www.dailymail.co.uk/news/article-1231538/Mephedrone-menace-The-deadly-drug-thats-cheap-order-pizza–totally-legal.html. Accessed on Feb 2010.

[2] D M Wood. D Susannah, M Puchnarewicz, J Button, R Archer, H Ovaska, J Ramsey, T Lee, D W Holt, P I Dargan. "Recreational use of Mephedrone (4-Methylmethcathinone, 4-MMC) associated sympathetic Toxicity". *Journal of Medicinal Toxicology*, in press.

Method Development for Analysis of Lactose Aerodynamic Particle Size Distributions in Dry Powder Inhaler Products

Victoria Heath, Wenan Lu

Inhalation and Devices Centre of Emphasis, Pfizer Global R&D, Sandwich, UK

Abstract – **A method was required to analyse the aerodynamic particle size distribution (APSD) of lactose in dry powder inhalers (DPI) from a single shot using a next generation impactor (NGI). There are many separation and detection techniques available, however each have their limitations. Two techniques which showed the most theoretical potential, ion chromatography-Pulsed Amperometric Detector (IC-PAD) and liquid chromatography-mass spectrometry (LC-MS), were investigated to evaluate their suitability. The most challenging aspect of this method development was to achieve acceptable sensitivity, due to the dose being distributed across 10 NGI stages.**

INTRODUCTION

The APSD is typically assessed via the use of an NGI which separates the DPI shot over 10 stages. The majority of the lactose deposits within the first two stages (the mouth/throat and preseparator) and then decreases across each subsequent stage (S1 to S8). The ideal method should be able to:

1. Analyse samples produced from a typical NGI method and not require further manipulation.

2. Be sensitive enough to allow approximately 1% of the lactose fines content to be detected, which (for example) corresponds to 13 µg per stage for a product containing 10% fines at a 13 mg fill weight.

3. Have a fast analysis due to there being 10 samples produced per NGI determination.

Lactose is a sugar and cannot be measured by conventional HPLC with a UV detector because it does not have a chromophore. It is also very polar and therefore very soluble in water.

There are many techniques available to analyse lactose, such as anion chromatography because lactose can be ionised at high pH, also by hydrophilic interactive liquid chromatography (HILIC)[1], which stationary phases include amine bonded to silica and bare silica.

The commonly used detectors for sugar are: Evaporative Light Scattering Detector (ELSD), Corona Charged Aerosol Detector (CCAD) and Electrochemical Detection (e.g, PAD[2]). MS has not been commonly used, however is a highly specific and sensitive detector. ELSD and CCAD had been previously tried and failed to meet the required sensitivity, therefore PAD and MS were selected to be investigated in this study.

MATERIALS AND METHODS

LC/MS separations were performed on a Luna NH$_2$ (50 × 2.0 mm ID; 3.0 μm particle size) column which was eluted with mobile phase containing acetonitrile/water (80:20) at a flow rate of 0.3 mL/min for 3 mins using a Agilent 1200 binary pump and coupled to a AB SCIEX API4000 triple quadrapole mass spectrometer equipped with a Turbo-Ion spray source operating in negative ion mode and at a source temperature of 400°C. The capillary voltage was maintained at 45000 V. Detection of lactose and internal standard mannitol was achieved using multiple reactions monitoring (MRM), 341.0/161.4 and 181.2/89.2 were MRM transitions for lactose and mannitol respectively.

Sample preparation for LC-MS: 10 mL of diluent of water/methanol (80:20) was added into each NGI cup and then rocked for 5 mins. Finally each extraction was diluted 10 times with diluent of water/methanol (10:90).

IC-PAD separations were performed on a 250 × 4 mm CarboPac PA10 column which was eluted with 100 mM KOH at a flow rate of 1 mL/min for 9 mins using a IC3000 pump. Lactose was detected with Pulsed Amperometric Detection with quadruple – potential waveform.

Sample preparation for IC-PAD method: 5–10 mL of diluent was added into each cup and rocked for 5–10 mins.

RESULTS AND DISCUSSION

Both methods were able to quantify less than 5 μg of lactose on the NGI cups (0.5 μg/ml). The IC-PAD method is capable of analysing samples generated from typical NGI methods without further dilution. Linearity has been shown for samples containing up to 100 μg/ml therefore covering the sample concentration range for all samples generated from 1 shot at a 13 mg fill weight. The main disadvantage of this method is the run time of 9 minutes for each injection which results in the analysis of 1 NGI determination taking approximately 2 hours.

The LC-MS method has a much quicker run time when compared to the IC-PAD method. This results in the analysis of 1 NGI determination taking approximately 30 minutes. The sensitivity of the LC-MS method is approximately 4 times greater than the IC-PAD method. However, the method requires dilution of the NGI cups' extraction; also a standard curve has to be generated for each run, therefore sample preparation for LC-MS method is more cumbersome than IC-PAD method.

CONCLUSIONS

Each method has its advantages and disadvantages over the other method, however both methods can detect lactose to the required sensitivity and therefore both are suitable techniques to analyse lactose in DPIs.

REFERENCES

[1] G. Karlsson, S. Winge and H. Sandberg, "Separation of monosaccharides by hydrophilic interaction chromatography with evaporative light scattering detection". *Journal of Chromatography A*, **1092** (2005) 246–249.

[2] R.D. Rocklin, "Improved long term reproducibility for pulsed amperometric detection for carbohydrates via a new quadruple-potential waveform" *Anal Chem.* **70** (1998) 1496–1501.

Micellar Chromatographic Partition Cofficients – an Alternative to Tradition

L.J. Waters

Division of Pharmacy and Pharmaceutical Science, University of Huddersfield, UK.

INTRODUCTION

Classically, partition coefficients are determined using octanol and water (P$_{ow}$) to mimic movement of drugs through biological membranes. An alternative system is proposed using chromatography to determine micelle/water partition coefficients (P$_{mw}$) for pharmaceutical compounds. It is proposed that using a micellar system provides an interesting alternative to the traditional method that is experimentally faster, equally precise yet most importantly achieves a higher level of accuracy when attempting to correlate with an *in vivo* situation. This work initially focuses on four drugs with a comparative study between literature P$_{ow}$ and measured P$_{mw}$ values, this is followed by a comparative study of column and surfactant selection.

MATERIALS AND METHODS

For the majority of experiments, the mobile phase consisted of an aqueous solution of sodium dodecyl sulfate (SDS), ranging from 10–30 mm. Two other surfactants were also considered, namely dodecyltrimethylammonium bromide (DTAB) and N,N-Dimethyl-N-dodecylglycine betaine (Empigen BB). The mobile phase was then pumped through a standard HPLC set-up with a reverse phase cyanopropyl (RCN), amino, C8 or C18 column, maintained at 298 K. Four drugs were investigated in this study, all with established literature P$_{ow}$ values: these were caffeine, ibuprofen, ketoprofen and procaine. From these results it was possible to calculate P$_{mw}$ for each drug through plotting the SDS concentration (after subtraction of the CMC) with the inverse of the capacity

Table 1. Calculated partition coefficient values for four drugs using micellar liquid chromatography

Drug	Column	$\log P_{mw}$ (Exp)	$\log P_{ow}$ (Lit)
Caffeine	RCN	1.3 (± 0.1)	−0.07[2]
Ibuprofen	RCN	1.9 (± 0.2)	2.5[3]
Ketoprofen	RCN	1.0 (± 0.1)	3.2[4]
Ketoprofen	Amino	3.0 (± 0.2)	3.2
Procaine	RCN	2.5 (± 0.1)	2.1[5]
Procaine	Amino	3.0 (± 0.2)	2.1

factor. The plots were linear ($R^2 \geq 0.99$) with the slope/intercept equal to P_{mw}[1].

RESULTS AND DISCUSSION

Micellar liquid chromatography (MLC) was used to determine P_{mw} values for all four drugs with three separate surfactants and four different columns. Firstly, the two more hydrophilic columns (RCN and amino) provided P_{mw} values mainly higher than those reported for P_{ow} (Table 1) using the anionic surfactant SDS. However, this was not the case for ketoprofen which may indicate a significant difference in the drug-surfactant interaction.

The two significantly more hydrophobic columns (C8 and C18) did not produce data suitable for mathematical analysis and therefore no P_{mw} values were derived.

This was also true when considering a further two surfactants with differing head group charges (cationic DTAB and zwitterionic Empigen BB) in that data was not analysable. Provided with this information it can be established that for MLC to provide P_{mw} values requires an appropriate selection of mobile phase surfactant and column choice.

CONCLUSIONS

In conclusion, a novel method for obtaining partitioning data has been investigated and optimised with respect to column and surfactant selection. It is proposed that this system provides a closer mimic of the *in vivo* reality of biological membranes compared with the traditional octanol/water system.

ACKNOWLEDGMENTS

REFERENCES

[1] M.G. Khaledi and E.D Breyer, "Quantitation of hydrophobicity with micellar liquid chromatography" *Anal. Chem.*, **61** (1989) 1040–1047.

[2] S. Hansen et al., "In silico model of skin penetration based on experimentally determined input parameters" Eur. J. Pharm. Biopharm. 2008;68: 352–367.

[3] T. Scheytt, P. Mersmann, R. Lindstadt and T. Herberer, "1-octanol/water partition coefficients of 5 pharmaceuticals from human medical care" *Water, Air and Soil Poll.,* **165** (2005) 3–11.

[4] M. Fujii et al., "Effect of fatty acid esters on permeation of ketoprofen through hairless rat skin" *Int. J. Pharm.,* **205** (2000) 117–125.

[5] H. Matsuki, T. Hata, M. Yamanaka, S. Kaneshina, "Partitioning of uncharged local anaesthetic benzocaine into model biomembranes" *Colloids Surf. B.,* **22** (2001) 69–76.

Synthesis and Validation of RP-HPLC Method for the Indole Hydroxyhexanamide as Potential Histone Deacetylase Inhibitor

A. Puratchikody[1]*, A. Umamaheswari[1], P. Sudhakar[1], P. Senthamilselvan[1], S.M.M. Rahman[2]

[1]Department of Pharmaceutical Technology, Anna University Tiruchirappalli,Tiruchirappalli 620024, India

INTRODUCTION

Hydroxamic acid based differentiating and antiproliferative agents were among the first compounds to be identified as histone deacetylase inhibitors [1]. Suberoyl anilide hydroxamic acid (SAHA) has anticancer activity against hematologic and solid tumours [2] and has been approved by the FDA for the treatment of cutaneous T-cell lymphoma [3]. There are a few number of views available in literature which summarises recent classes of indole sulfonamide derivatives disclosed ultimately as effective tumour cell growth inhibitors, [4] or for the treatment of different types of cancer. In the present study, 6-{[(5-chloro-*1H*-indol-3-yl) sulfonyl] amino}-N-hydroxyhexanamide was synthesised chemically based on the nucleus of SAHA. Various analytical methods were used of which high-performance liquid chromatography (HPLC) methods are one of the most useful techniques for the determination and quantification of synthesised compound.

MATERIALS AND METHODS

The final compound was synthesised and extracted with ethyl acetate, and further dried with sodium sulphate and evaporated. The title compound was confirmed by ^{1}H NMR and LC–MS. RP-HPLC methods have been developed and validated for the synthesised compound. Chromatographic separations were performed on a column of Eclipse XDB C18 (250 mm × 4.6 mm), 5 μ, in isocratic mode. The mobile phase consists of 0.1% trifluoroacetic acid and methanol in
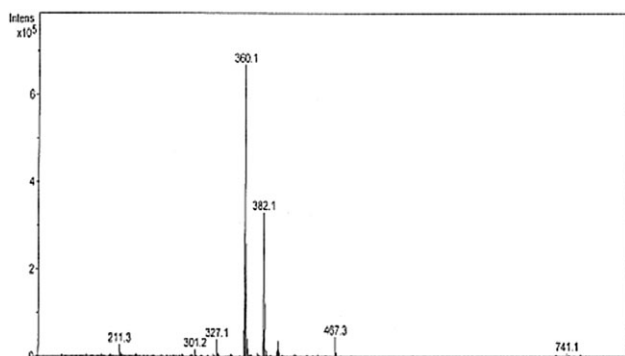
Fig.1. LCMS of compound 6-{[(5-chloro-*1H*-indol-3-yl)sulfonyl] amino-N-hydroxyhexanamide.

the ratio of (45:55, v/v) with flow rate set at 1 mL min^{-1}. The detection was carried out at 230 nm and the injection volume was maintained as 5.0 µL.

RESULTS AND DISCUSSION

The current method demonstrates good linearity over the range of 15–75 µg mL^{-1} and regression co-efficient (r^2) was found to be 0.998, the limit of detection and limit of quantification was found to 4 µg mL^{-1} and 15 µg mL^{-1} respectively. A simple, reproducible and sensitive isocratic RP-HPLC method proposed was found to be accurate, precise, robust and linear across the analytical range and cost effective in accordance with the ICH guidelines.

CONCLUSIONS

Indole containing amide derivative was chemically synthesised according to the scheme designed and RP-HPLC method was preferred for determining the reliability of the method for the synthesised compound in routine analysis. It can be effectively applied for routine quantitative analysis of indole hydroxyhexanamide derivatives in research institutions, industries, approved testing laboratories. In addition to that the proposed method will be employed in BA/BE studies and clinical pharmacokinetic studies in near future.

ACKNOWLEDGMENTS

REFERENCES

[1] D. Yujia et.al., Indole amide hydroxamic acids as potent inhibitors of histone deacetylases, Bioorganic and Medicinal Chemistry Letters, 13(11) (2003) 1897–1901.

[2] R. Codd, N. Braich, J. Liu, CZ. Soe, AA. Pakchung, Zn(II) dependent histone deacetylase inhibitors: suberoylanilide hydroxamic acid and trichostatin A, Int J Biochem Cell Biol, 41(4)(2009) 736–9.

[3] D. Madeleine, V. Jenny, Vorinostat: a new oral histone deacetylase inhibitor approved for cutaneous T-cell lymphoma, Expert Opinion on Investigational Drugs, 16 (7), (2007), 1111–1120.

[4] V. M. Richon et. al., Second generation hybrid polar compounds are potent inducers of transformed cell differentiation, Proc. Natl. Acad. Sd. USA. 93 (1996), 5705–5708.

Terahertz in-line sensor for perforated pan film coaters

R.K. May[1], M.J. Evans[2], S. Zhong[3], I. Warr[4], L.F. Gladden[1], Y.C. Shen[3], J.A. Zeitler[1]

[1]Department of Chemical Engineering and Biotechnology, University of Cambridge, Cambridge, UK.
[2]TeraView Ltd, Cambridge, UK.
[3]Department of Electrical Engineering and Electronics, University of Liverpool, Liverpool, UK
[4]Oystar Manesty, Merseyside, UK

INTRODUCTION

While film coating traditionally used to be performed for aesthetic or taste masking purposes, recent development efforts are directing coating technology more towards functional coatings for controlled release applications. However, better process understanding is desirable to improve the quality of coated products and realise new product opportunities for the pharmaceutical industry [1]. In recent years, terahertz pulsed imaging has been introduced as a powerful technology for the characterisation of pharmaceutical coating structures [2–3]. To date this technology is only available for reference measurements in research and development laboratories.

MATERIALS AND METHODS

An in-line terahertz sensor was developed and installed on a production-scale side-vented tablet coater (Premier 200, Oystar Manesty, Merseyside, UK). The sensor was externally mounted onto the perforated coating pan as such that the surfaces of tablets moving inside the rotating coating pan are presented at the focus of a continuous train of terahertz pulses. The system was tested during a five hour coating trial in which film coating was applied to 10 mm diameter, bi-convex tablets. Reflected time-domain waveforms were recorded at a rate of 120 Hz. Not all recorded waveforms contain suitable tablet reflections and signal processing was used to identify those that do. In order to validate the in-line measurements,

terahertz pulsed imaging (TPI) measurements were made on sample tablets removed during the coating trial, using a TPI Imaga 2000 (TeraView Ltd., Cambridge, UK). In addition, weight gain measurements were carried out.

RESULTS AND DISCUSSION

The coating thickness measurements using the in-line terahertz sensor agree very well with both the off-line TPI and weight gain measurements (Fig. 1). The in-line measurements, though obtained only from a single spot of individual moving tablets in the coating pan, are in excellent agreement with the average thickness as determined over the entire surface of the corresponding tablets by TPI.

In the current configuration the measurement sensor is able to measure the coating thickness of up to 100 individual tablets per minute. The measurements provide a good indication of the coating thickness distribution during the coating process within the pan coater (see insert in Fig. 1).

The terahertz sensor provides a direct measurement of the coating thickness [1,2] and no multivariate calibration is required for this method. The measurement is highly selective to coating thickness and quite robust to subtle formulation changes: after 180 minutes the colour of the coating suspension was changed and this had no influence on the coating thickness quantification (Fig. 1).

CONCLUSIONS

We have developed and evaluated a new in-line sensor technology for quantitative film coating thickness measurements of individual tablets during film coating in a perforated pan coater. The technology has considerable potential for PAT and QbD applications in film coating development.
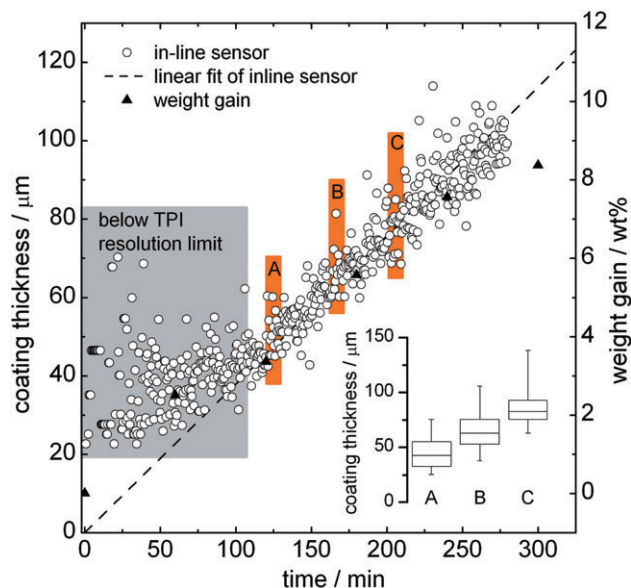
ACKNOWLEDGMENTS

Fig. 1. Coating thickness measured by the in-line process sensor during process time (open circles). For clarity the measurements are subdivided into bins of 30 second duration. Each data point corresponds to the average thickness during a 30 second bin. The closed black triangles indicate the average weight gain of 20 tablets. The insert shows the coating thickness distribution in the 10 minute intervals marked A, B and C of the main plot (the borders of the box indicate the 25th and 75th percentiles while the limits of the error bars represent the 5th and 95th percentiles)

REFERENCES

[1] L.A. Felton, S.C. Porter, Editorial, Drug Dev. Ind. Pharm., 36 (2010) 127–127.

[2] J.A. Zeitler et al., Analysis of coating structures and interfaces in solid oral dosage forms by three dimensional terahertz pulsed imaging, J. Pharm. Sci., 96 (2007) 330–340.

[3] Y.C. Shen, P.F. Taday, Development and Application of Terahertz Pulsed Imaging for Nondestructive Inspection of Pharmaceutical Tablet, IEEE J. Sel. Top. Quantum Electron, 14 (2008) 407–415.

The use of photocalorimetry to assess the photostability of nifedipine solutions

L. Almeida e Sousa[1], A. Beezer[1], D. Clapham[2], L. Hansen[3], S. Gaisford[1]

[1]Department of Pharmaceutics, The School of Pharmacy, University of London, London, UK.
[2]GlaxoSmithKline R&D, Ware, UK.
[3]Brigham Young University, Provo, UT, USA

INTRODUCTION

The desire to have a piece of equipment capable of performing quick, quantitative photostability tests led to the development of a new photocalorimeter. The work presented here aims to demonstrate the suitability of such an analytical tool to assess the photostability of pharmaceuticals. The basic structure of the photocalorimeter comprises light-emitting

diodes (LEDs) as the light source adapted to a multi-cell differential scanning calorimeter (MCDSC) which can be set to run at isothermal conditions.

The photodegradation of nifedipine in solution, a model photolabile drug, was chosen as the test reaction.

MATERIALS AND METHODS

Solutions of nifedipine were prepared in ethanol in different concentrations (1% and 1.33%) and different volumes (0.5 ml, 0.75 ml and 1 ml) were used with the calorimetric ampoules. The photo-MCDSC was set to run at a constant temperature of 25^0C for approximately 10 hours.

An HPLC assay was performed on these samples to quantify the amount of nifedipine that was being degraded with time and compare it with the quantitative data obtained with the photocalorimeter.

RESULTS AND DISCUSSION

The photodegradation of nifedipine in ethanol follows zero-order reaction kinetics observed as a constant heat flow deflection from baseline (Figure 1). Because the reaction went to completion during the experimental time it was possible to determine the total heat output and calculate the reaction enthalpy. This value was -160.15 KJ/mol.

The reaction rate constant was also determined using the calorimetric equation that describes zero-order kinetics in solution. The average rate constant determined for all experiments was 2.73×10^{-6} mol/dm^3.s. This value was confirmed with an HPLC assay, which returned a rate constant value of 1.73×10^{-6} mol/dm^3.s.

The enthalpies of reaction for different reaction pathways was estimated using Salmon and Dalmazzone's prediction method and, comparing these with the value determined calorimetrically, a mechanism of reaction using oxygen as a reactant was proposed [1, 2].

CONCLUSIONS

The photocalorimeter that was developed here allows the quantitative determination of reaction parameters which is
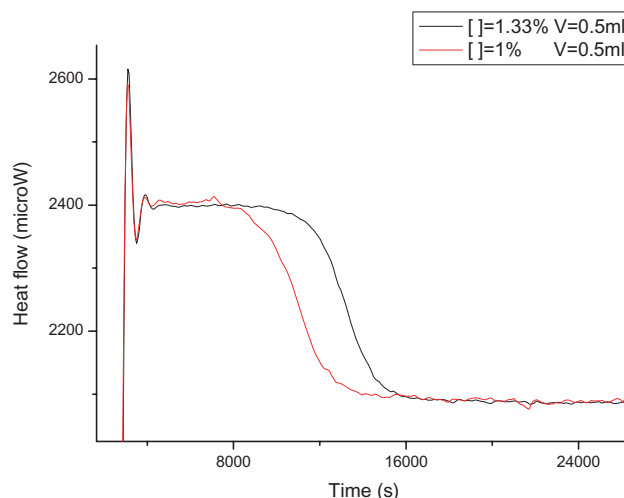

Figure 1. Graph showing the influence of the sample concentration on the calorimetric output.

very important for the assessment of photostability of pharmaceuticals. A reaction pathway for the photodegradation of nifedipine in solution was also proposed based on the enthalpy of reaction determined with the photocalorimeter.

ACKNOWLEDGMENTS

REFERENCES

[1] A. Salmon and D. Dalmazzone, "Prediction of enthalpy of formation in the solid state (at 298.15 K) using second-order group contributions. Part 1. Carbon-Hydrogen and Carbon-Hydrogen-Oxygen Compounds" *J. Phys. Chem. Ref. Data,* **35** (2006) 1443–1457.

[2] A. Salmon and D. Dalmazzone, "Prediction of enthalpy of formation in the solid state (at 298.15 K) using second-order group contributions. Part 2. Carbon-Hydrogen and Carbon-Hydrogen-Oxygen, and Carbon-Hydrogen-Nitrogen-Oxygen Compounds" *J. Phys. Chem. Ref. Data,* **36** (2007) 19–58.

A Novel Formulation for Oral Delivery of Live Bacterial Vaccines

Alexander D. Edwards* and Nigel K. H. Slater

Department of Chemical Engineering and Biotechnology, University of Cambridge, Cambridge, UK.
*Current address: Reading School of Pharmacy, University of Reading, UK

Abstract **– Most vaccines are injected, need refrigeration during distribution, and require challenging manufacturing processes. Live Bacterial Vaccines (LBV) offer the potential for oral administration, stability without refrigeration, and simple manufacture. Heterologous antigen delivery using LBV vectors could be used to target a wide range of pathogens. Most research to date has focused on LBV strain attenuation and on methods of introducing heterologous antigens (i.e. genetic engineering). For LBV to fulfill their promise, however, optimal formulation and**

delivery is also critical. Our research focuses on production, stabilisation and delivery of LBV. We are developing chemically defined media for fermentation, and use ambient-temperature drying with disaccharide stabilisation to make room-temperature stable LBV. To improve delivery efficiency, we invented a novel formulation block bile toxicity that utilises Bile Adsorbing Resins. After optimisation, this novel formulation can release up to 4000-fold more live cells into a bile solution than unprotected dried LBV.

INTRODUCTION

Live bacteria illustrate many challenges for biopharmaceutical formulation and delivery, being unstable, difficult to dry, and sensitive to temperature and moisture. Surprisingly, we found that when stabilised using trehalose, dried LBV are sensitive to intestinal bile, and highly sensitive to acid [1]. Although stomach acid can be bypassed using enteric coatings, subsequent release directly into the intestine risks loss of viability in bile. We invented a novel formulation to protect dried LBV from bile using Bile Adsorbing Resins (BAR) which are safe, orally administered ion-exchange resins previously used to lower cholesterol levels [2]. Initial studies showed 250-fold more live bacteria were recovered in a bile solution when BAR was added to LBV tablets, compared to control tablets where most cells died. Current work is focused on optimising this formulation and achieving maximal bile protection [3].

MATERIALS AND METHODS

For dissolution testing, a stabilised dried powder of the mouse LBV *S.* Typhimurium SL3261/pAH34L [3] was mixed with the filler microcrystalline cellulose. Powder was either mixed with 25% w/w of the BAR cholestyramine (Sigma, Poole UK) and filled into Vcaps Plus™ quick-release HPMC capsules, or weighed directly into a test tube. 20 ml of a 4% solution of ox bile in phosphate buffer pH7.0, or buffer alone, was added to replicate samples and incubated for 1 h at 37°C. Samples were taken, diluted and plated followed by overnight incubation and determination of viable cell counts.

RESULTS AND CONCLUSIONS

To optimise the BAR formulation for maximal protection from bile, a quantitative imaging system was developed which predicted that maximal protection could be achieved with a larger dosage, using 25% w/w of the BAR cholestyramine which has a small particle size. The results of the imaging system were used to develop a simple model of bile
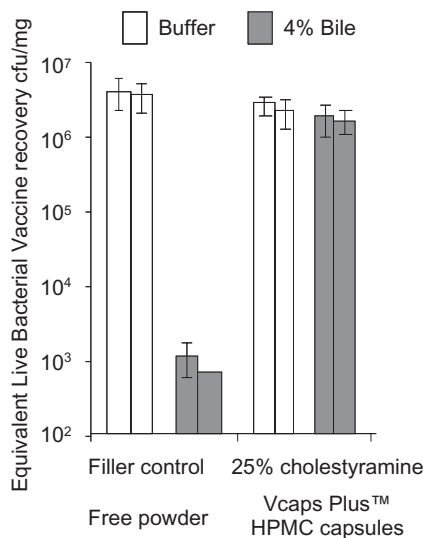

Fig. 1. Protecting dried LBV from bile solutions using an optimised formulation.

adsorbtion within oral dosage forms containing BAR that predicts the effects of varying BAR type and proportion, dose size and geometry.

The predictions of the imaging and modelling were tested by comparing live cell recovery in buffer vs. bile from LBV powder vs. an optimised oral dose comprising capsules with BAR. Although x4000 less live cells were recovered in bile with LBV powder, no loss was seen with BAR capsules, demonstrating 4000-fold more LBV recovery with the optimised formulation (fig. 1 and [3]).

ACKNOWLEDGMENTS

REFERENCES

[1] A.D. Edwards and N.K. Slater "Formulation of a live bacterial vaccine for stable room temperature storage results in loss of acid, bile and bile salt resistance", *Vaccine* 2008 Oct 23;26(45):5675–8

[2] A.D. Edwards and N.K. Slater, "Protection of live bacteria from bile acid toxicity using bile acid adsorbing resins", *Vaccine,* 2009 27(29):3897–3903.

[3] A.D. Edwards, P. Chatterjee, K. Mahbubani, C. Reis, N.K.H. Slater "Optimal Protection of Stabilised Dry Live Bacteria from Bile Toxicity in Oral Dosage Forms by Bile Acid Adsorbant Resins", Chemical Engineering Science, 2010, in press.

Bio-inspired Vectors for Gene Therapy

H.O. McCarthy[1,2], A.V. Zholobenko[1], J.A. Coulter[1], H.D. McKeen[1], D.G. Hirst[1], T. Robson[1], A. Hatefi[2]

[1]School of Pharmacy, Queen's University Belfast, 97 Lisburn Road, Belfast BT9 7BL Northern Ireland.
[2]Department of Pharmaceutical Sciences, Centre for Integrated Biotechnology, Washington State University, WA, USA

INTRODUCTION

Gene therapy is perceived as a revolutionary technology with the promise to cure almost any disease, provided that we understand its genetic or molecular basis. Undoubtedly the progress of gene therapy has been impeded by the lack of a suitable delivery vehicle. For systemic administration of therapeutic genes, a suitable vector for clinical applications should have low cytotoxicity/immunogenicity, high transfection efficiency, tissue specificity and be cost effective. Unfortunately, all currently available vectors have significant limitations. Despite this, a precedent for the use of cancer gene therapy has been set, with several gene therapy trials showing some success [1].

The inspiration for designing multifunctional bio vectors comes from viruses that can efficiently perform several functions to overcome many biological barriers. Bio-inspired vectors contain multiple sequences that perform a discrete function necessary for effective DNA transport [2]. We have designed such a vector, the Designer Biomimetic Vector (DBV) which is composed of several discrete motifs encoding a) a DNA condensing motif (DCM) obtained from the adenovirus mu peptide, b) a ZR-75–1 breast cancer cyclic targetting peptide (TP) for specific delivery of the nanoparticles, c) an endosomal disruption motif (EDM) that mimics the influenza virus fusogenic peptide and d) a nuclear localisation signal (NLS), rev, obtained from the human immunedeficiency virus type-1 [3]. A cathepsin D substrate (CS) was also engineered into the vector structure to facilitate dissociation of the targetting peptide from the vector within endosomes, where cathepsin D is abundant.

Here we describe the delivery of the cytotoxic iNOS gene *in vitro* and a GFP reporter gene *in vivo* to ZR-75–1 tumours, using our novel DBV.

MATERIALS AND METHODS

The DBV was expressed in E.coli, extracted with affinity chromatography and purified using size exclusion chromatography. The DBV was complexed to piNOS to form nanoparticles which were used either for characterisation via electrophoretic mobility shift assays, serum stability assays or dynamic light scattering analysis. ZR-75–1 breast cancer cells were transfected with DBV/piNOS nanoparticles and toxicity was quantified using the WST-1 cell toxicity and clonogenic assays. Over expression of iNOS was also confirmed via western blotting and Greiss test. Finally, ZR-75–1 intradermal tumours were grown using SCID models and the DBV/pEGFP-N1 nanoparticles were delivered both intratumourally and intravenously. Tumours and organs were excised and the GFP distribution was determined.

Figure 1: Schematic diagram illustrating the domains of the Designer Biomimetic Vector (DBV). These include a nuclear localisation signal (NLS), a DNA condensing motif (DCM), an endosomal disruption motif (EDM), a cathepsin substrate (CS) and a cyclic targetting peptide (TP).

RESULTS AND DISCUSSION

DBV was expressed in *E.coli* at approximately 3 mg/litre yield. Spherical nanoparticles formed when the DBV condensed piNOS between N:P ratios of 4–10. At N:P 9, DBV/piNOS produced particles with an average size of 75 nm. Transfection with the DBV/piNOS nanoparticles resulted in 62% cell kill. Total nitrite levels were in the range of 18 μM thus confirming iNOS overexpression. Forty eight hours after i.v. injection of the DBV /pEGFP-N1 nanoparticles, GFP protein was detected in all the organs. The addition of Chloroquine (50 mg/kg I.P) did not enhance the expression of GFP indicating functionality of the EDM. Furthermore the addition of nocodazole (3 mg/kg I.P.) resulted in a reduction in GFP expression again indicating NLS functionality *in vivo*.

CONCLUSIONS

There was significant cytotoxicity with the DBV/piNOS nanoparticles in ZR-75–1 breast cancer cells and with less than 20% transfection this indicates a bystander effect. Despite a lack of tumour targeting by the DBV vector *in vivo*, the data indicates that the DBV/pEGFP-N1 nanoparticles do not aggregate and can travel through the bloodstream with confirmation of gene expression in all the organs. Further studies will concentrate on using the human osteocalcin promoter (hOC) to transcriptionally target the iNOS plasmid to ZR-75–1 breast tumours [4]. The advent of designer biomimetic vectors heralds a new era of vectors that are composed of several discrete functional motifs that can be modified at a molecular level to carry out a distinct function.

REFERENCES

[1] S. Levy, B. Zhou, N. Ballian, Z. Li, S.H. Liu, M. Feanny, X.P. Wang, D.K. Blanchard, and F.C. Brunicardi. Cytotoxic gene therapy for human breast cancer *in vitro*. *J. Surg. Res.* **136** (2006) 154–60.

[2] H.O. McCarthy, Y. Wang, S.S. Mangipudi and A. Hatefi. Advances with the use of bio-inspired vectors towards creation of artificial viruses. *Expert Opin. Drug Deliv.* **7** (4) (2010) 497–512.

[3] S.S. Mangipudi, B.F. Canine, Y. Wang, and A. Hatefi. Development of a genetically engineered biomimetic vector for targetted gene transfer to breast cancer cells. *Mol. Pharm.* **6** (2009) 1100–9.

[4] H.O. McCarthy, J.A. Coulter, J. Worthington, T. Robson, and D.G. Hirst. Human osteocalcin: a strong promoter for nitric oxide synthase gene therapy, with specificity for hormone refractory prostate cancer. *J. Gene. Med.* **9** (2007) 511–520.

Design of Experiments: What parameters make an effective liposome-DNA delivery system in vitro?

S.E. McNeil, S. Carter, T. Parekh and Y. Perrie

Aston Pharmacy School, Aston University, Birmingham, B4 7ET, UK.

INTRODUCTION

It is well established that cationic liposomes are the most widespread non-viral method for efficiently delivering antigenic material for use in therapeutic and vaccine applications [1]. The cationic lipids within the liposomes electrostatically interact with the anionic DNA, thereby condensing the plasmid DNA and forming liposome-DNA complex systems. Formation of these complexes and ultimately, the delivery of genes to mammalian cells, is influenced by numerous factors including; type of cationic lipid, lipid to DNA ratio and lipid composition.

Design of experiment (DoE) was applied as it is a systematic approach for evaluating the effect of different factors and variables on the outcome of a process. By considering all possible combinations, factorial design allows extensive exploration into the interactions between variables, i.e. type of cationic lipid, cationic lipid : helper lipid ratio and DNA concentration and the overall effect on the final outcome. The program selectively generates a list of experimental parameters, significantly reducing the number of experimental preparations required for evaluation. The aim of this work was to assess and apply a DoE programme to obtain greater precision at estimating the overall main factors which may affect the characteristics of small unilamellar vesicles (SUV) and SUV-DNA complexes, and subsequently influences the cytotoxicity and transfection efficiency of SUV-DNA complexes *in vitro*.

MATERIALS AND METHODS

Factorial design and the evaluations were performed by the software MODDE 8.0 (Umetrics, Sweden). Liposome-DNA complexes consisting of a cationic lipid, either cholesterol 3β-*N*-(dimethylaminoethyl)carbamate (DC-Chol) or 1,2-Dioleoyl-3-Trimethylammonium-Propane (DOTAP) and the helper lipid, L-alpha-Dioleoyl Phosphatidyl ethanolamine (DOPE) were prepared at various lipid ratios and concentrations of gWIZ plasmid DNA which were selected from the DoE program and systematically tested. The physicochemical characteristics of each experimental formulation were measured and transfection efficiency and cytotoxicity to COS-7 cell line were assessed.

RESULTS AND DISCUSSION

By applying the DoE program, MODDE, the influence of various parameters/factors on the overall responses i.e. size, surface charge, transfection efficiency and cytotoxicity, were analysed and the outcome clearly shows that the most critical parameter influencing the mean size and zeta potential of liposomes-DNA complexes is the concentration of the cationic lipid component for both cationic lipids tested, DC-Chol and DOTAP, whereby particle size decreases with an increase in cationic lipid content.

The concentration of plasmid DNA is also shown to be a contributing factor. Cationic liposome-DNA complexes form spontaneously upon mixing DNA with positively charged liposomes and the complex system formed is dependent on the charge ratio. Comparison between the formulations
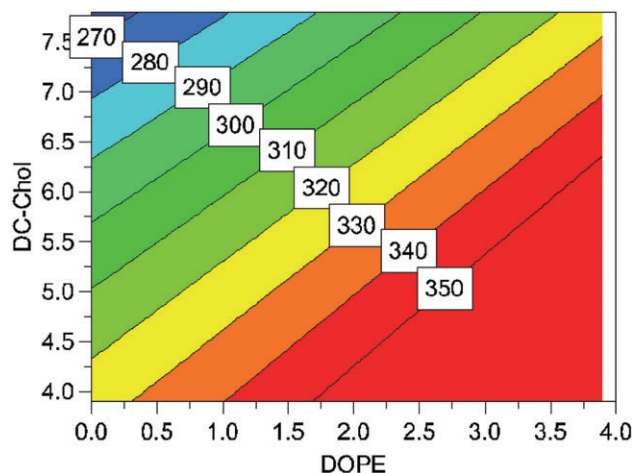

Figure 1: Response contour plot showing the effect of lipid composition on the final particle size of SUV-DNA complexes upon the addition of low quantities of DNA.

revealed that DC-Chol formulations exhibited slightly higher levels of cell viability than DOTAP formulations, presumably due to the presence of quaternary amine head groups within DOTAP, which are shown to be more toxic towards cells than tertiary amine head groups within DC-Chol [2].

CONCLUSIONS

By screening numerous input factors and analysing the output responses, the outcomes obtained by the application of DoE, demonstrate that the parameter which affects and determines the mean complex size and zeta potential is the concentration of the cationic component for both cationic lipids tested.

REFERENCES

[1] Li, S. and Huang, L., (2000) Non-viral gene therapy: Promises and challenges. *Gene Therapy* 7: 31.
[2] McNeil, S. E. and Perrie, Y. (2006) Gene Delivery using cationic lipids. *Expert Opin. Ther. Patent.*, 16: 1371–1382.

Development of Methods for the Detection of Protein Aggregation Propensity

O.W. Croad[1], C.J. Roberts[1], D.J. Scott[2], S. Rigby-Singleton[3], S. Allen[1]

[1]School of Pharmacy, University of Nottingham, UK.
[2]School of Biosciences, University of Nottingham, UK.
[3]Molecular Profiles Ltd, Nottingham, UK.

The rapid development of biopharmaceutical therapies is held back in part by extensive formulations analysis and optimisation steps. The current difficulty in predicting which molecules are susceptible to aggregation is a particular barrier within this process. This project aims to address the need for new analytical approaches to overcome this issue, by exploring the ability of single molecule force measurements to detect the early stages of protein aggregation. Such approaches could form the basis of new methods to screen molecules for their propensity to aggregate at an early stage within biopharmaceutical development.

INTRODUCTION

The delicate structures of the actives (e.g. proteins, peptides and nucleic acids) within biopharmaceutical formulations are crucial for their required therapeutic effect. Aggregation of these molecules has been shown to have adverse effects on their efficacy, and can result from structural alterations within the active biomolecular species; many theoretical aggregation mechanisms have an initial step which involves a partial deviation from the native state as the precursor to aggregation [1].

Force spectroscopy measurements have the potential to detect aggregation at the molecular level. Within this project, experiments are being performed, using an automated force spectroscopy platform (JPK ForceRobot300 [FR300]), to determine the features of force measurements that could be employed as indicators of early stage aggregation.

MATERIALS AND METHODS

Samples were prepared by adsorbing a 1 mg/ml solution of bovine serum albumin (BSA (Sigma-Aldrich) in phosphate buffer saline (PBS, pH 7.4)) onto mica substrates (Agar Scientific). Substrates were incubated for approx. 60 minutes to achieve at least monolayer surface coverage (confirmed by atomic force microscopy (AFM) imaging).

Measurements were performed in a temperature controlled, enclosed liquid cell, also in PBS. A maximum probe-sample contact force of 600 pN and a measurement speed of 1 μm/s were employed. The AFM tips used were silicon nitride MLCT probes (Veeco), with spring constants of approx. 35 pN/nm (calibrated using the thermal method [2].)

RESULTS AND DISCUSSION

Force spectroscopy measurements recorded with standard AFM tips on BSA functionalised surfaces, revealed that the AFM tip showed an increasing propensity to adhere to the protein surface with increasing temperature. Fig. 1 shows data where 10–20 surface locations (10 force curves/point) were assessed for adhesion for each temperature. This trend is consistent with an increased tendency to mechanically unfold the protein with the AFM tip, as the measurements are performed closer to the unfolding temperature of the BSA (around 58°C) [3].

CONCLUSIONS

As the partial/complete unfolding of proteins can lead to aggregation [1], these preliminary results hold promise in using this technique for the detection of protein aggregation susceptibility. More detailed experiments are currently underway to explore its potential as a new screening process within biopharmaceutical optimisation and development i.e. by exploring reversibility of the measurement, and the effects of other changes in experimental environment (e.g. denaturing salts and formulation excipients).
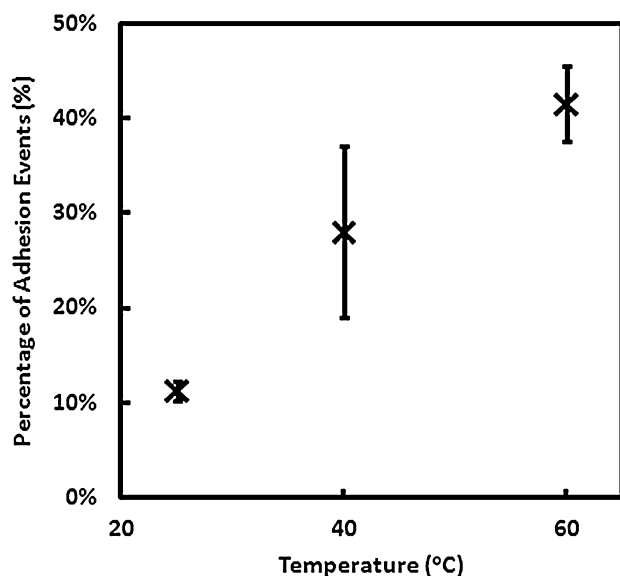
Fig.1. The percentage of probe-sample adhesion events as a function of temperature (recorded between standard AFM tips and BSA coated substrates).

REFERENCES

[1] A.M. Morris, M.A. Watzky, R.G. Finke, "Protein aggregation kinetics, mechanism, and curve-fitting: A review of the literature" *Biochimica et Biophysica Acta* 1794 (2009) 375–397

[2] M-S Kim, J-H Choi, J-H Kim, Y-K Park "Accurate determination of spring constant of atomic force microscope cantilevers and comparison with other methods" *Measurement* 43 (2010) 520–526

[3] G. Navarra, D. Giacomazza, M. Leone, F Librizzi, V Militello, P-L. San Biagio, "Thermal aggregation and ion-induced cold-gelation of bovine serum albumin" *Eur Biophys* 38 (2009) 47–446.

Efficient siRNA delivery and gene silencing by unsymmetrical fatty acid amides of spermine

Abdelkader A. Metwally, Charareh Pourzand, and Ian S. Blagbrough

Department of Pharmacy and Pharmacology, University of Bath, Bath, BA2 7AY, UK

INTRODUCTION

Gene silencing by siRNA i.e. synthetic dsRNA of 21–24 nucleotides, is already an important biological tool in the study of gene function and it also has many potential therapeutic applications for difficult-to-treat diseases [1].

Long-chain fatty acid amides of the naturally occurring polyamine spermine have previously been synthesised and evaluated in our research group for both pDNA and siRNA delivery [2–5]. Our SAR studies of long- (C18) and very-long (C20 and longer) fatty acid [6] conjugates of spermine are important in investigating the enhancement of siRNA delivery and of gene silencing.

AIMS

To study the SAR of novel unsymmetrical long- and very-long chain fatty acid spermine conjugates that will be evaluated for their efficiencies of siRNA delivery and gene knock-down.

MATERIALS AND METHODS

N^4-Arachidonoyl-N^9-oleoylspermine (AOS), N^4-lignoceroyl-N^9-oleoylspermine (LIGOS), and N^4-linoleoyl-N^9-oleoylspermine (LINOS) were prepared using DCC coupling of the corresponding carboxylic acids, after di-N-phthalimido protection of the primary amines. All transfection studies were carried out in the presence of foetal calf serum (FCS), 10% in DMEM on HeLa cells stably expressing enhanced green fluorescent protein (EGFP). siRNA concentration in each well of 24-well plates was 15 nM. Mean geometric fluorescence intensity of Alexa Fluor® 647 labelled-siRNA and EGFP was measured by FACS analysis 48 h post transfection. The alamarBlue® assay [7] was used to evaluate cytotoxicity. 6000 cells/well were incubated for 44 h post transfection then alamarBlue® reagent was added to the culture media and cells were incubated for a further 3.5 h.

RESULTS AND DISCUSSION

Gated FACS analysis (of living cells) showed that LIGOS has the highest siRNA delivery as measured by the normalised geometric mean fluorescence of Alexa Fluor® 647 (4-fold more compared to AOS and LINOS). However, more reduction in EGFP expression, in HeLa cells stably expressing EGFP, was achieved on siRNA delivery with AOS (to 34%, N/P = 21) and LINOS (to 29%, N/P = 11) compared to a reduction to 56% achieved with LIGOS (N/P = 18). Unsaturated fatty acid amide (linoleoyl; 18:2; arachidonoyl;

20:4) spermine conjugates showed higher knock-down efficiencies compared to (saturated) lignoceroyl (24:0) spermine conjugates.

This knock-down effect might be due to the ability of unsaturated chains to enhance fusion with endosomal membranes and thereby to facilitate endosomal escape [2], a key factor in the efficiency of siRNA mediated knockdown by lipoplexes [2–6]. Although LIGOS gave better siRNA delivery, its relatively low knockdown (to 56%) means that whilst saturated fats might enhance delivery, unsaturated fats specifically enhance endosomal escape of the delivered siRNA.

AlamarBlue® cytotoxicity evaluation showed that LINOS was less cytotoxic to HeLa cells (72% cell viability) compared to AOS (32%) and LIGOS (63%). The lower cell viability obtained with AOS may be attributed to the increased number (4) of C = C double bonds which has been reported to be a cause of cytotoxicity [8]. Under the same experimental settings, Lipofectamine™ 2000 reduced EGFP expression to 34%, with cell viability of 82%.

CONCLUSIONS

N^4-Linoleoyl-N^9-oleoylspermine (LINOS) is an efficient vector for the delivery of siRNA producing effective gene silencing even in the presence of FCS.

ACKNOWLEDGMENTS

REFERENCES

[1] I.S. Blagbrough and C. Zara, "Animal models for target diseases in gene therapy – using DNA and siRNA delivery strategies" *Pharm. Res.*, **26** (2009) 1–18.

[2] O.A. Ahmed, C. Pourzand, and I.S. Blagbrough, "Varying the unsaturation in N^4,N^9-dioctadecanoyl spermines: nonviral lipopolyamine vectors for more efficient plasmid DNA formulation" *Pharm. Res.*, **23** (2006) 31–40.

[3] D. McLaggan, *et al.*, "Pore forming polyalkylpyridinium salts from marine sponges versus synthetic lipofection systems: distinct tools for intracellular delivery of cDNA and siRNA" *BMC Biotechnol.* **6**, (2006).

[4] M.K. Soltan *et al.*, "Design and synthesis of N^4,N^9-disubstituted spermines for non-viral siRNA delivery – structure-activity relationship studies of siFection efficiency versus toxicity" *Pharm. Res.*, **26** (2009) 286–295.

[5] H.M. Ghonaim, S. Li, and I.S. Blagbrough, "N^1,N^{12}-diacyl spermines: SAR studies on non-viral lipopolyamine vectors for plasmid DNA and siRNA formulation" *Pharm. Res.*, **27** (2010) 17–29.

[6] H.M. Ghonaim, S. Li, and I.S. Blagbrough, "Very long chain N^4,N^9-diacyl spermines: non-viral lipopolyamine vectors for efficient plasmid DNA and siRNA delivery" *Pharm. Res.*, **26** (2009) 19–31.

[7] R. Asasutjarit, *et al.*, "Effect of solid lipid nanoparticles formulation compositions on their size, zeta potential and potential for in vitro type pHIS-HIV-Hugag transfection" *Pharm. Res.*, **24** (2007) 1098–1107.

[8] T.M. Lima, C.C. Kanunfre, C. Pompéia, R. Verlengia, and R. Curi, "Ranking the toxicity of fatty acids on Jurkat and Raji cells by flow cytometric analysis" *Toxicol. In Vitro*, **16** (2002) 741–747.

Immunological Regulation in the Tumour Microenvironment

H.K. Angell[1], D.G. Blount[1], S.A. Watson[2], R.W. Wilkinson[3], D.I. Pritchard[1]

[1]Immune Modulation Research Group, School of Pharmacy, University of Nottingham, Nottingham, UK.
[2]Division of Pre-Clinical Oncology, School of Medical and Surgical Sciences, University of Nottingham, Nottingham, UK.
[3]Cancer Infection Research Area, AstraZeneca Pharmaceuticals, Alderley Park, UK.

Regulatory T cells have been implicated in suppressing the anti-tumour immune response, resulting in tumour progression. Despite several mechanisms of suppression being suggested, effects of regulatory T cells upon tumour-killing cells, such as natural killer cells, remains unclear. We describe the development of an *in vitro* regulatory T cell suppression model, investigating the interactions of regulatory T cells with natural killer cells within the tumour microenvironment.

INTRODUCTION

Regulatory T cells (Tregs) co-exist with tumour cells, suppressing the anti-tumour immune response, resulting in tumour progression. Natural killer (NK) cells are able to elicit an anti-tumour immune response and are an important arm in the defence against tumours [1]. Tumour cell recognition by NK cells is orchestrated by activating signals mediated by natural killer group 2 member D (NKG2D).

It is hypothesised that NKG2D can be negatively regulated by transforming growth factor (TGF)-β and therefore NK cell surface expression of TGF-β receptors renders them vulnerable to control by soluble or cell-associated TGF-β.

It is proposed that TGF-β secreting Tregs within the tumour microenvironment suppress NK cell killing, enabling tumour escape.

MATERIALS AND METHODS

1) *K562 Model Killing Assay:* K562 tumour cells were stained with 5(6)-carboxyfluorescein diacetate N-succinidyl ester (CFSE). Peripheral blood mononuclear cells (PBMCs) and Tregs were isolated from a healthy volunteer (Miltenyi beads) and co-cultured at different ratios with the stained tumour cell line. Cultures were counter stained with propidium iodide (PI) to assess cell viability and cell-killing was expressed as percentage of $CFSE^+PI^+$ to $CFSE^+PI^-$.

2) *NKG2D and TGF-β RII analysis:* PBMCs were isolated from a healthy volunteer and stained with anti-human; CD4, CD3, CD8, CD56, TGF-β RII, and NKG2D antibodies, at different required combinations. Cells were fixed prior to running on a Beckman Coulter FC 500 and analysed using Weasel software.

2) *ULBP-2 and MICA analysis:* 1×10^6 cells of various tumour cell lines were blocked in 1% BSA-PBS and stained with anti-human MICA and anti-human ULBP-2 (R&D Systems).

RESULTS AND DISCUSSION

A significant reduction in the percentage of K562 cell killing was observed when Tregs were introduced at a 1:30:60 K562:PBMC:Treg cell ratio. This confirms that Tregs are having a suppressive effect on a population of cells within PBMCs that cause tumour cell killing.

Studies to support the proposed hypothesis that this cell population includes NK cells have included looking at the expression of NKG2D and TGF-β RII. In addition we have shown the expression of NKG2D ligands MICA and ULBP2
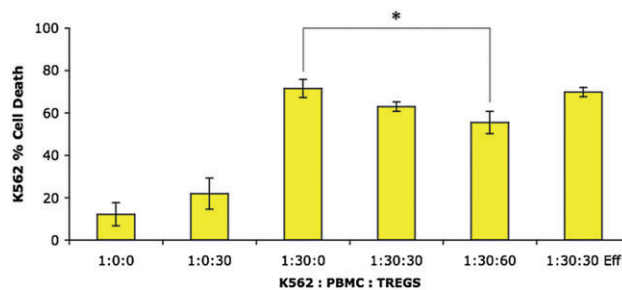

Fig. 1. Treg Mediated Suppresion of K562 Cell Killing Assay with PBMCs.

on the following tumour cell lines; SW602, DMS 114, LNCaP and MCF7.

CONCLUSIONS

Our study adds new data to the ongoing discussion on the role of Tregs in malignant diseases. Accumulating evidence points to a critical interaction between Tregs and NK cells in tumour progression.

Further investigation using a neutralising TGF-β RII and NKG2D antibody will aid in determining the role of Tregs in modulating NK cell tumour killing, and improve knowledge of the mechanisms of suppression of anti-tumour immunity. This model will then be employed to screen for inhibition of molecular targets associated with regulatory T cell activity.

ACKNOWLEDGMENTS

REFERENCES

[1] J. Zimmer, E. Andres, and F. Hentges. "NK cells and Treg cells: a fascinating dance cheek to cheek" *Eur. J. Immunol.,* **38** (2008) 2942–2945.

Understanding and Tailoring the Flow Properties of Biopharmaceutical Formulations

A. Gonçalves[1], C. Alexander[1], P. Patel[2], J. Pathak[3], C.J. Roberts[1], S. Uddin[2], S. Allen[1]

[1]School of Pharmacy, University of Nottingham, Nottingham, NG7 2RD, UK.
[2]Bioprocess Development, MedImmune Ltd, Cambridge, CB21 6GH, UK.
[3]Drug Delivery and Devices, Formulations Sciences Group, MedImmune LLC, Gaithersburg MD 20878, USA.

INTRODUCTION

New biopharmaceutical products are increasingly being developed as high concentration formulations, to overcome bioavailability issues and to attain reduced patient administration frequencies. However, under crowded conditions problems of aggregation, limited solubility and stability arise in protein formulations. For example, high protein concentration formulations (exceeding 50 mg mL^{-1}) can suffer reversible self-association and/or (irreversible) protein aggregation, as

well as other factors such as opalescence. Viscoelasticity can also become problematic at increased protein concentration. All these factors are relevant to both biopharmaceutical manufacture and delivery [1].

Stable protein formulations of tractable viscosity can be prepared either with small molecule additives or more complex molecules (e.g. surfactants/polymers). This project aims to investigate the impact of such additives on the rheology of high protein concentration formulations (above 50 mg mL^{-1}), and to improve understanding of the molecular origins of this behaviour. Our long term objective is to utilise such understanding to tailor the rheology of biotherapeutic formulations.

MATERIALS AND METHODS

Recombinant Human Albumin (rHA), Recombumin®, in its formulation buffer, was used as a model protein. Steady shear rheology was performed on a stress-controlled Anton-Paar MCR301 rheometer equipped with a 50 mm diameter cone-plate geometry (angle 1°), at 20°C ± 0.1°C, and a solvent trap to minimise fluid evaporation.

Dynamic light scattering (DLS) (802 Viscotek, Malvern; scattering angle 90°; HeNe laser) was performed at 20°C ± 0.1°C using a 12 μL quartz cuvette to monitor protein aggregation.

RESULTS AND DISCUSSION

The Krieger-Dougherty model [2] (Eq. 1) describes the viscosity of suspensions of spherical and other shaped particles.

$$\frac{\eta}{\eta_o} = \left[1 - \frac{\phi}{\phi_{\max}}\right]^{-[\eta]\phi_{\max}}$$
(Eq. 1)

Where η, η_o, ϕ, $[\eta]$ and ϕ_{max} denote solution viscosity, solvent viscosity, protein volume fraction, intrinsic viscosity and maximum packing volume fraction, respectively.

Eq. 1 was found to fit to rHA solution viscosity data well (Fig. 1), with fit parameters $[\eta]$ = 5.7 ± 0.25 and ϕ_{max} = 0.27 ± 0.02. Our $[\eta]$ value is sensible, given the large aspect ratio (elongated shape) of rHA [3]. Generally, as aspect ratio grows, $[\eta]$ increases and ϕ_{max} decreases [4].

DLS data indicated that rHA remains as a monomer in solution (>99%), even at 200 mg mL^{-1} concentration.
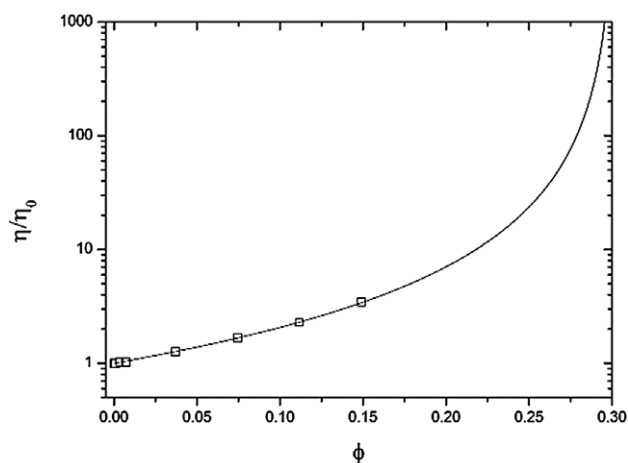

Fig. 1 – Relative viscosity as a function of rHA volume fraction. Experimental data – open squares; fit curve – solid line (r^2 = 0.997).

CONCLUSIONS / FUTURE WORK

The Krieger-Dougherty equation describes the concentration dependence of rHA solution viscosity. Even at 200 mg mL^{-1}, where the solution is three times more viscous than the buffer, rHA remains a monomer. Ongoing studies on rHA are focused on understanding the linear and non-linear viscoelasticity at the molecular level. We are also studying highly concentrated monoclonal antibody solutions to investigate how reversible self-association influences solution viscoelasticity, and the effects of small molecule/macromolecular additives on solution rheology.

ACKNOWLEDGEMENTS

REFERENCES

[1] Shire, S.J., Shahrokh, Z., Liu, J., *J. Pharm. Sci.*, **2004**, 93(6), 1390 1402.

[2] Krieger, I. M. & Dougherty, T.J., *Trans. Soc. Rheol*, **1959**, III, 137–152.

[3] Monkos, K., *Biochem. Biophy. Acta.*, **2004**, 1700, 27–34.

[4] Larson, R. G. "Particulate suspensions" in *The Structure & Rheology of Complex Fluids*, Oxford Univ. Press, NY, 1999, ch. 6.

A preliminary assessment of the dynamic gastric model (DGM) to predict the *in vivo* performance of a complex dosage form

J. Mann, S. Pygall, D. Murray, J. Hearn, C. Seiler, G. Pearce, R. Saklatvala, S. Fitzpatrick

Development Laboratories, MSD, Hoddesdon, Hertfordshire, UK

INTRODUCTION

Correlating *in vitro* performance t*o in vivo* behaviour is a critically important and cost-effective objective for the pharmaceutical industry. It is imperative to develop understanding of the conditions of the gastrointestinal environment and its influence on drug liberation phenomena from pharmaceutical dosage forms. Whilst fully characterising the complexity of the gastrointestinal tract may remain an elusive goal, understanding the key parameters to predict dosage form behaviour can be, achieved.

This work reports the assessment of an enhanced and robust *in vitro* screening method to direct formulation development and improve the probability of success for human *in vivo* studies.

MATERIALS AND METHODS

A range of formulations for a combination product containing two different APIs (A and B) was investigated. Subsequently, the dissolution performance was assessed and rank ordered using standard USP dissolution methods (I, II, III and IV). In parallel, samples were tested in the Dynamic Gastric Model (DGM) (figure 1). This is a fully automated, computer controlled model of the human stomach. The PK performance of the formulations was subsequently evaluated in a human study.
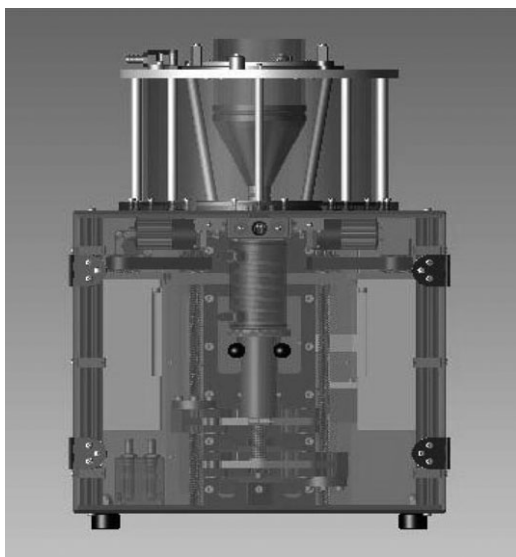
The DGM is a sophisticated *in vitro* dissolution technique. The dosage form is added with or without food to simulate fed or fasted states. The DGM "digests" by homogenising using biorelevant hydrodynamics with the addition of simulated gastric fluid and enzymes. Samples are taken at intervals as the model empties, the intervals are determined by the composition of the meal dosed. These samples are then extracted and analysed for drug content. A potential benefit over standard USP II dissolutions in SGF is that the DGM uses hydrodynamics that are much closer to that experienced in the human stomach and has realistic gastric emptying.

RESULTS AND DISCUSSION

The initial formulation screening using conventional USP methods afforded some indication of a desirable design space with respect to the composition of the formulations but neither USP II or USP III could reproducibly rank order the formulations to previously discerned human pharmacokinetic (PK) parameters.

It was possible to discriminate the majority of probe formulations using USP IV in the open loop configuration, with a low flow rate and a challenging dissolution media with respect to pH for one of the drugs. The DGM validated the USP IV data and found a broadly similar rank ordering in the probe formulations (figure 2) with respect to cumulative drug release. This allowed identification of lead formulations that were taken in human PK studies in order to determine the validity of the *in vitro* screening. The *in vivo* human data confirmed the validity of the predictions made using the
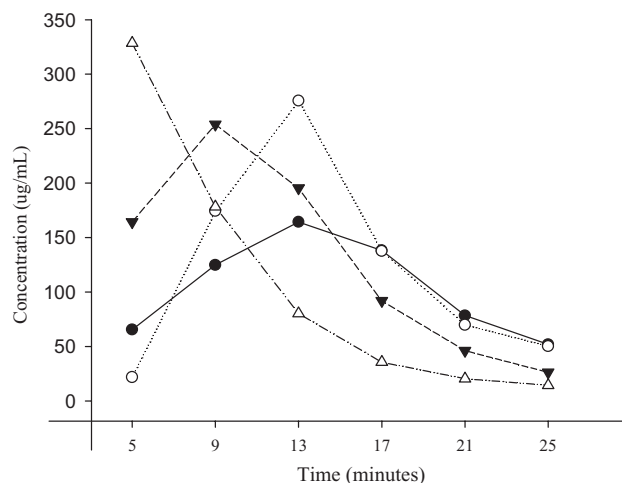

Figure 1. The Dynamic Gastric Model (DGM)

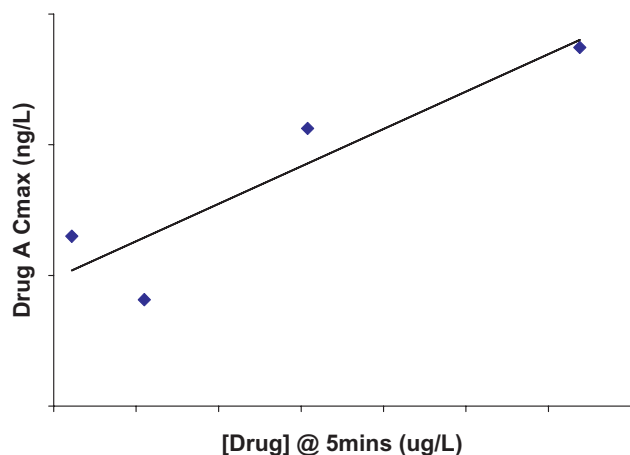**Figure 2.** Cumulative release of Drug A in the DGM

Figure 3. Correlation plot of Drug A Cmax against Drug A concentration in the DGM at 5 minutes

PBL-DGM by exhibiting the same rank ordering with respect to Cmax and drug released at the 5 minute time-point (figure 3).

CONCLUSIONS

This study has shown some evidence that by decreasing the reliance on conventional USP methods, innovative technology may potentially afford levels of insight and prediction of *in vivo* performance that are not readily attainable by other techniques.

ACKNOWLEDGMENTS

Characterisation of ATP-binding cassette (ABC) transporters in the Calu-3 human bronchial epithelial cell culture model

V. Hutter[1], C. Hilgendorf[2], A. Brown[3], V. Zann[4], A. Cooper[4], D. Pritchard[3], C. Bosquillon[1]

[1]Division of Advanced Drug Delivery and Tissue Engineering, School of Pharmacy, University of Nottingham, UK. [2]AstraZeneca R&D Mölndal, Sweden. [3]Division of Molecular and Cellular Science, School of Pharmacy, University of Nottingham, UK. [4]AstraZeneca R&D Charnwood, Loughborough, UK.

Abstract – **Expression and functionality of ATP-binding cassette (ABC) transporters were assessed in Calu-3 cell monolayers cultured at an air-liquid interface. Transporter gene expression was in agreement with published data in human lungs with the exception of BSEP which was over-expressed in Calu-3 cells. Net secretory transport of the ABC substrate ^{3}H-digoxin was reduced in presence of the inhibitors verapamil, PSC833 and MK571. However, the transporter(s) involved could not be identified.**

INTRODUCTION

Calu-3 human bronchial epithelial cell monolayers exhibit morphological and permeability characteristics similar to those of the native epithelium when cultured on permeable supports at an air-liquid interface [1]. Inconsistent and limited published data exists regarding ABC transporters in the lung and Calu-3 cells [2, 3]. This work aims to characterise the expression and functionality of ABC transporters in Calu-3 cells and thus assess their suitability as an *in-vitro* model to identify drug molecules actively transported across the bronchial epithelium.

MATERIALS AND METHODS

Calu-3 cells were seeded on 12-well Transwell® inserts at a density of 1×10^5 cells/cm^2 and cultured at an air-liquid interface for 21 days. ABC transporter expression was assessed at both the gene and protein levels using a real-time PCR low density TaqMan array and western blot, respectively. Permeability of the ABC substrate ^{3}H-digoxin alone and in the presence of a panel of inhibitors was obtained in both apical to basolateral (AB) and basolateral to apical (BA) directions.

RESULTS AND DISCUSSION

Gene expression levels were in accordance with those in human lungs, except for BSEP which was over-expressed in Calu-3 cells (Table 1). Western blot analysis confirmed the absence of MRP2 and the presence of either MDR1 or BSEP compared with positive cell controls, HEK-MRP2 vesicles, Caco-2 (MDR1) and Sf21-BSEP vesicles (data not shown).

Net secretory transport of ^{3}H-digoxin in Calu-3 cell layers resulted in efflux ratios of 11.6 ± 2.6 at passage 25–30 and

Table 1: Gene expression levels of selected ABC transporter proteins in Calu-3 layers (passage 35) normalised against large ribosomal protein (RPLP0) and major vault protein (MVP). Data compared with published gene expression levels in healthy lung tissue [4]. Key: ++ moderate, + low, − absent gene expression

Gene	Protein	Relative Gene Expression	Assigned Expression Level	Published Expression Level
ABCB1	MDR1	0.031	+	−
ABCB11	BSEP	0.314	++	−
ABCC1	MRP1	0.071	+	++
ABCC2	MRP2	0.003	−	−
ABCC3	MRP3	0.410	++	++
ABCC4	MRP4	0.176	++	+
ABCC5	MRP5	0.052	+	++
ABCC6	MRP6	0.014	+	+
ABCG2	BCRP	0.004	−	++

Figure 1: Efflux ratios for ^{3}H-digoxin at low (25–30) and high passage (45–50). Data are presented as the mean ± SD (n = 3–4) and compared with control using a one way ANOVA test. * $p < 0.01$.

3.1 ± 0.4 at passage 45–50. ^{3}H-digoxin efflux ratios were significantly reduced to <2.3 (low passage) and <1.5 (high passage) by the inhibitors PSC833, MK571 and verapamil (Figure 1). The efflux ratio of ^{3}H-digoxin in the presence of 1 mM probenecid was not significantly different from control at either of the passages tested.

CONCLUSIONS

Permeability studies with ^{3}H-digoxin confirmed the presence of functional ABC transporter system(s) in Calu-3 cell layers and highlighted variations in transporter subtypes and/or expression levels with passage number. The transporter(s) involved could not be identified using a panel of chemical inhibitors due to non-specific inhibition. The functionality of BSEP in Calu-3 cells will be determined due to its over-expression at the gene and protein levels. Elucidation of active transport mechanisms in Calu-3 layers may be key to understanding the trafficking and absorption of inhaled drug therapeutics across the bronchial epithelial barrier.
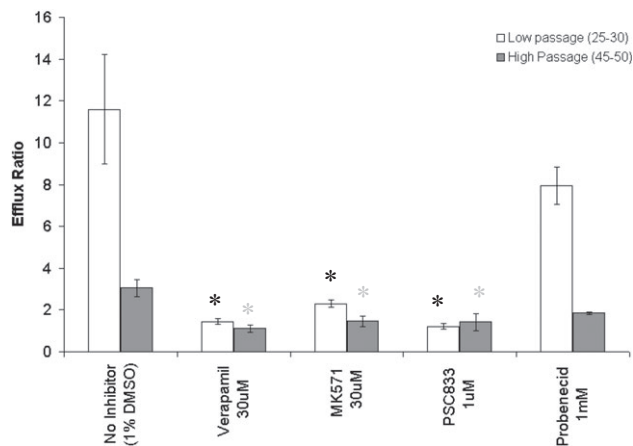
REFERENCES

[1] C.I. Grainger, L.L. Greenwell, D.J. Lockley, *et al.* "Culture of Calu-3 cells at the air interface provides a representative model of the airway epithelial barrier" *Pharm Res,* **23** (2006) 1482–1489.
[2] M. Maldova, C. Bosquillon, D. Asker, *et al.* "*In-vitro* respiratory drug absorption models possess nominal functional P-glycoprotein activity" *J Pharm Pharmacol* **61** (2009) 293–301.
[3] C. Bosquillon, "Drug transporters in the lung–do they play a role in the biopharmaceutics of inhaled drugs?" *J Pharm Sci* **99** (2010) 2240–2255.
[4] K. Bleasby, J.C. Castle, C.J. Roberts *et al.* "Expression profiles of 50 xenobiotic transporter genes in humans and pre-clinical species: a resource for investigations into drug disposition." *Xenobiotica*

Doxycycline Tissue Levels in Abdominal Aortic Aneurysm (AAA) Patients

N.J. Medlicott[1], S. Chary[1], G. Johnstone[1], G. Jones[2]

[1]School of Pharmacy, and [2]Department of Medical and Surgical Sciences, University of Otago, Dunedin.

Abstract – **A reversed phase HPLC assay was developed for doxycycline in plasma and AAA tissue. Plasma concentrations ranged from 1.63–2.88 μg/mL and aneurysm tissue concentrations were 1.82–10.0 μg/g in nine patients who received 100 mg doxycycline twice daily for four weeks prior to AAA surgery. The mean tissue to plasma concentration ratio was 2.2 ± 1.2.**

INTRODUCTION

Doxycycline, a commonly used antibiotic, has broad spectrum matrix metalloproteinase (MMP) inhibitor activity and is currently being trialled as a therapeutic agent to slow abdominal aortic aneurysms (AAA) growth [1]. The aim of this study was to quantify doxycycline concentrations in

plasma and AAA tissue in patients treated with a normal doxycycline dosage prior to AAA repair.

MATERIALS AND METHODS

A C18 Luna (5 µm), 250×3 mm column was used (Phenomenex, New Zealand). Mobile phase was 20:80v/v acetonitrile: 0.025% oxalic acid. Flow rate was 0.8 mL/min. Injection volume was 50 µL. Detector wavelength was 347 nm. Column temperature was 30°C.

Plasma (0.5 mL) was mixed with 50 µL phosphoric acid (8.5%) and 50 µL internal standard (10 µg/mL chlortetracycline, I.S.). Then vortexed, incubated for five minutes on ice, and centrifuged. Supernatants (600 µL) were transferred to StrataX columns (30 mg/1 mL, Phenomenex) pre-conditioned with methanol and water. Washed with 5% methanol (600 µL, three times); then eluted with 500 µL 30:70v/v acetonitrile:0.025% oxalic acid or 2×400 µL 75% acetonitrile. Acetonitrile samples were evaporated to dryness and reconstituted with 200 µL mobile phase.

Aortic tissue samples (ca.50 mg) were homogenised in 400 µL McIlvaine buffer (pH4, 0.09 M EDTA). 20 µL 20% trichloroacetic acid, 50 µL I.S. and 400 µL water were added. Samples were vortexed, centrifuged and supernatant (800 µL) transferred to StrataX columns as above. Elution was with 75% acetonitrile and reconstitution volume was 120 µL.

Patients received 100 mg doxycycline twice daily for four weeks prior to AAA surgery and four weeks post-operatively. Blood samples (10 mL) were collected prior to surgery. Aortic tissues removed during aneurysm repair were frozen in liquid nitrogen and stored at −80°C. Ethical approval was from the Lower South Regional Ethics Committee (New Zealand).

RESULTS AND DISCUSSION

Recovery of doxycycline from spiked plasma was around 80% for samples eluted with 30:70 v/v acetonitrile:0.025% oxalic acid. The assay was linear over 0.1–5 µg/mL doxycycline ($R^2 > 0.995$). Within-run variability at 0.2, 1.5 and 3.0 µg/mL was less than 10% (CV, n = 5). Between-run variability was less than 10% at 1.5 and 3.0 µg/mL, and 14% at 0.2 µg/mL (n = 3). For samples eluted with 70% acetonitrile, recovery at 2 µg/mL was 82%. The assay was linear over 0.05–5 µg/mL doxycycline ($R^2 > 0.995$) and assay variability was reduced.

Recovery of doxycycline from spiked aortic tissue was 72–83% and the assay was linear over 0.1–15 µg/g doxycycline ($R^2 > 0.995$).

The mean plasma doxycycline concentration at the time of surgery was 2.03 µg/mL (range:1.63–2.88 µg/mL, n = 9) and the mean AAA tissue concentration was 4.53 µg/g (range:1.82–10.0 µg/g). The mean tissue to plasma concentration ratio was 2.23 (range:1.1–4.8).

CONCLUSION

AAA tissue concentrations appeared low compared with those reported to inhibit collagenase (IC_{50} 16–18 µM (7–8 µg/mL)) or gelatinase (IC_{50} 30–50 µM (13–22 µg/mL)) [2]. This information may help interpret findings of effects of doxycycline treatment on MMP levels and clinical effect in AAA.

ACKNOWLEDGMENTS

REFERENCES

[1] Newman KM, Ogata Y, Malon AM, *et al*. Identification of Matrix Metalloproteinases 3 (Stromelysin-1) and 9 (Gelatinase B) in Abdominal Aortic Aneurysm. *Arterioscler. Thromb.*, **14** (1994) 1315–1320.

[2] Golub LM, Sorsa T, Lee H-M, *et al.* Doxycycline inhibits neutrophil (PMN)-type matrix metalloproteinases in human adult periodontitis gingiva. *J. Clin. Periodontol.*, 22 (1995), 100–109.

Dry Powder CriticalSorb™ Formulations Promote the Absorption of Macromolecules Across the Nasal Mucosa of Rabbits

A.L. Lewis, F.M. Jordan, L. Illum

Critical Pharmaceuticals Ltd., BioCity Nottingham, Pennyfoot Street, Nottingham, NG1 1GF.

Abstract – **The ability of various intranasal CriticalSorb formulations to promote human growth hormone (hGH) absorption across the nasal mucosa was assessed. Bioadhesive dry powder formulations were manufactured by spray drying, administered intranasally to conscious rabbits and the pharmacokinetics investigated. Protein integrity was demonstrated on storage for 13 weeks. An optimum formulation was found that gave a relative bioavailability of hGH of 43%. In conclusion, CriticalSorb™ has the potential to be a very efficient nasal delivery system for peptides and proteins.**

INTRODUCTION

The nasal cavity provides an excellent opportunity for non-invasive systemic drug delivery of hydrophilic drugs [1]. To

improve absorption across the nasal mucosal barrier, a number of permeation enhancers have been employed. However, new absorption enhancers with improved tolerability are needed [2].

We have recently discovered a novel permeation enhancer – CriticalSorb™ – able to promote the absorption of proteins and peptides across the nasal mucosal membrane. In the current study, we developed a range of dry powder formulations of hGH – a 22 kDa protein – and investigated the effect of varying the ratio of CriticalSorb: hGH on nasal bioavailability in conscious rabbits.

MATERIALS AND METHODS

hGH (Sandoz) was spray dried with a bioadhesive excipient and CriticalSorb, varying the ratio of absorption enhancer:protein. 1 mg/kg hGH was administered to conscious rabbits (n = 6) intranasally or subcutaneously, and blood samples collected from the marginal ear vein. Bioanalysis was performed on an Immulite 1000 (Siemens Diagnostics). hGH integrity was assessed using SEC and RP-HPLC methods after storage in glass vials with a nitrogen headspace at −20°C over 13 weeks.

RESULTS AND DISCUSSION

A range of bioadhesive dry powder hGH formulations containing CriticalSorb were produced and protein integrity was demonstrated upon manufacture and storage for 13 weeks at −20°C as assessed by SEC, RP-HPLC and native-PAGE (Table 1).

The best intranasal formulation achieved a bioavailability of 43% (F_{0-2h}) relative to a subcutaneous injection (Table 2) with very rapid absorption.

CONCLUSIONS

Intranasal dry powder CriticalSorb™ formulations have been developed that achieve exceptionally high bioavailabilities of

Table 1: hGH Integrity on Manufacture and Storage ND = Not Determined

	Week 0	Week 4	Week 13
% Monomer	99.5 ± 0.1	99.2 ± 0.0	99.6 ± 0.2
% Undegraded	95.3 ± 0.4	ND	96.7 ± 0.2

Table 2: Effect of CriticalSorb (CS):hGH Ratio on Bioavailability

	hGH s.c.	CS:hGH Ratio 1	CS:hGH Ratio 2	CS:hGH Ratio 3	CS:hGH Ratio 4
F_{0-2h} vs sc (%)		43.1 ± 14.6	17.1 ± 3.24	1.4 ± 0.41	0.9 ± 0.5
Tmax (h)	1 ± 0.4	0.25 ± 0.05	0.5 ± 0.2	1 ± 0.1	1 ± 0.2
C_{max} (ngml^{-1})	806.8 ± 23.4	520.2 ± 202.3	258.3 ± 50.6	18.3 ± 7.66	8.7 ± 4.2

hGH, and that were stable on storage. These studies show that CriticalSorb™ has the potential to be a very efficient nasal delivery system.

ACKNOWLEDGMENTS

REFERENCES

[1] L. Illum. Nasal drug delivery-possibilities, problems and solutions. Journal of Controlled Release 87, 2003, 187–198.

[2] H.R Costantino *et al*, Intranasal delivery: Physicochemical and Therapeutic Aspects. Int. J. Pharm. 337, 2007, 1–24.

Evaluating the Role of Dosage Size and Feeding on Gastric Retention in the Dog

Emma McConnell[1], Anita Lalloo[2], Jin Lan[2], Simon Hill[1], Richard Elkes[1], Henry (Yunhui) Wu[2]

[1]Devlab, MSD, Hertford Road, Hoddesdon, UK, [2]Biopharmaceutics, PR&D Merck, West Point, PA, USA

There are numerous approaches to try to achieve gastroretention (GR), one of which is the use of size-increasing systems. Here we investigate that concept by dosing controlled release (CR) dosage forms of differing sizes to the dog and assessing their transit/PK parameters. Dosage forms which had greatly different size and swelling profiles behaved similarly in the dog. This data, along with studies on the effect of food, suggest that gastroretention is mediated mainly by calorific/fat content taken with a CR dosage form, and the actual size of the dosage forms is less important.

INTRODUCTION

Gastroretention has been identified as a potential approach to achieve controlled release for drug molecules with a narrow absorption window. Retention of a dosage form in the stomach

(wherein dissolved drug is slowly released and emptied into the proximal small intestine) would ideally provide better bioavailability than conventional controlled released systems. Swelling (or size increasing) tablets are hypothesised to work on the premise that a tablet can avoid gastric emptying by virtue of having a size greater than the dimensions of the pylorus (~15 mm man/ ~5 mm dogs) and having sufficient mechanical strength to avoid disintegration by the muscular contractions of the stomach. In vitro techniques such as time-lapse photography (to assess swelling) are useful to rank such dosage forms and this used to select dosage forms of contrasting size and swelling characteristics. These formulations were dosed to dogs and the transit and PK parameters were evaluated.

Figure 1 *Swelling profile of 1000 mg) and 200 mg polymer tablets*

MATERIALS AND METHODS

Tablets were prepared using direct compression of blends of hydroxypropyl methylcellulose (HPMC), polyethylene oxide (PEO), lactose, microcrystalline cellulose and magnesium stearate. These were loaded with 20 mg of metformin. The tablets were assessed for swelling using time-lapse photography in simulated USP II conditions and the images converted to 2-dimensional surface area values. Metformin release was measured using USP II apparatus in simulated gastric fluid. To measure the transit of the tablets, barium-impregnated spheres or threads were added to the blend before compression. Dog studies were designed to understand the effect of food (low and medium fat diets) and dosage form size on the PK profiles of metformin. Transit of the dosage forms was followed using X-ray imaging.

RESULTS AND DISCUSSION

To elucidate the effects of formulation size on transit and PK parameters in the dogs, formulations were designed to have different size and swelling profiles, but similar drug release rates. A range of polymeric tablets were investigated. An HPMC/ PEO matrix tablet (1000 mg caplet shaped, 20 mg metformin) and a HPMC matrix tablet (200 mg round, 20 mg metformin) showed the most favourable characteristics in vitro. The 1000 mg tablet swelled quickly to a large size (in contrast to the 200 mg tablet which had a small size and low swelling rate, Fig.1). The HPMC/PEO matrix eroded in vitro after ~12 hours which is desirable to prevent accumulation of GR dosage forms. These formulations had similar drug release rates (data not shown).

The in vivo gastric emptying times of the 1000 mg and 200 mg tablets were similar using the medium fat diet (5.5 ± 2.1 and 5.0 ± 0.0 hours respectively). Barium impregnated spheres were used as markers and they had a similar gastric emptying time (3–6 hour range). This is despite the smaller dosage form and the spheres being of smaller diameter than the dog pylorus. This suggests that there is limited evidence of size-mediated gastroretention in the dog. Gastric residence could, however, be modified by changing the fat value of the food as expected (3.3 hours with low fat diet and >6 hours with 1000 mg tablet with high fat). The similar transit times
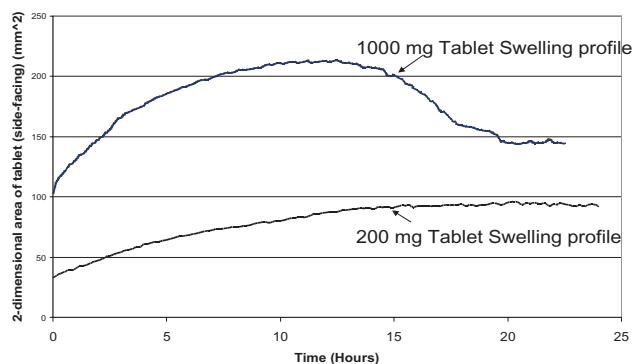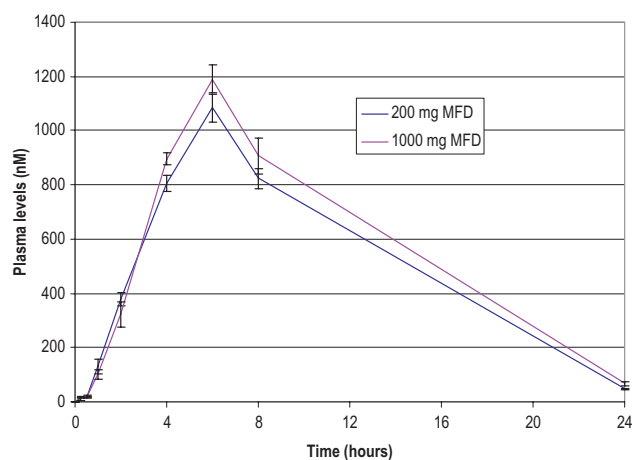

Fig 2 *PK parameters after dosing 1000 mg HMPC/PEO matrix tablet or 200 mg HMPC matrix tablet containing metformin (beagle dogs, n = 6) with a medium fat diet (MFD).*

of the small and large dosage forms translated to similar PK parameters (similar AUC, Tmax and Cmax, Fig 2).

CONCLUSIONS

The data suggests that there is limited effect of a size-mediated mechanism on gastroretention, and gastroretention is mediated to a greater extent by the reaction of the fed stomach to non-disintegrating dosage forms. However, increasing the size may increase the probability of longer retention in the stomach, which may not be reflected in this small study. The dog model should be used with caution when investigating gastric retention where size-increase is the primary mechanism under investigation.

ACKNOWLEDGMENTS

Evaluation of the rat airway epithelial RL65 cell line as a novel *in-vitro* model for screening inhaled drug candidates

V. Hutter[1], N. Tang[1], V. Zann[2], A. Cooper[2], D.I. Pritchard[3], C. Bosquillon[1]

[1]Division of Advanced Drug Delivery and Tissue Engineering, School of Pharmacy, University of Nottingham, UK
[2]AstraZeneca R&D Charnwood, Loughborough, UK.
[3]Division of Molecular and Cellular Science, School of Pharmacy, University of Nottingham, UK.

Abstract – **The rat airway epithelial cell line RL65 was assessed for its potential as an *in-vitro* permeability screening tool of inhaled compounds. Cells were grown on Transwell® cell culture supports at an air-liquid interface in serum-free medium. Cell layers exhibited transepithelial electrical resistance (TEER) values >200Ω.cm^2 after 14 days in culture when seeded at a density of 1×10^4 cells/ cm^2. A coefficient of apparent permeability (P_{app}) ~2.5×10^{-6} cm/s was obtained for the paracellular markers, fluorescein sodium and ^{14}C-mannitol. No vectorial transport was observed for the drug transporter substrates rhodamine 123 and ^{3}H-digoxin.**

INTRODUCTION

A rat airway epithelial *in-vitro* model is needed to bridge the gap between rat *in-vivo* and human *in-vitro* models currently used in early clinical development of inhaled drug candidates [1] as well as to gain an understanding of inter-species variations in drug absorption from the lungs. The cell line RL65 was isolated from normal neonatal rat lung and shows morphological and biochemical characteristics similar to bronchial/bronchiolar epithelial cells [2]. The aim of this work was to assess the suitability of RL65 cells as a model for *in-vitro* permeability screening.

MATERIALS AND METHODS

The rat lung cell line RL65 was purchased from the ATCC at an unknown passage (x). Cells were cultured in Dulbecco's Modified Eagle's Medium/Ham's F12 nutrient mixture 1:1 supplemented with 85 nM selenium, 2.5 µg/ml bovine insulin, 5.4 µg/ml human transferrin, 0.03 mM ethanolamine, 0.1 mM phosphoethanolamine, 500 nM hydrocortisone, 5 µM forskolin, 50 nM retinoic acid, 0.15 mg/ml bovine pituitary extract, 100 UI/ml penicillin and 100 µg/ml streptomycin.

Cells were seeded at a density between 1×10^4 and 1×10^5 cells/cm^2 on 12-well Transwell® cell culture inserts and cultured at an air-liquid interface 24 hours after seeding. The development of the barrier properties of the cell layers was assessed by TEER measurements. Permeability studies (passage x + 9–12) were performed in Hank's Balanced Salt Solution 14 days after seeding using the paracellular markers fluorescein sodium (0.1 mg/ml) and ^{14}C-mannitol (6.56 µM). The model was assessed for the presence of functional transporter systems using rhodamine 123 (5 µM) and ^{3}H-digoxin
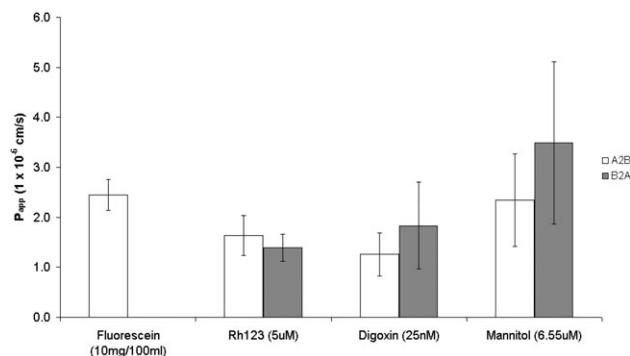

Figure 1: P_{app} (10^{-6} cm/s) of various permeability markers in RL65 cell layers (passage x + 9 – 12). Cells were seeded at 1×10^4 cells/cm^2 and cultured at an air-liquid interface for 14 days. Data are presented as mean ± SD (n = 3 – 4).

(25 nM) as model substrates trafficked by a variety of transporters.

RESULTS AND DISCUSSION

RL65 cell layers exhibited a measurable TEER after four days in culture. TEER values increased with time in culture to reach a peak of 165 ± 1 Ω.cm^2 after 8 days at a seeding density of 1×10^5 cells/cm^2, of 156 ± 1 Ω.cm^2 after 10–11 days when seeded at 5×10^4 cells/cm^2 and 220 ± 64 Ω.cm^2 after 13–14 days at a density of 1×10^4 cells/cm^2 (n = 3).

P_{app} values of the paracellular markers ^{14}C-mannitol and fluorescein sodium were ~2.5×10^{-6} cm/s (Figure 1). The permeability of rhodamine 123 and ^{3}H-digoxin was similar in the apical to basolateral (AB) and BA directions (Figure 1).

CONCLUSIONS

The rat airway epithelial RL65 cell line forms layers with sufficiently tight barrier properties, as indicated by TEER and permeability of paracellular markers which are in the same range as in the established human bronchial epithelium cell line, 16HBE14σ [3]. Therefore, RL65 cell layers are a promising novel rat respiratory cell culture model for inhaled drug permeability screening. However, no active transport mechanisms appeared to be functional under the investigated conditions. Permeability measurements will be reproduced in layers at a higher passage number to assess transporter activity in older cells.

REFERENCES

[1] M.Sakagami, "In vivo, in vitro and ex vivo models to assess pulmonary absorption and disposition of inhaled therapeutics for systemic delivery", *Adv.Drug.Deliv.Rev.*, **58** (2006) 1030–1060.

[2] P.E.Roberts, D.M.Phillips, J.P.Mather, "A novel epithelial cell from neonatal rat lung: isolation and differentiated phenotype", *Am.J.Physiol.*, **259** (1990) L415-L425.

[3] H.Wan, H.L.Winton, C Soeller et al, "Tight junction properties of the immortalised human bronchial epithelial cell lines Calu-3 and 16HBE14o-*"Eur Respir J"*., **15** 2000 1058–68.

Impact of Biopharmaceutics Properties on Clinical Performance of Simple 'Powder in Capsule' Formulations

J. Bennett, J. Davis, M. McAllister, J. Morris

Pfizer Global R & D, Sandwich, Kent, UK.

INTRODUCTION

A number of compounds within Pfizer have been progressed to the clinic using 'powder in capsule' (PIC) formulations which simply comprise of bulk drug in a hard gelatin capsule. This minimalistic approach has obvious advantages in terms of speed and resource, though could be seen to pose significant risk, as lack of formulation optimisation may adversely impact clinical performance. Studies were undertaken to understand how the biopharmaceutics properties of a drug impacted on the 'success' of PIC formulations in the clinic. An analysis of 21 compounds progressed to the clinic as PIC formulations was conducted to understand the influence of solubility, permeability and dose number on clinical performance and success [1].

MATERIALS AND METHODS

Criteria for 'clinical success' were defined and based primarily on pharmacokinetic parameters. A scoring system was developed to ensure clinical data for each compound were assessed and weighted in a similar way. Compounds were classified as clinically 'successful' or 'non-successful' (represented graphically as grey closed and open symbols, respectively). A 'confidence score' was also devised which shows the relative amount of clinical data available to make the assessment. The size of the data points on the graphs are larger for compounds in which there is greater confidence (i.e. more data available) for assigning the 'success' and 'non-successful' categorisation.

Solubility data was generated largely by shaking bulk drug in SGF (without enzymes) and Fassif for > 16 hrs prior to filtering and assay by LC-MS-UV. The highest solubility that this methodology can determine is 0.3 mg/ml. The lowest solubility value generated over the physiological pH range was used in the data plot.

Permeability (Papp) data was obtained from in vitro MDCK/Caco-2 cell monolayer studies conducted at pH 7.4.

RESULTS AND DISCUSSION

The data shows that 14/21 (66%) and 5/21 (23%) compounds were regarded as clinically 'successful' and 'non-successful', respectively. The confidence in the assignment was relatively high for 8 of the 'successful' and 2 of the 'none successful' compounds. The biopharm properties of the compounds progressed as PIC formulations were found to span the BCS classes with both high and low permeability and solubility compounds progressed to the clinic [2]. No relationship between clinical success and permeability was found. Clinically 'non-successful' compounds were only observed, though not exclusively, with low solubility compounds (solu-
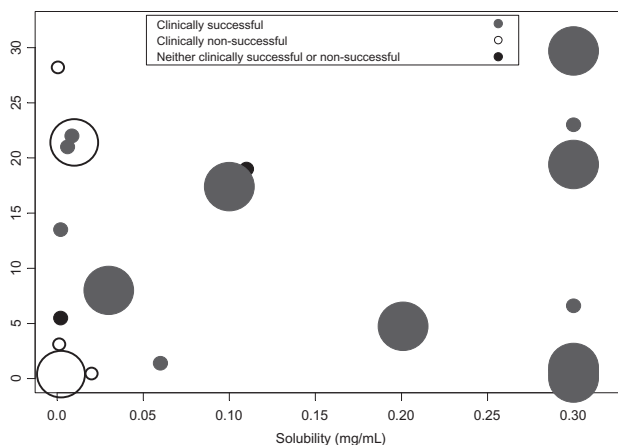

Fig. 1. Influence of permeability and solubility on 'clinical success' of PIC formulations.

bility < 0.03 mg/ml). Compounds which were regarded as 'clinically successful' had dose numbers as high as at least 5.

CONCLUSIONS

PIC formulation is a useful approach to progress compounds reducing time and resource in early development. Application of PIC formulation is not limited to BCS class and maybe appropriate for all classes. Solubility and dose number are likely to be important factors in limiting clinical success, though the boundaries of these are wider than those established for high solubility by the BCS classification system. Contribution of additional factors such as wettability and dissolution rate also merit consideration.

ACKNOWLEDGMENTS

REFERENCES

[1] G.L. Amidon, H. Lennernas, V.P. Shah and J.R. Crison "A theoretical basis for a biopharmaceutic drug classification: the correlation of in vitro drug product dissolution and in vivo bioavailability" Pharm. Res.,**12**, 3 (1995) 413–420.

[2] Food and Drug Administration Guidance for industry, "Waiver of in vivo bioavailability and bioequivalence studies for immediate release solid oral dosage forms based on a biopharmaceutics classification system", Centre for Drug Evaluation and Research, (2000).

In vitro, in vivo and simulation tools to improve safety and tolerability profile in clinical studies: PhI experience for a new chemical entity

M. Petrone[1], S. Beato[2], A. Casazza[2], R. Gomeni[1], F. A. Gray[3]

[1]GlaxoSmithKline, Clinical Pharmacology Modelling and Simulation, Verona, Italy
[2]GlaxoSmithKline, Pharmaceutical Development, Verona,
[3]GlaxoSmithKline, Clinical Pharmacology and Discovery Medicine, Harlow, UK

Abstract – **Population model derived from Phase I studies can be integrated backwards to simulation tools, in vitro data and physico-chemical information on a new chemical entity (NCE), together with physiology knowledge of gastrointestinal (GI) tract. The benefit of this approach is to identify the optimal experimental strategy to modulate the pharmacokinetic profile in order to improve the safety and tolerability properties.**

INTRODUCTION

The quantitative integration into modeling and simulation of anatomy/physiology, *in silico*, *in vitro* and *in vivo* systems for describing pharmacokinetics (PK) and pharmacodynamics (PD), has been widely advocated for accelerating candidate drug development and reducing attrition [1]. The present communication describes a simulation-based approach to improve the safety and tolerability profile of a new chemical entity (NCE) acting *via* the noradrenergic-serotoninergic-dopaminergic pathways, which has been proposed for the treatment of obesity, integrating physiological, *in vitro* and *in vivo* information on biopharmaceutical, pharmacokinetic and tolerability properties.

MATERIALS AND METHODS

Early clinical information of a NCE obtained in a first-time in human (FTIH) study in 23 healthy subjects were used to generate a population pharmacokinetic model [2]. The relationships between model-derived metrics of systemic exposure (e.g. absorption rate and rate to peak levels) and safety and tolerability findings were assessed using PK-PD models. Simulations based on the population PK model parameters were conducted with the aid of the software program Gastroplus™ [3,4,5], which allows the integration of physico-chemical data of the NCE (permeability, solubility and its pH dependency) with the physiology of the human gastrointestinal tract. Simulations were made using different absorption rates resulting from modified release profiles of the NCE in the gastrointestinal (GI) tract.

RESULTS AND DISCUSSION

A simulated PK profile where absorption constant was 10-fold lower than estimated during FTIH study (Figure 1) allowed improving the safety and tolerability of the NCE. Absorption in the distal GI tract was a requirement for maintaining the
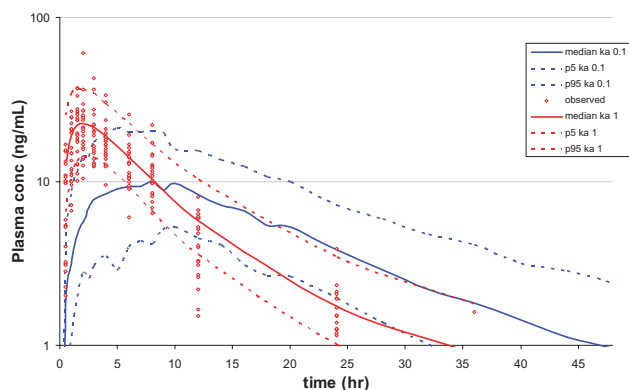
Fig. 1. Population PK at 60 mg dose: observed (red profiles) vs predicted (blue profiles) data at a simulated absorption rate

overall exposure. Physico-chemical properties of the molecule allow its formulation as modified release so that absorption rate can be modulated by release of the drug from the formulation.

CONCLUSIONS

The proposed simulation-based approach indicated that an extended release could provide a pharmacokinetic profile able

to control the peak-related side effects without influencing the overall therapeutic effect of the NCE. The integration of *in-vitro* and *in-vivo* data in simulation tools can be implemented successfully to modulate the pharmacokinetic profile in order to improve the safety and tolerability properties of new compounds.

REFERENCES

[1] Aarons, L. Karlsson, M.O. et al; European Journal of Pharmaceutical Sciences: Vol 13 (2001), 115–122.
[2] Guidance for Industry: Population Pharmacokinetics. U.S. Department of Health and Human Services, Food and Drug Administration 1999.
[3] Wei, H.; European Journal of Pharmaceutics and Biopharmaceutics 2008 ISSN: 0939–6411 Vol. 69 Issue: 3, 1046–1056.
[4] Parrott, N.; Molecular Pharmaceutics 2008 ISSN: 1543–8384 Vol. 5 Issue: 5, 760.
[5] Balaji A, Woltosz W, Bolger MB. Advanced Drug Delivery Reviews 2001, 50:S41–S67.

Influence of Pioglitazone on Solubility of Glimepiride: Approaches to In-Vivo and In-Vitor

Prashant B. Musmade*, Shriram Pathak, A. Karthik, K. M. Bhat and N. Udupa

Dept. of Pharmaceutical Quality Assurance, Manipal College of Pharmaceutical Sciences, Manipal University, Manipal-576104, India.

Abstract **– Pioglitazone and glimepiride is a well known fixed-dose combination (FDC) therapy used in Type 2 diabetes mellitus. If drugs are formulated in the fixed dose combination, it is necessary to determine the solubility and permeability of the drugs in combination as well as individually. In the present study we found the problem of variable solubility of glimepiride at different pH along with pioglitazone compare with alone. The bioavailability of glimepiride in animal model is also altered by the FDC.**

INTRODUCTION

Fixed dose combination regimens are attractive in conditions like hypertension and diabetes due to improved efficacy which can translate into better therapeutic outcomes. Solubility and permeability are the major biopharmaceutical factors that affect the rate and extent of absorption of orally administered drugs. Pioglitazone and glimepiride is the most widely used fixed dose combination worldwide. Solubility

data at simulated gastrointestinal pH conditions of pioglitazone and glimepiride in individual as well as in combination is not well reported.

The present study was aimed to evaluate saturation solubility of pioglitazone, glimepiride and in combination and also to understand the extent of absorption of pioglitazone, glimepiride and in combination in rats.

MATERIAL AND METHOD

The saturation solubility (*in-vitro*) of glimepiride, pioglitazone alone and in combination was carried out in buffer of pH 1.0, 1.5, 2.0, 6.4 and 7.4 using the shake flask method at $37 \pm 1°C$ for 24 hrs. The solubility sample analysis was carried out by HPLC method. IR spectroscopy was used to study the interaction between glimepiride and pioglitazone.

In vivo pharmacokinetic study of glimepiride (dose −20.0 mg/kg), pioglitazone (2.0 mg/kg) and in combination was carried out in rats.

RESULT AND DISCUSSION

The present study found that solubility of glimepiride and pioglitazone is pH dependent. Glimepiride solubility increased from pH 1.0 to 6.4 and decreased at pH 7.4 In the case of pioglitazone, high solubility was observed at pH 1.0. The results found that there was a significant ($p < 0.05$) increase in solubility of glimepiride in presence of pioglitazone compared to glimepiride alone at pH 1.0, 1.5, 2.0 and 7.4 and significantly decreased at pH 6.4. In the case of pioglitazone there was no alteration of solubility in the presence of glimepiride compared to pioglitazone alone. The increase in the solubility may be due to interaction between glimepiride and pioglitazone. The *in vivo* pharmacokinetic results showed that there was a 1.86 fold increase in the relative bioavailability of glimepiride in presence of pioglitazone compared with glimepiride. The cause for this alteration in the bioavailability needs to be investigated further.

CONCLUSION

The present study showed significant enhancement of pharmacokinetic parameters and relative bioavailability of glimepiride in the presence of pioglitazone compared with glimepiride, whereas the same interaction was not observed for pioglitazone in the presence of glimepiride. This may be due to altered solubility, permeability or enzymatic activity.

ACKNOWLEDGMENT

REFERENCES

1. G. Derosa, "Pioglitazone plus glimepiride: a promising alternative in metabolic control" *Int. J. Clin. Pract.,* **61** (2007), suppl. 153, 28–36.
2. M. Hanefeld, "Pioglitazone and sulfonylureas: effectively treating type 2 diabetes", *Int. J. Clin. Pract.,* **61** (2007), suppl. 153, 20–27.
3. J. Waugh, G.M. Keating, G.L. Plosker, S. Easthope, and D.M. Robinson, 2006, "Pioglitazone: a review of its use in type 2 diabetes mellitus", Drugs, **66** (2006) 85–109.
4. T.T. Mariappan and S. Singh, "Regional gastrointestinal permeability of rifampicin and isoniazid (alone and their combination) in the rat" *Int. J. Tuberc. Lung Dis.,* **7**(2003) 797–803.
5. M. Nahar and N.K. Jain, "Formulation and evaluation of saquinavir injection", *Indian J. Pharm. Sci.,* **68**(2006) 608–614.

Pharmacokinetics, Biodistribution, Acute Toxicity and In Vivo Anti-tumour Efficacy of Paclitaxel Solid Dispersion

Xiangrui Liu[1,3], Jiabei Sun[1], Xiaomei Chen[1], Shudong Wang[2], Xuan Zhang[1], Qiang Zhang[1]

[1]Department of Pharmaceutics, School of Pharmaceutical Sciences, Peking University, Beijing 100083, China
[2]School of Pharmacy and Centre for Biomolecular Sciences, University of Nottingham, University Park, Nottingham NG7 2RD, UK.
[3]Present address: School of Pharmacy and Centre for Biomolecular Sciences, University of Nottingham, University Park, Nottingham NG7 2RD, UK.

INTRODUCTION

Paclitaxel is a naturally occurring alkaloid that has shown clinical activity against several tumours. However, due to its low aqueous solubility, Cremophor EL (polyoxyethylated castor oil) and ethanol are used as excipients in the most widely used commercial formulation TAXOL. Serious clinical side effects have been attributed to Cremophor. A novel Cremophor-free paclitaxel solid dispersion was prepared with PVP-K30 (polyvinylpyrrolidone) in our laboratory previously. The primary aim of this study was to evaluate the pharmacokinetics, biodistribution, acute toxicity and *in vivo* antitumour efficacy of paclitaxel solid dispersion compared with TAXOL.

METHODS

Sprague-Dawley rats were used to examine the pharmacokinetics and tissue distribution of paclitaxel after intravenous administration (5 mg/kg). The acute toxicity was studied in ICR mice by calculating LD50 (median lethal dose). In vivo anti-tumour efficacy was evaluated in nude mice bearing human ovarian adenocarcinoma (SKOV-3) xenograft in a schedule of single administration of TAXOL (15 mg/kg) or paclitaxel solid dispersion (15 mg/kg or 30 mg/kg) on the first, fourth and seventh day, respectively. The animal experiments were approved by the Institutional Animal Care and Use Committee of Peking University.

RESULTS

The plasma AUC of paclitaxel solid dispersion was 5.84-fold lower than that of TAXOL and the Vd and Cl of paclitaxol solid dispersion were increased by 8.70- and 4.90-fold, respectively. However, no significant differences between paclitaxol solid dispersion and TAXOL were observed in tissue distribution. The LD_{50} was 34.8 mg/kg for TAXOL

whereas no death was observed at the highest dose of 160 mg/kg of paclitaxol solid dispersion. Paclitaxol solid dispersion showed similar anti-tumour activity as TAXOL at a dose of 15 mg/kg. Most importantly, the improved tolerance of paclitaxel solid dispersion enabled a higher administrable dose of paclitaxel, which resulted in improved anti-tumour activity.

CONCLUSIONS

Paclitaxel solid dispersion produced more rapid paclitaxel clearance in bloodstream but showed similar distribution and residence time in tissues tested. Paclitaxol solid dispersion had similar *in vivo* antitumour efficacy as TAXOL, but significantly improved tolerance.

The Effect of Cross-Linking on the *In Vitro* Disintegration of Hard Gelatin Capsules

M.J. St.Clair, J. Purdie, Y. Hu and P. McGeough

Department of Analytical Chemistry, Encap Drug Delivery Ltd., Livingston, UK.

Abstract – **A study was conducted to compare dissolution methods for overcoming cross-linking of hard gelatin capsules. A formulation known to express cross-linking of hard gelatin capsule shells was used under varied stress conditions to produce different degrees of cross-linking.**

INTRODUCTION

The relative merits and limitations of hard gelatin capsules are well documented. Gelatin has the ability to form highly suitable films, capable of dissolving readily in the stomach. It has been observed that certain conditions, especially the existence of aldehydes or hot and humid storage, can render the capsule partially insoluble in water due to cross-linking of the gelatin [1].

The aim of this work is to compare the differences in different media used to generate dissolution profiles of a product where the capsule shells have been modified by inducing cross-linking of the gelatin by inclusion of a proprietary Pharmaceutical NCE, also suitable for determination in solution by UV Spectroscopy.

METHODS

Capsules were stored for 3 months at 5°C, 25°C/60%RH and 40°C/75%RH in order to induce differing levels of cross-linking of the gelatin; classed as mild, moderate and severe respectively. The comparison was conducted by measuring the rate of release of the included active material; using USP dissolution apparatus II at 75 rpm. The dissolution media compared were:

1) Water (as a control).
2) Intestinal Fluid, Simulated, SIF – using 10 g/L of Pancreatin.
3) Gastric Fluid, Simulated, SGF – using 3.2 g/L of Pepsin.
4) Intestinal Fluid SIF *two tier* – using 0.05 g/L of Pancreatin (USP < 711 > *two-tier* testing)
5) Gastric Fluid SGF *two tier* – using 75000units/L of Pepsin (~0.8 g/L)(USP < 711 > *two-tier* testing)

RESULTS AND DISCUSSION

Fig. 1 demonstrates that for mild cross-linking there are no significant differences between the media although small experimental variation is present, this is due to occlusion of the media due to the enzyme concentrations.

Fig. 2 demonstrates that with moderate levels of cross-linking both SIF and SGF have similar releases to each other and to the mild cross-linking (Fig. 1). The *two-tier* SIF and SGF demonstrate significant retardation although are still similar to each other. This demonstrates the equivalency of the *two-tier* enzyme concentrations. The water demonstrates retardation only slightly slower than the *two-tier* equivalents.

Fig. 3 shows that with severe levels of cross-linking the *two-tier* enzyme concentrations are no longer sufficient to promote release and there is no difference to water. The high concentration of enzyme in SIF still promotes release at the initial rate. The concentration of enzyme in SGF however now demonstrates retardation.

CONCLUSIONS

The study illustrates that only for mild cross-linking will the USP < 711 > *two-tier* system aid in improving release profile but it also demonstrates the equivalency of the enzyme levels
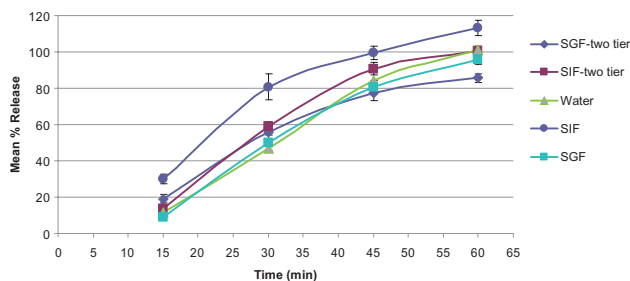

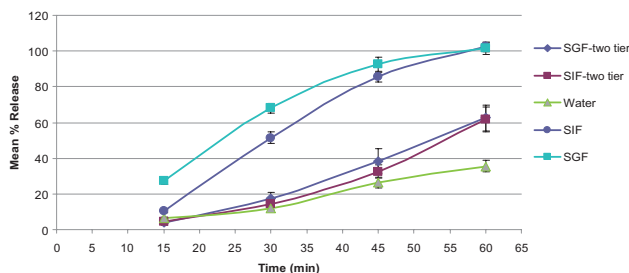**Fig. 1.** Mild cross-linking (error bars showing standard deviation)

Fig. 2. Moderate cross-linking (error bars showing standard deviation)
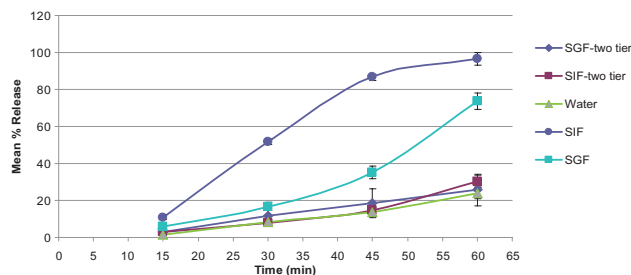

Fig. 3. Severe cross-linking (error bars showing standard deviation)

stated. Higher enzyme concentrations do promote release of more significantly cross-linked capsules but it is yet to be proved what the *In-Vivo* correlation concentrations are.

REFERENCES

[1] G.A. Digenis, T.B. Gold, and V.P. Shah. "Cross-linking of Gelatin capsules and its relevance to their *in vitro – in vivo* performance" J.Pharm. Sci. **83**: 915–921 (1994).

[2] V.A. Gray. "Two-tier dissolution testing. AAPS: Hard and soft gelatin capsules: issues, research and outcome" *Boston* (1997).

Using TNO gastro-Intestinal Model (TIM1) to screen potential formulations for a poorly soluble development compound

S. E. David[1], M. M. Strozyk[2], T. A. Naylor[1]

[1]Pharmaceutical Development, GSK, Harlow, CM19 5AW. [2] Pharmaceutical Development, GSK, Poznan, Poland

Abstract – **The bio-relevant TNO Gastro-Intestinal Model (TIM1) [1,2] was used to evaluate various formulations of drug GSK-X. GSK-X is a poorly soluble compound with adequate permeability; studies were performed using biorelevant media in fed and fasted conditions. The formulations tested were 100 mg dosage units of: (A) GSK-X Gelucire® 44/14 capsule, (B) GSK-X PolyEthyleneGlycol (PEG) 3350 tablet, (C) milled GSK-X wet granulated tablet, (D) micronised GSK-X wet granulated tablet and (E) GSK-X wet bead milled/spray dried capsule (WBM/ SD). The results demonstrate an elevated dissolution and Cmax in the fed state compared to the fasted state for all formulations tested. The highest Cmax was demonstrated for the WBM/SDP capsule.**

INTRODUCTION

The aqueous solubility of GSK-X is 1.0 µg/ml and is required to be dosed at 100 mg. The permeability of GSK-X has been measured at $P_{app(A\ B)}$ 34.6 10^{-6} cm/s at 1 µM in Caco-2 cell systems but is predicted to be P_{eff} 3.44×10^{-4} at ph 7.4 using the measured LogD. It is likely that particle size reduction or bioenhancement will be required in vivo to deliver a dose of 100 mg.

MATERIALS AND METHODS

(A) GSK-X was milled (x90 65 µm) and suspended in molten Gelucire 44/14® at a loading of 33% w/w and filled into size 0, hpmc capsules at 65°C.

(B) GSK-X was milled (x90 65 µm) and granulated (high shear) with PEG 3350 (30% w/w). The granule was compressed into 350 mg tablets.

(C) GSK-X was milled and wet granulated (high shear). The granules were dried in a fluid bed drier and compressed into 350 mg tablets.

(D) Micronised GSK-X (x90 6.8 µm) was processed as (C)

(E) GSK-X was suspended in aqueous media and milled using a single chamber Nylacast mill using 0.65 mm and 0.40 mm Yttrium Stabilised Zirconia grinding beads then spray dried using a MobileMinor. The powder (x90 1.1 µm) was blended and filled into size 0 capsules.

The dosage form was introduced to the TIM1 at the start of the experiment with the relevant meal. Samples were taken
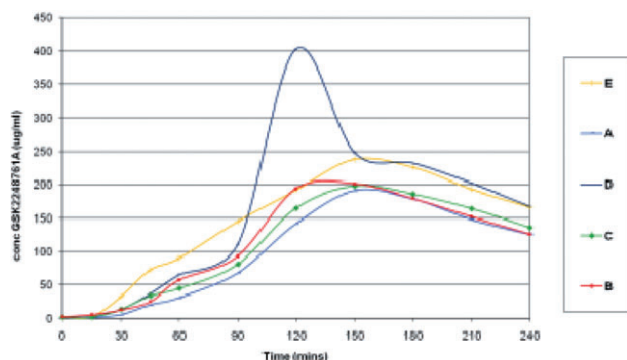
Figure 1 TIM1-TNO dissolution in the fed state

Figure 2 TIM1-TNO dissolution in the fasted state

at regular intervals for 4 hrs. The samples were analysed by HPLC.

RESULTS AND DISCUSSION

Dialysis sampling was not possible due to very low recoveries; therefore direct sampling from the separate compartments was used. In the fed state (Figure 1) formulation **E** has the highest rate and extent of dissolution. The 120 min timepoint for the micronised tablet is an anomaly. In the fasted state formulation **A** performed significantly better than the other formulations (Figure 2).

CONCLUSIONS

There is a significantly higher dissolution rate and Cmax in the fed state compared to the fasted state for all formulations.
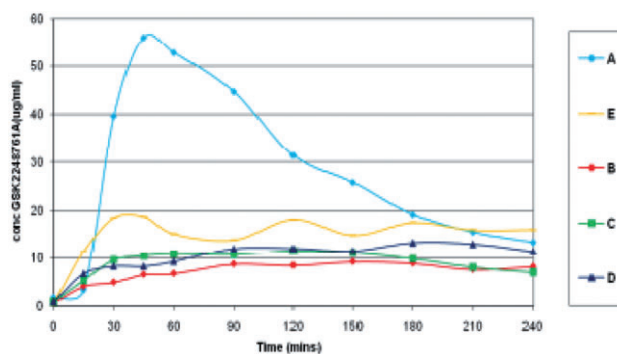
The highest dissolution rate was demonstrated for the WBM/SDP capsule formulation compared to all the other formulations. These results were predictive of the results obtained from a human relative biostudy in the fed state.

ACKNOWLEDGEMENTS

REFERENCES

[1] M. Minekus, P. Marteau, R. Havenaar, and J. H. J. Huis in't Veld. "A multicompartmental dynamic computer-controlled model simulating the stomach and small intestine". *Atla* 23 (1995) 197–209

[2] R. Havenaar and M. Minekus. ˝In vitro model of an in vivo digestive tract˝. JP US European Patent PCT/NL93/00225 (1994)

Transverse fingernail curvature: a quantitative evaluation, and an exploration into the influence of gender, age, handedness, height and hand size

Sudaxshina Murdan

Department of Pharmaceutics, School of Pharmacy, University of London, UK

Abstract – **The transverse curvature of healthy fingernails were measured in 183 individuals to provide baseline values. Regression analysis showed that nail plates were flatter in men, in older individuals, and in those with wider hands. In addition, in dextral (but not in sinistral) subjects, the fingernails of the dominant hand were flatter than their opposites in the non-dominant hand.**

INTRODUCTION

Healthy nail plates are curved both longitudinally and transversely, although overcurvature can indicate a disorder.

Research into the transverse nail curvature has been very limited. The aim of this study was therefore to measure the transverse curvature of healthy adult fingernail plates and thereby provide baseline values for 'normal' nail plates, and to explore the possible influences of a subject's gender, age, height, handedness, hand length and hand breadth on fingernail curvature.

MATERIALS AND METHODS

The study was approved by The School of Pharmacy's (University of London) ethics committee, and participants (92
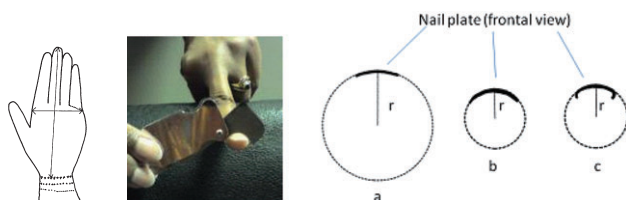
Figure 1. Positions at which hand length and breadth were measured. Transverse nail curvature was measured using a radius gauge. Flat nails (a) have a large radius, while curved nails (b) have smaller radii. The radius of the topmost part of the nail was recorded, as shown (c).

Table 1: Transverse nail curvature of the different digits

	Radius of nail curvature (mm)				
	thumb	index	middle	ring	little
Male	12.9 ± 2.0	10.8 ± 2.2	10.4 ± 2.1	8.4 ± 1.8	6.7 ± 1.2
Female	10.2 ± 1.9	8.2 ± 1.9	8.0 ± 1.6	6.5 ± 1.4	5.3 ± 0.9

male and 91 female adults, aged 21–90 years old) were recruited. The participants were asked for their age, height, mass and dominant hand, while the length and breadth of both hands was measured on the palmar side (Figure 1). Nail transverse curvature was expressed as the radius of the circle whose curve most closely approximates that of the nail plate (Figure 1), and was measured (by the author) using stainless steel radius gauges. The radius gauge was placed against the surface of the nail plate, mid-way along its length (Figure 1), and the gauge whose curvature most closely matched that of the nail plate was identified. It must be noted that because nail plates are rarely part of perfect circles, the methodology is not exact, but gives a close estimate. In all cases, the curvature of the topmost part of the nailplate was recorded, as shown in Figure 1. For each participant, the curvature of all healthy fingernails was measured; nails that were bitten or damaged in any way were excluded from the study.

RESULTS AND DISCUSSION

Transverse fingernail curvatures are shown in Table 1. Bearing in mind that large radius of curvature equates to flatter nails, the radius of curvature had the following order:
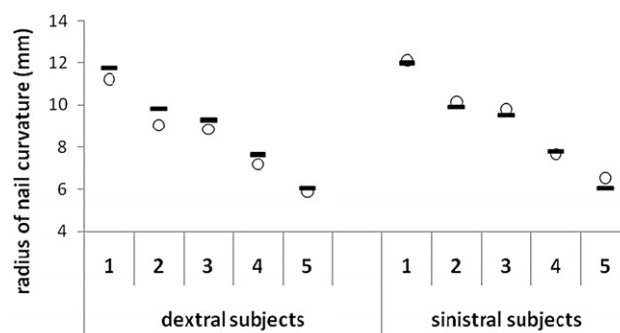

Figure 2. Curvature of the fingernails of digits 1–5 of the right (−) and left (o) hands in dextral and sinistral subjects. Means are shown, N = 160 – 164 for dextral subjects and 17–18 for sinistral subjects.

thumb > index > middle > ring > little finger. The dominant hand's fingernails were flatter than their opposites in the non-dominant hand, though the difference was greater (and only statistically significant) in dextral individuals compared to sinistral ones (Figure 2).

To investigate correlation between subjects' nail curvature and their gender, age, height, and hand length and breadth, hierarchical multiple regression was performed, entering gender first. Only gender, age and hand width were statistically significant ($p < 0.005$) with standardised ß coefficients of 0.35, 0.32 and 0.31 respectively. The whole model explained 56% of the total variance in nail curvature, $F(5, 176) = 45.1$, $p < 0.001$. Using the unstandardised B coefficients, a regression equation linking nail curvature with gender, age and hand breadth may be written as:

Mean nail curvature = 0 − 2.0 + 1.23*(Gender) + 0.03*(Age) + 0.89*(Hand breadth)

where Gender = 0 for females; 1 for males; and curvature, age and breadth are in mm, years and cm respectively.

CONCLUSIONS

Gender, age and hand breadth influence nail curvature, nail plates being flatter in men, in older individuals, and in those with wider hands.

The author is deeply grateful to all the volunteers.

A Hydrocortisone Nanoparticle Dosage Form

S. Zghebi, M. De Matas, M. Denyer, N. Blagden

Pharmaceutical Innovation Research Group, University of Bradford, Bradford, UK.

INTRODUCTION

Of particular importance in recent years has been the development of techniques for producing nanoparticles (NPs) of

poorly-water soluble drugs with dimensions less than 1000 nm for which their high surface area can lead to improvements in bioavailability. Furthermore, the small size of these particles can also enable cellular uptake, particularly for positively

charged systems. Therefore, an overall objective of this part of the project was to produce nanoparticles with different levels of positive surface charge using the bottom-up method.

MATERIALS AND METHODS

Nanosuspensions of the poorly-water soluble steroid drug hydrocortisone (Hc) were prepared by antisolvent precipitation technique using a micro channel reactor [1]. A 1% w/v solution of Hc in ethanol was combined with an anti solvent in a Y-micro channel reactor (internal diameter 0.5 mm). The solute and anti solvent aqueous solutions were combined at flow rates of 1 and 3.5 ml/min respectively to drive precipitation. In addition, to achieve suspension stability the anti solvent contained hydroxypropyl methyl cellulose (HPMC), polyvinylpyrolidone (PVP) and sodium lauryl sulphate (SLS) at concentrations of 0.2, 0.2 and 0.1% w/v respectively. Surface charge was tuned by adsorption of one of two quaternary ammonium cationic surfactants, namely didodecyldimethylammonium bromide (DMAB) and cetyltrimethylammonium bromide (CTAB) at concentrations in the range 0.01 – 0.2% w/v. The anionic surfactant SLS was omitted in the preparation of coated nanoparticles. Overall, positively-charged Hc nano-particles suitable for cell uptake studies were generated. Nanoparticle suspensions were evaluated for their stability by monitoring their size and ζ-potential up to 28 days using the Zetasizer Nano (Malvern Instruments, Worcestershire, UK).

RESULTS AND DISCUSSION

Particle size of uncoated Hc nanoparticles was in the range of 446.0 to 468.3 nm with ζ-potential between −1.46 and −2.06 mV. These particles showed no marked growth over 21 days. Nanoparticles coated with different concentrations of DMAB ranged in size from 148.8 to 739.3 nm with ζ-potential values between +27.7 and +76.1 mV (Fig. 1). ζ-potential was dependant on the initial surfactant concentration (0.01 – 0.2% w/v). CTAB-coated nanoparticles' diameter ranged from 155.8 to 237.9 nm and ζ-potential values were between +5.6 and +52.0 mV (Fig. 2). Both surfactants exhibited a similar ζ-potential profile as surfactant concentration was varied. Surfactant–coated NPs demonstrated adequate particle and suspension stability over 28 days.

CONCLUSIONS

These studies clearly show that with the prudent manipulation of the adsorption of cationic surfactants the micro channel
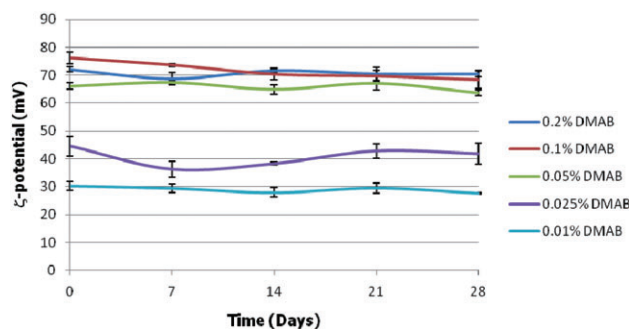

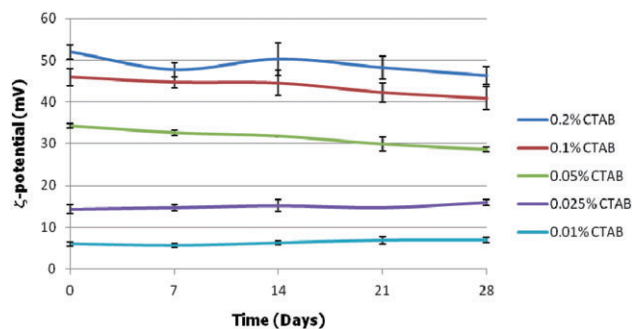**Fig. 1.** ζ-potential for DMAB – coated NPs over 28 days

Fig. 2. ζ-potential for CTAB – coated NPs over 28 days

precipitation route yielded nanoparticles with a tuneable surface charge. Such novel stabilised nano-medicines open up the potential for direct translocation across cell membranes. In the future, an *in vitro* evaluation of cellular uptake will be undertaken.

ACKNOWLEDGMENT

REFERENCE

[1] H.S.M. Ali, P. York and N. Blagden, "Preparation of hydrocortisone nanosuspension through a bottom-up nanoprecipitation technique using microfluidic reactors" *Int. J. Pharm.*, **375** (2009) 107 – 113.

A new model for *in vitro* finite dose permeation studies

M. Machado, J. Hadgraft, M.E. Lane

The School of Pharmacy, University of London, U.K.

Abstract **– Finite dose studies have shown some limitations in simulating what really happens when applying a formulation on the skin. This work aims to develop a new protocol that could better simulate the application of a formulation to the skin surface. The new protocol simulated short time contact conditions and correlated well with previous *in vivo* studies.**

INTRODUCTION

Previous studies were carried out to assess how different solvents affect the *stratum corneum* (SC) barrier properties *in vivo* by measuring the onset time of erythema following the application of a model drug -methyl nicotinate (MN). The aim of this work is to develop a method for *in vitro* permeation studies that simulates, as closely as possible, the same protocol carried out in *in vivo* studies. The new method should overcome some limitations of the commonly used protocols for *in vitro* permeation studies.

MATERIALS AND METHODS

The *in vitro* permeation of MN through human epidermis was investigated using Franz-type diffusion cells. The epidermis was positioned between the two compartments with the SC facing the donor compartment. The receptor phase used was a solution of PBS pH 7.4. The experiments were performed after immersing the Franz-type diffusion cells in a $32 \pm 1°C$ water bath. MN in each vehicle was applied on the skin surface at the same thermodynamic activity of 0.1 M MN in water (adjusted depending on the partition coefficient in solvent / water) for 30 seconds to an area of 1 cm^2 of skin using a pre-soaked filter paper. After 30 seconds the filter paper was removed and the SC gently cleaned with a cotton-bud and a filter paper. Five replicates were performed for each formulation. All samples were analysed by HPLC. The amount of MN applied was estimated by mass balance studies. For this study single solvents – water, isopropyl myristate (IPM), isopropyl isostearate (IPIS), propylene glycol (PG), propylene glycol monolaurate (PGML) and propylene glycol dicaprylocaprate (PGMC); binary systems – IPIS + lauryl alcohol, IPIS + benzyl alcohol, PGMC + lauryl alcohol and PGMC + benzyl alcohol; and ternary systems – PGMC + benzyl alcohol + PG and PGML + IPIS + PG were investigated.
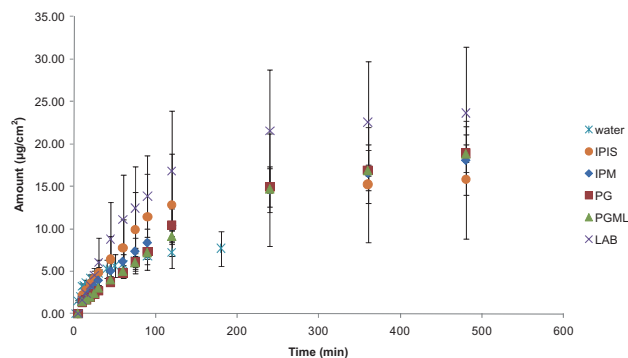

Figure 1 – Example of a permeation profiles of MN (from single solvents) after a 30 second application using a pre-soaked filter paper.

RESULTS AND DISCUSSION

Sigmoidal permeation profiles (Figure 1) were obtained for all the formulations reflecting the short contact time of the drug with the skin. A plateau was reached which means that no more drug is available for permeation.

When comparing the *in vitro* permeation profiles and the previously obtained *in vivo* results the same trend was confirmed for each solvent system. In both studies MN permeated faster from water than from the lipophilic solvents.

Furthermore, it should be noted that the amount of drug permeated was much lower than the amount of MN initially applied which may reflect the evaporation of the drug throughout the experiment.

CONCLUSIONS

This innovative protocol simulated short time contact of a drug with the skin.

This method should be useful not only for monitoring drug permeation from formulations (finite dose studies) but also in other areas that aim to study short time exposure of solvents to the skin.

ACKNOWLEDGMENTS

A Novel 3D Immuno-Competent Co-Cultured Skin Model to Investigate the Allergenic Potential of Chemicals

D.Y.S. Chau[1]*+, C. Johnson[2]*, P.A. Cato[1], S. MacNeil[2], J.W. Haycock[2], A.M. Ghaemmaghami[1]+

[1]Allergy Research Group, School of Molecular Medical Sciences, University of Nottingham, Queen's Medical Centre, NG7 2UH, UK. [2]Tissue Engineering Group, Kroto Research Institute, University of Sheffield, Sheffield, S3 7HQ, UK. *authors contributed equally to this work. +corresponding authors: amg@nottingham.ac.uk; david.chau@nottingham.ac.uk

Abstract – **The aim of this project is to develop a perfusable and immunocompetent 3D human skin model comprising of keratinocytes, fibroblasts and antigen presenting cells (APC). It is anticipated that such a model will efficiently mimic the native microenvironment in which these cells co-exist *in vivo*, and therefore provide an effective *in vitro* tool for the prediction of the allergenic/therapeutic potential of novel chemicals. Furthermore, this model system will allow the identification of the key pathways and mechanisms initiated during chemical-induced skin sensitisation and allow characterisation.**

INTRODUCTION

There has been an increasing number of allergy-related incidents over the past few decades which are predicted to rise further to 50% by 2015 [EU Commission Research statistics]. Furthermore, current implementation of the 7th Amendment to the EU Cosmetics Directive (76/768/EEC) prohibits the testing and marketing of products tested on animals. As such, the establishment of a reliable and accurate *in vitro* test for the assessment of new and novel drugs/chemicals is urgently needed due to the limited biological relevance and ethical consideration of animal models/testing. Human skin constitutes the first immune defence barrier with a highly organised structure that protects the body from harmful environmental toxins and infections. It is composed of three primary layers: the epidermis, dermis and hypodermis of which the function-specific keratinocytes, APC and fibroblasts cells reside respectively. Dendritic cells (DC) are a specialised type of APC which serve as sentinels that capture antigens at the site of entry, transport them to the local lymph nodes and consequently process them through the immune/inflammation response cascade.

MATERIALS AND METHODS

Human primary skin keratinocytes and fibroblasts were cultured individually on a novel pre-treated microfibre-based scaffold as a submerged culture before being assembled together and cultured at an air-liquid (A-L) interface for an additional 7 days. Monocyte-derived dendritic cells (mDC) were differentiated and cultured in complete media supplemented with 50 ng/ml GM-CSF and 250 U/ml IL-4 for 6 days before being incorporated within an agarose-fibronectin gel. The completed 3D construct was achieved by *sandwiching*
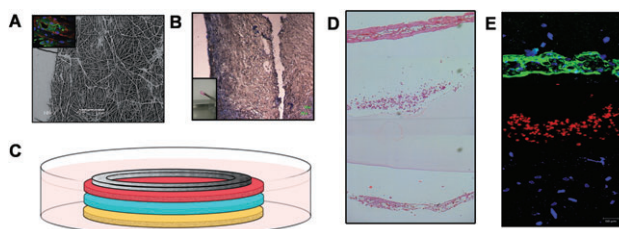

Figure 1: Construction and development of 3D immuno-competent skin model (A) individual keratinocyte cell layer on novel scaffold (B) mDC incorporated within agarose-fibronectin gel (C) schematic of complete 3D model (D) H&E staining of cell and gel layers within 3D construct (E) confocal imaging of cell and gel layers within 3D construct: upper layer; keratinocytes labelled with pancytokeratin and DAPI, middle layer; mDC labelled with CellTracker Red, bottom layer; fibroblasts labelled with DAPI

the gel between the two scaffold cell layers using CellCrowns™ and incubated at an A-L interface for up to 14 days. Individual keratinocytes, fibroblasts and mDC cell layers and the complete co-cultured construct were analysed by confocal microscopy, SEM and IMH. mDC were challenged using lipopolysaccharide (400 ng/ml LPS, 24 h) and cell distribution, morphology, surface phenotype and endocytic ability were assessed using a combination of biochemical assays, histology, imaging and flow cytometry. Cytokine expression profiles were obtained by Multiple Analyte Detection FlowCytoMix™ (Bender Medsystems, Vienna, Austria) and ELISA.

RESULTS AND DISCUSSION

A 3D co-culture model based on human skin keratinocytes, fibroblasts and mDC has successfully been established and cultured in a common media. The model demonstrates an intact epithelial structure with positive staining for pancytokeratin, involucrin and cytokeratin-10.

Dendritic cells maintain the expected phenotype [based on CD1a, CD11c, CD86, CD207 (Langerin), CD208 (DC-LAMP), CD209 (DC-SIGN) and CD324 (E-Cadherin) expression] alongside a characteristic DC-cytokine expression profile (IL-6, IL-8, IL-10, IL-12, IFN-α and TNF). Stimulation and endocytic behaviour are maintained/enhanced following recovery from the "immune layer sandwich" (agarose-fibronectin gel).

CONCLUSIONS

It is anticipated that this novel 3D co-cultured model system represents the native *in vivo* microenvironment in which these cells co-exist and thus may be exploited as a screening tool in the (bio)pharmaceutical industry for new drugs/therapeutics.

A Novel Polymeric Microneedle Formulation for the Transdermal Delivery of Bacteriophages

E.M. Ryan, B.F. Gilmore, S.P. Gorman, R.F. Donnelly

School of Pharmacy, Queen's University Belfast, Belfast, UK.

Abstract **– The aim of this work was to develop an optimised formulation for stabilisation and successful transdermal delivery of a model bacteriophage, T4, *in vitro*. Many bacteriophages including T4 are acid- sensitive and cannot be delivered orally. An alginic acid/trehalose formulation was found to provide ample mechanical strength, and a suitable environment, to maintain T4 viron stability. T4 phage was rapidly released from the microneedle and delivered across a Silescol® membrane, which mimics the *stratum corneum*, *in vitro*.**

INTRODUCTION

Microneedle (MN) mediated transdermal drug delivery is a minimally invasive, simple and effective method of delivery. Recently polymeric microneedles have been used in controlled release delivery (Fig 1) [1]. Bacteriophages were first used as an antibacterial therapy in the early 20th century. However, they became unpopular in the western world following the discovery of antibiotics. Increasing antibacterial resistance has provided a renewed interest in phage therapy [2]. In this study, bacteriophage T4 was stabilised within a suitable polymeric system and delivered *in vitro*.

MATERIALS AND METHODS

1) *Bacteriophage double layer assay technique*: Phage viability was assessed using the phage double layer assay. Dilutions of the phage preparations were mixed with a host bacterium and dispersed evenly onto solid medium and incubated. Virus particles which infected the host lawn were enumerated [3].
2) *Microneedle fabrication and characterisation*: A range of water soluble polymers were used to make microneedle (MN) arrays using silicone moulds prepared by laser engineering. The microneedles were characterised using a TA.XT- plus Texture Analyser (Stable Micro Systems Ltd, Surrey, UK). Microneedles were visualised before and after this process using a light microscope (GXMGE-5 digital microscope, Laboratory analysis Ltd, Devon, UK).

3) *In vitro bacteriophage delivery:* Penetration of the bacteriophages across a Silescol® membrane (Barloworld Scientific Ltd, Staffordshire, U.K.) was investigated using a Franz-cell apparatus (PermeGear Inc, Bethlehem, PA, U.S.A) at 37°C. Silescol® membranes mimic the barrier properties of the *stratum corneum*. T4 release from the microneedles was examined over a 24 hour period.

RESULTS AND DISCUSSION

Stability studies of T4 phage, were carried out prior to incorporation into a suitable polymeric carrier. It was found that T4 exhibits pH and temperature sensitive stability, with a pH range of 6–8 and storage at and below 4°C being most suitable. Incorporation of T4 into a wide range of commonly used anionic and non ionic polymers resulted in rapid deactivation of the virus. An optimised alginic acid formulation with added trehalose maintained virus stability for up to 2 months.

Increasing the trehalose : alginic acid ratio increased the microneedle strength. A 1:20 ratio gave an average 29.7 ± 4.7 % reduction in height, whereas a 1:2 ratio resulted in a 22.7 ± 4.6 % reduction in height (n = 27, mean ± SD). High con-
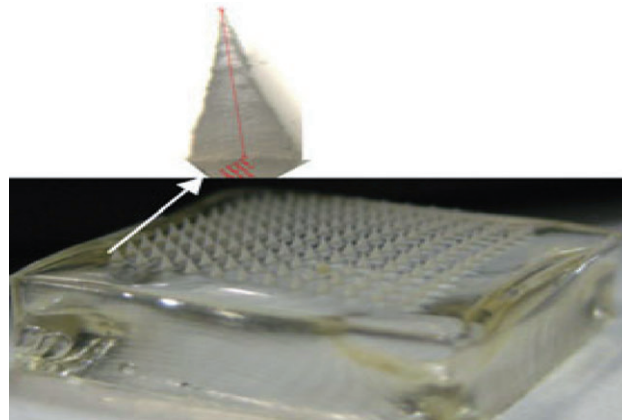

Figure 1: Digital photograph of polymeric laser micro-moulded microneedle array

centrations (>80% of total loadings) of bacteriophages were rapidly delivered (over 2 hours) across Silescol® *in vitro*.

CONCLUSIONS

In this work, a mechanically robust and phage compatible polymeric microneedle formulation has been developed to deliver a model bacteriophage *in vitro*. We are currently investigating delivery of bacteriophages *in vivo* using this optimised microneedle formulation.

REFERENCES

[1] J.H. Park, M.G. Allen, M. R. Prausnitz, "Polymer Microneedles for Controlled-Release Drug Delivery" *Journal of pharmaceutical research*, **23** (2006) 1008–1019

[2] A. Sulakvelidze, Z Alavidze, J. Glenn Morris Jr. "Bacteriophage Therapy" *Antimicrobial agents and chemotherapy*, 45 (2001) 649–659

[3] M.H. Adams. "Bacteriophages" in Bacteriophages: Methods and protocols, Humana Press, New York, publisher, 2009 ch7 pp 69–76

A polyamide-based membranous device for specialised drug delivery

T. Govender[1], V. Pillay[1*], Y.E. Choonara[1], L.C. du Toit[1], G. Modi[2], D. Naidoo[3]

[1]University of the Witwatersrand, Dept. of Pharmacy and Pharmacology, 7 York Road, Parktown, Johannesburg, 2193
[2]University of the Witwatersrand, Dept. of Neurosciences, Division of Neurology, 7 York Road, Parktown, Johannesburg, 2193
[3]University of the Witwatersrand, Dept. of Neurosciences, Division of Neurosurgery, 7 York Road, Parktown, Johannesburg, 2193
*Correspondence: viness.pillay@wits.ac.za

INTRODUCTION

This study is aimed at investigating the design and development of a novel polyamide-based polymeric membrane for implantable drug delivery.

MATERIALS AND METHODS

1) *Preparation of polymeric membranes:* Polymeric membranes were prepared by a precipitation reaction. Novel polyamide 6,10 (PA 6,10) synthesised by modified interfacial polymerisation reaction [1], was firstly dissolved in formic acid. The solution was placed under magnetic stirring at 3000rpm and the temperature was raised to 65°C until all PA 6,10 dissolved. Another solution comprising ethylcellulose (EC) dissolved in acetone was prepared. The PA 6,10-formic acid solution was then added to the EC-acetone solution while under magnetic stirring. Stirring continued until the formation of a homogenous solution. The solution was left to stir for approximately an hour and upon completion of stirring, double de-ionised water was added to the solution. This resulted in the formation of a white gel-like precipitate at the interface. The precipitate was collected by filtration with a Buchner apparatus with the continuous addition of double de-ionised water. Following filtration, the precipitate was collected, appropriately moulded and left to dry under a fume hood for 24 hours. Resultant membranes were round, regular and exhibited surface porosity.

2) *FTIR Spectrophotometric Analysis:* Fourier transform infrared (FTIR) spectroscopy was undertaken on the resultant membranes to assess any structural variations in the polymeric membranous device, as a result of any interactions in the formulation.

3) *Morphological characterisation of polymeric membrane:* Surface morphology was characterised by Scanning Electron Microscopy (SEM). Photomicrographs were taken at different magnifications and samples were prepared after sputter-coating with gold. Morphological characterisation of the membranes revealed the shape, surface morphology and structure of the device.

4) *Textural profile analysis:* Textural analysis was used to determine the physicomechanical properties of the membranes in terms of their Brinell Hardness and deformation energy. This was compared to Brinell Hardness values obtained from a PA 6,10-EC disc, compressed with a Carver Hydraulic Press.

RESULTS AND DISCUSSION

Structural characterisation was performed on the PA 6,10, EC and the PA 6,10-EC membrane synthesised by precipitation reaction. Results confirmed the presence and integrity of a combination of both PA 6,10 and EC functional groups in the membranes produced by precipitation reaction. This thus confirmed the formation of a novel PA 6,10-EC membranous device. SEM images of the novel polymeric membrane at varying magnifications confirmed that membranes were irregular and highly porous. Textural profiling confirmed the integrity of the synthesised membranous matrices with BHN values ranging from 2.42–2.54 N/mm^2. BHN values of the compressed PA 6,10-EC discs ranged from 3.09–4.01 N/mm^2. The lower BHN values of the PA 6,10-EC membranes are indicative of a device that is non-crystalline and potentially more favourable for implantation.

CONCLUSIONS

The PA 6,10-EC membranes were successfully synthesised. Furthermore, resultant membranes were regular and of consistent size, rigid and displayed no evidence of easy breakage.

ACKNOWLEDGMENTS

REFERENCES

[1] O.A. Kolawole, V. Pillay and Y.E. Choonara, "Novel Polyamide 6,10 Variants Synthesised by Modified Interfacial Polymerisation for Application as a Rate-Modulated Monolithic Drug Delivery System" *Journal of Bioactive and Compatible Polymers,* **22** (2007) 281–313.

A Randomised Open Label Comparison of Tiotropium and Ipratropium in Chronic Obstructive Pulmonary Disease

Reema Thomas[1], Adepu Ramesh[2], Mahesh Padagudru.Anand[3],
Gurumurthi Parthasarathi[2], Sabin Thomas[2]

[1]School of Pharmacy and Tech Mgmt, NMIMS, Mumbai, India
[2]JSS College of Pharmacy, JSS University, Mysore, India
[3]JSS medical college, Mysore, India

INTRODUCTION

Chronic obstructive pulmonary disease (COPD) is a chronic disease of the lungs characterised by expiratory airflow obstruction [1]. The Indian Council of Medical Research evaluated an incidence of COPD to be 3.9 million each year among tobacco users [2]. Tiotropium bromide is a relatively new anticholinergic agent, with bronchodilating activity lasting for 24 hours or more, compared to ipratropium. It has been developed as a metered dose inhaler (MDI) and suitable for once daily administration and thereby increases medication adherence in COPD patients [3]. The study aimed to compare safety and efficacy of tiotropium and ipratropium in COPD patients among the south Indian population.

MATERIALS AND METHODS

A total of 70 patients were selected at random for a 3 month prospective study, of these, 60 patients completed the study period: 30 in each group. During the run-in period of 1 week, the patients were given inhaled beclomethasone 400 mcg on a regular basis and salbutamol inhaler 100 mcg as and when required. After the run-in period, the patient's PFT was recorded to get baseline data and were randomised into either tiotropium 18 mcg once daily or ipratropium 40 mcg four times daily both via MDI (brands of Cipla Pharmaceuticals India Ltd). Outcome measures were lung functions tests (spirometry), baseline dyspnoea index (BDI), transition dyspnoea index (TDI) and use of concomitant salbutamol. Follow up data was recorded on 15th, 30th, 60th and 90th days of the study.
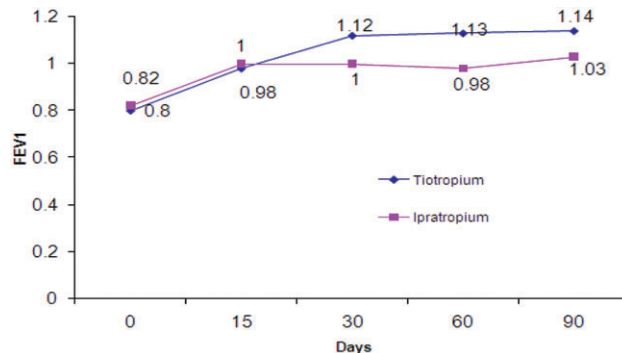

Figure 1: Changes in FEV_1 among two treatment groups at different stages of the study

RESULTS AND DISCUSSION

During treatment both groups showed improvements in lung functions ($p < 0.05$). The improvements in lung functions in tiotropium group was better than in ipratropium group, though this was not supported statistically (110 ml) ($p > 0.05$).

Improvements in dyspnoea was observed in patients of both the groups. However compared to ipratropium, tiotropium group showed a statistical improvement in dyspnoea indices ($p < 0.05$) on 15th day follow-up. The concomitant use of salbutamol was also lower in the tiotropium group ($p > 0.05$). The most common drug related adverse event was dry mouth (tiotropium 57%, ipratropium 30%), which was not statistically significant ($p > 0.05$).

Table 1: Baseline dyspnoea index (BDI)

Domains	Tiotropium	Ipratropium
Functional impairment	1.88	1.91
Magnitude of task	1.8	1.91
Magnitude of effort	18	1.85
Focal score	**1.82**	**1.89**

Higher focal scores improves dyspnoea

Figure 2: Changes in the transition dyspnoea scores at different follow-ups

CONCLUSION

Tiotropium in a dose of 18 mcg once daily via MDI showed improvement in dyspnoea and lung functions compared to ipratropium 40 mcg four times daily. The differences in improvement in lung functions detected between the two groups were insignificant. However, tiotropium's once daily dosing might have a better impact on patient adherence.

ACKNOWLEDGMENTS

We are grateful to JSS Mahavidyapeetha, Principal JSS College of Pharmacy and Medical superintendent JSS Medical College for permitting to conduct the study.
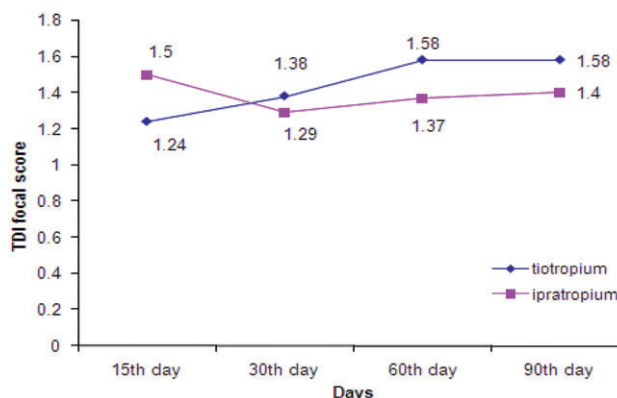
REFERENCES

[1] Ohri CM, Steiner MC. COPD the disease and non drug treatments. *Hospital Pharmacist* 2004; 11: 359–76.

[2] Kumar S. India steps up anti-tobacco measures. *Lancet* 2000; 356: 1089.

[3] Joos GF et al. Tiotropium Bromide: A Long-Acting Anticholinergic Bronchodilator for the Treatment of patients with COPD. *IJCP* December 2003; Vol 57: Pg 906–908.

Addition of immunostimulatory components to DDA-TDB adjuvant delivery system

R. Kaur[1], A. Milicic[2], A. Reyes-Sandoval[2], A. Hill[2], Y. Perrie[1]

[1]Medicines Research Unit, Aston University, Birmingham, B4 7ET, UK.
[2]The Jenner Institute, University of Oxford, Old Road Campus Research Building, Oxford, OX3 7DQ, UK.

Abstract **– Cationic liposomes based on dimethyldioctade-cylammonium (DDA) and trehalose 6,6'-dibehenate (TDB) have been evaluated and have been shown to be promising as vaccine adjuvants for a number of vaccination purposes [1]. The aim of the study was to incorporate additional immunostimulatory components to DDA-TDB liposomes, the adjuvant system.**

INTRODUCTION

Cationic liposomes are of interest as delivery vehicles for vaccine antigens as they possess positive charge and are able to carry the antigen to and interact with the negatively charged surface of the antigen presenting cells (APCs) [2]. In this study we investigated the versatility of cationic liposomes based on DDA-TDB in combination with different immunostimulatory ligands including, polyinosinic-polycytidylic acid (Poly IC, TLR3 ligand), and CpG (TLR9 ligand) in combination with DDA-TDB.

MATERIALS AND METHODS

The DDA-TDB liposomes were prepared by the lipid-hydration method as described previously [3] or the dehydration-rehydration method [4]. In all formulations the final OVA concentration in a 50 µl dose was 20 µg, and the final concentration of DDA and TDB was 250 µg and 50 µg, respectively. All liposomal formulations were measured for vesicle size and zeta potential.

RESULTS AND DISCUSSION

Incorporation of immunostimulatory components was found to affect the particle size and surface charge (Figure 1). Empty DDA-TDB liposomes were found to be 572.6 ± 50.4 nm in size with a positive surface of 59.9 ± 10.5 mV. The adsorption of OVA resulted in an increase in size to 1047.1 ± 135.8 nm, whereas with the addition of CpG and PolyIC to the DDA-TDB OVA liposomes made no further significant
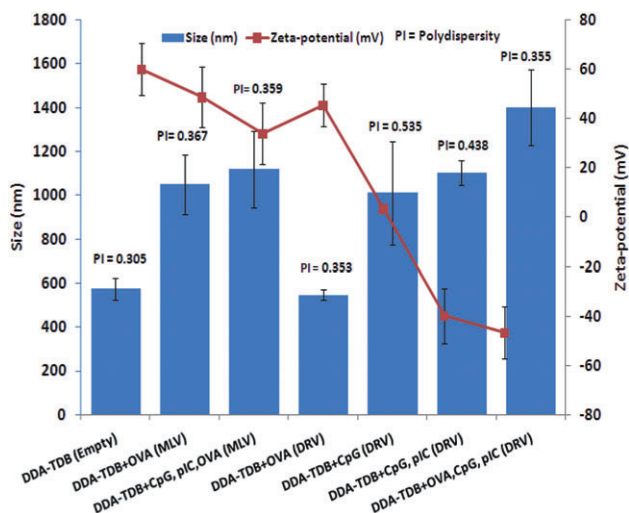
Figure 1. Size (nm), polydispersity (PI) and zeta potential (mV) of liposomes.

difference in the size (1116.9 ± 176.0 nm) with no significant effect on the zeta potential in both cases at the concentrations used.

When the dehydration-rehydration method was used to incorporate the OVA within the liposomes, the size of the liposomes was 546 ± 23.7 nm, significantly smaller than vesicles prepared with surface complexed OVA. In contrast with the entrapment of only CpG within the DDA-TDB DRV the size of the liposomes significantly increased to 1010 ± 235 nm and zeta potential significantly reduced to near neutral (3.4 ± 1.32 mV) suggesting a reconfiguration of the system compared to the DDA-TDB entrapping OVA. However, the addition of PolyIC in combination with CpG resulted in vesicles of a similar size (1101.9 ± 55.79 nm) but with a negative zeta potential (-39.9 ± 11.1 mV). Finally, the addition of the three components OVA, CpG and PolyIC resulted in no further significant change in zeta potential but a slight increase in size to 1399.2 ± 172.5 nm.

CONCLUSIONS

The incorporation of different immunomodulating compounds into these liposomes on the immune response will be determined.

REFERENCES

[1] D. Christensen et al. *Journal of Liposome Res.* **19** (2009) 2–11.
[2] E.M. Agger, et al. *PLoS ONE.* **3** (2008) e3116.
[3] J. Davidsen et al. *Biochim Biophys Acta.* (2005) 1718, 22–31.
[4] C.Kirby and G.Gregoriadis. *Bio/Technology.* **2** (1984) 979- 984.

An in vivo determination of the human nail plate pH

Sudaxshina Murdan, Gesmi Equizi, Geeta Goriparthi

Department of Pharmaceutics, School of Pharmacy, University of London, London, UK.

Abstract **– The in vivo pH of healthy finger and toenail plates, measured using a skin pH metre, was 5.1 (±0.6) and 5.4 (±0.8) respectively. Toenail pH was higher than that of fingernail, while the subject's gender and age, hand/foot side (right or left) had no influence on pH. Handwashing increased nailplate pH, although the increase was not sustained with time. Tape stripping of the nail plate showed a slightly lower pH inside the nail plate compared to its surface.**

INTRODUCTION

While there is much information on skin pH, there is none, to our knowledge, on nail pH. It is possible that the latter influences nail plate colonisation by pathogens, like the situation in skin [1]. It is also known that fungal spore formation is influenced by the pH of the medium [2]. In this context, we measured the pH of healthy nail plates, in an attempt to explore whether the skin pH metre could be used to measure nailplate pH, and to establish baseline values. Nail plate pH is here defined as the pH measured by a flat glass electrode at the nail plate surface with a hydrated nail-electrode interface, in an analogous manner to the definition of skin pH [3].

MATERIALS AND METHODS

Following approval by the London School of Pharmacy's ethics committee, 30 adult volunteers (11 females and 19 males) with healthy nails were recruited. All measurements were conducted in a temperature controlled room, where the ambient temperature and relative humidity were between 20.0–25.2°C and 22–38% respectively. Volunteers washed their hands with warm tap water and Cussoms Carex® anti-bacterial (sensitive) handwash, wiped dry using tissue paper and equilibrated in the temperature-controlled room for 20 minutes prior to any measurements. The nailplate pH was measured using the Skin pH meter PH-905® (Courage and Khazaka GmbH, Germany) as is performed for skin pH measurement [3]. D-Squame Cuderm (polyacrylate adhesive discs) was used for tape stripping nail plates.

RESULTS AND DISCUSSION

Following washing, drying and equilibrating for 20 minutes, the pH of fingernails (digits 1–5) and toenails (big toenails) in 22 volunteers was as shown in Table 1. Multiple regression was used to investigate the influence of gender, age, nature (i.e. finger or toe nail) and side (i.e. right or left) on the nail plate pH. Preliminary analyses showed no violation of the assumptions of normality, linearity, multicollinearity and homoscedasticity. Only the nature, i.e. finger or toe, was significant, with a beta value of −0.2 (p = 0.002) – finger and toe nailplates have statistically different pH. The model explained only 5% of the variance in nail plate pH.

It is known that washing increases skin pH. This was also found for nailplate pH (paired t test, p < 0.0005); pH of fingernail plates in 14 individuals (10 fingernails each) being 5.11 (±0.44) and 5.28 (±0.49) before and after handwashing respectively. The increase in pH was not however sustained with time, as shown in Figure 2 when pH continued to be measured in four individuals.

Tape stripping of the 2 thumbnail plates in 11 individuals showed a lower pH inside the nail plate compared to that of the nail plate surface (pH before washing = 5.1 ± 0.5; pH after washing = 5.3 ± 0.7; pH following 20 tape strippings after handwashing = 4.8 ± 0.6).

CONCLUSIONS

Fingernail pH is different to toenail pH. Washing increases nail pH, while tape stripping reveals a lower pH inside the nail plate.

REFERENCES

1. P Agache, P Humbert. Measuring the Skin. Springer 2004. Pp 28–29; 272–280.

Table 1. Finger and toe nailplates pH. Mean pH (sd, N) are shown

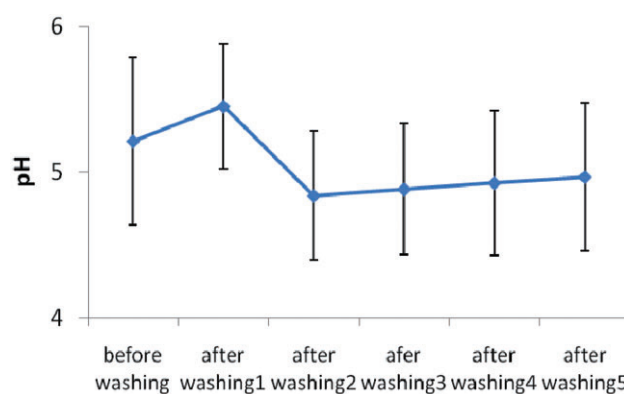|		Fingernails	Toenails
Mean pH		5.1 (0.6, N = 204)	5.4 (0.8, N = 33)
Influence of:			
Gender	M	5.1 (0.5, N = 125)	5.3 (0.7, N = 20)
	F	5.1 (0.6, N = 79)	5.6 (1.0, N = 13)
Hand/Foot side	R	5.0 (0.6, N = 105)	5.4 (1.0, N = 16)
	L	5.1 (0.6, N = 99)	5.4 (0.7, N = 17)
Digits	1	5.1 (0.6, N = 42)	Only big toenails could be measured
	2	5.0 (0.6, N = 43)	
	3	5.2 (0.6, N = 40)	
	4	5.0 (0.5, N = 41)	
	5	5.1 (0.5, N = 38)	

Fig. 1: pH change with washing and time subsequently

2. SA Yazdanparast, RC Barton, 2006. J. Med. Microbiol. 55, 11, 1577–1581. 3.J Fluhr, L Bankova, S Dikstein, Handbook of non-invasive methods and the skin. 2nd ed. 2006 pp 411–427.

An investigation into the surface energy of human fingernail plates

S. Murdan, Chitranjan Poojary, Dilan R. Patel, João Fernandes, Angie Haman and Zara Sheikh

Department of Pharmaceutics, School of Pharmacy, University of London, London, UK.

Abstract – **The surface energy of human fingernail plates (dry, hydrated and filed) were measured using the acid-base (van Oss) method.**

INTRODUCTION

Topical ungual (i.e. pertaining to the nail) drug formulations include solutions, paints, lacquers and nail patches. Interfacial energies between such formulations and the nail plate are expected to govern nail-formulation contact and thereby ungual drug permeation. Interfacial phenomena is also expected to influence the adhesion of microorganisms onto the nail plate and subsequent invasion.

Despite the important role of such interfacial phenomena, there is no currently no literature on the nail plate's surface energy.

Our aim was therefore to measure the surface energy of nail plates. The surface energy of normal, filed and hydrated nail plates, as patients would normally apply topical nail medicines to filed nail plates, and such formulations could increase nail hydration due to occlusion. The surface energy of bovine hoof membranes was also measured as these are often used as models for nail plates.

MATERIALS AND METHODS

Following approval by the London School of Pharmacy's ethics committee, 11 adult volunteers with healthy nails were recruited, and the surface energy of their nail plates was measured using the acid-base (van Oss) method, i.e. firstly the contact angles formed between drops of two polar and one apolar liquid, and the nail plate was measured using a goniometer (FTA 1000, First Ten Angstroms, USA), and subsequently the van Oss-Chaudhary-Good equation was used to calculate the nail plate's surface energy. The liquids used were water, glycerol, diiodomethane and formamide.

Nails were hydrated by immersing the nail in distilled water for 10 minutes then wiping with paper towels. Filing (3 strokes) was performed using the file provided in a pack of Loceryl®.

RESULTS AND DISCUSSION

Contact angles formed by a drop of water, glycerol, diiodomethane and formamide on normal (dry), hydrated and filed fingernail plates are shown in Table 1. N ≥ 102 for all liquids.

Repeated measures ANOVA, conducted to determine whether hydration and filing of the nail plate altered the contact angle made by a liquid droplet on the nail plate, revealed that this depended on the nature of the liquid. While there was no difference in contact angle for the polar glycerol and water, there were significant ($p < 0.05$) changes for the apolar diiodomethane, and formamide, as shown in Table 1, using the symbols * and +. The same symbol next to two

Table 1: Contact angle of the liquids on the nail plate.

	Mean contact angle (sd) on nail		
	normal	**hydrated**	**filed**
Diiodomethane	50.4 (6.6)*	50.9 (6.6)+	43.5 (7.3)*+
Formamide	58.8 (8.0)*	61.4 (7.0)*+	55.8 (8.4)+
Glycerol	71.8 (8.7)	74.6 (8.7)	74.9 (8.3)
Water	74.2 (7.2)	73.8 (7.9)	74.6 (6.9)

Table 2: Surface energy of nail plates

	Surface energy (mJ/m²)
Normal nail plate	34.8
Hydrated nail plate	33.5
Filed nail plate	38.2

angles shows that these two angles are significantly different from each other. For example, for diiodomethane, normal angle is different from filed angle, and hydrated angle is different from filed angle.

The surface energy of normal, hydrated and filed nail plates is shown in Table 2. The surface energy of bovine hoof membranes was found to be 31.9 mJ/m². This, being fairly similar to the surface energy of in vivo human nail plate, shows that the bovine hoof membrane could be used as a model for the nail plate for certain investigations.

CONCLUSIONS

Hydration and filing altered the contact angles made by some, but not all, the liquids on the nail plate. The surface energy of normal, hydrated and filed nail plates were determined.

ACKNOWLEDGEMENTS

We are extremely grateful to all the volunteers who participated in this study.

Anticancer Activity of *Dendrophthoe Flacata* on Ehrlich's Ascites Carcinoma Treated Mice

Richard Lobo[1,*] Nipun Dashora[1], Vijay Sodde[1], Kirti. S. Prabhu[1]

[1]Department of Pharmacognosy, Manipal College of Pharmaceutical Sciences, Manipal University, Manipal-576 104, Karnataka, India

Abstract – **The plants belonging to the family loranthaceae are attributed traditionally for anticancer activity. *Dendrophthoe falcata* (Loranthaceae), commonly known as 'Mistletoe' in English, is a perennial climbing woody parasitic plant traditionally used in the treatment of swellings, wounds, ulcers, tumour and joint disorders [1]. Pattanayak et al., (2008) evaluated the activity of the aqueous extract of leaves of *D. falcata* growing on *Shorea robusta* for the antitumour activity on 7 12-Dimethylbenz[a] anthracene induced rat mammary tumour models and revealed a 24.934% reduction in the tumour size at the dose level of 400 mg/kg, which was less than that of standard drug tamoxifen [2]. Thus suggesting *D. falcata* as a source for anticancer drugs.**

INTRODUCTION

To study the anticancer activity of the aqueous extract of the *D. falcata* in Swiss albino mice against Ehrlich Ascites Carcinoma (EAC) cell line.

MATERIAL AND METHOD

The anticancer activity was evaluated in Swiss albino mice against EAC cell line at the doses of 200 and 400 mg/kg body weight orally. The extract at both doses was administered for 13 consecutive days. After the last dose of treatment, the mice were decapitated after an overnight fast and antitumour effect of extract was assessed by evaluating tumour volume, viable and nonviable tumour cell count, tumour weight and hematological parameters of EAC bearing host.

RESULTS

Aqueous extract showed significant decrease in (p < 0.0001) tumour volume, viable cell count, tumour weight and elevated the life span of EAC tumour bearing mice. Haematological profile such as RBC, haemoglobin and WBC count reverted to a normal level in treated mice.

CONCLUSION

The result showed that the extract had potent dose dependent anticancer activity and that is comparable to that of cisplatin.

REFERENCES

[1] P.K. Warrier, V.P.K. Nambiar and C. Ramankutty, "Indian Medicinal Plants – a Compendium of 500 Species", **2** (1993) India, Orient Longman

[2] Pattanayak, P. Mitra Mazumder, and, P. Sunita, *Dendrophthoe falcata* (L.f) ettingsh: A consensus review. *Phcog. Mag.,* **4** (2008) 359–368.

Application of Biophysics and Bioengineering to the Assessment of Barrier Function

Q. Yang, S. Cordery and R.H. Guy

Department of Pharmacy and Pharmacology, University of Bath, Bath, UK.

Abstract **– Atopic dermatitis is related to impaired skin barrier function. Skin on the face is thinner and the corneocytes of the stratum corneum are smaller [1]. This work aims to characterise skin barrier function on both the forehead and the forearm using bioengineering techniques. The results to-date reveal that the stratum corneum of forehead skin has less natural moisturising factor and intercellular lipids which are more disordered than that of the forearm. Forehead skin may therefore be considered to have a less competent barrier function.**

INTRODUCTION

The loss-of-function mutation of filaggrin gene has been firmly linked to predisposition to atopic dermatitis [2]. As a result, lower levels of natural moisturising factor (NMF) are generated in atopic skin and this is thought to contribute to an impaired barrier function [3]. The stratum corneum (SC) on the face is thinner, and the surface area of the corneocytes smaller, resulting in a shorter path-length for transport and a noticeably higher permeability. Therefore, it is proposed that forearm and forehead skin from healthy volunteers may be used to model the distinction between a competent SC and one pre-disposed to AD. The goal of this project is to apply different bioengineering methods to screen SC barrier function on the forehead and forearm of healthy volunteers and to identify markers for its impairment.

MATERIALS AND METHODS

NMF components were extracted from the forearm and forehead of 6 healthy volunteers using reverse iontophoresis, passive diffusion and tape-stripping. The extracted samples were analysed by LCMS to identify and quantify the amounts of 22 components of NMF. Transepidermal water loss (TEWL) measurements were taken before and after each tape-strip and the results were used to derive the thickness of the SC [4]. The SC was also examined by attenuated total reflectance-Fourier transform infrared spectroscopy (ATR-FTIR) before and after each tape-strip to probe lipid quantity, composition and organisation at the two anatomic sites considered.

RESULTS AND DISCUSSION

SC thickness on the forehead was significantly thinner than that on the forearm and TEWL values were correspondingly higher. The concentrations of most NMF components were similar on both sites but there was a much lower total amount of NMF extracted from the forehead. However, those NMF components normally present in forearm SC in small quantities (e.g., glutamine and glutamic acid) were found in higher concentrations on the forehead and, as a result, were more easily extracted by passive diffusion. IR absorbance from both forearm and forehead SC at ~2850 cm⁻¹ and 2920 cm⁻¹

shifted to lower frequencies as tape-stripping progressing indicating that lipids near to the skin surface were relatively disordered most probably due to the contribution from sebaceous constituents. This effect was much more marked on the forehead than on the forearm.

CONCLUSIONS

The results confirm that forehead SC may be considered a less competent barrier than that on the forearm, as characterised by the presence of lesser amounts of NMF and less-ordered lipids.

REFERENCES

[1] M. Machado, T.M. Salgado, J. Hadgraft, M.E. Lane, "The relationship between transepidermal water loss and skin permeability", *International Journal of Pharmaceutics* **384** (2010) 73–77.

[2] M.J. Cork, S.G. Danby, Y. Vasilopoulos, J. Hadgraft, M.E. Lane, M. Moustafa, R.H. Guy, A.L. MacGowan, R. Tazi-Ahnini, S.J. Ward, "Epidermal barrier dysfunction in atopic dermatitis" *J. Invest. Dermatol.* **129** (2009) 1892–1908.

[3] S. Kezic, P.M.J.H. Kemperman, E.S. Koster, C.M. de Jongh, H.B. Thio, L.E. Campbell, A.D. Irvine, I.W.H. McLean, G.J. Puppels, P.J. Caspers, "Loss-of-Function mutations in the filaggrin gene lead to reduced level of natural moisturising factor in the stratum corneum" *J. Invest. Dermatol.* **128** (2008) 2117–2119.

[4] L.M. Russell, S. Wiedersberg, M. Begoña Delgado-Charro, "The determination of stratum corneum thickness an alternative approach" *European Journal of Pharmaceutics and Biopharmaceutics* **69** (2008) 861–870.

Approaches to controlled release of antimicrobial tea tree oil (TTO) and silver ions (Ag⁺) by liposome encapsulation

W.L. Low[1], C. Martin[2,3], and M.A. Kenward[1,2]

[1]Research Centre in Applied Science (RCAS), [2]Department of Pharmacy, [3]Research Institute in Healthcare Science (RIHS), University of Wolverhampton, Wolverhampton, UK.

Abstract – **There is an increasing need for safe, alternative antimicrobial agents, to counteract current challenges in wound management due to antibiotic resistance in pathogens. This *in vitro* study assessed the feasibility of using liposomal TTO and Ag⁺ to achieve controlled delivery whilst maintaining microbiocidal activity.**

INTRODUCTION

Antimicrobial agents such as silver ions (Ag⁺) and tea tree oil (TTO) may be an effective alternative for topical infection treatment [1, 5]. Both agents however display side effects when used at elevated concentrations. One approach to reduce the development of side effects involves encapsulation in responsive, controlled release delivery systems [4]. Such technologies may be better able to manage the wound environment, speed up the healing process and minimise scarring [2]. Encapsulation of alternative antimicrobial materials, TTO and Ag⁺, within liposomes (lipo-TTO and lipo-Ag⁺) may reduce side effects associated with high drug loading at infection sites and also minimise toxicity to healthy tissues. This study investigated the efficacy and feasibility of delivering liposome encapsulated TTO and Ag⁺ to eliminate representative common skin pathogens *in vitro*.

MATERIALS AND METHODS

Minimum lethal concentration (MLC) of TTO and Ag⁺ was determined for *P. aeruginosa* (Gram negative), *S. aureus* (Gram positive) and *C. albicans* (yeast). The rate of killing for free and liposome encapsulated agents was assessed at concentrations (detailed in Fig. 1 legend) determined from the MLC for the free (unencapsulated) agent in broth cultures. Liposomes composed of phosphatidylcholine and cholesterol (2:1 molar ratio) were prepared by the Reverse-phase Evaporation Vesicles method (REV) [3]. The aqueous phase consisted of either: (i) 2.5% silver nitrate solution, or (ii) TTO emulsified with 1.0 % w/v $PVA_{30-70kDa}$ (TTO : PVA 40:60 v/v).

RESULTS AND DISCUSSION

Free Ag⁺, TTO : PVA, lipo-TTO and lipo-Ag⁺ killed large numbers of microorganisms (Fig. 1). The time kill experiments were conducted at concentrations determined from the MLC for each microorganism to allow collection of meaningful data. PVA-emulsified TTO helps to improve dispersion of TTO components thereby increasing antimicrobial activity. Encapsulated agents were released in a biphasic manner (data
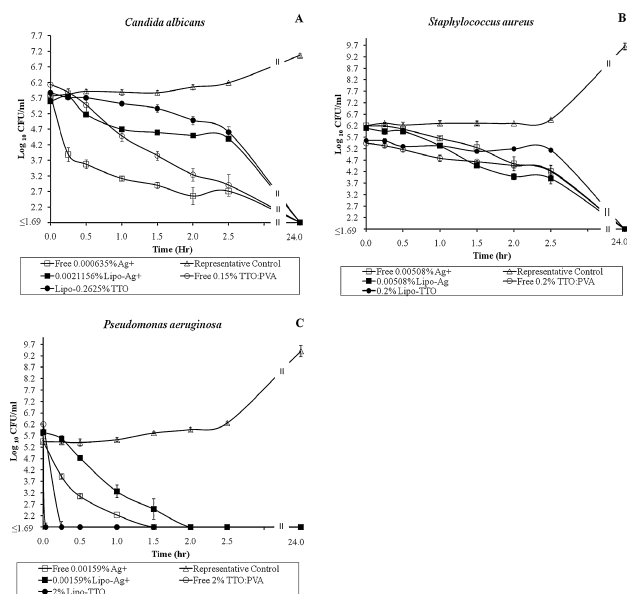
Figure 1. Time kill curves of A. *C. albicans* (NCYC 854), B. *S. aureus* (NCIB 6571) and C. *P. aeruginosa* (NCIB 8295) exposed to Lipo-TTO (●), Free TTO (○), Lipo-Ag$^+$ (■), Free-Ag$^+$ (□) at the indicated concentrations and to neither agents (△). The symbols represent the mean of 3 replicates ± SD. The lowest detectable limit was 1.69 log cycles or 50 CFU/ml.

not shown) and retained their antimicrobial activity. Despite the slower rate of kill (Fig. 1), the ability of lipo-TTO and lipo-Ag$^+$ to kill large numbers of cells demonstrated the ability of liposomes to effectively deliver TTO and Ag$^+$ to microbial cells. The larger size and different structural properties of yeast cells compared to bacteria may influence antimicrobial efficacy, bioavailability and distribution of the encapsulated agent; hence the varying amount needed for a microbiocial effect.

CONCLUSIONS

The results demonstrated the feasibility of liposomes as controlled release delivery systems for alternative antimicrobial agents (TTO or Ag$^+$). Future efforts to modify the physical characteristics of liposomes and encapsulate both agents in combination could provide useful information that may improve wound treatment and infection control approaches.

ACKNOWLEDGMENTS

REFERENCES

[1] C. F. Carson, S. Messager, K. A. Hammer and T. V. Riley, "Tea tree oil: a potential alternative for the management of methicillin-resistant *Staph. aureus* (MRSA)" *Hlthc. Infect.,* **10** (2005) 32–34.

[2] C. J. Beukelman, A. J. J. van den Berg, M. J. Hoekstra, R. Uhl, K. Reimer and S. Mueller, "Anti-inflammatory properties of a liposomal hydrogel with povidone-iodine (Repithel®) for wound healing *in vitro*" *Burns,* **34** (2008) 845–855.

[3] F. Jr. Szoka and D. Papahadjopoulos, "Procedure for preparation of liposomes with large internal aqueous space and high capture by reverse-phase evaporation" *Proc Natl Acad Sci USA.,* **75** (1978) 4194–4198.

[4] L. Zhang, D. Pornpattananangku, C. M. Hu, and C. M. Huang, "Development of nanoparticles for antimicrobial drug delivery" *Curr. Med. Chem.,* **17** (2010) 585–94.

[5] S. Silver, L.T. Phung, and G. Silver., "Silver as biocides in burn and wound dressings and bacterial resistance to silver compounds" *J. Ind. Microbiol. Biotechnol.,* **33** (2006) 627–634.

Aqueous-organic precipitation method resulting in polymorphism of α-lactose monohydrate

I.R.A. Al-Obaidi, H.N.E. Stevens, F.J. McInnes

Strathclyde Institute of Pharmacy and Biomedical Sciences, University of Strathclyde, Glasgow, UK

INTRODUCTION

Lactose has four polymorphs, α-lactose monohydrate, β-lactose, stable anhydrous α-lactose and unstable hygroscopic anhydrous α-lactose [1], and it is important to understand the effect of formulation processing on the formation of these polymorphs. In this study hydroxypropyl methylcellulose (HPMC) was used as a carrier to precipitate water soluble α-lactose monohydrate (ALM) microparticles using isopropyl alcohol (IPA) as a precipitating agent. The physical state of ALM within the microparticles was investigated.

MATERIALS AND METHODS

1) *Precipitation of microparticles*: Aqueous solutions of α-lactose monohydrate with HPMC K100LV polymer (alone and in combination), were prepared in concentrations ranging from 1% to 10% w/w. Solutions were

dropped in a controlled manner into IPA, and agitated using an electrical stirrer at a speed of 2000rpm to obtain microparticles which were collected by centrifugation.

2) *Zeta potential*: A zeta sizer was used to measure the zeta-potential for all microparticles to study the mechanism of HPMC-ALM interaction.

3) *Differential scanning calorimetry (DSC) and fourier transfer infrared analysis (FT/IR):* DSC and FT/IR were used to study the effect of process and formulation variables on the physical state of ALM in the microparticles (from 1% – 5% w/w solutions). For DSC, 15–240 °C was used with a 10°C/ min heating rate.

RESULTS AND DISCUSSION

DSC analysis showed a predominant melting point of the β-form of ALM at 230–240 °C following precipitation from IPA (without HPMC). FT/IR showed predominant peaks at 876.4 cm^{-1}, 891.9 cm^{-1}, 897.6 cm^{-1} and 949.7 cm^{-1} which are also an indication of β-lactose. This is assumed to be a result of the solvate and dehydration effect of IPA, which has been shown to induce polymorphism [3]. As the ALM concentration increased the extent of β-formation by IPA precipitation decreased.

Figure 1 shows that zeta-potential of the ALM: HPMC microparticles increased from −1.85 mV ± 0.31 to 11.3 mV ± 0.33 as the concentration of the mixture increased (1–10% w/w). This suggests there was increasing adsorption between lactose and HPMC, as HPMC would shield the negative charge of the hydroxyl groups of lactose, by increasing the distance between the particles surface and the shear plane [2].

DSC analysis showed predominant peaks of β-form (225°C-232°C) as HPMC concentration increased (Figure 2). The melting points obtained were slightly lower than those obtained by IPA processing, due to the plasticiser effect of HPMC. Infrared spectrum confirmed these results by comparing their regions of spectrum between 780–980 cm^{-1}, which can be an indicative part of the spectrum for α and β polymorphs of lactose. HPMC and ALM are structurally compatible for adsorption by a hydrogen bonding mechanism [4]. It is hypothesised that this permitted HPMC to modify and control the crystal growth of ALM and produce polymorphs as the HPMC concentration increased.

CONCLUSIONS

Both HPMC polymer and IPA precipitating agent in an aqueous-organic co-precipitation technique were responsible for polymorphism of α-lactose monohydrate.
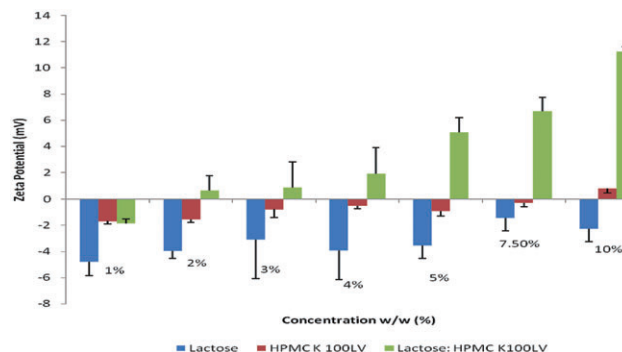
ACKNOWLEDGMENTS

Figure 1. Zeta-potential of individual excipients and microparticle formulations
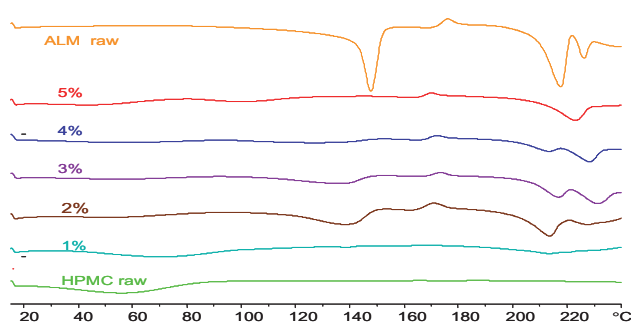

Figure 2. DSC spectrum of microparticles precipitated from different concentrations of lactose: HPMC

REFERENCES

[1] J. H. Kirk, S. E. Dann and C. Blatchford, "Lactose: A definite guide to polymorph determination." *International Journal of Pharmaceutics* **334** (2007) 103–114.

[2] Y. Yokoi, E. Yonemochi, k. Terada, **"**Effects of sugar ester and hydroxypropyl methylcellulose on the physicochemical stability of amorphous cefditoren pivoxil in aqueous suspension" *Int J Pharm,* **290** (2005) 91–99.

[3] D. Braga and F. Grepioni, "Making crystals from crystals: a green route to crystal engineering and polymorphism. "*Chem Commun,* **29** (2005) 3635–45.

[4] I. Katzhendler, R. Azoury, M. Friedman,"Crystalline properties of carbamazepine in sustained release hydrophilic matrix tablets based on hydroxypropyl methylcellulose" *Journal of Controlled Release,* **54** (1998) 69–85.

Biodegradable PLGA Nanoparticle for Sustained Ocular Drug Delivery

Himanshu Gupta*[1,2], M. Aqil[1], R.K. Khar[1], Asgar Ali[1], Aseem Bhatnagar[2], Gaurav Mittal[2]

[1]Department of Pharmaceutics, Faculty of Pharmacy, Jamia Hamdard (Hamdard University), New Delhi-110062, India
[2]Department of Nuclear Medicine, Institute of Nuclear medicine and Allied Sciences (INMAS), Defence R&D Organisation, Ministry of Defence, New Delhi-110054, India
*himanshu18in@yahoo.com

Abstract – **Poor ocular bioavailability of drugs (< 1%) from conventional eye drops (i.e. solution, suspension and ointments) is due mainly to the precorneal loss factor that include rapid tear turnover, non productive absorption, transient residence time in cul-de-sac and the relative impermeability of the drugs to corneal epithelial membrane. To overcome these problems, novel drug delivery system i.e. nanoparticles were explored. In our present work, we have developed PLGA nanoparticles and then evaluated for various parameters.**

INTRODUCTION

A variety of ocular drug delivery systems, such as hydrogels, microparticles, nanoparticles, liposomes and collagen shields have been designed and investigated for improved ocular bioavailability. Amongst them, polymeric nanoparticle is found as an interesting approach and proved to be a good carrier for ocular drug delivery due to their particle size of 500 nm. Sparfloxacin is a newer generation hydrophobic floroquinolone which is used as a model drug in present work. Nanoparticle system can be used to formulate poorly water soluble drugs as nanosuspension thus offers the best opportunity to enhance ocular bioavailability.

MATERIALS AND METHODS

Sparfloxacin encapsulated PLGA nanoparticles were prepared by the nanoprecipitation method. The formulation is characterised for various properties like particle size, zeta potential, morphology by Malvern and TEM respectively. The formulation is further characterised for in vitro drug release, stability etc. Microbiological assay was carried out against *Staphylococcus aureus* using cup-plate method. Precorneal residence time was studied on albino rabbits by gamma scintigraphy after radiolabelling of sparfloxacin by Tc-99 m. Ocular tolerance of developed formulation was also studied by HET-CAM method. [1]

RESULTS AND DISCUSSION

The developed nanoparticles give a mean particle size range of 199–205 nm with a zeta potential of −22 mv. An entrapment efficiency of 86% was obtained in this process with a nanoparticle recovery of 70%. In vitro release from developed nano formulation in simulated tear fluid, pH 7.4 showed an extended release profile of sparfloxacin. Microbial assay shows clear zone of inhibition and reveals prolong microbial efficacy of
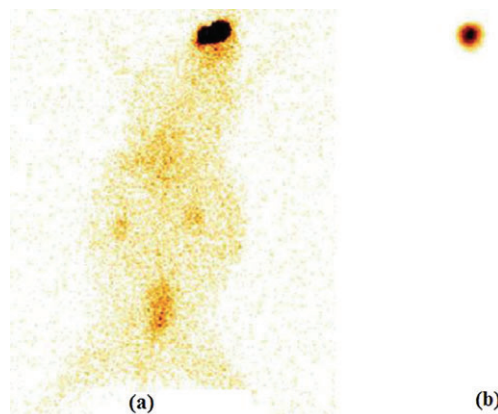

Fig. 1. Gamma scintigraphic whole body images after 5 h of administration (a) marketed formulation (b) sparfloxacin nanosuspension.

developed nanoparticles as compared to marketed eye drops. The observation of acquired gamma camera images showed good retention over the entire precorneal area for developed formulation as compared to marketed formulation. Marketed drug formulation cleared very rapidly from the corneal region and reached to systemic circulation through nasolachrymal drainage system, as significant radioactivity was recorded in the kidney and bladder after 2 h of ocular administration, whereas developed nano formulation cleared at a very slow rate (p < 0.05) and remained at corneal surface for longer duration as no radioactivity was observed in systemic circulation. HET-CAM assay further proves the non irritant property of developed nanosuspension. Formulation was non-irritant up to 8 h (mean score 0) while the mean score was found to be 0.33 up to 24 h. The developed lyophilised nanosuspension were found to be stable for a longer duration of time (**degradation constant of 1.4×10^{-4}**) imparting good shelf life to the product.

CONCLUSIONS

The developed sparfloxacin nanosuspension give extended control release with better tolerability and prolonged retention at corneal site. It is suitable for sustained ocular drug delivery and can go up to the clinical evaluation and application.

ACKNOWLEDGMENTS

REFERENCE

[1] Himanshu Gupta, M. Aqil, R.K. Khar, Asgar Ali, Aseem Bhatnagar, Gaurav Mittal, Sanyog Jain, "Development and characterisation of Tc-99m timolol maleate for evaluating efficacy of in situ ocular drug delivery system" *AAPS Pharm. Sci.*, **10(2009)** 540–546.

Chemical permeation enhancement strategies for improved topical caffeine delivery

H. Ab Hadi, M.E. Lane and J. Hadgraft

Department of Pharmaceutics, The School of Pharmacy, University of London, London, UK

INTRODUCTION

Caffeine is commonly used as a model hydrophilic compound in skin research, and it also has pharmaceutical and cosmetic applications [1,2]. Several topical products containing caffeine are currently marketed including anti-cellulite creams and gels, moisturisers, serums and shampoo. As skin permeation of this compound is expected to be low, the aim of this work is to investigate how topical delivery of caffeine may be optimised using chemical penetration enhancers.

MATERIALS AND METHODS

Solubility studies of caffeine in propylene glycol (PG), dimethyl isosorbide (DMI), isopropyl myristate (IPM), 1,2-Pentanediol (1,2-PENT), geraniol (GER), isopropyl isostearate (ISIS), and 1,8-cineole (CIN) were conducted at 32°C. Miscibility studies were conducted with binary and ternary solvent combinations of PG-DMI-IPM, PG-GER-IPM, DMI-ISIS-CIN, and PG-IPM-1,2-PENT. Infinite dose skin permeation studies were performed at 32°C in single solvents, binary and ternary solvent mixtures. Steady-state fluxes (J_{ss}) were determined by non-linear modelling using Scientist Version 3.0 (Micromath Scientist Software Tool, Inc., USA).

RESULTS AND DISCUSSION

Phase diagrams show the boundaries of the different phases as a function of the component composition (Figure 1).

Caffeine solubility and flux from the single solvents (PG, DMI and IPM) as well as binary and ternary combinations are summarised in Table 1.

The flux of caffeine was significantly (p < 0.05) enhanced in ternary systems (T1, T3 and T4) compared with the single solvents. This flux enhancement is because of the synergistic effect generally observed when more than one combination of solvents is used in a formulation. The ternary mixtures, T1, T3 and T4 showed significantly higher flux (p < 0.05) of caffeine compared with T2. This may be the result of more efficient uptake of the solvent into the skin and thus enhanced drug flux.
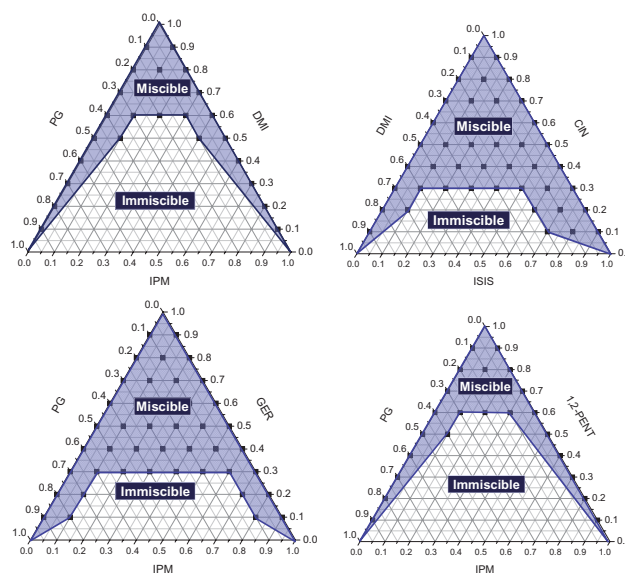

Fig. 1. Ternary phase diagram constructed from miscibility studies.

Table 1. Caffeine solubility and flux from different vehicles (mean ± SD; n ≥ 3)

Solvent	Caffeine solubility (mg/ml)	Flux (µg/cm²/h)
PG	15.89 ± 0.06	3.02 ± 0.22
DMI	22.6 ± 0.02	0.85 ± 0.14
IPM	1.12 ± 0.59	10.67 ± 0.77
PG:DMI	37.98 ± 4.27	2.57 ± 0.57
IPM:DMI	13.24 ± 0.89	5.59 ± 1.4
T1-PG:DMI:IPM	35.23 ± 1.11	29.57 ± 7.5
T2-PG:DMI:IPM	43.64 ± 3.22	7.52 ± 1.77
T3-PG:DMI:IPM	14.1 ± 0.84	26.61 ± 1.2
T4-PG:DMI:IPM	18.63 ± 3.57	23.22 ± 1.49

When compared with the flux of caffeine from simple aqueous systems (2.9 ± 0.7 µg/cm²/h) [3] all of the PG:DMI:IPM ternary mixtures which were evaluated demonstrate at least a 7-fold improvement in flux.

CONCLUSIONS

In conclusion, the flux of caffeine was optimised using ternary systems of PG:DMI:IPM. Solubility and permeation studies of caffeine from other solvents and their combinations are ongoing.

ACKNOWLEDGMENTS

REFERENCES

[1] Amato, M., Isenschmid, M., and Hüppi, P. "Percutaneous caffeine application in the treatment of neonatal apnea" *Eur. J. Pediatr.*. **150:** 8 (1991) 592–594.

[2] Rawlings, A.V. "Cellulite and its treatment" *Int. J. Cosmet. Sci.* **28** (2006) 175–190.

[3] Dias, M., Hadgraft, J., and Lane, M. E. "Influence of membrane-solvent-solute interactions on solute permeation in skin" *Int. J. Pharm.* **340:** 1–2 (2007) 65–70.

Comparative evaluation of bioadhesive propolis gel (B-Gel) for mouth ulcers

S.G. Gilda[1], R.S. Dhumal[2], J. Fearneley[4], A.R. Paradkar[2,3]

[1]Department of Pharmaceutics, Bharati Vidyapeeth University, Poona College of Pharmacy, Pune, India.
[2]Centre for Pharmaceutical Engineering, University of Bradford, Bradford, UK.
[3]Institute of Pharmaceutical Innovation, University of Bradford, UK.
[4]Nature's Laboratory, Whitby, North Yorkshire, YO22 5JR, UK

Abstract – **The objective was to characterise and perform comparative evaluation of a nanodroplet forming bioadhesive gel containing propolis (B-Gel®) with marketed products for similar application.**

INTRODUCTION

Propolis is a mixture of various amounts of beeswax and resins collected by the honeybee from plants, particularly from flowers and leaf buds. It contains flavonoids and phenolic acids or their esters, which often form up to 50% of all ingredients. Caffeic acid phenethyl ester (CAPE) is one of the important active ingredients. Propolis shows various pharmacological and therapeutic activities such as anti-inflammatory, anti-microbial, anti-viral, anticancer, immunomodulatory and local anaesthetic [1]. Since propolis has shown local anaesthetic as well as anti fungal activity it may serve as a good candidate for mouth ulcers. However, propolis has poor water solubility which hampers its therapeutic activity and has limited its commercial exploitation. Considering this need we have developed a water soluble propolis. The aim of this work is to formulate gel of water soluble propolis extract which can be easily applied to the affected area delivering the phytoconstituents locally.

MATERIALS AND METHODS

B-Gel is proprietary product developed for Nature's Laboratory. It contains propolis 1.5 % in a Carbopol base. This bioadhesive product has been supplied by Nature's Laboratory. B-Gel was characterised for CAPE content using RP-HPLC. Its local anaesthetic, bioadhesivity and antimicrobial activity were evaluated in comparison with Bongel and Soregel.

Bioadhesivity of the gels was determined using bioadhesivity tester on sheep oral mucosa. The gels were screened for in-vivo local anaesthetic activity using Randel selleto model and compared with marketed preparations. Anti microbial and antifungal activity was determined using plate method.

RESULTS AND DISCUSSION

The propolis B-Gel contains 0.52% of CAPE as determined by HPLC. The force of detachment required was used as an
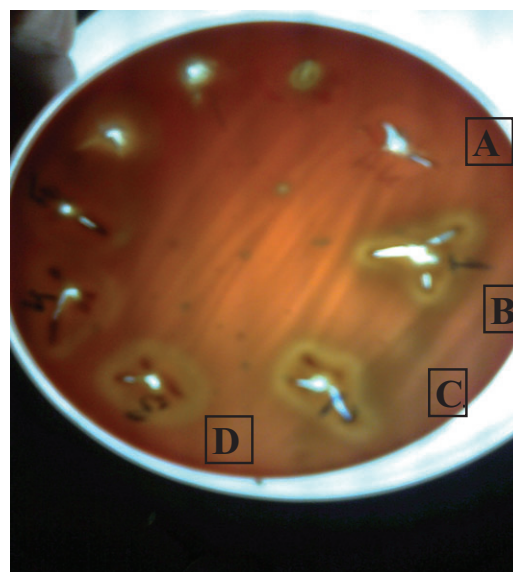

Figure 1. Plate showing zones of inhibition for Amikacin (A), Bonjela (B), Soregel (C) and propolis B-Gel (D).

Table 1: Local anaesthetic activity

Bonjela	Soregel	Propolis Gel (B-Gel)
45 ± 2.3 %	50 ± 2.61 %	61.66 ± 3.22 %

indicator of the bioadhesivity. B-Gel requires 1360 mN force while Bonjela requires 920 mN force of detachment indicating propolis nano gel has strong bioadhesivity compared to Bonjela. In-vivo local anaesthetic activity was studied using Randell selleto model. B-Gel showed superior local anaesthetic activity than Bonjela and Soregel (Table 1). Anti bacterial and antifungal activities of the gel were also compared with Bonjela and Soregel using Amikacin as control. The zones of inhibition were 13, 16, 21 and 13 mm^2 for Bonjela, Soregel, propolis anogel and Amikacin, respectively. This indicates superiority of B-Gel over both the marketed products and the control.

CONCLUSIONS

B-Gel has shown enhanced bioadhesive, local anaesthetic and antimicrobial activity compared to marketed formulations. Further work is going on to characterise the nano sized droplets generated and investigate its utility to provide faster onset of action.

ACKNOWLEDGMENTS

REFERENCE

[1] V. S. Bankova, S. S. Popov, N. L. Marekov, "A Study on Flavonoids of Propolis" J. Nat. Prod. **46** (1983) 471–474.

Crystallisation of furosemide using different solvents to enhance drug dissolution

T.O. Adeusi, R.R. Haj-Ahmad, A.A. Elkordy

Department of Pharmacy, Health and Well-Being, University of Sunderland, United Kingdom

The aims of this research were to: (i) prepare furosemide microcrystals from systems containing either acetone or ethanol in absence or presence of stabilising additives (hydroxypropyl-γ-cycoldextrin and copovidone), (ii) differentiate between drug microcrystals collected either by spray drying or filteration and (iii) study dissolution profiles of different furosemide microcrystals or solvates.

INTRODUCTION

Production of polymorphs or solvates of hydrophobic drugs may lead to enhancement of dissolution of these drugs and subsequently the development of hydrophobic drugs as pharmaceuticals in suitable oral dosage forms.

MATERIALS AND METHODS

Furosemide microcrystals were prepared by mixing drug (0.5%w/v) in either ethanol or acetone with stabilising agent aqueous solutions (0.25%w/v cyclodextrin or 0.25% copovidone or mixture of them). Drug microcrystals were precipitated and separated by either spray drying or filteration (followed by drying at ambient temperature).

Dried microcrystals were evaluated by yield determination; solubility test; differential scanning calorimetry (DSC); Fourier Transform Infra-Red (FT-IR); drug dissolution and polarised microscopy.

RESULTS AND DISCUSSION

The yield was highest for furosemide crystallised in ethanol (in the presence of cyclodextrin) than in acetone, suggesting the effect of solvent on the yield results. Crystallisation of the drug from ethanol enhanced the aqueous solubility of furosemide compared to that of the drug crystallised from acetone; the results were 42.58 (1.14) and 18.58 (0.62) μg/ml for furosemide in ethanol and in acetone respectively. The solubility of furosemide in water was 18.24 (0.47). In addition, the presence of the stabilising excipients increased the solubility of furosemide by about 2–3 folds.

For dissolution data, furosemide microcrystals form ethanol and in the presence of cyclodextrin improved the dissolution of the pure drug e.g. the drug released after 15 minutes was 48% versus 8% for microcrystals with cyclodextrin and pure drug respectively. The crystallisation of furosemide from ethanol in absence of additives produced 40% drug release after 15 minutes against only 24% drug release from drug microcrystallised in acetone, suggesting different polymorph formation. Additionally, furosemide with copovidone and cyclodextrin crystallised in ethanol gives a higher overall release compared to furosemide alone (p < 0.05).

To explain the results of drug dissolution, the differential scanning calorimetry data revealed that the microcrystals had a melting point which was higher than the pure drug and also the area under the curve was different, suggesting formation of different polymorphs, this was confirmed by microscopy analysis. FT-IR revealed interaction between the drug, solvent and excipients.

Comparing the two drying processes, the spray drying produced crystals which were different in their thermal behaviour compared to drug crystals collected by filteration.

CONCLUSIONS

These results show that ethanol and excipients lead to an improvement of furosemide dissolution.

Cyclodextrins with Pluronic®F-127 as Carrier Systems in Gene Delivery using Drying Technology

H.M. Beba and A.A. Elkordy

Department of Pharmacy, Health and Well-Being, University of Sunderland, Sunderland, SR1 3SD

The aims of this study were to: (i) prepare cyclodextrin containing DNA formulations and (ii) study the effects of Pluronic®F-127, Solutol®HS15 and folic acid on stability of freshly prepared and freeze dried cyclodextrin-DNA formulations.

INTRODUCTION

Gene therapy is a rapidly expanding field and it has applications in treatment for both genetic and acquired diseases. Delivery of a genetic product to a cell can be challenging. DNA is a bulky structure that has a negatively charged phosphate backbone at physiological pH. In order to deliver this type of molecule successfully, negative charge must be neutralised to avoid repulsion from anionic cell surfaces. Also, DNA must be condensed and protected against nuclease degradation [1]. Cyclodextrins as non-viral DNA carriers are of particular interest in gene delivery.

MATERIALS AND METHODS

Deoxyribonucleic acid (DNA), from calf thymus was used as a model. DNA solutions in phosphate buffer, pH 7.2 were prepared with carboxymethyl-β- cyclodextrin as the main non-viral carrier in gene formulations incorporating various excipients (Pluronic®F-127, Solutol®HS15 and folic acid) in ratios of 1:3:3 and 1:10:10, DNA : cyclodextrin : excipient. The solutions were characterised in fresh and freeze dried forms: (i) Ethidium bromide exclusion assays using fluorescence spectrophotometry determined the degree of DNA incorporated into cyclodextrin, (ii) Deoxyribonuclease (DNase) activity was assessed spectrophotometrically to determine the amount of DNA available for enzyme degradation, (iii) Fourier Transform Infrared Spectroscopy (FT-IR) was used to determine any structural changes in the formulations and (iv) Differential Scanning Calorimetry (DSC) was used to determine thermal stability of formulations. Also, charge measurement using Zeta PALS1 determined the suitability of formulations for cell transfection.

RESULTS AND DISCUSSION

The fluorescence assay revealed good incorporation of DNA into cyclodextrin for Pluronic®-F-127 stabilised formulations. In particular, Pluronic®F-127:cyclodextrin: DNA 10:10:1 formulation showed that it may lead to incorporation percentages exceeding 25% for freeze dried DNA samples and 35% for fresh DNA samples. The decrease in incorporation for freeze dried sample compared to fresh sample may be due to repulsive forces which form during freezing as all the components are drawn closer together i.e. solute concentration increased. For fresh sample of folic acid : cyclodextrin : DNA 10:10:1, the amount of DNA incorporated was 12% whilst freeze dried Solutol®HS15:cyclodextrin : DNA 10:10:1 sample showed a very small amount of DNA incorporation (0.6%). Comparing these results with cyclodextrins (in absence of stabilising excipients) as non-viral vectors see example [2], the percentage DNA incorporated depends on nitrogen : phosphate ratio for cyclodextrin: DNA and only at high ratios (100:1 or higher) DNA can be incorporated. This means that excipients used in this research, especially Pluronic®-F127, show promise for delivery of effective gene formulations.

It was found that formulations with Pluronic®-F127 and folic acid as stabilising excipients in freeze dried forms (Pluronic®-F127 (or folic acid):cyclodextrin : DNA 10:10:1) gave excellent protection to DNA from DNase (100% of incorporated DNA was protected from DNase degradation). The increase in stability shown from the freeze drying may be explained by favourable bonds being formed during the freeze drying process. This was confirmed by the FT-IR data. Formulations containing Solutol®HS15:cyclodextrin : DNA 3:3:1 protect DNA from nuclease enzyme in both fresh and freeze dried samples. Cyclodextrins are a type of sugar and it has been shown that stability of DNA complexes increases by increasing sugar concentration. It has been hypothesised that this was due to vitrification. Recently however, experimentation has proposed a more direct stabilisation technique between DNA and sugars.

FT-IR and DSC data confirm interactions between Pluronic®-F-127 and cyclodextrin-DNA complex. FT-IR

spectra demonstrated hydrogen bond formation and the possibility of covalent bonding between cyclodextrin and DNA in the presence of Pluronic®-F127 leading to the removal of the functional group responsible for the shift at ~1155 cm^{-1}, believed to be belonging to an alcohol group on the cyclodextrin ring. DSC results revealed that the presence of cyclodextrin with Pluronic®-F-127 increased the transition temperature of DNA (in DSC solid state) from 209°C to ~223°C. The transition temperature of the cyclodextrin: DNA 10:1 formulation was 216°C.

The presence of Pluronic®-F127 reduced the negative charge of DNA-cyclodextrin (-22.27 mV) in concentration dependent manner. The charge was −7.98 mV for Pluronic®-F127:cyclodextrin: DNA 10:10:1, although the charge was negative, which would not be favourable for cell transfection, but the increase of Pluronic®F-127 concentration may decrease negativity and overcome the barrier to cell transfection. The reverse trend was seen for the Solutol®HS15 formulations with the Solutol®HS15:cyclodextrin: DNA 3:3:1 formulation having a charge of −7.81 mV and the 10:10:1 formulation having a charge of −12.13 mV. The overall charge was positive (6.70 mV) in the case of the folic acid: cyclodextrin: DNA 3:3:1 formulation.

CONCLUSIONS

This research shows how the use of excipients (Pluronic®F-127, Solutol®HS15 and folic acid) and their concentrations with cylcodextrin (as a gene carrier) can impart stability to DNA formulations.

REFERENCES

[1] Abdelhady HG, Allen S, Davies MC, Roberts CJ, Tendler SJ, Willians PM, 2003. Nucleic Acids Res. 31: 4001–4005.
[2] Cryan, S-A, Holohan, A, Donohue, R, Darcy, R, O'Driscoll, CM. 2004. Euro J Pharm Sci. 21: 625–633.

Delivery of latex microsphere suspensions using nebulisers

A.M.A. Elhissi[1], I. Parveen[1], W. Ahmed[2]

[1]School of Pharmacy and Biomedical Sciences and [2]School of Computing, Engineering and Physical Sciences, University of Central Lancashire, Preston, UK

Abstract – The effect of particle size of latex microspheres (1, 4.5 or 10 μm) on the aerosols generated by four nebulisers was studied. The aerosols of the Pari (air-jet) and the Polygreen (ultrasonic) nebulisers were highly independent of the sphere size, and the output of the Pari was higher. However, the Aeroneb Pro (vibrating-mesh) performed better with the 4.5 and 10 μm spheres. By contrast, the Omron (vibrating-mesh) performed efficiently only when the 1 μm spheres were used.

INTRODUCTION

Air-jet and ultrasonic nebulisers are well-established in generating liquid aerosols. Vibrating-mesh nebulisers have been recently commercialised. They operate by extruding the liquid through a perforated plate to generate aerosol [1]. In this study, the ability of the vibrating-mesh nebulisers (Aeroneb Pro and Omron MicroAir) to deliver latex microspheres was evaluated and compared to air-jet (Pari LC Sprint) and ultrasonic (Polygreen) nebulisers.

MATERIALS AND METHODS

Size analysis of latex microspheres and determination of aerosol output: Polystyrene latex microspheres (Alfa Aesar, UK) having a size of 1, 4.5 or 10 μm were diluted to 1% w/v using phosphate buffer saline. Nebulisation of microspheres (5 ml) was performed in front of a twin impinger (TI) and samples were taken for size analysis using laser diffraction (Malvern Mastersizer 2000). The aerosol output was determined gravimetrically.

RESULTS AND DISCUSSION

The measured size (volume median diameter, VMD) was in high agreement with the expected size (Table 1). The Span values were very small, indicating that particles are monodispersed (Table 1).

Except for the Polygreen, all nebulisers delivered 1 μm spheres to the TI (Table 2). The Pari nebuliser caused aggregation of the spheres in the lower impinger (LI) since high VMD and Span values were obtained (Table 2). The 4.5 μm spheres were not delivered by the Polygreen or the Omron since no particles were detected in the TI (Table 2). However, the Polygreen nebuliser delivered the 10 μm spheres whilst

Table 1. Size (VMD) and size distribution (Span) of the latex microspheres before nebulisation (n = 3 ± sd)

Microspheres	VMD (μm)	Span*
1 μm	0.98 ± 0.02	0.37 ± 0.03
4.5 μm	4.79 ± 0.04	0.86 ± 0.2
10 μm	9.73 ± 0.03	0.30 ± 0.04

*Span = (90% undersize – 10% undersize) / VMD

Table 2. Size of microspheres collected from the nebuliser and Upper (UI) and lower (LI) stages of the TI at the end of nebulisation (n = 3 ± sd)

Nebuliser / Sphere size	VMD (μm)		
	Nebuliser	UI	LI
Pari / 1 μm	4.80 ± 1.21	1.52 ± 0.70	77.66 ± 2.94
Polygreen / 1 μm	2.32 ± 0.89	ND*	ND*
Omron / 1 μm	2.36 ± 1.04	0.98 ± 0.13	1.02 ± 0.00
Aeroneb Pro / 1 μm	1.08 ± 0.01	1.12 ± 0.07	2.76 ± 1.22
Pari / 4.5 μm	7.02 ± 1.68	4.50 ± 0.35	85.46 ± 54.67
Polygreen / 4.5 μm	4.26 ± 0.10	ND*	ND*
Omron / 4.5 μm	4.71 ± 0.23	ND*	ND*
Aeroneb Pro / 4.5 μm	4.28 ± 0.06	3.67 ± 0.33	13.65 ± 8.31
Pari / 10 μm	10.58 ± 1.48	10.09 ± 1.21	94.35 ± 18.99
Polygreen / 10 μm	9.59 ± 0.22	5.90 ± 3.41	128.57 ± 108.57
Omron / 10 μm	NAG**	NAG**	NAG**
Aeroneb Pro / 10 μm	9.72 ± 0.08	13.34 ± 5.52	5.73 ± 2.78

*ND = Not detected, **NAG = No aerosols generated

Fig.1. Aerosol output (%) of latex microsphere formulations (n = 3 ± sd)

no particles were delivered by the Omron (Table 2). The particles detected in the nebulisers indicate accumulation of some microspheres within nebulisers during aerosolisation.

Aerosol output of the Pari and Polygreen nebulisers was minimally affected by the sphere size; however the Pari produced much higher output (Fig.1). The Aeroneb Pro produced the highest output with 4.5 and 10 μm spheres and the Omron achieved approx 100% output for the 1 μm spheres, but poor or no aerosols were generated from the larger spheres (Fig.1). Fluid characteristics and nebuliser design can affect the properties of nebulised aerosols [2, 3].

CONCLUSIONS

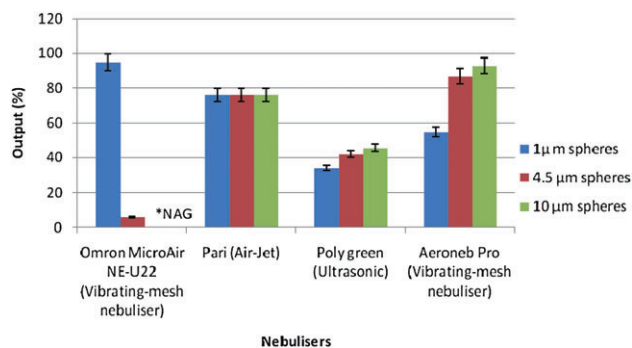Nebulisers performed differently with different microsphere sizes. Generally, the Aeroneb Pro and the Pari were the most reliable devices in delivery of the dispersions. However, the output produced by the Omron was almost 100% only with the smallest spheres.

REFERENCES

[1] R. Dhand, "Nebulisers that use a vibrating mesh or plate with multiple apertures to generate aerosol" *Respir. Care,* **47** (2002) 1406–1416.

[2] O.N.M. McCallion, K.M.G. Taylor, M. Thomas and A.J. Taylor, "Nebulisation of fluids of different physicochemical properties with air-jet and ultrasonic nebulisers" *Pharm. Res.,* **12** (1995) 1682–1688.

[3] T. Ghazanfari, A.M.A. Elhissi, Z. Ding and K.M.G. Taylor, "The influence of fluid physicochemical properties on vibrating-mesh nebulisation" *Int. J. Pharm.* **339** (2007)103–111.

Design and formulation of a novel polymer-based buccal film

F. Kianfar, B.Z. Chowdhry, M.D. Antonijevic, J.S. Boateng

School of Science, University of Greenwich at Medway, Chatham Maritime, ME4 4TB, UK
(farnoosh1354@gmail.com)

INTRODUCTION

The aim of this work was to develop a novel film for delivering amorphous drugs into the systemic circulation via the buccal mucosa. The advantage of the buccal mucosa over the sublingual, such as better systemic effects, has led to its exploration as a functional administration route [1]. Buccal formulations can be developed as films, freeze-dried wafers [2] which are suitable alternatives to deliver drugs promptly and safely.

MATERIALS AND METHODS

Materials: Poloxamer 407 and different polymer grades (911, 379, and 812) of carrageenan known for its bioadhesive viscous modifying properties, were used to select the most appropriate grade for drug loading, and PEG 600 and glycerol were used as plasticisers. Model soluble (paracetamol) and insoluble (ibuprofen and indomethacin) drugs known to exhibit polymorphism and with different log P values were chosen for investigating stable amorphous drug formation.

Method: Gels were prepared by dispersing carageenan in deionised water for 24 hours to allow complete hydration before homogenisation and poloxamer added. Films were obtained by pouring the gels into petri dishes and dried in an oven at 60°C for 24 hours. Two sets of films (diameter 90 mm) both containing poloxamer, PEG and carrageenan 911 with or without drug, were evaluated for tensile properties in triplicate by Texture Analysis (Stable Microsystems) to select optimum amounts and type of film components.

RESULTS

The results from formulation development demonstrated that the best condition for gel formation was to incubate carrageenan in aqueous solution for 24 hours to allow for complete hydration and uniform gel formation.

Carrageenan 911 was used to produce films with no entrapped air bubbles, and of acceptable transparency as well as flexibility (Fig.1). These characteristics were achieved by the addition of an appropriate plasticiser to obtain strong but reasonably flexible films, as shown by the tensile experiments. The most suitable choice of plasticiser, which also allowed an enhancement in the amount of drug incorporated, was PEG 600 (PEG 600:carrageenan 11:5). This ratio produced the required films with appropriate balance between flexibility and strength which are essential for physical stability of films during handling. Examination of the plots of PEG 600 concentration against film elongation and elastic modulus showed that 5.5 % w/w PEG 600 was the optimum formulation with an elastic modulus value of approximately 2.5 N/mm^2 (Fig.2). Generally increasing drug content resulted in a slight reduction in elastic modulus but not significantly.

Optimised ratios of the starting materials in the initial gel used to prepare the polymer films were 2.5% carrageenan 911, 5.5% PEG 600 and 4% (w/w) poloxamer 407 as well as one of the following drugs: 1.6% paracetamol, 0.4% ibuprofen, or 0.3% (w/w) indomethacin.

CONCLUSIONS

Solvent cast swellable buccal films containing optimised ratios of poloxamer, carrageenan and PEG that both maximises drug incorporation and produces a gel with right mechanical properties (right balance of strength and flexibility), have been designed and formulated.
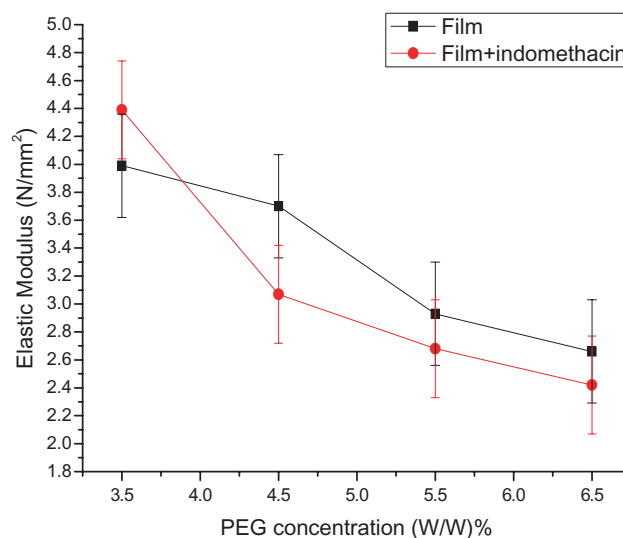

Fig.1. Developed buccal film.

Fig. 2. Tensile testing: the effects of PEG 600 concentration on the film's elastic modulus (n = 3).

REFERENCES

[1] R. P. Dixit, and S. P. Puthil, "Oral strip technology: Overview and future potential". *J. Control. Release*, **139** (2009) 94–107.

[2] A.M. Hillery, A. W. Lloyd, J. Swarbrick, "Drug delivery and targetting for pharmacists and pharmaceutical scientists". London, Taylor and Francis, 2001, **7**. 186–206.

Design and in-vitro evaluation of ultradeformable lipid vesicles (transfersomes) for transdermal delivery of Salmon Calcitonin

T. Toliyat[1], R. Hadian[2]

[1] Faculty of pharmacy, Tehran University of Medical Sciences, Tehran, Iran.
[2] Food and Drug Assistance, Mazandaran University of Medical Sciences, Sary, Iran.

INTRODUCTION

The aim of this study was investigating the ability of ultradeformable lipid vesicles (transfersomes) to transport Salmon Calcitonin (SCT) across the skin.

MATERIALS AND METHODS

Two formulations of transfersomes containing SCT were prepared from soybean phosphatidylcholine and different surfactants (sodium lauryl sulphate for formula F1 and sodium deoxycholate for formula F2) with a lipid/surfactant ratio of 86/14 by thin film hydration method and brought to the desirable size by homogenisation and ultrasonication. Conventional liposomes containing SCT and soybean phosphatidylcholine were made by the same method [1–4].

The in vitro skin permeation test was carried out using Franz diffusion cell. Phosphate buffer ph = 7.4 was used as acceptor compartment and rat abdominal skin was used as natural membrane [5]. Aliquots were taken from the acceptor compartment every hour for 10 hours and SCT was quantified using HPLC with a mobile phase consisting of acetonitrile and 0.05% v/v aqueous solution of Trifluoroacetic acid with a 70/30 ratio.

The entrapment efficiency of the lipid vesicles was determined by dialysis bag technique. The particle size distribution was measured by dynamic light scattering. The statistical analyses were performed using Microsoft Excel 2007, One-Way ANOVA and Tukey's test for comparison of values and $p < 0.05$ was accepted as denoting a statistical difference.

RESULTS AND DISCUSSION

The results are presented in tables I and II. All data are expressed as mean ± Standard deviation.

The results show no significant difference in average particle size of F1, F2 and conventional liposome, but both transfersome formulas show a higher amount of entrapment efficiency than liposome.

F2 has higher entrapment efficiency and it has also transported higher amounts of its associated SCT across the skin compared to F1. Neither Liposome nor SCT solution were able to transport any amounts of SCT across the skin.

Table I. Particle size and entrapment efficiency of different formulas.

Formula	Average particle diameter (μm)	Entrapment efficiency (%)
F1	7.72 ± 1.33	65.85 ± 2.32
F2	7.7 ± 1.31	74.95 ± 4.43
Liposome	5.72 ± 2.42	61.81 ± 1.45
Solution	–	–

Table II. Results of skin permeation test after 10 hours for different formulas

Formula	Amount of SCT crossed the skin surface area (μg/cm²)	Transepidermal flux of SCT (μg/cm²/hour)	Total amount of SCT crossed the skin (%)
F1	69.56 ± 5.41	10.37 ± 0.76	47.66 ± 3.71
F2	91.71 ± 3.50	11.31 ± 0.79	55.13 ± 2.12
Liposome	0.00	0.00	0.00
Solution	0.00	0.00	0.00

CONCLUSIONS

This study shows that transfersomes are able to transport considerable amounts of Salmon Calcitonin across the skin and thus, can be regarded as a new route for non-invasive administration of peptides.

REFERENCES

[1] G Cevc and G Blume, "New highly efficient formulation of diclofenac for the topical, transdermal administration in ultradeformable drug carriers, Transfersome" *Biochim Biophys Acta*., 1514(2001) 191–205.

[2] G Cevc and G Blume, "Biological activity and characteristics of triamcinolone acetonide formulated with the self regulating smart carriers, Transfersomes®" *Biochim Biophys Acta*., 1614(2003) 156–164.

[3] G Cevc, D Gebauer, J Stieber, A Shätzlein and G Blume, "Ultradeformable lipid vesicles, Transfersomes, have an extremely low pore penetration resistance and transport therapeutic amounts of insuln across the intact mammalian skin" *Biochim Biophys Acta*., 1368(1998) 201–215.

[4] I Sari güllü Özgüney, H Yesim Karasulu, J Kantarc, S Sözer, T Güneri and G Ertan, "Transdermal delivery of Diclofenac sodium through rat skin from various formulations" *AAPS PharmSciTech*., 7(4)(2006) Article 88 E1-E7.

Development of novel amphiphilic polymers for the oral delivery of insulin: Effects of graft on cellular interaction *in vitro*

C.J. Thompson[1], K. Skene[1], P. Gadad[1], W.P. Cheng[2] and R. Knott[1]

[1]School of Pharmacy & Life Sciences, Robert Gordon University, Aberdeen, UK.
[2]School of Pharmacy, University of Hertfordshire, Hatfield, UK.

Abstract – **Novel amphiphilic polymers based on a poly(allyl amine) backbone have been synthesised with either palmitoyl (Pa) or cetyl (Ce) grafts and quaternary ammonium moieties (Q). These polymers form polyelectrolyte complexes (PEC) with insulin. Their uptake and interaction with Caco-2 cells was shown to differ. QPa-insulin PEC were co-localised in the perinuclear area of cells regardless of external conditions. QCe-insulin PEC uptake was prevented by an active transport inhibitor. The difference in structure of the polymers must play a role in cellular interaction.**

INTRODUCTION

Oral delivery is the preferred route of administration for both patients and clinicians. However insulin cannot be delivered orally in its native state due to enzymatic degradation and its inability to pass through the gastrointestinal tract [1].

Our previous work showed that novel amphiphilic polymers (QPa and QCe) were able to protect insulin from *in vitro* enzymatic degradation [1, 2].

The aim of this study is to further elucidate the mechanism(s) by which these polymers are able to facilitate insulin uptake into Caco-2 cells and whether they can promote paracellular transport using the same cell model.

MATERIALS AND METHODS

QPa and QCe were made as before [1] and tagged with the fluorescent marker rhodamine (R) while insulin was labelled with fluorescein isothiocyanate.

Intracellular Uptake Study

Caco-2 cells were grown in 24 well polyester plates over 4 days using Eagle Minimum Essential Media (EMEM).

QPa or QCe (48 µg/mL), insulin (3 µg/mL) or polymer:insulin complexes (48:3 µg/mL) were incubated with Caco-2 cells for 1 h and images were recorded (n = 3). Cells were also pre-treated with Ca^{2+} free or insulin supplemented EMEM.

The above experiments were repeated after the addition of an active transport (sodium azide) inhibitor (n = 3).

Transepithelial Electrical Resistance (TEER) Study

Caco-2 cells were grown over 21 days in polycarbonate transwell plates.
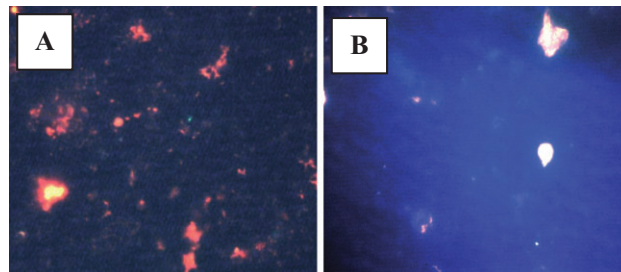

Fig. 1. Caco-2 cells pre-incubated with sodium azide. (A) QPa-insulin (48:3 µg/mL); (B) QCe-insulin (48:3 µg/mL) (Mag. x400).

QPa or QCe (48 µg/mL) or polymer-insulin complexes (48:3 µg/mL) in HBSS buffer were added to transwell plates and TEER measurements were taken over 4 h. Controls of insulin alone (3 µg/mL) and HBSS were used (n = 2).

RESULTS AND DISCUSSION

PEC were localised in the perinuclear area of cells except in the case of QCe-insulin PEC whose uptake was prevented when incubated with sodium azide (Fig. 1). Other conditions did not affect either QCe or QPa uptake. The lack of effect on uptake when using Ca^{2+} free media suggests that neither polymer was taken up due to endocytosis. Indeed, QPa PEC uptake did not appear to be affected by any of the conditions used. This difference in uptake would suggest that QCe PEC were taken up by a non-endocytotic, energy dependent process, while QPa PEC were taken up by a non-endocytotic, non-energy dependent process.

TEER data indicated that QCe was able to reduce TEER to a greater extent than QPa which would indicate that QCe may have a greater interaction with tight junction proteins than QPa (Fig. 2). PEC produced a lower reduction in TEER than QPa/QCe alone possibly due to a reduction in zeta potential on complexation [1, 2].

CONCLUSIONS

The change in structure between QPa and QCe alters the way in which the polymers interact and are taken up by Caco-2 cells.
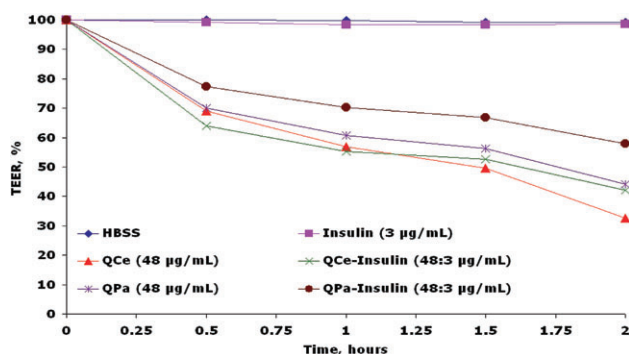
ACKNOWLEDGMENTS

Fig. 2. TEER measurements of Caco-2 cells in transwell plate after addition of QPa, QCe or polymer:insulin complexes.

REFERENCES

[1] C.J. Thompson, L. Tetley, I.F. Uchegbu, and W.P Cheng, "The complexation between novel comb shaped amphiphilic polyallyl-amine and insulin – Towards oral insulin delivery" *Int. J. Pharm.*, **376** (2009) 46–55.

[2] C.J. Thompson, L. Tetley, I.F. Uchegbu, and W.P Cheng, "The influence of polymer architecture on the protective effect of novel comb shaped amphiphilic poly(allyl amine) against in vitro enzymatic degradation of insulin – Towards oral insulin delivery" *Int. J. Pharm.*, **383** (2010) 216–22.

DNA lipoplex formulation: Effect of salt on characteristic properties

Behfar Moghaddam, Qinguo Zheng and Yvonne Perrie

School of Life and Health Sciences, Aston University, Birmingham, UK.

Abstract **– The influence of presence of electrolytes in the aqueous media on the formulation of lipoplexes and the characteristic properties of liposomes before and after complexation with DNA was investigated.**

INTRODUCTION

Previous research has shown cationic liposomes to be useful in delivery of nucleic acids both *in vitro* and *in vivo* [1,2]. However, liposomes prepared from cationic lipids have been shown to be influenced by salt concentrations and according to polyelectrolyte theory the presence of salt in formulation may affect conformational properties such as stability of polyelectrolytes, although recent studies have shown low concentration of salt does not have a destructive influence on formulation and its stability [3,4]. Indeed, recent studies [4] have shown that the addition of low concentration of salts to cationic liposomes during complex formation could lead to an improved vaccine adjuvant action [4]. The aim of the current research was to investigate the effect of salts on lipoplexes.

MATERIALS AND METHODS

Liposomes composed of 1,2-dioleoyl-*sn*-glycero-3-phosphoethanolamine (DOPE) or (1,2-distearoyl-*sn*-glycero-3-phosphoethanolamine) DSPE in combination with 1,2-dioleoyl-3-trimethylammonium-propane (DOTAP) or 1,2-stearoyl-3-trimethylammonium-propane (DSTAP) were prepared by the lipid hydration method. 8 µmol of DOPE as helper lipid was added to an equal amount of DOTAP or DSTAP. Similarly formulations were prepared from DSPE:DOTAP. Each of these formulations were prepared by

hydration in 1 ml of dH$_2$O or phosphate buffer saline (PBS; 7.4). To prepare small unilamellar vesicles the above liposomes were sonicated for up to 60 seconds. In all cases, DNA complexes were formed by mixing the cationic liposomes with DNA at various concentrations (2.5 to 200 µg) and left to stand for 30 mins. Their characteristics in terms of size and zeta potential were measured by photon correlation spectroscopy (Brookhaven Instrument Corporation) and DNA complexation was measured using Pico-green analysis (Invitrogen Ltd. UK).

RESULTS AND DISCUSSION

For all formulations tested the rehydration media was shown to influence both the size and zeta potential. Most notable was the inability to prepare DSPE:DOTAP liposomes in PBS. Additionally, rehydration of other formulations in PBS resulted in a decreased zeta potential compared to those prepared in dH$_2$O. In terms of the size, whilst no significant difference was measured for DOPE: DSTAP liposomes prepared in either of the two aqueous media, DOPE:DOTAP vesicle size was increased by hydration in PBS compared to dH$_2$O. In terms of DNA adsorption, DOPE:DOTAP lipoplexes showed high association of DNA irrespective of the hydration media.

CONCLUSIONS

Characterisation studies demonstrated that rehydration medium has a notable influence on the physiochemical characteristics of lipoplexes; depending on the lipid structure, not all cationic lipids can support liposome formation in the presence of salts. The choice of aqueous media influences both
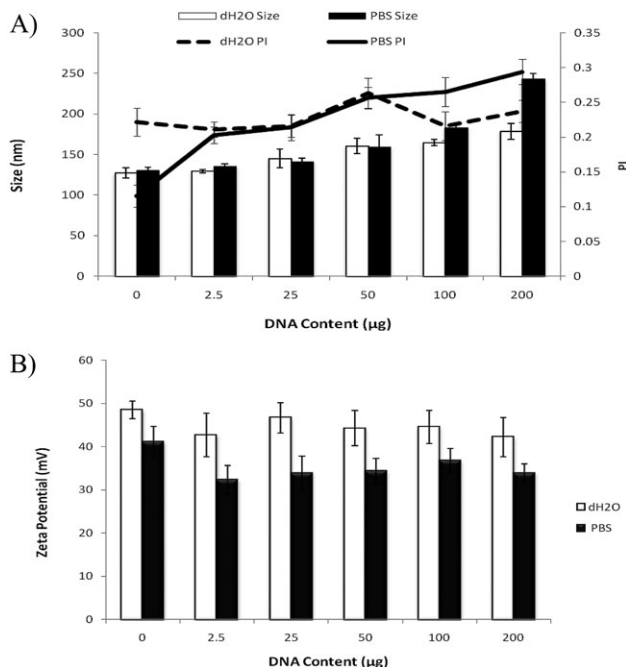
Figure 1: Vesicle size and Polydispersity Index (A) and Zeta potential (B) of DNA-Lipoplexes (DOPE:DOTAP) in distilled water and PBS and in various concentrations of DNA. Results denote mean ± SD, $n = 3$.

the vesicle size of the liposomes and their zeta potential however did not adversely influence their ability to complex DNA.

REFERENCES

[1] Yvonne Perrie and G.Gregoriadis, "Liposome-entrapped plasmid DNA: characterisation studies", *Biochimica et Biophysica Acta.,* 1475(2000) 125–132.

[2] A. Kim , E. Lee, S. Choi and C. Kim,"In vitro and in vivo transfection efficiency of a novel ultradeformable cationic liposome", *Biomaterials.,* 25(2004) 305–313.

[3] Davidsen et al., "Characterisation of cationic liposomes based on dimethyldioctadecylammonium and synthetic cord factor from M. tuberculosis (trehalose 6,6'-dibehenate)-a novel adjuvant inducing both strong CMI and antibody responses" *Biochimica et Biophysica Acta,* 1718(2005) 22 – 31.

[4] Yan and Huang, "The effects of salt on the physicochemical properties and immunogenicity of protein based vaccine formulated in cationic liposome." *Int J pharm*, 368(2009)56–62.

Effect of lyophilised wafer discs containing silymarin on the migration of microvascular endothelial cell

P.C. Gadad, K.H. Matthews, R.M. Knott

School of Pharmacy and Life Sciences, Robert Gordon University, Aberdeen, UK.

INTRODUCTION

Impaired angiogenesis is a contributory factor of delayed wound healing in diabetes [1, 2]. Lyophilised wafers are promising topical formulations for the management of chronic wounds [3]. The aim of this work was to prepare, characterise and study the effect of lyophilised wafer discs containing silymarin on the migration of microvascular dermal endothelial cells.

MATERIALS AND METHODS

The lyophilised wafer discs, with and without silymarin (equivalent to 50 µmol/L), were prepared using xanthan gum and non ionic surfactant Pluronic F68. The pre-lyophilised and reconstituted post-lyophilised gels were rheologically characterised. The wafer discs were gamma ray sterilised and the concentration of silymarin was quantified by HPLC before application in the endothelial cell model.

The migration of human microvascular endothelial cells of adult dermis (HMVECad) was studied under normal oxygen (20%) tension (normoxia) and below normal oxygen (5%) tension (hypoxia), in either 5 mmol/L or 20 mmol/L D-glucose and in the presence of silymarin wafer discs. HMVECad were seeded into circular rings of 4 mm diameter in six well plates. After 5 hours of incubation, rings were taken out and half of the resulting circular monolayer was removed before incubating the cells under the test conditions outlined above. An annotated image taken at 0 h was super imposed on a 48 h image and the migration distance was recorded for the intact and wounded edges of the semicircular monolayer.

RESULTS AND DISCUSSION

The pre- and reconstituted, post-lyophilised/gamma irradiated gels suggest that the viscosity coefficient and yield stress increased with increasing dose of radiation (Table 1). The quantity of silymarin present in the lyophilised wafer discs (89 to 90%), assessed by HPLC, was found to be less than expected (Table 2), based on the assumption of non-homogenous dispersion of silymarin in xanthan gel.

Table 1. Viscosity coefficient and yield stress of pre- and reconstituted post-lyophilised/gamma irradiated wafer gels

Gels	Viscosity coefficient (Pa.s)	Yield stress (Pa.s)
Pre lyophilised control gel	2.5	19
Gamma (25 KGy) irradiated control wafer gel	2.9	20
Gamma (40 KGy) irradiated control wafer gel	3.2	20
Pre lyophilised silymarin gel	2.2	19
Gamma (25 KGy) irradiated silymarin wafer gel	2.8	23
Gamma (40 KGy) irradiated silymarin wafer gel	3.6	33

Table 2. Quantification of silymarin present in gamma radiation sterilised lyophilised wafer discs by HPLC

Samples sterilised with γ rays	Weight of the wafer discs in HPLC solvent (mg/mL)	Measured concentration of silymarin (µg/mL)	Theoretical concentration of silymarin (µg/mL)
Sample 1 (0 KGy)	2.0	71.7	79.7
Sample 2 (25 KGy)	1.9	69.5	78.1
Sample 3 (40 KGy)	2.1	76.5	85.4

In the wound healing assay, ten measurements of migration distance from the intact and wounded edge were recorded for each of three monolayers. This was repeated on another occasion (n = 60). The migration of HMVECad was found to be significantly ($p < 0.001$) higher in the hypoxic conditions compared with normoxic conditions. Unlike untreated cells, silymarin wafer discs arrested the high glucose induced decrease in the migration of cells under both normoxic and hypoxic conditions.

CONCLUSIONS

The ionising gamma radiations did not adversely affect the consistency or yield stress of the gels upon reconstitution with distilled water. Silymarin wafers negated the effect of increased glucose concentration in both normoxic and hypoxic conditions on the migration of microvascular endothelial cells. The stability of silymarin within the lyophilised wafers is still to be determined although initial NMR analysis of gamma irradiated silymarin wafers suggest that no degradation occurs.

ACKNOWLEDGMENTS

REFERENCES

[1] H. Brem and M. Tomic-Canic, "Cellular and molecular basis of wound healing in diabetes" *The Journal of clinical investigation,* **117(5)** (2007)1219–1222.

[2] V. Falanga, "Wound healing and its impairment in the diabetic foot" *The Lancet*, **366(9498)** (2005) 1736–1743.

[3] K.H. Matthews, H.N.E. Stevens, A.D. Auffret, M.J. Humphrey and G.M. Eccleston, "Formulation, stability and thermal analysis of lyophilised wound healing wafers containing an insoluble MMP-3 inhibitor and a non-ionic surfactant" *International Journal of Pharmaceutic*s, **356(1–2)** (2008) 110–120.

Electrically assisted microneedle mediated transdermal drug delivery

Martin J. Garland, Hannah McMillan, A. David Woolfson, Ryan F. Donnelly.

School of Pharmacy, Queen's University Belfast, Belfast, UK.

Abstract **– This study describes, for the first time, an electrically responsive hydrogel, poly(methyl vinyl etherco-maleic anhydride) – polyethylene glycol (PMVE/MA-PEG), for microneedle (MN) mediated transdermal drug delivery. It was found that the rate of MN swelling and drug delivery was significantly enhanced in the presence of an electric current.**

INTRODUCTION

The aim of this study was to evaluate, for the first time, the combination of an electrical stimulus with *in situ* swellable poly(methyl vinyl etherco- maleic anhydride) – polyethylene glycol (PMVE/MA-PEG) microneedle (MN) arrays for transdermal drug delivery. In addition, optical coherence tomography (OCT) was used to evaluate the penetration characteristics of PMVE/MA-PEG MN arrays into neonatal porcine skin *in vitro*, following insertion using a custom designed spring-activated applicator.

MATERIALS AND METHODS

MN, comprised of 15% w/w PMVE/MA-7.5% w/w PEG 10,000, were prepared using a laser-based micromoulding

technique, to create an 11×11 MN array of 600 µm height, 300 µm width at base, and 300 µm interspacing at base. Optical coherence tomography (OCT) was used to assess the depth of MN penetration following insertion into excised neonatal porcine skin using a custom designed spring-activated applicator at a force of 4.4, 7.0, 11.0 and 16.4 N/array. The in-skin swelling of MN, with and without the application of a current (0.5 mA/cm^2), in full thickness neonatal porcine skin was determined over a 24 h period, by removing the MN from the skin at set time intervals, and measuring the increase in MN surface area using a digital microscope (GE-5 Digital Microscope, Laboratory Analysis Ltd, Devon, UK). The passive, iontophoretic (0.5 mA/cm^2, current duration 6 h), microneedle mediated, and microneedle mediated iontophoretic delivery of MB from a bioadhesive patch formulation across dermatomed neonatal porcine skin over a 24 h period was assessed using a vertical Franz cell set up, with MB analysed using UV spectroscopy.

RESULTS AND DISCUSSION

Using OCT, it was found that increasing the force used for MN application resulted in a significant increase in the depth of penetration achieved within neonatal porcine skin (Fig.1) ($p < 0.01$). MN were shown to swell effectively in full thickness neonatal porcine skin, with MN surface area increasing by approximately 150% after 24 h. Interestingly, the application of an electrical current led to a significantly greater rate of MN swelling ($p < 0.001$), with a 7-fold increase in MN surface area at 24 h in comparison to MN swollen in the absence of an electrical field. The permeation of MB across dermatomed neonatal porcine skin was found to be dependent upon the drug delivery strategy employed.

Whilst the use of iontophoresis alone led to a 2- fold increase in % of MB permeated at 24 h (22%), in comparison to the passive delivery (11%), the greatest enhancement was seen when either MN or a MN/ ITP combination strategy was
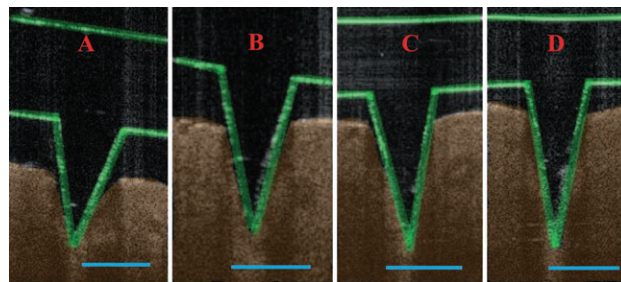

Fig. 1. 2D still images of MN following insertion into neonatal porcine skin at an application force of 4.4 N (A), 7.0 N (B), 11.0 N (C), and 16.4 N (D). (Scale bar represents 300 µm).

used. In particular, the use of hydrogel MN led to a 7-fold increase in the amount of MB released at 24 h (76 %), in comparison to passive delivery. However, the combination of MN and ITP led to a significantly accelerated rate of drug delivery ($p < 0.001$), with similar levels of MB detected at 6 h (72%) using this combination to that of 24 h with MN alone

CONCLUSIONS

Previously, the combination of ITP and MN has focused on the use of either solid MN that are used merely to puncture or sugar MN that are placed into the skin and deposit the drug during dissolution prior to ITP. In these cases the pores created in the skin could potentially close or become blocked, thus negating the length of benefit that may be obtained through the use of ITP. The use of hydrogel MN in this study could revolutionise the MN field as, in a one step process, they could create a continuously open aqueous pathway for drugs to migrate through, the rate of which could be accelerated through the application of an electrical current.

Enhanced Buccal Delivery of Fentanyl Citrate Using Buccal Patches

M.S. Salem[1], S.M. Assaf[1], R.T. Abu-Huwaij[2], A.A. Sallam[3]

[1]Faculty of Pharmacy, Jordan University of Science and Technology, Irbid, Jordan.
[2]College of Pharmacy and Medical Sciences, Al-Ahliyya Amman University, Amman, Jordan.
[3]T. Q. Pharma, Amman, Jordan.

INTRODUCTION

Fentanyl is a potent synthetic opiod analgesic used in the treatment of breakthrough pain [1]. It is susceptible to degradation by first-pass hepatic metabolism providing short duration of action (30–60 min after IV administration). This originates the need of an alternative route of delivery which can bypass the hepatic first-pass metabolism. The aim of the present study was to develop a buccal mucoadhesive patch containing fentanyl citrate, and to evaluate the effect of penetration enhancers on the in vitro permeation studies through porcine buccal mucosa.

MATERIALS AND METHODS

The following materials were used in the research project: fentanyl citrate, carbopol 971P, ethylene vinyl acetate copolymer (40 wt% vinyl acetate stabilised), propylene glycol monolaurate, poloxamer 407, oleic acid, polyethylene glycol 400,

dichloromethane (HPLC grade), glycerol, perchloric acid 60%, sodium hydroxide and ethanol absolute.

A freshly excised buccal tissue obtained from pigs weighing between 35 and 40 kg was used. Bi-layered patches were produced by casting from plasticised drug/polymer solutions in glass dishes. Moisture uptake was determined according to Arora and Mukherjee [2]. Circular patches containing different glycerol contents were used for water uptake studies. Fentanyl citrate was analysed using a validated high performance liquid chromatography (HPLC) method as described by Lambropoulos et al [3]. In vitro permeation studies were conducted using Franz diffusion cells with a diffusional area of 2.84 cm^2.
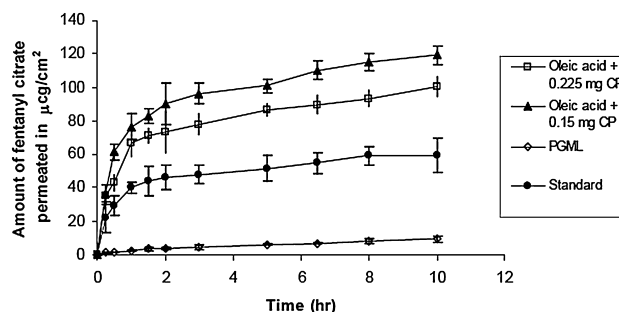

Fig. 1. Effect of penetration enhancers on in vitro permeation of fentanyl citrate from mucoadhesive patches across porcine buccal mucosa into PBS.

RESULTS AND DISCUSSION

New fentanyl citrate buccal patches comprising a drug-containing mucoadhesive layer and a drug-free backing layer were prepared. Carbopol-971P was used as the mucoadhesive polymer and ethylene vinyl acetate as the backing layer. In vitro permeation across porcine buccal mucosa was evaluated using Franz diffusion cell. Patches were designed to provide drug delivery in unidirectional fashion to the mucosa. It was demonstrated that these patches control drug permeation due to hydration and swelling of the mucoadhesive polymer. Patches showed an increase in hydration of up to 90 minutes, a plateau of equilibrium until 300 minutes, and then a level off in weight change suggesting complete hydration of patches. More prolonged diffusion was observed upon an increase in thickness of the mucoadhesive layer due to an increase in diffusion length. Oleic acid was a better penetration enhancer for fentanyl citrate than propylene glycol monolaurate. Significant increase in drug permeation occurred in presence of oleic acid as penetration enhancer whereas propylene glycol monolaurate resulted in retardation of fentanyl permeation (Fig. 1).

CONCLUSIONS

Fentanyl citrate is used as a pain killer, so rapid onset of action is required. The in vitro high initial release followed by consecutive slow release are promising results for carrying out in vivo studies. Therefore, in vitro results were fair enough to ascertain the feasibility of administering fentanyl citrate through buccal route, which is a useful alternative to the oral route, avoiding pre-systemic metabolism.

ACKNOWLEDGMENTS

REFERENCES

[1] P.A. MacIntyre, L. Margetts, D. Larsen, and L. Barker, "Oral transmucosal fentanyl citrate versus placebo for painful dressing changes: a crossover trial" *J. Wound Care*. **16** (2007) 118–121.

[2] P. Arora and B. Mukherjee, "Design, development, physicochemical and in vitro and in vivo evaluation of transdermal patches containing diclofenac diethylammonium salt", *J. Pharm. Sci*., **91** (2002) 2076–2089.

[3] J. Lambropoulos, G. Spanos and N. Lazaridis, "Development and validation of an HPLC assay for fentanyl, alfentanil, and sufentanil in swab samples", *J. Pharm. Biomed. Analysis*, **23** (2000) 421–428.

Enhanced solubility of beclometasone dipropionate using G4 PAMAM dendrimers

A.M.A. Elhissi, G. Martin, M. Najlah, Z. Zhou, A. D'Emanuele

School of Pharmacy and Biomedical Sciences, University of Central Lancashire, Preston, UK

Abstract **– G4 PAMAM dendrimers accommodating beclometasone dipropionate (BDP) were developed and characterised. The dendrimers had a biomodal size distribution and a neutral surface charge. Approximately 3% of the steroid was associated with the dendrimer structure which was calculated to be approximately 6% of the moles of the dendrimers.**

INTRODUCTION

Dendrimers are tree-like hyper-branched polymers that might act as carriers and solubilisers of poorly soluble drugs. Polyamidoamine (PAMAM) dendrimers are widely used in research as model dendrimers [1]. In this study, G4 PAMAM dendrimers accommodating the model antiasthma steroid

BDP were characterised in terms of particle size, surface charge and association efficiency of the steroid with the polymeric structure of the dendrimers.

MATERIALS AND METHODS

1) *Preparation of a steroid-dendrimer film*: A methanol solution of G4 PAMAM dendrimers was placed in a previously weighed round-bottomed flask which was then attached to a rotary evaporator. The vacuum was applied under rotation for approximately 2 h. After evaporation of methanol, the rotary evaporator was turned off and the flask reweighed to determine the weight of the dendrimers. BDP was added to constitute 10% of the dendrimer weight. The resultant mixture was dissolved in methanol followed by rotary evaporation to form a film of dendrimer-BDP.

2) *Inclusion of BDP in dendrimer structure:* Phosphate-buffered saline was added to the dendrimer film followed by stirring overnight. The resultant aqueous dispersion was centrifuged to sediment the unassociated steroid. The supernatant and the pellet were separately diluted using methanol. High performance liquid chromatography (HPLC) analysis of the steroid was performed using methanol and water (75 : 25 v/v) and a flow rate of 1.7 ml/min. Samples (20 µl) were injected through a C-18 column using an Agilent 1200 system. The association of BDP with the dendrimer was calculated as the association efficiency (AE) or association capacity (AC).

AE(%) = (amount of BDP associated / total amount of BDP) X 100%

AC(%) = (moles of BDP associated / moles of dendrimer) X 100%

3) *Size and surface charge analysis of the BDP-dendrimers:* Size and surface charge (zeta potential) analysis of the dendrimers-steroid were performed using Photon Correlation Spectroscopy and Laser Doppler

Velocimetry respectively by employing the Zeta Nano instrument (Malvern Instruments, UK).

RESULTS AND DISCUSSION

HPLC showed that a fraction of BDP was associated with the polymeric structure of the dendrimers. The AE of BDP was
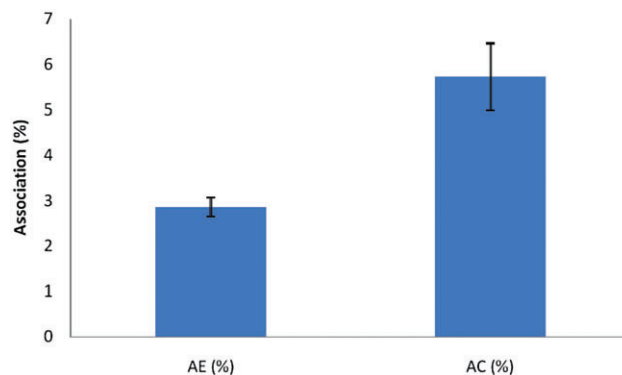

Fig.1. AE and AC of BDP in G4 PAMAM dendrimers as determined using HPLC (n = 3 ± sd)

Table 1. Size and zeta potential of dendrimers-steroid

Size (nm)		Zeta potential (mV)
First peak	Second peak	
7.53	183.40	−0.198

less than 3% (Fig.1). This figure was doubled when the association was calculated as the AC (Fig.1).

Size analysis showed that dendrimers had a bimodal size distribution. However, both peaks were in the nanometres range (Table 1). The larger peak possibly indicates that some dendrimers have aggregated. The surface charge (zeta potential) of the dendrimers was neutral (Table 1).

CONCLUSIONS

This study has shown that the model steroid BDP was successfully associated with the polymeric structure of the G4 PAMAM dendrimers. This prevented the precipitation of the steroid and hence enhanced its solubility.

REFERENCE

[1] A. D'Emanuele and D. Attwood, "Dendrimer-drug interactions" *Adv. Drug Del. Rev.* **57** (2005) 2147–2162.

Enteric Coating of a non-soluble Contrast Medium: A Road Well Travelled

J.E. Morris, A.C. Williams

School of Pharmacy, University of Reading, Reading, UK.

Abstract **– This project seeks to develop an orally administered formulation of barium sulphate, a contrast agent often used to image the bowel. Current delivery via enema is inconvenient and causes significant patient distress. Using pH responsive polymers, barium particles have been coated to permit targetting to the large bowel. Several coating methodologies were evaluated; particles produced by solvent emulsification had appropriate sizes and coating efficiencies to permit oral administration of this contrast agent.**
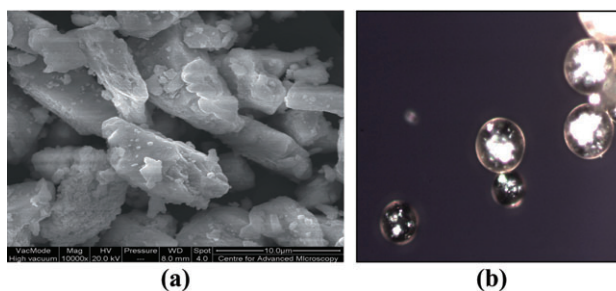
Fig. 1. SEM images of uncoated, preparatory barium sulphate (10000 mag) (a) Light microscopy image of barium sulphate encapsulated into Eudragit S microparticles by the solvent emulsion evaporation method (b).

INTRODUCTION

Imaging the large bowel for diagnostic purposes typically uses a radio-opaque contrast medium such as barium sulphate, administered by enema. The procedure – which incorporates the insufflation of the bowel by the addition of air – is often perceived by the patient as invasive, uncomfortable and embarrasing and results can sometimes be disappointing. This project seeks to develop an alternative formulation to permit oral dosing of this contrast medium based on enteric coatings.

MATERIALS AND METHODS

A pH responsive polymer, poly(methacrylic acid / methyl methacrylate) – Eudragit S (Degussa AG) was used to coat barium sulphate particles. Initialy, spray dried granules of $BaSO_4$ coated with Eudragit S were produced [1] using a Buchi 190 Spray Dryer. Various operating conditions were employed to improve yields and coating efficiencies, but typically used a mixed ethanol/water feed solution.

Additionally, $BaSO_4$ was encpasulated into Eudragit S microparticles using a solvent – emulsion – evaporation method [2]. The polymer (1 g) was dissolved in 10 ml ethanol before emulsification into liquid parafin BP (100 ml) containing 1%w/v sorbitan sesquioleate. $BaSO_4$ (0.2 g) was added. The mixture was homogenised overnight at 1200 rpm before particles were recovered by filtration and rinsed three times in 50 ml n-hexane.

Particles were analysed for size, size distribution and shape by light microscopy, SEM and dynamic light absorption technique.

RESULTS AND DISCUSSION

Spray drying generated fine, uniform sized free flowing particles with good characteristics for oral delivery. The $BaSO_4$ powder size, initially around 30 microns in diameter grew only marginally to approximately 40 microns after spray
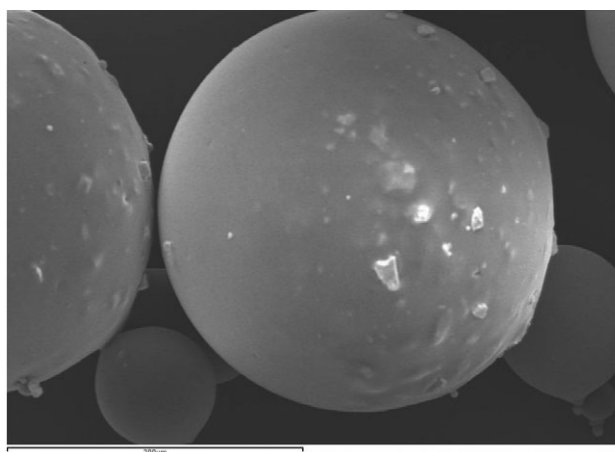
Fig. 2. SEM image of barium sulphate encapsulated into Eudragit S microparticles by the solvent emulsion evaporation method.

drying, suggesting a thin film of the polymer coat has been successfully applied. However, light microscopy images indicated that the particles had not been well coated, and indeed the process appeared to have caused significant attrition of some of the starting materials.

In contrast, images obtained for the solvent emulsification technique showed clearly that the $BaSO_4$ particles were indeed encapsulated in a polymer shell, and that these particles retained a size that is suitable for oral delivery, typically in the order of 33 microns diameter (Figures 1 & 2) with, on average 75% below 41.6 μm, 50% below 27.3 μm and 25% below 21% μm.

CONCLUSIONS

Coating barium sulphate with pH responsive polymers is not trivial and the results showed that spray drying was not suit-

able due to attrition during the manufacturing process and the variability in coating efficiency. Solvent emulsification methods on the other hand, generated particles with good characteristics in terms of powder flow and of a size suitable for delivery via the oral route. The encapsulation of the barium was clearly evident in the microscopic images and coating efficiency from the solvent method was superior to that by spray drying.

REFERENCES

[1] Shin Etsu, Japanese Pharmaceutical Excipients, Japan
[2] Nilkumhang S., Basit A.W. 'The robustness and flexibility of an emulsion solvent evaporation method to prepare pH-responsive microparticles' *Int. J. Pharm.* (2009), doi:10.10.16/j.ijpharm. 2009.03.024

Formulation and Evaluation of Colon Targetted Tablets Containing Simvastatin Solid Dispersion

B.S. Ahmed, H.K. Ibrahim*, A.A. Abd-Alrahman

Department of Pharmaceutics and Industrial Pharmacy, Faculty of Pharmacy, Cairo University, Cairo, Egypt.

Abstract **– This work aimed to deliver simvastatin to the colon in a presolubilised form in a trial to improve its poor bioavailability. Simvastatin colon targetting is promising due to the lower levels of cytochrome enzymes in the colon than in the small intestine. Solubilsation is necessary to ensure fast, reproducible and complete drug dissolution and absorption on reaching the colon.**

INTRODUCTION

Simvastatin is a well established oral antihypercholesterolemic agent, with a problem of low bioavailability due to its water-insolubility and intestinal metabolism by CYP3 enzyme [1]. A recent work proved the benefits of simvastatin colon targetting in improving its oral bioavailability [2]. Moreover, formulating simvastatin as delayed release formulations could gain an additional therapeutic advantage by coinciding with the circadian rhythm of cholesterol synthesis. However, dissolution could be problematic for the absorption of the insoluble simvastatin from the distal intestine.

MATERIALS AND METHODS

Solid dispersions of simvastatin with mannitol, Ineutic®, Poloxamer® F-68, polyethylene glycol 4000 and polyvinyl pyrrolidone K-30 were prepared at different drug to carrier ratios applying solvent evaporation technique. The prepared solid dispersions were evaluated using FT-IR, DSC and in vitro dissolution studies. The formula of choice was compressed into tablets applying different concentrations of Croscarmellose Na as a superdisintegrant. Tablets were evaluated for their disintegration and dissolution in pH 7.4. Colon targetting was achieved by coating with Eudragit S 100 as a pH-responsive polymer [3]. The effect of the coating level (2.5–15%) and plasticiser type (dibutylphthalate and triethylcitrate) on drug dissolution behaviour, in a sequence of dissolution media simulating the gastrointestinal physiological pH variation, were investigated.
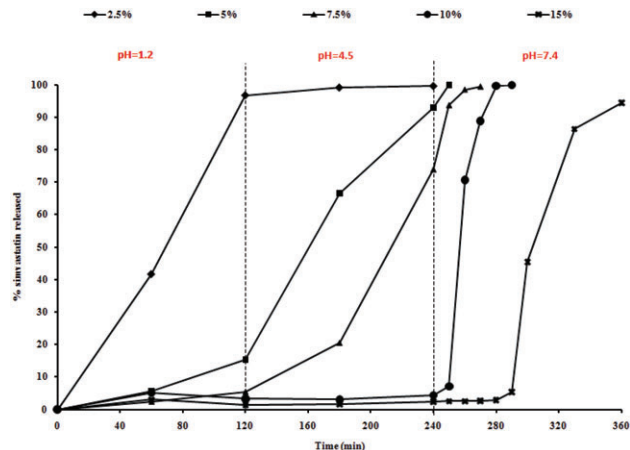
Fig. 1. Effect of coat level on simvastatin release profile from Eudragit S100 coated tablets.

RESULTS AND DISCUSSION

The 1:5 simvastatin/Poloxamer solid dispersion recorded the highest improvement in drug dissolution efficiency (12.2 fold). On tabletting, 5% Croscarmellose Na produced tablets with fast disintegration (90 sec.) and 100% drug release in 40 min. The release results from the coated tablets, indicated that the coating level is the critical factor in determining the duration of the lag-phase. The best results were given by the 10% (20:2:1 W/W) Eudragit S100/ triethylcitrate/ Talc) coat. This tablet formula achieved an adequate lag time for the intended colonic targeting (240 min), followed by an immediate release phase, $t_{50\%}$ = 245 min.

CONCLUSIONS

The optimised simvastatin tablets could be promising for reducing the drug dose and improving its bioavailability based on the protection from the intestinal metabolism.

Additional studies are needed to assess its performance in vivo.

REFERENCES

[1] J.B. Robinson, "Simvastatin: present and future perspectives" *Expert Opin Pharmacother.*, **8** (2007) 2159–2172.

[2] M.T. Grozdanis, J.M. Hilfinger, G.L. Amidon, J.S. Kim, P. Kijek, P. Staubach and P. Langguth, "Pharmacokinetics of the CYP 3A Substrate Simvastatin following Administration of Delayed Versus Immediate Release Oral Dosage Forms" J. *Pharm. Res*, **25** (2007) 1591–1600.

[3] Z.Z. Piao, M.K. Lee and B.J. Lee, "Colonic release and reduced intestinal tissue damage of coated tablets containing naproxen inclusion complex," *Int. J. Pharm.*, **350** (2008) 205–211.

Formulation and *In vitro* evaluation of Amphotericin-B nanoparticle for ocular delivery

Swarnali Das*[1], Preeti Suresh[2],

[1]School of Pharmacy and Technology Management, NMIMS University, Mumbai, India
[2]Institute of Pharmacy, Pt. Ravi Shankar Shukla University, Raipur, Chattisgarh, India

Abstract **– The general aim of this work was to develop a formulation that would be better tolerated in the eye with Amphotericin B, without using an irritating surfactant. Therefore, a nanoparticle of Amphotericin B eye drop formulation was developed by using 2 different polymers. It was evaluated for particle size,** *in vitro* **drug release, % yield, zeta potential etc. A promising result was obtained for all the parameters. Since patients with ocular infections require several months of treatment, the stability of the nanoparticle had to be considered. For this reason, stability studies was carried out for 6 months at room temperature and at 2–6° C. Results were supporting to earlier data of fresh formulations. Furthermore, drug content remained constant, indicating that no leakage or release occurred in the final concentrated suspension. These results show the feasibility of an ophthalmic preparation based on nanoparticle amphotericin B.**

Figure 1: TEM image of nanoparticle formulation

INTRODUCTION

Local fungal infections with *Candida*, *Fusarium*, *Curvularia* and *Aspergillus* can lead to serious ulceration of the cornea and must be treated rapidly. The current treatment consists of 0.15% (w/v) amphotericin B eye drops prepared from Fungizone®, containing deoxycholate, an irritant for the cornea, which reduces patient compliance. Eye drops based on liposomal amphotericin B (AmBisome®) would be a convenient alternative; but a drawback is instability [1]. As we know nanoparticles have many advantages including good ocular retention property, increased bioavailability, reduction in dose and others, so nanoparticle suspension of this drug was considered.

MATERIALS AND METHODS

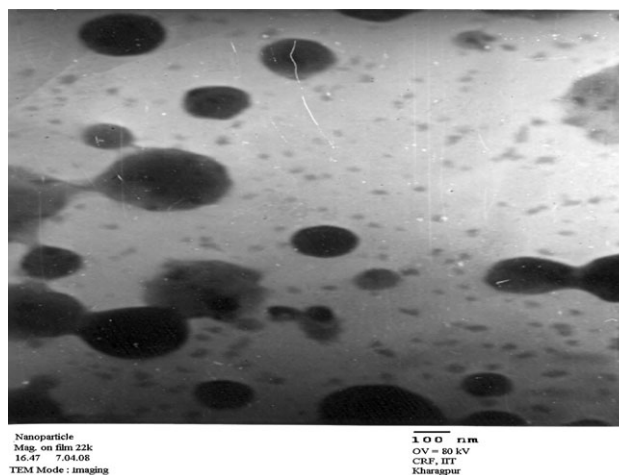Amphotericin-B (AmB) was kindly supplied as a gift sample by Asence Pharma Pvt. Ltd., India. Eudragit® RS100 and Eudragit® RL100 were gifted by FDC Ltd., India. Acetone, Polyvinyl alcohol (PVA), dimethyl sulfoxide (DMSO) and methanol were purchased from S. D. Fine Chemical Limited, India and were used as received.

The AmB-loaded NPs was prepared by solvent displacement process [2]. Two different polymers were used – Eudragit RS 100 and RL 100. 18 different formulations were prepared with the 2 variables including

Drug and Polymer weight ratio and solvent and non-solvent volume ratio.

RESULTS AND DISCUSSION

The *in vitro* drug release data was best explained by Higuchi's equation and almost 60 % drug was released in 24 hrs. Drug release rate was more for RL formulation than RS. The drug entrapment efficiency varied from 60 to 80 %. Good polydispersity index values were also obtained for most preparations (0.2–0.8).

The systems obtained with Eudragit® RL, which contains a higher amount of quaternary ammonium groups, had more positive zeta potential (24–38 mV) with respect to Eudragit® RS nanoparticles (20–28 mV). Six months of stability studies indicated that no marked differences were observed in the nanoparticles for all the *in vitro* parameters. Average size increased a little with respect to the initial values (130–300 nm), probably because of particle aggregation. This type of phenomenon has been also reported earlier (Pignatello *et al*., 2002b).

CONCLUSIONS

An optimised Eudragit retard polymer containing different amounts of AmB was successfully prepared using nanoprecipitation method. Good ocular retention property was found due to unique particle size and positive zeta potential. Good stability was also noted after 6 months at various conditions. All the results imply that nanoparticles can be used for ocular delivery of AmB.

REFERENCES

1. R.L. Juliano, C. Grant, K.R. Barber, M. Kalp, "Mechanism of the selective toxicity of amphoterictn B incorporated into liposomes" *Mo.l Pharmacol.,* 31(1987) 1–11.
2. H. Fessi, F. Puisieux, J.P. Devissaguet, N. Ammoury, S. Benita, "Nanocapsule formation by interfacial polymer deposition following solvent displacement" *Int. J. Pharm.,* 55(1989) R1-R4.
3. R. Pignatello, C. Bucolo, P. Ferrara, A. Maltese, A. Puleo, G. Puglisi, "Eudragit RS100® nanosuspensions for the ophthalmic controlled delivery of ibuprofen" *Eur. J. Pharm. Sci.,* 16 (2002) 53–61.

Formulation optimisation for the topical delivery of active agents in traditional medicines

P. Thitilertdecha[1,2], P. Akkarasereenont[1], T. Laohapand[1], M.G. Rowan[2], R.H. Guy[2]

[1]Centre of Applied Thai Traditional Medicine, Faculty of Medicine Siriraj Hospital, Mahidol University, Bangkok, Thailand
[2]Department of Pharmacy and Pharmacology, University of Bath, Bath, UK

Abstract **– The objective of this study is to determine bioavailability of naturally active substances in optimised topical dosage forms of *Acanthus ebracteatus* Vahl and *Clerodendrum petasite* S. Moore. Vanillic acid, chrysin and verbascoside were found in ethanolic extracts of both plants and were quantified by high performance liquid chromatography (HPLC) coupled with ultraviolet (UV) and/or mass spectrometric (MS) detection.**

INTRODUCTION

A. ebracteatus Vahl and *C. petasites* S. Moore have been widely used for at least 25 years in Thai traditional medicine for the treatment of skin problems, such as rashes and abscesses. Only the plants themselves and powders there from are available on the market with poor reliability in quality, safety and efficacy. Few chemical studies have been made of these plants and, not surprisingly, there have been no clinical trials concerning the topical delivery of these medicines.

MATERIALS AND METHODS

Ethanolic extracts of the plants were examined by HPLC, using photodiode array (PDA) UV and MS detection. Skin penetration of active components of these extracts are to be evaluated by *in vitro* diffusion cell experiments using excised pig skin. The bioavailability of these compounds will then be determined *in vivo* in human volunteers using tape-stripping methodology.

The HPLC-PDA and HPLC-UV-MS conditions optimised in this study were based on four natural phenolic compounds (caffeic acid, vanillic acid, chrysin and verbascoside) with known antioxidant activity. The assay employed a Dionex Acclaim®120 column (C_{18}, 5 μm, 150 × 4.6 mm i.d.), gradient elution using a mobile phase containing acetonitrile and 0.1% aqueous acetic acid at a flow rate of 0.5 ml min⁻¹, and detection by MS or PDA. *In vitro* percutaneous permeation tests of the plant extracts formulated as saturated solutions (50 mg ml⁻¹) in 50% aqueous ethanol were performed over 24 hours.

RESULTS AND DISCUSSION

Maximum wavelengths of the phenolic standards were selected by HPLC-PDA to apply to HPLC-UV-MS as follows: 260 nm for vanillic acid and chrysin, and 330 nm for caffeic acid and verbascoside. With respect to robustness of the optimised HPLC method, the intra-day and inter-day relative standard deviations (RSD) of the standards were less than 1.5% and their correlation coefficients (r^2) were >0.95 over six concentrations of standards ranging from 0.2 to 20 μg ml⁻¹. Vanillic acid, chrysin and verbascoside were detected in ethanolic extracts of both species. Then, saturated solutions of the plant extracts were tested in *in vitro* diffusion cell experiments using porcine skin. It was found that vanillic acid penetrated through the skin at a rate consistent with its predicted maximum flux of ~12 μg.cm⁻².h⁻¹ [1]. However, skin absorption of chrysin and verbascoside was limited by their

low levels in the plant extracts and by their less favourable physiochemical properties compared to vanillic acid (including molecular weight, log P, and solubility in oil and in water).

CONCLUSIONS

Qualitative analysis showed that vanillic acid, chrysin and verbascoside were present in both plants. Of these, only vanillic acid penetrated through the skin. Vanillic acid and chrysin have not previously been identified in either of the plants considered, while verbascoside has been reported in *A. ebracteatus* Vahl. Although these three phenolic compounds have been widely used in the cosmetic and pharmaceutical fields, their topical bioavailability has not yet been quantified.

REFERENCES

[1] Potts RO, Guy RH. Predicting skin permeability. *Pharm Res* (1992) 9: 663–669.

Freeze-dried thiolated chitosan formulations for protein delivery via the buccal mucosa

I. Ayensu, J.C. Mitchell, J.S. Boateng

School of Science, University of Greenwich at Medway, Chatham Maritime, ME4 4TB, UK

INTRODUCTION

The buccal mucosa has received increased attention in recent years for the delivery of proteins/peptides as an alternative to the currently used parenteral route [1]. Although limited by molecular size, hydrophobicity and low permeability of membranes, thiolated chitosan derivatives have however been identified to deliver proteins/peptides across the buccal mucosa because of their mucoadhesive, penetration enhancing and peptidase inhibition properties [2]. This project aims to develop freeze-dried thiolated chitosan formulations for protein delivery via the buccal mucosa and to determine the effectiveness of cryoprotection and annealing on the stability of the protein drug.

MATERIALS AND METHOD

Chitosan-4-thiobutylamidine (C-TBA) was synthesised, purified and thiol content determined [3]. Matrix formulations with C-TBA incorporating glutathione as enzyme inhibitor, glycerol as plasticiser, mannitol as cryoprotectant and bovine serum albumin (BSA) as a model protein drug [Table 1] were freeze-dried using a Virtis Advantage Freeze Dryer. A novel lyophilisation cycle incorporating an annealing process was developed based on preliminary thermal characterisation by DSC. The process involved freeze treatment from room temperature to −55°C (2 hours), annealing to −35°C (2 hours) and finally freezing back to −55°C (2 hours). The effect of the annealing process and cryoprotectant on the stability of the freeze dried protein formulation was evaluated using SEM, XRD and Raman spectroscopy.

Table 1 Matrix formulations

	Form. A (mg/mL)	Form. B (mg/mL)	Form. C (mg/mL)
C-TBA	10.0	10.0	10.0
Glutathione	0.5	0.5	0.5
Glycerol	1.0	1.0	1.0
Mannitol	1.0	–	1.0
BSA	5.0	5.0	–

RESULTS AND DISCUSSION

The thermal events observed during the DSC characterisation of the formulation components were used to select the annealing temperature. The annealing process during the freezing stage prevented premature crystallisation of mannitol and led to growth of both solute crystals and ice crystals which resulted in faster water vapour transport and shorter primary drying time of 12 hours. In addition to acting as plasticiser, glycerol allowed the formulation to swell instead of instant disintegration when it came in contact with dissolution medium. A high magnification SEM (Fig. 1) showed a micrograph of a flexible and non brittle freeze-dried wafer with wool-like spongy network which was morphologically stable.

XRD analysis of the annealed freeze dried C-TBA formulation confirmed the stability of the amorphous model protein drug (BSA) formulated with the cryoprotectant mannitol.

The Raman spectroscopic data showed no significant changes in the nature of the model drug. Further research is underway to determine the release profile and storage stability of the novel freeze-dried protein formulations.
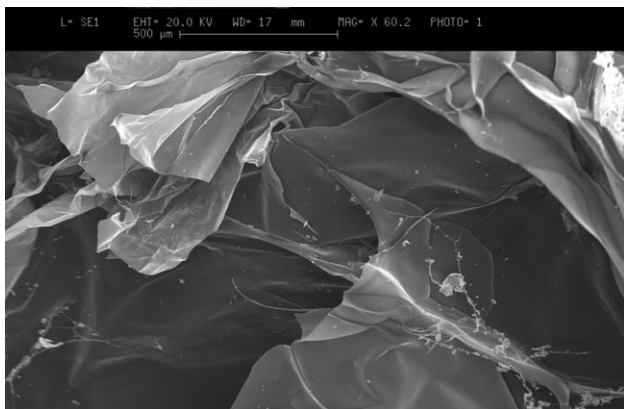
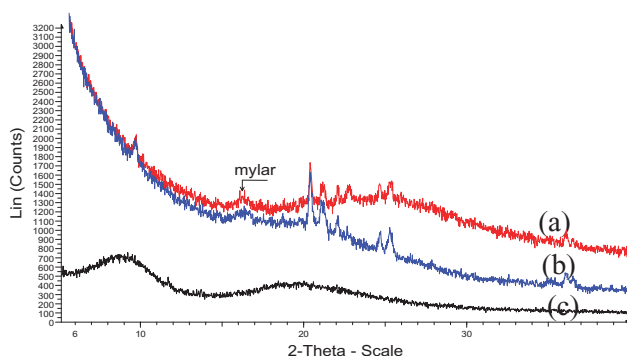**Fig. 1.** SEM image of C-TBA freeze-dried formulation

Fig. 2. XRD of BSA loaded freeze-dried formulation: (a) C-TBA-BSA (b) C-TBA and (c) BSA

CONCLUSION

A stable thiolated chitosan based system for potential protein delivery via buccal mucosa has been developed. Annealing and cryoprotection helped stabilise the freeze-dried chitosan-4-thiobutylamidine protein formulation.

ACKNOWLEDGEMENT

REFERENCES

[1] Y. Sudhakar, K. Kuotsu, A.K. Bandyopadhyay. ''Buccal bioadhesive drug delivery – A promising option for orally less efficient drugs''. *J. Control. Rel.* **114**, (2006) 15–402.

[2] A. Bernkop-Schnurch, D. Guggi, and Y. Pinter. Thiolated chitosans: development and in vitro evaluation of a mucoadhesive, permeation enhancing oral drug delivery system. *J. Control. Rel* **94** (2004) 177–186. [3] N. Langoth. *et al.* Thiolated chitosans: design and *in vivo* evaluation of a mucoadhesive buccal peptide drug delivery system. *Pharm. Res* **23**, [2006] 573–579.

Freeze-dried Tablets for Mucosal Administration of Vaccine/Microbicide; Comparison of Drug Release with Gel Formulations

U. Anekwe, G. Andrews, K. Malcolm, V.L. Kett

School of Pharmacy, Queen's University Belfast, Belfast, UK

INTRODUCTION

Mucosal administration of HIV microbicides and vaccines is of great interest. Generally gels are used, but these have drawbacks such as difficulty with administration and poor retention. We have developed freeze-dried tablets (FDTs) that reconstitute in vivo to form mucoadhesive gels and offer improved ease of administration and retention. In this research we have compared drug release from FDTs, obtained by freeze-drying mucoadhesive gel formulations, with their gel counterparts. The four gels tested are based on hydroxyethylcellulose (HEC) and polyvinylpyrrolidone (PVP) plus another mucoadhesive polymer and either bovine serum albumin (BSA) or the HIV microbicide dapivirine (dap).

MATERIALS AND METHODS

The four formulations contained 4% PVP, 3% HEC plus 3% of either polycarbophil (Noveon AA1, N), Chitosan (Ch), sodium carboxymethycellulose (NC) or poly(methyl vinyl ether/maleic anhydride) (Gantrez, G) and drug loading of 1% . FDTs were manufactured by dispensing the corresponding gel into tablet blister packs and freeze-drying over 24 hours using an Advantage Freeze-dryer (VirTis NY, USA) and required no further processing. Mucoadhesion testing and texture profile analysis (TPA) were performed on the gels and reconstituted FDTs using a Stable Micro Systems texture analyser (Model TA-XT2). For TPA a 10 mm probe was compressed twice into each formulation at 2 mms^{-1} to a

15 mm depth. For mucoadhesion testing a mucin disc (1) was brought into contact with the gel and then held in contact with a force of 0.1 N for 30 s before removal at 1 mm/s. Drug release rates from FDTs and gel counterparts were determined (100 ml release medium, 37°C, 60 rpm n = 4) under sink conditions to compare their drug release profiles, and evaluate the effect of the mucoadhesive components and drug type on drug release. Drug release data (first 60% release) were fitted to the semi-empirical Korsmeyer equation (2) to obtain plots that could be used to determine the mechanism of drug release. Values of k, the kinetic constant and n, which is indicative of the release mechanism, were determined from regression analysis of the plots.

RESULTS AND DISCUSSION

Drug release profiles for the dap formulations showed faster release for N-dap, Ch-dap and NC-dap compared with their freeze-dried counterparts up to 8 hrs (Figure 1). While for the BSA systems G-bsa and Ch-bsa showed the fastest release profile up to 8 hrs indicating that both freeze-drying and drug type have an effect on release profile. The n values obtained (Table 1) indicate that for the dap systems a Super Case II transport mechanism occurs while for the BSA systems the release mechanism is "anomalous transport" i.e. non-Fickian kinetics corresponding to coupled diffusion/polymer relaxation.

Freeze-drying reduced the mechanical properties of NaCMC and chitosan formulations and increased their mucoadhesive strengths but increased both the mechanical and mucoadhesive properties of gantrez formulations. While the drug release data was acceptable for the chitosan formulations TPA showed that they might not be suitable for delivery of BSA, since they exhibited the lowest mechanical properties. For example, the hardness of both Ch-bsa-FD and Ch-bsa gels were significantly lower than Ch-dap-FD (P < 0.05 & P < 0.01 respectively).

CONCLUSIONS

Our studies confirmed that FDTs could be used to formulate proteins and microbicides for controlled release. Furthermore, the nature of the drug: polymer interaction had affected both the drug release profile and the physical properties of the tablets.
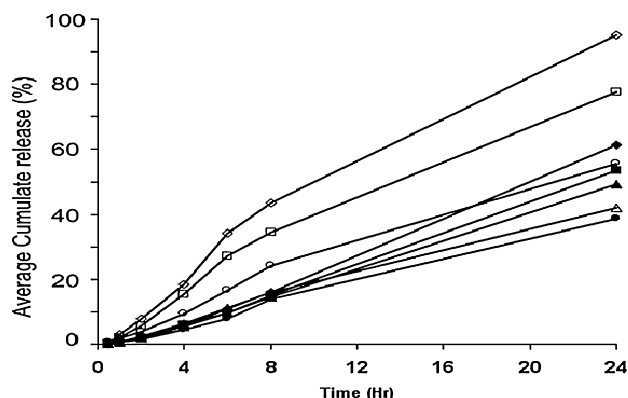

Figure 1. Release profiles of dapivirine from the FDT and gel systems ◆N-dap-FD, ■Ch-dap-FD, ▲NC-dap-FD, ●G-dap-FD, ◇N-dap, □Ch-dap, △NC-dap, ○G-dap,

Table 1. Analysis of dapivirine / BSA release mechanism from the FDT and gel systems.

FDT	n	R^2	Gel	n	R^2
N-dap-FD	1.32	0.9934	N-dap	1.57	0.8861
Ch-dap-FD	1.34	0.9960	Ch-dap	1.58	0.8917
NC-dap-FD	1.35	0.9919	NC-dap	1.49	0.9652
G-dap-FD	1.31	0.9863	G-dap	1.16	0.9905
N-bsa-FD	0.69	0.9955	N-bsa	0.54	0.9401
Ch-bsa-FD	0.75	0.9735	Ch-bsa	1.04	0.9676
NC-bsa-FD	0.93	0.9870	NC-bsa	0.83	0.9734
G-bsa-FD	0.81	0.9816	G-bsa	0.91	0.9933

ACKNOWLEDGMENTS

REFERENCES

1. D. Jones, A.D. Woolfson, A.F. Brown, M. J. O'Neill, 1997 "Mucoadhesive, syringeable drug delivery systems for controlled application to the periodontal pocket: release kinetics, syringeability, mechanical and mucoadhesive properties". J. Cont. Rel., 49, 71–79.
2. R. Korsmeyer, R. Gurny, E. Doelker, P. Buri, N. Peppas, 1983. Mechanisms of solute release from porous hydrophilic polymers. Int. J. Pharm. 15, 25–35.

Heterocyclic N^4, N^9-Diacyl Spermines: Nanoparticle Lipopolyamine Vectors for Efficient pDNA and siRNA Delivery

Hassan M. Ghonaim[1,2], Mostafa K. Soltan[1,3], and Ian S. Blagbrough[1]

[1]Department of Pharmacy and Pharmacology, University of Bath, Bath, BA2 7AY, UK
[2]Faculty of Pharmacy, Suez Canal University, Ismalia, Egypt
[3]Faculty of Pharmacy, Zagazig University, Zagazig, Egypt

Abstract – **We are designing and developing lipid-polyamines based upon changes in a series of four N^4,N^9-diacyl spermines (myristoyl, palmitoyl, stearoyl, and oleoyl) each end-capped with the weakly basic nitrogen-containing heterocycles imidazole, pyridine, and quinoline for the efficient delivery of genes for gene therapy [1], and also for the delivery of siRNA to knock-down gene expression [2, 3].**

INTRODUCTION

Our goals are to design and develop novel non-liposomal gene and siRNA delivery systems [1–3]. Heterocyclic N^4,N^9-diacyl spermines bring about controlled self-assembly into a scaffold and also facilitate absorptive endocytosis and/or fusion with cell membranes through the two lipid regions. They spontaneously neutralise and condense DNA and siRNA, leading to efficient nanoparticle formation.

MATERIALS AND METHODS

• Measurement of particle size

Particle size of the lipoplexes was measured by laser light scattering using a NANOSIGHT LM10.

• Transfection experiments

We used a human primary skin fibroblast cell line (FEK4) and a human cervix carcinoma, HeLa derived and transformed cell line (HtTA). The complex was incubated with the cells. Levels of fluorescence were detected by gated FACS. The transfection efficiency was calculated based on the percentage of positive cells (green fluorescence, Fig. 1) in the total number of cells.

• Cytotoxicity (MTT) assay

Lipoplexes were added in the same way as in the above transfection protocol using the MTT assay. The % viability related to control is calculated by: $100 \times$ test absorbance/control absorbance.

• Confocal microscopy visualisation

Used with one labelling solution containing cell membrane labelling (red) and nuclei labelling (blue).

RESULTS AND DISCUSSION

The heterocyclic substituted lipospermines show higher transfection and delivery efficiencies over simple lipospermines giving
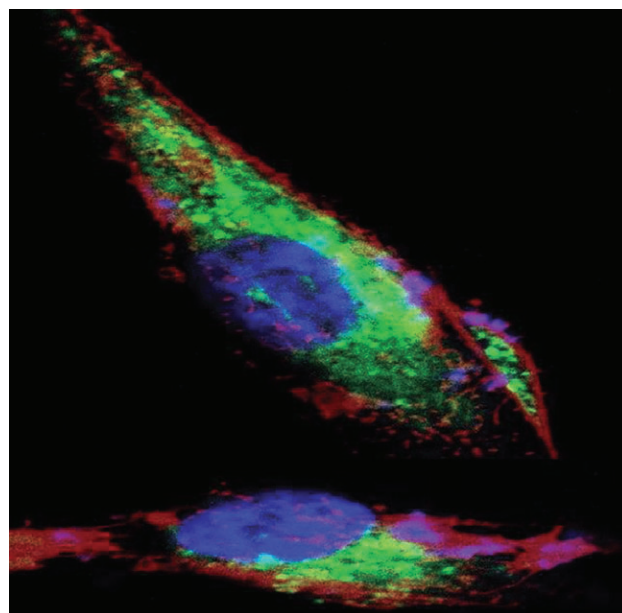

Fig. 1. Confocal microscope image showing green fluorescent protein inside FEK4 cells transfected with pEGFP delivered with di-4-imidazolylmethyl-N^4,N^9-dioleoyl spermine.

the same biological results at 50% lower concentrations. Their higher delivery potential is due to the increase in the pK_a of the vector, adding the basic nitrogen atoms in the two terminal heterocycles that can be protonated as the endosome acidifies.

CONCLUSIONS

We have demonstrated that di-4-imidazolylmethyl N^4,N^9-dioleoyl spermine, a synthetic cationic lipid, is an efficient pDNA and siRNA delivery vector, incorporating nitrogen-containing heterocycles into the cationic lipid. This novel vector is non-toxic at the required low concentration for controlled self-assembly. This new non-viral, non-liposomal delivery vector facilitates absorptive endocytosis and/or fusion with cell membranes through its lipid moiety whilst having a higher basic nitrogen atom capacity in order to assist endosome escape.

ACKNOWLEDGMENTS

REFERENCES

[1] H.M. Ghonaim, O.A.A. Ahmed, C. Pourzand, and I.S. Blagbrough, "Varying the chain length in N^4,N^9-diacyl spermines: non-viral lipopolyamine vectors for efficient plasmid DNA formulation" *Mol. Pharm.* **5** (2008) 1111–1121.

[2] M.K. Soltan et al., "Design and synthesis of N^4,N^9-disubstituted spermines for non-viral siRNA delivery – structure-activity relationship studies of siFection efficiency versus toxicity". *Pharm. Res.* **26** (2009) 286–295.

[3] H.M. Ghonaim, S. Li, and I.S. Blagbrough. N^1,N^{12}-Diacyl spermines: SAR studies on non-viral lipopolyamine vectors for plasmid DNA and siRNA formulation. *Pharm. Res.* **27** (2010) 17–29.

Investigation of Empty Bilosomes for Oral Vaccine Delivery using Design of Experiments

Jitinder Wilkhu[1], Sarah E McNeil[1], David Anderson[2], Yvonne Perrie[1]

[1]School of Life and Health Sciences, Aston University, Aston Triangle, Birmingham, UK,
[2]Variation Biotechnologies INC, 1740 Woodroffe Avenue, Ottawa, Ontario

Abstract **– Bilosomes are vesicles which are prepared from non-ionic surfactants with the incorporation of bile salts to aid their stability through the gastro-intestinal tract (GIT). The aims are to investigate the different lipid ratios and how they influence bilosome characteristics.**

INTRODUCTION

Oral vaccines offer significant benefits over traditional vaccines due to their ease of administration, improved patient compliance and potentially enhanced mucosal immune responses. Bilosomes have been investigated as vaccine delivery systems where inclusion of bile salts within the bilosome construct has been shown to have a stabilising role after oral administration, by preventing degradation in the GIT, and subsequently can act as carriers for oral vaccines [1].

MATERIALS AND METHODS

The software Modelling and Design of experiments (MODDE, Umetrics) was used for the generation and evaluation of the statistical experimental design. A range of bilosome formulations were prepared by high shear homogenisation using different blends of monopalmitoyl-glycerol, cholesterol, Dicetyl-phosphate (DCP) and bile salts. The lipids were heated to 120 °C for 10 minutes in an oil bath and an emulsion was created by the addition of 25 mM sodium bicarbonate buffer pH 7.6 and homogenised for 2 minutes. While homogenising 100 mM bile salt was added and homogenised for a further 8 minutes, upon cooling, the bilosome formulation was incubated for 2 hours with gentle shaking at 220 rpm.

The responses measured include vesicle size analysis using a sympatec helos particle sizer, pH and zeta potential measured in double distilled water at 25 °C on a Zeta Plus Brookhaven Instrument.
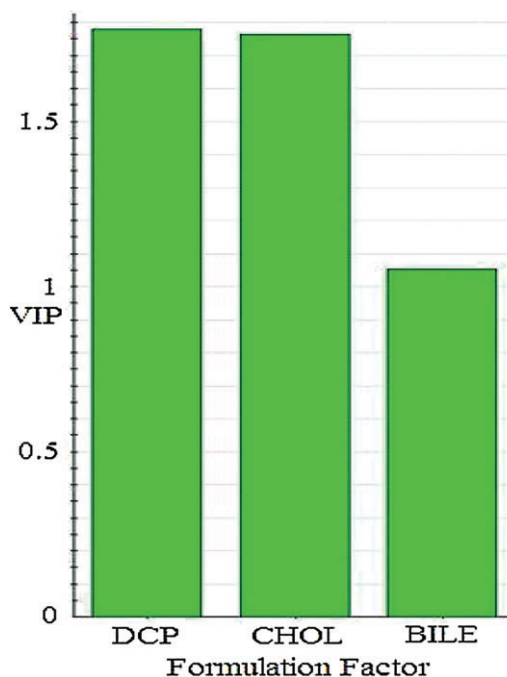

Fig. 1. Variable importance plot (VIP) showing the effects of the formulation factors upon pH, size and zeta potential. A value of 1 shows average importance and a value greater than 1 shows significant importance.

RESULTS AND DISCUSSION

Data obtained from the experiments was entered back into the MODDE software allowing graphs to be generated and to optimise the specific responses in relation to the characteristics of bilosomes.

Results from the experiment show that the DCP and cholesterol ratios employed to prepare the bilosomes are the

major factors which determine the pH and zeta potential. Increased DCP use results in a lowering of the pH.

The VIP plot (Fig .1) for the factors are correlated in response to the suspension pH, vesicle size and vesicle zeta potential of the bilosomes. The plot confirms the findings from the experiment for the specific responses where, the DCP content is of the highest importance.

CONCLUSIONS

The DCP lipid has shown to be the controlling factor in the manufacture of bilosomes as it has a significant impact on the pH which reflects the zeta potential. To achieve optimised bilosomes in terms of vesicle size for oral vaccine delivery, the bilosome formulation should comprise of monopalmitoylglycerol, cholesterol and DCP in a ratio of 5:4:1 together with incorporation of bile salts.

REFERENCE

[1] Daniel A Norris., Navneet Puri, Patrick J. Sinko (**1998**). "The effect of physical barriers and properties on the oral absorption of particulates." Advanced Drug Delivery Reviews 98: 135–154.

Investigation of protease activated drug release from hydrogels conjugated with a V8 protease-sensitive fluorogenic substrate

W. Chen, B. Walker, C.P. McCoy, D.S. Jones, S.P. Gorman, B.F. Gilmore

School of Pharmacy, Queen's University Belfast, UK.

INTRODUCTION

Biofilm formation is a problem common to all indwelling medical devices [1]. Formation of the biofilm gives rise to increased tolerance and phenotypic resistance to antimicrobial agents making such infections difficult to eradicate. Strategies aimed at overcoming this problem include the development of antimicrobial drug-loaded biomaterials [2]. However, these strategies suffer a number of drawbacks including 'burst release' of antimicrobial agents followed by prolonged, sub-therapeutic release of drug, potentially selecting for a more resistant phenotype. Ideally, release of antimicrobial agents should be coordinated with the presence of infecting organisms. Therefore, we have developed novel hydrogel coatings whereby antimicrobial release is triggered by bacterial proteases, such as *S. aureus* V8 protease, expressed during colonisation and biofilm formation. The aims of this study is to investigate the ability of V8 protease to diffuse into hydrogel networks and effect release of a 'cargo' molecule from hydrogels bearing protease-labile linkers, using a novel fluorimetric assay.

METHODOLOGY

Fluorogenic substrate, Ac-LLD-AMC and substrate monomer, Acryloyl-(PEG)$_2$-LLD-AMC were synthesised based on Fmoc-Asp(Wang resin)-AMC, using Fmoc-solid phase synthesis protocols. HATU and DIPEA were used as coupling reagents.

The sensitivity of Ac-LLD-AMC against V8 protease from *S. aureus* (Sigma-Aldrich) was determined using a microtitre-based fluorimetric assay. Hydrolysis of Ac-LLD-AMC by V8 protease (2 U/mL) was carried out in PBS (pH7.4) at 37 °C and the release of AMC (λex 380 nm, λem 460 nm) was measured in a FLUOstar OPTIMA plate reader.

V8 protease-sensitive fluorogenic hydrogels, p(100HEMA-*co*-0.5Acryloyl-(PEG)$_2$-LLD-AMC) and p(60HEMA-*co*-40MAA-*co*-0.5Acryloyl-(PEG)$_2$-LLD-AMC) were prepared by free radical polymerisation. Briefly, a mixture of HEMA, MAA and substrate monomer were polymerised at 90 °C in glass moulds, using benzoyl peroxide initiator, and ethylene glycol dimethacrylate as cross-linking reagent.

The glass transition temperature (T_g) of the hydrogels was examined using modulated temperature differential scanning calorimeter (MTDSC).

Hydrogels (3 mm disc) were incubated with or without 2 U/mL V8 protease in 0.3 ml PBS at 37 °C and 100 rpm. At each time point, the sample solutions (100 μL) were transferred to a black 96-well microtiter plate and the release of the cleaved AMC from the hydrogels determined by fluorescence intensity (λex 380 nm, λem 460 nm), the sample solutions (100 μL) were returned for the duration of the experiment. The V8 protease was refreshed every 98.5 h.

RESULTS

Fluorescence assay of Ac-LLD-AMC in the presence of V8 protease demonstrated that this substrate exhibited cleavage by V8 protease with a K_m of 1085 μM and a V_{max} of 0.56×10^{-6} M/s, which demonstrated that Ac-LLD-AMC is a suitable V8 protease-sensitive substrate for ongoing studies. Thermal analysis indicated that the hydrogels were properly copolymerised (single T_g). Diffusion studies revealed that V8 protease diffused deeper into p(60HEMA-*co*-40MAA-*co*-0.5Acryloyl-(PEG)$_2$-LLD-AMC) than p(100HEMA-*co*-0.5Acryloyl-(PEG)$_2$-LLD-AMC) and caused a maximum of
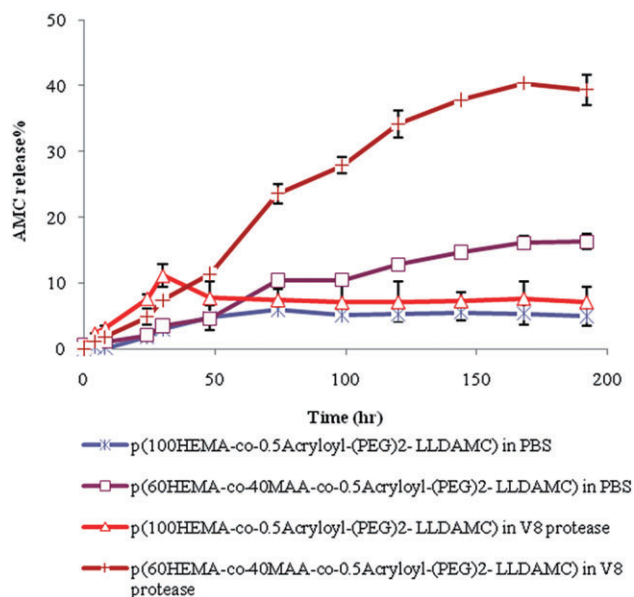
Fig.1. Release of the cleaved AMC from the hydrogels conjugated with Acryloyl-(PEG)$_2$-LLDAMC in the presence/absence of 2 U/mL V8 protease in PBS pH7.4 at 37 °C

approximately 25% and 8% AMC release, respectively, from these two different compositions (Fig. 1).

CONCLUSIONS

We have developed V8 protease-sensitive hydrogels by covalently incorporating a V8 protease-sensitive substrate monomer (Acryloyl-(PEG)$_2$-LLD-AMC) to investigate the V8 protease diffusion behaviour within the HEMA/MAA based hydrogel network. Ongoing work will examine the ability of a number of bacterial proteases, including V8 protease, to release therapeutically useful concentrations of antimicrobial at the hydrogel surface in a protease-stimulated manner to prevent initial bacterial adherence and early biofilm formation events.

REFERENCES

[1] R. McCrory, D.S. Jones, C.G. Adair and S.P. Gorman, "Pharmaceutical strategies to prevent ventilator-associated pneumonia" *J. Pharm. Pharmacol.*, **55** (2003) 411–428.

[2] M.E. Rupp, T. Fitzgerald, V. Helget, S. Puumala, J.R. Anderson and P.D.Fey, "Effect of silver-coated urinary catheters: Efficacy, cost-effectiveness and antimicrobial resistance" *Am. J. Infect. Control.*, **32** (2004) 445–450.

Investigation of skin permeation using ATR-FTIR spectroscopic imaging and multivariate target factor analysis

K.T. Mader[1], J. Tetteh[1], W.J. McAuley[2], M.E. Lane[2], J. Hadgraft[2], J.M. Andanson[3], S.G. Kazarian[3]

[1]Medway Sciences, University of Greenwich, Medway, UK
[2]School of Pharmacy, University of London, London, UK
[3]Department of Chemical Engineering, Imperial College, London, London, UK

Abstract **– ATR-FTIR spectroscopic imaging permeation experiments of a model formulation across stratum corneum (SC) were conducted to acquire further understanding of the mechanism of drug permeation. Quantitative iterative target transformation factor analysis (QITTFA) was used for the analysis of the complex and highly overlapping spectroscopic data generated.**

of ambiguity of the MCR results due to richer information in the data set and the possibility of qualitatively and quantitatively compare experiments [5]. In this work ATR-FTIR imaging together with quantitative iterative target transformation factor analysis (QITTFA) is used to acquire further understanding of the mechanism of drug and solvent permeation.

INTRODUCTION

The use of multivariate data analysis can enhance the range of application of ATR-FTIR to study membrane permeation of a wide range of molecules [1]. It also allows the simultaneous measurement of solvent and solute permeation in complex systems [2]. In particular, Multivariate curve resolution (MCR) methods have been proven valuable in analysing spectroscopic imaging data [3, 4]. Furthermore, iterative MCR techniques can be used to analyse augmented data sets. The major benefits of such merged matrices are the reduction

MATERIALS AND METHODS

Stratum corneum (SC) samples were provided by the School of Pharmacy, University of London. The SC samples were originally obtained from human abdominal skin from the Human Tissue Bank (UK). Ethical approval was given for the project by Trent MREC, reference number 06/MRE04/37. The diffusion imaging data sets were provided by the Imperial College London. A detailed description of the experimental methodology and equipment used for this experiment is given in reference [6]. A saturated solution of around 10% benzyl

nicotinate (BN) in 10% polyethylene glycol 400 (PEG 400), 10% ethanol and 70% (mass) water was prepared. IR spectra were collected using a focal plane array (FPA) detector with 64×64 pixels in a wavenumber range of 875–4000 cm^{-1} with a spectral resolution of 4 cm^{-1} and 64 co-additions. Thirty one ATR-FTIR images (total image size of this system was 550×600 μm^2) were collected subsequently to monitor the permeation of the model formulation over a period of about 24 hours. QITTFA was used to extract distribution maps of major formulation components as well as SC lipid and proteins. Additionally, the permeation of the formulation components was investigated at three locations (L1, L2, L3) covering regions which show high, low and medium relative concentrations of BN. The data matrices for each location were augmented and analysed simultaneously.

RESULTS AND DISCUSSION

Figure 1A shows distribution maps of SC protein and lipids as well as ethanol and BN of the image measured after 1370 minutes. Evolution profiles of BN extracted from location L1, L2 and L3 are shown in Figure 1B.

CONCLUSIONS

The results demonstrate the power of QITTFA to monitor both spatial and time domain profiles of several formulation and SC components. This opens up the possibility of obtaining detailed local mechanistic insight into diffusion processes on a molecular level, with the potential to link spatial compositional differences of the sample to the extracted evolution profiles.

ACKNOWLEDGMENTS

Figure 1: **A. Distribution maps of predicted relative concentrations of SC protein, SC lipids, ethanol and BN at each pixel of the FPA detector (blue = low relative concentration; red = high relative concentration). B. Evolution profiles of BN at the three different locations L1, L2, L3.**

REFERENCES

[1] McAuley, W.J., Lad, M.D., Mader, K.T., Santos, P., Tetteh, J., Kazarian, S.G., Hadgraft, J., Lane, M.E., *Eur. J. Pharm. Biopharm.*, 2010. 74(2): 413–419.

[2] Russeau, W., Mitchell, J., Tetteh, J., Lane, M.E., Hadgraft, J., *Int. J. Pharm.*, 2009. 374(1–2): 17–25.

[3] Tetteh, J., Mader, K.T., Andanson, J.-M., McAuley, W.J., Lane, M.E., Hadgraft, J., Kazarian, S.G., Mitchell, J., *Anal. Chim. Acta*, 2009. 642(1–2): 246–*256*.

[4] de Juan, A., Maeder, A. M., Hancewicz, T., Tauler, R., *Trends in Analytical Chemistry*, 2004. 23(1):70–79.

[5] Gemperline, P.J., Zhu, M., Cash, E., Walker, D.S., *ISA Transactions*, 1999. 38: 211–216.

[6] Andanson, J.-M., Hadgraft, J., Kazarian, S.G., *Biomed. Opt.*, 2009. 14(3): 034011–8.

In-*vitro* aerodynamic particle size distribution of the Symbicort® Turbuhaler® at different inhalation flows using an anderson cascade impactor

Almeziny, M[1]. and Clark, B.[1]

School of Pharmacy, University of Bradford, Bradford, UK.

INTRODUCTION

Symbicort® Turbuhaler® is an inhaled drug. It is a combination of budesonide and formoterol. Budesonide is a glucocorticoid. It is provided as a mixture of two epimers, 22R and 22S. The budesonide epimer R is known to be 2 to 3 times more potent than the budesonide epimer S. In addition, formoterol is a long-acting selective beta-2 adrenoceptor agonist. The influence of flow rate on drug delivery by dry powder inhalers (DPIs) has been established. Also, the flow rate of each component may be di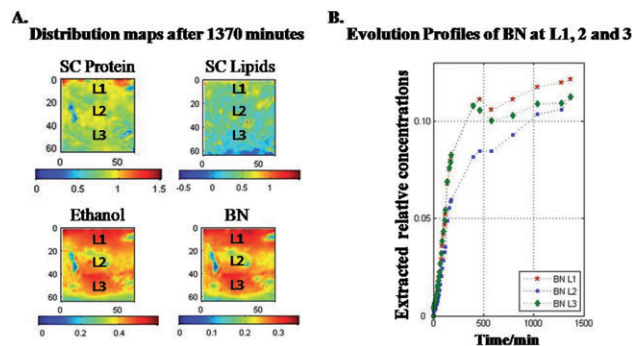fferent and therefore the pharma-cological ratio may vary in delivery to the patient. As a result, it is essential to keep the combination ratio constant.

The aim of the study was to examine the effect of the flow rate on this combination.

MATERIALS AND METHODS

Methods and instrumentation: The aerodynamic characteristics of the emitted dose were measured by an Anderson cascade impactor (ACI).

Equipment and Inhalation device: A GAST 1023 Pump, 0–100 L/min (GAST, Brook Hampton, Doncaster, UK); Electronic digital flow meter Model DFM (Copley Scientific Ltd. Nottingham UK); Andersen MKII cascade impactor (Copley Scientific Ltd.); Critical Flow Controller Model TPK. (Copley Scientific Ltd.); and Copley Inhaler Testing Data Analysis Software (CITDAS) (Copley Scientific Ltd).

High-performance liquid chromatography (HPLC) analysis: The amount of drug deposited in each stage was measured using the HPLC method of analysis

Fine particle analysis: All the aerodynamic calculation was conducted using the Copley software (CITDAS version 2).

Statistical analysis: The one-way ANOVA with the Bonferroni effect test was used to compare the aerodynamic particle size characterisation of the different flow rate using SPSS V15.0 (SPSS Inc., Chicago, USA).

RESULTS AND DISCUSSION

There were statistically significant differences for formoterol, budesonide R and budesonide S between 28.3 L/min and 60 L/min in Total Emitted Dose (TED). The comparison of aerodynamic particles size characterisation results from the Symbicort® Turbuhaler® device showed that the Fine Particle Dose (FPD) increases as the flow rate is increased, this difference was statistically significant $p < 0.001$. Also, there was a statistical difference between flow rate 28.3 L/min and 60 L/min in the Mass Median Aerodynamic Diameter (MMAD) where it decreases with increasing the flow rate. On the other hand, the effect of flow rate on Fine Particle Fraction (FPF) was statistically significant, $p < 0.001$, and the high flow rate increases the FPF Table (1). The combination ratio was constant at all flow rates in term of FPD, MMAD and throat deposition for formoterol, budesonide R, and budesonide S. Furthermore, the STDEV of fine particles distribution reduced as the flow rate was increased which indicates an improvement in dosage form uniformity. Besides that, as the flow increased, there was a decrease in the amount of formoterol, budesonide R, and budesonide S deposited in the throat induction (port and the pre-separator).

Table (1). A comparison of percentages for formoterol, budesonide R and budesonide S deposited on each stage of ACI at two different flow rates from Symbicort® Turbuhaler® device divided by number of dose

L/ mint	Formoterol		Budesonide R		Budesonide S	
	28.3	**60**	**28.3**	**60**	**28.3**	**60**
	AVG	AVG	AVG	AVG	AVG	AVG
Induction port [%]	33.48	34.33	33.54	34.92	36.77	32.06
Pre-separator [%]	44.63	6.88	45.9	6.92	52.23	7.55
TED [%]	88.58	103.5	78.42	101.33	76.37	98.71
FPF [%]	19.16	52.48	20.77	50.15	36.79	55.34
MMAD [mm]	3.62	2.3	3.48	2.35	3.46	2.31
GSD	1.43	1.93	1.44	1.83	1.55	1.86

CONCLUSIONS

Device design should minimise patient factors such as flow rate effects, this will ensure that the patient receives a safe and efficacious dose.

Furthermore, the flow-dependent particle deposition results emphasise the need for the Pharmacopoeias to use a variety of inhalation flow rates for in-vitro tests rather than one that is determined according to the resistance of the dry powder inhaler.

REFERENCES

ALMEZINY, M. and CLARK, B. (2007) High performance liquid chromatography assay method for simultaneous quantitation of formoterol and the two epimers of budesonide. Journal of Pharmacy And Pharmacology, 59, 74.

TARSIN, W., ASSI, K. H. and CHRYSTYN, H. (2004) In-Vitro Intra- and Inter-Inhaler Flow Rate-Dependent Dosage Emission from a Combination of Budesonide and Eformoterol in a Dry Powder Inhaler. Journal of Aerosol Medicine, 17 (1), 25–32.

ZANEN, P., VAN SPIEGEL, P. I., VAN DER KOLK, H., TUSHUIZEN, E. and ENTHOVEN, R. (1992) The effect of the inhalation flow on the performance of a dry powder inhalation system. International Journal of Pharmaceutics, 81 (2–3), 199–203.

In-Vitro Evaluation of Carboxymethylcellulose-based Inhalable Microparticles

M. Mishra and B. Mishra

Department of Pharmaceutics, Institute of Technology, Banaras Hindu University, Varanasi -221005.

INTRODUCTION

Sodium carboxymethylcellulose (SC) has been widely utilised in drug delivery systems via oral [1] and nasal mucosa [2]. However, they have not been studied extensively as a carrier for pulmonary route of administration. Thus, the aim of the present work was to evaluate the suitability of SC based microparticles for inhalation delivery of Levofloxacin hyaclate (LX). LX is a broad-spectrum antibiotic used in the treatment of both acute and chronic respiratory tract infections.

Preparation of spray dried microparticles: Aqueous ethanolic solution (30%v/v) containing LX and sodium car-

boxymethylcellulose [ratio1:1(batch LX1SC1), 1:2 (batch LX1SC2) and 1:3 (batch LX1SC3)], leucine (30 %w/w) and lactose or mannitol (batch mLX1SC2) was spray dried (Advanced spray drier, Labultima, LU-227, India). The operating parameters were set as follows: inlet temperature 120 °C, outlet temperature 45 °C, aspirator 40 % and feed rate of 1 rpm.

Characterisation of Microparticles: The fabricated microparticles were evaluated in terms of particle morphology (Scanning Electron Microscopy, QUANTA 200 FEI), aerosolisation behaviour (eight stage, nonviable Andersen cascade impactor with a preseparator, USA) and thermal characteristics (Differential Scanning calorimetry, DSC-60, Japan). For in vitro cytotoxicity studies, H1299 mammalian alveolar cells were seeded (5000 cells/well) into 96- well plate and incubated overnight at 37°C and 5% CO_2 atmosphere. The cells were treated with sterile, aqueous microparticles suspension (0.01–1.0 mg/ml) and sodium lauryl sulphate (1% as positive control). After 24 h of incubation, cell viability was determined using MTT (3-(4,5-dimethyl-thiazol-2-yl)-2,5-diphenyltetrazolium bromide) assay [3]. *In vitro* drug release from the microparticles (equivalent to 10 mg LX) was studied by dialysis (membrane thickness 0.025 mm) against phosphate buffer saline pH 7.4. Aliquot samples were analysed by spectrophotometry (JASCO 7800, Tokyo, Japan) at 291.6 nm.

RESULTS

The prepared microparticles were spherical in shape (Fig. 1). The fine particle fractions (<5 µm) generated for LX1SC1, LX1SC2, LX1SC3 and mLX1SC2 were 27.5, 33.8, 31.2, and 43.5 % respectively. The DSC scan of batch LX1SC2 showed two broad diffuse endothermic peaks around 30°C and 110°C indicative of water loss and a sharp endothermic peak at 234°C indicative of a melt of LX. No cell cytotoxic effects were observed in the tested concentrations (Fig. 2). The incorporation of SC into microparticulate systems inhibited drug release rate 6–10 times than that obtained from pure drug solution in the first hour.

CONCLUSION

This study supports the approach of using spray dried SC based microparticles for safe inhalation delivery. Increasing the proportion of SC did not affect the aerosolisation properties but resulted in a more prolonged drug release profile in vitro.
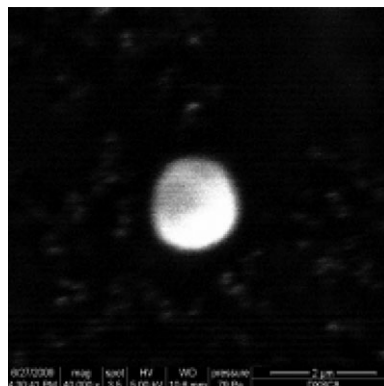

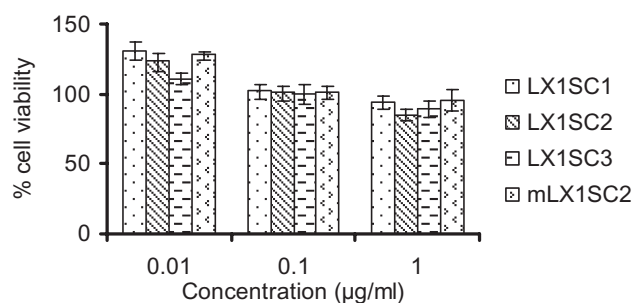**Fig 1:** SEM photomicrograph of SC based spray dried microparticle.

Fig. 2: Cell viability of SC based spray dried microparticles after 24 h (n = 3)

ACKNOWLEDGEMENTS

REFERENCES

[1] J. Ali, R. Khar, A. Ahuja, and R. Kalra, "Buccoadhesive erodible disk for treatment of oro-dental infections: design and characterisation" *Int. J. Pharm.*, **238** (2002) 93–103.

[2] B. Mishra, C. Sankar and M. Mishra, "Polymer based Solutions of Bupranolol Hydrochloride for Intranasal Systemic Delivery" *J. Drug Target.* in press.

[3] A. Grenha, C. I. Grainger, L.A. Dailey, B. Seijo, G.P. Martin, "Chitosan nanoparticles are compatible with respiratory epithelial cells in vitro" *Eur. J. Pharm. Sci.*, **31** (2007) 73–84.

Ionised Salbutamol Transport in the Presence of Counterions

A. Patel[1,2], C.P. Page[1], M.B. Brown[3,4], S.A. Jones[2]

[1]The Sackler Institute of Pulmonary Pharmacology, Pharmaceutical Science Division, King's College London,
150 Stamford Street, London, SE1 9NH, UK
[2]Pharmaceutical Science Division, King's College London, 150 Stamford Street, London, SE1 9NH, UK
[3]MedPharm Ltd, 50 Occam Road, Surrey Research Park, Guildford, Surrey, GU2 7YN, UK
[4]School of Pharmacy, University of Hertfordshire, College Lane, Hatfield, Herts, AL10 9AB, UK

INTRODUCTION

Inhaled drug delivery can be facilitated by presenting the active agent as a pharmaceutical salt. For example, salbutamol is commonly administered as a sulphate salt in order to prevent crystal agglomeration and thus enhance its aerosolisation efficiency [1]. However, the affinity of the drug and the counterion once in solution is often unknown. If an active and its co-formulated counterion are both ionised they may form an ion pair in solution which could influence transport into the tissue of the lung [2]. The aim of this work was to assess how salbutamol transport across a model membrane was influenced by the presence of a counterion.

MATERIALS AND METHODS

Transport experiments were carried out in individually calibrated upright Franz cells (MedPharm Ltd, UK) with an average receiver volume of 9.79 cm^3 and an average surface area of 2.11 cm^2. The effect of counterions on the transport of salbutamol (Cipla Ltd, India) was investigated by measuring flux across regenerated cellulose dialysis tubing, 12–14 k molecular weight cut-off (Medicell International, London, U.K). Samples were taken from the Franz cells every fifteen minutes for a 2 hour period and sample content was determined using high pressure liquid chromatography (HPLC). Salbutamol transport studies were carried out in the presence of a hydrophilic salt, sulphate and a hydrophobic salt, 1-hydroxy-2-napthoic acid (1H2NA).

RESULTS AND DISCUSSION

Using the HPLC assay (LOD = 1.25 µg/ml and LOQ = 4.15 µg/ml, between 1.0 and 100 µg/ml with a CV < 2%) the transport rate of salbutamol across RCM was 0.89 ± 0.13 µg/cm^2/min. A 2 fold enhancement in salbutamol transport (1.90 ± 0.15 µg/cm^2/min) was observed in the presence of sulphate. Salbutamol in the presence of 1H2NA showed no significant increase (P > 0.05, one way ANOVA) in transport (Figure 1).
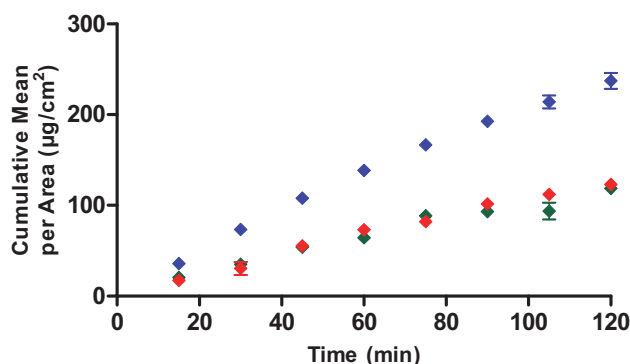

Fig. 1. Cumulative mass of salbutamol permeated per unit area of the regenerated cellulose membrane for base (green), salbutamol in the presence of sulphate (blue) and salbutamol in the presence of 1H2NA (red) (n = 5). Each bar represents the mean ± standard deviation.

CONCLUSIONS

Salbutamol transport across regenerated cellulose membrane was increased by changing the associated counterion in solution. The lipophilicity of the counterion appeared to influence the transport of salbutamol.

ACKNOWLEDGMENTS

REFERENCES

[1] T.-Z. Tzou, R.R. Pachuta, R.B. Coy and R.K. Schultz, "Drug form selection in albuterol-containing metered-dose inhaler formulations and its impact on chemical and physical stability" *J. Pharm. Sci.*, **86** (1997) 1352–1357.

[2] V. Sarveiya, J.F. Templeton and H.A.E. Benson, "Ion-pairs of ibuprofen: increased membrane diffusion" *J.Pharm.Pharmacol.*, **56** (2004) 717–724.

Liposomes: a tool for extended release of drugs in preclinical development

Maria Marlow, Jonathan Wollacott, Janet Fisk, Amanda Berry and Anne Cooper

[1]AstraZeneca R&D Charnwood, Bakewell Road, Loughborough, UK.

Abstract **– This paper describes a simple method of preparation for a liposome formulation, that can be applied to drugs in the discovery phase of development and then when dosed gives extended release in the lung in a preclinical rat model. The simple manufacturing methodology allows for manipulation of small quantities of water soluble drugs as exemplified by sodium cromoglycate.**

INTRODUCTION

Liposomes have been used extensively for the controlled release of drugs in particular giving extended release in the lung [1]. This paper describes a simple method of preparation for a liposome formulation, that can be applied to drugs in the discovery phase of development and then when dosed gives extended release in the lung in a preclinical rat model.

MATERIALS AND METHODS

The liposomes were prepared by dissolving dipalmitolyphosphatidyl choline (DPPC) in ethanol then injecting the lipid/ethanol solution into buffer containing the drug. The drug and liposomes with encapsulated drug were separated using gel size exclusion chromatography. The liposomes were then extruded to give a size of approximately 200 nm.

A liposome formulation and a control formulation with exactly the same drug loading (0.3 mg/ml) were dosed by the intratracheal (i.t.) route at 1 ml/kg to male Sprague Dawley rats under recovery anaesthesia. At various time points after dosing the animals were terminated and the lungs excised and analysed for drug by LC-MS.

RESULTS AND DISCUSSION

Drug loadings were in the order of 0.2 to 0.5 mg with a lipid content of 10 mg DPPC ml for both salbutamol and sodium cromoglycate liposome formulations which allowed appropriate dosing in the preclinical rat model. A liposome formulation of these water soluble drugs was easily achieved by this methodology but it proved more difficult to achieve appropriate drug loadings of more lipophilic drugs.

The results for sodium cromoglycate dosed at 0.3 mg/kg in a liposome formulation and as a control solution in saline
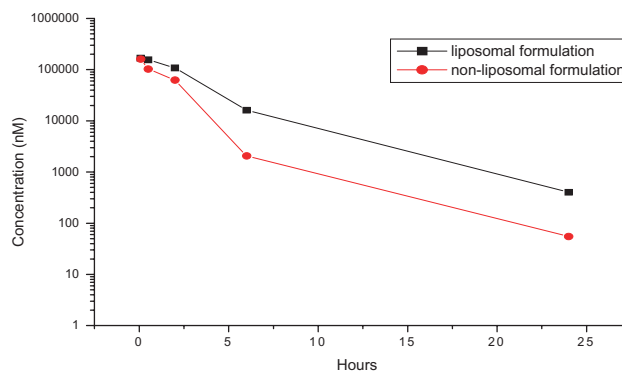

Fig. 1. Comparison of sodium cromoglycate dosed i.t. to rats at 0.3 mg/kg in a liposome formulation and in solution (n = 2)

are shown in Figure 1. The liposome formulation retained the drug in the lung for longer than the control formulation. The area under the lung concentration/time curve (AUC) for the liposome formulation over the 24 hour period post dosing was approximately twice that of the control solution. The results are in agreement with a similar formulation dosed to human volunteers [2], where drug was detected in the plasma 24 hours post nebulisation.

CONCLUSIONS

The results described herein demonstrate that it is possible to use liposomes as a tool in the preclinical drug development to retain drugs within the lung. The simple manufacturing methodology allows manipulation of small quantities of drug at this stage of development

REFERENCES

[1] I.W. Kellaway and S.J. Farr, "Liposomes as drug delivery systems to the lung", *Advanced Drug Delivery Reviews,* 5 (1990) 149–161 149.

[2] K.M.G. Taylor, G. Taylor, I.W. Kellaway and J. Stevens, (1989) The influence of liposomal encapsulation on sodium cromoglycate pharmacokinetics in man. *Pharm. Res.* **6** (1989) 633–636.

Membrane investigations using biophysical methods and multivariate target factor analysis

S.J. Chavda, M.E. Lane, J. Hadgraft

Department of Pharmaceutics, The School of Pharmacy, University of London.

Abstract – **One of the major challenges in (trans)dermal research is to improve the amount of drug delivered to and through the skin. One approach to increase the flux of active agent in the skin is the use of chemical penetration enhancers (CPEs). The study investigates the effect of CPEs using ATR-FTIR spectroscopy. The technique is successfully calibrated and correlated with the more traditional Franz diffusion cells using multivariate target factor analysis.**

INTRODUCTION

Attenuated Total Reflectance Fourier Transform Infrared (ATR-FTIR) spectroscopy and Franz diffusion cell studies are established techniques to study the effects of CPEs and may be used to estimate drug diffusion and partition parameters in permeation studies. The aims of this research are:

1) To examine the structural features of a series of CPEs (isostearyl isostearate (ISIS), isopropyl isostearate (IPIS), isopropyl myristate (IPM), hexanol, octanol and decanol) with different physicochemical properties and understand their influence on the permeation characteristics of the model compounds, methylparaben (MP) and butylparaben (BP) through silicone membrane.
2) To attempt absolute quantitative calibration of the ATR-FTIR system in order to calculate absolute partition coefficients and subsequently the permeability coefficients, k_p (KD/h).
3) To compare the permeability coefficients obtained by Franz diffusion cells with those obtained by ATR-FTIR, with the use of chemometrics to deconvolute the complex spectral data from ATR-FTIR.

MATERIALS AND METHODS

Both ATR-FTIR and Franz diffusion cell experiments were performed using saturated drug solutions under infinite dose conditions at ambient temperature (21˚C + 2˚C). The silicone membranes were presoaked in each solvent for 24 hours. Sink conditions were maintained throughout the experiment. The receptor solution used was PBS. The amount of parabens permeated was quantified using HPLC. Solvent uptake was determined gravimetrically.

ATR-FTIR spectroscopic diffusion experiments were performed using a Nicolet Avatar 360 spectrometer fitted with an ATR accessory ZeSe crystal. Data analyses were performed using OPUS (version 5.5) and Scientist® (version 3.0) software. The spectral data from ATR-FTIR was deconvoluted using chemometrics, multivariate target factor analysis, Insight® software (DiKnow Ltd, UK).
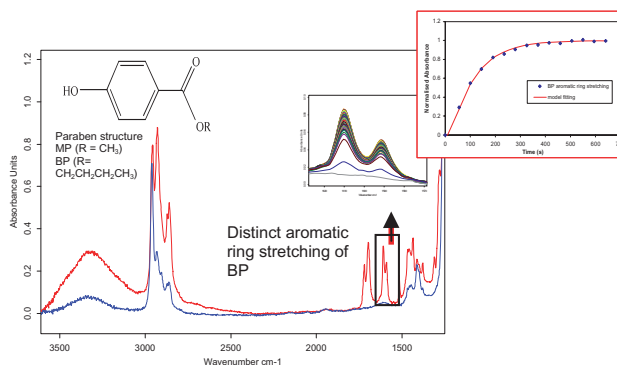

Figure 1. Diagrammatic overview of mathematical modelling using Scientist® of a permeation profile obtained using ATR-FTIR spectroscopy.
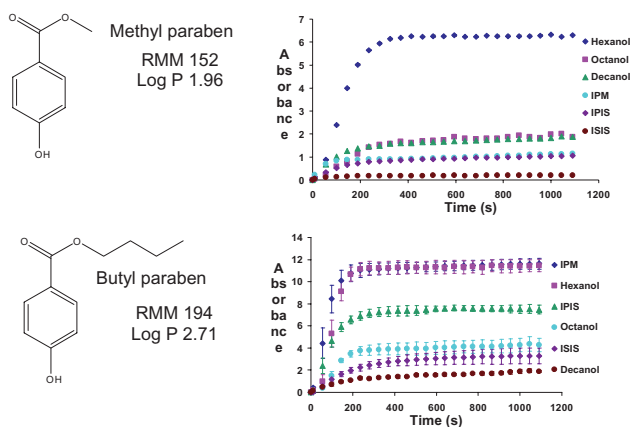

Figure 2. Diffusion profiles of parabens in different solvents.

RESULTS AND DISCUSSION

Vehicles which were highly sorbed by the membrane altered its properties, increasing the diffusion coefficient of the permeant.

Significant differences in the plateau absorbance values of parabens in the different vehicles were observed. These values are related to the concentration of parabens in the membrane and were thus strongly influenced by the solubility of the permeant in the vehicle and the uptake of vehicle into the membrane. An absolute quantification of the ATR-FTIR system was obtained. A correlation between permeability coefficients, k_p measured using Franz diffusion cell and ATR-FTIR spectroscopy after chemometrics, were obtained.

CONCLUSIONS

The absolute calibration of the ATR-FTIR enabled direct quantification and correlation of permeation data from the two techniques. Future work will aim to further probe the influence of structure activity relationships on the permeation of molecules through human skin. Knowledge attained from these initial experimental designs will be applied in the development of future formulations to optimise drug delivery through the skin.

ACKNOWLEDGMENTS

METROLOGY OF THE STRATUM CORNEUM

D. Mohammed[1], J. Hadgraft[1], M.E. Lane[1], P.J. Matts[1,2]

[1]The School of Pharmacy, University of London, UK.
[2]Procter and Gamble, Egham, UK.

INTRODUCTION

The purpose of this study was to investigate, assess and compare corneocyte maturity and size, protease activity and protein content and TEWL as a function of stratum corneum depth of the mid ventral forearm in subjects varying in gender and race.

MATERIALS AND METHODS

Twenty-two healthy volunteers aged 20–58 were recruited with informed consent (13 males, 9 females [12 Caucasian and 10 Black subjects]). A circle of 2.2 cm diameter was delineated within the centre of mid ventral left forearm. Standard D-Squame[(R)] tape was applied using a constant pressure of 225 g cm^{-2} (D-Squame pressure instrument) for 5 seconds. Twenty consecutive tape strippings were performed. TEWL measurement was conducted before and after each tape strip. Protein content from each tape was measured using SquameScan 850A [1].

To examine maturity and size [2], corneocytes were extracted from tape 1, 8 and 15 using 1 ml of buffer consisting of 2% sodium dodecyl sulphate, 20 mM DL-dithiothreitol, 5 mM EDTA in 0.1 M Tris-hydrochloride buffer (pH 8.0) and heated for 10 minutes. After centrifugation, corneocytes were double-stained using Nile Red and anti-human involucrin. The fluorescence was monitored with a fluorescence microscope equipped with a Fuji S2 pro camera. ImageJ image analysis software was used to differentiate Nile Red and involucrin-stained corneocytes and to determine corneocyte size.

To examine protease activity [3], corneocytes were extracted using a buffer composed of 0.1 M Tris-HCl and 0.5% Triton X-100 at pH 8.0. Fluorogenic peptide substrates, either KLK5 or KLK7 or Tryptase, were added. The reaction was stopped with 1% v/v acetic acid. HPLC with a fluorescent detector was used to quantify protease activity. To improve the HPLC signal and peak shape, tape strip numbers 2–4, 5–7, 9–11, 12–14 and 16–18 were combined.

RESULTS AND DISCUSSION

Corneocyte maturity and size, stratum corneum protease activity and protein content reduced significantly (ANOVA, one way, $p < 0.001$) with depth. In contrast, TEWL measurement increased significantly (ANOVA, one way, $p < 0.001$) with depth. Mature hydrophobic corneocytes with rigid envelopes were larger and isolated from the outermost layer of stratum corneum. Higher protease activity and protein content were also observed on the outer surface of stratum corneum. The activity of trypsin-like enzyme such as KLK5 was higher at all depths compared with chymotrypsin-like enzyme such as KLK7. There was no statistically significant effect of race or gender.

CONCLUSIONS

Corneocyte maturity, size and protease activity can be used to probe the stratum corneum at a molecular level.
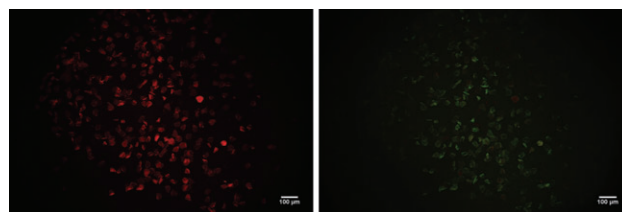
ACKNOWLEDGMENTS

Fig. 1. Comparison between Nile Red and immuno-stained corneocyte images obtained from 1st tape strip of the mid left forearm of White origin female.

REFERENCES

[1] Voegeli, R., J. Heiland, S. Doppler, A.V. Rawlings, and T. Schreier, *Efficient and simple quantification of stratum corneum proteins on tape strippings by infrared densitometry.* Skin Res Technol, 2007. 13(3): p. 242–251.

[2] Hirao, T., M. Denda, and M. Takahashi, *Identification of immature cornified envelopes in the barrier-impaired epidermis by characteri-* sation of their hydrophobicity and antigenicities of the components. Exp Dermatol, 2001. 10(1): p. 35–44.

[3] Voegeli, R., A.V. Rawlings, S. Doppler, J. Heiland, and T. Schreier, *Profiling of serine protease activities in human stratum corneum and detection of a stratum corneum tryptase-like enzyme.* Int J Cosmet Sci, 2007. 29(3): p. 191–200.

Modelling of drug permeation in human skin *in vitro* from finite dose applications

R. Vieira[1], M.E. Lane[1], J. Hadgraft[1], Y. Anissimov[2], A.C. Watkinson[3]

[1]Department of Pharmaceutics, The School of Pharmacy, University of London, London, UK
[2]Griffith University, Queensland, Australia
[3]Acrux Ltd, West Melbourne, Victoria, Australia

Abstract – **A diffusion model for percutaneous absorption was constructed, based on Laplace transformations, for the specific case of delivery of finite drug doses to the skin. Experimental data for *in vitro* human skin diffusion studies were generated and fitted to the model. The effective dose available for permeation was always predicted to be lower than the actual dose applied for the range of finite dose formulations studied.**

INTRODUCTION

In vitro skin permeation studies with finite dose application are frequently used to gain insight into drug permeation *in vivo*. Because of the small amounts of drug employed in such studies and the depletion of the drug over the course of the experiment it is not a trivial exercise to model the resulting flux data. In this work a numerical inversion of a Laplace domain solution was used to solve Fick's second Law of diffusion and thus determine effective dose, apparent partition and diffusion parameters for a range of formulations studied under finite dose conditions [1].

MATERIALS AND METHODS

In vitro finite dose diffusion studies using human skin were conducted using five model formulations of a lipophilic drug. Saturated amounts of drug were used in all cases. Permeation studies were performed using Franz diffusion cells over 48 hours. A Laplace model was constructed to solve Fick's second Law of Diffusion. The drug permeation profiles were fitted to Equation 1, using Scientist software, version 3.0, (Micromath® Scientist Software Tool, Inc.). Subsequently, values for the partition parameter P_1, and the diffusion parameter P_2, and also effective dose were obtained from Equations 2 and 3.

$$\bar{Q} = \frac{Dose\sqrt{s.td}}{s\left(V_n.s.td.\sinh\left(\sqrt{s.td}\right) + \sqrt{s.td}.\cosh\left(\sqrt{s.td}\right)\right)} \quad (1)$$

$$V_n = \frac{V}{K.h.A} = \frac{V}{P_1.A} \quad (2) \qquad\qquad td = \frac{h^2}{D} = \frac{1}{P_2} \quad (3)$$
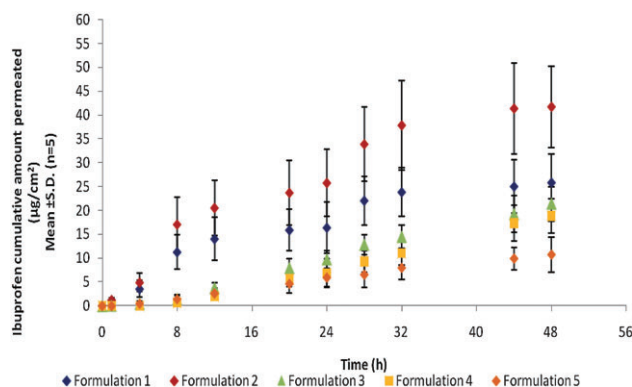

Figure 1. Cumulative amount of drug permeated across human skin, from five different model formulations, under finite dose conditions (3.6 μL application). Each data point represents mean ± S.D.(n = 5).

td: time parameter related to the diffusion time; Vn: donor volume number (i.e. the effective volume of the formulation compared to the skin, representative of the partition coefficient parameter); s: Laplace variable; V: volume of the applied formulation; K: partition coefficient; h: diffusion path length; A: diffusion area; P_1: partition parameter; D: diffusion coefficient; P_2: diffusion parameter.

RESULTS AND DISCUSSION

Figure 1 shows the experimental data obtained from the *in vitro* drug permeation studies across human skin. The apparent partition coefficient (P_1) and diffusion coefficient (P_2) obtained allowed an assessment of formulation influence on drug partitioning and diffusion, respectively. The "effective dose" available for permeation was determined from the best fits of the data to the model and was lower than the actual dose applied for all formulations. The Model Selection Criterion (MSC), which describes the "goodness of fit" of the model to the data was clearly affected by the actual and "effective" dose applied which varied for each formulation. Crystallisation of drug on the skin surface or inside the skin,

after application may explain limited drug penetration across the skin.

CONCLUSIONS

A diffusion model for percutaneous absorption was constructed to which finite dose drug permeation profiles were fitted. The theoretical model demonstrated the differences between the actual dose and effective dose for skin permeation. The results demonstrate the difficulties encountered for the analysis of permeation data in finite dose experiments. Future studies will focus on elucidating the reasons why the

effective dose is always lower than the applied dose and the actual disposition of the drug in the skin.

ACKNOWLEDGMENTS

REFERENCE

[1] Anissimov, Y.G. and Roberts, M.S., Journal of Pharmaceutical Sciences, 1999. **88**: p. 1201–1209.

Nanoparticle Engineering of Water Insoluble APIs *via* Spray-Drying

Nina Schafroth[2], Umesh Y. Jadhav[1], Sushil Makne[1] and Dennis Douroumis[1]

[1]University of Greenwich, School of Science, Chatham Maritime, ME4 4TB, Kent,
[2]BÜCHI Labortechnik AG, Meierseggstrasse 40, 9230 Flawil, Switzerland

INTRODUCTION

The aim of the current study was to engineer biodegradable PLGA nanoparticles of poorly water soluble drugs (Cyclosporine, CyA and Dexamethasone, DEX) by using spray–drying. Process parameters were investigated in order to optimise the particle size and the produced yield. More than 40% of active substances during formulation development by the pharmaceutical industry are poorly water soluble. Lately, spray-drying has drawn interest for the development of novel drug delivery systems [1].

MATERIALS AND METHODS

Prior the spray-drying process drug/polymer blends (1/5 w/w) were dissolved in dichloromethane/Et-OH (70:30) with 1–2% total solid content and spray–dried using a B – 90 spray dryer. The spray-dryer was supplied with CO_2 (1.5 bars) to build the electrical field required for particle separation and N_2 (1.5 bars) to dry the produced particles. Pure active substances, polymers and drug loaded particles were fully characterised.

RESULTS AND DISCUSSION

Spray–drying was implemented to produce PLGA nanoparticles of poorly soluble drugs. The obtain particle size was related to the process parameters and the grade of the PLGA polymers.

The applied pressure, head temperature and the spray rate showed significant effect on the obtained particle size and yield.

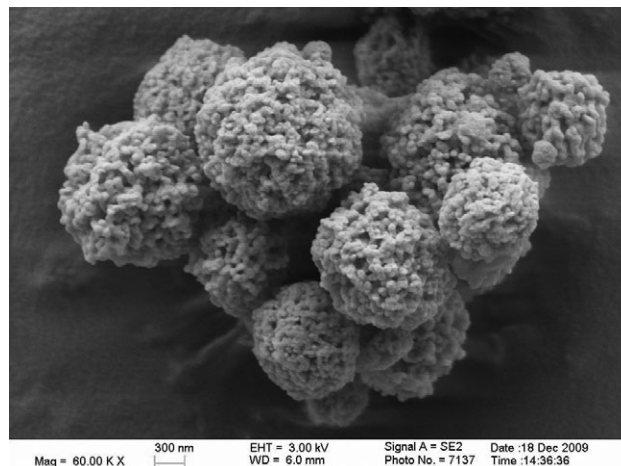The drug loaded nanoparticles showed an average particle size of 850 nm (Fig. 1) in most cases with drug loadings (DL)

Fig. 1. SEM image of DEX/PLGA (concentration of 2%), spray cap with mesh of 5.5 micron, spray rate of 90%.

up to 25% and yields up to 60%. The produced powders were characterised by DSC and XRD studies. Interestingly, CyA/PLGA nanoparticles showed the existence of amorphous CyA in all samples. Fig. 2 shows the absence of the CyA endothermic peak at 120°C (XRD confirmed this observation). In contrast, XRD studies showed the existence of both amorphous and crystalline DEX states.

The DSC thermograms presented a shift of DEX melting peak towards lower temperatures.

The release kinetics showed an initial burst release for both CyA and DEX followed by sustained release over 15 days as shown in Fig. 4. The burst release was attributed to the rapid diffusion of the drug on the particle surface.
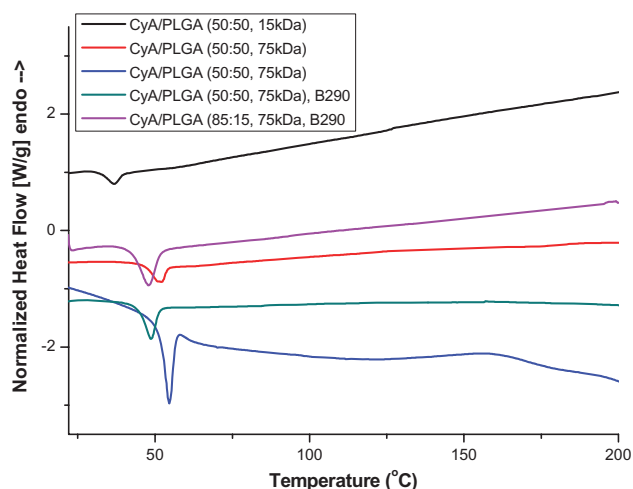
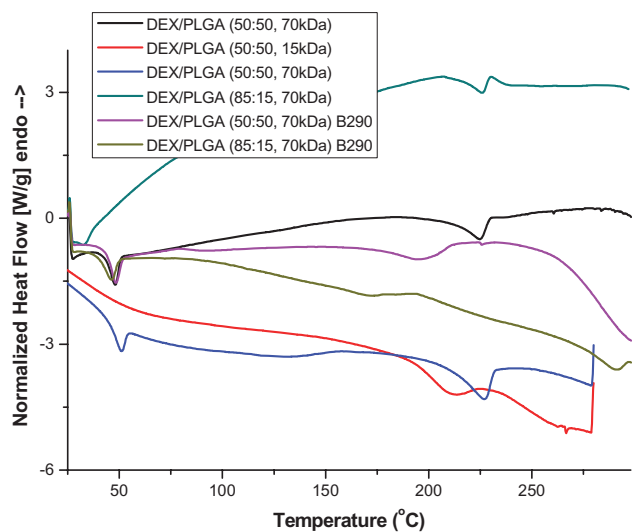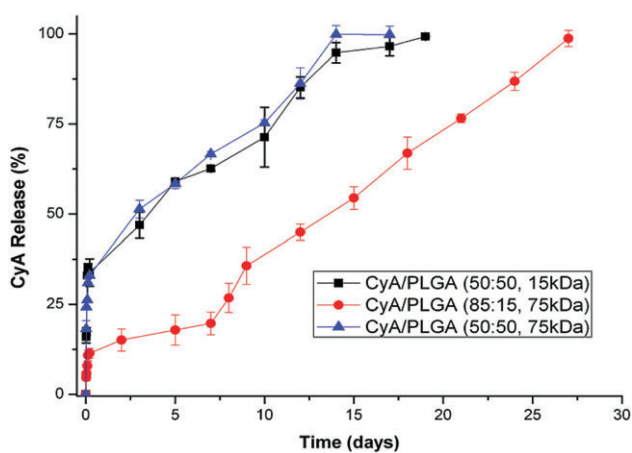**Fig. 2.** DSC thermograms of spray–dried CyA/PLGA nanoparticles

Fig. 4. Release profiles of CyA encapsulated in various PLGA grades.

CONCLUSIONS

In conclusion, spray–drying was successfully used to produce nano- and micro- CyA and DEX loaded particles with high encapsulation efficiencies and sustained release patterns.

REFERENCE

[1] R. Vehring. Pharmaceutical particle engineering via spray–drying. Pharm. Res. 25, 999–1022, (2008)

Fig. 3. DSC thermograms of spray – dried DEX/PLGA nanoparticles

Organic Cation Transporters are Functional in Layers of the Human Bronchial Epithelial Cell Line Calu-3

M. Mukherjee[1], T. Calande[1], J. Cheung[1], D.I. Pritchard[2] and C. Bosquillon[1]

[1]Division of Drug Delivery and Tissue Engineering,
[2]Division of Molecular and Cellular Science, School of Pharmacy, University of Nottingham, Nottingham, UK.

Abstract **– Functional expression of Organic Cation Transporters (OCT) was investigated in Calu-3 cell layers. Patterns of mRNA expression similar to those in human lungs were observed. Uptake studies using the fluorescent cationic dye ASP⁺ demonstrated the presence of an *in vitro* OCT activity, partially inhibited by common inhaled drugs. Calu-3 layers were proven suitable for the investigation of drug-OCT interactions in the bronchial epithelium.**

INTRODUCTION

Layers of the human bronchial epithelial Calu-3 cell line have developed as a model of the airway epithelium for *in vitro* permeability measurements [1]. The range of native functional transporters expressed in the cell line remains however ambiguous. OCTs are present in human lungs and common inhaled drugs have been reported to interfere with these trans-

porters [2]. The aim of this work was to evaluate the expression and functionality of OCT in differentiated Calu-3 layers as well as the ability of inhaled drugs to interact with these transporters in that cell culture model.

MATERIALS AND METHODS

Calu-3 cells (passage 27–33) were seeded at a density of 10^5 cells/cm^2 on 12-well polyester Transwell® cell culture supports and cultured at an air-liquid interface for 21 days. The expression of OCTs was assessed by reverse transcription polymerase chain reaction (rt-PCR). Their functionality was evaluated by quantifying the intracellular uptake of the cationic fluorescent dye [4-(4-(diethylamino)styryl)-N-methylpyridinium iodide (4-Di-2-ASP)] (ASP$^+$, 10 µM) in presence or absence of the non-selective OCT inhibitor tetraethylammonium (TEA, 5 mM) and selective OCTN2 inhibitor L-Carnitine (10 µM). The influence of the inhaled drugs formoterol, salbutamol, ipratropium (500 µM) and budesonide (30 µM) on ASP$^+$ internalisation was also measured.

RESULTS AND DISCUSSION

rt-PCR analysis showed OCT1, OCT3, OCTN1 and OCTN2 were expressed at different levels in Calu-3 layers (Fig. 1) while OCT2 mRNA could not be detected. OCTN2 expression was the highest, which is in accordance with levels quantified in human lung tissue [2].

The uptake of ASP$^+$ was reduced by 80% in the presence of TEA, which demonstrated OCT functionality in Calu-3 layers (Fig.2). L-carnitine decreased the internalisation of the dye by 40% (Fig.2). This indicates that OCTN2 is functional in Calu-3 layers and that one or several other members of the same family of transporters contribute to the OCT activity. All tested inhaled drugs reduced ASP$^+$ uptake (Fig. 2), confirming their inhibitory effect on OCTs in differentiated bronchial cell layers.

CONCLUSIONS

It was established that OCTN2 and at least another member of the OCT family of transporters were functionally active in Calu-3 cell layers. The OCT activity was partially inhibited by common inhaled drugs. This study shows Calu-3 layers are a suitable respiratory *in vitro* model to investigate inhaled drugs-OCT interaction in the bronchial epithelium.
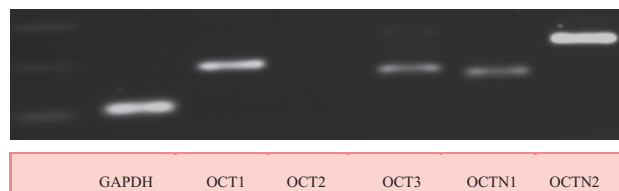

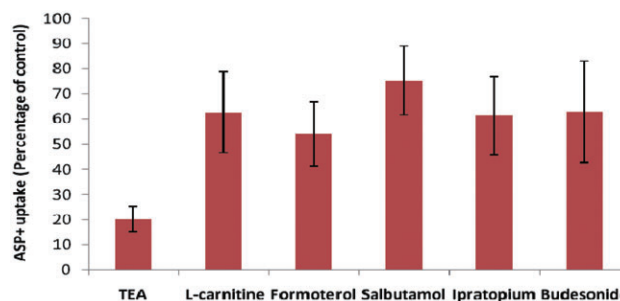**Fig. 1. rt-PCR analysis of OCT expression in differentiated Calu-3 cell layers. GAPDH was used as the housekeeping control**

Fig. 2. ASP$^+$ uptake (% of control) by Calu-3 cell layers in presence of OCT inhibitors and inhaled drugs. Data are presented as mean ± standard error on the mean (n = 3–4 layers)

ACKNOWLEDGMENTS

REFERENCES

[1] Forbes, B. and C. Ehrhardt, 'Human respiratory epithelial cell culture for drug delivery applications'. *European Journal of Pharmaceutics and Biopharmaceutics*, 2005. **60**(2): p. 193–205.

[2] Bosquillon, C. "Drug transporters in the lungs – do they play a role in the biopharmaceutics of inhaled drugs?" *J.Pharm.Sci.,* published online on 30 Nov 2009.

[3] Bleasby, K., et al., "Expression profiles of 50 xenobiotic transporter genes in humans and pre-clinical species: A resource for investigations into drug disposition." *Xenobiotica,* 2006. **36**(10–11): p. 963–988.

pH responsive liposome-in-microsphere formulations for drug delivery to the colon

M.J. Barea[1], M. Jenkins[2], R.H. Bridson[1]

[1]School of Chemical Engineering, University of Birmingham, Birmingham, UK.
[2]School of Metallurgy and Materials, University of Birmingham, Birmingham, UK.

Abstract – **A formulation has been developed that incorporates sub micron liposomes in pH responsive polymer microspheres for drug delivery to the ileocaecal junction of the GI tract. Eudragit S100 microspheres were produced using a double emulsion technique and used to encapsulate liposomes. To withstand the solvent used within the microsphere production route, the liposomes were coated with chitosan. The model drug 5-ASA was incorporated into the liposomal formulations with release being explored in simulated GI tract conditions.**

INTRODUCTION

The use of liposomes for sustained and targetted drug release has been a widely investigated concept. As yet there are no liposomal formulations for oral colonic drug delivery and therefore the aim of this work was to develop a drug delivery system that can be orally administered but which also remains stable throughout the upper GI tract. The stomach and small intestine are perceived as hostile environments (e.g. for macromolecules) and therefore it can be beneficial to target the colon for systemic and local treatments.

MATERIALS AND METHODS

Neutral liposomes encapsulating the model drug 5-ASA were produced using egg phosphatidycholine and cholesterol. The liposomes were then coated with 1 % chitosan in acetic acid and subsequently incorporated into Eudragit S100 microspheres via a double emulsion solvent evaporation method to produce liposomes-in- microspheres (LIMs) [1]. Characterisation techniques for liposomes and LIMs included zeta potential analysis, laser diffraction sizing, light microscopy, fluorescence microscopy and cryo-SEM. Drug release trials were completed *in vitro*, using a number of representative GI tract conditions for the stomach, small intestine and large intestine.

RESULTS AND DISCUSSION

The presence of a chitosan coating layer on the liposomes was shown through an increase in vesicle zeta potential from – 1.4 mV to +45 mV. Further results indicating the presence of a coating layer and its stability in solvent included an increase in mean size, fluorescence imaging of labelled chitosan coated liposomes and the use of cryo-SEM (Fig 1). Similar techniques were used to identify the presence of chitosan coated liposomes within the Eudragit microspheres. Subsequent drug
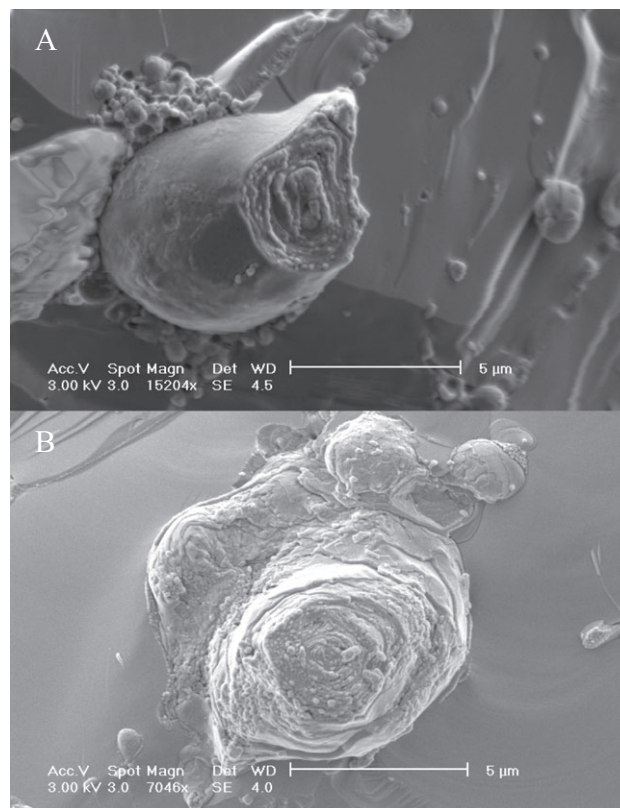

Fig. 1. Cryo-SEM images of uncoated (A) and chitosan coated (B) liposomes for incorporation into Eudragit S100 microspheres

release trials indicated that significant drug release would likely occur in and downstream of the ileocaecal region when simulating GI tract conditions *in vitro*.

CONCLUSIONS

The incorporation of liposomes into Eudragit S100 microspheres has been successful with the use of a protective chitosan coating layer for the liposomes. Subsequent drug release trials have shown results indicative of ileocaecal/colonic region targetting and therefore the LIMs may be useful for treatment of the large bowel or delivery of systemically-acting molecules.

ACKNOWLEDGMENTS

REFERENCE

[1] S. S. Feng, G. Ruan, Q. T. Li, "Fabrication and characterisations of a novel drug delivery device liposomes-in-microspheres (LIM)" *Biomaterials*, **25** (2004) 5181–5189

Poly-caprolactone (PCL) based nanospheres for the delivery of lansoprazole

A. Shabir[1], Y. Perrie[1], S. Begum[2] and A. Mohammed[1]

[1]Aston Pharmacy School, Aston University, Birmingham, B47ET, UK
[2]Apex Healthcare Ltd., UK

Abstract – **The polymer to drug ratio plays a major role in the characterisation and drug loading of nanoparticles produced using the solvent displacement technique. Using a 5:1 ratio, successful nanoparticle formulation of lanso-prazole using poly-(caprolactone) were produced.**

INTRODUCTION

Currently there is great interest in nanostructure-mediated drug delivery (colloidal), which can be used to reformulate licensed drug products into liquid oral formulations for use in the treatment of paediatric and geriatric patients. The objective of the current work was to study the suitability of poly-caprolactone (PCL) in nanosphere systems for the reformulation of a poorly soluble drug, lansoprazole, into a liquid formulation.

Lansoprazole, a proton pump inhibitor, is a hydrophobic drug that is currently only formulated in a tablet form. For this reason there is a need for the drug to be reformulated in oral liquid form, for ease of administration to the specified target market.

MATERIALS AND METHODS

The nanosphere preparation was carried out using the solvent displacement technique. Briefly, an organic solution of PCL, at varying concentrations, was added to 10 mg of lansoprazole. This acetonic solution was then added to 10 mL of 0.25% (w/v) Pluronic F127, under magnetic stirring. The nanoparticle dispersion was concentrated to 10 mL under reduced pressure, with the non-encapsulated drug being separated by centrifugation. The lansoprazole-loaded pellets were then re-dispersed in 10 mL of distilled water, and characterised for size, particle charge and amount of drug entrapped.

The preparations were characterised for particle size using a light scattering Zetasizer (Brookhaven UK) at a set temperature of 25°C, the results for which were represented as a mean +SD. Quantification of loaded-nanoparticles was carried out by HPLC analysis.
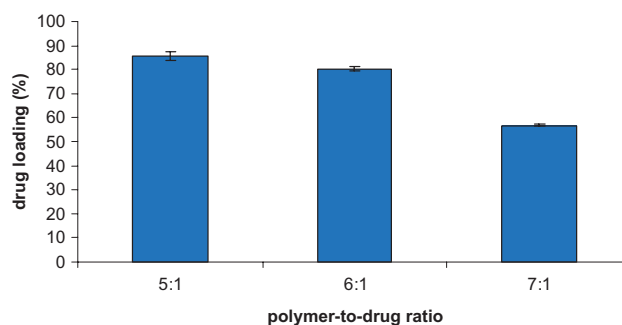

Fig. 1. Drug loading characterisation of PCL-coated nanoparticles

RESULTS AND DISCUSSION

The nanoparticles were prepared at varying polymer-to-drug ratios: 5:1, 6:1 and 7:1. The 5:1 nanoparticle preparation showed a particle size of 271.6 + 4.8 nm, which was seen to increase with increasing polymer concentration (7:1 nanoparticle preparation displayed particle size of 308.7 + 19.5 nm ($P < 0.05$)). The difference between the 5:1 and 7:1 polymer to drug ratios can be attributed to an increase in the viscosity of the organic phase as the polymer concentration increases. Viscosity is explained by the coacervate phase, where the removal of acetone under reduced pressure induces the separation of small liquid droplets rich in solvent and polymer. Hence as the separation of nano-droplets increases, the viscosity of the suspension also increases.

It can also be said that the differences seen between the 5:1 and 7:1 nanoparticle preparations can be directly related to the compositions of PCL. PCL has relatively weak coiling capabilities, thus as the concentration of PCL increases it causes the nanoparticles to increase in size slightly due to the minimum flexibility of the PCL chain, and this in turn causes the repulsive forces between the particles to lessen.

As seen from Figure 1 the entrapment values for the preparations of 5:1 (85.5 + 1.8%), 6:1 (80.38 + 0.66%) and 7:1 (56.88 + 0.21%) polymer-to-drug ratios were significantly different, with the major difference being between the 5:1 and

7:1 nanoparticle preparations. This decrease in lansoprazole entrapment with increasing polymer concentration can be attributed to the increase in viscosity of the formulation as the polymer concentration increases. This is as an increase in viscosity results in an increase in the resistance for the drug to enter into the hydrophobic domains of the polymeric environment, and thus resulting in a decrease in the drug entrapment.

CONCLUSIONS

These results show that PCL-based systems can provide a practical alternative for the reformulation of lansoprazole as an oral liquid-based medicine. However, optimisation of polymer to drug ratio is vital in order to produce nanoparticles with a high drug loading percentage.

It can be concluded that the polymer to drug ratio of 5:1 resulted in high drug loading ($85.5 + 1.8\%$) with the smallest particle size ($271.6 + 4.8$ nm).

Preparation of sustained release polymeric microspheres containing rifampicin

M.A. Darbandi[1], M. Zandkarimi[1], A. Rouholamini[2], K. Gilani[2], H. Tajerzadeh[2]

[1]School of Pharmacy, Zabol University of Medical Sciences, Zabol, Iran
[2]School of Pharmacy, Tehran University of Medical Sciences, Tehran, Iran

INTRODUCTION

Tuberculosis is one of the major infectious diseases around the world [1]. Targetting antituberculosis drug to the lung will increase local therapeutic effects and reduce systemic side effects.

In this study, rifampicin, an antituberculosis drug, was loaded in poly lactide-co-glycolide(PLGA) microspheres using spray drying method.

MATERIALS AND METHODS

Rifampicin, PLGA 50:50, and PLGA 75:25 was purchased from sigma chemical.

1) *Spray drying:* Rifampicin and polymer solutions were spray dried, using a lab scale spray drier (Buchi 191) with an inlet and outlet temperature of 50°C, and 45°C, respectively. For spray drying the polymer:drug ratio was 2:1 and the concentration of the PLGA set at 0.5%. PLGA and drug were dissolved in dichloromethane (DCM) or solvent mixture of DCM and ethyl acetate (DCM/EA). DCM/EA ratio was set at 80:20 and 33:67.

2) *In-vitro experiments***:** The particle size distribution of samples was determined using laser light scattering. Content uniformity and in vitro lung deposition was determined by spectrophotometer at 475 nm. Scanning electron microscopy (SEM) was done at 25 keV. The bulk density was determined by graduated cylinder and helium pycnometer. In vitro deposition was determined by Andersen cascade impactor.

3) *In-vivo experiments:* Microspheres were instilled into the rat lung through the obtuse syringe. Blood samples were taken after 24, 36, 48, 60, 72 and 96 h; centrifuged; collected; stored at −30 °C; and analysed by microbiological method [2].

RESULTS AND DISCUSSION

Density of the microspheres and process yield increased when higher fraction of EA was used (Table 1). These observations

Table 1. Physicochemical properties of the microspheres

Polymer	Solvent	Bulk density	Size (μm)	% Yield
PLGA 50:50	DCM(100)	0.095 + 0.009	7.23 + 0.02	30 + 1
PLGA 75:25	DCM(100)	0.121 + 0.007	7.21 + 0.03	35 + 2
PLGA 75:25	DCM/EA(80:20)	0.225 + 0.008	7.35 + 0.05	55 + 4
PLGA 50:50	DCM/EA(67:33)	0.151 + 0.007	7.30 + 0.04	42 + 2
PLGA 75:25	DCM/EA(67:33)	0.275 + 0.011	7.28 + 0.02	48 + 1

could be explained by the higher solubility of polymer in DCM and hence longer distance between polymer chains in dispersion. By using EA in the solvent mixture, distance between polymer chains decreases and adhesion of the polymer chains improves during spray drying process.

SEM pictures shown using EA/DCM mixture as solvent improved the spherical shape of the microspheres. Slower solvent evaporation rate of EA leads to the decreasing solvent removal velocity from the polymer matrix and formation of more spherical microspheres.

Addition of EA in pure DCM reduced release rate. Again, this behaviour could be explained by the decreasing distance between polymeric chains and therefore producing a more structured polymer after drying.

In-vivo results were shown that the addition of 33% EA to the pure DCM in the PLGA 75:25 microspheres increases the T_{max} value from 36 to 48 h, mean absorption time (MAT) from 7.1 to 14.8 h, decrease C_{max} from 0.53 to 0.43 μg/ml, decrease K_a from 0.14 to 0.071/h and decrease AUC from 35.40 to 29.94 μgh/ml ($p < 0.05$). These observations could be correlated to the similar release rate decreasing observed in in-vitro studies. In all microspheres the plasma concentrations of drug remained above the minimal inhibitory concentration (MIC) up to 96 h. Using slow release rifampicin microspheres could improve patient compliance and decreases

systemic side effects due to reduction of total dose, C_{max}, and dose frequency.

CONCLUSIONS

In-vivo studies were demonstrating potential therapeutic efficiency of the rifampicin microspheres administered by intra tracheal route. Results demonstrate that EA is an excellent low toxic solvent that could be added in DCM for decreasing release rate of rifampicin microspheres.

REFERENCES

[1] J.L. Ho, L.W. Riley. "Defences against tuberculosis" in The Lung, R.G. Crystal and J.B. West, Philadelphia, Scientific foundations Lippin Cott-Raven Publishers, 1997, pp. 2381–2394.

[2] H. Saito, H. Tomioka, "Therapeutic Efficacy of liposome-entrapped rifampin against mycobacterium avium complex infection induced in mice" Antimicrobial Agent Chemoter., 33 (1989) 429–433.

Pulmonary delivery of α-chymotrypsin via novel polyester microparticles

H.M. Tawfeek[1,2], S.H. Khidr[2], E.M. Samy[2], S.M. Ahmed[2], A. Shabir[3], A.R. Mohammed[3], G.A. Hutcheon[1], I. Saleem[1]

[1]School of Pharmacy and Biomolecular Sciences, Liverpool John Moores University, Liverpool, UK.
[2]Department of Industrial Pharmacy, Assiut University, Assiut, Egypt.
[3]School of Life and Health Sciences, Aston University, Birmingham, UK

INTRODUCTION

Pulmonary delivery of therapeutic agents is an attractive, convenient and effective route for treatment of many pulmonary disorders [1]. Poly(glycerol adipate-co-ω-pentadecalactone), PGA-co-PDL, is a novel polyester and has recently shown promise as a delivery system for hydrophilic macromolecules [2]. The aim of this study was to investigate PGA-co-PDL and its pegylated co-polymer poly(ethylene glycol), PEG-PGA-co-PDL, as sustained release microparticle carriers for pulmonary delivery of macromolecules, using α-chymotrypsin (α-CH) as a model protein, for treatment of local lung diseases, such as cystic fibrosis.

MATERIALS AND METHODS

1) P*reparation*: Microparticles were prepared via w/o/w double emulsion/spray drying utilising a mini-spray dryer (Büchi B-290, Switzerland). The inlet and outlet temperature was 100 and 47°C, feed rate 6 ml/min and the aspirator 38 m³/h. 1.5%w/w leucine was added to the external phase prior to spray drying as a despersibility enhancer.

2) C*haracterisation*: Microparticles were characterised for their spray drying yield, encapsulation efficiency, geometric particle size and zeta potential (Zetaplus, Brookhaven particle sizer), true density (Qunatachrome instruments® Multi-pyconometer) and morphology using scanning electron microscopy (SEM).

3) I*n vitro study:* 10 mg microparticles were placed in an eppendorf with PBS buffer (1 ml) at pH 7.4 for 24 h. At selected time-points the supernatant was collected following centrifugation (5 min at 13500 rpm, accuSpin Micro 17) and analysed by UV at 280 nm.

3) *Aerosolisation studies*: Microparticle samples (20 mg) were loaded into HPMC capsules (size 2), and aerosolised (60 L/min for 4 s) via a Handihaler® into a Next Generation Impactor (NGI), coated with 1% glycerol:methanol solution. Samples were collected by washing with DCM/water (1:2) and analysed by UV as above. The fine particle fraction (FPF) and mass median aerodynamic diameter (MMAD) were determined [3].

RESULTS AND DISCUSSION

Produced microparticles had yields of 46.5 ± 2.1 and 51.2 ± 1.5, with low encapsulation efficiency for PGA-co-PDL (14.8 ± 2.5) and PEG-PGA-co-PDL (12.1 ± 0.3) due to the hydrophilic nature of the enzyme partitioning in the external aqueous phase. PEG-PGA-co-PDL (-20.4 ± 0.8) showed a higher zeta-potential indicating an enhanced stability compared with PGA-co-PDL particles (-13.6 ± 2.1). SEM images showed regular spherical particles with smooth surface and minimum points of contact due to the addition of leucine (Fig.1).

A steady release pattern of α-CH was obtained from both microparticles with a slightly higher percentage released from PEG-PGA-co-PDL particles over 24 h (Fig. 2).

The low density and small MMAD of both microparticles resulted in high FPF and deep deposition of α-CH in lower NGI stages. However, the MMAD values are more than double the geometric particle size indicating some aggregation upon aerosolisation (Table 1).

CONCLUSIONS

PEG-PGA-co-PDL shows promise as sustained release carriers for pulmonary delivery of proteins, with better aerosolisation and protein release properties. Further investigations will involve optimising the encapsulation, release and integrity of α-CH.
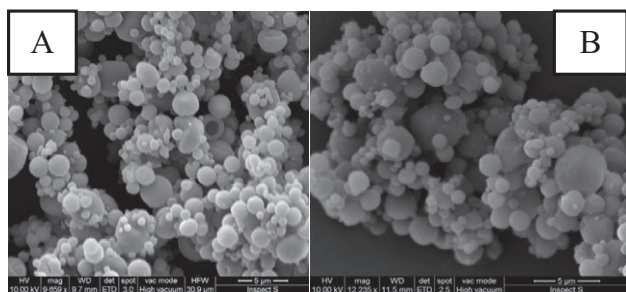
Fig. 1. SEM images of A) PGA-co-PDL and B) PEG-PGA-co-PDL spray dried α-CH loaded microparticles.
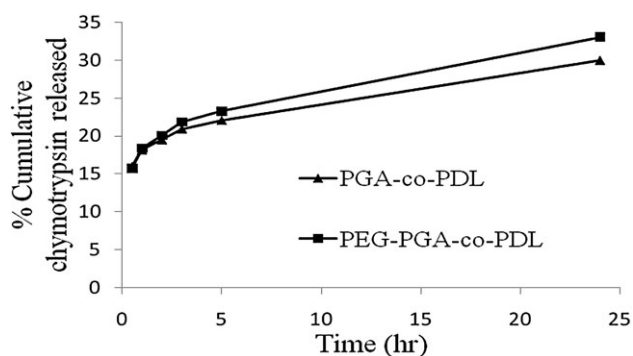
Table 1. The true density, geometrical particle size (PS), (FPF) and (MMAD) for spray dried α-CH loaded microparticles.

Polymer	Density	PS	FPF	MMAD
PGA-co-PDL	0.51 ± 0.01	1.32 ± 0.1	44.4 ± 5.9	3.09 ± 0.08
PEG-PGA-co-PDL	0.61 ± 0.09	0.72 ± 0.2	46.8 ± 5.3	1.94 ± 0.08

REFERENCES

[1] E.M. Westerman et al., "Dry powder inhalation of colistin in cystic fibrosis patients: a single dose pilot study" J Cyst. Fibros., **6** (2007) 284–292.

[2] E.E. Gaskell, G. Hobbs, C. Rostron, G.A. Hutcheon, "Encapsulation and release of alpha-chymotrypsin from poly(glycerol adipate-co-omega-pentadecalactone) microparticles" J. Microencapsulation., **25** (2008) 187–195.

[3] M.R. Feddah, K.F. Brown, E.M. Gipps, N.M. Davies, "In-vitro characterisation of metered dose inhaler versus dry powder inhaler glucocorticoid products: influence of respiratory flow rates" *J. Pharm. Sci.*, **3** (2000) 317–324.

Fig. 2. In-vitro release of α-CH from spray dried PGA-co-PDL and PEG-PGA-co-PDL microparticles.

Self-assembled Complex Formulations of Lipid-Aminoglycoside Conjugates: Nanoparticles for Efficient Gene and siRNA Delivery

Hassan M. Ghonaim[1,2], Yuxi Chen[1], Charareh Pourzand[1], and Ian S. Blagbrough[1]

[1]Department of Pharmacy and Pharmacology, University of Bath, Bath, BA2 7AY, UK
[2]Faculty of Pharmacy, Suez Canal University, Ismalia, Egypt

Abstract – **We are designing and developing lipid-polyamines based upon aminoglycoside cationic head-groups linked to a lipid moiety, e.g. cholesterol, for the efficient delivery of genes for gene therapy [1, 2], and also for the delivery of siRNA to knock-down gene expression [2, 3]. The conjugation of neomycin B to cholesterol provides an "intelligent" material which may well overcome problems found in poly-nucleic acid delivery.**

INTRODUCTION

Our goals are to design and develop gene and siRNA delivery systems [1–3], based upon aminoglycosides, e.g. neomycin, and lipids, e.g. cholesterol, covalently bound as non-viral vectors which can cause the self-assembly of lipoplexes of pDNA and/or siRNA.

MATERIALS AND METHODS

- **Measurement of particle size**

Lipoplex particle size was measured by laser light scattering using a NANOSIGHT LM10.

- **RiboGreen intercalation assay**

RiboGreen solution was added to each well containing free siRNA or complexed with NeoChol and measured with a Microplate Reader.

- **Transfection experiments**

A human primary skin fibroblast cell line (FEK4) and a human cervix carcinoma, HeLa derived and transformed cell line (HtTA) were used. The complex was incubated with the cells. Levels of fluorescence were detected by gated FACS. The transfection efficiency was calculated based on the per-

centage of positive cells (green fluorescence, Fig. 1) in the total number of cells.

- **Cytotoxicity (MTT) assay**

NeoChol complexes were added in the same way as in the above transfection protocol using the MTT assay. The % viability related to control is calculated by: 100 x test absorbance/control absorbance.

RESULTS AND DISCUSSION

3β-[5″-(Aminoethanethiol)-neomycin B] carbamoyl cholesterol (NeoChol) was synthesised and showed the required LSIMS HR accurate mass data. The average particle size was 200 nm for pDNA and 120 nm for siRNA. siRNA shows condensation as a function of N/P charge ratio (nitrogen to phosphate ratio). Neomycin B did not transfect the primary cells. However, NeoChol, as a function of increasing N/P charge ratio, showed efficient DNA transfection.

NeoChol shows efficient transfection with good viability, comparable with the commercial transfecting agents LipoGen (DNA delivery) and TransIT (siRNA delivery).

CONCLUSIONS

We have shown that NeoChol, a synthetic cationic lipid, a conjugate derived from neomycin B antibiotic and cholesterol is efficient for the in vitro delivery of pDNA and fluorescent siRNA. NeoChol spontaneously neutralises and condenses negatively charged DNA and RNA leading to efficient nanoparticle formation. This controlled self-assembly of a scaffold also facilitates absorptive endocytosis and/or fusion with cell membranes through the lipid moiety.

ACKNOWLEDGMENTS

We acknowledge Prof R.M. Tyrrell (University of Bath) for the FEK4 and HtTA cell lines.
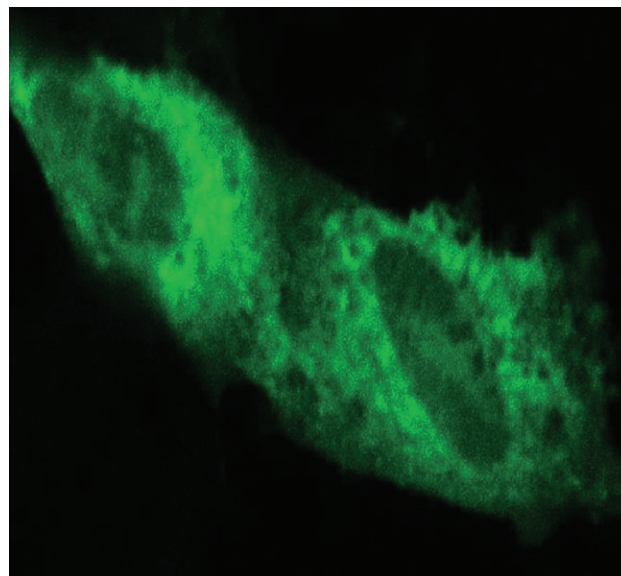

Fig. 1. Confocal microscope images showing green fluorescent protein inside FEK4 cells.

REFERENCES

[1] H.M. Ghonaim, O.A.A. Ahmed, C. Pourzand and I.S. Blagbrough, "Varying the chain length in N^4,N^9-diacyl spermines: non-viral lipopolyamine vectors for efficient plasmid DNA formulation" *Mol. Pharm.* **5** (2008) 1111–1121.

[2] I.S. Blagbrough and H.M. Ghonaim, Polyamines and their conjugates for gene and siRNA delivery. In G. Dandrifosse (Ed.), "*Biological aspects of biogenic amines, polyamines and conjugates*", Transworld Research Network, India, 2009, 81–112.

[3] H.M. Ghonaim, S. Li and I.S. Blagbrough, "Very long chain N^4,N^9-diacyl spermines: Non-viral lipopolyamine vectors for efficient plasmid DNA and siRNA delivery" *Pharm. Res.* **26** (2009) 19–31.

Size-tunable conjugated CdS quantum dots with high photoluminescence yield

Pranav Bhujval[1], Sudha Rajaram[1], Marco E. Favretto[2], Dennis Douroumis[1]

[1]University of Greenwich, School of Science, Chatham Maritime, ME4 4TB, Kent,
[2]University of Kent, School of Pharmacy, Chatham Maritime, ME4 4TB, Kent

INTRODUCTION

In the last decade nanocrystalline semiconductor structures called quantum dots (QDs) have been an area of great research interest. We have synthesised size-tunable, QDs with high photoluminescence (PL) following chemical functionalisation of the particle surface conjugated with human transferring (Tf). Cytotoxicity and cellular uptake of conjugated Tf-QDs were studied *in vitro* in 3T3 endothelial cells and LNCaP prostate cancer cells.

MATERIALS AND METHODS

CDs QDs were synthesised using a standard [1,2] procedure. Freshly prepared and conjugated QDs were further characterised.
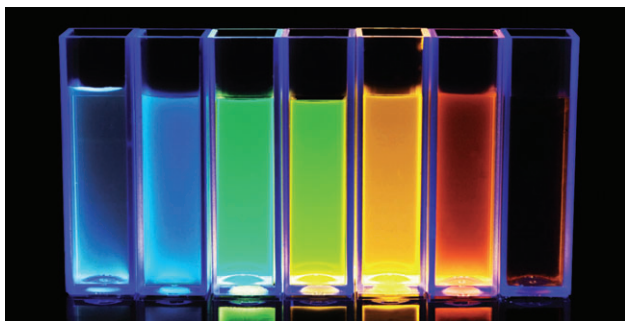
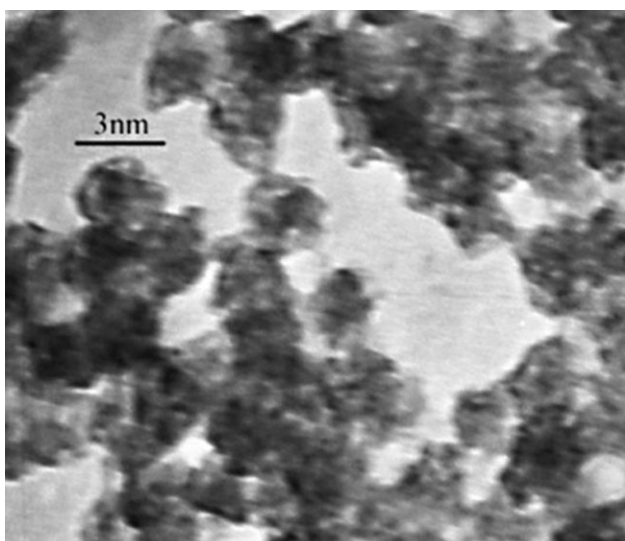**Fig. 1.** Aqueous CdS qdots of different sizes exited with UV lamp.

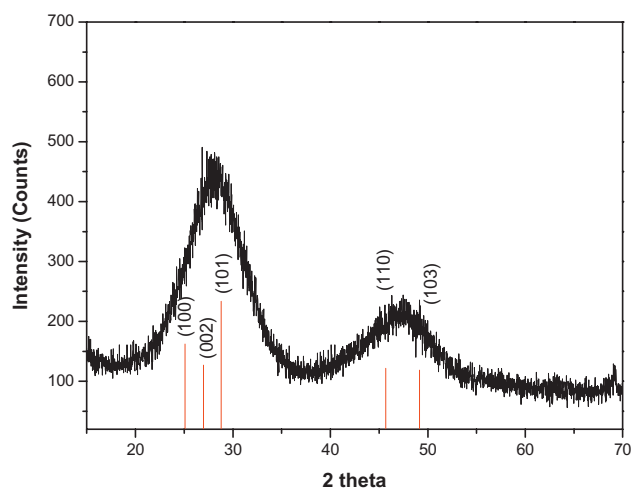**Fig. 2.** TEM micrograph of CdS nanoparticles

Fig. 3. XRD pattern of wurtzite CdS qdots

RESULTS AND DISCUSSION

By adjusting the Cd/S molar ratio we were able to produce QDs with size–tunable emission (Fig. 1) and high lumines-
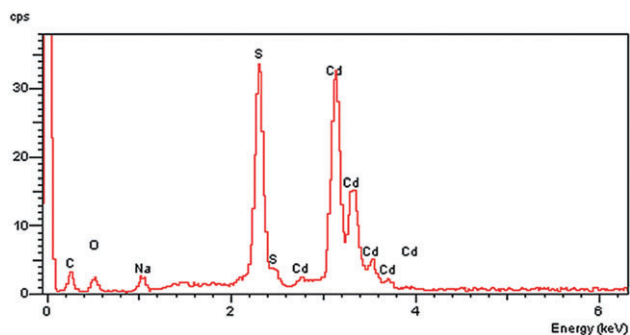

Fig. 4. Typical EDX spectra of water soluble CdS qdots.
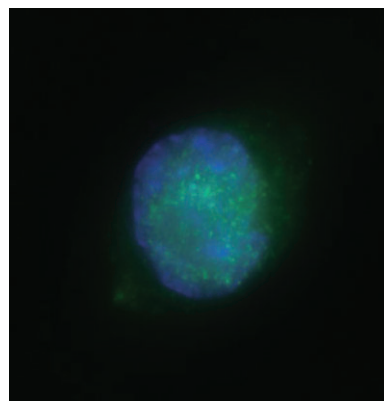

Fig. 5. Cellular uptake of Tf-CdS in prostate cancer cells (2 hr, LNCaP).

cence with emission width 2–10 nm (half width at half maximum, HWHM).

TEM studies illustrated in Fig. 2 showed nearly monodispersed, spherical particles. The image shows QDs with a good uniformity in size and shape of ~3 nm

Fig. 3 depicts the X-ray powder diffractogram obtained from CdS QDs synthesised under optimal conditions, which showed broad peaks at 2θ values of 25°, 26°, 28°, 44° and 47°, corresponding to the crystal planes (100) (002) (101) (110) and (103) of wurtzite structure CdS QDs. The EDX spectrum in Fig. 4 shows the existence of elemental Cd and S at 3.1 KeV and 2.3 KeV respectively with 1:1 stoichiometric ratio, indicating that the nanoparticles are composed of pure CdS.

Tf-QDs (green labelling) were found to be non-toxic, compared to bare QDs, and presented excellent endocytic uptake after 2 hrs (Fig. 5)

CONCLUSIONS

Conjugated Tf-QDs with enhanced cellular uptake have been successfully used to target prostate cancer cells and can be used for imaging purposes in future.

REFERENCES

[1] P. Bhujbal, S. Rajaram, M.E. Favretto, D. Douroumis **A facile synthesis route of size tunable CdS quantum dots with high photoluminescence yield. J. Nanosci. Nanotech. (in Press)**

[2] G.T. Hermanson. Bioconjugate Techniques, Elsevier, 2008.

Soluble PMVE/MA Microneedle Arrays as a Potential Transdermal Delivery System for Metronidazole

Rita Majithiya[1], David Woolfson[1], Ryan F. Donnelly[1]

[1]School of Pharmacy, Queen's University Belfast, Belfast, UK.

Abstract **– The aim of this study was to fabricate and evaluate soluble polymeric PMVE/MA [poly (methylvinylether-co-maleic acid)] MN (Microneedle) arrays containing hydrophilic model drug metronidazole. MN arrays showed significant increase in *in vitro* permeation of metronidazole as compared to passive diffusion.**

INTRODUCTION

MN arrays are minimally invasive devices that can be used to by-pass the *stratum corneum* barrier and thus achieve enhanced transdermal drug delivery. MN's consisting plurality of microprojections (50–900 μm in height) with diverse geometries have been produced from silicon, metal, carbohydrates and polymers using various microfabrication techniques. Application of such MN arrays to biological membranes can create transport pathways of micron dimensions. Micro pores readily-permit the transport of a wider range of therapeutics including hydrophilic drug and macromolecules to and across the skin by piercing the *stratum corneum* [1], which is considered to be the main barrier for permeation of hydrophilic drug across skin.

MATERIALS AND METHODS

In this study, polymeric PMVE/MA MN arrays were fabricated using silicone micromoulds prepared by a novel galvanometer-based laser micromachining method (11 × 11 array, MN height 600 mm, interspacing of 300 μm).

Soluble MN arrays and a soluble patch were formulated using 20% w/w aqueous blends of PMVE/MA to which metronidazole was added at a loading of 3.5% w/w. Soluble MN arrays with 10%w/w pore forming agent (sodium bicarbonate) were also prepared to enhance solubility of the matrix by increasing the size of the void space in the matrix by increasing the porous structure which will promote the diffusion of solute and thereby permeation of the drug.

The MN arrays were characterised in terms of fracture force. The skin permeability of metronidazole from polymeric patch, soluble MN arrays containing metronidazole and soluble MN arrays with sodium bicarbonate containing metronidazole across neonatal porcine skin (dermatomed to 350 μm thickness) was investigated *in vitro* using modified Franz cells

RESULTS AND DISCUSSION

MN arrays were found to possess very good mechanical strength. The percentage reduction in MN height for a com-
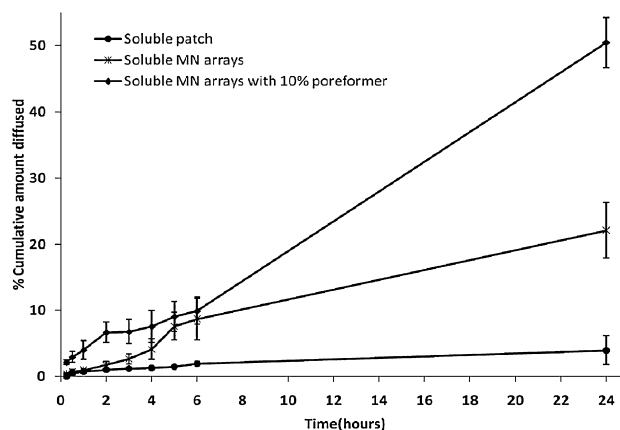

Figure 1: *In vitro* permeation of metronidazole from soluble MN arrays containing metronidazole with and without pore forming agent across dermatomed neonatal porcine skin. Each value represents the mean ± SD of 4 experiments.

pression force of 0.36 N/needle was found to be approximately 20%. Addition of sodium bicarbonate to PMVE/MA MN arrays had no significant effect on the % reduction in height of MN arrays following compression at 0.36 N/needle, whereas metronidazole addition resulted in only a slight increase in % reduction in height of MN arrays.

The *in vitro* permeation profiles of metronidazole permeated from a PMVE/MA patch and a PMVE/MA MN array (with and without pore forming agent) are shown in Figure 1. A 7-fold increase in % cumulative amount permeated was found with soluble MN arrays which further increased to 15-fold when pore forming agent was added to soluble MN arrays as compared to passive diffusion over a period of 24 hours.

CONCLUSIONS

Soluble MN arrays proved to be a promising transdermal drug delivery system for enhancing permeation of the highly hydrophillic drug metronidazole across the hydrophobic barrier of the skin; *stratum corneum*. MN treatment created aqueous channels and, thereby, significantly enhanced drug diffusion. Soluble MN arrays with pore forming agent proved to be even more efficient in terms of permeation enhancement. Further *in vivo* studies in animal models and clinical trials are ongoing to prove efficacy and safety of the above mentioned system. This novel technology will allow the transdermal market to be expanded beyond the present con-

fines imposed by physicochemical properties of the drug molecules in relation to skin permeation leading to benefits for patients, healthcare providers and pharmaceutical industry.

ACKNOWLEDGMENTS

REFERENCE

[1] Prausnitz M.R "Microneedles for transdermal drug delivery" *Adv Drug Deliv Rev.* **56** (2004) 581–587.

Studies on drug-in-adhesive acrylic layers containing ibuprofen and poloxamer 188

W. Saddique, K. Dodou

Sunderland Pharmacy School, University of Sunderland, Sunderland, UK.

Abstract – **The integration of poloxamer 188 and ibuprofen into acrylic layers was studied using three different incorporation methods. Layers prepared by mixing the molten binary mixture with the liquid adhesive showed lower crystalline content compared with layers prepared by incorporation of the physical and solid dispersion binary mixtures.**

INTRODUCTION

Preliminary *in-vitro* studies of acrylic layers containing binary mixtures of ibuprofen and poloxamer 188 showed enhanced ibuprofen release when prepared with molten binary mixtures compared with layers prepared with physical and solid dispersion binary mixtures and layers containing ibuprofen alone [1]. Our aim was to further investigate this finding.

MATERIALS AND METHODS

Preparation of adhesive layers: Ibuprofen: poloxamer 188 binary mixtures at ratios of 30:70, 40:60, 50:50 and 60:40 were incorporated into acrylic layers either as physical mixtures (PM), solid dispersions (SD) or molten mixtures (MM). The layers were examined in the following sequence:

Polarised microscopy: The presence of crystals in the layers was established using an Olympus BH2 microscope with an Olympus lens fitted with a camera (AxioCam MRc-Zeiss, UK) and AxioVision vs4.4 image analyser software.

Differential Scanning Calorimetry (DSC): Enthalpy of fusion (ΔHf) values and melting temperatures (n = 3) were recorded in hermetic pans using a standard DSC (Q1000, TA Instruments, USA) heat/cool/heat cycle from 0°–100°C at 5°C/min. Precalibration was via indium standard.

Rheological measurements: These were conducted according to a previously described method [2].

Fourier Transform Infra Red (FTIR): The IR spectra of ibuprofen, poloxamer 188 and all layer combinations were recorded using a Spectrum BX FTIR (Perkin Elmer, US) at 4 cm^{-1} resolution.
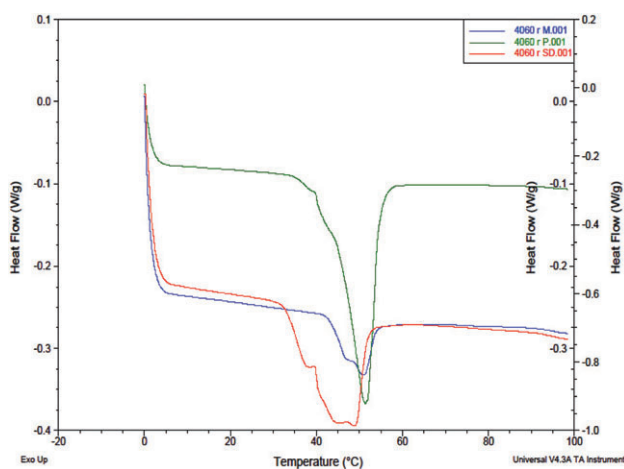

Fig. 1. Example of melting endotherms obtained from MM (blue), PM (green) and SD (red) layers.

RESULTS AND DISCUSSION

DSC analysis showed melting endotherms from the binary crystalline mixture but not from pure ibuprofen, regardless of layer preparation method (Fig. 1). FTIR analysis confirmed the absence of ibuprofen crystal dimers in all layers. MM layers at all ratios had the lowest enthalpy values compared to PM and SD layers, indicating low crystalline binary content, also demonstrated by polarised microscopy (Fig 2).

Rheological measurements showed that all layers complied with the required adhesive performance criteria [2].

CONCLUSIONS

Incorporation of molten binary mixtures of ibuprofen: poloxamer 188 in acrylic adhesive resulted in the formation of ibuprofen crystal-free layers of high thermodynamic activity.
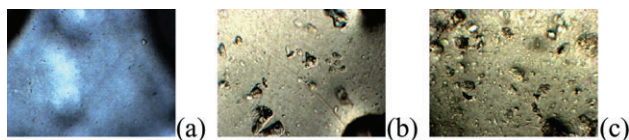
Fig. 2. Polarised microscopy (100x magnification) of 50 : 50 layers prepared by MM (a), PM (b) and SD (c).

ACKNOWLEDGMENTS

REFERENCES

[1] A. Sutton, "Formulation and dissolution studies on transdermal drug-in-adhesive layers with the addition of drug solubilising polymer" Final year project 2006/7 (supervisor: Dr Kalliopi Dodou), unpublished.

[2] K.Y. Ho and K. Dodou, "Rheological studies on pressure-sensitive silicone adhesives and drug-in-adhesive layers as a means to characterise adhesive performance" *Int. J. Pharm.*, **333** (2007) 24–33.

Study of role of ethosomes in topical delivery of an antifungal agent

A.P. Pawar[1], K.S. Shaikh[1]

[1]Department of Pharmaceutics, Poona College of Pharmacy, Bharati Vidyapeeth University, Pune, India-411038

INTRODUCTION

Conventional topical therapy fails to treat the deep seated fungal infections leading to a recurrence of symptoms [1, 2]. Liposomes and niosomes are useful in topical delivery of drugs wherein the drug overcomes the skin barrier, and achieves maximum concentration and residence in the skin's deeper layers [3, 4]. Similarly, ethosomes can be a key to topical delivery of drugs in fungal skin infections. The present study was undertaken to assess the role of ethosomes in topical delivery of the antifungal, ciclopirox olamine (CPO).

MATERIALS AND METHODS

CPO ethosomes containing Phospholipon 90H (0.5%, 0.7%, 0.9%w/v) and ethanol (10%, 20%, 30%v/v) were prepared by the hot method according to 3^2 factorial design and characterised for particle size, entrapment efficiency and zeta potential to study the effect of lipid and ethanol concentrations on the physicochemical characteristics. The drug deposition in and flux across membrane, both, were determined by in-vitro and ex-vivo methods.

RESULTS AND DISCUSSION

Ethosomes are lipid vesicles containing high amount of ethanol. Spherical or slightly oval vesicles of mean diameter in the range of 186 to 608 nm as measured by laser light scattering were obtained. They possessed a negative zeta potential (Zetasizer 300 HSA). The maximum entrapment efficiency, determined by Sephadex minicolumn centrifugation and further fluorescence spectroscopy, was about 92%. Increasing ethanol concentration favoured entrapment of the drug but thereafter the vesicle rigidity was reduced by high amount of ethanol leading to lower entrapment (Fig. 1).
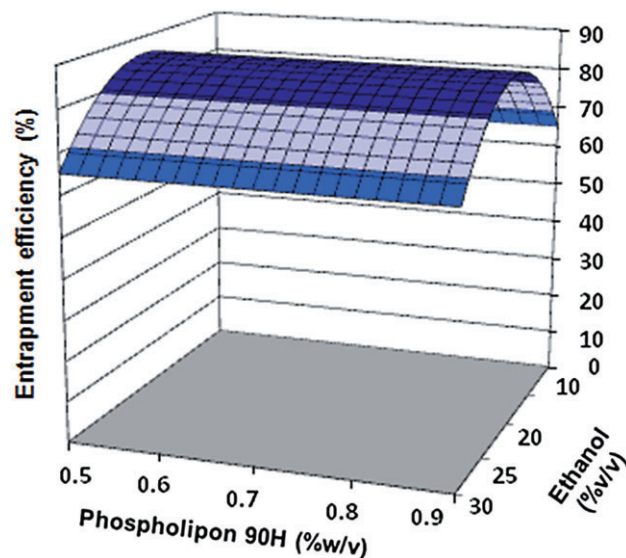
Fig. 1. Effect of phospholipid and ethanol on entrapment efficiency of ethosomes.

Increasing ethanol concentrations also diminished the vesicle size (Fig. 2).

In-vitro, the ethosomes displayed a maximum drug deposition of 68% and in some cases a cumulative amount of about 60 % was released across the membrane during 24 hours. The ex-vivo study demonstrated a higher drug deposition (65.2% ± 2.0) and % cumulative amount permeated (29.23 ± 1.9) for the ethosomal dispersion while that of CPO solution in water-methanol mixture (9:1) was 37.13% ± 3.9 and 21.80% ± 3.1 respectively.

The increase in drug deposition and cumulative release across the skin was primarily due to ethanol. Lipid vesicles

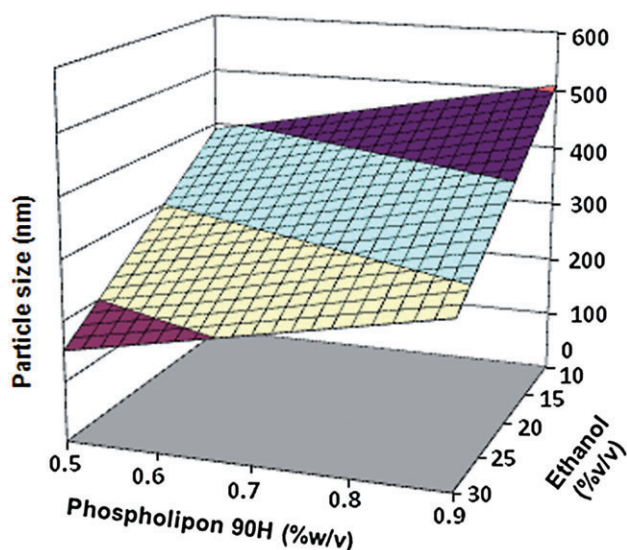**Fig. 2.** Effect of phospholipid and ethanol on particle size of ethosomes.

fuse with the skin lipids and release enclosed drugs into the skin. Ethanol serves as a penetration enhancer by altering the fluidity of the lipid structure of the skin, thereby allowing the transport of drug molecules across the skin. Also, high flexibility imparted to the vesicles by ethanol allows them to squeeze through the skin layers and traverse the deeper skin layers thus enhancing skin accumulation and permeation.

CONCLUSIONS

Ethanol predominantly regulates the physicochemical characteristics of ethosomes. Through the present study, the potential of ethosomes as carriers of CPO for treatment of fungal skin infections is established.

REFERENCES

[1] M.A. Pfallera and D.A. Sutton, "Review of in-vitro activity of sertaconazole nitrate in the treatment of superficial fungal infections" *Diagn. Micr. Infec. Dis*., 56(2006) 147–152.

[2] M.H. Schmid and H.C. Korting, "Therapeutic progress with topical liposome drugs for skin disease" *Adv. Drug Deliv. Rev*., 18(1996) 335–342.

[3] K.S. Shaikh and A.P. Pawar, "Liposomal delivery enhances cutaneous availability of ciclopirox olamine" *Latin Am. J Pharm.*, in press.

[4] K.S. Shaikh, C. Bothiraja and A.P. Pawar, "Studies on non-ionic surfactant bilayer vesicles of ciclopirox olamine" *Drug Dev. Ind. Pharm.*, in press.

Surface Coated Lactose Carrier Dry Powder Inhalation Particles using a Fluid Bed System

I.Y. Saleem[1], T. Patel[1], M. Roberts[1]

School of Pharmacy and Biomolecular Sciences, Liverpool John Moores University, Liverpool, UK.

INTRODUCTION

Carrier particles play an integral role in dry powder inhalation (DPI) formulations, which include modulating drug-drug interactions during blending, improving powder flow and aiding the powder dispersion properties [1]. Accordingly, the drug particles must adequately separate from the carrier surface and thus the surface morphology plays a significant role in the dispersion properties of DPIs. Here we report on an alternative method for modifying the surface morphology of lactose carriers using a Ventilus® 1 fluid-bed system, to improve the aerosol dispersion properties of DPIs.

MATERIALS AND METHODS

1) *Surface Coating of Lactose Carrier*: Approximately 250 g of lactose carrier, Pharmatose 200M (P200M) (DeMelkindustrie Veghel Co, Netherlands) was placed into a Ventilus® 1 (Innojet, Germany) fluid-bed system and surface coated with an aqueous solution of 1% HPMC (Pharmacoat 603, Shin-Etsu Chemical Co. Ltd, Japan) 0, 5 and 10% P200M, and distilled water to 100%, using the IRN 2V spray nozzle for 3 h. The operating conditions (spraying rate, product temperature, airflow, spray air pressure and support pressure) of the fluid-bed system were optimised from preliminary experiments. After coating, the lactose-coated carrier powder was sieved using a Test Sieve Shaker (Endecotts Limited, UK) and collected on a 63 μm sieve.

2) *Preparation of Dry Powder Blend*: 2%w/w of micronised salbutamol sulphate was blended with sieved lactose-coated/uncoated carrier in a 10 ml vial and mixed using a Turbula® mixer (WAB, Switzerland) for 30 min (n = 3). The drug content was determined by UV at 276 nm.

3) *Aerosolisation Performance*: 20 mg of blended powder were placed into HPMC capsules (size 2) and aerosolised via a HandiHaler® into a next generation impactor at a flow rate of 60 L/min. Samples were collected by washing with distilled water and analysed by UV as above. The fine particle fraction (FPF) and mass median aerodynamic diameter (MMAD) were determined (n = 9) [2].

4) *Physical Characterisation*: Particle morphology was analysed using scanning electron microscopy (SEM) (FEI

Table 1. Physical Characteristics of Lactose-Coated/Uncoated Carrier

Carrier	Spray solution (%)		True Density (g/cm³)	Surface Area (m²/g)
	HPMC	P200M		
1	0	0	1.095 ± 0.125	11.034
2	1	0	1.167 ± 0.118	10.026
3	1	5	1.233 ± 0.077	9.060
4	1	10	1.244 ± 0.354	8.161

Table 2. Aerosol and Dispersion Properties of Salbutamol Sulphate from Different Lactose Carriers (n = 9)

Carrier	FPF	MMAD (μm)
1	7.60 ± 1.44	5.00 ± 1.00
2	11.43 ± 3.69	3.84 ± 1.05
3	19.37 ± 1.33	3.12 ± 0.41
4	15.57 ± 1.71	2.96 ± 0.54
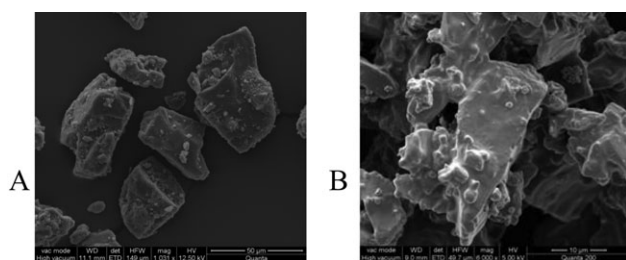
Fig. 1. SEM of Lactose-Uncoated (A) & Lactose-Coated (B) Carrier

Quanta 200, Japan). True density was measured using a Multipycnometer (Quantachrome Instruments, UK). The surface area of lactose-coated/uncoated carrier was determined using BET gas adsorption method.

RESULTS AND DISCUSSION

Increasing the concentration of spray solution enhanced the adhesion of the coating material, resulting in more P200M being coated onto the surface of the lactose carrier and hence a decrease in surface area (Table 1).

Furthermore, increasing the concentration of spray solution decreased the surface roughness of lactose-coated carrier compared to uncoated lactose, as represented by SEM (Fig 1). Increasing the spray solution concentration potentially resulted in more spray liquid coating the surface and filling the depressions.

The FPF was significantly higher than formulations containing the lactose-uncoated carrier (Table 2). This was due to the coating of the lactose carrier resulting in a smoother surface with minimum surface depressions and hence reduced drug particles being embedded in crevices/depressions on the surface, plus reduced adhesion forces between carrier and drug.

CONCLUSION

Surface coating of lactose carriers using the fluid-bed system, prior to drug blending, may be an alternative method of modifying the surface morphology to improve DPI dispersion.

REFERENCES

[1] A.J. Hickey et al, Physical characterisation of component particles included in dry powder inhalers. I. Strategy review and static characteristics. *J Pharm Sci.,* **96** (2007)1282–1301.

[2] M.R. Feddah, K.F. Brown, E.M. Gipps, N.M. Davies, "In-vitro characterisation of metered dose inhaler versus dry powder inhaler glucocorticoid products: influence of respiratory flow rates" *J. Pharm. Sci.,* **3** (2000) 317–324.

Sustained release HPMC microparticles for nasal delivery, prepared by a co-precipitation technique

I.R.A. Al-Obaidi, H.N.E. Stevens, F.J. McInnes

Strathclyde Institute of Pharmacy and Biomedical Sciences, University of Strathclyde, Glasgow, UK

INTRODUCTION

The nasal cavity is an attractive route for systemic absorption because of its large surface area, high blood perfusion and low enzymatic activity [1]. However, mucociliary clearance is the main problem of this route, clearing administered substances in approximately 21 minutes [2]. This study investigated a co-precipitation technique to produce sustained release polymer-drug bioadhesive microparticles, using hydroxypropyl methylcellulose (HPMC) as a bioadhesive polymer and metformin HCl (MH) as a model drug.

MATERIALS AND METHODS

1) *Preparation of microparticles*: Aqueous gels of HPMC (K100LV) alone and in combination with MH were prepared in two concentrations, 3% and 4% w/w (1:1 polymer:drug ratio). The gels were dropped in a controlled manner into acetone agitated using an electrical mixer at 8000 rpm to obtain microparticles. Microparticles were collected in a dry form by filtration.

2) *Microparticle loading efficiency*: Percentage of drug loading was measured by weighing 5 mg of each formula-

tion, dissolving in 20 ml of distilled water, then measuring absorbance using UV spectrophotometry at 233 nm.

3) *Moisture uptake measurement*: HPMC raw polymer and blank microparticles (prepared from a 4% solution) were stored at different relative humidities (43% RH, 65% RH and 85% RH using saturated salt solutions) at 25°C for 16 days. Thermo-gravimetric analysis (TGA) was performed for these samples to study the weight lost with heating from 20–240°C at a rate of 10°C/min.

4) *Dissolution study:* The release profiles of MH: HPMC microparticles (containing 1 mg MH according to loading efficiency), physical mixtures in the same ratio and 1 mg raw MH were studied using a Franz-cell diffusion apparatus. Water (20 ml) was used in the receptor compartment, 0.5 ml samples were withdrawn at regular intervals, and substituted rapidly with fresh media. Samples were analysed for MH content using UV spectrophotometry at 233 nm.

RESULTS AND DISCUSSION

Loading efficiency for MH was 53% and 45% for the 4% and 3%w/w formulations respectively. TGA results (Table 1) illustrate that raw HPMC took up significantly more water at 85% RH in comparison to 65% RH and 43% RH. This was expected due to the presence of hydrogen bonding groups in HPMC. Blank HPMC microparticles however, were affected by all humidities similarly.

The release profile of raw MH, and drug: polymer physical mixtures achieved 100% after 5 minutes, while both microparticle formulations demonstrated controlled release up to one hour (Figure 1). This is thought to be a result of the use of a matrix forming polymer in addition to altered water uptake by the formulation (as evidenced by TGA).

CONCLUSIONS

Sustained release MH: HPMC microparticles were obtained that achieved controlled release of a model drug. This is thought to be a result of modification of water uptake properties, which should be confirmed with further studies.

Table 1 Percentage water uptake at different relative humidities, determined by TGA

Formulation	Relative humidity		
	43%	65%	85%
HPMC raw powder	2.1	2.6	5.4*
Blank HMPC microparticles	3.3	3.8	3.3

*Significant ($P < 0.05$)
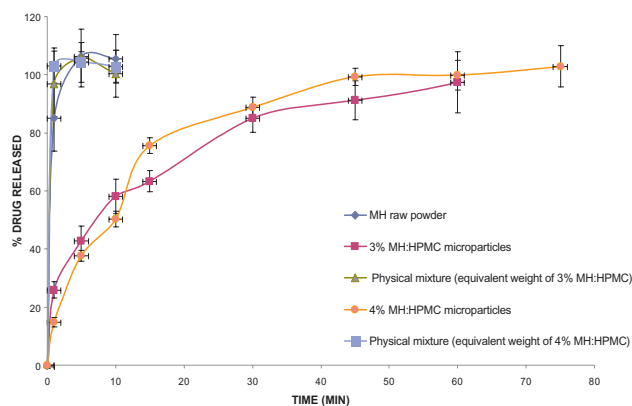
Figure 1. The release profile of MH from different formulations

ACKNOWLEDGMENTS

REFERENCES

[1] A.M. Hillery, A. W. Lioyd and J. Swarbrick, "Nasal Drug Delivery" in *Drug delivery and targetting for pharmacists and pharmaceutical scientists*, London and NewYourk, Taylor & Francis, 2001, ch. 9, pp. 215–243.

[2] P. Arora, S.H. Sharma and S. Garg, 'Permeability Issues in Nasal Drug Delivery' *Res. Focus,* **7** (2002) 967–975.

Sustained release of chlorhexidine from lyophilised wafers

O. Labovitiadi, A. Lamb, K.H. Matthews

School of Pharmacy and Life Sciences, Robert Gordon University, Aberdeen, UK.

Abstract – **A quantitative *in vitro* method for measuring the release of chlorhexidine digluconate (ChD) from a series of lyophilised wafers fabricated from natural polymers including sodium alginate (SA), xanthan gum (XG), karaya gum (KaG) and guar gum (GG) was undertaken. A free-standing dissolution raft (FSDR) designed and manufactured in-house was used. Results in PBS (pH 7.4) at 36.5°C indicated that the concentrations of ChD in PBS after eight hours ranged from 2.3 μg/mL for SA to 5.6 μg/mL for XG. These values were respectively 10 to 30-fold in excess of the minimum biocidal concentration (MBC = 0.4 μg/mL) for methicillin-resistant *Staphylococcus aureus* (MRSA). This demonstrated the potential of antimicrobial wafers for the topical treatment of wound infection.**

INTRODUCTION

Lyophilised wafers have been developed as topical vehicles for the delivery of therapeutic agents to suppurating wounds [1]. Inclusion of precise amounts of broad spectrum antimicrobial compounds may offer the possibility of effective dosing beyond the minimum biocidal concentrations of common wound pathogens such as MRSA. A reproducible quantitative method for determining the efficacy of antimicrobial wafers against planktonic colonies of bacteria, based on a modified Franz diffusion cell, has been reported [2]. There was a requirement to further quantify antimicrobial release in an enclosed dissolution apparatus that roughly modelled the topical wound environment.

MATERIALS AND METHODS

Shaped wafers containing a clinical concentration (0.5%v/v) of ChD were produced from solutions and gels of SA, XG, KaG and GG by freeze-drying in polystyrene plates (used as moulds). A dissolution apparatus (FSDR) was constructed as indicated (Fig.1). Wafers and gels were placed on the membrane in contact with the dissolution medium for the duration of the test. Samples (3 mL) were removed at hourly intervals for eight hours and [ChD] determined by UV analysis at 254 nm (Fig.2).

RESULTS AND DISCUSSION

The concentrations of ChD detected after eight hours varied from 8.30 ± 0.31 µg/mL for SA wafers, the slowest overall release, to a notable 68.63 ± 3.35 µg/mL for GG gel. The apparent decrease in [ChD] from 8–24 hrs for the latter sample was attributed to degradation of ChD with time. Most wafer samples, however, released ChD at a decreasing rate partly due to sink conditions enforced by the membrane and the low percentage of drug released (3.4–7.0% at 8 hrs for SA and GG wafers respectively). Clearly, a combination of equilibrium swelling and ChD/polymer interactions within the enclosed FSDR resulted in the bulk of the antimicrobial compound remaining in the swollen gel network. This is desirable behaviour for an *in situ* topical delivery system designed to adhere to a suppurating wound bed, especially when it is appreciated that the minimum biocidal concentration (MBC) for ChD against MRSA is 0.4 µg/mL.

CONCLUSIONS

Antimicrobial wafers appear fit for purpose with respect to the release of effective amounts of antimicrobial ChD in a simulated wound environment.
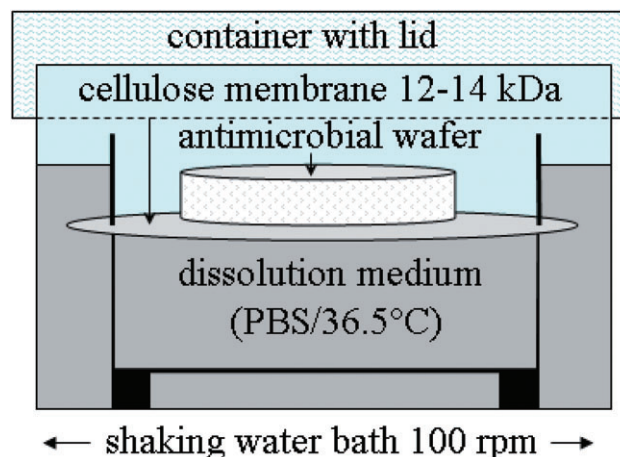
Fig.1. Schematic diagram of FSDR.
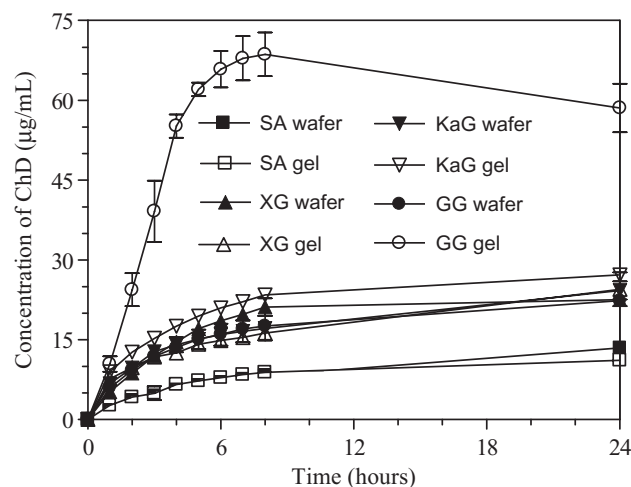
Fig.2. Release of ChD from wafers and gels (n = 3, SD)

REFERENCES

[1] K.H. Matthews, H.N.E. Stevens, A.D. Auffret, M.J. Humphrey and G.M. Eccleston, "Lyophilised wafers for wound healing" *Int.J.Pharm*, **289** (2005) 51–62.

[2] O. Labovitiadi, K. Matthews and A. Lamb, "Modified Franz diffusion for the *in vitro* determination of the efficacy of antimicrobial wafers against methicillin-resistant *S. aureus* (MRSA)" *J. Pharm. Pharma.*, **61**(supplement) (2009) A-19, 27.

Swelling, network parameters and permeability of poly (ethylene glycol)-crosslinked poly (methyl vinyl ether-co-maleic anhydride) hydrogels containing pore-forming agent

Thakur Raghu Raj Singh, A. David Woolfson, Ryan F. Donnelly

Queen's University Belfast, Belfast, Northern Ireland, BT9 7BL, UK

Abstract – **The swelling behaviour, network parameters and solute permeation of poly (ethylene glycol) (PEG)-crosslinked poly (methyl vinyl ether-co-maleic acid) (PMVE/MA) hydrogels containing pore-forming agent was investigated. Hydrogels with higher content of pore-forming agent showed higher percentage swelling and average molecular weight between crosslinks, *Mc*. Solute permeation increased with increasing pore-former concentration in the hydrogels.**

INTRODUCTION

In the present study, the effect of a pore-forming agent, sodium bicarbonate ($NaHCO_3$) on the swelling kinetics, network parameters and bovine serum albumin (BSA) permeation was investigated. Hydrogels were prepared from aqueous blends of 15% w/w of poly (methyl vinyl ether-co-maleic anhydride) (PMVE/MA) and 7.5% w/w of poly (ethylene glycol) (PEG 10,000 Daltons) containing 0, 1, 2, or 5% w/w of $NaHCO_3$ were evaluated for swelling and network parameters. In addition, the permeability of BSA through the equilibrium swollen hydrogels containing different percentages of $NaHCO_3$ was also investigated. The ultimate aim of this research was to develop hydrogels for controlled delivery of proteins.

MATERIALS AND METHODS

Aqueous polymeric blends of 15% w/w PMVE/MA and 7.5% w/w PEG 10,000 containing 0, 1, 2, or 5% w/w of $NaHCO_3$ were cast into films as described previously [1–3]. Films (1×1 cm^2) were crosslinked at 80°C for 24 h and were swollen in phosphate buffer saline (PBS) at pH 7.4 for 24 h at room temperature. Mechanism of water diffusion into the hydrogels was determined by the dynamic swelling studies.

Parameters, such as percentage equilibrium water content (% EWC), % swelling, molecular weight between crosslinks (M_c), crosslink density (q) and Flory-Huggins polymer-solvent interaction parameter were determined by mathematical treatment of swelling results. A modified Franz-cell setup was used to investigate the diffusion of BSA across swollen hydrogels.

RESULTS AND DISCUSSION

In general, increase in $NaHCO_3$ content increased the swelling of hydrogels. For example, the % EWC was 731, 860,
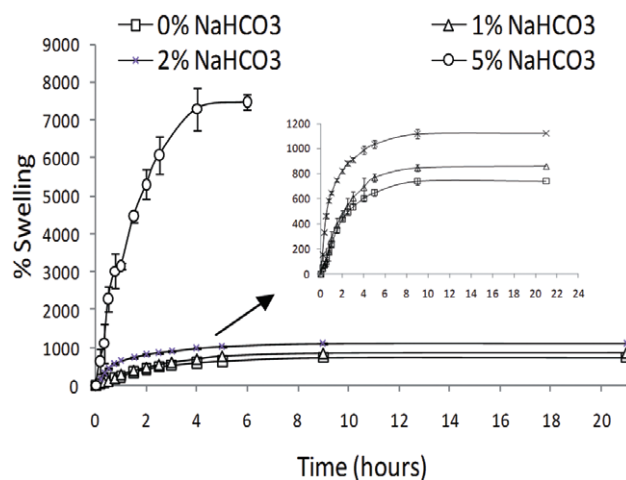

Figure 1. Percentage swelling of PEG-crosslinked PMVE/MA hydrogels containing different concentrations of $NaHCO_3$. Inset shows magnified view of swelling of hydrogels containing 0, 1 and 2% of $NaHCO_3$. Mean ± SD, N = 3.

1109 and 7536 % and the M_c was 8.26, 31.64, 30.04 and 3010.00 × 105 g mol^{-1} for hydrogels containing 0, 1, 2, and 5% w/w of $NaHCO_3$, respectively.

Furthermore, the crosslink density (q) of the hydrogels decreased with increase in $NaHCO_3$ content.

Permeation of BSA through the swollen hydrogels increased with increasing $NaHCO_3$ content, as shown in Figure 1. For example, the mean percentage cumulative permeation of BSA after 24 h was 14.71, 18.07, 33.56, and 63.05 % across hydrogels containing 0, 1, 2 and 5% w/w of $NaHCO_3$, respectively.

CONCLUSIONS

In conclusion, increase in the content of pore-forming agent in the hydrogels extensively affected their swelling properties which, in turn, resulted in increased pore size (determined from M_c values). In addition, a significant increase in the permeation of a model high molecular weight protein (i.e. BSA) was achieved. We are currently evaluating these systems for use as rate controlling membrane in sustained release drug delivery devices.

REFERENCES

[1] Thakur, R.R.S., McCarron, P.A, Woolfson, D.A., Donnelly, R. F, "Investigation of swelling and network parameters of poly (ethylene glycol)-crosslinked poly (methyl vinyl ether-co-maleic acid) hydrogels" *Eur Polym J*. **45** (2009) 1239–1249.

[2] Thakur, R.R.S., McCarron, P.A, Woolfson, D.A., Donnelly, R. F., 2009. "Investigation of solute permeation across hydrogels composed of poly (methyl vinyl ether-co-maleic acid) and poly (ethylene glycol)" *J. Pharm Pharmcol*. **62** (2010) 1–9.

[3] Thakur, R.R.S., McCarron, P.A, Woolfson, D.A., Donnelly, R. F, "Physicochemical characterisation of polyethylene glycol-plasticised poly (methyl vinyl ether-co-maleic acid) films". *J Appl Polym Sci*, **112** (2009) 2792–2799.

The effect of polymer architecture on polymer-lipid interactions within biological membranes

R.J. Green, H. Burnhams, J. Howgego, N. Gitonga, S. Odubanjo and F. Greco

School of Pharmacy, University of Reading, Reading, RG6 6AD, UK.

Abstract **– Towards controlling drug delivery, polymeric drug carriers can be developed into sophisticated delivery systems. To further understand polymer binding behaviour to lipid membranes, we have used biophysical methods to investigate the role of polymer architecture on lipid binding properties. In these studies, differences in polymer binding to lipid surfaces have been related to lipid surface charge and polymeric structure.**

INTRODUCTION

The increasing need for "smart" therapeutics (i.e. therapeutic agents that act solely at the desired site of action) has prompted the development of very sophisticated drug carriers. Amongst others, dendrimers (polymers characterised by a regular branching) are arousing significant interest as drug carriers due to their favourable characteristics (low polydispersity, possibility of different functional groups, high loading capacity). However, whenever medical applications are foreseen, it is vital to prove that these systems are non toxic and biocompatible. We have used biophysical methods (surface pressure measurements and external reflection FTIR spectroscopy) to investigate the interaction between a series of PAMAM and PEI polymers to lipid surfaces with the aim to assess how polymeric architecture influences the biomembrane binding behaviour of polymeric drug carriers.

MATERIALS AND METHODS

A Langmuir trough was used to prepare compressed monomolecular layers of anionic and zwitterionic phospholipids at the air/liquid interface. Polymer solutions were subsequently added to the aqueous subphase below the stabilised lipid surface [1]. Changes in surface pressure as a result of polymer addition indicated penetration of the polymer into the lipid layer. Using this experimental set up, external reflection (ER) FTIR spectroscopy at the air/liquid interface was also used to monitor polymer-lipid interactions and provided information regarding lipid layer structure and polymer adsorption.

RESULTS AND DISCUSSION

Differences in lipid binding of linear, branched and dendritic structures were investigated through varying both molecular weight and polymer concentration. It was found that both PAMAM and PEI interacted strongly to anionic lipid surfaces due to electrostatic interactions, leading to penetration into the lipid layer at all polymer concentrations studies (2–600 µg/ml). Binding to zwitterionic lipid surfaces was observed, however lipid layer penetration occurred only at high polymer concentrations (0.6 mg/ml). ER-FTIR spectroscopy confirmed interaction between the polymer and lipid layer at concentrations where lipid layer penetrations was not observed. Surprisingly, the effect of molecular weight and polymer architecture was less pronounced, with little observed difference between different PAMAM generations and different molecular weights of branched and linear PEI. The dendritic structure of PAMAM led to lipid binding occurring rapidly within the first 10 minutes of binding. However, the surface pressure continued to increase throughout the measurement time for branched and linear PEI suggesting further binding and penetration into the lipid layers beyond the initial interaction (Figure 1).

CONCLUSIONS

Differences in polymer binding as seen by surface pressure curves are linked to differences in the extent of polymer penetration into the lipid layer and rate of binding and can be related to polymeric characteristics, in particular flexibility. These observations impact on the polymer's potential role as an effective drug carrier.
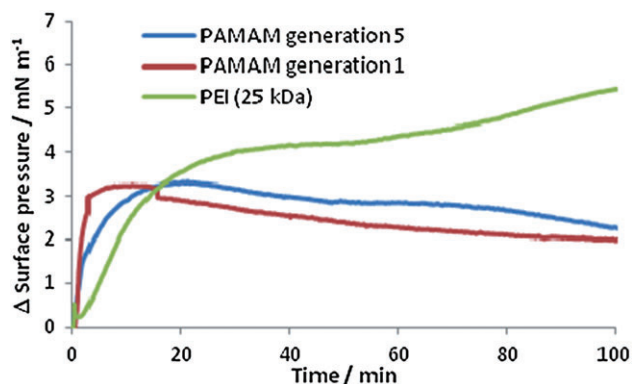
Figure 1. A graph of surface pressure verses time for PAMAM (Gen 1 and 5) and branched PEI binding to an anionic lipid layer (compressed to 20 mN m^{-1}). Polymer concentration in the aqueous subphase was 12 µg/ml in buffer (pH 7, 20 mM).

REFERENCE

[1] M. D. Lad, F. Birembaut, L. A. Clifton, L.A., R. A. Frazier, J. R. P. Webster & R. J. Green "Antimicrobial peptide-lipid binding interactions and binding selectivity" *Biophys. J.* 92 (2007) 3575–3586.

The Effect of Protectant/Anti-Adherent Concentration on the Liposomes throughout spray-drying

K.H. Chen, C.P. McCoy, R.K. Malcolm, V.L. Kett

School of Pharmacy, Queen's University Belfast, Belfast, UK

INTRODUCTION

Spray-drying is used to produce liposomal formulations as aerodynamic dried powders for inhalation, with minimal adverse effects on hydrolysis and oxidation of phospholipids [1]. The aim of this study was to investigate the effect of varying concentrations of disaccharide protectants sucrose or trehalose dihydrate and the anti-adherent L-leucine on key characteristics of liposomes containing the model indometacin that were prepared by both the ethanol injection and proliposome method.

MATERIALS AND METHODS

The liposomal dispersions composed of 25 mg/mL Soy phosphatidylcholine (≥80% purity, Lipoid) and 2.875 mg/mL Cholesterol (PhEur grade, Sigma-Aldrich), were prepared by both ethanol injection and proliposome methods. The effect of protectants concentration was firstly investigated, Hydration buffer containing 2.5, 5, 7.5, 10 and 15% (w/w) of sucrose or trehalose.dihydrate were used. Once the optimal sucrose or trehalose.dihydrate level had been determined then the effect of the addition of anti-adherent (L-Leucine) was investigated using concentrations of 0.25, 0.5 and 1% (w/w).

Spray-drying was performed with a Mini Spray-dryer Büchi 190 and the applied spraying parameters were: inlet temperatures 100 °C, outlet temperature 70 °C, spray-flow 600 Nl/h, aspirator setting 20, pump setting 2.5–3 ml/min.

Liposome size was determined with a ZetaSizer 3000HS (Malvern, UK). Encapsulation efficiency was determined by using Sephadex G-50 gel filtration & HPLC method. Phospholipid content was estimated by the Stewart assay. MDSC studies were performed to determine the glass transition temperature (Tg) of the spray-dried powders and TGA. *In vitro* release was performed by using a dialysis technique (dialysis membrane MWCO 7 kDa) and compared with release of unencapsulated drug. Morphology of the dried liposomes was observed by SEM.

RESULTS AND DISCUSSION

0.5% (w/w) L-Leucine was determined to be the optimal anti-adherent concentration since this revealed no significant change in liposome sizes before and after spray-drying ($p < 0.05$) (Fig 1.). Table 1 shows the characteristics of the optimal trehalose/L-leucine formulations produced by both methods. Similar values were seen for the formulation containing 10% (w/w) sucrose and 0.5% (w/w) L-Leucine. However, there were key differences in the Tg properties of the products; the optimal sucrose formulations exhibited Tg values of 46.21 ± 3.10 °C (ethanol injection) and 48.95 ± 4.97 °C (proliposome). While those formulated with 15% (w/w) trehalose.dihydrate and 0.5% (w/w) L-Leucine showed higher values of 70.81 ± 1.93 °C (ethanol injection) and 70.66 ± 3.08 °C (proliposome). SEM images showed that the liposome powders formulated with sucrose consisted of
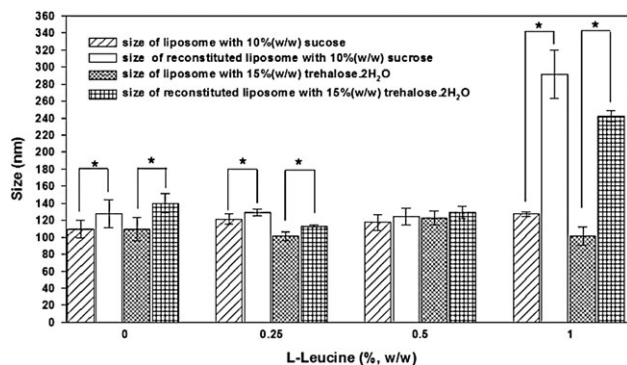
Fig 1. Effects of varying concentration of L-Leucine in combination with 10% (w/w) sucrose or 15% (w/w) trehalose.2H$_2$O on the liposome size prior to spray-drying and after reconstitution. *denotes P < 0.05 (t-test).

smooth spherical particles while those formulated with trehalose displayed shrinkage. Drug release studies showed that the liposomal formulations released circa 55% drug through the dialysis membrane over 24 hr compared with 80% over 4 hr for the unencapsulated drug.

CONCLUSIONS

Our studies confirmed that the inclusion of either 10% (w/w) sucrose and 0.5% (w/w) L-leucine or 15% (w/w) trehalose. dihydrate and 0.5% (w/w) L-Leucine could effectively protect liposomes from damage caused by spray-drying.

REFERENCE

[1] P. Goldbach, H. Brochart and A. Stamm, "Spray-Drying of Liposomes for a Pulmonary Administration. I. Chemical Stability of Phospholipids." *Drug Dev Ind Pharm.*, 1993. 19(19):2611–2622.

Table 1. The characterisation of liposomes with 15% (w/w) trehalose.dihydrate and 0.5% (w/w) L-Leucine.* denotes P < 0.05 (t-test).

Preparative methods	Ethanol injection		Proliposome	
	Before spray-drying	After reconstitution	Before spray-drying	After reconstitution
Liposome with 15% (w/w) trehalose.dihydrate and 0.5% (w/w) L-Leucine				
Liposome size (nm) & (PI index)	130.7 ± 2.7 (0.31 ± 0.03)	132.7 ± 4.2 (0.36 ± 0.02*)	138.5 ± 4.8 (0.52 ± 0.04)	127.3 ± 3.6* (0.40 ± 0.03*)
Encapsulation efficiency (%)	37.42 ± 6.41	42.46 ± 3.78	49.67 ± 7.12	51.95 ± 7.04
Encapsulated drug content (μg/mL)	165.3 ± 27.4	181.8 ± 16.5	447.5 ± 67.7	449.05 ± 66.0
Loading Efficiency (μg drug/ mg Lipid)	6.29 ± 0.93	7.18 ± 0.69	15.11 ± 2.24	15.69 ± 1.95
Liposome with 10% (w/w) sucrose and 0.5% (w/w) L-Leucine				
Liposome size (nm) & (PI index)	113.8 ± 14.7 (0.23 ± 0.04)	118.2 ± 10.9 (0.27 ± 0.04*)	137.9 ± 4.9 (0.48 ± 0.02)	134.0 ± 8.2 (0.39 ± 0.03*)
Encapsulation efficiency (%)	33.30 ± 3.90	45.04 ± 8.06*	45.40 ± 0.95	45.91 ± 2.3
Encapsulated drug content (μg/mL)	143.5 ± 9.9	183.1 ± 21.9*	397.6 ± 8.3	366.3 ± 23.7
Loading Efficiency (μg drug/ mg Lipid)	5.92 ± 0.45	8.15 ± 1.33*	14.44 ± 0.60	14.30 ± 1.81

The formulation and evaluation of a dry powder for pulmonary delivery in cystinosis

B.E. Buchan[1], G. Kay[1], K.H. Matthews[1], M.P. Ramsey[2], D. Cairns[1]

[1]School of Pharmacy and Life Sciences, The Robert Gordon University, Aberdeen, UK, AB10 1FR.
[2]GSK, Ware, Hertfordshire, UK, SG12 0DP.

Abstract – **Cystinosis is a rare genetic disease, the oral treatment for which currently requires the administration of capsules every six hours. This treatment causes frequent nausea, vomiting and the odorous metabolites present in the breath and sweat. Administration by inhalation may reduce this effect; therefore respiratory microspheres containing cysteamine were prepared and evaluated. The microspheres are within the size range 0.5–5 μm, show instant release and can travel to the levels representative of deep lung tissue. These results offer the possibility of a dry powder inhaler for the systemic treatment of cysteamine bitartrate.**

INTRODUCTION

Cystinosis is a rare autosomal recessive disease characterised by raised intracellular levels of the amino acid, cystine. The disease affects most organs in the body. Treatment for cystinosis involves the 6-hourly oral administration of cysteamine (Cystagon™), an aminothiol which possesses an offensive taste and smell [1]. A dry powder inhaler for systemic delivery could eliminate the foul taste and disruptive dosage regime that is experienced with the current oral treatment.

MATERIALS AND METHODS

Cysteamine bitartrate was synthesised and spray-dried with poly (D,L-Lactide) in ethyl acetate. The resulting powder was blended in various ratios with lactose (63–90 µm). SEM analysis was performed on the microspheres. Dissolution studies were undertaken using thiol specific DTNB reagent, in 50 ml of media (90% deionised water, 10% Tris buffer), stirred at 100 rpm and sampled every 5 mins. Testing was performed at 37°C.

Drug content in the microspheres was measured in parallel. Aerodynamic particle size was analysed using an Anderson Cascade Impactor (ACI).

RESULTS AND DISCUSSION

Microspheres were found to be spherical and in the size range of 0.5–5 µm (Fig 1), the size range required for optimal deep lung targetting. Cysteamine bitartrate was released instantly from the polymer, and 100% release was achieved within 2 minutes.

Microspheres were found to contain 50.33% cysteamine bitartrate. Initial ACI results show that microspheres can travel to the levels representative of deep lung tissue; 6.1% have an aerodynamic size of 4.1 µm.

CONCLUSIONS

Micro particles in the size range required for deep lung targetting were manufactured and characterised for drug content,
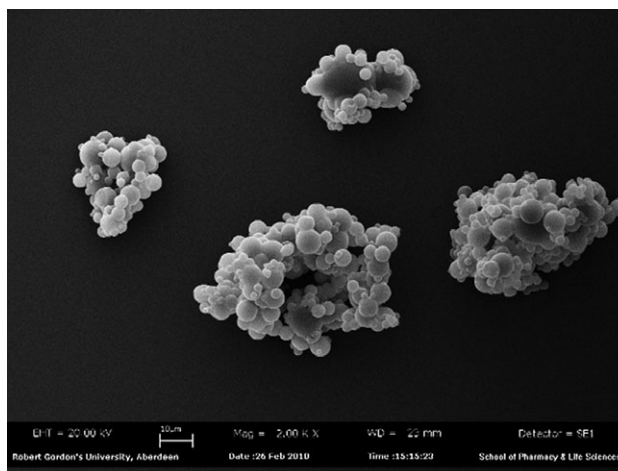

Fig. 1. Scanning electron microscopy (SEM) image of spray dried cysteamine bitartrate microspheres.

surface characteristics, dissolution and aerodynamic particle size. The microspheres were found to possess potentially ideal characteristics for delivering cysteamine through the lung. Further investigation will be required to confirm systemic delivery in the clinical setting.

ACKNOWLEDGMENTS

REFERENCE

[1] E. Levtchenko, M. Besouw, H. Blom, A. Tangerman, A. de Graaf-Hess, "The origin of halitosis in cystinotic patients due to cysteamine treatment" *Mol. Gen. Met.*, **91** (2007) 228–233.

The influence of sodium halides on the output and fine particle fraction of aerosols generated using air-jet and vibrating-mesh nebulisers

A.M.A. Elhissi[1], A. Vali[1], W. Ahmed[2]

[1]School of Pharmacy and Biomedical Sciences and [2]School of Computing, Engineering and Physical Sciences, University of Central Lancashire, Preston, UK

Abstract – **The presence of Na halides in solution highly affected the properties of the aerosols generated using a Sidestream air-jet nebuliser or an Aeroneb Pro vibrating-mesh nebuliser. In presence of halides, the Aeroneb Pro generated aerosols having greater output and higher fine particle fraction (FPF).**
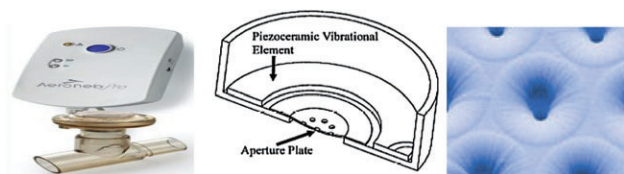
1310

Fig. 1. An Aeroneb Pro nebuliser (left) which operates using a perforated plate connected to a vibrational element (middle) to generate aerosols from dome-shaped apertures (right)

Fig. 2. Aerosol mass output of the halides using a Sidestream air-jet or Aeroneb Pro vibrating-mesh nebulisers

Fig. 3. FPF of the halide aerosols generated using a Sidestream air-jet or Aeroneb Pro vibrating-mesh nebulisers

INTRODUCTION

Air-jet nebulisers are well-established in generating liquid aerosols for pulmonary drug delivery. Alternatively, vibrating-mesh nebulisers have been recently commercialised. One model is the Aeroneb Pro which extrudes liquid through a mesh plate connected to a vibrational element to generate the aerosol (Fig.1) [1]. We found that dissolved NaCl markedly increased the aerosol output and reduced droplet size using vibrating-mesh nebulisers [2]. In this work, we studied the effect of halide type and concentration on the properties of the aerosols using air-jet and vibrating-mesh nebulisers.

MATERIALS AND METHODS

1) *Preparation of the halide solutions and determination of aerosol output*: HPLC-grade water was used to prepare NaCl or NaI (0.1%, 1% or 2% w/v) solutions. Nebuliser was filled with 5 ml of solution and nebulisation commenced to "dryness". The aerosol mass output was determined gravimetrically. The nebulisers investigated were the Sidestream-Freeway elite air-jet nebuliser (Respironics, UK) and the micropump Aeroneb Pro vibrating-mesh nebuliser (Aerogen Ltd, Ireland).

2) *Aerosol droplet size analysis*: Nebulisation of solutions was performed across a laser beam using the Spraytec laser diffraction size analyser (Malvern Instruments, UK). The fine particle fraction (FPF) of the aerosol was recorded. FPF is the fraction of aerosol that is likely to deposit in the peripheral respiratory airways (i.e. respiratory bronchioles and alveolar region).

FPF = Aerosol output X Aerosol fraction ≤5.41 μm

RESULTS AND DISCUSSION

The aerosol output of the Sidestream nebuliser was highly unaffected by the presence of Na halides. By contrast, even very small halide concentrations significantly increased ($P < 0.05$) the aerosol output of the Aeroneb Pro nebuliser which exceeded the output produced by the Sidestream device (Fig.2).

Na halides increased the FPF for both nebulisers. Except for deionised water, the Aeroneb Pro produced similar or higher FPF than the S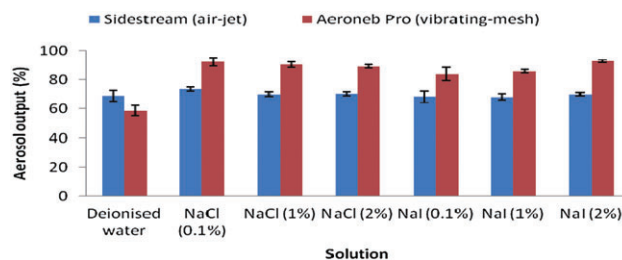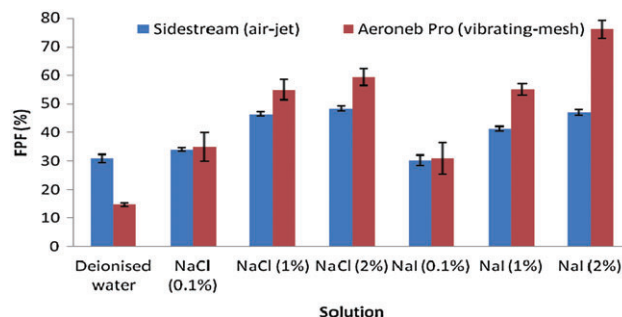idestream especially at high halide concentrations (Fig.3). Moreover, for the Aeroneb Pro nebuliser, NaI was more capable to increase the FPF when compared to NaCl (Fig.3). This might be attributed to the higher tendency of the iodide ions to concentrate at the air-water interface [3].

CONCLUSIONS

Aeroneb Pro nebuliser produced higher aerosol output and FPF than the Sidestream nebuliser when halides were included. The Aeroneb Pro nebuliser was more dependent on halide type and concentration.

ACKNOWLEDGEMENTS

We thank Aerogen Ltd, Ireland for supplying us with the Aeroneb Pro nebuliser.

REFERENCES

[1] R. Dhand, "Nebulisers that use a vibrating mesh or plate with multiple apertures to generate aerosol" *Respir. Care* **47** (2002) 1406–1416.
[2] T. Ghazanfari, A.M.A. Elhissi, Z. Ding and K.M.G. Taylor, The influence of fluid physicochemical properties on vibrating-mesh nebulisation. *Int. J. Pharm.* **339** (2007)103–111.
[3] P. Jungwirth and D.J. Tobia, "Ions at the air/water interface" *J. Phys. Chem.*, **106** (2002) 6361–6373.

The use of mathematical modelling to describe fluid flow within the colon

A. Timmis[1], D.J. Smith[1], R.H. Bridson[2], M.J.H. Simmons[2], S.P. Decent[1]

[1]School of Mathematics, University of Birmingham, Edgbaston, B15 2TT, UK.
[2]School of Chemical Engineering, University of Birmingham, Edgbaston, B15 2TT, UK.

Abstract – **Very few physical or theoretical models have been developed to assist with product development for oral colonic drug delivery. The aim here is to develop a theoretical mathematical model to describe the geometry of the colon and the fluid flows within it. This is part of a project which aims to predict the distribution and residence time of dosage forms in the colon e.g. whether they will reach the mucosal layer of the colon wall.**

INTRODUCTION

Oral colonic drug delivery may be utilised for both topical and systemic treatment. For the latter, relatively long residence times, low enzymatic activity and a mucus layer with a slower rate of turnover than the small intestine are advantageous.

Despite the importance of colonic mixing processes in health and drug delivery, there has been little research into the physical modelling of the colon. The physical movements can be divided into small oscillating 'haustral contractions', which occur regularly, and 'mass movements', which occur briefly several times per day. The current study is concerned with the haustration process, and the prediction of the flow and pressure gradients that will result from a simple model oscillation.

METHODS

A thorough search of the literature provided a starting point for describing the physiology and motion of the colon. We discuss the characteristic frequencies, pressures and flow velocities occurring in the colon, and how these parameters are used in our mathematical model.

The muscular contractions are represented by considering the wall of the colon as a solid oscillating boundary with a periodic pattern made up of oscillating 'sections' which drives the flow. The mathematical form of the model oscillation preserves the volume of fluid in a section. The flow is assumed to be axisymmetric, i.e. it does not vary significantly around the axis of the colon, a reasonable assumption given that the smooth muscle contracts as a ring.

Analytical methods then employed to determine properties of the fluid flow are lubrication theory and small amplitude analysis methods [1,2], with the no-slip boundary conditions on the moving colon wall.

RESULTS AND DISCUSSION

An initial expression for an oscillation which will preserve fluid volumes is given by
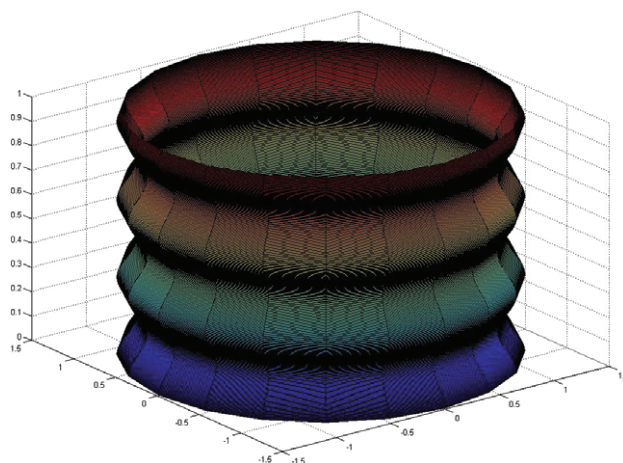

Fig. 1. Boundary representation with $R_0 = 1$, $a = 0.2$, $\lambda = 2$ and $T = 1$.

$$R = R_0 \sqrt{1 + a \cos\left(\frac{2\pi}{\lambda} z\right) \cos\left(\frac{2\pi}{T} t\right)},$$

where R_0 is the mean radius; a is the amplitude of the oscillation; λ is its wavelength; and T is its period. Figure 1 is a diagram of this oscillation at time $t = 0$.

Using this expression for the boundary of the colon, components of velocity were found for a Newtonian fluid in both the radial (towards/away from the tube axis) and the longitudinal (along the axis) direction in terms of the pressure profile. From our expression for the oscillation, the pressure can be calculated, and hence the flow field can be predicted.

CONCLUSIONS

Using a variety of established theories adapted to the physics of the colon it has been possible to find a mathematical representation of the wall of the colon and hence model the flow of a Newtonian fluid through this using two different analytic techniques in order to find the velocities and pressure of the fluid. Future work will include modelling particle tracking, and taking into account complex mucus and luminal fluid properties [3], as well as the consideration of multiscale models including the relationship between adsorption to the surface layers of the mucosa and the bulk flow within the lumen.

REFERENCES

[1] D.J. Acheson, *Elementary Fluid Dynamics*, Oxford, Oxford University Press, 1990.

[2] H. Ockendon and J.R. Ockendon, *Viscous Flow,* New York, Cambridge University Press, 1995.

[3] F.A. Morrison, *Understanding Rheology*, New York, Oxford University Press, 2001.

Transcutaneous Immunisation using Colloidal Carriers

Teerawan Rattanapak, Thomas Rades, Sarah Hook

School of Pharmacy, University of Otago, Dunedin, NZ.

Abstract **– The aim of this study was to formulate and characterise a number of immunogenic colloidal vaccine delivery systems capable of enhancing immune responses to a peptide vaccine. Cubosome formulations showed the highest skin retention *in vitro* (as compared to ethosomes, transfersome and liposomes) and stimulated both CD8 and CD4 responses in mice. Therefore, cubosomes appear to be the most promising colloidal carrier for TCI.**

INTRODUCTION

Transcutaneous immunisation (TCI) has many potential advantages over traditional immunisation however there is still the obstacle of delivering vaccine antigen through the stratum corneum (SC). The SC is the uppermost skin layer composed of densely packed corneocytes and provides a formidable barrier to peptide vaccine antigens. A range of approaches have been used in order to enhance TCI, here we have investigated the ability of colloidal carriers (liposomes, tranfersomes, ethosomes [1] and cubosomes [2]) to deliver a peptide vaccine to the skin both *in vitro* and *in vivo*.

MATERIALS AND METHODS

Formulations: *Liposomes and transfersomes* – phosphatidlycholine (PC, 20 mg/mL), tween 80 (20 mg/mL, for transfersomes) +/− monophosphoryl lipid A (MPL, 0.2 mg/mL) were dissolved in chloroform and evaporated to dryness. The thin film was rehydrated with an aqueous solution of a dye-labelled model peptide (TMR-SIINFEKL, 1 mg/mL) +/− Quil A (0.4 mg/mL). The resulting vesicles were extruded. *Ethosomes* **–** PC +/− MPL were dissolved in chloroform and evaporated to dryness. The thin film was dissolved in ethanol (30%v/v). An aqueous solution of peptide +/− Quil A was added gradually to the stirred lipid solution. *Cubosomes* – phytantriol (20 mg/ml), poloxamer 407 (3 mg/ml) +/− MPL were dissolved in chloroform and evaporated to dryness. A concentrated solution of peptide +/− Quil A was added and mixed until it was visually homogenous. Water (5 ml) was added and the formulation was vortexed for 10 min. **Skin retention**: 100 μL samples of formulation were applied onto still-born piglet skin mounted on Franz diffusion cells which were then covered with tinfoil and Parafilm. Samples were taken at predetermined intervals and retention determined. The amount of peptide in the skin extract was determined by fluorescence spectroscopy. For confocal microscopy skin was examined using Zeiss LSM 510 confocal laser scanning microscope. **In vivo immunogenicity:** C57Bl/6 mice were adoptively transferred with transgenic OT-I and OT-II cells. On day 0 and 14, 100 μL of formulation was applied to shaved, depilated skin which was then covered with an occlusive dressing for 24 hours. Expansion of antigen reactive cells and antibody titres were measured on day 17 by flow cytometry (BD FACSCanto) and ELISA respectively [3].

RESULTS AND DISCUSSION

Characterisation of formulations: All lipid carriers possessed a negative charge and a vesicle size in the range of 100–200 nm. High entrapment efficiency of model peptide was achieved with liposomes, transfersomes and ethosomes (>65%). The lower entrapment in cubosomes (~20%) was likely due to the presence of open water channels and the small size of the peptide. **Skin retention:** The cubosome and ethosome formulations showed the highest skin retention (Figure 1). The low penetration with the transfersome formulation may be due to occlusion negating any hydration gradient. The inclusion of the adjuvants MPL and Quil A in the formulations increased retention.

Confocal microscopy showed that with all the formulations the peptide predominantly co-localised with hairs. However more diffuse staining of the skin was apparent for the cubosome formulation. **In vivo immunogenicity**: Peptide vaccines delivered in colloidal carriers stimulated immune
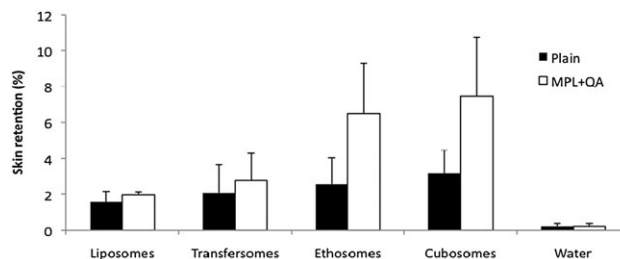

Figure 1. Skin retention is expressed in term of percentage of peptide in the skin.

responses greater than those stimulated by peptide plus adjuvant in water. The cubosome formulation stimulated the largest response with both CD8 and CD4 activation being detected.

CONCLUSIONS

The skin retention of all lipid carrier systems was higher than reference vehicle, however the model peptide was found mostly bound to the SC and hair. Inclusion of adjuvants increased retention most likely due to the penetration enhancing effect of Quil A [4]. Cubosomes stimulated both CD4 and CD8 immune responses demonstrating the potential of these carriers for TCI.

REFERENCES

[1] J. Myschik, T. Rades and S. Hook, "Advances in Lipid-Based Subunit Vaccine Formulations" *Curr. Immunol. Rev.*, **5** (2009) 42–48.

[2] S. Rizwan, Y. Dong, B. Boyd, T. Rades and S. Hook, "Characterisation of bicontinuous cubic liquid crystalline systems of phytantriol and water using cryo FESEM" *Micron,* **38** (2006.) 478–485.

[3] W. McBurney, D.G. Lendemans, J. Myschik, T. Hennessy, T. Rades and S. Hook, "In vivo activity of cationic immune stimulating complexes (PLUSCOMs)*" Vaccine*, **26** (2008) 4549–4556.

[4] H. Madsen, P. Ifversen, F. Madsen, B. Brodin, I. Hausser, and H. Nielsen, "In vitro cutaneous application of ISCOMs on human skin enhances delivery of hydrophobic model compounds through the stratum corneum" *AAPS Journal*, **11** (2009) 728–739.

Triple-layered Solid Matrix Tablet Configurations for Constant Multiple Drug Delivery

K. Moodley[1], V. Pillay*[1], Y.E. Choonara[1], L.C. Du Toit[1]

[1]University of the Witwatersrand, Department of Pharmacy and Pharmacology, 7 York Road, Parktown, 2193, Johannesburg, South Africa.
*Correspondence: viness.pillay@wits.ac.za

INTRODUCTION

The purpose of the study was to establish an optimal triple-layered tablet formulation that is capable of providing zero-order release of three different water soluble drugs. Drug release profiles were compared to those depicted by commercial drug products SLEEPEZE-PM® containing diphenhydramine (DPH), Ranihexal® containing ranitidine (RDH) and Phenergan® containing promethazine (PMZ).

MATERIALS AND METHODS

1) *Experimental design:* A Box-Behnken experimental design template comprising 17 formulations was generated using Minitab® V15 software after obtaining formulation variables during preformulation.

2) *Preparation of formulations*: Drug-loaded triple-layered tablet (TLT) matrices were prepared by direct compression according to the design template with varying polymer and salt quantities. Polymers employed were polyamide 6,10 (PA6,10), PEO WSR 301 and salted-out PLGA (s-PLGA). Sodium sulphate (SS) was combined with PA6,10. Model drugs loaded into the TLT formulations were DPH, PMZ and RDH.

3) *In vitro dissolution testing:* Formulations were subjected to *in vitro* dissolution testing using a USP 25 rotating paddle method in a dissolution apparatus (Caleva Dissolution Apparatus, model 7ST; G.B. Caleva Ltd., Dorset, UK) at 50 rpm with 900 mL simulated gastric fluid (SGF) (pH 1.2; 37°C) and 900 mL phosphate-buffer solution (PBS) (pH 6.8; 37°C High performance liquid chromatography (HPLC) was employed to analyse *in vitro* dissolution samples.

4) *Textural profile analysis:* A calibrated TA.*XTplus* Texture Analyser (Stable Microsystems, UK) was used to determine the Brinell Hardness Number (BHN) of various formulations.

5) *Morphological characterisation:* Scanning electron microscopy (SEM) was utilised to ascertain the surface morphology of the matrices after compression.

RESULTS

In vitro dissolution results revealed capability to provide zero-order drug release of all three drugs from certain TLT formulations. Drug release profiles from these formulations illustrated linear release of DPH, PMZ and RDH over 24 hours. A trend was observed that showed a higher PA6, 10 to SS ratio presented with a more linear release of DPH and higher BHN values, which may be explained by a higher mechanical stability [1] due to a more efficient compact matrix allowing for adequate retardation of drug release, while a lower s-PLGA to PEO ratio presented with a more linear release of RDH from the outer layer and higher BHN values, the s-PLGA may control the swelling of PEO resulting in uniform drug release. The formulations containing PA6,10 within the range of 200–350 mg and s-PLGA within the range of 50–100 mg illustrated more desirable linear release profiles. The middle (second) layer was kept constant at 350 mg of PEO. The optimised formulation profile depicted a significant superior release of DPH, PMZ and RDH as compared to the respective commercial products. The disintegration times of SLEEPEZE-PM® tablets, Ranihexal® tablets and Phenergan® tablets were approximately 1 hour, 1 hour and 30 minutes respectively. SEM showed irregular surfaces with minimal pores.

CONCLUSIONS

This study has provided evidence that the TLT formulations are capable of providing improved uniform release of three different water soluble drugs which may be greatly beneficial for further application in combination therapy for various disease states.

ACKNOWLEDGEMENTS

REFERENCE

[1] R. Patel, V. Pillay, Y.E. Choonara and T. Govender, "A Novel Cellulose-Based Hydrophilic Wafer Matrix for Rapid Bioactive Delivery" *Journal of Bioactive and Compatible Polymers,* **22** (2007) 119–142.

Understanding the Cause of Increasing Dose Through Life from a Pressurised Metered Dose Inhaler (pMDI)

A.C. Colombani, F. Chambers, K. Lee, R. Jansen, D. Hodson

AstraZeneca, Medicines Development, Loughborough, UK.

Abstract **– The root causes of increased dose through life of the rapid fill/rapid drain type of valves was investigated. The primary cause of rise is probably a wash back effect.**

INTRODUCTION

The conventional metering valves, used for pressurised Metered Dose Inhalers, store the next dose in the valve metering chamber. In an alternative type of valve, called rapid fill/ rapid drain (RF/RD) valves, the metering chamber stays open to the bulk when the valve is in resting position. The metered-dose is only separated from the bulk during actuation. Different variants of the RF/RD valves were thoroughly evaluated for function and pharmaceutical performance [1]. All valves performed well in terms of pressure filling, water ingress and other mechanical requirements; however they all had one major flaw. In every case the delivered dose was found to increase through the life of the inhaler.

MATERIALS AND METHODS

Four 1.6 mg/mL budesonide suspension formulations and 2 beclometasone dipropionate solution formulations (~60% and 30% of the saturated solubility) were prepared and pressure-filled in cans crimped with a 50 μL RF/RD valve [2]. The delivered dose was tested through the life of the product. A multi-way experimental design was used to study the effect of shake technique, shake velocity, automated waste firing (between sampling points), canister orientation during storage and firing force [1].

Table. 1. Effect of formulation type on dose increase through life

Formulation type	Creaming Suspension		Sedimenting Suspension		Solution	
	Slow	Fast	Slow	Fast	Conc.	Diluted
Dose increase % RTL	32	28	26	18	30	14

RESULTS AND DISCUSSION

One of the leading theories to explain the dose rise was that the drug was flocculating and the larger flocculates were prevented from entering the metering chamber due to the complex flow path. However, several studies with different valve designs and formulations proved this to be unlikely. As an example, some solution formulations still exhibited a high rise through life (RTL, Table 1).

Three suspension formulations yielded similar dose rise through life. The lower RTL of the fast sedimenting formulation could be explained by an increased concentration in the metering chamber, opposing the process which increases bulk concentration. Secondly, the concentrated solution formulation was close to saturated solubility and had the potential to crash out of solution during actuation. Finally, the use of automated waste firing systems reduced the dose rise through life of the slowly creaming suspension tested by approximately 5% compared to manual waste firing.

In an RF/RD valve, if part of the dose is not delivered, it is not retained within the metering chamber and the drug is potentially washed back into the bulk, causing a steady rise in concentration. To test this theory an RF/RD valve was
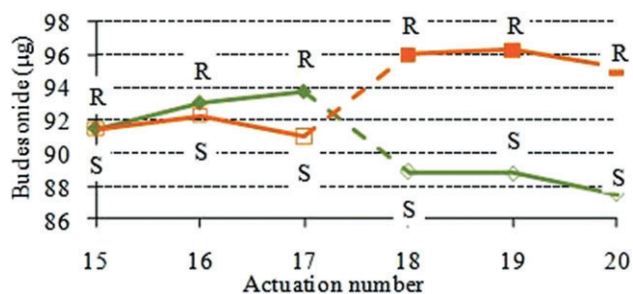
Fig. 1. Dose from an RF/RD valve fired in Standard mode **S** and Retention mode **R**

tested in 'retention mode' – i.e., the valve stem was kept depressed during shaking so that any retained drug could not be re-dispersed into the bulk, except during the turbulent refill event. The RTL dropped by 15% when the valve was used in retention mode.

A theoretical model was developed to predict the RTL and calculate the percentage of compound retained within the chamber at the end of the actuation.

Using a RTL of 29% and a target dose of 80 µg/act, the model calculates that 13.6% of the dose is not delivered and

washes back to the bulk after each actuation. The dose is predicted to rise from 70 µg/act to 90 µg/act, which fits the data. The same calculation was made for the RF/RD valve actuated in retention mode, which exhibited a mean RTL of 14%. The washback dropped from 13.6% to 5.9% of the dose. The difference corresponds to the 5 µg/act shown in Figure 1, where the actuation modes are switched.

CONCLUSIONS

The primary mechanism for the observed increase in delivered dose through life with an RF/RD valve is probably an incomplete delivery of the dose, leading to drug retention in the valve metering chamber and followed by a washback to the bulk. Incomplete transfer of drug from the bulk is a secondary mechanism, related to the size and buoyancy of the flocculates in specific types of formulations.

REFERENCES

[1] Wilby M. (2005), "Increasing Performance consistency of pMDIs", *Drug Del. Technol*., **5** (9), p58
[2] Purewal T.S., "Formulation of Metered-Dose inhalers", Purewal T.S. and Grant D.J.W. (Eds), *Metered Dose Inhaler Technology* (1998), Interpharm Press, Inc., Buffalo Grove, Illinois

Versatile Solid Lipid Nanoparticles for Controlled Drug Delivery

J. Chana, B. Forbes, S.A. Jones

Pharmaceutical Science Division, King's College London, 150 Stamford Street, London, SE1 9NH, UK.

INTRODUCTION

Nanoparticles are promising drug delivery carriers as they can improve chemical stability, control drug release and alter drug pharmacokinetics. However, it is extremely difficult to manufacture non-toxic nanocarriers with low polydispersity and an appropriate abundance in suspension to meet the dosing requirements of many therapeutic agents [1]. Phase inversion of emulsions is capable of generating concentrated solid lipid nanoparticle (SLN) suspensions [2]. Using this process particles are fabricated by precipitation from emulsions of oil, water and surfactant. The resultant particles comprise a solid phospholipid shell surrounding a liquid triglyceride (oil) core and are stabilised by an exterior surfactant layer. Although these SLNs have potential for controlled delivery, the dependency of particle formation on emulsion composition has not previously been reported in detail. The aim of this work was to understand how changes in emulsion composition affect the particle size distribution of SLN suspensions.

MATERIALS AND METHODS

Triglycerides (Labrafac®), sodium chloride 3 % w/v in water and the surfactants macrogol hydroxystearate (Solutol®) and

soyabean lecithin (Phospholipon®) were mixed at room temperature and then subjected to several controlled heating and cooling cycles, between 60 °C and 85 °C, at a rate of 4 °C/min. The temperature cycling converted an oil-in-water nano-emulsion to and from a water-in-oil nano-emulsion (phase inversion), due to the thermo-dependent orientation of Solutol®. The subsequent addition of cold water, causing solidification of the Phospholipon® shell, resulted in a nanoparticle suspension. SLNs were purified of excess excipients and larger particulate matter using centrifugation at 100,000 *g* for 60 min. The purified particles were diluted with water for size distribution analysis using photon correlation spectroscopy (Beckman Coulter Delsa Nano C). Data represent the mean particle size ± the standard deviation to indicate the particle size distribution.

RESULTS AND DISCUSSION

SLN with a size of 48.9 ± 9.3 nm were generated when a 1:1 mass ratio of Labrafac® to Solutol® was used (figure 1). Both the particle size and dispersity increased (81.3 ± 46.4 nm) when the oil loading was increased from 17 % w/w to 25 % w/w whilst the surfactant was maintained at 17 % w/w. Increasing the surfactant to 25 % w/w to provide a 1:1 mass
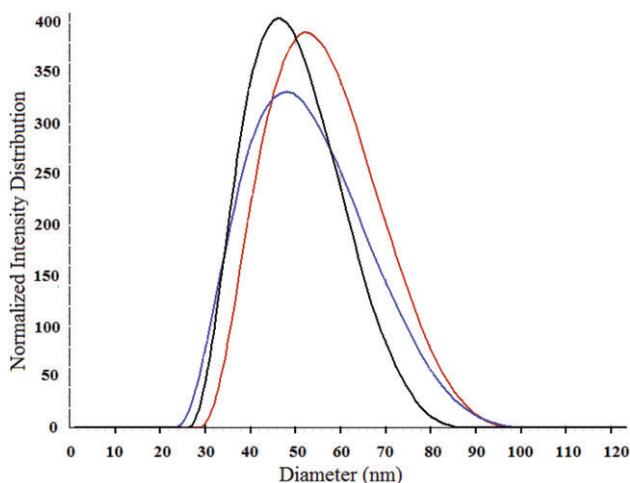
Fig.1. Intensity distribution for SLN generated from an emulsion containing 17% Labrafac® and 17% Solutol®. Size analysis performed in triplicate using photon correlation spectroscopy.

ratio restored the SLN size to 50.0 ± 11.1 nm. Replacing the medium chain triglyceride, Labrafac®, with a more hydrophobic long chain triglyceride, soybean oil, caused phase separation at an oil loading of 17 % w/w and 1:1 oil:surfactant ratio. Reduction of the loading of the soybean oil to 15 % w/w and

increasing surfactant concentration to 19 % w/w was required to form the SLN with a size of 47.4 ± 21.4 nm.

CONCLUSIONS

The ratio of oil and surfactant phases within this system has a marked influence on the size and polydispersity of the SLNs generated. The surfactant plays a crucial role in stabilising the system by coating oil droplets and minimising surface free energy. An increase in oil loading or hydrophobicity must be supported by a corresponding increase in surfactant concentration to maintain emulsion stability. Particle fabrication from the emulsions generated concentrated SLN suspensions. The ability of the system to accommodate changes in composition demonstrates a versatility that makes this SLN platform well suited for controlled drug delivery.

ACKNOWLEDGMENTS

REFERENCES

[1] A. A. Date and V.B. Patravale, "Current strategies for engineering drug nanoparticles" *Current Opinion in Colloid & Interface Science*, **9** (3) (2004) 222–235.

[2] B. Heurtault, P. Saulnier, B. Pech, J.E. Proust and J.P. Benoit, "A novel phase inversion-based process for the preparation of lipid nanocarriers" *Pharmaceutical Research*, **19** (2002) 875–880.

Esterase activity in the Human Bronchial Epithelial Calu-3 Cell Line

F. Bayard[1], T. Calande[2], D.I. Pritchard[3], W. Thielemans[4], S. Young[5], S. Paine[6], C. Bosquillon[2]

[1]Doctoral Training Centre in Targeted Therapeutics, School of Pharmacy
[2]Division of Drug Delivery and Tissue Engineering, School of Pharmacy
[3]Molecular and Cellular Sciences, School of Pharmacy
[4]School of Chemistry and Process and Environmental Research
University of Nottingham, University Park, Nottingham, NG7 2RD
[5]Bioscience
[6]Department of Drug Metabolism and Pharmacokinetics, AstraZeneca R&D Charnwood

Abstract – **The presence of an esterase activity in Calu-3 cells was demonstrated by quantifying the extracellular conversion of p-nitrophenyl acetate into p-nitrophenol. This initial study allowed the calculation of Vmax = 93. 7 pmol.min^{-1} per μg of proteins and the Michaelis-Menten constant Km = 1265 μmol.L^{-1}.**

INTRODUCTION

The human bronchial epithelial cell line Calu-3 is extensively used as an in vitro model of the airway epithelium [1]. A large range of esterases are well known to be present in the lungs [2]. Therefore, the aim of this work was to determine whether Calu-3 cells exhibit any esterase activity.

MATERIALS AND METHODS

Calu-3 cells (passage 37) were grown on 24-well plates for 7 days, at 37°C and in 5% CO_2. Cells were washed with Hanks' Balanced Salt Solution (HBSS) and the medium was replaced by p-nitrophenyl acetate (100 to 2000 μmol.L^{-1}) or p-nitrophenol solutions. The two compounds were dissolved in DMSO to prepare solutions in HBSS/DMSO 0.1% (v/v). Fifty μL of solution were sampled after 21, 42, 75 and 144

minutes, they were diluted with 50 μL of NaOH 10^{-6} M and the absorbance was read at 410 nm. Total protein content was quantified after cell membrane disruption using a RC DC protein assay. Autohydrolysis of p-nitrophenyl acetate was assessed in HBSS/DMSO after 144 minutes of incubation at 37°C. Accuracy of measurement was tested by applying a solution of p-nitrophenol onto the cells and measuring the concentration after 144 minutes of incubation. Km and Vmax were calculated using the Lineweaver-Burk plot (Equation 1).

$$\frac{1}{V_0} = \frac{K_m}{V_{max}}\frac{1}{[S]} + \frac{1}{V_{max}}$$ (*Equation* 1)

RESULTS AND DISCUSSION

Autohydrolysis of p-nitrophenyl acetate in absence of cells was quantified as 5–8% of the initial concentration, after 144 minutes. Only 60% of initial p-nitrophenol applied at the surface of the cell layer was recovered after 144 minutes of incubation, for two different concentrations. Further investigation is needed to determine whether p-nitrophenol is absorbed or metabolised by the cells.

The amount of p-nitrophenol assayed in the incubation medium per micrograms of proteins following exposure of Calu-3 cells with p-nitrophenol acetate versus the time is shown on Figure 1. The plot suggests Michaelis-Menten kinetics. Vmax was determined as 93.7 pmol.min^{-1} per μg of protein and Km as 1265 μmol.L^{-1}.

CONCLUSIONS

This initial study demonstrates the presence of an esterase activity in Calu-3 cells and indicates the cell line might be a suitable model for metabolic studies in the bronchial epithelium. However, a more in-depth investigation is needed to explain the apparent loss of material measured when a p-nitrophenol solution of a known concentration is applied
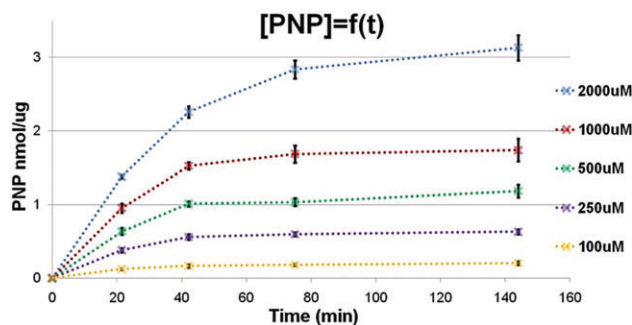

Figure 1: Amount of p-nitrophenol per micrograms of proteins measured in the incubation medium throughout the time for different initial concentrations of p-nitrophenyl acetate. Data are presented as mean ± SD (n = 3 wells)

onto the cells. Vmax and Km must be recalculated at high concentrations of p-nitrophenyl acetate that saturate Calu-3 esterase activity and both intra and extracellular concentrations of the hydrolysed product must be measured.

ACKNOWLEDGMENTS

REFERENCES

[1] B. Forbes and C. Ehrhardt, "Human respiratory epithelial cell culture for drug delivery applications" in *5th International Conference and Workshop on Cell Culture and In Vitro Models for Drug Absorption and Delivery: Feb 25-Mar 05 2004; Saarbrucken, GERMANY*, Elsevier Science Bv (2004) 193–205.

[2] A. E. Vatter, O. K. Reiss, J. K. Newman, K. Lindquist and E. Groeneboer, "Enzymes of the lung. I. Detection of Esterase with a New Cytochemical Method" *Journal of Cell Biology*, **38** (1968) 80–98.

A novel nanoscale approach for studying the structure and stability of solid dispersions

M. Bunker[1], J. Zhang[1], <u>A. Parker</u>[1], C.E. Madden-Smith[1], and C.J. Roberts[1].

[1]Molecular Profiles, 8 Orchard Place, Nottingham Business Park, Nottingham, NG8 6PX, UK.

INTRODUCTION

Formation of a solid solution or dispersion of a drug in a water-soluble polymer is one of the primary techniques for improving the dissolution rate and bioavailability of a poorly water soluble drug. Characterising the state of the drug inside a polymer matrix is important since issues such as stability, safety and efficacy can be greatly affected.

Here we present a novel application of nanothermal analysis (nano-TA) to investigate the heterogeneity of model drug/polymer formulations with the purpose of developing a

detailed understanding of the stability of a drug polymer solid solution using nano-TA supported by atomic force microscopy (AFM) imaging. Felodipine-poly(vinyl pyrrolidone) (PVP) solid dispersions were studied at different concentrations and after storage at different relative humidities (RH).

MATERIALS AND METHODS

Nano-TA is a localised, nanoscale thermal analysis technique combining high resolution AFM imaging with the characteri-
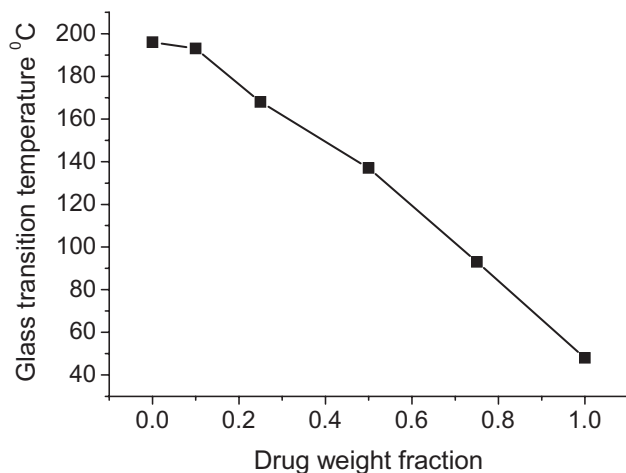
Figure 1. Plot of T_g against drug weight fraction for felodpine-PVP solid dispersions measured using nano-TA.

sation of thermal properties based on a physical deflection of a micro cantilever mounted probe in response to the sample as it is heated. Solid dispersions were prepared at varying drug concentrations from solution by spin coating. The stability of a sample with 25% drug was tested after stressing by exposure to 60% and 75% RH for up to 3 days.

RESULTS AND DISCUSSION

Nano-TA was used to measure the glass transition temperature (T_g) of dispersions with varying amounts of felodipine, showing an approximately linear decrease with increasing drug content (Figure 1).

AFM imaging was used to track the evolution of surface morphology of the 25% drug loaded formulation during exposure to high RH. A homogenous surface consistent with a solid solution was initially observed. Further imaging showed that whilst exposure to 60% RH had no influence on surface morphology, 75% RH causes changes in surface features with the appearance of distinct heterogeneity. AFM phase imaging shows a clear contrast indicating differences in material properties, and highlighting the early stages of nucleation and the subsequent growth of needle shaped crystals of felodipine within the polymer matrix.

CONCLUSIONS

Nano-TA in combination with AFM imaging provides a novel approach to study the behaviour of drug-polymer dispersions. Here we can use the technique to measure the Tg of such systems at varying drug concentrations under stressed conditions. AFM imaging reveals the very earliest stages of felodipine nucleation and crystal growth upon storage at high RH. Hence, this approach is able to study the critical point of the onset of instability in the felodipine-PVP dispersion system, and is suitable for rapid stability screening of different drug loadings and storage conditions of solid solutions, with a minimum of drug sample required.

An Investigation into the Structural Properties of Trehalose in Relation to Cryoprotection: Analysis of Thermal Transitions of Trehalose Dihydrate

Bahijja Raimi-Abraham[1], Susan Barker[1] and Duncan Craig[1]

[1]School of Pharmacy, University of East Anglia, Norwich, UK.

INTRODUCTION

The cryoprotectant activity of trehalose is thought to be related to its glass forming ability. As trehalose exists in multiple forms, interconversion between forms may have significant impact on its functionality. Here we have used DSC with extremely slow and fast heating rates to study the interconversion profile of crystalline trehalose dihydrate (TD).

MATERIALS AND METHODS

TD was purchased from Sigma-Aldrich. Modulated Temperature DSC (MTDSC) was carried out using TA Instruments DSC Q2000 with heating rates of 0.5 to 2.0°C/min (+/− 0.212°C modulation, 60 second period) in pin-holed pans. High speed DSC (HyperDSC®) was carried out using Perkin Elmer 8500 with 2nd generation HyperDSC® technology with heating rates of 50 to 750°C/min. Thermogravimetric analysis (TGA) was carried out using a TA instruments Hi-Res 2950 instrument at a rate of 2°C/min from 30°C to 250°C in open pans.

RESULTS AND DISCUSSION

Slow (0.5°C/min) MTDSC experiments showed a single endothermic peak at ~94°C; the modulated signal and slow rate allowed measurement of the heat capacity through the process itself. No further transitions were seen up to 150°C. On cooling, T_g was seen at 119.5°C which was observed on reheating, followed by crystallisation and melting shown in
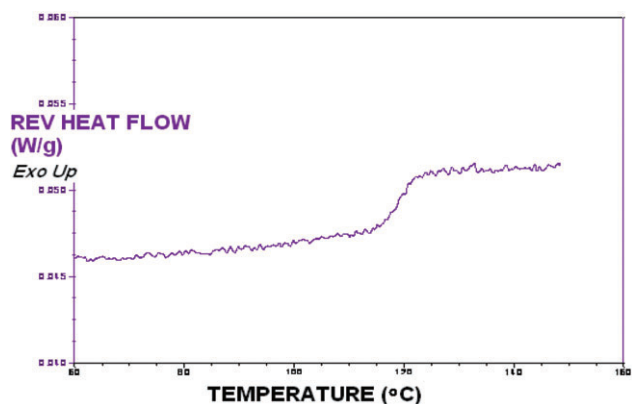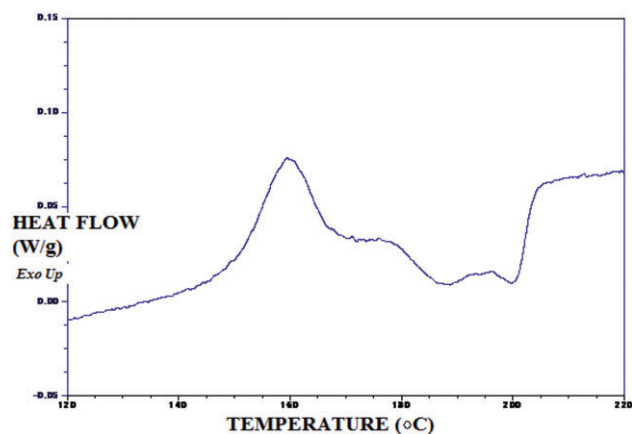
Fig.1 TD MTDSC Cooling 0.5°C/min

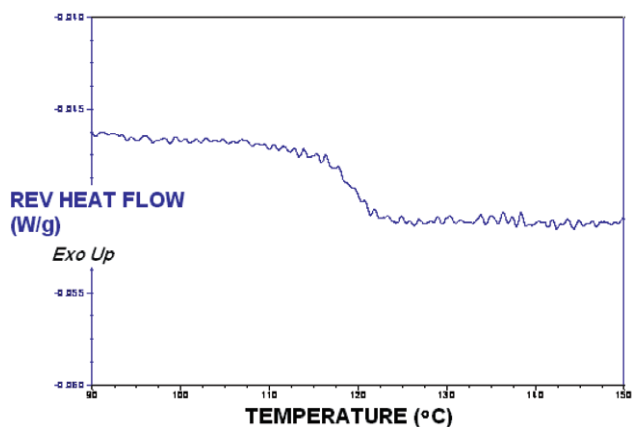
Fig.2 TD MTDSC 2nd heating at 0.5°C/min

Fig. 3 TD MTDSC 2nd heating at 0.5°C/min
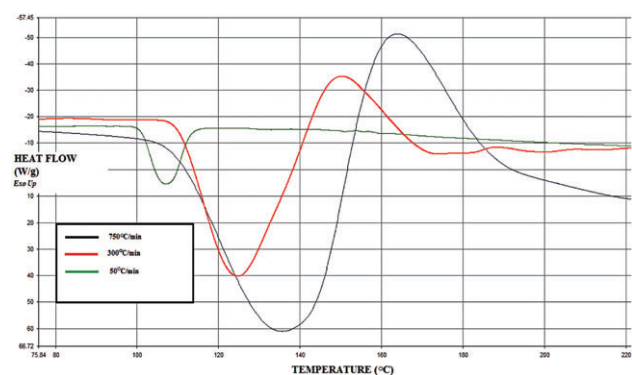
Fig. 4: TD HyperDSC® 1st heating

figures 1–3. TGA indicated water loss of 8.5%w/w, lower than predicted value for TD, suggesting that a plasticised liquid state is formed through the transition. The first heating period responses at rates of up to 750°C/min all demonstrated an endotherm at 90–110°C; however with rates in excess of 300°C/min an additional exotherm was seen between 150°C and 165°C which we ascribe to re-equilibration of the baseline (Fig.4). After cooling, the second heating ramp exhibited a T_g at ~134°C.

CONCLUSIONS

The study suggests that low heating rates allow processes to be observed in quasi-equilibrium states while also facilitating measurement of heat capacity changes through transitions. We suggest that TD undergoes partial dehydration and structural collapse to a hydrated liquid state at slow rates. In contrast, fast rates allow near negation of processes occurring during scanning but care is required in interpreting data due to baseline re-equilibration effects.

Application of Thermal Methods to the Study of Structural- and Stereo-Isomeric Amino Acids in the Solid-State

Anthony J. Cherry, Babur Z. Chowdhry, Stephen A. Leharne and Milan D. Antonijevic*

School of Science, University of Greenwich at Medway, Chatham Maritime, Kent, ME4 4TB, UK

INTRODUCTION

Thermal Analysis (TA) techniques measure a specific property of a sample as a function of temperature (or time), and are used in the pharmaceutical industry to study the solid-state properties of APIs and drug excipients [1].

The use of only one type of TA technique is unlikely to provide a complete, coherent analysis of a sample; thus, a number of TA techniques must be simultaneously employed.

In the case of amino acids, their study using TA is somewhat rare, with the prevalent themes in literature focusing on spectroscopic techniques [2] or biological studies.

This study aims to demonstrate the useful information TA can provide with reference to the solid-state properties of amino acids, with structural- and stereo-isomeric properties being a key theme throughout.

MATERIALS AND METHODS

Alanine was the material of choice for this research work; a small molecular weight amino acid ideal for comparative studies as it exists in three forms (L-α, D-α and β), displaying both structural- and stereo-isomerism.

Four TA methods were employed: HSM (Hot Stage Microscopy), TGA (Thermogravimetric Analysis), DSC (Differential Scanning Calorimetry) and TSC (Thermally Stimulated Current spectroscopy). The latter technique of TSC is likely to be unfamiliar in the context of pharmaceuticals. TSC is a novel form of dielectric analysis essentially measuring the current generated by the temperature activated relaxation of molecular scale dipoles within a sample [3], imparting information regarding the molecular motions of molecules as they are heated.

Figure 1: TG curves of D -, L-, β- and a physical mixture of L/D-alanine at 2°C/min. Onset is the extrapolated onset temperature. Mass loss is the total percentage mass loss from 30–600°C.
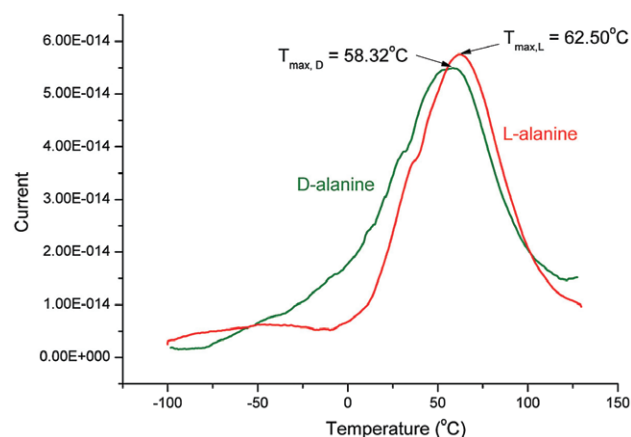
Figure 2: TSC curves of D- and L-ala. T_p = 50°C, t_p = 2 min, E_p = 20 V/mm, T_0 = −100°C, t_0 = 1 min, q = 10°C/min, T_f = 130°C.

RESULTS AND DISCUSSION

Preliminary TGA results (Fig. 1) show a clear, reproducible difference in the shape of the TG curves for the three forms of alanine, indicating a definitive variation in their solid state properties. A sharp and almost complete loss of mass for L- and D-alanine agree with HSM findings that a sublimation process is occurring between 220–230°C. The two-stage mass loss of β-alanine indicates it degrades via an alternative route. HSM images show an initial volatile loss, followed by a melting or softening process, and a final degradation stage. A preliminary study of a 1:1 molar physical mixture of L- and D-alanine shows a noticeable reduction in the onset of the sublimation process, indicating a solid state interaction of the two forms.

Preliminary TSC results (Fig. 2) show a noticeable difference in curve shape as well as a shift in T_{max}. The curve for D-ala is broader and exhibits a gentler incline than the curve for L-ala, indicating a greater distribution of relaxation times for the D- form. Further tests using thermal windowing and relaxation map analysis will provide a greater understanding of their solid state properties.

CONCLUSIONS

It is clear from preliminary results that TA shows a great deal of potential in identifying, qualifying and quantifying solid-state properties of amino acids, as well as differentiating structural- and stereo-isomeric forms.

REFERENCES

[1] Craig, D. Q. M., Reading, M. 2007. Thermal Analysis of Pharmaceuticals. Edited by Duncan Q. M. Craig and Mike Reading. *ChemMedChem,* 3, 1139–1140.

[2] Caroline, M. L., Sankar, R., Indirani, R. M. & Vasudevan, S. 2009. *Materials Chemistry and Physics,* 114, 490–494.

[3] Antonijevic, M. D., Craig, D. Q. M. & Barker, S. A. 2008. *International Journal of Pharmaceutics,* 353, 8–14.

Biodegradable Microparticles for the Delivery of Bioactive Molecules

J.S. Law[1], A.C. Ross[2], F.J. McInnes[1]

[1]Strathclyde Institute of Pharmacy and Biomedical Science, University of Strathclyde, Glasgow, UK.
[2]Controlled Therapeutics (Scotland), East Kilbride, UK.

INTRODUCTION

Biodegradable segmented polyurethanes can be utilised in a range of medical applications. This is a result of the wide variation in the microstructure that occurs due to phase separation into hard and soft segment domains. The constituents of the hard and soft segments and their respective ratios influence the mechanical properties [1] and the rate of drug release [2].

The focus of this work is to physically characterise three biodegradable polyurethanes as the initial step towards the preparation of biodegradable microparticles.

MATERIALS AND METHODS [3]

1) *Preparation of polymer*: PEG (M_n = 400, 2000 or 8000) and ε-caprolactone were reacted with stannous octoate as a catalyst to form three different pre-polymers. The three pre-polymers were reacted with polycaproloactone-diol and butane diisocyanate to form the final biodegradable polyurethanes, labelled PU_{400}, PU_{2000} or PU_{8000}.

2) *Tensile testing:* Dogbone shaped polymers were tested in an Instron Model 3343, with a 500N load cell at a rate of 200 mm/sec.

3) *Stability studies*: Pessaries formed from the polymers were incubated in phosphate buffered saline for 1 day, 1 week, 1 month and 2 months at 37°C and 50°C (n = 4). The pessaries were weighed to determine swelling and dried in a desiccator. The pessaries incubated at 50°C for one month were analysed for mass loss using gel permeation chromatography (GPC). The degree of swelling was analysed using a Kruskal-Wallis test with a Mann-Whitney U test for post-hoc analysis.

RESULTS AND DISCUSSION

Tensile data (Figure 1) shows that PU_{400} and PU_{2000} demonstrated a segmented structure, with the first peak of the curve (inset) showing the stress required to break bonds in the hard segment of the polymer, and an elongation portion (negligible increase in stress with a large increase in elongation) showing the influence of the soft segment on elasticity. PU_{8000} shows
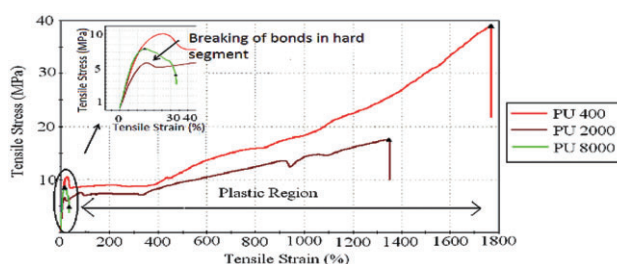

Figure 1. Stress-strain curve for three biodegradable polyurethanes

Table 1. GPC data for polyurethanes after swelling

Sample	Mw Polymer (g/mol)	Mw After Swelling (g/mol)	Mass lost (g/mol)
PU400	158 124	116 456	41 668
PU2000	132 238	115 138	17 110
PU8000	100 009	–	–

no real plastic elongation region, suggesting that there is no microphase separation in the polymer chains.

During swelling experiments PU_{8000} completely broke down in PBS and could not be analysed for swelling. PU_{2000} showed a higher degree of swelling than PU_{400} for all time points at both 37°C and 50°C (P < 0.05), with an average swelling of 29.3% and 0.7% (50°C, 2 months) for PU_{2000} and PU_{400} respectively.

PEG is hydrophilic, resulting in water influx and hydrolysis of ester bonds of caprolactone. Hydrolysis of ester bonds is responsible for the decrease in mw (Table 1). PU_{8000} contains a high % weight of PEG and a lower % weight of PCL, meaning that there is a higher capacity for water influx and less ester bonds to break. PU_{400} contains less PEG than PU_{2000}, resulting in less swelling being observed.

GPC data (Table 1) shows a drop in mw of both PU_{400} and PU_{2000} following incubation at 50°C for one month, with PU_{400} showing a greater decrease in mw than PU_{2000}. This did not correlate with swelling data, therefore suggesting different mechanisms of erosion.

CONCLUSIONS

The novel polyurethanes studied here have the potential to be utilised in controlled drug delivery vehicles by tailoring chemical composition to achieve desired mechanical properties and biodegradation timescales [2].

REFERENCES

[1] J. Zuidema, B. van Minnen, M.M. Span, C. E. Hissink, T.G. van Kooten and R.R.M. Bos, "*In vitro* degradation of a biodegradable polyurethane foam, based on 1,4-butandiisocyanate: A three-year study at physiological and elevated temperature" *J Biomed Mat Res Pt A,* **90** (2008) 920–930.

[2] H. B. Ravivarapu, K. Burton and P. P. DeLuca, "Polymer and microsphere blending to alter the release of a peptide from PLGA microspheres" *Eur J Pharm Biopharm* **50** (2000) 263–270.

[3] D. M. Nicolson, J. A Halliday, J. Touminen and A. Zurutuza, "Bioresorbable polyurethanes based on polyalkylene glycols, polycaprolactone diols, and diisocyanates" EU Patent no EP2076556 (2008).

Characterisation of the mechanical properties of ionic liquid incorporated endotracheal tube biomaterials

D.J. Kinnear[1], C.P. McCoy[1], D.S. Jones[1], G.P. Andrews[1], S.P. Gorman[1], K. Bica[2].

[1]School of Pharmacy, Queen's University Belfast, UK. [2]Institute of Applied Synthetic Chemistry, Vienna University of Technology, Austria.

Abstract – **Poly(vinyl chloride) possesses ideal properties for use as a biomaterial with the exception that it is susceptible to microbial colonisation. Incorporation of novel antimicrobial ionic liquids (ILs), which may overcome this issue, is shown here to significantly alter the mechanical properties of resulting PVC materials.**

INTRODUCTION

Nosocomial infections are currently of significant interest in both the literature and in the media, due to the frequency of occurrence and associated high level of mortality. One of the most severe of these is ventilator-acquired pneumonia (VAP), which results from intubation with an endotracheal (ET) tube and accounts for up to 60% of all nosocomial infections [1]. As with other medical devices, the ET tube may become colonised by pathogenic bacteria and biofilm formation occurs, leading to infiltration of body tissues by the pathogen and development of pneumonia. The biofilm forming capabilities of these pathogens make them resistant to many antibiotic regimens and thus treatment is difficult [2] [3] and in some cases impossible. Alternative strategies are needed for prevention of VAP, which we aim to address by modification of the ET tube with antimicrobial ILs. This however may alter the mechanical properties of the biomaterial, such as strength and flexibility.

MATERIALS AND METHODS

PVC resin (MW 43,000) was purchased from Sigma-Aldrich UK and tetrahydrofuran (GPR) was obtained from VWR International Limited, Poole. Quaternary ammonium ILs were synthesised by metathesis. Unplasticised poly(vinyl chloride) films were prepared by the solvent cast method, incorporated with one of three room temperature ILs. Dumb-
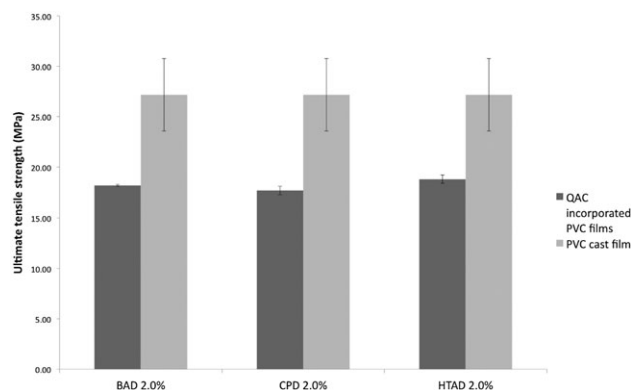
Figure 1: Chart showing ultimate tensile strength of QAC incorporated biomaterials with PVC controls. Results are plotted as mean ± standard deviation.

bell shaped replicates were cut from each film using a Ray-Ran hand operated cutting press and tensile properties characterised after 1 and 3 weeks using a Stable Micro Systems TA.XT plus texture analyser and Texture Exponent 32 software. Values for ultimate tensile strength, Young's Modulus and percentage elongation were calculated from the data.

RESULTS AND DISCUSSION

Figure 1 shows how incorporation of 2.0% of each IL affects the ultimate tensile strength of each material, which was significantly reduced in comparison to PVC.

So too were the values for Young's modulus, which were >98% lower than that of PVC. This demonstrated that the ionic liquids act as plasticisers within the material, facilitating the movement of the polymer chains past one another and

increasing the flexibility of the material. This disruption of the polymer network has also lead to a decrease in the strength of the material, allowing breakage under a lower applied force.

CONCLUSIONS

Incorporation of quaternary ammonium compounds has a significant effect on the mechanical properties of PVC, reducing the ultimate tensile strength but increasing the flexibility of the material. This indicates that room temperature ILs act as a plasticiser for PVC.

ACKNOWLEDGMENTS

REFERENCES

[1] H. Wagh and D. Acharya. "Ventilator Associated Pneumonia: an Overview" *BJMP* 2009:2(2) 16–19.

[2] A. Torres, S. Ewig, H. Lode and J. Carlet. "Defining, treating and preventing hospital acquired pneumonia: European perspective" *Intensive Care Medicine* 2009 (35); 9–29.

[3] A. Michalopoulos et al. "Aerosolised colistin as adjunctive treatment of ventilator-associated pneumonia due to multidrug-resistant Gram-negative bacteria: a prospective study" *Respiratory Medicine* 2008 (102); 3; 407–412.

Characterising the surface properties of pharmaceutical tooling components with atomic force microscopy

M. Bunker[1], J. Zhang[1], A. Parker[1], R. Blanchard[2] and C.J. Roberts[1].

[1]Molecular Profiles, 8 Orchard Place, Nottingham Business Park, Nottingham, NG8 6PX, UK.
[2]I Holland, Meadow Lane, Nottingham, NG10 2GD, UK.

INTRODUCTION

The aim of this study is to develop an atomic force microscopy (AFM) based approach to study the adhesive interaction forces between tabletting punches and a model formulation ingredient (lactose), that can be used to understand and predict issues such as sticking during tabletting compression.

MATERIALS AND METHODS

Adhesive interactions were measured, and their variation studied, between single lactose particle probes and tablet punches with different surface coatings. Arrays of force-distance curves were recorded on punch surfaces under controlled conditions and lateral spacing using an EnviroScope AFM (Veeco Instruments). The influence of relative humidity (RH) was studied by measuring adhesion at 10%, 30% and 60%RH. The influence of surface roughness was investigated by comparing two punches differing only in surface finish. The adhesion force was also spatially mapped to indentify 'hot spots' of high adhesion on the punch surfaces. In addition, roughness parameters were measured with AFM imaging and a modelling approach was considered for predicting the influence of roughness on adhesion.

RESULTS AND DISCUSSION

Surface roughness was found to play a significant role in the adhesion distribution across the punch surface. This difference between different punches can be correlated to observations on performance from their use in industry. Adhesion forces were spatially mapped to indentify 'hot spots' of high adhesion.

Figure 1A and 1B shows the adhesion force distributions measured on punches coated with CN+ and CN finishes respectively and which differ only in surface roughness. Each represents the variation in adhesion measured across a 10 μm x 10 μm area of the surface (n = 2500). The data is reasonably well fitted with a Gaussian distribution (solid lines) for both samples. The corresponding mean adhesion forces are 14.2 nN for the CN+ and 19.2 nN for the CN. Note that the same lactose particle probe was employed for both CN and CN+ punches in order to eliminate a possible variation in contact area induced by different particle probes and to allow direct comparison of the distributions. Since the adhesion data was recorded in a defined grid pattern across the surface, it is also possible to plot the data as an adhesion force map, as shown in Figure 2.

A modelling approach is also discussed whereby the relative adhesion of different surfaces can be predicted from
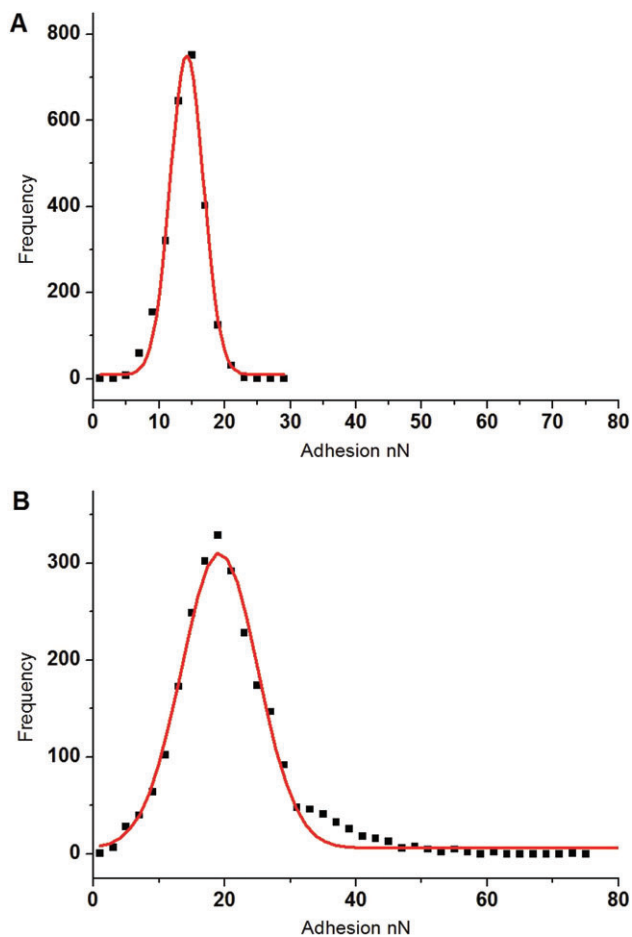
Figure 1a (top) and **1b** (bottom) showing adhesion force distributions between lactose-CN and lactose-CN+ punch coatings respectively.

Figure 2 showing adhesion force maps between lactose-CN (top) and lactose-CN+ (bottom) punch coatings.

roughness data. The adhesion of lactose particles to tablet punches was significantly affected by RH, for one type of punch causing a greater than 3x increase in adhesion as the RH is increased from 30% to 60%. Interestingly, different punch face materials showed different RH-adhesion behaviour, which can be linked to punch surface hydrophilicity.

CONCLUSIONS

The work introduces a new method for screening tablet punch materials and tabletting conditions and highlights important factors which need to be considered when evaluating adhesive interactions in tablet compression and how potential sticking problems may be affected. Correlations are observed between AFM adhesion results on different punches and their observed tabletting behaviour during manufacture. This provides a promising basis for a predictive approach towards combating tabletting issues.

Characterisation of Co-Solvent Effects in Poly(Vinyl Alcohol) Gels by Oscillatory Rheology

E.J. Wright, D.S. Jones, G.P. Andrews

School of Pharmacy, Queen's University Belfast, Belfast, UK.

Abstract – **Poly(vinyl alcohol) is an extremely versatile polymer but its uses in the gel state can be limited by the syneresis (ageing) shown in gels with water as the only solvent. To improve the ageing and, therefore, functionality of PVA gels they need to be made with water and co-solvents.**

INTRODUCTION

Poly(vinyl alcohol) (PVA) is a semi-crystalline, hydrophilic, water soluble polymer. These properties arise from strong intra- and inter-molecular hydrogen bonding due to the regular hydroxyl groups [1]. The strong hydrogen bonding also aids in the dissolution and gelation of the polymer in water and with other co-solvents [2]. Co-solvents are required as gels made with water only show syneresis and age quickly by losing water and increasing crystallinity, making them difficult to characterise with rheology [3]. The co-solvents being investigated are dimethyl sulphoxide (DMSO), propylene glycol (PG), dipropylene glycol (DPG), *N*-methyl pyrrolidone (NMP) and 2-pyrrolidone.

MATERIALS AND METHODS

The PVA of molecular weight 13,000–23,000 (98% hydrolysed) was purchased from Sigma-Aldrich. PG, DPG and 2-pyrrolidone (GPR) were purchased from Sigma-Aldrich and the DMSO and NMP (GPR) were purchased from VWR.

Gels are produced by dissolving PVA in water or water/solvent mixes and heating and stirring at 90 °C for 24 hours. They were then allowed to cool to room temperature and characterised by oscillatory rheometry at 37°C within 72 hours of manufacture.

RESULTS AND DISCUSSION

Two polymer concentrations (20 and 30%) and two solvent concentrations (10 and 20%) were investigated. Upon manufacture, two of the gels could not be characterised as they had already undergone a form of syneresis and could not be removed from the storage vessel, the 30% PVA, 20% DMSO and 30% PVA, 20% PG gels.

The solvent combination of water and DMSO always produces a more elastic, stronger PVA gel than water only. Both NMP and 2-pyrrolidone consistently produce weaker, more viscous, gels than water only solvent. The 2-pyrrolidone gels at both PVA concentrations are more elastic than NMP but less elastic than water only gels. For PG, the 20% PVA gels are stronger than water only gels and increasing solvent con-
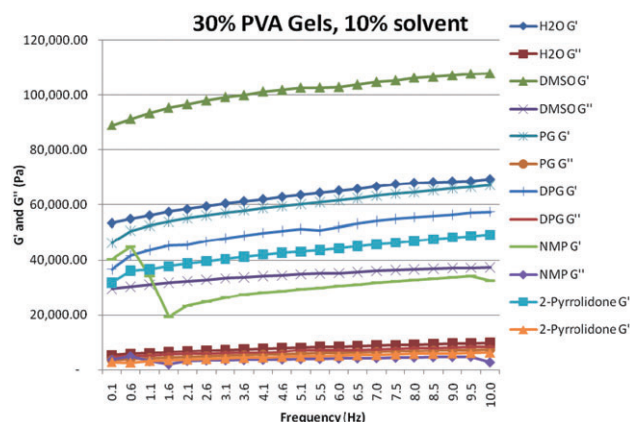

Fig. 1. Graph showing oscillatory rheology G′ and G″ data for gels manufactured with 30% PVA and 10% solvent in water.

centration has no significant effect. At 30% PVA and 10% PG the gel is weaker than a water only gel yet the gel containing 20% PG was so strong it could not be characterised. DPG at 20% PVA concentration shows an increase in elasticity as the solvent concentration increases, with both gels stronger than water only gels. At the higher polymer concentration, 30%, the DPG gels at both solvent concentrations are weaker/more viscous than the water only gels.

CONCLUSIONS

The size of the solvent molecule appears to play a significant role in the number of cross-links that can be formed and therefore how strong the gel is. Larger solvents disrupt the cross-linking between polymer chains and produce weaker gels compared to water alone. The smallest solvent molecule produces the strongest gel as it assists in the formation of cross-links, producing gels that are stronger than those made in water only.

REFERENCES

[1] S.I. Song and B.C. Kim, "Characteristic rheological features of PVA solutions in water-containing solvents with different hydration states" *Polymer*, **45** (2004) 2381–2386

[2] P.D. Hong, C.M. Chou and C.H. He, "Solvent effects on aggregation behaviour of polyvinyl alcohol solutions" *Polymer*, **42** (2001) 6105–6112

[3] J.C.J.F. Tacx, H.M. Schoffeleers, A.G.M. Brands and L. Teuwen, "Dissolution behaviour and solution properties of polyvinylalcohol as determined by viscometry and light scattering in DMSO, ethyleneglycol and water" *Polymer*, **41** (2000) 947–957

Effect of drug salt selection on the physiochemical properties of hot-melt extruded eudragit RL PO insoluble matricies

D.L. Caldwell[1], D.S. Jones, G. Andrews

[1]Department of Pharmacy, Queen's University Belfast, UK.

Abstract **– Two commercially available salt forms of quinine (hydrochloride and sulphate) were compared to the free base form of the drug to determine the effect of salt type on miscibility and in-vitro release properties within a eudragit RL PO hot-melt extruded matrix. The free base was found to have highest miscibility and solubility within the molten matrix and exhibited slowest release from the matrix, while the hydrochloride showed poorest miscibility but fastest release profile. This was proposed to be attributed to varying sites of polymer-drug interactions which was in turn influenced by the quinine salt counter-ion.**

INTRODUCTION

It is estimated that half of all drug molecules used in medicine are administered as salts and the formation and selection of a suitable salt form of a drug candidate is recognised as an essential step in drug development.

The aim of this work was to ascertain if salt form of the selected model drug (quinine) had an influence on physiochemical properties and in-vitro release profile of an extruded dosage form containing eudragit RL PO.

MATERIALS AND METHODS

1) Hot melt extrusion

Physical mixtures were fed into a prism (Eurolab) 16 mm twin-screw extruder (Thermo Scientific, Stone, UK). Screws were co-rotated at a speed of 100 rpm and the temperature applied was 150°C.

2) Differential scanning calorimetry

Samples were subjected to conventional DSC at thermal ramp of 10°C/min from 20–200°C

3) In-vitro dissolution

A Caleva 8ST dissolution apparatus (n = 5) was used. The samples were tested in 900 ml of phosphate buffered saline (Ph 7.3 ± 0.2) at 37°C at a paddle rotation speed of 100 rpm. Concentration of drug was determined by UV analysis at 330 nm.

4) Infra-red analysis of extrudates

FT-IR spectroscopy was performed using a perkin elmer spectrum One FT-IR spectrometer and the KBR method in the 4000–400 cm^{-1}

RESULTS AND DISCUSSION

DSC was used to provide a quantitative measurement of the solubility of the drug within the molten polymer. This method can be used since the portion of solubilised drug does not contribute to the melting endotherm so quantification of that dissolved can be enabled[1]. Quinine free base had the highest solubility within (circa 26%) while the sulphate and hydrochloride salt forms had a significantly lower solubility with the molten matrix (18% and 7.5% respectively). 5% and 30% drug loaded extrudates were assessed since both salt forms and free base were in a solid solution at 5% and a solid dispersion at 30%. There was no statistically significant difference in the release profiles of all three solid solutions, however there was a significant difference when the salts were in a solid dispersion. Approximately only 10% of the free base form was released after 6 hours, while 60% of the sulphate was released and just under 100% of the hydrochloride. This showed that aqueous solubility of the salt was the dominant factor influencing release. FT-IR showed differences in the sites of interaction between the free base and the salt forms.

CONCLUSIONS

Salt forms of an API are frequently used to improve aqueous solubility. Hot melt extrusion is also a technique often used to enhance solubility of a poorly solubility API. This work has shown that salt form selection had a significant influence on eudragit RL PO dosage forms prepared by hot melt extrusion.

REFERENCE

[1] Crowley M.M *et al*. Drug Development and Industrial Pharmacy 33 (9): 909–926

[2] Glaessi B., Siepman F., Tucker I., Siepman J., Rades T. Journal of Pharmaceutics and Biopharmaceutics, 2009, 73 (3): 366–372

Effect of excipients on the performance of orally disintegrating tablets

M. Grachet[1], V. Morris[1] and G. Bajwa[1]

[1]Pharmaceutical Development, Pfizer Global R&D, Sandwich Laboratories, UK.

INTRODUCTION

Orally disintegrating tablets (ODTs) are designed to disintegrate or dissolve rapidly on contact with saliva, thus eliminating the need to chew the tablet, swallow an intact tablet, or take the tablet with liquids. This mode of administration is beneficial to paediatric and geriatric patients, to people with conditions related to impaired swallowing, and for treatment of patients when compliance may be difficult (e.g. for psychiatric disorders).

ODTs can be manufactured via direct compression (DC). The drug is blended with superdisintegrants, water soluble excipients and sweeteners and then compressed. This allows conventional tabletting equipment to be used for processing. It is necessary to ensure that excipients have the functionality required to formulate a DC ODT that fulfils the following criteria: disintegration time <30 s [1], friability <1%.

AIM

The objective of this study is to investigate the effect of formulation variables, including different superdisintegrants, binder and glidant levels and different co-processed fillers on the performance (disintegration time and friability) of the ODTs. The particle size, flow properties and compactability of the fillers was also determined.

MATERIALS AND METHODS

A number of co-processed excipients have been developed and supplied specifically for use in ODTs, they include Pharmaburst XP-500 and Parteck ODT (refer to Table 1 for composition). A comparison with spray-dried mannitol (Pearlitol 200SD) was also undertaken. The following superdisintegrants were investigated in this study: Ac-Di-Sol, Explotab and Kollidon CL-SF at three different concentrations. A 14 run placebo design of experiment (DOE) was completed.

The ODTs were compounded at laboratory scale (200 g) using the Natoli Hand Press to a target weight of 400 mg, using standard round concave 11 mm tooling to tablet hardness levels of 4–5 or 7–8 kp.

RESULTS AND DISCUSSION

All the fillers studied exhibited good flow properties (Carr's index <20). Pearlitol 200SD has a larger mean particle size than Pharmaburst XP-500 and Parteck ODT (Table 1).

Filler and superdisintegrant type were found to have the most significant impact on tablet disintegration time ($p < 0.05$). Pearlitol 200SD and Pharmaburst XP-500 exhibited a faster disintegration time than Parteck ODT. Tablets containing the disintegrant Kollidon CL-SF disintegrated faster than those containing Explotab or Ac-Di-Sol (Figure 1).

Tablet hardness level did not impact the disintegration time, however a significant improvement in tablet friability was observed for tablets manufactured at 7–8 kp (friability
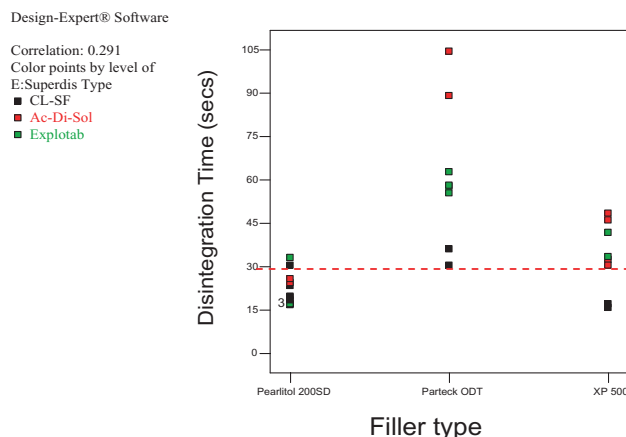
Figure 1. Plot of disintegration time against filler type, coloured by superdisintegrant

Table 1. Summary of filler properties

Composition	Trade name	Manufacturer	Particle size ($d_{4,3}$ μm)	Flow properties (Carr's index)
Contains polyols & superdisintegrants	Pharmaburst XP-500	SPI Pharma	110–125	15.6
D-mannitol & croscarmellose sodium	Parteck ODT	Merck	70–120	19.5
Spray-dried mannitol	Pearlitol 200 SD	Roquette	180	16.1

<0.2%). Co-processed excipients and the addition of binder (microcrystalline cellulose) also produced less friable tablets.

Lower compression forces were required to compress ODTs when using Parteck ODT, Pharmaburst XP-500 and Kollidon CL-SF. These excipients demonstrated good compression characteristics.

CONCLUSIONS

This study suggested that at a laboratory scale (200 g), ODTs prepared with Pearlitol 200SD or Pharmaburst XP-500 as filler, Kollidon CL-SF (5%), MCC (5%) and glidant (1%) displayed acceptable disintegration and friability at the different hardness levels.

REFERENCE

[1] FDA, "Guidance for Industry: Orally Disintegrating Tablets", accessed 2009.

Effects of Drug Solubility and Concentration on Phase Transformations of Hydroxypropyl Cellulose Aqueous Solutions

Terry Ernest[1], Luigi Martini[2], Matthew Roberts[3] and James L Ford[3]

[1]GlaxoSmithKline, Pharmaceutical Development, Harlow
[2]GlaxoSmithKline, Pharmaceutical Development, Ware
[3]School of Pharmacy & Biomolecular Sciences, Liverpool John Moores University, Liverpool

INTRODUCTION

Hydroxypropyl cellulose (HPC) is a commonly used suspending agent in liquid dosage forms. Aqueous solutions of HPC are known to undergo phase transformations at elevated temperatures [1]. To investigate the potential application of this phenomenon in developing paediatric medicines, the effect of temperature and drug concentration on viscosity and UV transmission were determined for a range of molecular weight HPC grades. The concentration effects of two commonly prescribed paediatric drugs with different solubilities, paracetamol and ranitidine, when dissolved in 5% w/w HPC grade EF aqueous solutions were determined.

MATERIALS AND METHODS

Aqueous solutions of HPC (Klucel® (Aqualon)) grades EF, LF, JF and GF were prepared by dissolving the required type and quantity of HPC in purified water. 5% w/w HPC EF solutions containing ranitidine at concentrations of 2.5, 5, 50 and 100 mg/ml and paracetamol at concentrations of 5, 10 and 15 mg/ml concentrations were used.

The viscosities were determined at various temperatures using a water bath and Brookfield LVDV III viscometer. A small sample adaptor was used to measure samples. Viscosity was measured from ambient temperature to 60°C at 5°C intervals.

UV transmission of the solutions was determined at 2°C intervals until 0% transmission was reached at 540 nm using a 1 cm cuvette and a jacketed cuvette holder.

RESULTS AND DISCUSSION

An increase in temperature of the HPC solutions resulted in a decrease in viscosity. Minimum viscosity was reached at ~50–60°C. All grades of HPC showed a similar trend with the more viscous grades showing the greatest change in viscosity.

The UV transmission of HPC solutions without drug decreased as sample temperature increased. Percent UV transmission for HPC solutions reached near zero at 33°C to 36°C depending upon HPC grade. These data indicate that increasing temperature caused the dehydration and precipitation of HPC [1].

An increase in paracetamol concentration reduced the viscosity of the HPC solutions whilst an increase in ranitidine concentration increased viscosity. Solutions containing a higher concentration of paracetamol also reached near zero UV transmission at lower temperatures whilst a higher concentration of ranitidine reached its zero UV transmission at higher temperatures. These data indicate that drug concentration and drug solubility influence the phase transformation exhibited by HPC.

An example of these data is provided in Table 1.

CONCLUSIONS

Increase in temperature reduces HPC solution viscosity and causes precipitation of HPC.

The 'sparingly soluble' [2] drug paracetamol (<15 mg/ml) decreased the temperature of dehydration and precipitation

Table 1. Influence of temperature and drug concentration on HPC solution viscosity and %UV transmission.

Temperature °C	5% EF HPC Solution		5% EF HPC containing 15 mg/g Paracetamol		5% EF HPC containing 100 mg/g Ranitidine	
	% UV Trans	Viscosity (cP)	% UV Trans	Viscosity (cP)	% UV Trans	Viscosity (cP)
30	83.3	47.0	71.6	77.8	92.3	52.2
34	28.9	–	1.7	–	97.7	–
36	0		0.1		98.9	
40	0	37.1	0.2	14.6	–	39.4
42	0		–		1.9	
45	0	28.3	–	10.6	0.2	30.9
50	–	11.3	–	7.7	–	11.3
55	–	5.0	–	5.5	–	5.3
60	–	3.6	–	4.0	–	3.9

onset and the 'freely soluble' [2] drug ranitidine (>100 mg/ml) increased the temperature of dehydration and precipitation.

It is believed that salting in by ranitidine of HPC is similar to salting effects observed with other drugs in solution with hypromellose [3].

The impact of temperature on HPC hydration shown here will be explored in future work.

REFERENCES

[1] S. A. Vshivkov and E. V. Rusinova, "Phase Diagrams of a Hydroxypropyl Cellulose–Water System under Static Conditions and in the Shear Field", *Polymer Science,* Ser. B, 2007, Vol. 49, Nos. 7–8, pp. 209–212.

[2] The British Pharmacopoeia (BP) 2009 Volume I and II, General Notices, Published August 2008.

[3] K. Mitchell *et al,* "The influence of additives on the cloud point, disintegration and dissolution of hydroxymethylcellulose gels and matrix tablets", *Internat. J. Pharm.,* 1990, Vol. 66, pp 233–242.

Effects of polymer type and drug/polymer interactions on the supersaturated celecoxib solutions

O.A. Abu-Diak[1], D.S. Jones[1], G.P. Andrews[1]

[1]Drug Delivery Group, School of Pharmacy, Queen's University of Belfast, UK.

INTRODUCTION

The low physical stability of amorphous drugs and their spontaneous tendency to re-crystallise often negate their advantage of high solubility [1]. To achieve the full benefit of amorphous drugs, it is necessary to stabilise the supersaturated drug solutions achieved during dissolution of amorphous solid dispersions. This study aims to characterise the effects of polymer type on the supersaturated celecoxib (CX) solutions.

MATERIALS AND METHODS

Amorphous solid dispersions of CX based on Eudragit® 4155F or polyvinylpyrrolidone (PVP K25) were prepared by hot-melt extrusion (HME) using a co-rotating twin-screw extruder at a screw speed of 100 rpm. CX/Eudragit® 4155F binary system at 1:9, 3:7, 1:1, and 7:3 mass ratios were extruded at a temperature of 170 °C, whereas only CX/PVP mass ratios of 3:7, 1:1 and 7:3 were possible to be extruded. A temperature of 150 °C was used to extrude the CX/PVP

(1:1 and 7:3), whereas 3:7 ratio was extruded at 170°C. *In vitro* drug release studies on solid dispersions containing equivalent amount of 50 mg CX were conducted under non-sink conditions using phosphate buffer pH 7.4 (PBS 7.4) (500 mL) and a temperature of 37°C ± 0.2°C. Solution proton nuclear magnetic resonance (^{1}H NMR) was used to characterise any drug/polymer interactions that might occur during dissolution of the amorphous solid dispersions.

RESULTS AND DISCUSSION

All the amorphous solid dispersions generated supersaturated drug concentrations i.e. above the equilibrium solubility of crystalline CX (1.58 ± 0.04 μg/mL) up to 72 h. CX/PVP solid dispersions at 3:7 ratio maintained a drug concentration of 21.92 ± 0.07 μg/mL after 72 h, which was slightly higher than the theoretical solubility of amorphous CX predicted by Parks model [2] (19 μg/mL). These results suggest the high stabilising effects of PVP on the supersaturated solutions of CX with no considerable enhancement in its solubility. Conversely, Eudragit® 4155F showed significant solubilising

effects on CX. For example, a nearly complete drug release (99.23 ± 1.01 µg/mL) was achieved by CX/Eudragit® 4155F solid dispersions at 1:9 ratio after 1 h, which maintained up to 72 h at 100.67 ± 0.6 µg/mL.

Physical mixtures of CX with Eudragit® 4155F showed significant increases in its solubility, whereas no such effects have been observed with PVP. Conversely, PVP showed high inhibitory effects against CX re-crystallisation from supersaturated drug solutions generated by concentrated methanolic drug solutions in PBS 7.4 containing different concentrations of the polymer, whereas Eudragit® 4155F has not shown any considerable stabilising effects.

^{1}H NMR spectra of Eudragit® 4155F solid dispersions showed downfield shifts to higher values (deshielding) in all aromatic protons containing sulfonamide group, whereas some of these protons were shielded and the others were deshielded in the PVP solid dispersions suggesting differences in the type of drug/polymer interactions formed during drug dissolution.

CONCLUSIONS

Supersaturated CX solutions were generated by dissolution of amorphous solid dispersions as a result of the stabilising effects of PVP and the solubilising effects of Eudragit® 4155F. These different polymer effects may be related to the differences in the type of drug/polymer interactions formed during dissolution of the solid dispersions.

REFERENCES

[1] B. C. Hancock and G. Zografi, "Characteristics and significance of amorphous state in pharmaceutical systems" J. Pharm. Sci., 86 (1997) 1–12

[2] G. S. Parks, H. M. Huffman, F. R. Cattor, "Studies on glass. II: the transition between the glassy and liquid states in the case of glucose" J. Phys. Chem., 32: 1366–1379

Enhancement of Solubility of Nateglinide by Solid Dispersion Technique

J. Ravi Kumar Reddy, C.Madhusudhana Chetty

Department of Pharmaceutics, Annamacharya College of Pharmacy, Rajampet, India.

INTRODUCTION

The solubility behaviour of drugs remains one of the most challenging aspects in formulation and development.[1] The greater understanding of dissolution and absorption behaviour of drugs with low aqueous solubility is required to successfully formulate them into bioavailable drug products. In the present study an attempt was made to enhance the solubility of Nateglimide, as it has poor solubility in water. Solid dispersions were prepared using Mannitol, Citric acid, PEG6000 hydroxypropyl-β-cyclodextrin.

MATERIALS AND METHODS

Nateglimide solid dispersions were prepared by solvent evaporation method. Scanning of solid dispersions was performed to evaluate whether there is any interference in UV detection of solid dispersions compared to control (drug) which can depict the drug polymer interaction. The solubility of Nateglinide as bulk drug and its solid dispersions were determined in simulated gastric fluid, distilled water and 6.8 pH phosphate buffer.

RESULTS AND DISCUSSION

Various solid dispersions were prepared using Mannitol, Citric acid, PEG6000 hydroxypropyl-β-cyclodextrin, in 1:1, 1:2 and 1:3 w/w ratio for initial optimisation of polymer. The solubility and dissolution results revealed that there was an increase in solubility and dissolution of all the solid dispersions as com-
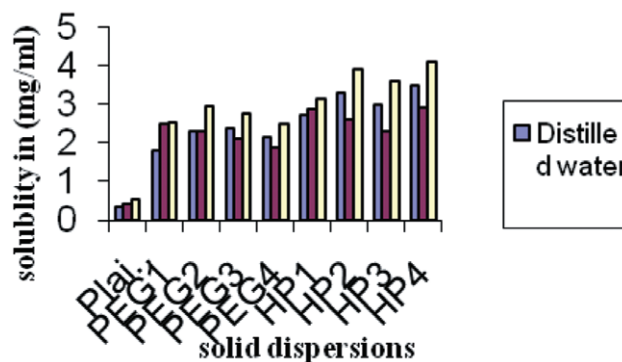

Fig 1. Solubility of Nateglinide from various solid dispersions in simulated gastric fluid (SGF), distilled water and 6.8 pH phosphate buffer.

pared to pure drug but was highest in case of HP3 (1:3) ratio of drug: hydroxypropyl-β-cyclodextrin which revealed hydroxypropylbetacyclodextrin was more effective as compared to the other three polymers. Further combinations were prepared by increasing the content of hydoxypropyl -β-cyclodextrin i.e. the solid dispersions were prepared with 1:4 and 1:5 ratio of drug:hydoxypropyl-β-cyclodextrin.

CONCLUSION

The dissolution and solubility studies of HP3 (1:3) ratio of drug: hydroxypropyl-β-cyclodextrin, solid dispersion revealed that in both cases the solubility and dissolution was

increased, and thus formulation HP3 was optimised as the most promising solid dispersion.

REFERENCES

[1] Leuner, C. and Dressman, J., (2000), Improving drug solubility for oral drug delivery using solid dispersions. **Eur. J. Pharm. Biopharm.** 50, 47–60

[2] Cilurzo, F., Minghetti, P., Casiraghi, A. and Montanari, L., 2000. Characterisation of nifedipine solid dispersions. **Int. J. Pharm.** 242, 313–317.

[3] Pawar, S. P., Gudsoorkar, V. R. and Shete, J. S., 1995. Solid dispersions of trimethoprin. **The Eastern Pharmacist**. XXXVIII (450), 147–149.

Fmoc hydrogels from aromatic carbohydrate amphiphiles

A.A. Edwards[1], L.S. Birchall[2], V. Jayawarna[2], S. Roy[2], M. Hughes[2], T. Tuttle[2], N. Saudi[1], G. Okorgheye[1], R.V. Ulijn[2]

[1]Medway School of Pharmacy, Universities of Kent and Greenwich at Medway, Kent, UK.
[2]Department of Pure and Applied Chemistry, University of Strathclyde, Glasgow, UK.

INTRODUCTION

Numerous low molecular weight (LMW) hydrogels have been reported but only a small number of these are carbohydrate based.[1–3] LMW gelators are typically amphiphilic molecules where the alignment of hydrophobic and hydrophilic regions facilitates gel formation. Most carbohydrate based LMW gelators form organogels and the hydrophobic element is commonly introduced by modification of a sugar hydroxyl group[1,2] although there are a few exceptions.[4] Shinkai *et al* have also demonstrated that the chiral diversity inherent in a monosaccharide can be used to manipulate gelation properties *e.g.* organogelation and/or hydrogelation.[5] Aromatic carbohydrate amphiphiles, based on galactosamine and glucosamine, were therefore prepared to assess the effect of different aromatic groups and the manipulation of chirality on gelation. The primary goal of this work is to develop galactose-based hydrogels for 3D cell culture of hepatocytes.

MATERIALS AND METHODS

The potential gelators were prepared in one synthetic step by the introduction of an aromatic group to an amino sugar in solution phase at room temperature. Aromatic groups were attached to the amino group of the hydrochloride salts of either D-galactosamine (GalNH$_2$) or D-glucosamine (GlcNH$_2$) *via* carbamates (Fmoc) or amide bonds (napthyl, fluorenyl, phenyl) (Fig. 1). The Fmoc group was introduced by the use of Fmoc-Cl whereas the fluorenyl, phenyl and napthyl groups were introduced using the corresponding acids and standard peptide coupling reagents. The isolated compounds were heated to 75–80 °C in water then cooled to establish if gelation could be thermally triggered. Hydrogels were only obtained from GalNHFmoc and GlcNHFmoc and were characterised using rheology and imaged by AFM.
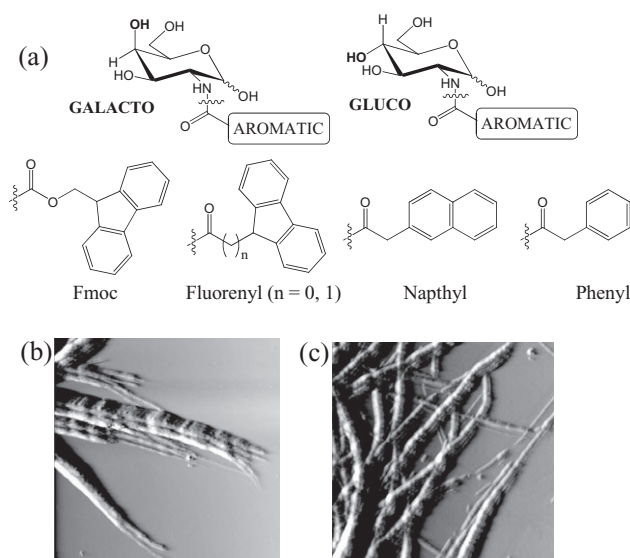

Fig. 1. Aromatic carbohydrate amphiphiles: potential gelators (a) and AFM images (5 × 5 μm) of the hydrogels from GalNHFmoc (b) and GlcNHFmoc (c)

RESULTS AND DISCUSSION

Five different hydrophobic groups were selectively coupled *via* the amino group of GalNH$_2$ or GlcNH$_2$. Hydrogels were formed by GalNHFmoc and GlcNHFmoc at 5 mM and 10 mM concentrations respectively. All other compounds formed precipitates.

The formation of a hydrogel with Fmoc but by neither fluorenyl group is surprising. Presumably the increased distance of the aromatic group from the amino sugar facilitates better intermolecular interactions. This is consistent with the

lack of hydrogelation for the napthyl and phenyl derivatives.

Both Fmoc derivatives formed relatively stiff hydrogels, as determined by rheology studies, at both pH 7 and under physiological conditions. These gels were also stable to repeated heating and cooling cycles. AFM images show that the larger bundles of fibres present are formed from individual fibrils which are visible at the ends.

Gelation is widely reported by Fmoc-peptides[6] but these Fmoc gels have no peptide component therefore it is likely that self assembly will occur *via* a different mechanism, perhaps driven by carbohydrate aromatic interactions.[7] Further experiments (fluorescence, IR, XRD, TEM and DSC) and molecular modelling are in progress to determine the precise mode of assembly.

CONCLUSIONS

The Fmoc derivatives are effective hydrogelators although the mechanism of gel formation has yet to be established. The

bond distance between the amino group and the aromatic moiety appears to play a significant role in gel formation.

REFERENCES

[1] A recent example: Q. Chen, Y. Lv, D. Zhang, G. Zhang, C. Liu and D. Zhu *Langmuir* **26** (2010) 3165–3168.
[2] M. de Loos, B. L. Feringa, and J. H. van Esch, *Eur. J. Org. Chem.* (2005) 3615–3631.
[3] L. A. Estroff and A. D. Hamilton, *Chem. Rev.* **104** (2004) 1201–1217.
[4] Z. Yang, G. Liang, M. Ma, A. S. Abbah, W. W. Lu and B. Xu *Chem. Commun.* (2007) 843–845.
[5] O. Gronwald, S. Shinkai, *Chem. Eur. J.* **7** (2001) 4329–4334.
[6] A recent example: G. Liang *et al.* *Langmuir* **25** (2009), 28419–8422.
[7] M. S. Sujatha, Y. U. Sasidhar and P. V. Balaji *Biochemistry* **44** (2005) 8554–8562.

Formation of Cocrystals by Spray Drying

Amjad Alhalaweh[1] and Sitaram P. Velaga[1]*

[1]Department of Health Sciences, Luleå University of Technology, Luleå, SE-971 87, Sweden

Abstract – **Spray drying is a widely used technique for material processing and scale-up. The cocrystals formation by spray drying is studied. In contrast to solvent evaporation method, spray drying of stiochiometric solutions of incongruently saturating cocrystals had generated pure cocrystals. The formation phenomena in spray drying could be kinetically controlled or mediated by glassy state.**

INTRODUCTION

Pharmaceutical cocrystals are becoming increasingly interesting in the drug product development [1]. The cocrystal formation in the equilibrium solution methods is dependent on the saturation condition of cocrystals i.e. congruent or incongruent. Generally, congruently saturating systems are thermodynamically stable during slurrying while an incongruently saturating cocrystal transforms (not stable) [2–3]. However, these methods are non-stoichiometric and require efficient control of thermodynamic and kinetic factors. These drawbacks have encouraged us to test cocrystallisation by spray drying.

Spray drying is a method of producing dry powders from solution by rapid evaporation of the solvent with a hot air stream in one step. This is one of the widely used methods for material processing and scale-up in the pharmaceutical and food industries. In this study, we set out to explore the formation of cocrystals by spray drying and to understand the role of thermodynamic and kinetic factors in the formation by this technique. The cocrystallisation pathway for incongru-

ent systems in the spray drying in relation to the solvent evaporation method are discussed. To the best of our knowledge, the formation of cocrystals using spray drying has not been systematically studied to date.

MATERIALS AND METHODS

All materials used in the entire study were sourced from Sigma-Aldrich and used without further purification.

Solutions of 1:1 molar ratio of drug and coformers were prepared. Processing conditions including air flow 357 L.h-1, aspiration rate 100 % (only 70 % used for water sample), and solution feed rate 5 ml.min^{-1} were applied for all systems. The inlet temperature was 70–75 °C and 120 °C for organic solvents and water respectively. PXRD studies were conducted on Siemens DIFFRACplus 5000. Samples were scanned up to 40° in 2θ with 0.01° step size and 2 second step time.

RESULTS AND DISCUSSION

A mixture of solid phases resulted from the solvent evaporation as expected, following the thermodynamic pathway for incongruent systems (Table 1). In contrast, contrary to what can be expected from a fast evaporation in spray drying, cocrystals were formed. Similar results were obtained from the spray drying of congruently saturating systems (results not shown).

Table 1: Incongurent systems investigated and resulting solid phases from solvent evaporation at the room temprature and spray drying as confirmed by the PXRD. The selcted cocrystal were of 1:1 stoichiometry. *new cocrystal. †amorphous after spary drying but converted to cocrystal upon storage

Cocrystal	Solvent	Solvent evaporation	Spray Drying
Carbamazepine-Glutaric acid	Ethanol	Drug, coformer, and Cocrystal	Cocrystal
Theophylline-Nicotinamide	Ethanol	Drug, coformer, and Cocrystal	Cocrystal
Urea-Succinic acid	Water	2:1 cocrystal and coformer	Cocrystal*
Indomethacin-Nicotinamide	Methanol	Drug, coformer, and Cocrystal	Cocrystal†

The cocrystal formation in spray drying was controlled by kinetic phenomenon i.e. via preferencial nucleation of cocrystals or via glassy state.

CONCLUSIONS

◆ Pure cocrystals were generated in the spray drying from the stoichiometric solutions of inconguent and congruemt solutions.
◆ The formation of cocrystals under incongruent saturation conditions undermines the importance of thermodynamic formation phenomena.
◆ Spray drying is a suitable technology for the preparation and scale-up of cocrystals.

REFERENCES

[1] N. Schultheiss and A. "Newman, Pharmaceutical Cocrystals and Their Physicochemical Properties". Cryst. Growth Des., 9 (2009) 2950–2967.
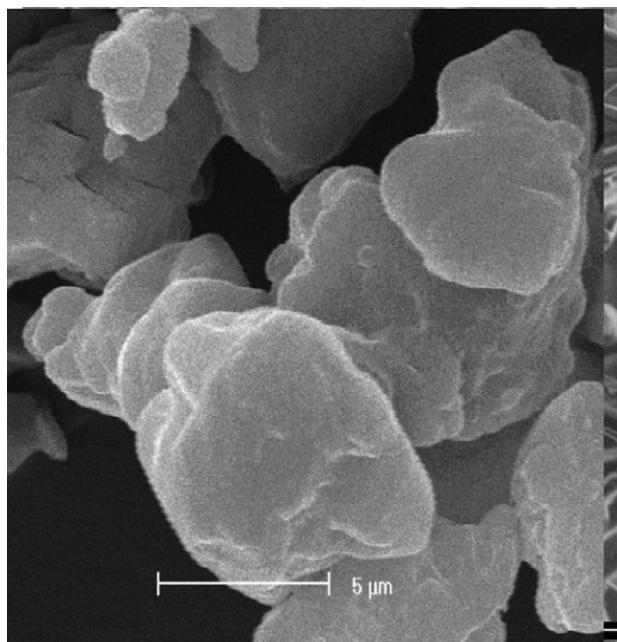

Figure 1. SEM pictures of spray-dried cocrystals of Carbamazepine-Glutaric acid (left) and Urea-Succinic acid (right)

[2] D.J. Good and N. Rodriguez-Hornedo, "Solubility Advantage of Pharmaceutical Cocrystals". Cryst. Growth Des., 9 (2009) 2252–2264

[3] R. Chiarella, R. Davey, and M. Peterson, "Making Co-CrystalsThe Utility of Ternary Phase Diagrams". Cryst. Growth Des., 7 (2007) 1223–1226.

[4] E. Gagnière, et al. "Formation of co-crystals: Kinetic and thermodynamic aspects". J. Cryst. Growth., 311 (2009) 2689–2695.

Generation and characterisation of new anhydrous polymorph of theophylline

D. Khamar[1], L. Seton[1], I. Bradshaw[1], G. Hutcheon[1].

[1]School of Pharmacy and Biomolecular Sciences, Liverpool John Moores University, Liverpool, UK.

Abstract – **A previously unreported anhydrous polymorph of theophylline was generated and characterised. The stability behaviour of a new solid form was studied by solubility determination, crystallisation, slurry equilibration and thermal analysis. This new anhydrous Form IV has been observed as the most stable form at room temperature and it is enantiotropically related to Form II. Moreover, the enantiotropic relationship in between Form I and Form II was also investigated by thermal analysis and slurry equilibration method.**

INTRODUCTION

Theophylline is a bronchodilator drug used in the treatment of asthma. Theophylline is known to exist as a monohydrate and three different anhydrous (Form I, Form II and Form III) forms [1]. The crystal structures are known for only Form II and monohydrate form. The anhydrous Form II has been considered as the most stable form at room temperature, which converts to Form I at 268.6 ± 2.2°C [2]. Form III has been regarded as a highly metastable form which converts to

Form II [3]. The interconversion, stability and crystallisation behaviour of different anhydrous forms of theophylline are not very clear. This is mainly due to the unavailability of crystal structure data and their inter transformation behaviour for all anhydrous forms.

MATERIALS AND METHODS

Generation of different anhydrous forms: Form II is available as bulk material from Sigma Aldrich, UK and used as such. Form I was generated by heating Form II in quick-fit glass vials at 260°C for 2 hours. Form IV was obtained from slurrying experiments with either Form II or Form I in methanol for 15 days.

Solubility determination of anhydrous theophylline was carried out by withdrawing samples from agitated suspensions and determining the concentrations by UV spectroscopy. Solubility determination in methanol was conducted by gravimetric methods. For the slurrying experiments, suspensions of anhydrous theophylline (I/ II/ I + II) in methanol were agitated at constant speed and samples withdrawn at frequent time intervals and analysed by Powder X Ray Diffraction (PXRD), optical microscopy and Scanning Electron Microscopy (SEM). Thermal analysis was carried out by Differential Scanning Calorimetry (DSC) at different heating rates in semi sealed pans and by Hot Stage Microscopy (HSM).

RESULTS AND DISCUSSION

Slurrying experiments starting with either Form II or Form I generated a new anhydrous form which was named as Form IV [4]. Solubility experiments from both water and methanol showed that Form IV is the most stable form as it has lower solubility than Form II. Cooling crystallisation of theophylline follows "Ostwald's rule of stages" [5] and generates Form II from methanol which eventually converts to Form IV over several days. Thermal analysis showed that Form IV to II transition is a solid state transition whereas Form II generates Form I via melt recrystallisation. Both Form I and II converted to Form IV through solvent mediated transformation. The crystal structure of Form IV showed theophylline dimers (Fig. 1) in the crystalline lattice and potentially this hydrogen bond motif imparts thermodynamic stability by strong hydrogen bonds compared to Form II where no such strong hydrogen bond motifs were seen.
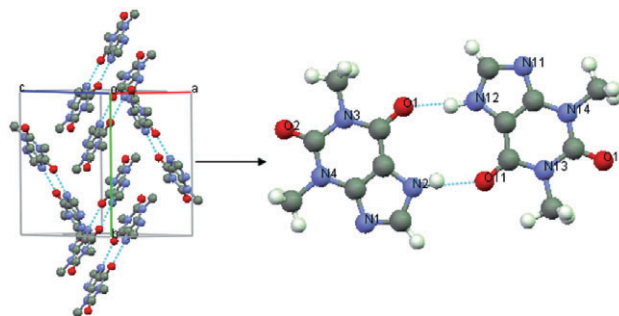

Fig. 1. Crystal structure of Form IV showing theophylline dimers.

CONCLUSIONS

This work thoroughly investigates the stability and interconversion of different anhydrous forms of theophylline. The most stable anhydrous polymorph (Form IV) of theophylline was generated and crystal structure for this form was reported. The stability order at room temperature for anhydrous forms is IV > II > I.

ACKNOWLEDGMENTS

REFERENCES

[1] A. M. Amado, M.M. Nolasco, and P.J.A. Ribeiro-Claro, "Probing pseudopolymorphic transitions in pharmaceutical solids using Raman spectroscopy: Hydration and dehydration of theophylline" *J. Pharm. Sci.,* **96** (2007) 1366–1379.

[2] B. Legendre, and S.L. Randzio, "Transitiometric analysis of solid II/ solid I transition in anhydrous theophylline" *Int. J. Pharm.*, **343** (2007) 41–47.

[3] N.V. Phadnis, and R. Suryanarayanan, "Polymorphism in anhydrous theophylline – Implications on the dissolution rate of theophylline tablets". *J. Pharm. Sci.*, **86** (1997) 1256–1263.

[4] L. Seton, D. Khamar, G. Hutcheon, I. Bradshaw, "The solid state forms of theophylline: presenting a new anhydrous polymorph" *Cryst. Growth Des.,* in press.

[5] J.W. Mullin, *Crystallisation*, 4th ed. Butterworth Heinemann, London, UK, 2001, pp. 214–215.

Granule stress characterisation for wet high shear granulation: model validation

E.L. Chan[1], G.K. Reynolds[2], B. Gururajan[3], M.J. Hounslow[1], A.D. Salman[1]

[1]Department of Chemical and Process Engineering, University of Sheffield, Mappin Street, Sheffield, UK
[2]AstraZeneca, Charter Way, Silk Road Business Park, Macclesfield, Cheshire, UK
[3]AstraZeneca, Bakewell Road, Loughborough, Leicestershire, UK

Abstract – **A model for granule stress due to the impeller in a high shear mixer is proposed based on the inertial force of a rotating granular bed. The model is validated using pressure films to measure the stress at the impeller tip in a high shear granulator. Results for the tested formulation yield a linear correlation between the measured stress and the calculated values from the model.**

Fig. 1. Plot of measured tip stress versus granule stress model (Eq. 1)

INTRODUCTION

In the high shear granulation process, the stress exerted by the impeller affects granule deformation and growth and also leads to granule breakage. Earlier work on granule growth and breakage characterisation estimated this stress from the granule velocity and granule density [1–2], but the effects of impeller geometry and granule bed properties could not be seen explicitly from their model. In this work, a new model for the granule stress due to the impeller in a vertical axis high shear mixer is proposed and validated.

THEORY

Assuming a rectangular and constant angular velocity granular bed profile [4] and taking only the inertial contribution of the stress, the stress of the granule bed (Eq. 1) proposed depends on the granule bed properties, impeller blade geometries and rotational velocities. For the model validation, the stress at the impeller tip is investigated in particular.

$$\sigma_{total} = C_{IS} \frac{H_G}{h_I} \frac{\rho_G}{(1-\varepsilon_G)} \omega_{I-G}^2 r^2 (1-\cos\theta_I) \qquad \text{Eq. 1.}$$

MATERIALS AND METHODS

Wet high shear granulation of Lactose 450M and HPMC powders with water was performed in a 10 L Zanchetta Roto Junior high shear mixer.

1) *Tip stress measurement*: Fujifilm pressure films (Teckscan) which produce colour patches upon pressure application were affixed to the impeller tip. The colour densities were analysed using a stereo microscope for stress determination. Measurements were taken in the steady granule growth regime.
2) *Granule bed surface velocity measurement*: A Photron Fastcam Viewer high speed camera was used to monitor the granule bed surface velocity at 1000 fps.
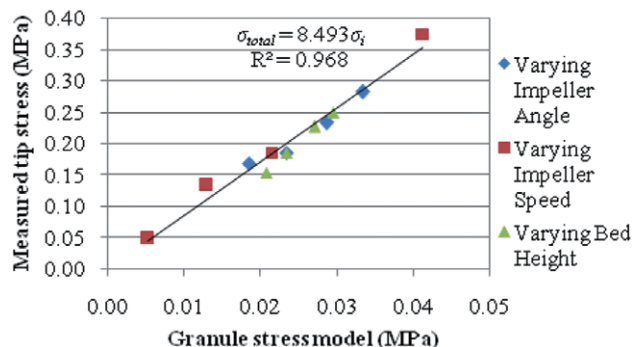
RESULTS AND DISCUSSION

The effect of impeller speeds, impeller blade, inclined angles and powder fill heights on the tip stress were investigated. The measured tip stress increased with these variables as predicted by Eq. 1. Regression was applied to the measured data to obtain the best fit and the coefficient of determination (R^2 value) determines how well the fitting is. From this analysis, the measured stress increases proportionally with the calculated values from Eq. 1 (Fig. 1). The proportionality constant C_{IS} can vary for different formulations and equipments since the granule bed frictional properties are neglected in the model development. This can also explain the difference in the magnitudes between the measured stress and the calculated values. Furthermore, the pressure film method measures the continuous build-up of stress from the onset of granulation rather than the instantaneous pressure.

CONCLUSIONS

A semi-empirical linear model for granule stress in a high shear granulator is found (Eq. 2) where the material/equipment constant, $C_{IS,}$ is determined experimentally using a fairly simple and effective pressure film method.

SYMBOL LIST

σ_{total}	: granule stress	ε_G	: granule bed porosity
C_{IS}	: material constant	ω_{I-G}	: relative velocity
H_G	: granule bed height	r	: radial position
h_I	: impeller height	θ_I	: impeller angle
ρ_G	: granule bed density	σ_i	: granule inertial stress

REFERENCES

[1] P. Vonk, C.P.F. Guillaume, J.S. Ramaker, H. Vromans and N.W.F. Kossen, "Growth mechanisms of high shear pelletisation" *Eur. J. Pharm. Biopharm.*, **157** (1998), 93–102.

[2] H. Vromans, H.G.M. Poels Janssen and H. Egermann, "Effects of high shear granulation on granulate homogeneity" *Pharm. Dev. Technol*, **4** (1999), 297–303.

[3] P.C. Knight, J.P.K. Seville, A.B. Wellm and T. Instone, "Prediction of impeller torque in high shear powder mixers", *Chem. Eng. Sci.*, **56** (2001), 4457–4471.

Incorporation of solid and liquid long chain triglyceride oils into non-ionic oil-in-water micro- and nanoemulsions

P. Wasutrasawat[1,2], W.Warisnoicharoen[2], H. Al-Obaidi[1], M.J. Lawrence[1]

[1]Pharmaceutical Science Division, King's College London, London SE1 9NH, UK and [2] Department of Pharmaceutical Technology, Faculty of Pharmaceutical Sciences, Chulalongkorn University, Bangkok 10330, Thailand

Abstract – **The formation, stability and solubilisation capacity of oil-in-water microemulsions (ME) and nanoemulsions (NE) stabilised by the non-ionic surfactant, $C_{18:1}E_{10}$ and containing either the liquid triglyceride, soybean oil (SBO), or the solid triglyceride, tripalmitin (TPN). Although there was little difference observed in the extent of the area of ME and NE existence, droplet size and stability, solubilisation of the poorly water-soluble drug was reduced in the TPN-containing ME and NE, most probably because of the "solid-like" nature of the TPN in some of the ME and all of the NE.**

INTRODUCTION

ME and NE have attracted considerable attention for use in a wide variety of industrial applications, including pharmaceuticals as drug delivery vehicles. Superficially ME and NE both contain oil and water, generally in the form of small surfactant-stabilised droplets of narrow size distribution. As a result of their very small droplet size – roughly 5–100 nm for ME, and 20–200 nm for NE – preparations are either transparent or slightly translucent, they have differences in their stability, with ME thermodynamically stable and NE kinetically stable. However, as some NE exhibit extended stability, it may be possible to gain pharmaceutical advantage from use of NE as opposed to ME in terms of improved drug solubilisation and reduced surfactant concentration.

The present study – focused on the effect of the state of the oil on the physico-chemical behaviour of the resulting ME and NE – involved investigation of the formation, stability and solubilisation capacity of oil-in-water (o/w) ME and NE stabilised by $C_{18:1}E_{10}$ and containing either the liquid triglyceride, SBO, or the solid triglyceride, TPN.
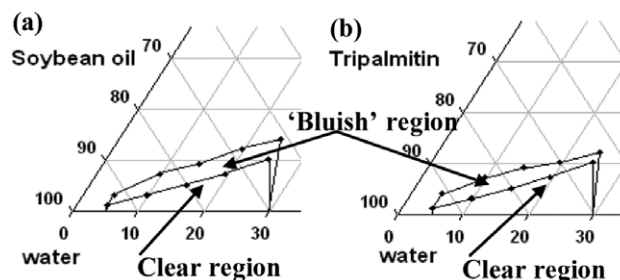

Fig. 1. Partial triangular phase diagrams for $C_{18:1}E_{10}$ stabilised o/w systems containing (a) soybean oil and (b) triplamitin 298 K.

MATERIALS AND METHODS

Samples were prepared as described in [1]. Clear samples were classified as ME, while bluish/translucent ones were denoted as NE. The areas of existence of o/w ME and NE stable for 1 month (as assessed by visual inspection and dynamic light scattering) were plotted on partial triangular diagrams. Solubilisation of the poorly water-soluble drug, testosterone propionate (TP), was determined in ME and NE comprising 10 wt% $C_{18:1}E_{10}$ with various amounts of tripalmitin (TPN) or soybean oil (SBO) as previously determined [1]. The melting points of the oils in ME and NE were determined by DSC.

RESULTS AND DISCUSSION

The areas of ME existence (Fig. 1) were identical for both oils and agreed with that previously reported by us for SBO [2]. However, the SBO-containing NE systems exhibited a

Table 1. Solubilisation of testosterone propionate in o/w microemuslions and nanoemulsions stabilised using 10 wt% $C_{18:1}E_{10}$ at 298 K. Figures in parenthesis give ± SD of the mean of 3 individual measurements

Mean Solubility wt% (± SD)							
Oil wt%	1	2	3	4	5	6	7
Tripalmitin	0.30	0.31	0.33	0.35	0.40	0.41	0.41
(C16)	(0.01)	(0.01)	(0.02)	(0.01)	(0.04)	(0.05)	(0.03)
Soybean	0.32	0.43*	0.52*	0.57*	0.66*	0.78*	0.78*
($C_{18:1}$)	(0.01)	(0.03)	(0.02)	(0.01)	(0.01)	(0.02)	(0.04)

* indicates a significant difference ($p < 0.05$) between solubilisation in the microemuslions and nanoemulsions at the same oil concentration

larger area of existence than the TPN-containing ones – for example, NE-stabilised by 20 wt% $C_{18:1}E_{10}$ incorporated 12 wt% SBO as opposed to only 10 wt% TPN. The size of the ME and NE droplets containing the same wt% of oil were very similar. Samples containing 3 wt% or less oil were clear ME (droplet size < 15 nm), while samples containing >3 wt% oil were classified as NE (droplet sizes in the range 17–46 nm). Regardless of ME and NE composition, the droplets remained stable over a period of 1 month.

Table 1 shows the results of the solubilisation study. As can be seen, the solubility of TP increases with increasing oil concentration, although the increase in TP solubility levels off at 6 wt% SBO and 1 and 5 wt% TPN.

Interestingly, DSC studies showed that in ME containing 2 wt% or less oil, most, if not all, of the TPN was in a liquid state, while in contrast most, if not all of the TPN was in a solid form when present in NE at 4 wt% or greater. Regardless of SBO concentration, the oil was in a liquid state in the ME and NE.

CONCLUSIONS

The greatest level of TP solubilisation occurred in the SBO-containing ME and NE. NE solubilised more TP than their corresponding ME.

REFERENCES

[1] C. Malcolmson, C. Satra, S. Kantaria, A. Sidhu, M.J. Lawrence "Effect of oil on the level of solubilisation of testosterone propionate into nonionic oil-in-water microemulsions" *J. Pharm. Sci.* **87** (1998) 109–116.

[2] W. Warisnoicharoen, A.B. Lansley and M.J. Lawrence, "Nonionic oil-in-water microemulsions: the effect of oil type on phase behaviour" *Int. J. Pharm.*, **198** (2000) 7–27.

Influence of crystallisation conditions on the morphology of ibuprofen crystals

M.H. Shariare, N. Blagden, M. de Matas and P. York

Institute of Pharmaceutical Innovation, University of Bradford, Bradford, BD7 1DP, UK

INTRODUCTION

Crystallisation is a widely used technique for purification and manipulation of the final crystal form of therapeutic agents. In particular, potential exists to control the mechanical properties of ibuprofen through control of crystal habit. The aim of this study was therefore to understand the influence of crystallisation conditions on the morphology of ibuprofen to enable production of crystals with different habits.

MATERIALS AND METHODS

Two batches of ibuprofen (Et-Ibu and Hex-Ibu) were crystallised using a cooling crystallisation technique with ethanol and hexane as solvents. Crystallised ibuprofen (Et-Ibu and Hex-Ibu) was characterised by scanning electron microscopy (SEM), optical microscopy, powder avalanching, thermogravimetric analysis (TGA), differential scanning calorimetry (DSC), powder x-ray diffraction (PXRD), dynamic vapour sorption (DVS) and inverse gas chromatography (IGC).

RESULTS AND DISCUSSION

Results showed that aspect ratio of ibuprofen crystals was related to the polarity (dielectric constant), solubility parameter and different types of bonding capacity of solvents. Ibuprofen crystallised from ethanol (dielectric constant = 30 and solubility parameter = 26.1) which has high polar and hydrogen bonding capacity (polar = 11.2 and hydrogen = 20) demonstrated plate like crystals with low aspect ratio of 2.5. Ibuprofen crystallised from non-polar hexane (dielectric constant = 2 and solubility parameter = 14.9) with high disper-
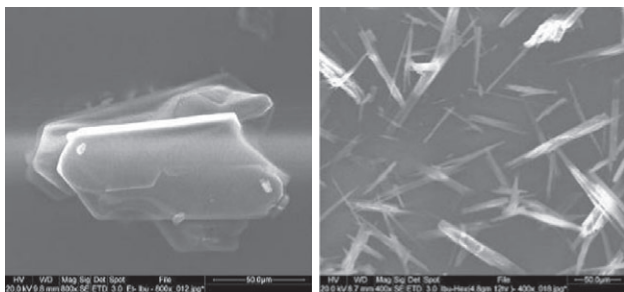
Fig 1. Scanning electron microscopy images of Et-Ibu and Hex- Ibu.

sion bonding capacity produced needle like crystals with high aspect ratio of 8.4. A linear relationship was observed between solubility of ibuprofen in a solvent and the cooling rate required to achieve the same supersaturation ratio.

Relationships were also observed between supersaturation ratio and induction time in both solvents, indicating that as supersaturation increases, induction time decreases. After a certain stage, there was no change in induction time although the supersaturation was increased. TGA and DSC data showed no difference in the thermal behaviour of the two crystallised batches and PXRD data showed that all the batches of ibuprofen comprised the same polymorphic form. DVS data

however showed differences in equilibrium moisture content at 95% RH (Et-Ibu 0.24% ± 0.01 and Hex-Ibu 0.14% ± 0.01), which is possibly due to differences in molecular orientation at the major habit faces of these two batches. IGC data also support the results obtained by DVS, which showed higher specific energy in THF for Et-Ibu compared to Hex-Ibu (Et-Ibu- 3.4 kJ/mol ± 0.35 and Hex-Ibu- 2.85 kJ/mol ± 0.18).

It also showed differences in dispersive surface energy (Et-Ibu = 30.05 mJ/m^2 ± 2.14 and Hex-Ibu = 36.40 mJ/m^2 ± 1.78), which is probably due to high aspect ratio of Hex-Ibu crystals. Ibuprofen crystallised from ethanol was less cohesive and free flowing (mean avalanche time Et-Ibu = 2.48 sec ± 2.13 and Hex-Ibu = 6.04 sec ± 4.75) than ibuprofen crystallised from hexane measured by powder avalanching. This is possibly also related to the lower aspect ratio of Et-Ibu crystals which decreases the contact area between crystals and increases the flow ability of the powder.

CONCLUSIONS

Crystallisation conditions can be manipulated to control the size, morphology and the powder properties of ibuprofen crystals which can be potentially used to control the processing characteristics of this compound.

Influence of Hydration State and Homologue Composition of Magnesium Stearate on the Properties of Liquid Paraffin Lipogels

Sheikh K.A.[1,2], Rouse J.J.[2], Kang Y.B.[1] and Eccleston G.M.[2]

[1]International Medical University (IMU), School of Pharmacy, 57000, Kuala Lumpur, Malaysia
[2]University of Strathclyde, Strathclyde Institute of Pharmacy and Biomedical Sciences (SIPBS), G4 0NR Glasgow, Scotland, UK

INTRODUCTION

Drugs and excipients often exhibit polymorphism. Transformation from one polymorphic form to another during processing can affect the physical chemical properties of the dosage form. Magnesium stearate (MgSt) exists as polymorphs and may be composed of either pure or mixed homologues. The aim of this work was to investigate the influence of the crystal state and the homologue composition of MgSt on the physical chemical properties of lipogels prepared from them using different methods of preparation.

MATERIALS AND METHODS

Five forms of MgSt were used to prepare the lipogels. Pure anhydrous magnesium stearate obtained by heating magnesium oxide and pure stearic acid (~97% C$_{18}$) (S1) on hydration formed the trihydrate (S2). Commercial mixed homologue MgSt was used as received (S3) and dried to form a mixed

homologue anhydrate (S4), which was rehydrated to yield mixed homologue dihydrate (S5).

Thirty (30) lipogels were prepared by dispersing ~12.5% MgSt (S1–S5) in liquid paraffin, heating to 110°C at a rate of 10°C/min, holding at 110°C for 1 hour and upon cooling (~0.1–0.2°C/min) to room temperature either adding ~1–4% water (method 1), homogenising (method 2) or cooling without water or homogenisation (method 3). The lipogels were characterised by visual inspection, polarised microscopy, DSC, and XRD.

RESULTS AND DISCUSSION

Lipogels prepared from the three samples of mixed homologue MgSt (S3-S5) formed stable semisolids when prepared by methods 1 and 2, but gave unstable solids (syneresis of oil over time) when prepared by method 3.

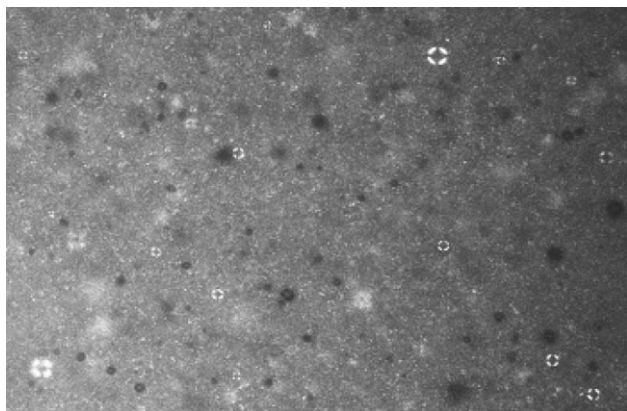Systems containing pure MgSt (anhydrous or trihydrate) prepared by methods 1–3 were generally structured fluids.

Fig. 1: Photomicrograph of the stable semisolid lipogel prepared by method 1 using MgSt (S3) and liquid paraffin.

The exception was the lipogel containing pure MgSt trihydrate (S2) prepared by method 3, which was initially semisolid, but reverted to a liquid when stirred gently, implying pressure sensitivity.

The stable semisolid lipogels showed "Maltese crosses" between cross–polars (Fig.1) which are indicative of lamellar phases. In contrast, unstable solids and fluids did not show "Maltese crosses", but rather crystals. The pressure sensitive semisolid from pure MgSt (method 3, S2) contained both plate-like crystals and lamellar structures; the latter only disappeared on stirring.

All mixed homologue semisolid lipogels prepared by methods 1 and 2 showed similar thermal properties suggesting that the microstructures were similar.

In contrast, the thermal properties of the unstable solids formed with mixed homologue MgSt (method 3) and the fluids formed with pure homologue Mg St were different from each other and from stable semisolid lipogels, implying differences in their structures. This observation was supported by XRD which indicated significantly more amorphous MgSt in the unstable solids compared to the mainly crystalline stable semisolids.

CONCLUSIONS

The formation of stable semisolid lipogels depends on the type of magnesium stearate used and method of preparation. Mixed homologue MgSt was essentially in the crystalline state in semisolid lipogels containing lamellar phases. In contrast, MgSt was mainly in the amorphous state in unstable solids.

ACKNOWLEDGEMENTS

Investigating solid state microstructure and interactions in lactose:PVP pharmaceutical granules

B. Crean[1], S. Banks[1], D. Le Roux[2], A. Parker[2], C.E. Madden-Smith[2], C.D. Melia[3] and C.J. Roberts[4].

[1]AstraZeneca Charnwood Pharmaceutical Development, Bakewell Road, Loughborough LE11 5RH, UK
[2]Molecular Profiles, 8 Orchard Place, Nottingham Business Park, Nottingham, NG8 6PX, UK
[3]Formulation Insights, School of Pharmacy, University of Nottingham, Nottingham NG7 2RD, UK
[4]Laboratory of Biophysics and Surface Analysis, School of Pharmacy, University of Nottingham, Nottingham NG7 2RD UK

INTRODUCTION

X-ray micro computed tomography (XMCT) was used in conjunction with confocal Raman mapping to measure the intragranular pore size, binder volumes and to provide spatial and chemical maps of internal granular components in α-lactose monohydrate granules formulated with different molecular weights of polyvinyl pyrrolidone (PVP). Infrared spectroscopy was used to understand the molecular association of binder domains.

MATERIALS AND METHODS

Granules were prepared by high shear aqueous granulation from α-lactose monohydrate and PVP K29/32 and K90.

XMCT was used to visualise the granule microstructure, intra-granular binder distribution and measure intra-granular porosity, which was subsequently related to intrusion porosimetry measurements. Confocal Raman microscopy and infrared microscopy were employed to investigate the distribution of components within the granule, and explore the nature of binder substrate interactions.

RESULTS AND DISCUSSION

XMCT datasets of internal granule microstructure provided values of residual porosity in the lactose:PVP K29/32 and lactose:PVP K90 granules of $32.41 \pm 4.60\%$ and $22.40 \pm 0.03\%$, respectively. The binder volumes of the lactose:PVP K29/32 and lactose:PVP K90 granules were

2.98 ± 0.10% and 3.38 ± 0.07% respectively, and were attributed to PVP rich binder domains within the granule. Example tomography and binarised images isolating the PVP rich binder domains are shown in Figure 1.

Confocal Raman microscopy revealed anisotropic domains of PVP between 2 μm and 20 μm in size surrounded by larger particles of lactose, in both granule types. Raman data showed that PVP domains contained various amounts of lactose. A Raman peak shift for the PVP amide group was further investigated using IR microscopy to examine granules before and after heating at 110 °C for 45 minutes. The vibrational peak shift position remained the same, which indicated that the PVP was molecularly associated with lactose, likely through hydrogen bonding, rather than residual water that may have been present from the wet granulation. The combination of physical and chemical analytical methods clearly showed four different structural regions are present within both granule types, independent of PVP molecular weight. The localised analysis at the micron length scale using confocal Raman microscopy indicated structural regions consisting of (i) PVP coated lactose with PVP in excess, (ii) PVP coated lactose in which PVP was depleted and (iii) lactose only domains. Structures (i) and (ii) can be interpreted in terms of different layer thicknesses of PVP on lactose crystals, and (iii) is probably an artefact of sample sectioning. Binarisation image analysis from the XMCT data showed that at the granular level, there were also (iv) discreet and isolated domains of PVP, which may represent PVP that was incompletely processed during the granulation step.

Figure 1. Representative XMCT images of lactose:PVP granules. Cross-sectional images are shown in the left hand column (A: lactose:PVP K29/32 and B: lactose:PVP K90) and intra-granular binder distributions calculated from binarised images in the right-hand column (C: lactose:PVP K29/32 and D: lactose:PVP K90) (Scale bars = 200 μm).

CONCLUSIONS

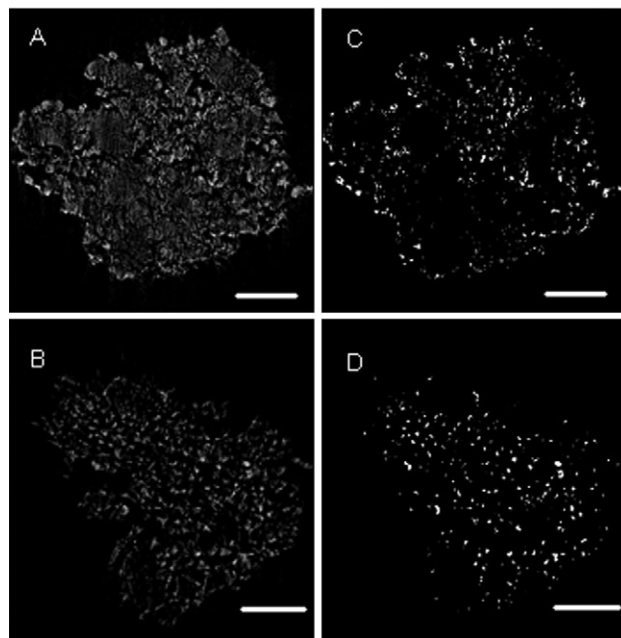XMCT can be applied to investigate granular microstructure and resolve the porosity and the excipient and binder volumes. Combining this technique with vibrational techniques provides further structural information and aids the interpretations of the XMCT images. When used complementarily, these techniques highlighted that porosity and binder volume were the most significant microstructural differences between the α-lactose monohydrate granules formulated with the different grades of PVP.

Investigation into the cause of blistering on tablets

J.C. Hooton, P. Lee, S.R. Holland, D.J. Murphy, T. Harris.

Pharmaceutical Development, AstraZeneca, Macclesfield, UK.

Abstract – **In order to investigate the cause of blistering on tablets, small scale granulations of formulation variants was performed. It was found that crospovidone was responsible for the blistering problem, and that the problem could not be resolved by either changing grade or reducing the level of the excipient in the formulation.**

INTRODUCTION

During the development of a formulation for a novel compound (Formulation A), it was observed that upon storage at elevated humidity, tablet surfaces became raised and uneven (a problem known as 'blistering'). While the blistering effect did not affect tablet performance, their appearance was unacceptable. An initial investigation with MRI imaging indicated that the formulation component present in the blistering penetrated into the tablet core and was therefore related to an excipient present in the formulation. A subsequent SS-NMR and TOF-SIMS investigation indicated that crospovidone was the cause, possibly due to swelling. While these analytical techniques suggested crospovidone was implicated, to test the hypothesis and potential methods of solving the problem, a series of formulation variants were manufactured using small scale processing equipment, and then stored under elevated temperature and humidity conditions to facilitate the onset of 'blistering'.

MATERIALS AND METHODS

Small scale granulations were performed using a Mi-Pro high shear mixer granulator (Pro-C-epT, Zelzate, Belgium). Parameters used were scaled down from the current manufacturing process. Granules were dried using a Vector fluid bed dryer and compressed using an instrumented F-Press.

The formulation components are shown in Table 1. Small scale wet granulation was used to make tablets with lactose and MCC instead of drug (to investigate if API affected blistering) and with no crospovidone (to prove disintegrant was the cause). Tablets manufactured were stored in open bottles at 40°C/75%RH for 28 days, and then visually examined for evidence of blistering.

Subsequent experiments were then performed to see if the blistering effect could be mitigated by using lower levels of crospovidone in the formulation, or by changing the disintegrant grade to one with a lower particle size.

RESULTS AND DISCUSSION

Table 2 shows that blistering was observed for all tablets, with the exception of the formulation containing no crospovidone. This indicated that crospovidone was the cause of the problem.

As the disintegrant is important in fragmenting of tablets, it is possible that changing the amount could adversely affect the dissolution of the tablet. Tablets were therefore dissolution tested and it was found that the absence of crospovidone had an effect upon this. Attempts to mitigate the blistering problem by using lower levels or different grades of crospovidone also proved unsuccessful in eliminating the problem.

Table 1. Formulation components

	Component	Function
Drug	Active ingredient	
Lactose	Filler	
Microcrystalline cellulose (MCC)	Filler	
Crospovidone	Disintegrant	
Povidone	Binder	

Table 2. Amount of hydrate formed during experiments

Experiment	Blistering observed
Lactose instead of drug	Yes
MCC instead of drug	Yes
No crospovidone	No
Reduced crospovidone	Yes
Different crospovidone grade	Yes

CONCLUSIONS

The presence of crospovidone was deemed to be the cause of the blistering problem. It was found that the problem could not be mitigated by either changing grade or reducing levels of the excipient.

ACKNOWLEDGMENTS

Investigation of the interaction between poloxamer 407 and poly (ethylene glycol) 600

F. Kianfar, B.Z. Chowdhry, J.S. Boateng, M.D. Antonijevic

School of Science, University of Greenwich at Medway, Chatham Maritime, Kent ME4 4TB, UK (fk30@gre.ac.uk)

INTRODUCTION

The aim of this study was to evaluate the interactions between poly (ethylene glycol) (PEG) 600 and poloxamer 407 prior to their use in a pharmaceutical formulation.

Chemical interactions between various ingredients alter the stability of pharmaceutical product [1]. Investigating the interaction between starting materials is a pre-requisite to develop a stable high quality pharmaceutical formulation. Changes in melting point [2] directly influence the stability of a product. One of the fundamental changes that might modify the melting point of a compound and consequently alter the stability of the system is the interaction between excipient(s) and API(s). The formation of a mixture following the interaction between component compounds, influences the characteristics of the system which therefore need to be determined.

MATERIALS AND METHODS

Materials: Poloxamer 407 (a block copolymer of ethylene oxide and propylene oxide with molecular weight (MW) between 9,760 to 13,200 and melting point of 56°C) and PEG (average MW about 570 to 600 and melting point between 20 and 25°C).

Analytical techniques: A Q2000 DSC instrument (TA Instruments) was employed to investigate the interaction between PEG 600 and poloxamer 407. Samples were prepared by physical mixing of PEG 600 and poloxamer 407 at
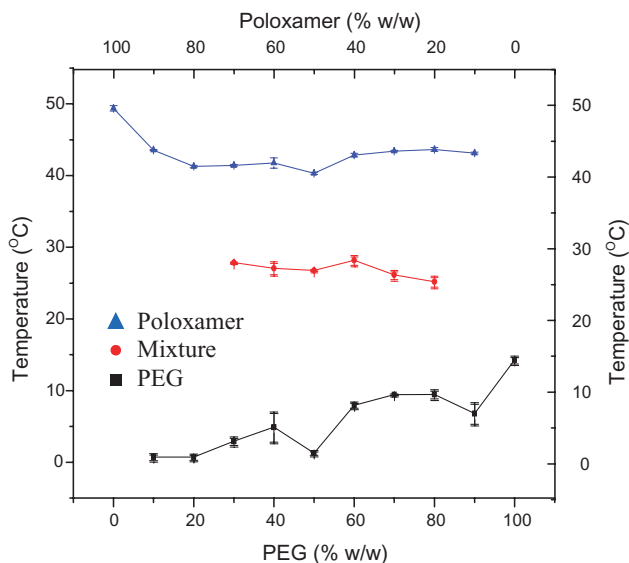
Fig.1. DSC transition onset values for mixture of 0/100 (%w/w) to 100/0 (%w/w) of PEG/poloxamer.

percentage of poloxamer, the melting point of PEG is decreased from 14.2°C to 0.7°C for pure PEG and 10/90 mixture (PEG/poloxamer) respectively. However, the same effect has not been observed with the change in melting point of poloxamer. After addition of 20% of PEG, poloxamer reaches its minimum melting point of 41.2°C and remains fairly constant with further increase of PEG/poloxamer ratio. The most interesting finding is the formation of what is believed to be a complex (mixture) of PEG/poloxamer at ratios of 30/70; 40/60 up to 80/20 with the melting point of the complex being relatively uniform (26.7 °C). This additional transition confirms not only that the two compounds physically interact but also form a unique entity that has characteristic properties i.e. melting behaviour.

CONCLUSIONS

The results of the DSC analyses showed significant changes in melting points values between the individual samples of PEG 600 and poloxamer and the mixture. This finding confirms that an interaction occurs between the two polymers. However, the extent of interaction varies and depends on the ratios of two compounds in the various mixtures.

REFERENCES

[1] W. R. Young. "Accelerated Temperature Pharmaceutical Product Stability Determinations" Drug Dev. Ind. Pharmacy. **16** (1990) 551–569.
[2] J. R. Davis. "Handbook of Thermal Spray Technology" in thermal technology, ASM Internationals, Material Park, Ohio, 2004, ch 1.pp 1–36.

ratios of (0/100) up to (100/0 %w/w) of PEG/poloxamer at 10% increments followed by solidification. The parameters for the DSC experiments were as follows:

1st heating −40°C to 80°C @ 10°C/min
2nd heating −40°C to 80°C@ 10°C/min
3rd heating −40°C to 80°C @ 10°C/min

Cooling after each heating cycle was at 40°C/min

RESULTS AND DISCUSSION

Figure 1 shows the melting point values for a series of PEG/ poloxamer mixtures. It is evident that with an increase in

Lactose fluidisation properties and their relationship to dry powder inhaler performance

H. Kinnunen[1], J. Shur[1], G. Hebbink[2], A.S. Muresan[3], R. Price[1]

[1]Pharmaceutical Surface Science Research Group, Dept. of Pharmacy and Pharmacology, University of Bath, Bath, UK.
[2]DMV-Fonterra Excipients, Borculo, Netherlands.
[3]FrieslandCampina Research, Deventer, Netherlands.

Abstract – **Adding lactose fines to a dry powder inhaler (DPI) formulation is hypothesised to increase the tensile strength of the powder thus resulting in higher fluidisation energy and consequentially in improved drug delivery. The aim of the study was to test the hypothesis. The results show that an increase in fluidisation energy corresponds to an improved DPI performance in the case of micronised fines. With milled fines no such clear link between fluidisation energy and DPI performance was seen.**

INTRODUCTION

Adding lactose fines to a dry powder inhaler (DPI) formulation enhances the performance of the formulation. Traditionally active site [1] and drug-fines agglomerates [2] theories have been used for explaining the phenomenon. Recently, a third possible mechanism for how the lactose fines improve the performance of DPI formulations was introduced, according to which adding lactose fines increases the tensile strength of the formulation. As a consequence, the fluidisation process is more energetic once it occurs after the tensile strength of the powder has been overcome, thus resulting in an increased number of particle-particle and particle-device collisions, and consequentially better de-agglomeration of the drug [3].

The aim of the study was to provide support for the third mechanism by showing that the addition of lactose fines makes the carrier more cohesive, and consequently results in higher fluidisation energy and therefore in improved drug delivery.

MATERIALS AND METHODS

Pre-blends of lactose were prepared by mixing lactose fines (Lactohale grades LH300 (microfine), LH230 and LH210) with LH100 (Coarse carrier). All the lactose materials used in the study were received from DMV-Fonterra Excipients (Borculo, Netherlands).

The powder flow and fluidisation properties of the pre-blends were characterised on a FT4 powder rheometer (Freeman Technology, Welland, UK). The lactose pre-blends were formulated with budesonide and the *in vitro* performance of the formulations was assessed on a Next Generation Impactor (Copley Scientific, Nottingham, UK) using Rotahaler, Cyclohaler and Handihaler devices.

RESULTS AND DISCUSSION

As shown in Fig. 1, adding lactose fines increased the fluidisation energy (FE) of the lactose pre-blends. LH300 was efficient in improving DPI performance in terms of fine particle fraction of emitted dose (FPF_{ED}) with all the devices. LH230 and LH210 proved to have less impact on the *in vitro* performance of the formulations despite having increased the fluidisation energy of the pre-blends. However, LH230 and LH210 provide better stability for the end product and therefore these milled grades of lactose are widely used in industry.
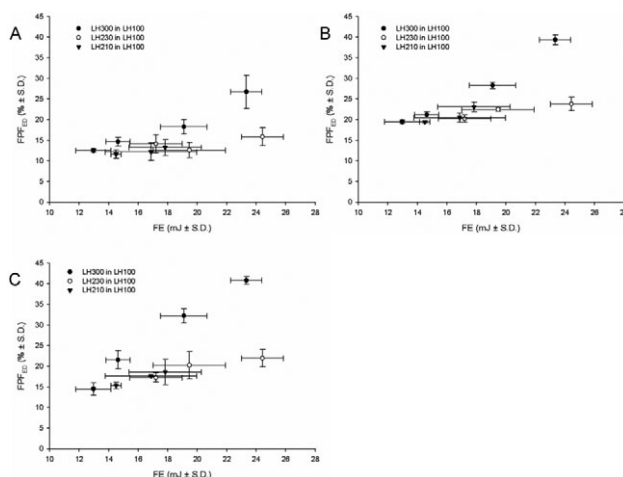

Fig. 1. Fine particle fraction of emitted dose as a function of fluidisation energy for the formulations tested on A) Rotahaler B) Cyclohaler and C) Handihaler

CONCLUSIONS

When a DPI product is designed, the combination of the formulation and the device used for delivering the medication has to be carefully considered so that the desired outcome in terms of drug delivery is achieved. Also the processing history of the lactose fines has to be taken in to account, as clear differences in the performance of micronised and milled fines were seen despite all of them exhibiting very similar fluidisation properties.

ACKNOWLEDGMENTS

REFERENCES

[1] D. Ganderton. "The generation of respirable clouds from coarse powder aggregates" *J Biopharm Sci.* **3**(1992), 101–105.
[2] Lucas, K. Anderson, and J.N. Staniforth. "Protein deposition from dry powder inhalers: Fine particle multiplets as performance modifiers" *Pharm. Res.* **15**(1998), 562–569.
[3] J. Shur, H. Harris, M.D. Jones, J.S. Kaerger, and R. Price. "The role of fines in the modification of the fluidisation and dispersion mechanism within dry powder inhaler formulations" *Pharm. Res.* **25**(2008), 1931–1940.

Nano-characterisation of phase separation in pharmaceutical solid dispersion films

F S. Qi, J. Moffat

School of Pharmacy, University of East Anglia, Norwich, Norfolk, NR4 7TJ UK

Abstract – **Humidity induced phase separations in solid dispersion films containing a poorly soluble drug and a hydrophilic polymer were investigated at a micron to submicron scale using pulsed force AFM (PFM-AFM), nanothermal analysis and photothermal microspectroscopy (PT-MS). Phase separations with micron to submicron dimensions were observed using PFM-AFM. The localised identification of drug/drug rich and polymer rich domains was achieved using nano-thermal analysis and PT-MS. PT-MS allowed the quantitative analysis of the drug distributions of the films.**

INTRODUCTION

Solid dispersion has been widely used for the purpose of enhancing dissolution of poorly water-soluble drugs. Phase separation is one of the direct causes of the physical instability of solid dispersions. Humidity induced phase separation is of particular importance to hydrophilic polymer based solid dispersions since it is an environmental stress more likely to occur during product storage than high temperature stress. Recent developed nano-characterisation tools allow detailed and highly localised physicochemical characterisation of solid dispersions.[1–3] This study employed scanning probe based localised characterisation methods including PFM-AFM, nano-thermal analysis and PT-MS to study the humidity induced phase separation of solid dispersion films.

MATERIALS AND METHODS

The films were prepared using a SCS G3P-8 lab scale spin coater (Cookson Electronics, Rhode Island, USA). Felodipine and PVP K29/32 with ratio of 1:1 were dissolved in a 1:1 dichloromethane/ethanol. The fresh films were tested within 2 hours of preparation. The humidity tests were performed at room temperature and 40%, 75%, and 94% RH. PFM-AFM imaging was performed using a pulse force mode AFM probe (Veeco, CA, USA) coupled with a Witec PFM module (Witec, Ulm, Germany). Localised nano-thermal analyses were performed using a Nano Thermal Analyser (Anasys Instruments, Santa Barbara, USA) with a Veeco diCaliber scanning probe microscope head and a thermal nanoprobe. PT-MS analysis was implemented by integrating a dedicated optical interface, a Thermomicroscopes Explorer AFM equipped with a Wollaston thermal probe and a FTIR spectrometer (Bruker Optics limited, Coventry, UK).

RESULTS AND DISCUSSION

The PFM-AFM images of the freshly prepared felodipine-PVP films showed no phase separation at submicron resolution. The nanothermal analysis of the fresh film revealed a highly reproducible single glass transition (T_g) at $100 \pm 2°C$. The N-H stretching at 3290 cm^{-1} observed in the PT-MS spectra of the fresh films indicated the drug-polymer hydrogen bonding.[4]

After exposure to humidity, cellular-like structures with dimensions of 50–100 μm were observed on the films. The PFM-AFM images revealed the significant roughness of the nuclei-like centre of each cellular unit. These nuclei are likely to be the separated drug during drying after humidity treatment. Localised nano-thermal analyses on the humidity treated films showed double T_gs at 50–60°C and 115–130°C which are associated with the glass transition of drug-rich domains and polymer rich domains respectively. The drug content in the polymer rich domains can be estimated using the Gordon-Taylor equation to be around 23–25% (w/w). No crystalline drug melting was detected even for the film treated at 94%RH for 24 hours (without drying). The N-H stretching at 3290 cm^{-1} (fresh) shifted to 3340 cm^{-1} (humidity treated) indicating the presence of cohesive hydrogen bonding between felodipine molecules, and the disruption of drug-polymer interaction.[4]

In addition to the detection of phase separation, the distribution of drug in the film before and after the humidity treatment was analysed using PT-MS. The result indicates that after humidity treatment, the drug distribution is highly uneven across the film. This is caused by migration of drug molecules during phase separation.

CONCLUSION

Nano-characterisation methods including PFM-AFM, nanothermal analysis, and PT-MS revealed the micron to submicron size phase separation in the felodipine-PVP films induced by humidity. In addition to the size and chemical makeup of the phase separations, the combined use of these novel techniques also allows the evaluation of drug/phase distribution across the solid dispersion films during aging which can bring new insights into the dynamic process of phase separation in solid dispersion formulations.

ACKNOWLEDGMENTS

REFERENCES

1. S. Qi, A. Gryczke, P. Belton, D.Q.M. Craig, Int. J. Pharm. 2008, 354(1–2) 158–167

2. L. Harding, S. Qi, G. Hill, M. Reading, D.Q.M. Craig, Int. J. Pharm. 2008, 354(1–2) 149–157

3. X. Dai, J.G. Moffat, A.G. Mayes, M. Reading, D.Q.M. Craig, P.S. Belton and D.B. Grandy, Analy. Chem. 2010 82(1) 91–97

4. P.J. Marsac, A.C.F. Rumondor, D.E. Nivens, U.S. Kestur, L. Stanciu, L.S. Taylor, J. Pharm. Sci. 2010, 99(1) 169–185

Optimisation of hydrogel microneedle design for transdermal drug delivery

Martin J. Garland, Laura Rodriguez Gallego, David Woolfson, Ryan F. Donnelly.

School of Pharmacy, Queen's University Belfast, Belfast, UK

Abstract – **This study describes the use of *in situ* swellable hydrogel microneedle (MN) array for transdermal drug delivery. For the first time, the effect of MN geometry upon the resulting in-skin swelling and drug permeation profiles across neonatal porcine skin from a hydrogel MN array were investigated. It was found that the rate of MN swelling, and ultimately drug delivery, was dependent upon MN array design.**

INTRODUCTION

Microneedle arrays are minimally invasive devices that can be used to by-pass the *stratum corneum* barrier and thus achieve enhanced transdermal drug delivery. Microneedles (MN) (50–900 μm in height, up to 100 MN cm^{-2}) in diverse geometries have been produced from silicon, metal, carbohydrates and polymers using various microfabrication techniques [1, 2]. In this present study we describe the use of *in situ* swellable MN arrays, based upon a cross-linked poly(methyl vinyl etherco- maleic anhydride) – polyethylene glycol (PMVE/MA-PEG) hydrogel. Once inserted into the skin this MN system will absorb interstitial fluid to form a swollen hydrogel, creating a continuously open aqueous pathway for drugs to migrate through. The aim of this study was to evaluate, for the first time, the effect of microneedle geometry upon the resulting in-skin swelling and drug permeation profiles from PMVE/MA-PEG MN arrays.

MATERIALS AND METHODS

MN, comprised of 15% w/w PMVE/MA-7.5% w/w PEG 10,000, were prepared using a laser-based micromoulding technique, to create a range of arrays of varying geometry (Table 1). The in-skin swelling of MN in full thickness neonatal porcine skin was determined over a 24 h period, by removing the MN from the skin at set time intervals, and measuring the increase in MN surface area using a digital microscope (GE-5 Digital Microscope, Laboratory Analysis Ltd, Devon, UK). The microneedle mediated delivery of methylene blue (MB), using a range of MN variables (Table 1) across dermatomed neonatal porcine skin (350 μm thick) over a 24 h period was assessed using a vertical Franz cell set up, with MB analysed using UV spectroscopy at 664 nm (Biotek Powerwave XS Microplate Spectrophotometer, BioTek, Bedfordshire, UK).

Table 1. The % of MB released at 6 h across dermatomed neonatal porcine skin from a range of hydrogel microneedle designs (Mean ± SD, n = 5).

	Variable	% MB released at 6 h
MN Height (μm)	350	16.1 ± 0.91
MN width and interspacing 300 μm	600	29.5 ± 1.74
	900	35.58 ± 2.28
MN density (no. of MN/ cm^2)	121	29.5 ± 1.74
MN height 600 μm, *MN width 300* μm	196	43.6 ± 3.92
	361	59.18 ± 4.41
PEG MW (Da)	200	14.3 ± 1.19
MN height 600 μm, *MN width 300* μm, *interspacing 300* μm	10,000	29.5 ± 1.74

RESULTS AND DISCUSSION

Table 1 shows the effect that MN design, both in terms of geometry and formulation composition, have upon the permeation profiles of MB through the hydrogel MN material and across dermatomed neonatal porcine skin. It was found that the geometry of the MN array used plays an important role in the rate of drug permeation, with statistically higher release observed as the height of the MN was increased ($p < 0.001$), as well as with an increase in MN density ($p < 0.001$). Interestingly, this was found to correlate with statistically different rates of swelling for these designs, with an increase in swelling rate noted as the MN height ($p < 0.001$) and MN density ($p < 0.001$) were increased. In addition, the cross-link density of the hydrogel material was found to affect the release and in-skin swelling of the MN array, with a higher cross-linked density (PEG 200) causing a reduced rate of drug release and MN swelling in comparison to a more open hydrogel network when PMVE/MA is crosslinked with PEG 10,000 ($p < 0.001$).

CONCLUSIONS

This study has highlighted, for the first time, the ability to alter the rate of drug diffusion from a hydrogel MN array through adjustment of either MN geometry and/or cross-linking density. The use of hydrogel MN in this study could revolutionise the MN field as, in a one step process, they

could create a continuously open aqueous pathway for drugs to migrate through, the rate of which could be tailored to meet the requirements for a specific drug or patient profile through simple adjustment of array design.

REFERENCES

[1] S. Henry, D.V. McAllister, M.G. Allen, M.R. Prausnitz, Microfabricated microneedles: a novel approach to transdermal drug delivery, *J. Pharm. Sci.* **87** (1998) 922–925.

[2] M.R. Prausnitz, Microneedles for transdermal drug delivery, *Adv. Drug Deliv. Rev.* **56** (2004) 581–587

Patterning the Mechanical Properties of Hydrogen Silsesquioxane (HSQ) Films Using Electron Beam Irradiation for Application in Mechano Cell Guidance

Mathieu Lanniel[1], Bingrui Lu[2], Yifang Chen[2], Stephanie Allen[1], Lee Buttery[1], Phil Williams[1], Ejaz Huq[2] and Morgan Alexander[1]

[1]Laboratory of Biophysics and Surface Analysis, School of Pharmacy, University of Nottingham, Nottingham NG7 2RD, UK.
[2]Rutherford Appleton Laboratory, Harwell Campus, Didcot, OX11 0QX, UK.

Abstract **– The effects of electron beam dose on the topography and the mechanical properties of Hydrogen Silsesquioxane (HSQ) are characterised using atomic force microscopy (AFM). The changes of the HSQ stiffness and roughness of a "development step" used to remove uncured material employing trimethylamine (TMA) are investigated. The attachment of human mesenchymal stem cells (hMSC) cultured on HSQ coated with plasma polymerised allylamine is demonstrated.**

INTRODUCTION

Studies on mesenchymal stem cells have revealed that these cells commit to different lineages according to the stiffness of the substrate used for cell culture [1, 2]. Cell attachment to materials has also been shown to depend on the surface chemistry and topography of the material [3]. It has been noted that amino groups are particularly favourable for the immobilisation of adhesive proteins promoting cell adhesion [4]. This study explores the potential of hydrogen silsesquioxane (HSQ) coated with plasma polymerised allylamine (ppAAm) as a material for studying the effect of surface stiffness on stem cell differentiation.

MATERIALS AND METHODS

Commercial hydrogen silsesquioxane solution was spin-coated onto silicon wafers. Electron beam exposure of HSQ was carried out within a wide range of doses (19.4 μC cm^{-2} to 2000 μC cm^{-2} for the developed HSQ array, 7 μC cm^{-2} to 5000 μC/cm^2 for the undeveloped HSQ array). Development was then carried out on one HSQ array for 2 minutes using TMA. To allow cell attachment, the HSQ arrays were coated with plasma polymerised allylamine and hMSCs were seeded on the arrays. AFM nanoindentation measurements were performed to determine the Young's modulus of the samples.
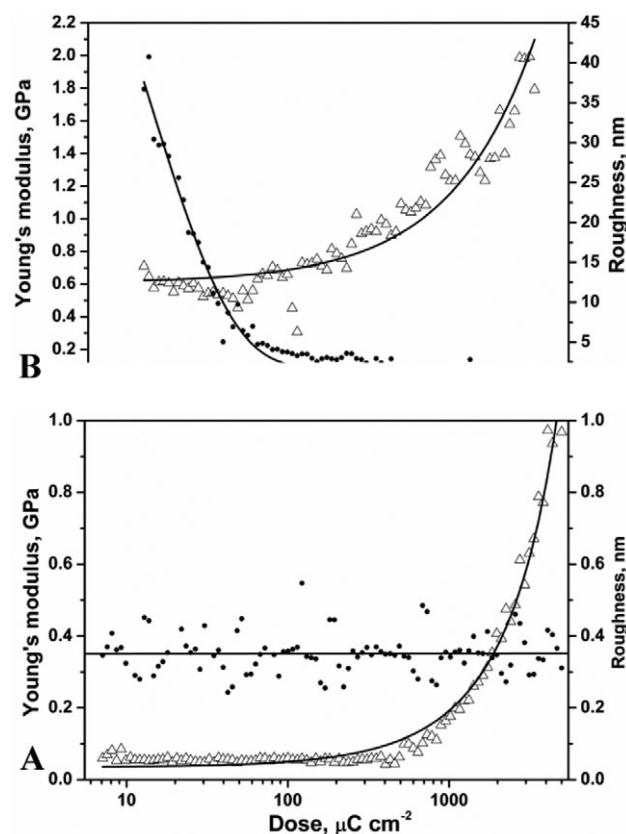

Figure 1. Young's modulus (Δ) and RMS roughness (·) of the undeveloped (A) and developed (B) HSQ arrays as a function of electron beam exposure.

RESULTS AND DISCUSSION

For undeveloped HSQ samples, Young's modulus values ranged from 0.06 GPa for a pristine sample to 1 GPa for the

highest electron beam exposure. The root-mean-square (RMS) roughness varies between 0.2 nm and 0.6 nm (Figure 1.A). For the developed HSQ sample (Figure 1.B), modulus values were comprised between 0.7 GPa for the lowest exposure to 2 GPa for the highest one. The RMS roughness shows a decrease from 40.7 nm for the lowest electron beam exposure to 0.32 nm for the highest one. Surface coating with ppAAm facilitates adhesion of hMSCs to HSQ sample of variable modulus for 1 week of culture.

CONCLUSIONS

It was observed that electron beam curing of HSQ is able to control the surface Young's modulus over a large range of stiffness values, with highly controlled feature geometry and spatial distribution.

Mesenchymal stem cells were cultured on the HSQ samples after coating with ppAAm illustrating the potential of this system to spatially control cell response.

REFERENCES

[1] A.J. Engler, S. Sen, H.L. Sweeney, D.E. Discher, Cell 126/4 (2006) 677.
[2] A.S. Rowlands, P.A. George, J.J. Cooper-White, Am J Physiol-Cell Ph 295/4 (2008) C1037.
[3] M. Li, Glawe, J.D., Green, H., Mills, D.K., McShane, M.J., (2000).
[4] A.S.C. Curtis, C.W.D. Wilkinson, B. Wojciak, Abstr Pap Am Chem S 207 (1994) 269.

Production of amorphous dispersions of sulfonamides/polyvinylpyrrolidone by ball milling

Caron V., Tajber L., Corrigan O.I., Healy A.M.

School of Pharmacy and Pharmaceutical Sciences, Trinity College, Dublin 2, Ireland.

Abstract – **This work reports on the production of amorphous dispersions by milling initially crystalline sulphonamide drugs with polyvinylpyrrolidone.**

INTRODUCTION

At the present time, most solid drug formulations use the active pharmaceutical ingredient (API) in the crystalline state. A promising way to improve the bioavailability of APIs is to produce amorphous forms which present increased apparent solubility compared to the crystalline forms. One way to stabilise amorphous APIs is to make molecular dispersions of drugs in a polymer glassy matrix. Among the different ways to produce these dispersions, ball milling is a solid state and solvent-free route which makes it attractive for poorly soluble drugs that cannot be dissolved in a suitable (harmless) solvent.

MATERIALS AND METHODS

Sulfadimidine (SDM), sulfadiazine (SDZ), sulfamerazine (SMZ) and sulfathiazole (STZ) are antibacterial drugs belonging to the sulfonamide group. SDM and SDZ present only one crystalline form while SMZ and STZ present respectively two and five polymorphs. Polyvinylpyrrolidone (PVP) is an amorphous polymer. Powders were processed with a ball mill (Retsch PM 100). The systems were characterised by Powder X-Ray Diffraction (PXRD), Differential Scanning Calorimetry (DSC), Infrared Spectroscopy (FTIR), Scanning Electron Microscopy (SEM) and powder rheometry (repeatability and flowability tests using a FT4 Rheometer).

RESULTS AND DISCUSSION

PXRD patterns (Figure 1) show that SDM/PVP, SDZ/PVP and STZ/PVP mixtures must contain between 60% and 70% of PVP to produce amorphous systems on co-milling while SMZ/PVP requires only 30% of PVP to produce an amorphous composite system. DSC scans reveal that the amorphous mixtures present a single glass transition (Tg) located between the Tg of the pure compounds, indicating that API and PVP are truly mixed at a molecular level during co-milling for these concentrations. FTIR spectra seem to indicate API-PVP interactions. For concentrations of PVP less than the level required to get fully amorphous systems, the solid-state nature of the material depends on the API: PXRD patterns show that SDM and SDZ present a reduction in intensities and a broadening of their Bragg peaks, consistent with partial amorphisation and increased crystalline defects. PXRD patterns of milled STZ are quite complex to analyse and seemed to reveal the presence of forms III and IV along with amorphous material. SMZ undergoes a polymorphic transition from metastable to stable polymorph, showing a remarkable counterintuitive example of stabilisation (lowering of Gibbs free energy) of a system upon milling. SEM pictures show that, for all milled systems, the particles present
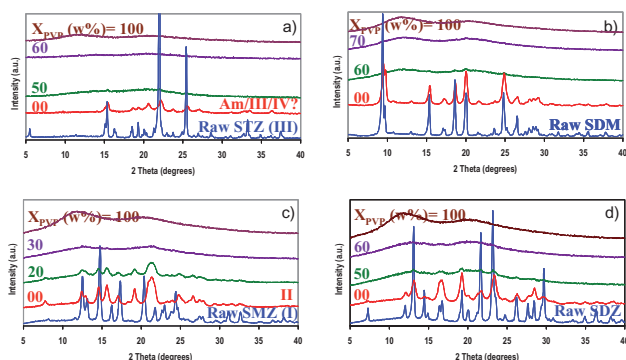
Fig 1. PXRD patterns of comilled composites: a) STZ/PVP, b) SDM/PVP, c) SMZ/PVP, d) SDZ/PVP.

irregular and crushed shapes. Powder rheometry shows that milled systems present irregular flowability.

CONCLUSIONS

For all the systems under investigation, ball milling enabled amorphous dispersions to be obtained, given a sufficient load of PVP. Compared to other techniques, ball milling has the advantage of avoiding solvent usage and also avoiding potential thermal degradation of the pharmaceutical compounds. However, particle morphology is poor and may pose processing problems (e.g. conveying, flowability . . .) as shown by powder rheometry.

ACKNOWLEDGMENTS

Scrutiny of controlled release protein loaded PLGA microspheres using surface analytical techniques

A. Rafati[1], A. Boussahel[1], A.G. Shard[2], K.M. Shakesheff[1], P.T. Whiteside[3], S. Rigby-Singleton[3], C.J. Roberts[1], X. Chen[1], D.J. Scurr[1], M.R. Alexander[1], M.C. Davies[1]

[1]School of Pharmacy, University of Nottingham, Nottingham, UK
[2]National Physical Laboratory, London, UK
[3]Molecular Profiles Ltd., Nottingham, UK

Abstract **– PLGA microspheres encapsulating lysozyme as a model of a controlled release formulation are analysed using ToF SIMS. We show for the first time a discontinuous surfactant film on the surface of the microspheres which is removed upon sputtering with C_{60} ions. Confocal Raman provides ready information on the internal structure of the particles which is supplemented by ToF-SIMS of sectioned microspheres.**

INTRODUCTION

Controlled release formulations such as polymer microspheres allow for the sustained efficacious delivery of protein therapeutics. To gain an understanding of the distribution of the protein and excipients such as surfactants within individual microspheres, we have employed the complementary techniques of ToF-SIMS and confocal Raman spectroscopy.

MATERIALS AND METHODS

Poly(lactic-co-glycolic acid) (PLGA) was used with hen egg white lysozyme and polyvinyl alcohol. A double emulsion production method was used as outlined previously [1].

Lysozyme concentrations of 1.5%, 3%, 5% and 10% (w/w) were investigated.

ToF SIMS was carried out using an ION-TOF, ToF-SIMS IV with a bismuth source, using the burst alignment mode of operation, and a buckminsterfullerene source for sputtering.

Confocal Raman used a WITec CRM200, a 40 μm^2 area was mapped and 11 μm was scanned in the z-axis in order to obtain a 3D understanding of the chemical distribution of polymer and protein drug.

RESULTS AND DISCUSSION

The ToF-SIMS analysis of sectioned microspheres in Figure 1a showed large porous voids within the microsphere, some of which showed protein present. In addition, discrete spherical protein-rich domains are seen within the PLGA which measure approximately 2 μm in diameter (indicated with an arrow in Figure 1a and b). These findings are complemented by the Raman data in Figure 1b where the larger pores show the presence of lysozyme on their walls and smaller ones appear to be filled. The internal microsphere architecture and the distribution of protein, have their origin in the water in oil in water emulsion production process.
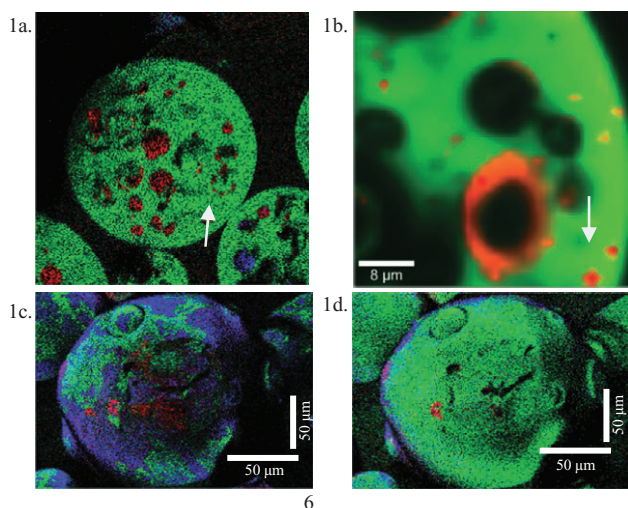
Fig. 1a. ToF-SIMS of asectioned microsphere. Green indicates PLGA (m/z 71/73/87/89), red shows protein (m/z 42) and blue indicates PVA (m/z 59). **Fig. 1b.** shows a confocal **Raman** map, the arrows in a and b indicate pores concentrated with protein measuring ~2 μm. **Fig. 1c** and d. ToF SIMS of an intact microsphere before and after sputtering

ToF-SIMS analysis revealed a discontinuous PVA surfactant layer on the PLGA microsphere surface in Figure 1c with low levels of protein appearing at the surface. AFM

profilometry (not shown) reveals the surfactant layer to be 4 nm thick. C_{60} etching of the surface readily etched this away to reveal the underlying PLGA (Figure 1d).

CONCLUSIONS

The complementary application of confocal Raman analysis and ToF-SIMS has revealed that protein is distributed in the porous structure of the microsphere, either in protein rich domains or on the walls of larger pores. In contrast, the microparticle surface is composed primarily of a discontinuous, 4 nm thick coating of PVA surfactant on the PLGA surface. This is the first example of high resolution chemical imaging of surfactant films on such a system.

ACKNOWLEDGMENTS

REFERENCE

[1] S. Ravi, *et al.*, Development and Characterisation of Polymeric Microspheres for Controlled Release Protein Loaded Drug Delivery System. Indian Journal of Pharmaceutical Sciences 70(3) (2008) 303–309.

Solid Dispersions – Molecular Distribution and Crystal Habit Modification

W.K. Ali[1], C.F. Rawlinson[1], A.C. Williams[1]

[1]School of Pharmacy, University of Reading, Reading, RG6 6AD, UK

Abstract – **Here, the mechanisms by which poloxamer (PX) interacts with ibuprofen (IB) in solid dispersions (SD) are investigated. SEM and Raman mapping provide evidence for molecular distribution of IB at low drug loading and modified crystalline habit at higher ratios.**

INTRODUCTION

SDs can be used to improve dissolution and hence bioavailability of poorly-water soluble drug. By this process drugs can be dispersed in molecular, amorphous, or crystalline form of reduced size and altered crystalline habit. Understanding the drug form present is important due to the resulting influence on apparent dissolution. We have previously reported molecular distribution of IB within PX 407 SD systems dependent on molar ratio of drug to polymer; at 2:1 ratios hydrogen bonding mediated molecular distribution (as evidenced with FT-InfraRed, Differential Scanning Calorimetry and Powder X-ray Diffraction)[1]. At higher drug ratios both crystalline and molecular forms were detected. Dissolution rate advantages were identified for all systems.

Here we aim to explore the influence of drug-polymer ratio on the spatial distribution of IB within the SD, and the form and particle size of residual crystalline fractions.

MATERIAL AND METHODS

SD (employing fusion methods) and physical mixtures of IB and poloxamer 407 were prepared at 3% (2:1 molar ratio), 10%, 33% and 50% IB w/w. Samples were coated with gold (Edwards sputter coater S 150 B for 2 minutes at 25 MA) and examined using scanning electron microscopy (600 F SEM) under vacuum using FEI Quanta 20 kV accelerate voltage. Compressed discs of solid dispersions and physical mixture were prepared and their surface mapped using Raman Microscopy (Renishaw).

RESULTS AND DISCUSSION

SEM images 10%, 33%, and 50% SD all showed evidence of crystals of reduced size and altered habit compared to unproc-

essed IB: needles in unprocessed samples, flatter plates in SDs. Low levels of very fine IB crystals were observed in the 3% system at high magnification power (15000 X).

Crystalline IB spectroscopic features were absent from Raman microscopy images collected for 3% SD. All SD samples showed evidence consistent with IB-PX hydrogen bonding at PX terminal groups. This evidence was absent in physical mixtures; mapping indicated macroscopic mixing of the two components.

At 10%, 33% and 50% loadings additional crystalline features of IB (including dimer hydrogen-bonding and crystal lattice moieties) were visible in the individual spectra, and upon mapping indicated small localised areas of high concentration of IB crystals.

These results confirm conclusions from previous data of hydrogen bonding mediated molecular dispersion at 3% IB. However SEM provided evidence that limited nucleation/re-crystallisation has occurred even in this low drug loaded sample. At higher drug loading, extensive IB re-crystallisation has occurred. However, observations relating to habit and crystal size indicate that PX is moderating the physical presentation of all IB. Accordingly, differences from starting IB materials and physical mixes may offer mechanisms for a dissolution rate advantage in all SD samples.

CONCLUSIONS

IB was predominantly dispersed in a molecular form in the 3% SD. At 10%, 33% and 50% IB is additionally present as small localised areas of IB plate crystals. The molecular dispersion, reduced crystal size, crystal habit and intimate mixing with PX may all contribute to the improved dissolution profiles previously reported for these systems.

ACKNOWLEDGMENTS

REFERENCE

[1] W.Ali, A.C. Williams, C.F.Rawlinson, "Stochiometrically governed molecular interactions in drug: poloxamer solid dispersions" *Int.J. Pharm.,* **391** (2010) 162–168

Sucrose / glucose molecular alloys by cryogenic milling

A.J. Megarry[1], J. Booth[2], J. Burley[1]

[1]School of Pharmacy, University of Nottingham, UK
[2]AstraZeneca, Macclesfield, UK

Abstract – **Molecular alloys are a relatively new concept but have shown great promise as an emerging formulation platform [1]. A new sucrose / glucose molecular alloy is reported here as a model system to study the interesting properties of molecular alloys. We demonstrate that amorphous material can be prepared by cryogenic milling without melting. The glass transition temperature can be precisely tuned over a 40 °C range by changing the composition of the molecular alloy.**

INTRODUCTION

Low aqueous solubility of drugs can lead to poor bioavailability and present a significant challenge to formulation scientists. Solubility can be increased by formulating drugs as amorphous solids, however, because such systems are typically metastable and more reactive, drug stability can be compromised [2]. Multi-component molecular alloys, prepared by cryomilling, offer a mild and generic approach to the preparation of amorphous formulations, without the drawbacks associated with more established solvent and heat-based processing methods commonly used to produce amorphous solid dispersions. The formation of single phase amorphous materials without solvents and heat minimises the risk of drug instability and provides the possibility of producing molecular dispersions with genuinely tunable physical properties.

MATERIALS AND METHODS

Sucrose and glucose were purchased from Sigma Aldrich and used as received.

Cryogenic milling was performed with a SPEX Sample Prep 6870 Freezer/Mill. Samples were precooled for 5 minutes, milled for 2 minutes at 15 cycles per second and cooled for 1 minute. All samples were milled for 1 hour. Samples were allowed to return to room temperature before analysis.

Differential Scanning Calorimetry (DSC) was performed using a TA Q2000, using Tzero low mass pans. All samples were heated at a rate of 10 °C / minute.

X-Ray Powder Diffraction (XRPD) was performed with a Bruker D8.

RESULTS AND DISCUSSION

XRPD data (not shown) revealed that the samples were initially crystalline and 'x-ray amorphous' after milling. DSC showed that sucrose has a glass transition temperature (Tg)
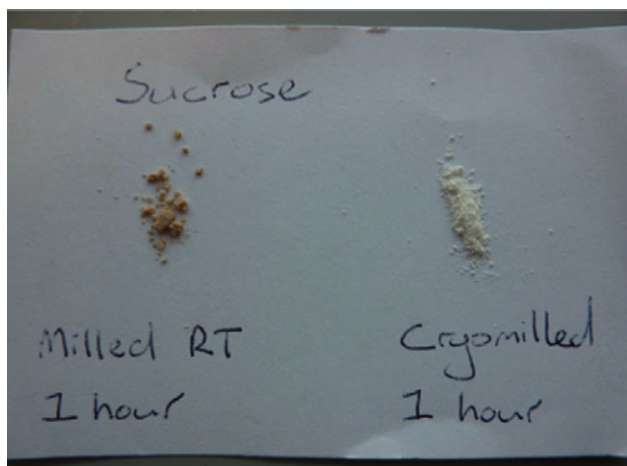
Fig. 1. Sucrose after room temperature and cryogenic milling for 1 hour.

Fig. 2. Sucrose / glucose molecular alloy variation of glass transition temperature with time.

of 60 °C after 60 minutes of cryogenic milling. Interestingly, sucrose that had been milled for the same time at room temperature showed significant caramelisation (Fig. 1). This shows that the amorphisation on milling occurred without melting. Mixtures of glucose (Tg: 20 °C) and sucrose were also made and subjected to cryogenic milling. By DSC, they showed a single relaxation event, suggesting they have been mixed at a molecular level. By changing the composition of the molecular alloy, it is possible to rationally tune the Tg (Fig. 2).

CONCLUSIONS

Cryogenic milling is a very mild method to prepare amorphous material without melting. It can be used to form molecular alloys with tunable, predictable physical properties.
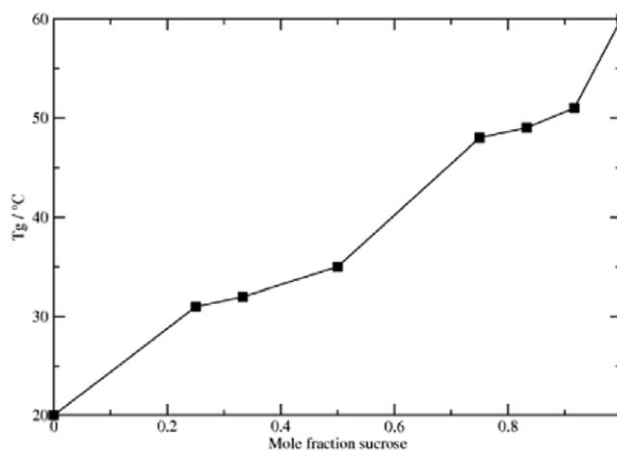
These molecular alloys appear to be very promising as a new formulation platform for poorly soluble and thermally sensitive drugs.

REFERENCES

[1] M. Descamps, J. F. Willart, E. Dudognon, and V. Caron. Journal of Pharmaceutical Sciences, 96(5):1398–1407, 2007.
[2] G. Zografi, B. C. Hancock. Journal of Pharmaceutical Sciences, 86(1):1–12, 1997.

Tensile Analysis and Swelling Characterisation of Co-Solvent Effects in Poly(Vinyl Alcohol) Films

E.J. Wright, R. Byrne, G.P. Andrews, D.S. Jones

School of Pharmacy, Queen's University Belfast, Belfast, UK.

Abstract **– Poly(vinyl alcohol) and co-solvent effects have been extensively studied in the gel state but not in films. It is possible to manipulate the mechanical and swelling properties of the PVA films using co-solvents and annealing for specific purposes, such as urethral catheter coatings and drug delivery systems.**

INTRODUCTION

Poly(vinyl alcohol) (PVA) is a hydrophilic, water soluble polymer that forms both gels and films. It exists in a semi-crystalline state as a result of the strong intra- and inter-molecular hydrogen bonding due to the regular hydroxyl groups [1]. This hydrogen bonding also aids in the dissolution and gelation of the polymer in water and with co-solvents [2], the effects of which have previously been studied in gels. The solvents under investigation are dimethyl sulphoxide (DMSO), propylene glycol (PG), dipropylene glycol (DPG), *N*-methyl pyrrolidone (NMP) and 2-pyrrolidone. The PVA films are characterised for use in the pharmaceutical or medicinal field as catheters or drug delivery systems.

MATERIALS AND METHODS

The PVA of molecular weight 13,000–23,000 (98% hydrolysed) was purchased from Sigma-Aldrich. PG, DPG and 2-pyrrolidone (GPR) were purchased from Sigma-Aldrich and the DMSO and NMP (GPR) were purchased from VWR.

Films were manufactured by dissolving PVA in water/solvent mixtures at 90°C and stirring for 24 hours. The films were cast in Petri dishes and allowed to cool and dry over 5 days and then half the films were annealed in an oven at 90°C for 15 minutes.

The tensile testing was carried out using TA XT.plus Texture Analyser and films, cut in a 'dog bone' shape, were stretched at a rate of 1 mm/s for up to 200 mm or until they snapped. The force and distance required to break were measured. The equilibrium swelling study was carried out over 48 hours at 25 °C in deionised water.

Fig. 1. Chemical structure of polymer and solvents.

RESULTS AND DISCUSSION

The tensile results show that there is no clear pattern across all solvents. For instance annealed 30% PVA films using NMP have a higher Young's Modulus than the same non-annealed films and higher concentrations of NMP will produce stronger films. DPG films also show higher Young's Modulus when films are annealed, with the highest Young's Modulus recorded for 20% PVA and 10% DPG annealed film. At low polymer concentrations with DMSO the annealed films produce higher Young's Moduli and at higher polymer concentrations the non-annealed films produce higher values. For PG films in all but one circumstance the annealed films are stronger, except with 30% PVA and 10% PG were the non-annealed film is stronger.

There is also variation in the results from the swelling studies. At 20% PVA concentration the films containing less solvent (10%) swell more than those containing more (20%) regardless of whether the film is annealed or non-annealed. At 30% PVA concentration the films which have not been annealed swell more when they also contain less solvent. H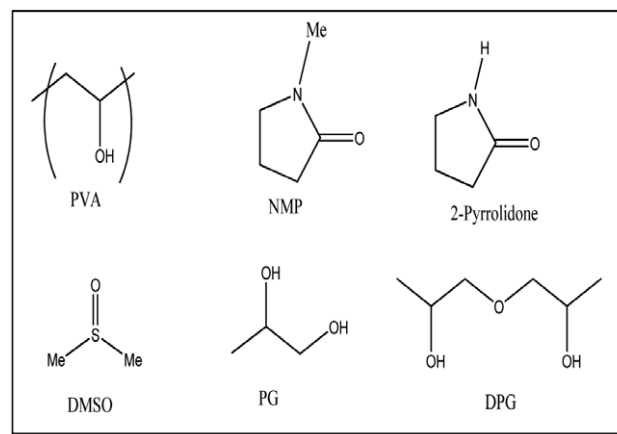owever at the higher polymer concentration and when the films are annealed the pattern is largely the same, although the DPG film with more solvent swelled more than the films containing less solvent.

CONCLUSIONS

The annealed films in most conditions produce a higher Young's Modulus and swell less. The annealing process allows polymer chains to arrange in a more favourable conformation making them stronger and unable to take up water and swell to the same extent as non-annealed films.

REFERENCES

[1] S.I. Song and B.C. Kim, "Characteristic rheological features of PVA solutions in water-containing solvents with different hydration states" *Polymer*; **45** (2004) 2381–2386

[2] J.S. Park, J.W. Park and E. Ruckenstein, "On the viscoelastic properties of poly(vinyl alcohol) and chemically crosslinked poly(vinyl alcohol)" *J. Appl. Polym.Sci.*, **82** (2001) 1816–1823.

The Characterisation of Slow Crystallisation of Lipidic Solid Dispersion Systems using Quasi-Isothermal MTDSC

S.O. Otun[1], E. Meehan[2], S. Qi[1] and D.Q.M. Craig[1]

[1]School of Pharmacy, University of East Anglia, Norwich, UK.
[2]AstraZeneca, Macclesfield, UK.

INTRODUCTION

Quasi-isothermal modulated temperature DSC is a technique by which the sample material is subjected to modulations about a constant temperature for a prolonged period of time. This temperature is incrementally increased or decreased through a thermal transition, minimising the kinetic effects of the heating programme and meaning that the isothermal data sequence obtained illustrates the true transition temperature of the sample (Manduva et al 2008). In this study this method has been used to investigate the crystallisation process of lipid-based solid dispersion systems. In particular, it is recognised that slow or incomplete crystallisation is a significant manufacturing issue, but very little information is available

on this phenomenon. Here we suggest a novel means by which it may be quantitatively monitored.

MATERIALS AND METHODS

Samples of Gelucire 44/14 and the formulated solid dispersion systems, in the weight range 1.97 to 2.25 mg, were prepared into aluminium Tzero pans and analysed using a TA Q2000 DSC. After complete melting at 60°C for Gelucire alone and a maximum of 220°C for the model drug systems to allow for any crystalline drug melting, the samples were run using Quasi-Isothermal MTDSC, cooling at 1°C increments from 35 to 5°C for Gelucire 44/14 alone and 25 to 0° for solid dispersions, with an isotherm of 20 minutes at each increment, an amplitude of ± 1°C and a period of 60 seconds.

Solid dispersions of Gelucire 44/14 with the model crystalline drugs ibuprofen, indomethacin and piroxicam were prepared via the melt method at 60°C and allowed to cool at 20°C for 48 hours prior to analysis.

RESULTS AND DISCUSSION

Quasi-Isothermal MTDSC Lissajous analysis of the polymer Gelucire 44/14 illustrates obvious crystallisation on cooling at 31°C. Observation of the reversing heat capacity as a function of time, however, demonstrates crystallisation onset during the 33°C modulation, continuing until the conclusion of the experiment at 5°C, thus suggesting incomplete crystallisation (Fig 1).

Solid dispersion formulation of Gelucire 44/14 with the selected model drugs appears to significantly reduce the polymer crystallisation temperature. Those systems containing 5% w/w ibuprofen reduced the crystallisation temperature to 25°C, with increasing drug loading reducing the temperature further still (Fig 2). At 50% w/w ibuprofen no obvious crystallisation occurred, however in all cases the reversing heat capacity steadily decreased over time suggesting that equilibrium was not reached and crystallisation was therefore incomplete.

Indomethacin and piroxicam solid dispersions with Gelucire 44/14 were also found to have a much reduced crystallisation onset at 21, 25 and 21 for indomethacin 24, 21 and 25°C for piroxicam 5, 10 and 15% w/w drug loadings respectively. Again the 50% w/w systems for both model drugs did not demonstrate an obvious crystallisation peak however, as with all cases, there was a steady decrease in heat capacity over time, becoming more pronounced at 7°C in the case of piroxicam.

We believe the model drugs present in the solid dispersions to be crystalline, as a melt transition can be seen for the higher drug loadings on heating. Typically one would expect drugs to either promote crystallisation (via nucleation) or to have no effect, hence the counterintuitive observation of retardation is of interest and practical significance. The presence of un-dissolved drug particles is known to affect the overall crystal growth rate of the polymer (Long et al 1995). In the present case, however, we suggest that dissolved drug may be suppressing either nucleation or growth.
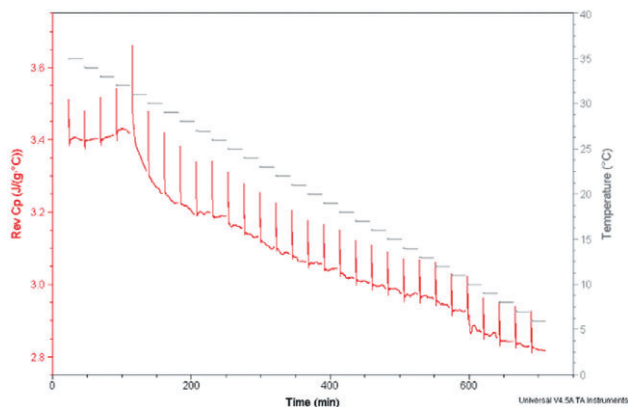

Fig. 1. QIMTDSC reversing Cp of Gelucire 44/14 20 minute modulations on cooling as a function of time.
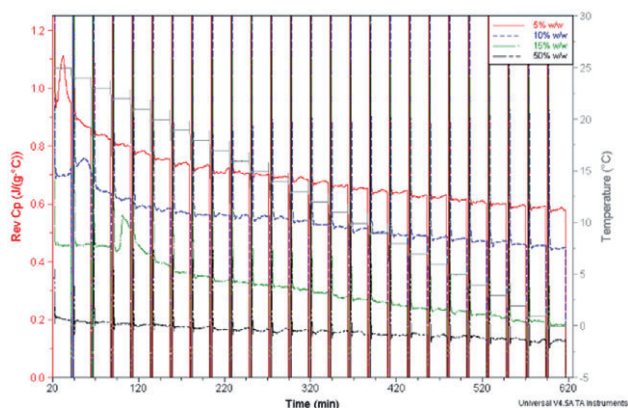

Fig. 2. QIMTDSC reversing Cp of ibuprofen and Gelucire 44/14 solid dispersion 20 minute modulations on cooling as a function of time.

CONCLUSIONS

Quasi-isothermal MTDSC appears to be a promising tool in the investigation of the crystallisation process. The combination of drug with polymer in solid dispersion systems appears to reduce the crystallisation temperature quite significantly if not eradicating it altogether. It is imperative to have an understanding of this process in order to predict its impact on the physicochemical properties of the final product.

ACKNOWLEDGMENTS

REFERENCES

[1] R. Manduva, V. L. Kett, S. R. Banks, J. Wood, M. Reading and D. Q. M. Craig, *J. Pharm. Sci*, **97** (2008) 1285–1300.

[2] Y. Long, R. A. Shanks and Z. H. Stachurski, *Prog. Polym. Sci*, **20** (1995) 651–701.

The Effect of Solvents on the Morphologies of Disulfiram Copper (II) Complex

J.Z. Tang[1], Z. Naqvi[1], N. Akhtar[1], S. Ali[1], W. Wang[2]

[1]The Pharmacy Research Group (PRG) and [2]The Cancer Research Group
The Research Institute in Healthcare Science (RIHS), University of Wolverhampton, Wolverhampton, WV1 1LY, UK

Abstract – **Different solvent systems were studied for forming the disulfiram copper (II) complex. The objectives of this study are to find the solvent system that facilitates high yield of the complex and induces forming fine crystals. A dark crystal of the disulfiram copper (II) complex was formed and characterised in terms of melting point (mp), infrared (IR) spectroscopy, UV-VIS analysis, and inductively coupled plasma (ICP) spectroscopy. The morphologies and particle sizes were assessed using light and scanning electron microscopes. The solvent systems in this study are 1) alcohol related, 2) acetone related, and 3) DMSO related. The acetone related solvent system is the best solvent system for the highest yield of the copper (II) complex while the DMSO related solvent system is the best solvent system for preparing the finest particle of the crystal.**

INTRODUCTION

Disulfiram is the active pharmaceutical ingredient (API) of Antabuse, an oral tablet used for alcohol aversion therapy for over 50 years [1]. Recent investigations reported that disulfiram, potentiated by metal ions has shown high and selective toxicity towards cancer cells [2]. It suggests that the active agent is likely a Cu complex, bis (diethyldithiocarbamate) Cu(II) or $Cu(deDTC)_2$, which is formed in situ [3]. Although the disulfiram Cu(II) complex was referred in the publications, this complex is actually a mixture of disulfiram and Cu(II), either in 1:1 mole ratio or Cu(II) in excess. It is of interest in preparing and purifying the disulfiram Cu(II) complex for developing new dosage form.

MATERIALS AND METHODS

Disulfiram from Acros Organics, UK and $CuSO_4 \cdot 5H_2O$ from Avocado Research Chemical LTD were used in preparing the disulfiram Cu(II) complex. Briefly, 22.5 mg of $Cu SO_4 \cdot 5H_2O$ was dissolved in saline solution and then added drop wise into 10 mg of disulfiram dissolved in a specific solvent system. The mixture was filtered after 48 h. The dark crystal, dried and weighed, was characterised in terms of melting point (mp), infrared (IR) spectroscopy, UV-VIS analysis, and inductively coupled plasma (ICP) spectroscopy. The morphologies and particle sizes were assessed using light and scanning electron microscopes.

RESULTS AND DISCUSSION

The results demonstrate that the crystal of the copper (II) disulfiram complex has a melting point in the range of 180–186°C. The IR spectra of the complex differ from those of
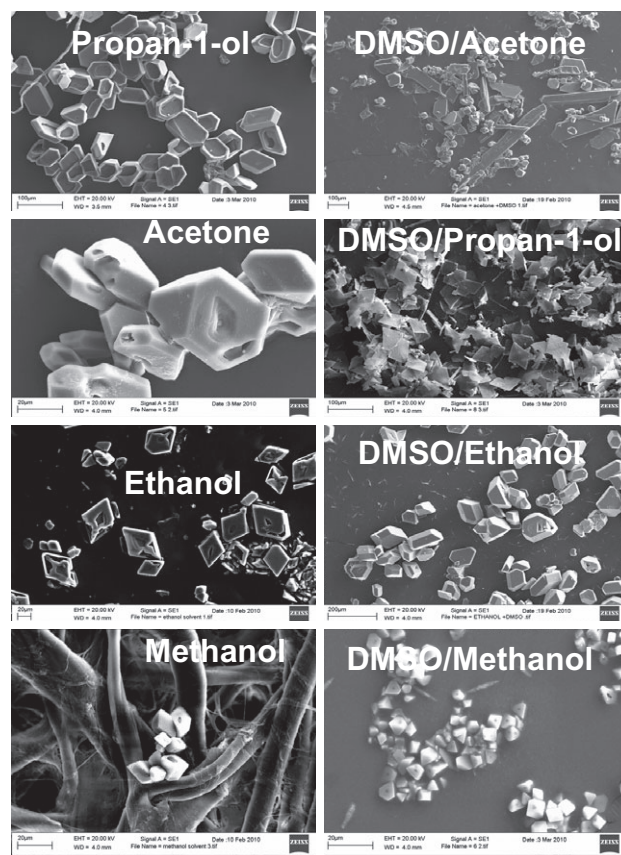

Fig. 1 Scanning electron microscopy images of the complex crystals from different solvent systems

disulfiram with new absorptions at 1206 cm^{-1} and 845 cm^{-1} against the reported absorption at 914 cm^{-1} for disulfiram [4]. The UV-VIS analysis exhibits a new absorbance at 437 nm for the copper (II) disulfiram complex [5]. The ICP copper content is approximately 17.00% (17.78% theoretical value of Cu(II)). The solvent systems in this study are 1) alcohol related, 2) acetone related, and 3) DMSO related. The acetone related solvent system is the best t solvent system for the highest yield of the copper (II) complex while the DMSO related solvent system is the best solvent system for preparing the finest particle of the crystal. Variety of crystal morphologies was observed, the elongated hexagon was produced from propan-1-ol and the diamond shape was from ethanol (Fig.1). The non-alcohol solvent systems were unable to produce crystals in a regular shape and the DMSO related solvent system might slow the crystal growth into a regular shape.

CONCLUSIONS

DMSO is a solvent frequently used for preparing disulfiram solution. The particle size of in situ formed disulfiram Cu(II) complex in DMSO might influence the growth of the cancer cells.

REFERENCES

[1] Sauna ZE, Shukla S, Ambudkar SV, "Disulfiram, an old drug with new potential therapeutic uses for human cancers and fungal infections" *Molecular BioSystems* 2005; 1: 127–134

[2] Cvek B, Dvorak Z, "Can the old drug, disulfiram, have a bright new future as a novel proteasome inhibitor?" Drug Discovery Today 2008; 13(15/16): 716–722

[3] Walker MB, Edwards K, Farmer PJ, "Disulfiram, metal, and melanoma" *J Chem Edu* 2009; 86(10): 1224–1226

[4] Ökçelìk B, Atay O, "Quantitative determination of disulfiram-containing pharmaceuticals by IR spectroscopy and high pressure liquid chromatography methods" *FABAD J Pharm Sci* 2003; 28: 193–200

[5] Sharma VK, Aulakh JS, Malik AK, "Fourth derivative spectrophotometric determination of fungicide thiram tetramethyldithiocarbamate in commercial sample and wheat grains using copper (II) sulphate" *EJEAF Che* 2003; 2(5): 570–576

The influence of API isolation and drying methods post crystallisation on API properties and performance during drug product processing

A. Balasundaram, M. Boukerche, C. Davies, N. Dawson, and P.L. Goggin

Pfizer Global Research & Development, UK
E-mail: neil.dawson@pfizer.com, arulsuthan.balasundaram@pfizer.com, moussa.boukerche@pfizer.com

INTRODUCTION AND OBJECTIVES

Wet granulation processes can increase the processability (e.g. flow) of active pharmaceutical ingredients (API) which have physical and mechanical properties that mean they cannot be successfully processed into drug product by other manufacturing methods. In addition, APIs that are wet granulated often have cohesive properties and hence can adhere to manufacturing equipment and restrict flow.

The purpose of this study is to understand how the drying of the API from the crystalliser impacts the physical properties of the API and subsequent downstream drug product performance following wet granulation. A series of drying conditions were investigated to produce variation of API properties.

MATERIALS AND METHODS

Total of 8 API lots were dried using either tray or agitated filter drying (AFD).

1) *Crystallisation and Isolation:* The crystallisation process was developed using parallel conditions in 50 ml-scale crystalliser (MultiMax). Optimised conditions were then scaled up in a 1 L scale crystalliser (LabMax) to assess the robustness of the crystallisation process. Thereafter multiple batches were processed at 1 kg scale in a 20 L fixed rig. These batches were dried using various operating conditions in an AFD to deliver different API particle properties. The resultant API was used to investigate the robustness of the wet granulation process.

2) *API physical properties:* The following particle and bulk powder properties were determined (Table 1).

Table 1: API physical propertie

Test	Technique
Degree of agglomeration	Imaging/light and scanning electron microscopy[1]
Particle size	Low angle laser light scattering (laser diffraction – USP429)
Bulk and tap density	Copley bulk and tap – USP28-NF23 method II

3) *Drug product:* High shear wet granulation experiments were conducted in the Fukae Powtec high speed mixer (250 g batch size) using standardised conditions.

The following quality attributes of the drug product were compared:

- Powder flow and density
- Compact radial tensile strength (RTS) at 0.85 solid fraction (SF)
- Compact hardness
- Compact disintegration time
- Compact dissolution

RESULTS AND DISCUSSION

During the drying process, agglomerates are formed. Increased drying time increased the degree of agglomeration and densification of the API. Tray dried batches typically had minimal agglomeration, a relatively low particle size (D[v,0.9]) and low bulk density compared to batches which were agitated filter dried. Fewer agglomerates of API led to poor blend flow

and wet granulation processability issues. Controlling the agglomeration state through the AFD conditions resulted in improved API bulk powder densification, defined by the API particle size distribution and bulk density. These were identified as important quality attributes of the API from a wet granulation processing perspective. The drying process did not have any impact on compact RTS, hardness, disintegration and dissolution. The compacts achieved a high RTS and this in turn formed tablets with high crushing strength. Targetted compact disintegration time of less than 15 minutes were met and the dissolution profiles showed 75% release at 15 minutes, meeting the criteria.

CONCLUSION

Control of agitator filter dryer conditions were identified as a key step in the drying process of the API improving the processability of a wet granulated drug product.

REFERENCE

[1] G. Nichols *et al* "A review of the terms agglomerate and aggregate with a recommendation for nomenclature used in powder and particle characterisation" *Int. J. Pharm.*, **91** (2002) 2103–2109.

The Synthesis of New Microgel Particles Based On 2-Hydroxyethyl(meth)acrylates

M. Cope[1], J.P. Cook[1], V. Khutoryanskiy[1]

[1]School of Pharmacy, University of Reading, Whiteknights, Reading, RG6 6AD, UK.

Abstract **– Microgel particles based on 2-hydroxyethylacrylate (HEA) and 2-hydroxyethylmethacrylate (HEMA) were synthesised by surfactant-free emulsion copolymerisation. The particles were characterised by dynamic light scattering and electron microscopy and it is anticipated that they could have applications in ocular therapeutics.**

INTRODUCTION

Random copolymers consisting of varying ratios of 2-hydroxyethylmethacrylate (HEMA) and 2-hydroxyethylacrylate (HEA) have previously been synthesised [1]. These polymers have demonstrated promising thermal and biological properties, with polymers with a HEMA content of 0–100% being found to be non-irritating with respect to mucosal tissues, and the temperature response being dependent on the HEMA/HEA concentration. In this research, cross-linked microgel particles have been synthesised as a possible injectable delivery vehicle, a novel application for these copolymers.

MATERIALS AND METHODS

The method of synthesis used was surfactant-free emulsion polymerisation (SFEP) [2]. In this method the monomer(s) and cross-linker, in this case ethylene glycol dimethacrylate (EGDMA), are added to water at a low weight fraction of around 1%. The mixture is heated and continuously stirred. Following the addition of a suitable initiator, such as ammonium persulphate, a cloudy dispersion of microgel particles is obtained. Unreacted monomer was removed from the particle dispersion by dialysis. Particles were synthesised with nominal relative HEMA/HEA ratios of 0–100 mol% and nominal cross-linker contents of 2 and 5 mol%.
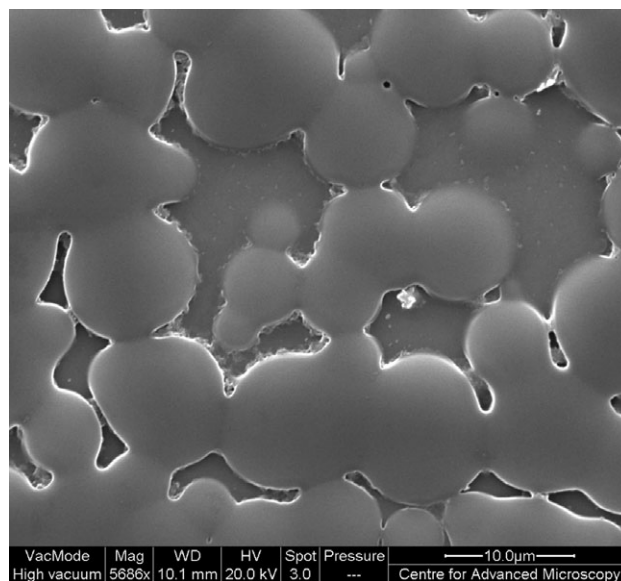

Fig. 1. Typical SEM image of HEMA microgel particles cross-linked with 5 mol% EGDMA.

RESULTS AND DISCUSSION

Dynamic light scattering was used to measure the mean hydrodynamic diameter of the microgel particles. Variations in the HEMA/HEA ratio in the reaction mixture were found to result in significantly different reaction yields and particle sizes, with all samples having a significant degree of polydispersity (see Fig. 1). The largest particle sizes, around 1 μm, were observed at the highest HEMA contents, 90–100%, suggesting that HEMA is incorporated preferentially into the

particles. This is probably because HEMA is more hydrophobic than HEA and thus better suited to the surfactant-free method.

The 'dry' particle diameters are significantly larger than the 'dispersed' particle diameters due to flattening of the particles onto the substrate surface as they dry, known as 'pancaking' [2]. The more hydrophilic particles, with higher HEA content, flatten to a larger extent as they have a higher water content in dispersion. Given the established use of HEMA in contact lens materials, and even for the delivery of drugs to the eye [3], these particles may also find applications in ocular therapeutics.

CONCLUSIONS

New microgel particles of HEMA and HEA cross-linked with EGDMA have been synthesised using an established method, surfactant-free emulsion polymerisation. These particles are likely to be highly biocompatible, as copolymers of HEMA and HEA have previously shown good biocompatibility [1]. The established use of HEMA in contact lens manufacture suggests these particles could be particularly suitable for ocular therapeutics.

REFERENCES

[1] Khutoryanskaya, O.V.; Mayeva, Z. A.; Mun, G. A.; Khutoryanskiy, V. V. *Biomacromolecules* **9** (2008) 3353–3361.

[2] Nerapusri, N.; Keddie, J.L.; Vincent, B.; Bushnak, I.A. *Langmuir* **22** (2006) 5036–5041.

[3] Gulsen, D.; Chauhan, A. International Journal of Pharmaceutics **292** (2005) 95–117.

Thermal decomposition of chlorogenic acid in different atmospheres

Samuel K. Owusu-Ware, Babur Z. Chowdhry, Stephen A. Leharne and Milan D. Antonijevic*

School of Science, University of Greenwich at Medway, Chatham Maritime, Kent ME4 4TB, UK

INTRODUCTION

Chlorogenic acid (CGA) is of significant scientific interest because of its potential pharmacological properties [1], which are the subject of on-going investigations.

The compound is known to be labile when exposed to air [1], which can present manufacturing problems. However, despite the foregoing interest there are limited TGA and DSC data describing the thermal decomposition behaviour of CGA.

In addition to comparing the decomposition behaviour of this compound in different atmospheres, this work aims to illustrate the importance of using a combination of thermal techniques in decomposition studies.

MATERIALS AND METHODS

Experiments were conducted (using a TGA 2950 instrument) in nitrogen and air atmospheres at a flow rate of 50 mL/min; 3–4 mg of sample was heated in the range of 160 to 600°C at various heating rates in a 100 μL aluminium crucible.

Samples were also subjected to multiple heating cycles, in which a single sample is heated to the end temperature of the first process, cooled back to the starting temperature and reheated to the end temperature of the succeeding process. This cycle was continued until the final process was removed from the system.

DSC studies were conducted using a METTLER DSC823 under nitrogen purge at 50 mL/min.

RESULTS AND DISCUSSION

Four decomposition processes were observed in nitrogen and air atmosphere. A previous TGA study in a helium atmosphere [2] indicated two mass loss processes; in addition, ~60% mass loss from ambient to 500°C was reported. This is similar to that observed in nitrogen; however, decomposition in air atmosphere resulted in ~95% change in mass.

The first decomposition process is identical in both atmospheres (*Figure 1*). However, there were significant differences in the mass loss profiles beyond this process. The 2nd and 3rd processes observed in nitrogen were not resolved in air atmosphere. Furthermore, the final process was the most dominant in air. The differences in the TGA profiles were possibly due to the oxidative condition, caused by the presence of oxygen in air.

The first event observed on the DSC output is due to a melt *(Figure 2)*. The reason is that this event is thermodynamically controlled and HSM studies show that melt precedes decomposition. The second event is kinetically controlled as it is heating rate dependant. This observed process is due to the formation of a lactone as the sample melts, resulting in the removal of a water molecule.

The two endothermic events were the only distinctive processes observed in the DSC studies. This therefore indi-
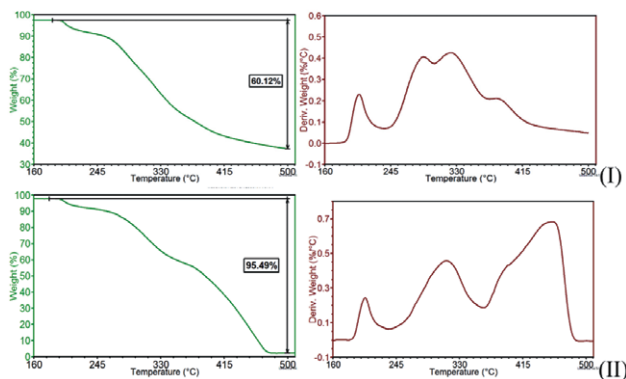
Figure 1. *TGA and DTG profile of CGA heated at 1°C/min; (I) in air atmosphere and (II) in a nitrogen atmosphere.*

Figure 2. *DSC curve overlay of CGA heated from 160 to 240°C at different heating rates (1°C/min (top), 3°C/min (middle), 5°C/min (bottom))*

cates the limitations in using DSC alone in the decomposition study of CGA.

the use of both methods for decomposition studies is recommended.

CONCLUSIONS

There is a significant difference in the decomposition behaviour of CGA in different atmospheres. More decomposition was observed in air; however, a nitrogen atmosphere provided better resolution between decomposition processes. Moreover, the presence of oxygen in air resulted in dominating oxidative processes.

TGA can be used to detect some processes at lower heating rates that are not detectable by DSC and *vice versa*. Hence,
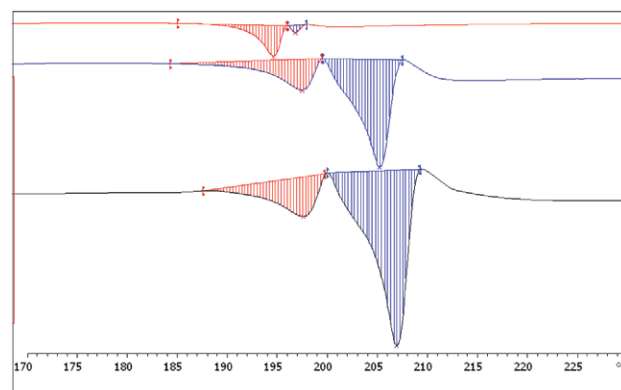
REFERENCES

[1] Zhao, M., Wang, H., Yang, B., Tao, H. (2010). Identification of cyclodextrin inclusion complex chlorogenic acid and its antimicrobial activity. *Food Chemistry*, **120**, 1138–1142.

[2] Sharma, R.K., Fisher, T.S., Hajaligol, M.R. (2002). Effect of reaction conditions on pyrolysis of chlorogenic acid. *Journal of Analytical and Applied Pyrolysis*, **62**, 281–296.

Towards the Rational Design of Crystalline Material for Pulmonary Delivery

M.J. Davies[1], L. Seton[1] & N. Tiernan[1]

[1]The School of Pharmacy and Biomolecular Sciences, Liverpool John Moores University (LJMU), Byrom Street, Liverpool, L3 3AF.

Abstract **– This study describes an approach to crystallise theophylline monohydrate via application of Langmuir monolayers representative of material within the deep lung. Monomolecular films are well suited to investigate crystal nucleation and growth due to the ordered array of surfactant molecules within their structure. This strategy may aid in the rational development of crystalline material displaying complementarity with pulmonary surfactant and thereby optimise disease management via the respiratory route.**

INTRODUCTION

This study outlines an approach to generate theophylline monohydrate crystals via Langmuir monolayers. Previous work has demonstrated that such monolayers facilitate epitaxial nucleation and crystal growth [1]. The model compound, theophylline, is prescribed to manage respiratory disease and has been subject to extensive study. This work aims to develop current understanding of crystal growth processes with respect to pulmonary surfactant monolayers, thus providing a foundation on which to engineer particulates with enhanced interaction profiles for delivery to the lung.

MATERIALS AND METHODS

Crystallisation was conducted underneath surfactant monolayers at pH 7 / ambient conditions, using a Nima Technology 102M Langmuir trough. The surfactant dipalmitoylphosphatidylcholine (DPPC) was dissolved in chloroform (1 mg/ml) and 10 µl were spread across an aqueous subphase containing theophylline (5.7 mg/ml); 10 minutes were allowed for solvent evaporation and formation of the surfactant monolayer. Subsequently, surface pressures were set to 5 mNm^{-1}
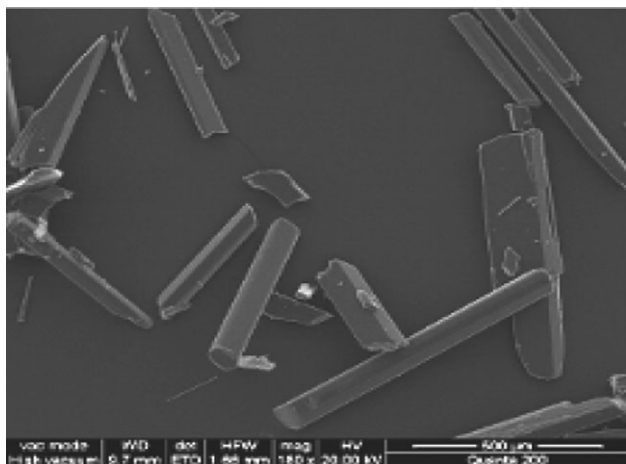
Fig. 1. SEM analysis of theophylline monohydrate formed under a DPPC monolayer at 55 mNm^{-1}

(G phase) and 55 mNm^{-1} (LC phase). The compressed monolayers were left to stand for 18 hours. Reference systems (i.e. batch crystallisation) were also prepared. The crystalline material was analysed using scanning electron microscopy (SEM), differential scanning calorimetry (DSC) and powder x-ray diffraction (PXRD).

RESULTS AND DISCUSSION

Variation in the DPPC LB isotherm when theophylline was dissolved in the subphase indicated monolayer-theophylline interaction [2]. Samples grown from water were confirmed as theophylline monohydrate and those from methanol as Form II anhydrous theophylline by DSC and PXRD. SEM analysis revealed that theophylline monohydrate presented as needle-like crystals (Fig. 1).

The anhydrous theophylline sample prepared by batch crystallisation contained crystal agglomerates of irregular morphology and a cohesive nature. Variation in the morphology between sample types was a result of epitaxial nucleation on the monolayer surface. PXRD verified that monolayer surface pressure influenced the crystal faces presented. Mercury 2.2 software [3] enabled visualisation of crystal packing and provided an insight into the chemical complementarity between surfactant monolayer and the crystal surfaces.

CONCLUSIONS

This study supports the application of compressed surfactant monolayers in the generation of therapeutic crystals at the air-water interface. Data suggest that when dissolved in solution, theophylline will interact with a DPPC monolayer. Here, the principal mode of interaction is believed to be an ion-dipole association. Potential exists to exploit this strategy for the rational design of therapeutics for pulmonary delivery and consequently advance disease management.

ACKNOWLEDGMENTS

REFERENCES

[1] S. Choudhury, N. Bagkar, G. K. Dey, H. Subramanian and J. V. Yakhmi, "Crystallisation of prussian blue analogues at the air-water interface using an octadecylamine monolayer as a template" *Langmuir*, **18** (2002) 7409–7414.

[2] Y. Mu *et al.*, "Effects of pH and surface pressure on morphology of glycine crystals formed beneath the phospholipid Langmuir monolayers" *Journal of Crystal Growth*, **284** (2005) 486–494.

[3] Cambridge Crystallographic Data Centre, UK.

Use of a Sacrificial Probe for Singlet Oxygen in Photodynamic Biomaterials

R.A. Craig, C.P. McCoy, S.P. Gorman

School of Pharmacy, Queen's University Belfast, Northern Ireland

INTRODUCTION

Recently, we described a series of novel porphyrin-impregnated hydrogels capable of producing biocidal singlet oxygen ($^1O_2$) on photoactivation [1]. This has been indirectly assessed using microbiological techniques, but a direct measurement of the $^1O_2$ produced by each hydrogel has not yet been performed on such materials due to the known associated problems with direct physical methods. Anthracene-9,10-dipropionic acid (ADPA) is known to degrade to an endoperoxide on reaction with $^1O_2$, resulting in photobleaching of its UV absorbance maximum [2]. This reaction has been utilised to provide a quantitative measure of $^1O_2$ generation at the surface of hydrogels, and gives an indication of their potential to act as infection-resistant biomaterials.

MATERIALS AND METHODS

ADPA was dissolved in a methanol/water solution. Porphyrin-incorporated and untreated polymer samples [1] (20×5 mm) in this solution were subjected either to a white light source
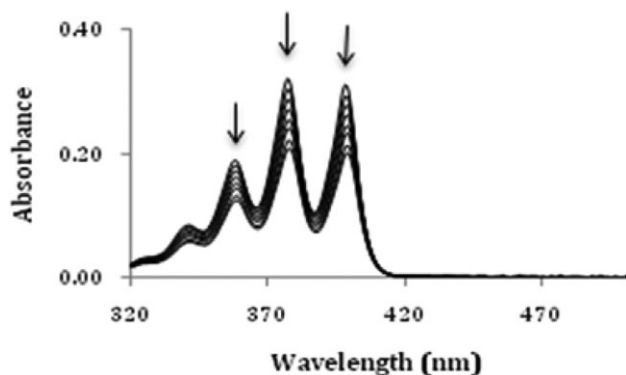
Fig. 1. The decrease in absorbance maxima of ADPA with irradiation time in the presence of porphyrin-incorporated hydrogel.
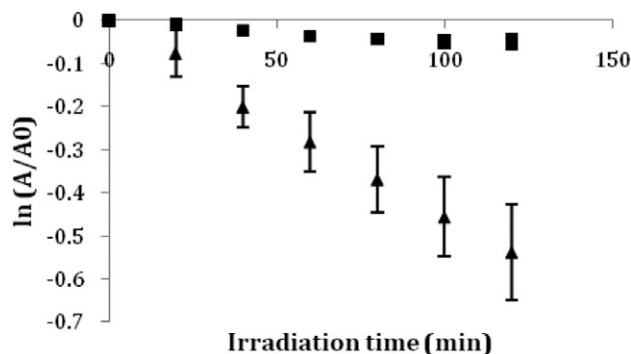

Fig. 2. A representative first order plot, illustrating the difference between porphyrin-incorporated hydrogels tested in dark (■) and light (□) conditions. Error bars show ± SD.

(4000 lux), at a fixed distance of 1cm, or to dark conditions, and UV analysis performed. The rate of photobleaching of ADPA was used to quantify $^1O_2$ production.

RESULTS AND DISCUSSION

Analysis of all studied polymers confirmed the requirement of light for the production of biocidal $^1O_2$. On irradiation of porphyrin-impregnated materials, clear decreases of the absorbance maxima of ADPA were observed (Fig. 1), and the first order plot of ADPA absorbance of porphyrin-incorporated materials during the tested time period illustrates the significantly greater reduction in ADPA absorbance in light conditions when compared to samples tested in the dark (Fig. 2).

Light is therefore required for $^1O_2$ production. A small ingress of ADPA into the untreated materials was observed, but not with porphyrin-incorporated materials. This may be explained by the formation of a layer of porphyrin at the surface of the materials, and neutralisation of the surface anionic charges, thus decreasing the porosity of the materials by facilitating a lower energy chain conformation and preventing ADPA ingress. The effect of ADPA uptake was accounted for when quantifying the $^1O_2$ generation by each material.

CONCLUSIONS

It has been demonstrated that exploitation of ADPA photobleaching provides a method for determining $^1O_2$ production at the surface of porphyrin-impregnated anti-infective biomaterials. Additionally, confirmation of the requirement of light for $^1O_2$ generation has been provided.

ACKNOWLEDGEMENTS

REFERENCES

[1] C. Parsons, C.P. McCoy, S.P. Gorman, D.S. Jones, S.E.J. Bell, C. Brady, et al. "Anti-infective photodynamic biomaterials for the prevention of intraocular lens-associated infectious endophthalmitis". *Biomaterials* **30** (2009) 597–602.

[2] B. Lindig, M. Rodgers, A. Schapp. "Determination of the lifetime of singlet oxygen in D_2O using 9,10-anthracene dipriopionic acid, a water-soluble probe". *J.Am.Chem.Soc.*, **102** (1980) 5590–5593.

Utility of Hansen Solubility Parameters in the Cocrystal Screening

Mohammad Amin Mohammad[1], Amjad Alhalaweh[2], Mais Bashimam[1], Mhd. Amer Al-Mardini[1] and <u>Sitaram Velaga</u>[2]*

[1]Department of Pharmaceutics and Pharmaceutical Technology, Faculty of Pharmacy, Damascus University, Damascus, Syria
[2]Department of Health Sciences, Luleå University of Technology, Luleå, SE-971 87, Sweden

Abstract – **The objective of this study was to test if the miscibility between drug and coformer, as predicted by solubility parameters, can be used as a tool in the cocrystal research. Hansen Solubility Parameters (HSPs) of a model drug, indomethacin and thirty coformers were calculated according to the group contribution method. The distances in HSPs between indomethacin and each cocrystal former were then calculated using three validated misci-**

bility tools. Twenty coformers were predicted and confirmed to be miscible with the drug. Interestingly, all cocrystals forming systems were miscible. Two new cocrystal systems were discovered through this approach. Therefore, the utility of the solubility parameters approach can enhance the efficiency of cocrystal screening.

INTRODUCTION

Pharmaceutical cocrystals are homogeneous crystalline solids with two or more neutral molecular components in the crystal lattice that are solids at room temperature and assemble through hydrogen bonding. The cocrystals are therefore miscible systems at molecular level. It is thus hypothesised that the miscibility between the drug and coformer can indicate cocrystal formation, and methods that predict the miscibility can be used as cocrystal screening tools.

Indomethacin, as a model drug and diverse coformers (including carboxylic acids, sugars, sweeteners etc) were selected. Hansen Solubility Parameters (HSPs) are suitable tools to predict the miscibility between drug and coformer.

Theory: Hansen partial solubility parameters (δ_d, δ_p and δ_h) were calculated using the group contribution method according to Hoftyzer and van Krevelen [1]. The miscibility was estimated using Van Krevelen approach (I), Bagley et al (II) and Greenhalgh et al (III) [1–3].

$$\Delta \bar{\delta} = \left[(\delta_{d2} - \delta_{d1})^2 + (\delta_{p2} - \delta_{p1})^2 + (\delta_{h2} - \delta_{h1})^2 \right]^{0.5} \quad \text{(I)}$$

$$R_{a(v)} = \left[4(\delta_{v2} - \delta_{v1})^2 + (\delta_{h2} - \delta_{h1})^2 \right]^{0.5} \quad \text{(II)}$$

where $\delta_v = (\delta_d^2 + \delta_p^2)^{0.5}$

$$\Delta \delta_{total} = \delta_{total,2} - \delta_{total,1} \quad \text{(III)}$$

where $\Delta \delta_{total}$ is the difference between the two components

MATERIALS AND METHODS

All the materials used are of analytical quality. $\Delta \bar{\delta}$, $R_{a(v)}$ and $\Delta \delta_{total}$ were calculated according to eq. I, II and III respectively. The drug/coformer systems with $\Delta \delta_{total} < 10$ $(J/cm^3)^{0.5}$ were tested for miscibility and cocrystal formation using differential scanning calorimetry (DSC). Drug/coformer systems with $\Delta \bar{\delta}_t < 5$ $(J/cm^3)^{0.5}$ and $R_{a(v)} < 5.6$ $(J/cm^3)^{0.5}$ were among the list having $\Delta \delta_{total} < 10$ $(J/cm^3)^{0.5}$. Based on the thermal behaviour of the systems, a secondary screening using liquid assisted grinding and reaction crystallisation methods was employed. Finally, cocrystalline phases were confirmed by thermal analysis, PXRD and Raman.

RESULTS

Table 1. Classification of coformers according to the miscibility criteria presented in [3]. Drug/coformer systems with $\Delta \delta_{total} < 7.5$ are suggested to be miscible.

$\Delta \delta_{total}(J/cm^3)^{0.5}$	Coformers	Miscibility
< 7.5	Cinnamic acid, Neotame, 4,4'-bipyridine, Benzoic acid, Glutaric acid, Fumaric acid, Maleic acid, Succinic acid, Nicotinamide, 4-aminobenzoic acid, Malonic acid, Cyclamic acid, Vanillic acid, Saccharin, Oxalic acid, 4-hydroxy benzoic acid, Urea, Citric acid, Malic acid, 4-aminobenzamide	Yes
7.5–10	Sucrose, 4-hydroxybenzamide	No
> 10	Tartaric acid, Arabinose (pyranose and furanose forms), Lactose, Maltose, Mannitol, Mannose, Glucose, Fructose (pyranose and furanose forms)	Not tested

Table 2. Coformers found to form cocrystals with indomethacin. Melting point of the drug 160 °C.

Coformers	Coformers Melting point (°C)	Eutectic Temperature (°C)	Cocrystal Formed
4,4'-Bipyridine	111.5	96.3	Yes/new
Cinnamic acid	133.3	110.9	Yes/new
Nicotinamide	128.4	98.8	Yes/reported[4]
Saccharin	228	147.7	Yes/reported[4]

CONCLUSIONS

◇ Drug/coformer systems with $\Delta \delta_{total} < 7.5$ $(J/cm^3)^{0.5}$ were found to be miscible with the drug. But $\Delta \bar{\delta}$ and $R_{a(v)}$ were more restrictive than $\Delta \delta_{total}$ in predicting the miscibility.

◇ The miscibility between the drug and coformers was demonstrated by the eutectic formation.

◇ All coformers that formed cocrystals were completely miscible with the drug, but not all the miscible systems formed cocrystals.

◇ Combined tools better rationalise the miscibility and cocrystal formation behaviour than any single tool alone. The solubility parameters approach can increase the efficiency of cocrystal screening by short listing the number of coformers.

◇ We are applying this hypothesis to other cocrystal forming drugs to verify its general applicability.

REFERENCES

[1] P.J. Hoftyzer, D.W. van Krevelen, Properties of Polymers, 4th edn. Elsevier, Amsterdam, 2009.

[2] E.B. Bagley, T.P. Nelson, and J.M. Scigliano, "Three-dimensional solubility parameters and their relationship to internal pressure measurements in polar and hydrogen bonding solvents" J. Paint Technol., 43 (1971) 35–42.

[3] D.J. Greenhalgh, A.C. Williams, P. Timmins, P. York, "Solubility Parameters as Predictors of Miscibility in Solid Dispersions" J. Pharm Sci., 88 (1999) 1182–1190.

[4] S. Basavoju, D. Boström, S.P. Velaga, "Indomethacin-Saccharin cocrystals: Design, synthesis and preliminary pharmaceutical characterisation" Pharm. Res., 25 (2008) 530–541; S. Bogdanova, D. Sidzhakova, V. Karaivanova and S. Georgieva, International Journal of Pharmaceutics., 163 (1998) 1–10.

Viscometric and Spectroscopic characterisation of Chitosan and Poly(methyl Vinyl Ether Maleic Acid)

L.B. AlKayyali[1], O.A. Abu-Diak[1], G.P. Andrews[1], D.S. Jones[1]

[1]Drug Delivery Group, School of Pharmacy, Queen's University of Belfast, UK.

INTRODUCTION

The use of Chitosan (CS) and Gantrez (GZ) alone as a gelling platform is restricted due to their poor rheological properties. Due to the electrostatic interactions between the charged groups along the polymer chain, polyelectrolytes solutions behave differently compared with neutral polymers regarding the viscosity [1]. This study focuses on the rheological properties of the CS and GZ dilute solutions and hydrogels.

MATERIALS AND METHODS

For rheological studies, the correct geometry was selected based on the properties of various formulations. A 40 mm parallel steel plate was used for CS-GZ hydrogels and a standard-size double concentric cylinder was used for dilute solutions.

For viscoelastic characterisation, CS-GZ hydrogels containing CS (1% w/w) and different concentrations of GZ (2.5, 5, 10% w/w) were prepared. The pH of the prepared hydrogels was adjusted at pH 2, 5 and 7 by sodium hydroxide (NaOH) solution.

For viscometric studies, dilute primary polymer solutions [0.0025–0.02% w/v of CS in 1% acetic acid (v/v) and GZ in glycerol: water (20:80)] were prepared, whereas dilute binary solutions of the polymers at a concentration range of 0.00125–0.012% w/v were prepared. FT-IR analysis was performed on samples of CS, GZ powders and CS-GZ hydrogels at a scanning range of 4000–400 cm^{-1}.

RESULTS AND DISCUSSION

Increasing GZ concentration in the binary hydrogel systems significantly increased the storage modulus (G′), loss modulus (G″) and dynamic viscosity, whereas the loss tangent was lowered. Conversely, increasing the pH of such systems from 2 to 7 resulted in reducing G′, G″, dynamic viscosity and increasing the loss tangent.

Viscometric studies based on Huggins model can be applied to determine the intrinsic viscosity of a polymer solution at low concentrations, where the reduced viscosity decreases linearly with decreasing polymer concentration (c). A linear plot for reduced viscosity (ηsp/c) versus concentration was obtained for CS and GZ primary solutions. Conversely, a pseudo hyperbolic pattern was obtained for CS-GZ binary systems [2], where a continual increase in molecular volume with dilution was observed. Therefore, Fuoss law was applied where the viscosity was proportional to the square root of polymer concentration [3]. This effect, known as a "polyelectrolyte effect", usually occurs as a result of the higher Coulombic repulsion between charged groups in dilute solutions causing an increase in the volume of macromolecules [1]. FT-IR studies showed a significant shift in the carbonyl group of GZ in the CS-GZ hydrogels compared to GZ powder from 1701 to 1709 cm^{-1} due to the interaction between the carbonyl group of GZ and the amine group of CS. With increasing the pH of the hydrogels to 5 and 7, a new peak was observed at around 1578 cm^{-1}, which was related to the carboxylate salt formed due to the interaction between the carboxylic acid of GZ and NaOH.

CONCLUSIONS

The viscoelastic properties of CS and GZ were improved as a result of the complex formation within the binary hydrogel systems which was confirmed using the viscometeric and FT-IR studies.

REFERENCES

[1] C. Kienzle-Sterzer, D. Rodriguez-Sanchez, and C. Rha, "Dilute Solution Behaviour of a Cationic Polyelectrolyte" Journal of Applied Science, 27(1982) 4467–4470

[2] C. K. Sato, P. R. Oliveira, R. L. Cunha, "Rheology of Mixed Pectin Solutions" Food Biophysics, 3 (1) (2008) 100–109

[3] S. Dragan, M. Mihai, L. Ghimici, "Viscometric study of poly (sodium 2-acrylamido-2-methylpropanesulfonate) and two random copolymers" European Polymer Journal, 39 (2003) 1847–1854

CDK9 inhibitor design, synthesis and biological evaluation

Shenhua Shi, Xiangrui Liu, Fankie Lam, Shudong Wang

Center for Biomolecular Sciences, School of Pharmacy, University of Nottingham, Nottingham, UK.

Abstract – **A library of 2,4,5-trisubstituted pyrimidine derivatives was designed and synthesised. Many of these compounds demonstrated potent anti-proliferative activity against human tumour cell lines. Examination of lead compounds in kinase assays has confirmed their CDK9 inhibitory activity. Lead compounds were evaluated for their ability to induce apoptosis in human cancer cells.**

INTRODUCTION

CDKs dysfunction has been recognised as the major contributor for abnormalities in cell cycle and transcription which underlie the majority of human cancers [1]. CDK9-cyclin T1 has an essential role in promoting RNA synthesis and anti-apoptotic protein production. With the findings in anticancer and antiretroviral research, it is strongly believed that CDK9 inhibition would be a useful therapeutic strategy [2–4]. Here we report the progress made in developing CDK9 pharmacological inhibitors as potential anti-cancer agents.

MATERIALS AND METHODS

A library of compounds was designed and synthesised as CDK9 inhibitor and a series of *in vitro* study was done to investigate its inhibitory mechanism.

RESULTS AND DISCUSSION

The compounds were tested for anti-proliferative activities against HCT-116 (colonic cancer cell line) and MCF-7 (breast cancer cell line) in MTT assay. Most compounds showed potency below 1 µM, the most potent compound exhibited best potency with IC_{50} around 10 nM. A set of compounds were tested against CDK1, 2, 7 and 9 and the preliminary structure activity relationship was established. In addition to CDK9, many compounds also inhibit CDK1 and 2, with various selectivity profiles against other CDKs. Cellular mode of action of lead compound was investigated and the correlation between CDK9 inhibition and anti-tumour activity was confirmed

CONCLUSIONS

The compounds described here represent a novel class of CDK9 inhibitors. These compounds demonstrated potent anti-proliferative activity against human cancer cell lines. Lead compounds' potent CDK9 inhibition was showed by both kinase and cell-based assays. Excellent anti-tumour activity against CLL clinical samples was observed.

REFERENCES

[1] Sausville, E. A. Complexities in the development of cyclin dependent kinase inhibitor drugs. *Trends Mol Med* **2002**, 8, S32–7.

[2] Kobor, M. S.; Greenblatt, J. Regulation of transcription elongation by phosphorylation. *Biochim Biophys Acta* **2002**, 1577, 261–275

[3] Schwartz, G. K.; Shah, M. A. Targetting the Cell Cycle: A New Approach to Cancer Therapy. In 2005; Vol. 23, pp 9408–9421

[4] Wang, S.; Fischer, P. M. Cyclin-dependent kinase 9: a key transcriptional regulator and potential drug target in oncology, virology and cardiology. *Trends Pharmacol Sci* **2008**.

Combretastatin A4 dimers: design, synthesis and biological evaluation.

M.A Casely-Hayford, T.A Omobolaji

Medway School of Pharmacy, Universities of Greenwich and Kent, Kent ME4 4TB, UK.

INTRODUCTION

The growth of a solid tumour is dependent on the growth of new blood vessels (angiogenesis) to meet its needs in terms of oxygen and nutrients. This neovasculature has become a primary target for the development of new anticancer drugs [1]. Several anti-angiogenic agents have entered clinical trials, among these is combretastatin A4, CA-4 **1** (Figure 1). Combretastatin A-4 was isolated from the bark of the African bush willow and has been shown to possess potent anticancer activity by inhibiting microtubule polymerisation and subsequently disrupting the neovasculature of tumours. The phosphate **2** with better water solubility is now in phase II clinical trials. The ability of 1 and 2 to damage tumour vasculature has made these compounds attractive lead compounds for the development of analogues with improved biological activity.

Multivalent interactions is fundamental to the regulation of many critical biological systems and involves cases where the ligand has two or more exclusive binding domains that can simultaneously bind to two or more distinct sites either on the same receptor or two distinct receptors.[11] Bivalent
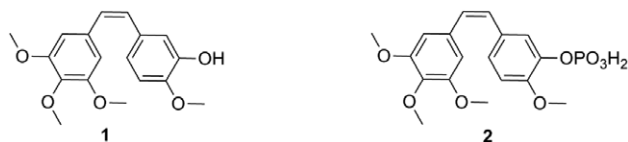
Figure 1: Structures of combretastatin A4 and the phosphate analogue.

interactions have been used in the past to enhance affinity, potency and selectivity.[11] Studies show that ligand homodimerisation is effective in increasing the selectivity and potency of relevant lead compounds.

OBJECTIVES

In this study we aim to synthesise combretastatin dimers with the view of improving their potency.

MATERIALS AND METHODS

Chemicals: 3-hydroxy-4-methoxybenzaldehyde, 3,4,5-trimethoxyphenylacetic acid, acetic acid and dibromoalkanes were purchased from Sigma-Aldrich.

The CA-4 core was synthesised using solution phase literature methods [2]. Thus, a mixture of 3-hydroxy-4-methoxybenzaldehyde (1 g, 6.58 mmol), 3,4,5-trimeth-oxyphenylacetic acid (2.97 g, 13.16 mmol), acetic acid (6 ml) and triethylamine (3 ml) were heated under reflux for 3 hours. Upon cooling, the reaction mixture was acidified with concentrated hydrochloric acid (9 ml), the mixture was left to crystallise. The resulting solid was filtered off and recrystallised from ethanol to give the propenoic acid derivative in 63% yield.

RESULTS AND DISCUSSION

A two step stereoselective method was used for the synthesis of the combretastatin core. The method included Perkin condensation of 3, 4, 5- trimethoxyphenylacetic acid **3** and 3-hydroxy-4-methoxybenzaldehyde **4** to give a propenoic acid intermediate. Decarboxylation of the propenoic acid intermediate was effected using powdered copper and quinoline at 200 °C in the presence of copper to give combretatsatin A4. Cis-combretastatin was isolated in good yield (68%).
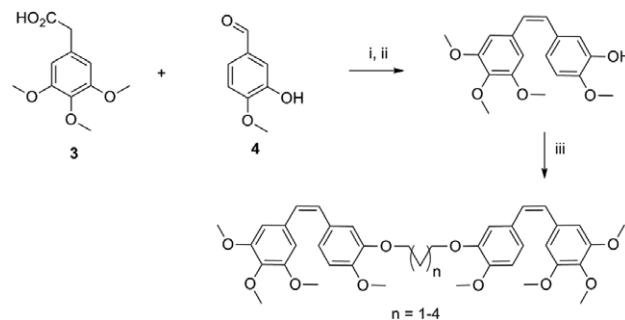

Figure 2: Synthesis of combretastatin dimers. (i) acetic anhydride, triethylamine. (ii) quinoline, copper powder. (iii) NaH, dibromoalkane

Dimerisation of CA-4 1 was achieved by initial treatment of CA-4 with NaH in DMF. The addition of the corresponding dibromoalkane then effected an SN2 type substitution leading to the dimeric compounds with yields between 55–78%. Characterisation was ascertained by ^{1}H/^{13}C, NMR and Mass spectrometry. Certain tubulin binding compounds also bind to DNA. Therefore with CA-4 and analogues in hand we proceeded to study their effect on super coiled plasmid DNA. Initial unwinding assays show that CA-4 and the dimeric compounds do not unwind DNA even at high concentrations.

CONCLUSIONS

CA-4 and the dimeric analogues were synthesised and characterised. Initial binding studies show that CA-4 and its dimers do not affect the structure of super coiled plasmid DNA, however the ultimate biological activity of the dimers is not yet known. Work is underway in our lab to fully characterise the biological activity of these dimers.

REFERENCES

[1] D. Neri, R. Bicknell. Tumour vascular targetting. *Nat. Rev. Cancer* **5**, (2005) 436–446.
[2] K. Gaukroger, J. Hadfield, L. Hepworth, N. Lawrence, A. McGown. Novel Syntheses of Cis and Trans Isomers of Combretastatin A-4. *Journal of Organic Chemistry.* **66** (2001) 8135–8138.

Construction of an SVM Model for Predicting Carcinogenicity of Diverse Chemicals

K. Tanabe[1], B. Lučić[2], D. Amić[3], T. Suzuki[4]

[1]Neuroscience Research Institute, National Institute of Advanced Industrial Science and Technology, Umezono 1-1-1, Tsukuba 305-8568, Japan
[2]NMR Center, The Rudjer Bošković Institute, P.O. Box 180, HR-10002 Zagreb, Croatia
[3]Faculty of Agriculture, The Josip Juraj Strossmayer University, P.O. Box 719, HR-31107 Osijek, Croatia
[4]Natural Science Laboratory, Toyo University, Hakusan 5-28-20, Bunkyo-ku, Tokyo 112-8606, Japan

Abstract **– To develop a QSAR model for predicting the carcinogenicity of a wide range of chemicals, the relationship between carcinogenicities and selected descriptors from molecular structures was analysed with support vector machines (SVMs). On the basis of the decision tree technique, SVM models for sub-structures counted by the Dragon software were serially created for 935 non-congenial chemicals, and were optimised for each subgroup.**

The resulting model was found to predict the carcinogenicity of a variety of chemicals with an overall performance of 83%, higher than any existing models.

INTRODUCTION

Data of carcinogenicity on numerous unascertained chemicals cannot be obtained by animal tests which are very laborious, time-consuming, costly and require many animals. Therefore, a reliable tool for predicting carcino-genicity of chemicals is highly desirable as a screening for animal tests, and QSAR approaches have been employed for predicting carcinogenicity of chemicals not tested experimentally. Although the existing approaches succeeded in modelling for congeneric chemicals, they work poorly for non-congeneric substances. In our previous study, the relationship between carcinogenicity data and descriptors for non-congenial chemicals was analysed with a support vector machine (SVM) method, and a parallel model based on grouping of chemicals into substructures was examined [1]. In this study, a serial model based on the decision tree technique was examined.

DATA AND METHODS

The carcinogenicity data and Dragon descriptors for 935 non-congenial (417 positive and 518 negative) chemicals created in our previous study [1] were applied in this study. The classification function (SVC) for weighted data in LIBSVM program [2] was used to classify chemicals into two carcinogenic categories (positive or negative), where weights were set depending on the reliabilities of the carcinogenicity data. The per-formance of the SVM model was measured with the overall accuracy counted as OA = (TP + TN) / (TP + TN + FP + FN) where TP is true positive, TN true negative, FP false positive, and FN false negative.

RESULTS AND DISCUSSION

A serial model based on the decision tree technique was examined. For the chemicals containing various can-didate substructures counted by the Dragon software, correlation coefficients between carcinogenicity and descriptor values were calculated. Using descriptors showing higher correlation coefficients, an SVM for each substructure was optimised and the overall accuracy was evaluated. The substructure showing the highest accuracy was selected. By using this procedure, the first substructure ArHC (aromatic hydrocarbons) was selected, and the accuracy for 54 chemicals containing ArHC was counted as 87.0%. For the chemicals without the selected substructure, the above procedures were repeated until the overall accuracy for the remaining chemicals exceeds the target value 75%. Using this model, 18 steps were repeated
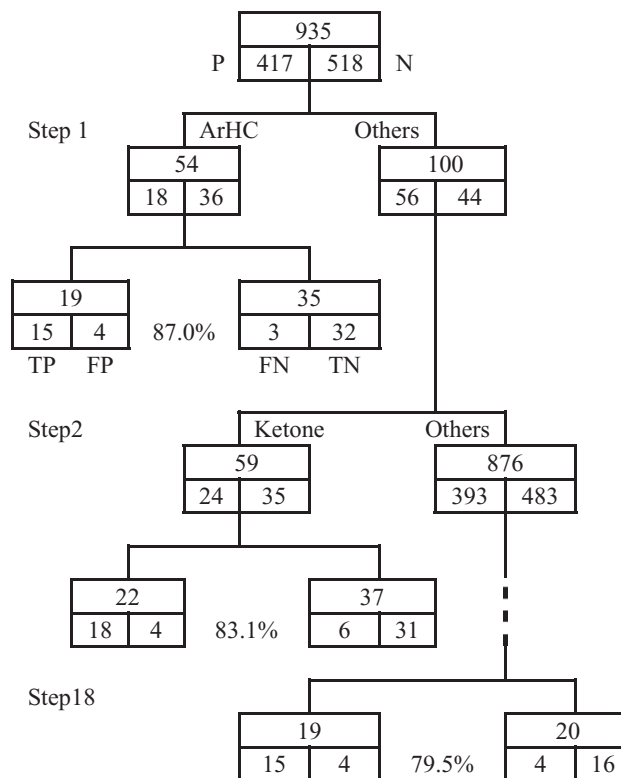

Fig. 1. Flow chart of the serial model in this study

as shown in Fig. 1, and in almost all steps, the overall accuracies higher than 80% were obtained for the selected substructures. Finally, the overall accuracy 83.3% with TP = 348, TN = 431, FP = 87, FN = 69 was attained, which demonstrates the satisfactorily high performance of the present model.

CONCLUSIONS

A serial model based on the decision tree technique was examined It was found that the model based on the combined use of chemical substructures and the decision tree method predicts the carcinogenicities of a wide variety of chemicals with a satisfactory overall accuracy of approximately 83%.

REFERENCES

[1] K. Tanabe, T. Suzuki, et al "Prediction of carcinogenicity for diverse chemicals based on substructure grouping and SVM modelling" *Molecular Diversity*, **14** (2010) in press.

[2] C. C. Chang and C. J. Lin, "LIBSVM–A library for support vector machines" *http://www.csie.ntu.edu.tw/~cjlin/libsvm/*

Design and synthesis of artesunate-anthraquinone hybrids as potential antitumour agents

L. K. Mberi Nsana, M. A. Casely-Hayford

Medway School of Pharmacy, Universities of Kent and Greenwich, Kent ME4 4TB, UK

INTRODUCTION

Artemisinin is a naturally occurring 1,2,4-trioxanesesquiterpene lactone with an endoperoxide bridge. It is extremely active against malaria including the deadly cerebral form. In addition to its antimalarial activity, artemisinin and its derivatives including artesunate (Fig. 1) have been shown to possess significant anticancer activity [1], involving iron (II) mediated cleavage of the endoperoxide bridge to generate toxic carbon centred free radicals able that interact with biomolecules leading to apoptosis [2].

Artemisinin analogues bearing DNA affinic chromophores such as acridone have been shown to have greater activity. 1,4-Disubstituted anthraquinones (Fig.1), which form the core structure of antitumour agents such as mitoxantrone and banoxantrone (AQ4N) [3], offer a unique opportunity for the development of artemisinin-anthraquinone hybrids with improved biological activity.

OBJECTIVES

In this study we aim to synthesise potential anticancer agents which combine the planar features of the intercalating anthraquinone skeleton with the trioxane based artemisinin to give bifunctional compounds with potential dual mechanism of action and greater potency.

MATERIALS AND METHODS

Artesunate and leucoquinizarin (Fig. 1) were bought from TCI Europe Ltd and all other reagents from Sigma-Aldrich. The hybrids were tested as DNA intercalators. The samples were electrophoresed in 1% agarose gel 50V for 3 h. The gel was stained with ethidium bromide and photographed using UV transilluminator.

Unwinding Assay: ΦX174 plasmid DNA (4 µg) was suspended in 108 µl of Tris-EDTA buffer (TEB) (pH 8.3, 50 mM) and 7 µl (0.25 µg) transferred into 8 Eppendorf tubes. Each agent concentration (1 µl) and TEB (2 µl) were added to each DNA solution. DMSO (1 µl) and TEB (2 µl) were added to the control. The mixture was incubated at 37 ° C for 2 h and their content loaded into the agarose wells with 20 % glycerol in TEB (4 µl).

RESULTS AND DISCUSSION

The mono/di-hybrids were successfully synthesised from leucoquinizarin and artesunate (Scheme 1).
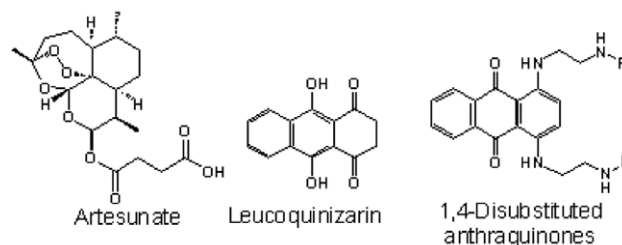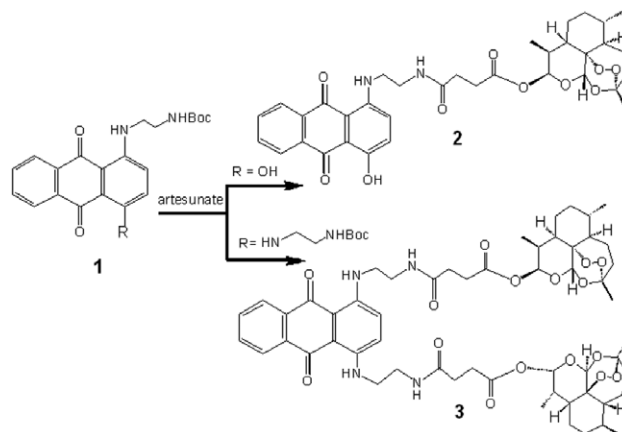

Figure 1

Scheme 1: Synthesis of anthraquinone-artesunate hybrids.

Condensation of leucoquinizarin with excess *N*-Boc-ethylenediamine gave **1** leading to mono and disubstituted anthraquinones. *N*-Boc deprotection using 2.5 M HCl/acetone and removal of solvents left the protonated derivative which was reacted with 10 fold excess of diisopropyl ethylamine, 5 fold excess of artesunate/HBTU over 17 h to give the di-hybrid **3**. The mono-hybrid **2** was obtained using 1 equivalent of artesunate/HBTU. Characterisation was ascertained by ^{1}H/^{13}C/2D COSY NMR and Mass spectrometry. Initial unwinding assays show that the di-hybrid does not unwind DNA even at high concentrations. No DNA strand cleavage was observed at these concentrations.

CONCLUSIONS

Although the di-hybrid **3** did not bind to DNA by intercalation it may possess antitumour properties via a different mechanism. Work is underway in our laboratory to fully characterise the biological activity of these hybrids.

REFERENCES

[1] Efferth, T., Dunstan, H., Sauerbrey, A., Miyachi, H., and Chitambar, C. R., 2001, "The anti-malarial artesunate is also active against cancer," International Journal of Oncoclogy, 18, p. 767.

[2] Wu, W. M., 1998, "Unified mechanistic framework for the Fe(II)-induced cleavage of qinghaosu and derivatives/analogues. The first spin-trapping evidence for the previously postulated secondary C-4 radical," Journal of American Chemical Society, 120, pp. 3316–3325.

[3] Loadman, P. M., Swaine, D. J., Bibby, M. C., Welham, K. J., and H., P. L., 2001, "A Preclinical Pharmacokinetic Study of the Bioreductive Drug AQ4N," Drug Metabolism and Disposition, The American Society for Pharmacology and Experimental Therapeutics, pp. 422–426.

Design and Synthesis of Novel EG5 Inhibitors

M. Abualhasan[1], O.B. Sutcliffe[1], F. Kozielski[2] and S.P. Mackay[1]

[1]Strathclyde Institute of Pharmacy and Biomedical Sciences, Glasgow, UK, [2] Beatson Institute for Cancer Research, Glasgow, UK.

INTRODUCTION

The currently available antimitotic drugs directly target the microtubule building blocks. These drugs induce adverse side-effects including neurotoxicity, and cancer cells can potentially develop resistance to them. New antimitotic drugs act indirectly on microtubules, these drugs have specific functions on phases of mitosis, and their inhibition may produce fewer side-effects than tubulin drugs.

Eg5 motors are a member of the kinesin family which are required for spindle bipolarity maintenance. Inhibition of these motors induces mono-asters cells. S-trityl-L-cysteine (STLC) is a specific and effective Eg5 inhibitor, the trityl group of the STLC binds to three hydrophobic sites inside the binding pocket [1].

Our aim is to design and synthesise high potency specific Eg5 inhibitors which have a higher inhibition activity than the STLC. Our suggested compounds have in general extended benzyl group, which is believed to be more flexible compared to the phenyl group of the STLC. It is also believed that the benzyl moiety will increase the hydrophobic binding to the Eg5 motors.

Figure 1: One of the our benzyl derivative compounds docked to Eg5 motor; docking shows it binds to the same binding pocket as STLC

The ATPase and cell-based bioassays test results demonstrated high inhibition for most of the synthesised compounds, some of them even have a higher inhibition activity compared to the STLC.

MATERIAL AND METHOD

First of all benzyl analogues of STLC were docked into Eg5 using the GOLD algorithm; ten different poses were scored.

The syntheses of the different benzyl analogues consist mainly of two steps; first the synthesis of the alcohol of the benzyl moiety using Grignard chemistry [2], the second is the coupling of alcohol to the cysteine conjugates.

The synthesised compounds were tested by ATPase and cell-based bioassays.

RESULTS AND DISCUSION

Molecular modelling shows that our suggested benzyl analogues bind to the same Eg5 binding site as STLC (Figure 1) and the GOLD scores showed good and promising results.
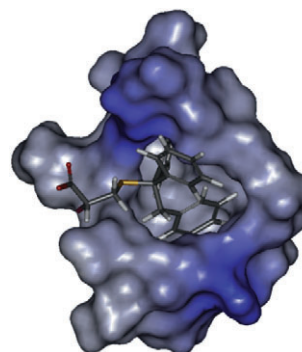
CONCLUSION

The synthesised benzyl derivatives have demonstrated a good inhibition activity by ATPase test in consensus with the modelling score results.

Future work is to synthesise more of benzyl analogues and also to determine the crystal structure of the most active compounds. This will give us a better understanding of the exact binding pattern of these compounds to the Eg5 motors.

REFERENCE

[1] S. Debonis et al J. Med. Chem. 2008; 51(5); 1115–1125.

[2] Manabu Hatano et al J. AM. CHEM. SOC. 128, 9998–9999.

Development of a novel molecular model and the rationalisation of a series of novel inhibitors of 17α-hydroxylase/17,20-lyase

P. Acharya, I. Shahid, C.P. Owen, S. Ahmed

School of Science, University of the West of Scotland, High Street, Paisley, Renfrewshire, Scotland, UK.

INTRODUCTION

The enzyme 17α-hydroxylase/17,20-lyase ($P450_{17\alpha}$) catalyses the conversion of C_{19} containing androgen precursors from the C_{21} containing steroids such as the pregnanes and progestins and involves an initial 17α-hydroxylation [via 17α-hydroxylase (17α-OHase)], followed by the cleavage of the C(17)-C(20) bond [via 17,20-lyase (lyase)] – both steps require NADPH and oxygen. We have previously reported halogenated derivatives of benzyl azole-based compounds which proved to be good inhibitors of $P450_{17\alpha}$ [1]. To rationalise the inhibitory activity of these compounds, we report the development (and use) of a new model for the active site of $P450_{17\alpha}$.

MATERIALS AND METHODS

The overall substrate, haem and inhibitors were constructed using CaChe. In the construction of the overall substrate-haem complex, we hypothesised that the attacking ferroxy oxygen species must be positioned within approximate attacking distance (and angle) to the appropriate C atom. In the construction of the lyase complex, the terminal oxygen of the Fe^{IV}-O• was bonded to the C(20) atom of 17α-hydroxypregnenolone. A representation of a group at the active site was bonded to the C(3)-OH of 17α-hydroxypregnenolone and the complex minimised using MM3 parameters; all the atoms were then locked. We then detached the FeO-C(20) bond and FeO-C(17) bond was formed with pregnenolone. A representation of a group at the active site was bonded to the C(3)-OH of pregnenolone and the complex minimised using MM3 parameters. The removal of pregnenolone resulted in the overall substrate-haem complex representation of $P450_{17\alpha}$.

RESULTS AND DISCUSSION

From the consideration of the results of the present study, we observe that the overall structure is an approximate deformed L shape with the two components being positioned as such that the angle between the two hydrogen bonding groups and the Fe atom in the centre of the haem is ~78°. The lyase component was found to possess the largest distance between the haem and the hydrogen bonding group attached to the C(3)-OH moiety of 17α-hydroxypregnenolone in comparison to the distance from the haem to the C(3)-OH moiety of pregnenolone. This result is therefore similar to that obtained using a homology based study [2].

Modelling known inhibitors of $P450_{17\alpha}$, we observed that some inhibitors were able to utilise one hydrogen bonding group whilst the highly potent inhibitors used both H-bonding groups, the additional interaction would therefore appear to allow these compounds to possess greater inhibitory activity in comparison to those only able to utilise one of the two hydrogen bonding groups.

CONCLUSIONS

We have therefore provided a model of the $P450_{17\alpha}$ active site since no crystal structure exists for this enzyme.

REFERENCES

[1] S. Ahmed, I. Shahid, S. Dhanani and C.P. Owen, "Synthesis and biochemical evaluation of a range of sulfonated derivatives of 4-hydroxybenzyl imidazole as highly potent inhibitors of rat testicular 17α-hydroxylase/17,20-lyase (P-450$_{17\alpha}$)", *Bioorg. Med. Chem. Lett.*, **19** (2009) 4698–4701.

[2] C.A. Laughton, S. Neidle, M.J.J.M. Zvelebil and M.J.E.A. Sternberg, "A molecular model for the enzyme cytochrome P450$_{17\alpha}$, a major target for the chemotherapy of prostate cancer" *Biochem. Biophys. Res. Comm.* **171** (1990) 1160–1167.

# Iron Chelation Therapy: An Expanding Horizon

R.C. Hider, X.L. Kong, S. Roy, Y.M. Ma and J. Preston

Division of Pharmaceutical Science, King's College London,
Franklin Wilkins Building, 150 Stamford St., London, SE1 9NH, UK

Abstract – **Iron chelation has been a life saving therapy for thalassaemia major patients over the past 30 years. With the introduction of orally active chelators, other diseases are now also being treated, for instance sickle cell disease, myeloma dysplasia and Friedreich ataxia. Indeed, iron chelators are showing potential for the retardation of various neurodegenerative disorders. This presentation will provide an update on the progress of such studies.**

INTRODUCTION

There are three iron chelators currently in clinical use, desferrioxamine (1), exjade (2) and deferiprone (3) [1]. Desferrioxamine is not orally active and by virtue of its rapid renal clearance has to be administered parentally for 6h periods. In contrast, both exjade and deferiprone are orally active. By virtue of the low molecular weight of both the free ligand and the iron complex, deferiprone (3) is able to remove excess intracellular iron, including mitochondrial iron [2, 3]. This endows deferiprone with the ability to remove excess
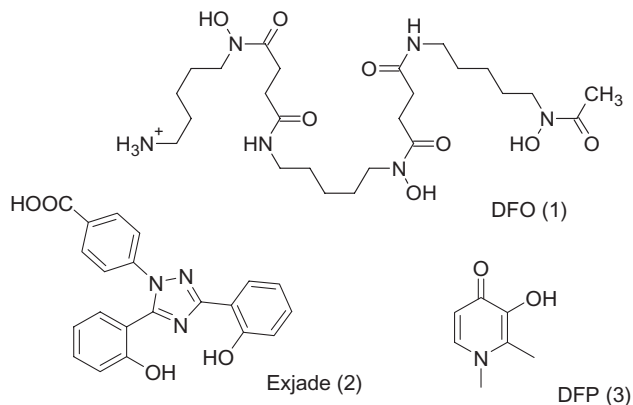
deposits of iron in cardiac, pancreatic and probably thymic tissue. Deferiprone is also capable of crossing the Blood Brain Barrier [4] but unfortunately is associated with a low incidence of agranulocytosis. In order to avoid this undesirable toxicity alternative hydroxypyridinone structures are being investigated.

RESULTS AND DISCUSSION

We have synthesised deferiprone analogues and have investigated their ability to penetrate the Blood Brain Barrier. Three of these compounds (F25, F29 and SR2B) have been investigated for their ability to alleviate Aβ peptide-induced toxicity in human neuronal cell cultures. 10 μM Aβ(1–40) induces a loss of neuronal cell viability after 24 h exposure
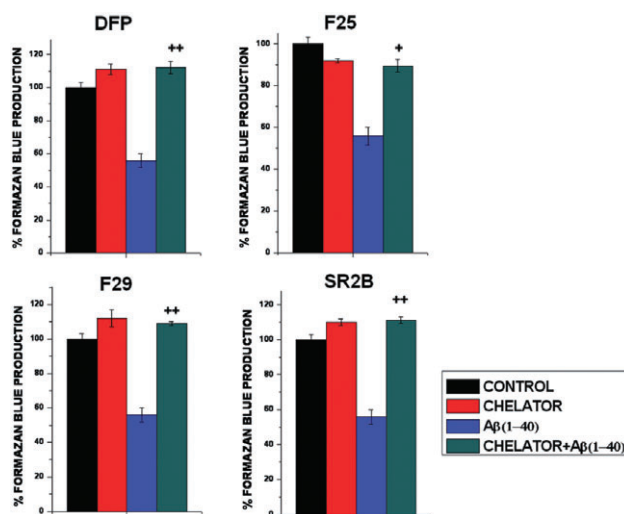

Figure 1 MTT assay of hydroxypyridinones in the presence of 10 μM Aβ(1–40). Formazan blue produced by control neurons was normalised to 100%. Chelator concn = 30 μM, 24 h incubation. $^+p < 0.05$ and $^{++}p < 0.01$ versus Aβ(1–40). All values are mean ± S.E.M from three independent experiments in quadruplicate.

as measured by a MTT-based bioassay (Figure 1). However in the presence of DFP (3), F25, F29 and SR2B this loss in viability was reduced and indeed completely reversed with F29 and SR2B.

CONCLUSIONS

Deferiprone which is being used clinically to treat Friedreich ataxia patients crosses the blood brain barrier and alleviates neuronal damage induced by Aβ(1–40). The deferiprone analogues F29 and SR2B cross the BBB more efficiently than deferiprone and possess similar neuroprotective properties.

ACKNOWLEDGMENTS

REFERENCES

[1] E. J. Neufeld. Oral chelators, deferasirox and deferiprone for transfusional iron overload in thalassaemia major: new data, new questions. Blood 107 (2006) 3436–3441.

[2] C. Borgna-Pignatti, M.D. Cappellini, et al. Cardiac morbidity and mortality in deferoxamine- or deferiprone-treated patients with thalassaemia major. Blood 107 (2006) 3733–3737.

[3] O. Kakhlon, H. Manning, et al. Cell functions impaired by frataxin deficiency are restored by drug-mediated iron relocation. Blood 112 (2008) 5219–5227.

[4] S. Roy, J.E. Preston, R.C. Hider and Y.M. Ma. Glycosylated deferiprone and its brain uptake. J. Med. Chem. *Submitted*.

Quartz crystal microbalance (QCM) studies for the investigation of ligand (IBM) interactions with major urinary protein (MUP)

J. Roy[#,*], C.A. Laughton[#], S. Allen[*]

*Laboratory of Biophysics and Surface Analysis, School of Pharmacy,
University of Nottingham, Nottingham, UK
#Division of Medicinal Chemistry and Structural Biology, School of Pharmacy,
University of Nottingham, Nottingham, UK

Abstract – **The major urinary protein (MUP) is a member of the lipocalin family that binds small ligands in a deeply buried hydrophobic pocket. Studies have shown that ligand binding is driven by enthalpic effects, not the entropic effects that are commonly associated with hydrophobic association. QCM-D studies have been used to show the flexibility of the binding site upon ligand binding on apo-MUP and Y120F Mutant MUP. However further analysis is now underway.**

INTRODUCTION

QCM techniques can provide unique insights into what drives protein-ligand association. Detailed calorimetric studies have shown that ligand binding is driven by enthalpic effects, not entropic effects[1]. Previous studies have shown that this is due to 'dewetting' of the binding site cavity even in the absence of ligands, and have also characterised the complex changes in molecular flexibility that accompany ligand binding-features that may be correlated with NMR data[2]. The binding cavity is dehydrated except for one water molecule which is bound to the tyrosine 120 of the binding cavity
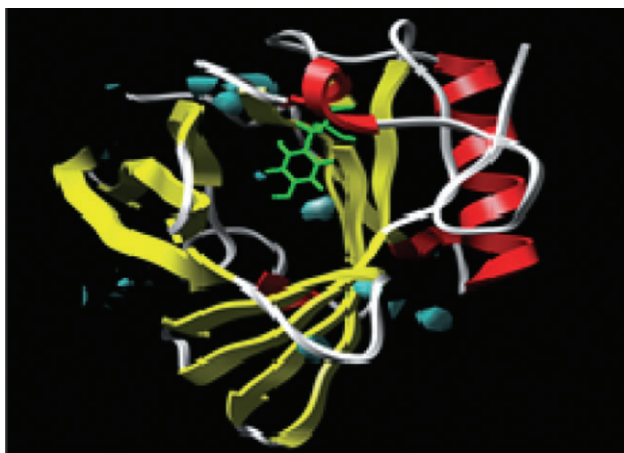

Figure 1: *MUP-IBM complex with 1 water molecule bound to residue tyrosine 120*

(figure 1). Mutating (tyrosine replaced by phenylalanine) this residue will allow us to obtain more information on the process of ligand-binding by MUP.

QCM-D is a well established derivative of the QCM which in addition to measuring the change in resonant frequency (f), can also probe energy dissipation (D) as a material is deposited on a gold-coated quartz crystal oscillator. The resonant frequency changes as a function of the mass of material deposited on the crystal surface [3], whereas the dissipation can provide information about the flexibility of the adsorbed layer. Here we are utilising QCM-D to explore IBM ligand binding to WT-MUP, and Y120F mutant MUP.

MATERIALS

All MUP and IBM solutions were made by adding degassed PBS solution at PH 7.3. The concentrations of MUP and IBM were made to 1 µM and 50 µM respectively.

RESULTS AND CONCLUSION

Molecule	ΔF_{MUP}	ΔD_{MUP}	ΔF_{IBM}	ΔD_{IBM}
WT-MUP	−95	0.713	−0.8	0.435
Y120F- MUP	−122	1.506	−0.74	0.31

ΔF_{MUP} is negative for both molecules which indicates a mass increase on the surface. The increase in D_{MUP} shows that a flexible layer of protein is formed on the crystal. F_{IBM} decreases by similar amounts for both proteins which indicates a mass increase due to the binding of the ligand to the protein however, the ΔD_{IBM} for WT-MUP is slightly higher than for Y120F-MUP. Therefore, the WT-MUP becomes more flexible then Y120F-MUP upon ligand binding. Further analysis is now underway.

ACKNOWLEDGMENTS

REFERENCES

[1] Bingham, R., Findlay, J. B. C., Hsieh, S., Kjellberg, A., Perazzolo, C., Phillips, S., Kothandaraman, S., Trinh, C.H., Turnbull, W.B., Bodenhausen, G., Homans, S.W. (2004) *J. AM. Chem. Soc.*, **126**: 1675–1681

[2] Barratt, E., Bronowska, A., Vondrasek, J., Cerny, J., Bingham, R., R., Phillips, S., Homans, S. W. (2006) *J. Mol., Biol.*, 362: 994–1003

[3] Sauerbrey, G. 1959. VERWENDUNG VON SCHWINGQUARZEN ZUR WAGUNG DUNNER SCHICHTEN UND ZUR MIKROWAGUNG. Zeitschrift Fur Physik 155:206–222.

Structural Studies on Glycosylated PAMAM Dendrimers

Teresa S. Barata[1], Steve Brocchini[1], Ian Teo [2], Sunil Shaunak[2], Mire Zloh[1]

[1]The School of Pharmacy, University of London, London, UK.
[2]Faculty of Medicine, Imperial College London, London, UK.

Abstract – **Dendrimers are hyperbranched molecules with many end groups. The glycosylation of PAMAM dendrimers induces immuno-modulatory properties. Molecular modelling studies were used to understand (i) why this surface modification may lead to this activity; (ii) how these dendrimers may interact with the biological target.**

INTRODUCTION

Dendrimers are macromolecules that are considered as potential medicines which display polyvalency but also share properties with low molecular molecules (e.g. low viscosity). Mono-saccharide modified polyamidoamine (PAMAM) dendrimers have been reported to have immuno-modulatory and anti-angiogenic activity that can prevent the progress of inflammatory responses[1]. It is thought that dendrimer interactions with the lipid polysaccharide (LPS) recognition system and, more specifically, with the cell membrane TLR4-MD2 complex may be responsible for its activity. End-group conjugation of the saccharide allows the loading of these dendrimers to be estimated between 8 and 9 glucosamine moieties per dendrimer. The position of the saccharides cannot be determined.

MATERIALS AND METHODS

The hyper-branched structure of PAMAM dendrimers is derived from a diaminobutane core. Repetitive units form the branches and carboxylate caps form the surface. The morphology of the dendrimer allows the structure to be seen as a sequence of interconnected monomers. The geometry and electronic properties of the monomers within the dendrimer are not known. Therefore, a set of *ab initio* and molecular mechanics calculations was conducted on various fragments of the dendrimers to evaluate geometric parameters of a 3D structure.

The electronic properties of these molecules were studied and the Frontier Molecular Orbital theory was used to understand the saccharide loading and distribution of the modified dendrimer surface. Conformational flexibility and consequent availability of the sugars were studied by the molecular dynamics of fully solvated molecules and molecular properties were estimated for all generated structures.

The representative conformations of flexible glycosylated dendrimers were used in rigid docking studies with MD2, using different software packages to understand the basis of their biological activity.

RESULTS AND DISCUSSION

Four basis monomers were defined to sequentially build the dendrimer structure; one diaminobutane core monomer, one monomer constituting the repetitive branch subunit, one monomer representing the carboxylated surface and a monomer for the glucosamine saccharide. Full parameterisation of the monomers and their combination were used to develop different force field parameters. Topology and parameter files were written and the 3D structures were generated with XPLOR-NIH.

Electronic properties determination and conformation flexibility assessments allowed for a better understanding of the distribution of the glucosamine molecules with a loading
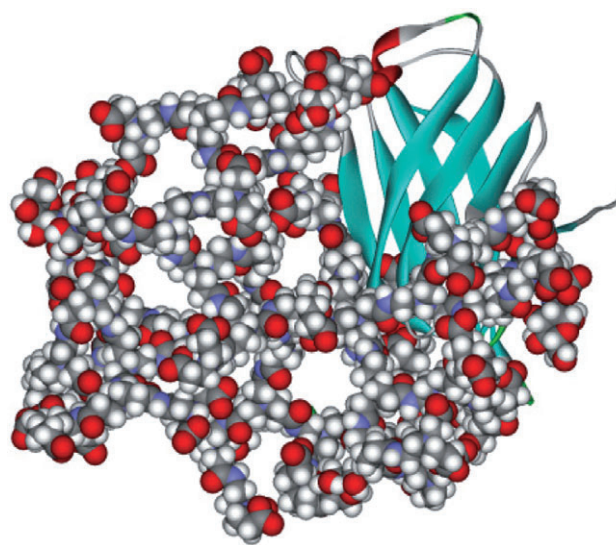

Fig. 1 Tentative model of MD2 and dendrimer with 8 glucosamine molecules. Docking study performed with PatchDock1.0 and visualised with DS Visualiser2.5.

range between 8 and 12 glucosamine molecules per dendrimer.

Finally, the ongoing interaction studies have revealed a possible mechanism for dendrimer activity through the interaction with the MD2 protein which is the accessory protein of the TLR4 cell receptor.

CONCLUSIONS

A method to generate 3D structures of dendrimer conjugates from a linear sequence has been developed. It enabled: (i) the study of loading and distribution of the glucosamine molecules on the dendrimers' surface and (ii) a proposal for a tentative mechanism of action of these molecules with the MD2 protein.

REFERENCE

[1] Sunil Shaunak, Sharyn Thomas, Elisabetta Gianasi, Antony Godwin, Emma Jones, Ian Teo, Kamiar Mireskandari, Philip Luthert, Ruth Duncan, Steve Patterson, Peng Khaw and Steve Brocchini (2004). *Nat. Biotechnol.* **22**: 977–984.

Structure-activity relationship of a series of inhibitors of aromatase (AR)

K. Shah, C.P. Owen, S. Ahmed

School of Science, University of the West of Scotland, Paisley, Renfrewshire, Scotland, UK.

INTRODUCTION

We have previously reported the development of a novel and theoretical modelling technique, the substrate-haem complex (SHC) approach, which has been used in the design and rationalisation of inhibitors of aromatase (AR) [1]. The crystal structure of AR was recently reported and in an effort to evaluate the validity of the SHC approach, we undertook a modelling study to compare the SHC with the crystal structure as well as undertaking a structure-activity relationship study of a number of inhibitors of AR using the crystal structure.

MATERIALS AND METHODS

The construction of the SHC has been reported previously and was based on the proposed final step of the aromatisation process where the C(1)-βH is abstracted whilst undergoing attack on the C(19) CHO moiety. In general, the steroid, haem and inhibitors were constructed within CaChe and the appropriate bonds formed between the appropriate functionalities. The overall structure was then minimised resulting in the formation of the SHC.

In the consideration of the binding of the inhibitors within the crystal structure of AR, the structure was downloaded from the PDB database and read into CaChe. The active site was identified and the substrate was deleted and the atoms locked. The inhibitors were constructed and bound to the Fe atom of the haem and the inhibitors minimised within the active site and areas about the active site identified which would be able to undergo hydrogen bonding with groups within the inhibitors. In the comparison of the SHC with the crystal structure, the substrates were identified and used to superimpose the SHC within the crystal structure.

RESULTS AND DISCUSSION

Consideration of the SHC and the crystal structure of AR, in particular, from the superimposing of the SHC onto the crystal structure, we discovered that the haem moiety within the SHC was positioned close to that in the crystal structure, the two Fe atoms were separated by 1.2 . Consideration of the hydrogen groups within the SHC suggests that these groups are incorrectly positioned and do not match the amino acids within the active site which are proposed to interact with the C(3) = O and C(17) = O moieties, namely, ARG115 and ASP309. Modelling compounds within the crystal structure supports previous molecular modelling studies undertaken by us. For example, we have previously suggested that the CGS-16949A binds within the active site as such that it utilises the hydrogen bonding group which would normally be utilised by the C(17) = O functionality within the substrate whilst binding to the haem via the imidazole moiety, this is indeed what we observe, i.e. this compound is able to utilise the ASP309 or MET374.

CONCLUSION

In conclusion, we have shown that the theoretically derived SHC closely matches the crystal structure, in particular, the positioning of the haem with respect to the substrate and is therefore an excellent representation of the AR active site.

REFERENCE

[1] S. Adat, C.P. Owen and S. Ahmed, "Inhibition of aromatase (AR) by benzyl azole-based compounds", *Lett. Drug Des. Disc.*, **4** (2007) 545–549.

Structure-Based Design, Synthesis, and SAR Exploration of Pyrrole-2-one Analogues as Inhibitors of the Annexin A2–S100A10 Protein Interaction: Potential Anti-angiogenesis therapeutics

Tummala R. K. Reddy, Chan Li, Guo Xiaoxia, Peter M. Fischer,
Lodewijk. V. Dekker*

Centre for Biomolecuar Sciences, Division of Medicinal Chemistry & Structural Biology, School of Pharmacy, University of Nottingham, Nottingham NG7 2RD

INTRODUCTION

Recent genetic studies have indicated that a complex between the Annexin II and the S100A10 is involved in angiogenesis. These proangiogenic factors support the progressive tumour growth. Peptide interference experiments indicate that the disruption of this complex is anti-angiogenic, leading to the arrest of tumour growth, making this an attractive target in growth factor directed anti-angiogenesis therapy [1, 2]. As yet no small molecule blockers of S100A10-Annexin II complex formation exist.

AIM

The goal of this research is to generate small molecules that can disrupt the formation of complex between the S100A10 and the Annexin II. Such molecules may exhibit anti-angiogenesis therapy leading to the arrest of the growth of the tumours. Thus anti-angiogenesis drugs can be used in combination with conventional chemotherapy in the treatment of cancer.

RESULTS AND DISCUSSION

An X-ray crystal structure of the complex between S100A10 and an annexin A2 N-terminal peptide (Figure 1) provides a plot form for the discovery of inhibitors through rational drug design [3]. We report the results from a virtual screening campaign of a small-molecule database containing over half a million compounds against an S100A10 structural model, as well as biological evaluation of predicted hit compounds. We present 13 inhibitor compounds, of which 7 compounds showed inhibitory potency in the low micromolar range using a fluorescence-based competitive binding assay between an N-terminal annexin A2 peptide and S100A10. We chose 3-hydroxy-1-(2-hydroxypropyl)-5-(4-isopropylphenyl)-4-(4-ethylbenzoyl)-1H-pyrrol-2(5H)-one as a promising starting point for exploratory hit-to-lead medicinal chemistry and prepared a total of 41 analogs. The most potent compounds were found to have similar inhibitory activity as the cognate annexin A2 peptide and overall the structure–activity relationships observed confirm the hypothetical binding mode from the virtual screen and point the way for further development of anti-angiogenic annexin A2–S100A10 inhibitors.
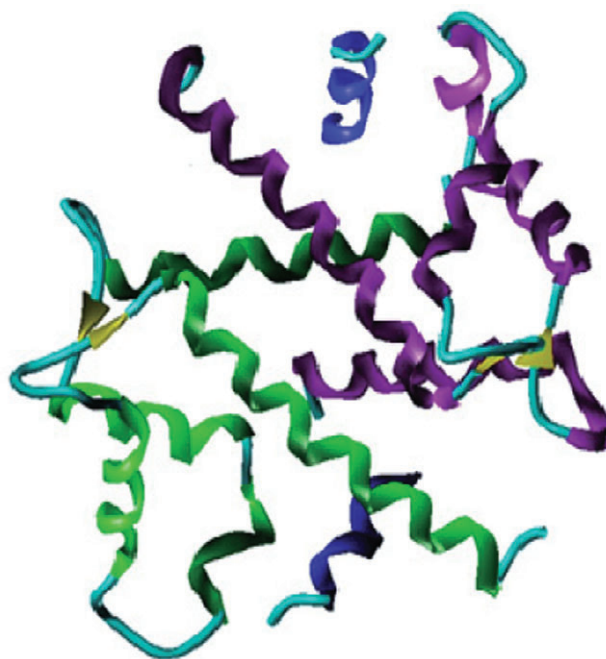

Figure 1: *X-ray crystal structure of the S100A10-Annexin-A2 N-terminal peptide complex. S100A10 is a dimer, its monomers are coloured in green and magenta. Annexin-A2 peptide which is in the concave pocket is coloured blue.*

CONCLUSIONS

We chose the 3-hydroxy-1H-pyrrol-2(5H)-one compound as a medicinal chemistry starting point. Systematic alteration of the 1H-pyrrol-2(5H)-one N1, C4, and C5 substituents resulted in distinct SARs that are in fairly good agreement with our hypothetical binding mode for the series. Although potency gain from the lead compound to the most potent derivatives was modest, the 1-substituted 4-aroyl-3-hydroxy-5-phenyl-1H-pyrrol-2(5H)-one pharmacophore represents a viable platform for further optimisation, which we are currently in the process of carrying out.

REFERENCES

[1] Tilmann Becker, Klaus Weber and Nils Johnsson. Protein-protein recognition via short amphiphilic helices; a mutational analysis of

the binding site of annexin II for p11. *The EMBO Journal*, 1990, 9, 4207–4213.

[2] Qi Ling, Andrew T. Jacovina, Arunkumar Deora, Maria Febbraio, Ronit Simantov, Roy L. Silverstein, Barbara Hempstead[2], Willie H. Mark and Katherine A. Hajjar Annexin II regulates fibrin homeostasis and neoangiogenesis in vivo. *The Journal of Clinical Investigation*, 2004, 113, 38–48.

[3] Stéphane Réty, Jana Sopkova, Madalena Renouard, Dirk Osterloh, Volker Gerke, Sébastien Tabaries, Françoise Russo-Marie & Anita Lewit-Bentley. The crystal structure of a complex of p11 with the annexin II N-terminal peptide. *Nature Structural Biology*, 1999, 6, 89–85.

Synthesis and ACE-inhibitory potency of captopril branched chain ester prodrugs

A. Chika[1], P. R. Gard[1], M.J. Ingram[1], G.P. Moss[2]

[1]School of Pharmacy and Biomolecular Sciences, University of Brighton, Brighton, UK.
[2]School of Pharmacy, Keele University, Keele, UK.

INTRODUCTION

Previously, a series of captopril straight chain ester derivatives were designed (using a QSPR approach), synthesised and characterised. They were shown to have enhanced skin penetration when compared to the parent drug [1]. This study has adapted the synthetic procedure used previously (for the straight chain esters) to facilitate the synthesis of a branch chain ester. In this case, 2-methylpropan-2-ol was chosen as a suitable candidate. The ACE-inhibitory potency of the branch chain derivative was then compared to the captopril straight chain ester equivalent.

Figure 1. Schematic representation of the esterification reaction of captopril with different alcohols [1].

MATERIALS AND METHODS

All chemicals, unless otherwise stated, were purchased from Sigma Aldrich Ltd. Angiotensin I, trifluoacetate, butan-1-ol and 2-methylbutan-2-ol were obtained from Acros Organics (Belgium). The prodrugs were synthesised by a modification of a previously published method [1]. Briefly, captopril (5 mmol, 1.09 g) was dissolved in the appropriate alcohol. Thionyl chloride (0.1 mL, 1.35 mmol) was then added drop-wise at 0°C. The reaction mixture was heated at 60°C for 4 h. The excess alcohol and thionyl chloride produced hydrogen chloride gas which was removed *in vacuo* to yield the ester. However, for the reaction with 2-methylpropan-2-ol the amount of thionyl chloride was increased to a molecular equivalent of captopril and the reaction time was decreased to 2.5 hours. This resulted in a 95%, or greater, yield. ACE-inhibitory potency of synthesised esters was measured using previously described methods [2].

Figure 2. Example of a captopril branch chain ester

RESULTS AND DISCUSSION

The method for synthesising the ester prodrug of captopril and of 2-methylpropan-2-ol was achieved by a minor modification of the published method [1]. The increased amount of the catalyst/reagent (thionyl chloride) required can be attributed to 2-methylpropan-2-ol being more sterically hindered than the previous straight chain alcohols. However, this had the advantage of decreasing reaction time. Initial ACE-inhibitory studies have indicated that the activity of the above prodrug is comparable to the straight chain analogue [2].
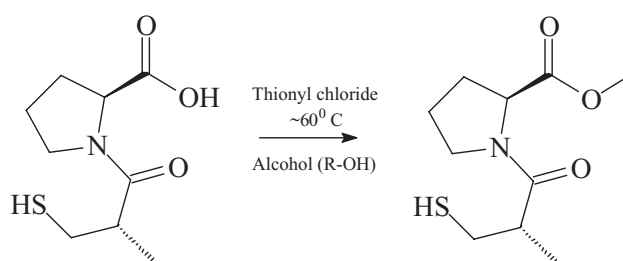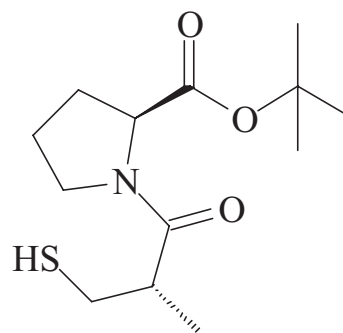
CONCLUSIONS

The branch chain ester prodrugs of captopril were successfully synthesised and characterised. Initial experiments suggest that captopril branch chain ester prodrugs seemed to be less pharmacologically active than captopril. Further investigations and *in vitro* evaluations are ongoing with respect to the ACE-inhibitory effects of branch chain ester prodrugs compared to straight chain prodrugs. Initial results of branch chain esters compare favourably to previous studies. Ongoing work will compare the percutaneous absorption of these prodrugs in *vitro* models.

REFERENCES

[1] G.P. Moss, D.R. Gullick, P.A.Cox, C. Alexander, M.J. Ingram, J.D Smart, W.J Pugh, Design, synthesis and characterisation of captopril prodrugs for enhanced percutaneous absorption. *J Pharm Pharmacol* **58** (2006) 167–177.

[2] D.R. Gullick, G.P. Moss, P.A. Cox, M. J. Ingram, P. R. Gard, J. D. Smart, W.J. Pugh., Metabolism of captopril carboxyl ester derivatives for percutaneous absorption. *J Pharm Pharmacol* **61**(2009) 159–165.

Synthesis and biochemical evaluation of 3,5-dibromo-4-hydroxyphenyl ketone-based compounds as inhibitors of 17β-hydroxysteroid dehydrogenase (17β-HSD)

S.N. Mashru, M.S. Olusanjo, C.P. Owen, S. Ahmed

School of Science, University of the West of Scotland, High Street, Paisley, Renfrewshire, UK.

INTRODUCTION

From our previous studies, we hypothesised that additional H-bonding group exists within the active site of type 3 of the 17β-hydroxysteroid dehydrogenase (17β-HSD) family of enzymes and which allow inhibitors to undergo hydrogen bonding interaction between the OH of the inhibitor and the active site [1]. We argued that the removal of this additional interaction would result in a reduction in the inhibitory activity within the 4-hydroxyphenyl ketone-based compounds. In an effort to evaluate our hypotheses with regards to the role of the additional hydrogen bonding interaction, we undertook the synthesis of dibrominated derivatives of a range of 4-hydroxyphenyl ketone-based compounds, and their subsequent biochemical evaluation.

MATERIALS AND METHODS

The synthesis of the target compounds was undertaken involving an initial Friedel-Crafts acylation using standard literature method [1]. The 4-hydroxy moiety was derivatised to the dibrominated derivative (Fig. 1) involving the use of bromine water.

The biochemical evaluation involved standard a literature method using rat testicular microsomal 17β-HSD3 and were undertaken in triplicate using ^{3}H-androstenedione [1].

RESULTS AND DISCUSSION

In the synthesis of the 3,5-dibrominated derivatives of 4-hydroxyphenyl ketone-based compounds, the latter series of compounds were initially synthesised according to the literature methodology previously reported by us [1]. The 4-hydroxyphenyl ketone-based compounds were then derivatised using bromine water (acetic acid was used as the reaction solvent). The reactions were found to proceed in moderate to excellent yield (typically between 40% and 60%) and in some cases with great difficulty, in particular, the dibrominated derivative of 4-hydroxyacetophenone (**1b**). The synthesis of **1b** proved to be extremely difficult and resulted in a number of by-products – the synthesis of the longer alkyl chain containing compounds proved to be less problematic.
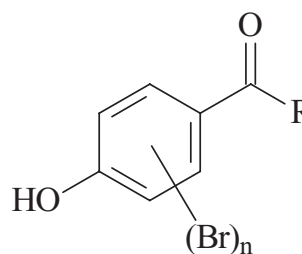

Fig. 1. Target compounds where n = 1 or 2; R = H or alkyl or cycloalkyl moiety.

From the consideration of the inhibitory data, we observed that the dibrominated derivatives of 4-hydroxyphenyl ketone-based compounds are extremely poor inhibitors of 17β-HSD3, in general, the compounds showed no inhibitory activity. For example, 4-hydroxynonanophenone (**2a**) was found to possess ~84% ai an inhibitor concentration of 100 μM, under similar conditions, the 3,5-dibromo-4-hydroxynonanophenone (**2b**) was found to lack inhibitory activity.

The acidity of the OH moiety was proposed to be a factor in the ability of the inhibitors to undergo hydrogen bonding with the enzyme active site. Determination of the pKa for the brominated and the non-brominated derivatives show that the dibrominated compounds are stronger acids, e.g. **2a** and **2b** were found to possess pKa values of 8.40 and 6.82 respectively. The biological activity therefore correlates well with the decrease in pKa.

CONCLUSIONS

In conclusion, our study suggests that the disruption of the ability of the OH moiety to undergo hydrogen bonding results in a decrease in inhibitory activity.

REFERENCE

[1] Lota, R., Olusanjo, M. S., Dhanani, S., Owen, C. P. and Ahmed, S., "Synthesis, biochemical evaluation and rationalisation of the inhibitory activity of a range of 4-hydroxyphenyl ketones as potent and specific inhibitors of the type 3 of 17β-hydroxysteroid dehydrogenase (17β-HSD3)", J. Steroid Biochem. Mol. Biol., 111 (2008) 128–137.

Synthesis and biochemical evaluation of sulfamated derivatives of 3,5-dibromo-4-hydroxyphenyl ketone-based compounds

B. Bhamare, C.K. Patel, M. Patel, C.P. Owen, S. Ahmed

School of Science, University of The West of Scotland, Paisley, Renfrewshire, UK

INTRODUCTION

We have previously reported ester derivatives of 4-[(aminosulfonyl)oxy]benzoate, which were found to be potent inhibitors of ES [1]. We postulated that the incorporation of groups into the phenyl ring system would stabilise the phenoxide ion leading to an increase in potency [2]. Here, we report the initial tentative results of our efforts to further increase the potency of a series of sulfamic acid alkanoyl/cycloalkanoyl-phenyl esters; their *in vitro* biochemical evaluation, and; the rationalisation of the inhibitory activity.

MATERIALS AND METHODS

The synthesis of the target compounds was undertaken involving an initial Friedel-Crafts acylation using standard literature method (using the appropriate acyl chloride and aluminium chloride in anhydrous dichloromethane). The 4-hydroxy moiety was derivatised to the sulfamate moiety (using aminosulfonyl chloride in dimethyl acetamide) followed by the dibromination of the sulfamic acid alkanoyl/cycloalkanoylphenyl ester using bromine water.
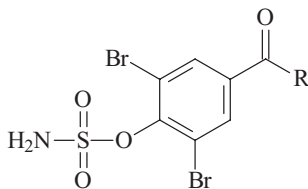

Fig. 1 The general structure of the target compounds where R = alkyl or cycloalkyl moiety.

The biochemical evaluation involved a standard literature method using human placental microsomal ES and were undertaken in triplicate [1] using ^{3}H-estrone sulfate and human placental microsomes.

RESULTS AND DISCUSSION

The synthesis of the target compounds proved to be extremely troublesome. That is, the bromination of the sulfamated derivative resulted in extremely poor yield of the target compound (in all cases the yield was less than 10% with the major by-product being the starting material). The reaction scheme was altered such that the sulfamoylation step was undertaken after the incorporation of the two bromine atoms within the phenylring. The reactions gave the target compounds in low yield – the compounds were, however, found to be unstable in solution form with the sulfamate moiety being found to be readily hydrolysed in solution.

The biochemical evaluation of the target compounds showed that the non-brominated derivatives were good inhibitors of ES, however, the results for the dibrominated derivatives proved to be inconclusive as we discovered that the target dibrominated derivatives were unstable in the assay mixture with prolonged standing.

However, a few of the compounds did show some potential, for example, sulfamic acid 4-nonanoylphenyl ester was found to possess 67% inhibitory activity at [I] = 10 µM whilst under similar conditions, sulfamic acid 2,6-dibromo-4-nonanoylphenyl ester was found to possess 95% inhibitory activity.

CONCLUSIONS

In conclusion, we have shown some data which appear to suggest that our hypothesis with regards to the increase in potency with the stabilisation of the phenoxide ion may have some validity, however, the target compounds were found to be unstable and require further investigation.

REFERENCES

[1] C.P. Owen, M. Patel, C. K. Patel, T. Cartledge and S. Ahmed, "Synthesis and *in vitro* biochemical evaluation of a series of compounds as potential inhibitors of estrone sulfatase (ES) and the role of pK_a in both the synthesis and the inhibitory activity of the potential inhibitors" *Lett. Drug Des. Discov.*, **4** (2007) 394–398.

[2] K. Aidoo-Gyamfi, T. Cartledge, K. Shah and S. Ahmed, "Estrone sulfatase and its inhibitors", *Anti-Cancer Agents Med. Chem.*, **9** (2009), 599–612.

Synthesis and biological evaluation of a range of thiosemicarbazone-based compounds as inhibitors of estrone sulfatase (ES)

S. Singh, A. Kumar, C.P. Owen and S. Ahmed

School of Science, University of the West of Scotland, High Street, Paisley, Renfrewshire, Scotland, UK.

INTRODUCTION

Thiosemicarbazone-based compounds have been reported as non-competitive inhibitors of estrone sulfatase (ES) [1]. However, the structure activity relationship (SAR) of the thiosemicarbazone-based compounds has not been rationalised. Here, we report our continued efforts into the synthesis and biochemical evaluation of a series of thiosemicarbazone-based inhibitors in an attempt to provide an insight into the SAR for these compounds.

MATERIALS AND METHODS

In the synthesis of the target compounds, benzaldehyde, propiophenone or butaphenone derivatives were refluxed in a solution of the appropriate thiosemicarbazide dissolved in absolute ethanol (EtOH) as the solvent and acetic acid as catalyst. The resulting solid was filtered and re-crystallised from aqueous EtOH to give the target compounds.

The biochemical evaluation involved the use of rat liver microsomal enzyme obtained from Sprague-Dawley ex-breeder male rats.

RESULTS AND DISCUSSION

The target compounds were obtained in moderate to excellent yield (ranging from ~30% to ~95%). In the initial synthesis of the hydroxyl derivatives, we discovered that the yield was greatly reduced, in particular, with the longer alkyl chain containing compounds, for example derivatives of butaphenone. We argued that the use of a weak acid may increase the yield as the protonation of the oxygen atom within the $C = O$ moiety would result in an increase in the dipole moment so as to favour the act of the carbonyl moiety by the thiosemicarbazide. The use of acetic acid as a catalyst did indeed result in an increase in yield. Furthermore, the hydroxy derivatives were found to be more soluble in EtOH in comparison to the halogen based derivatives and water was required to re-crystallise the target compound. No major problems were observed with the majority of derivatives of benzaldehyde.

In general, the thiosemicarbazone-based compounds synthesised within the current study were found to be weaker inhibitors of rat liver microsomal ES in comparison to the standard inhibitors used. For example, estrone-3-O-sulfamate was found to possess ~84% inhibition ([I] = 100 μM) whilst the most potent compound was found to be the hydroxy derivative (5-chloro-2-hydroxybenzaldehyde-N-cyclohexylthiosemicarbazone) which was found to possess ~80% inhibition whilst the weakest was found to possess ~30% inhibition. With regards to SAR, from an initial consideration of the initial screening data, it would appear that the ortho-substitution of the phenyl ring with functional groups able to undergo hydrogen bonding with groups at the active site has resulted in an increase in inhibitory activity. This is further supported by the observation that substitution with a halogen moiety at the ortho-position did not increase the inhibitory activity.

CONCLUSIONS

We have provided some novel inhibitors of ES and have undertaken limited SAR which has allowed the consideration of structural features so as to allow us to design further derivatives of this novel range of compounds.

REFERENCE

[1] P. Jütten, W. Schumann, A. Härtl, L. Heinisch, U. Gräfe, W. Werner, H. Ulbricht, "A Novel Type of Nonsteroidal Estrone Sulfatase Inhibitors" *Bioorg. Med. Chem. Lett,* **12** (2002) 1339–1342.

Synthesis and biological evaluation of pegylated-cysteamine compounds for the treatment of cystinosis

G. Kay[1], Z. Omran, A. Di Salvo, R.C. Mulrooney, M. MacKay, E. Hector, T. Mullen, R.M. Knott, D. Cairns

[1]School of Pharmacy and Life Sciences, The Robert Gordon University, Aberdeen, AB10 1FR, UK.

Abstract **– Cystinosis is a rare genetic disease, the oral treatment for which currently requires the administration of capsules every six hours. This treatment causes nausea, vomiting and the production of odorous metabolites in the breath and sweat. In an attempt to overcome these problems we have adopted a pegylation strategy. A library of pegylated derivatives of cysteamine has been synthesised and their ability to reduce the cystine burden of cystinotic cells was evaluated. One such compound, PD31, was found to be non-toxic and reduce the cystine levels in cystinotic cells.**

Scheme 1. Synthesis of pegylated cysteamine.

INTRODUCTION

Cystinosis is a rare autosomal recessive disease, where raised intracellular levels of the amino acid, cystine, causes crystals to form in every organ of the body. If left untreated death occurs within the second decade of life. Treatment involves the oral administration of cysteamine, an aminothiol which possesses an offensive taste and smell and, along with its metabolites, is excreted in breath and sweat causing halitosis and body odour as well as gastric irritation. This treatment is administered every 6 hours. As a result, patient compliance may be poor. [1]
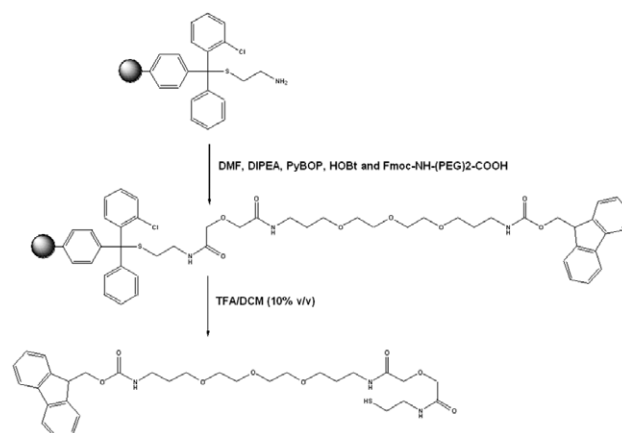
In order to overcome these problems a small library of novel pegylated derivatives of cysteamine has been synthesised and evaluated.

MATERIALS AND METHODS

A library of pegylated cysteamine compounds was synthesised and fully characterised. A combination of solid and solution phase organic chemistry was used. Purification was performed by preparative HPLC on a C18 column under isocratic conditions. The target compounds eluted with water (0.05 M TFA)/acetonitrile (25% : 75%). The targets were freeze-dried and characterised by ^{1}H and ^{13}C NMR.

Compound toxicity was undertaken using an Alamar blue reagent (Serotech, UK) based assay.

Intralysosmal cystine was measured using a thiol and sulfide detection kit (Molecular Probes, NL). Lysates were produced from cystinotic fibroblasts treated for 48 h with 1% DMSO (vehicle control), 50 µM cysteamine or 50 µM peg-derivative. Intralysosmal cystine was isolated from the lysates, converted to cysteine and the concentration measured on a multiwell plate reader.
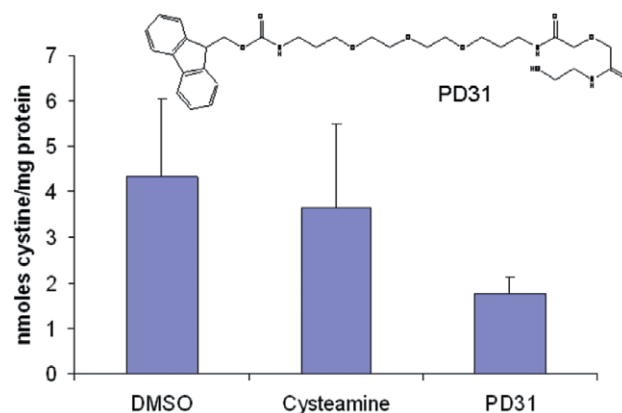

Fig. 1. Reduction of cystine in cystinotic cells measured at 48 hrs.

RESULTS AND DISCUSSION

A library of pegylated cysteamine compounds was synthesised in acceptable yield, Scheme 1.

Compounds were then evaluated for cellular toxicity and ability to reduce the cystine burden of cystinotic cells. PD31 was found to be non-toxic and to be 2-fold more effective than cysteamine at lowering lysosomal cystine (Fig. 1).

CONCLUSIONS

Pegylated derivatives of cysteamine have been synthesised and fully characterised. The ability of these agents to reduce

the cystine burden of cystinotic cells was evaluated using an in vitro procedure. One compound, PD31, was found to lower the cystine level of cultured cells by twice as much as the clinically used agent.

ACKNOWLEDGMENTS

REFERENCE

[1] Cairns D., Anderson R.J., Coulthard, M., Terry J., (2002). J. Pharm. 269: 615–616.

Synthesis and *in vitro* biochemical evaluation of 6-aminosulfonyl naphthanoate derivatives as potential inhibitors of estrone sulfatase (ES)

A. Kumar, C.K. Patel, C.P. Owen and S. Ahmed

School of Science, University of the West of Scotland, High Street, Paisley, Renfrewshire, Scotland, UK.

INTRODUCTION

The estrone sulfatase (ES) pathway becomes the major source of estrogen in postmenopausal women. This alternative route to the biosynthesis of estrone (E1) [and subsequently estradiol (E2)] allows the continued stimulation of estrogen-dependent breast cancer cells, thereby allowing the tumour to be stimulated via a non-aromatase pathway. Here, we report the synthesis of a series of ester derivatives of alkyl 6-aminosulfonyl naphthanoates (Fig. 1) and their *in vitro* biochemical evaluation.

MATERIALS AND METHODS

In the synthesis of alkyl 6-hydroxynaphthanoate, 6-hydroxy-2-naphthoic acid was initially reacted with the appropriate alkyl alcohol. The derivatisation of the OH moiety to the sulfamate derivative was undertaken using literature based methodology [1].

In the biochemical evaluation, we used human placental microsomes as the source of ES [2]. The substrate was radiolabelled estrone sulfate in tris-HCl buffer at pH 7.2. After the incubation, the reaction was quenched using toluene and the samples counted for 5 min for tritium.

RESULTS AND DISCUSSION

In the synthesis of the target naphthanoate-based compounds, the methodology described for the synthesis of the 4-[(aminosulfonyl)oxy]benzoate was used [2]. In general, the reactions were undertaken without any major problems and in moderate to good yield (typically between 45% to 70%).

Consideration of the IC50 values show that, in general, the naphthanoate-based compounds are weaker inhibitors than both the previously reported range of compounds based on the 4-hydroxybenzoic acid backbone as well as the standard
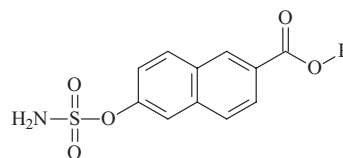

Fig. 1 Structure of the target compounds (R = alkyl chain).

compounds previously reported, namely, COUMATE, 667-COUMATE and EMATE [3].

With regards to the range of naphthanoates synthesised, the straight alkyl chain containing derivatives of naphthanoic acid were found to be more potent than the cycloalkyl moiety containing inhibitors. Indeed, the most potent inhibitor within the naphthanoate-based compounds was found to be compound cycloheptyl 6-aminosulfonyl-2-naphthanoate (IC50 = 2.7 ± 0.11 μM) which was found to be ~7.6 times more potent than the most potent straight chain containing compound, namely, cycloalkyl 6-aminosulfonyl-2-naphthanoate (IC50 = 20.6 ± 1.6 μM). In comparison, cycloheptyl 6-aminosulfonyl-2-naphthanoate was found to be approximately 16 times weaker than the most potent standard used within the current study, namely, cyclooctyl 4-aminosulfonyl benzoates (IC50 = 0.17 ± 0.007 μM).

CONCLUSIONS

In conclusion, we have synthesised a series of compounds which has further demonstrated that the active site of ES corresponding to the C(17) area is restricted in the volume of space available to inhibitors. We have also shown that the optimum logP within the current series of inhibitors of ES would appear to be approximately 3.3 and which closely matches our previous studies where the optimum logP was found to be ~3.6.

REFERENCES

[1] S. Ahmed, C.P. Owen, K. James, C.K. Patel and M. Patel, "Novel inhibitors of the enzyme estrone sulfatase (ES)" *Bioorg. Med. Chem. Lett*., **11** (2001) 841–844.

[2] S. Ahmed, K. James and C.P. Owen, "Inhibition of estrone sulfatase (ES) by derivatives of 4-[(aminosulfonyl)oxy] benzoic acid" *Bioorg. Med. Chem. Lett*., **12** (2002) 2391–2394.

[3] L.W.L. Woo, A. Purohit, B. Malini, M.J. Reed, B.V.L. Potter, "Potent active site-directed inhibition of steroid sulphatase by tricyclic coumarin-based sulphamates" *Chem. Biol*. **7** (2000) 773–791.

Synthesis and *in vitro* biochemical evaluation of a series of dialkyl esters of 5-aminosulfonyl isophthanoate

K. Shah, M. Akbarzadeh, C.K. Patel, C.P. Owen, S. Ahmed

School of Science, University of the West of Scotland, High Street, Paisley, Renfrewshire, Scotland, UK

INTRODUCTION

A number of steroidal and non-steroidal sulfamate-based inhibitors have been investigated as potent inhibitors of estrone sulfatase (ES). Here, we attempt to investigate the incorporation of electron withdrawing groups which we hypothesised would stabilise the phenoxide ion resulting in an increase in potency of the inhibitors. As such, we report the synthesis of a number of ester derivatives of dialkyl 5-aminosulfonyl isophthanoates and their *in vitro* biochemical evaluation.

MATERIALS AND METHODS

The dialkyl 5-aminosulfonyl isophthanoates were synthesised involving an initial esterification of the COOH moieties followed by the derivatisation of the OH moiety using aminosulfonyl chloride using dimethyl acetamide (DMA) as the solvent [1].

In the biochemical evaluation, we used literature procedure using human placental microsomes as the source of ES; using radio-labelled estrone sulfate in tris-HCl buffer at pH 7.2 [2]. After the incubation, the reaction was quenched using toluene and the samples counted for 5 min for tritium.

RESULTS AND DISCUSSION

The esters were formed by reacting the parent carboxylic acid (5-hydroxy isophthalic acid) with the appropriate alcohol in the presence of an acid catalyst. The esters were successfully synthesised in yields ranging from 60% to 90%, without any major problems. The dialkyl 5-aminosulfonyl isophthanoates were synthesised successfully using a literature based method previously reported by us, where the hydroxy ester was reacted with aminosulfonyl chloride and DMA, the reaction solvent. Moderate yields of the target compounds were obtained (30%–50%).

The phenoxide ion resulting from the hydrolysis of the sulfamate group is stabilised by the electron-withdrawing effect of the carbonyl group, therefore, the incorporation of a second carbonyl group within the phenyl ring would be expected to result in an increase in inhibitory activity. However, in the case of the alkyl 5-aminosulfonyl isophthanoate based compounds, they were shown to be very poor inhibitors of ES, all of the synthesised compounds being found to possess inhibitory activities less than 35% at 1000 μM inhibitor concentration. For example, the most potent compound within the current range was dipropyl 5-aminosulfonyl isophthanoate which was found to possess 31% inhibition at 1 mM.

We have rationalised the poor inhibitory activity and have postulated that the presence of the second carbonyl group on the phenyl ring increases the electron density about the O-Ar area. The electron-withdrawing ability of the second C = O is therefore reduced, preventing greater stabilisation of the phenoxide ion which results from the hydrolysis of the sulfamate group, and as a result a decrease in the inhibitory activity is observed.

CONCLUSIONS

Although we have not synthesised potent inhibitors of ES, we have nevertheless provided further support that the stability of the S-OAr bond is crucial to the potent inhibitory activity observed within potent inhibitors of ES.

REFERENCES

[1] S. Ahmed, C.P. Owen, K. James, C.K. Patel and M. Patel, "Novel inhibitors of the enzyme estrone sulfatase (ES)" *Bioorg. Med. Chem. Lett*., **11** (2001) 841–844.

[2] S. Ahmed, K. James and C.P. Owen, "Inhibition of estrone sulfatase (ES) by derivatives of 4-[(aminosulfonyl)oxy] benzoic acid" *Bioorg. Med. Chem. Lett*., **12** (2002) 2391–2394.

Synthesis of NO-releasing peptides and peptoids for stent coating

Z. Araim[1] M.J. Ingram[1], G.P. Moss[2] B. Patel[1], M. Santin[1], S. Meikle[1]

[1]School of Pharmacy and Biomolecular Sciences, University Brighton, Brighton, UK.
[2]School of Pharmacy, Keele University, Keele, Staffordshire, UK.

INTRODUCTION

Cardiovascular disease is the leading cause of death in the United Kingdom. Currently, stents and angioplasty are the primary therapeutic strategies for treatment of cardiovascular disease. However, many problems (such as restenosis and thrombosis) inhibit their use as long-term solutions. The release of nitric oxide (NO) in a localised area of the vasculature plays an important role in modulating cardiovascular cell homeostasis [1]. The addition of stents causes the loss of the multi-functional endothelium and so risks the progression and formation of a thrombus formed by platelet activation and aggregation. NO is a natural mediator of vascular homeostasis and is produced by endothelial cells. It has been known to reduce platelet adhesion and cause vasodilatation in the blood vessels. Extensive research has been conducted into solving the problems associated with restenosis and thrombosis. However, to date, this work has met with little success [2]. Attempts have also been made to tailor specific biomaterials for cardiovascular implant coatings, such as NO-releasing materials in the form of hydrogels and films. Such strategies have found success in reducing platelet adhesion and hyperplasia [2]. Synthesised nitroxylated derivatives of cysteine have been found to successfully release nitric oxide once placed on a metal stent-like material. In addition, we have used a previously synthesised of prodrug, S-nitroso captopril [3], as a comparator (peptoid) for this study.

MATERIALS AND METHODS

All materials, chemicals and solvents were obtained from Sigma-Aldrich. A metal disc (AISI 316 stainless steel disc, annealed temper, 0.25 mm thickness and 10 mm diameter) was used as a representation of a stent-like material. Synthesis of S-nitroso cysteine was achieved by using previously described methodology [3].

Stent material binding studies

A saturated solution of the product was made using a solution of (70:30) ethanol: water. The metal discs were placed in the solution and left to soak for 90 minutes at ambient temperature. The discs were removed and rinsed in a solution of ethanol:water (70:30) and left to dry in a vacuum desiccator for 30 minutes. The release of nitric oxide was tested using Greiss Reagent.

RESULTS AND DISCUSSION

S-nitroso cysteine was shown to release NO in the binding studies for the saturated solutions. In addition, S-
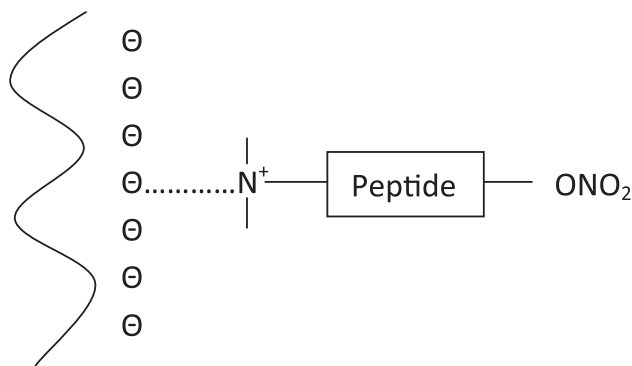

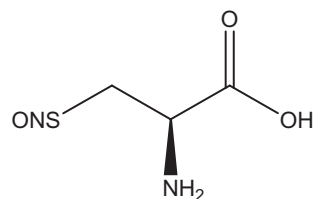**Figure 1.** Schematic diagram showing the arrangement of the NO-releasing peptides.

Figure 2. S-nitroso cysteine, which yielded 0.42 M of NO in the binding study (n = 3).

nitrosocaptopril yielded 0.45 M of NO from a saturated solution in the binding study.

CONCLUSIONS

The synthesis of NO donors that offer a new application for drug-eluting stents is presented. However, further research into attachment and release and considerations of safety, efficacy and tolerability needs to be considered.

REFERENCES

[1] Kumar GVP; Mathew L "New Stent Design for Percutaneous Aortic Valve Replacement". *Int. J Card Rev Med* **10** (2008) 121–4.
[2] M. Kushwaha et al "A nitric oxide releasing, self assembled peptide amphiphile matrix that mimics native endothelium for coating implantable cardiovascular devices", *Biomaterials* **31** (2009) 1502–8
[3] M J.Ingram and G Moss; "Synthesis of S-nitroso captopril" *J. Pharm Pharmacol*, **54** (2002) S67–68

The Drug Discovery Portal Library: a unique resource to enhance drug discovery in academia

N. Al-Shar'i, B. Al-Jaidi, B.F. Johnston, M.N. Robertson, S.P. Mackay and R.L. Clark[1]

[1]Strathclyde Institute of Pharmacy and Biomedical Sciences, University of Strathclyde, Glasgow, UK.

INTRODUCTION

The Drug Discovery Portal (DDP) at the University of Strathclyde was conceived by medicinal chemists to provide a resource that would enhance drug discovery collaborations between chemists and biologists in academia, while addressing the issues of novel chemical space and protectable IPR. Initiated in 2007, the DDP compound library was founded on a collection of physical compounds used in academic drug discovery programmes over a period of many years, which had never been adequately catalogued. The compounds are initially used *in silico* for virtual screening and are linked to the originating chemists so that samples are available for physical screening and analogues can be rapidly designed and synthesised in order to understand structure-activity relationships. Hence, you can go quickly from a novel hit to an optimised candidate.

We present an up-to-date principal components analysis (PCA) of the DDP compound library alongside a commercially available hit identification library, commercially available natural products and drugs with registered trade names. Our analysis suggests that the DDP offers a unique and invaluable resource for drug discovery in academia.

MATERIALS AND METHODS

Databases. The DDP compound database (14,800) was sourced from 132 chemists from 30 collaborating Institutions worldwide. The Zinc database of available natural products [1] contains unique compounds from seven commercial vendors, and was compared with the commercial hit library HitFinder [2] and trade name drugs [3].

Analysis. The structures were subjected to 2D standardisation using Scitegic Pipeline Pilot [4] then 184 2D molecular descriptors were calculated using the MOE Suite [5]. The descriptor fields were normalised and variables that were >90% correlated were discarded, the remaining descriptors then used to conduct PCA using SigmaP [6].

RESULTS AND DISCUSSION

An analysis of the core DDP compound library against a commercially available hit identification library, a commercially available natural products library and a subset of drugs with registered trade names has been conducted. Non-correlated molecular descriptors for each compound underwent PCA to highlight the chemical diversity of each library.

Approximately 50% of the variance can be described in two principal components (PC1 and PC2). The HitFinder and trade name drug libraries represent the extremes of chemical diversity, with HitFinder's compounds occupying a Lipinski-like [7] area of small molecules and the drugs with trade names extending to an area of heavier chemical space. It should be noted that whilst the trade name drugs occupy the largest area, the majority of compounds within this library can be found in areas occupied by the other libraries. The DDP academic library occupies a greater area of chemical space than the HitFinder library, with slightly heavier molecules. On both PC1 and PC2, the natural product libraries are the most chemically distinct. This is governed by an increasing number of chiral centres and lipophilicity. Unsurprisingly, the DDP library occupies this area of chemical space too, which reflects the research interests of many of the contributing academic researchers involved with the DDP. Despite the apparent overlap of libraries in the Lipinski-like region, the contents of each library are more than 99% unique and offer equal value for use in a screening campaign.

CONCLUSIONS

We believe the collation of this unique and previously untapped resource will be a valuable resource for the DDP which aims to facilitate the launch of many drug discovery projects. By identifying virtual then real hits from the DDP library we will facilitate the partnership of engaged chemists to the development of biologically active hit molecules identified by biologists.

ACKNOWLEDGMENTS

REFERENCES

[1] http://zinc.docking.org/vendor0/index_meta.shtml

[2] Maybridge HitFinder (version 7) database. September 2007. Maybridge, Trevillet, Tintagel, Cornwall, UK.

[3] Catalyst/World Drug Index Derwent 2005 database. Accelrys, Cambridge, UK.

[4] SciTegic Pipeline Pilot version 7.5.2, Accelrys; Accelrys: San Diego, 2009.

[5] Chemical Computing Group, Molecular Operating Environment, version 2008.10

[6] SigmaP11, Umetrics

[7] Lipinski, C.A. et al. "Experimental and computational approaches to estimate solubility and permeability in drug discovery and development settings" *Advanced Drug Delivery Reviews,* **23** (1997) 3–25

Toxicity modeling of a series of dyes by computational methods

T.Suzuki[1], S. Funar-Timofei[2], W.M.F. Fabian[3]

[1]Natural Science Laboratory, Toyo University, Tokyo, JAPAN.
[2]Institute of Chemistry of the Romanian Academy, Timisoara, Romania.
[3]Institut für Chemie, Karl-Franzens Universität Graz, Graz, Austria.

Abstract – **Dye toxicity, expressed as rat oral LD_{50} values, was correlated with dye descriptors by the multiple linear regression (MLR), artificial neural networks (ANN)s and support vector machines (SVMs). Dye structures were modeled by density functional theory (DFT) calculations, and structural descriptors were derived from the optimised structures. Specific dye structural features which influence the toxicity were derived.**

INTRODUCTION

Synthetic dyes are indispensable to the textile and dyeing industries. The use of dyes, as with most chemicals, can be hazardous. In this paper MLR, SVM and ANN methods, were applied to model dye toxicity and results were compared.

MATERIALS AND METHODS

A series of 30 textile and non-textile dyes of various types (acid, basic, direct, disperse, reactive, solvent and food) was considered, having the rat oral lethal dose (LD_{50}) [RTECS Database, MDL Information Systems, Inc., San Leandro, California U.S.A.] as dependent variable.

The molecular dye structures were built by the ChemOffice package [ChemBio3D Ultra 11.0, CambridgeSoft.Com, Cambridge, MA, U.S.A.] and energetically optimised by molecular mechanics calculations (MM2 force field) and further optimised by DFT calculations (B3LYP/6–31G(d)) using the Gaussian 03 program package [Gaussian 03, Revision B.04, Gaussian Inc., Wallingford CT, 2004]. Several descriptors were calculated from the minimum energy conformations by the various programs [Dragon Professional 5.5/2007, Talete S.R.L., Milano, Italy; by Winmostar v.3.59c, Winmostar by Delphi, Norio Senda; AlogPS 2.1 software, http://www.vcclab.org/lab/alogps/; Gaussian 03].

MLR calculations were performed by STATISTICA [STATISTICA 7.1, Tulsa, StatSoft Inc, OK, USA] and MobyDigs [R. Todeschini, D.Ballabio, V.Consonni, A.Mauri and M.Pavan (2004) MOBYDIGS, Version 1, TALETE srl, Milano, Italy] software. Conventional three-layer ANN with a single output neuron [Sanuk Co. Ltd., Tokyo, Japan] was employed. In SVM calculations, the regression function in the LIBSVM software [1] was used for analysing the correlation between the toxicity and the significant descriptor values.

RESULTS AND DISCUSSION

A training set of 24 compounds was used to develop the MLR model, which was validated by a test set of 5 dyes.

Variable selection was carried out by the genetic algorithm, using the Kubinyi fit criterion as constrained function to be optimised. The following MLR model was obtained:

$$\log LD_{50} = 2.3(\pm 0.06) + 0.12(\pm 0.04)nArNR2 + 0.24(\pm 0.05)nROH - 0.06(\pm 0.01)dipole$$

$N = 24$; $r^2 = 0.767$; $s = 0.167$; $F(3,20) = 21.94$; $q^2_{Loo} = 0.65$; $r^2_{adj} = 0.73$; $q^2_{boot} = 0.56$; $q^2_{ext} = 0.76$; $SDEP = 0.186$

Where nArNR2 is the number of tertiary amines, nROH is the number of hydroxyl groups, and dipole is the dipole moments, respectively

Dyes	MLR		SVM		ANN	
	training	test	training	test	training	test
RMSE	0.187	0.155	0.182	0.238	0.119	0.125

The best set of molecular descriptors included in the above MLR model was used to develop the nonlinear models by ANNs and SVMs. ANNs gave better results in comparison to the MLR model, contrary to the performance of the best SVM model. It might come from the fact that the optimisation of several parameters in SVMs was difficult for this data set.

CONCLUSIONS

Quantitative structure-toxicity relationship models were developed for 30 dyestuffs. Increased polarity, number of tertiary aromatic amines and number of hydroxyl groups of the dye molecules favour higher toxicity.

REFERENCE

[1] C.C. Chang and C. J. Lin, "A Library for Support Vector Machines." Software Available at http://www.csie.ntu.edu.tw/-cjlin/libsvm (2001.

In Silico Screening of Escort Molecules that Complex with Antibiotics

S.S. Rahman, S. Gibbons, M. Zloh

Department of Pharmaceutical and Biological Chemistry, School of Pharmacy, University of London,
29-39 Brunswick Square, London, WC1N 1AX

INTRODUCTION

Multidrug resistance (MDR) to antibiotics is a continuously evolving problem and occurs mainly due to the over-expression of efflux pumps. Efflux pumps are membrane-bound proteins that are involved with the removal of antibiotics from bacterial cells. One mechanism to inhibit these efflux pumps involves preventing the efflux pump activity using a broad range of structurally unrelated molecules that come from various sources (natural products, drugs, synthetic analogues etc) [1]. This mechanism of action occurs via binding of the inhibitor to the hydrophobic regions of the efflux pump in a competitive or non-competitive manner [2] or alternatively, the antibacterial drug might form a complex with an escort molecule which can bypass the efflux pumps responsible for MDR [3, 4]. The current study investigates complex formation between the efflux pump substrate and a small molecule using the *in silico* binding energies as a criteria for screening for suitable escort molecules that might potentiate the activity of antibacterial drugs.

MATERIALS AND METHODS

The online database Super Drug [5] was screened for molecules that contain moieties from known efflux pump inhibitors. Selected drugs from the screening were imported into VegaZZ where a 3000-step energy minimisation of each structure was applied.

The minimised drug molecules were subjected to docking protocols with norfloxacin (NOR) as the target using the GLUE software package. Ten drugs were then chosen to visualise the interactions within the complex, to predict various physical-chemical properties of the complexes and to calculate the molecular lipophilicity potential (MLP) surface using VegaZZ.

Minimum inhibitory concentration (MIC) assays and modulation assays were performed as described previously [3] to determine the antibacterial activity of the ten molecules against *Staphylococcus aureus* SA1199B and to verify whether any of these molecules can potentiate the activity of NOR.

NMR, UV and mass spectrometry were used to examine the presence of complex formation between these ten drugs and NOR.

RESULTS AND DISCUSSION

The Super Drug database [5] was searched for drugs that might potentially complex with NOR and 89 drugs with the highest Tanimoto coefficients were selected as potential escort molecules that might bind to NOR and hence act as modulators *in vitro*. These 89 drugs were subjected to docking studies and it was found that almost all of the molecules exhibited favourable binding energies with NOR (binding energy ≤ -10.0 kcal/mol).

The 3D structures of ten chosen drug-NOR complexes were visually analysed using VegaZZ and it was apparent that all ten exhibited aromatic face-to-face interactions that dominated the shape of the complex. Evaluating various physical-chemical properties of the all complexes suggested that that complexation would enable NOR to pass through the membrane with greater ease and hence result in a greater NOR concentration within the cell.

MIC assays confirmed that chlorpromazine and paroxetine exhibited antibacterial activity. The modulation activity assays established that chlorpromazine and apomorphine both possess weakly potentiating activity as they caused the MIC of NOR to decrease 2–4-fold. The lack of potentiating activity by paroxetine suggests that the modulation activity of chlorpromazine is unlikely to be due to an additive effect, although this cannot be completely ruled out.

The spectroscopy data acquired confirmed interactions between NOR and escort molecules, with apomorphine and chlorpromazine exhibiting the largest presence of complex formation in all spectroscopic studies, suggesting that these can act as escort molecules.

CONCLUSIONS

This study provides evidence of complex formation between efflux pump substrates (NOR) and escort molecules, and suggests that those complexes with good binding energies will exhibit the best potentiating activity and exhibit the greatest interactions.

ACKNOWLEDGMENTS

REFERENCES

[1] Nelson, M. L., "Modulation of Antibiotic Efflux in Bacteria" Curr. Med. Chem. **1** (2002) 35–54

[2] Ahmed, M., Borsch, C. M., Neyfakh, A. A. and Schuldiner, S., "Mutants of the Bacillus-Subtilis Multidrug Transporter Bmr with Altered Sensitivity to the Antihypertensive Alkaloid Reserpine" *J. Biol. Chem.* **268** (1993) 11086–11089

[3] Smith, E., Williamson, E., Zloh, M. and Gibbons, S., "Isopimaric acid from Pinus nigra shows activity against multidrug-resistant and EMRSA strains of Staphylococcus aureus" *Phytother. Res.* **19** (2005) 538–542.

[4] Zloh, M., Kaatz, G. W. and Gibbons, S., "Inhibitors of multidrug resistance (MDR) have affinity for MDR substrates" *Bioorg. Med. Chem. Lett.* **14** (2004) 881–885.

[5] http://bioinformatics.charite.de/superdrug/

Inhibition of Pseudomonas elastase, LasB, attenuates biofilm formation and increases antimicrobial susceptibility *in vitro*

B.F. Gilmore, G.R. Cathcart, and B. Walker

School of Pharmacy, Queen's University of Belfast, 97 Lisburn Road, Belfast BT9 7BL

INTRODUCTION

Pseudomonas Elastase (LasB) is a metalloprotease virulence factor of *Pseudomonas aeruginosa*, which plays a pivotal role in the infection process. It does so through enzymatic action on host tissues and biomolecules, and by proteolytic activation of a component of the biofilm formation pathway in the bacterial cell. The presence of biofilm is a negative prognostic indicator in pseudomonal infections such as the Cystic Fibrosis lung. The inhibition of LasB has therefore been undertaken as a means to inhibit biofilm formation.

A set of novel inhibitors of LasB have been applied to growing and established pseudomonal biofilms, in order to assess their ability to reduce biofilm formation. This strategy aims to attenuate this virulence mechanism without challenging bacterial cell viability, and hence without a direct selection pressure on the bacteria for the emergence of resistant strains.

MATERIALS AND METHODS

Previously, we have demonstrated that dipeptide N-mercaptoamides are potent inhibitors of lasB [1]. The most potent inhibitor was assayed for its ability to (i) reduce biofilm formation as a result of inhibition of NDK processing and reduced alginate formation (as confirmed by biomass crystal violet assay) and (ii) improving the sensitivity of P. aeruginosa biofilms to conventional antimicrobials.

RESULTS AND DISCUSSION

As shown in Figure 1, LasB inhibitor $HS\text{-}CH_2\text{-}Phe\text{-}Tyr\text{-}(NH_2)$ significantly reduced P. aeruginosa PA01 biofilm formation in vitro. This inhibitor was also shown to prevent the LasB-mediated degradation of its natural substrate NDK. Inhibitors were then used in combination with conventional antibiotics ciprofloxacin (CIP) and gentamicin (GEN), in order to determine whether 48 h biofilms grown in the presence of the inhibitor exhibited increased sensitivity to the antimicrobial challenge compared to control. The inhibitors were not shown to affect *Pseudomonas aeruginosa* viability.
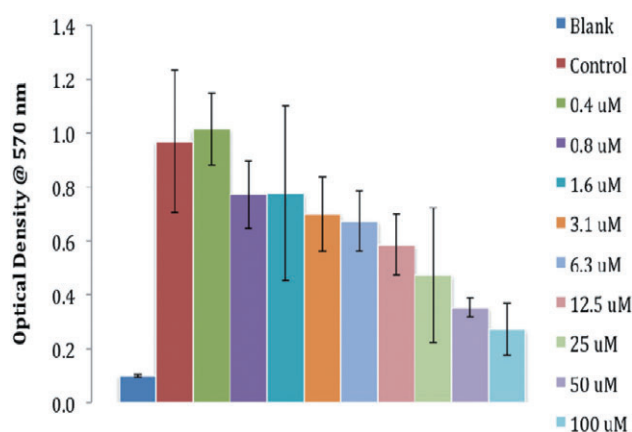

Figure 1. Reduction of *Pseudomonas aeruginosa* PA01 biofilm biomass formation by LasB inhibitor $HS\text{-}CH_2\text{-}CO\text{-}Phe\text{-}Tyr\text{-}(NH_2)$, Ki = 41 nM, after 24 hour challenge, at concentrations up to 100 µM. Biofilm is measured by crystal violet staining. An approximate maximum of 40 % reduction in formation of biofilm biomass is seen when the LasB inhibitor is used at 100 µM.

A checkerboard assay was used to determine suitable concentrations of CIP and GEN to significantly challenge established PA01 biofilms, without causing eradication. 50 µg / ml of each agent was chosen, and was used in combination with a range of concentrations of LasB inhibitor. LasB inhibitors again demonstrate a concentration-dependent effect. The eradication of biofilm is seen when the established biofilm is challenged with the LasB inhibitor at a concentration of 100 µM, in combination with CIP and GEN at the established (sub-eradication) concentrations.

CONCLUSIONS

Microbiological screening confirmed that LasB inhibitors did achieve an anti-biofilm effect against live *Pseudomonas* biofilms. Significant (i.e. greater than 90%) reductions in both viable biofilm cells, and total biofilm biomass were achieved when growing biofilms were challenged. These amounted to between one and four log cycles, or approximately 90–99.99

% overall reduction in viable cells, and approximately 40 % reduction in biomass. A total eradication of the biofilm was not achieved using LasB inhibitors alone. Using sub-eradication concentrations of standard antibiotics in combination with LasB inhibitor resulted in complete biofilm eradication

REFERENCE

[1] G.R. Cathcart, B.F. Gilmore, B. Greer, P. Harriott, B. Walker "Inhibitor profiling of the *Pseudomonas aeruginosa* virulence factor LasB using *N*-alpha mercaptoamide template-based inhibitors" *Bioorg. Med. Chem. Lett*. **19** (2009) 6230–6232

Inhibition of the bacterial metalloprotease, ZapA, a virulence factor of the opportunistic pathogen *Proteus mirabilis*

L. Carson[1], G.R. Cathcart[1], H. Ceri[2], S.P. Gorman[1], B.F. Gilmore[1]

[1]School of Pharmacy, Queen's University of Belfast, 97 Lisburn Road, Belfast BT9 7BL
[2]Department of Biological Sciences, University of Calgary, 2500 University Drive N.W., Calgary, Alberta, Canada T2N

INTRODUCTION

Proteus mirabilis, a Gram-negative opportunistic pathogen, possesses an array of virulence factors contributing to its ability to cause complicated urinary tract infection in patients who are undergoing long-term urethral catheterisation [1].

This study focuses on a specific virulence factor of *P. mirabilis*, the extracellular metalloprotease, ZapA, which has been reported to play a significant role in the establishment of chronic infection [2]. A focused library of 160 *N*-α mercaptoamide dipeptides were screened for inhibitory activity against ZapA, and inhibition kinetics determined. The *in vitro* ability of these inhibitors to preserve the integrity of host immune proteins, specifically Immunoglobulin A (IgA) has also been demonstrated.

MATERIALS AND METHODS

Purification of ZapA – *P. mirabilis* BB2000 was cultured in LB broth (200 ml) for 24 hours. ZapA was purified directly from clarified culture broth by Fast Protein Liquid Chromatography (FPLC) using the ÄktaPrime Plus apparatus with HiTrap PhenylHP column (GE Healthcare).

Inhibitor screening – *N*-α mercaptoamide dipeptide inhibitors, the synthesis of which has been described previously [3], were screened for inhibitory activity against ZapA using a micro-titre based assay with fluorogenic substrate, Aminobenzoyl-Ala-Gly-Leu-Ala-*p*-Nitro-Benzyl-Amide (Peptides International, Louisville, USA).

Degradation of IgA by ZapA – 2 µg of IgA from human colostrum (Sigma Aldrich, Dorset, UK) was denatured at 80°C for 15 minutes, then incubated for one hour at 37°C with 400 ng of ZapA in assay buffer (50 mM Tris HCl, 2 mM CaCl$_2$, pH 8.0), with and without the presence of inhibitor. To assess the extent of IgA digestion, SDS-PAGE with Coomassie blue staining was employed.

RESULTS AND DISCUSSION

A number of *N*-α mercaptoamide dipeptides have been identified as effective inhibitors of ZapA, showing K$_i$ values in the
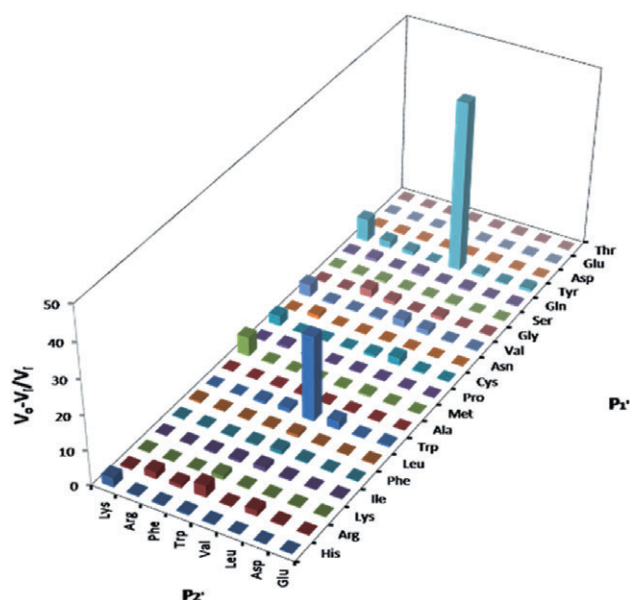

Fig. 1. Relative potency of *N*-α mercaptoamide dipeptide sequences as inhibitors of ZapA. Data is displayed as the fractional inhibition.

low micromolar range. SH-CO-CH$_2$-Y-V-NH$_2$ proved to be the most potent sequence with a K$_i$ value of 0.75 µM. The determinant of inhibitor potency appears to be the presence of Tyrosine (Y) or Tryptophan (W) in the P$_1$' position, suggesting that while the S$_1$' binding pocket of the active site will accommodate large aromatic residues, the ability of this residue to form hydrogen bonds with the active site is important for efficient binding.

The potential of inhibitor to preserve biological substrates, specifically IgA, against degradation by ZapA was displayed. SH-CH$_2$-CO-Y-V-NH$_2$ has conferred protection to IgA, preventing digestion by ZapA, with little or no degradation evident through SDS-PAGE analysis. Conversely, IgA has been extensively digested by uninhibited ZapA (Fig. 2).
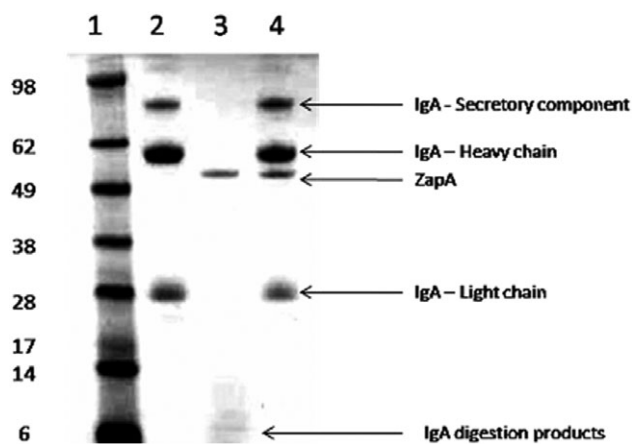
Fig. 2. SDS-PAGE analysis of IgA digestion by ZapA. Lane 1) MW marker. Lane 2) IgA control. Lane 3) IgA with ZapA. Lane 4) IgA with ZapA and SH-CH$_2$-CO-Y-V-NH$_2$ inhibitor.

CONCLUSIONS

Inhibition of bacterial virulence is an antimicrobial strategy which has recently gained momentum, as it is envisaged that non-destructive antimicrobials which attenuate the bacterial pathogen will not exert a strong selection pressure for the emergence of resistant strains [4]. Given that ZapA is an important virulence factor in establishment of chronic infection [2], successful inhibition may prove a novel antimicrobial strategy. Future studies shall further investigate the therapeutic value of ZapA inhibition in *P. mirabilis* infection.

REFERENCES

[1] A. Rozalski, Z. Sidorczyk, K. Kotelko "Potential virulence factors of Proteus bacilli" *Microbiol. Mol. Biol. Rev.* **61** (1997) 65–89

[2] V. Phan, R. Belas, B. F. Gilmore, H. Ceri "ZapA, a Virulence Factor in a Rat Model of *Proteus mirabilis*-Induced Acute and Chronic Prostatitis" *Infect. Immun.* **76** (2008) 4859–4864

[3] G.R. Cathcart, B.F. Gilmore, B. Greer, P. Harriott, B. Walker "Inhibitor profiling of the *Pseudomonas aeruginosa* virulence factor LasB using *N*-alpha mercaptoamide template-based inhibitors" *Bioorg. Med. Chem. Lett.* **19** (2009) 6230–6232

[4] L. Cegelski, G.R. Marshall, G.R. Eldridge, S.J. Hultgren "The biology and future prospects of antivirulence therapies" *Nat. Rev. Microbiol.* **6** (2008) 17–27

Investigating the Biotechnological Potential of Marine Bacteria

A. Busetti, B.F. Gilmore

School of Pharmacy, Queen's University, Belfast, UK.

Abstract **– This study aimed to investigate the caseinolytic, haemolytic, ureolytic, and quorum sensing inhibitory activity of culturable heterotrophic marine bacteria isolated from different samples collected in Irish and Northern Irish Marine coastal waters. A total of 150 strains were isolated and identified phenotypically and 110 strains were selected to be investigated phylogenetically by 16S rRNA gene sequence analysis.**

INTRODUCTION

Microbial symbionts of marine invertebrates have proven to be a rich source of bioactive compounds that can be valuable for biotechnological and pharmaceutical application.

Proteases with caseinolytic activity have been shown to play a role in biofilm formation and in some cases to possess antibiofilm properties [1].

Hemolytic activity is indicative of the production of haemolysins.

Ureolytic activity indicates the production of a urease enzyme capable of hydrolysing urea yielding as end products ammonium carbonate and ammonia.

Bacterial quorum sensing inhibiting compounds can attenuate virulence of pathogenic strains [2] or act as antibiofilm compounds, the leading cause of persistent chronic infections.

The objective of this study was to characterise culturable heterotrophic bacteria associated to various marine organisms and evaluate the potential of isolates to produce metabolites with biotechnological potential.

MATERIALS AND METHODS

150 bacterial isolates were purified based on colony morphology and stored in triplicate at −80°C to form a marine bacterial library. Isolation was performed by plating dilutions of various marine samples collected in the Strangford Lough intertidal zone on different media (LBA, MA) and incubating at 4, 28, 37 and 60°C. 110 isolates were further identified based on 16S rRNA sequence analysis (NCBI BLASTN) following genomic DNA extraction using GenElute™ Bacterial Genomic DNA Kit (Sigma-Aldrich), 16S rRNA (27F and 1492R universal bacterial primers) gene amplification and sequencing (Mwg Operon).

Sequences were aligned and used to construct a Maximum Parsimony phylogenetic tree (1500 bootstrap). Isolates were initially screened for caseinolytic activity by plating on 1% LB skim milk agar and examining for areas of clearing.
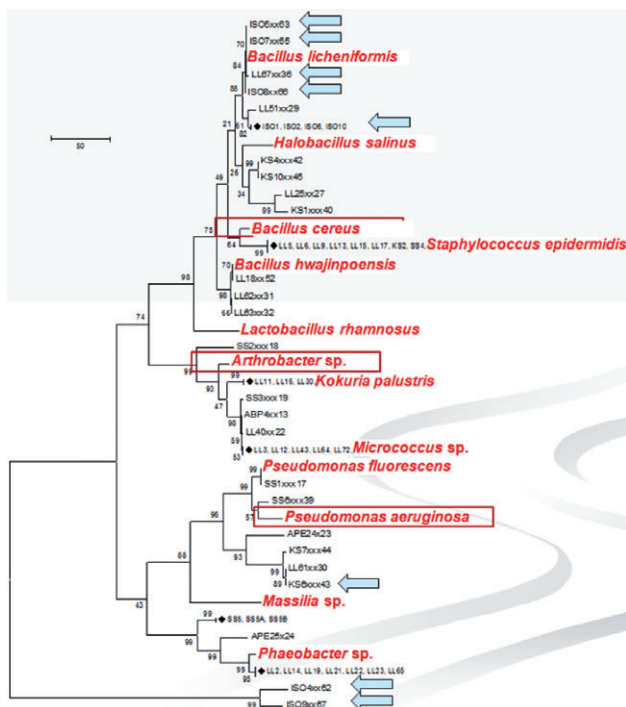
Fig. 1. MP phylogenetic tree of isolates based on 16S rRNA sequence.

Isolates were then screened for hemolytic activity by plating on Blood Agar and examining for α, β, and γ haemolysis. Isolates were screened for ureolytic activity by stabbing cultures in fast urea medium. Isolates were further screened using the overlay method [3], for the inhibition of quorum-sensing regulated pigment production in the indicator strains Chromobacterium violaceum ATCC12472, Serratia marcescens p48 NCIMB11857 and ATCC39006.

RESULTS AND DISCUSSION

A total of 150 isolates were purified from different marine specimens and investigated phenotypically. 110 isolates were characterised phylogenetically. Comparative 16S rRNA gene sequence analysis affiliated the isolates to diverse phylogenetic groups (Fig. 1).

53 isolates were found to degrade casein. 18 isolates showed haemolytic activity. 6 isolates showed strong QSI on indicator strains ATCC12472, ATCC 39006 and p48 NCIMB 11857. 16 strains showed ureolytic activity.

CONCLUSIONS

HPLC fractionation of culture broths followed by MS, ^{1}H NMR, ^{13}C NMR, and GC will be necessary to try and identify and characterise the bioactive molecules and attempt chemical synthesis.

REFERENCES

[1] Marti M, Trotonda MP, Tormo-Mas MA, Vergara-Irigaray M, Cheung AL, et al. Extracellular proteases inhibit protein-dependent biofilm formation in *Staphylococcus aureus*. *Microbes Infect*. 2010;12:55–64.

[2] Hentzer, M., Riedel, K., Rasmussen, T. B. et al. (2002). Inhibition of quorum sensing in *Pseudomonas aeruginosa* biofilm bacteria by a halogenated furanone compound. *Microbiology* **148**, 87–102.

[3] McLean, R.J., Pierson, L.S.,3RD and Fuqua, C., 2004b. A simple screening protocol for the identification of quorum signal antagonists. *Journal of microbiological methods,* **58**(3), pp. 351–360.

Isolation, Identification and Mechanistic Characterisation of Novel Proteases from Marine Bacteria

T. A. White, S. P. Gorman, B. F. Gilmore

School of Pharmacy, Queen's University Belfast, 97 Lisburn Road, Belfast, Northern Ireland, BT9 7BL

Abstract – **This study investigates protease production by marine derived bacteria, in order to develop an understanding of their various roles in pathogenesis and bacterial biofilm formation. By focussing on the inhibition of protease activity it may be possible to prevent and eradicate bacterial biofilms, which are known to be resistant to traditional antibiotics. This study reports on the discovery and identification of an EDTA sensitive, E-64 inhibited, protease produced by a known marine biofilm forming bacteria *Kocuria palustris*.**

INTRODUCTION

Biofilms are estimated to be involved in up to 80% of all chronic human infections, [3] imposing a heavy financial burden on the world health services [1] and significantly increasing patient morbidity and mortality. Previous work has confirmed protease involvement in the establishment of Pseudomonas biofilms and shown that potent inhibitors can significantly reduce biofilm formation. [2] This approach constitutes a novel anti-virulence therapy for bacterial biofilm-mediated infections.

The marine environment is an almost untapped resource in the field of pharmaceutical biotechnology. Pathogenic bacteria, found in both the marine and terrestrial environments, are known to produce proteases, increasing virulence and pathogenesis and in the interruption of innate host defences. Proteases are involved in a staggeringly diverse range of biological processes, including the colonisation step of biofilm formation, tissue damage during infection, interruption of cascade activation pathways, excision of surface cell receptors and inactivation of host protease inhibitors.[4]

METHODS

A broad-spectrum screen of a library of marine-derived bacteria (identified by 16S rRNA sequencing), for caseinolytic activity on skim milk agar was conducted. *K. palustris* showed positive caseinolytic activity, was grown in a pure culture and an extracellular protease was extracted from the supernatant. The protease was preliminary characterised as a cysteine or metalloprotease by conducting an azocasein assay, incorporating specific inhibitors. Purification using HIC, by FPLC, was followed by the determination of molecular weight using SDS-page.

RESULTS AND DISCUSSION

This report describes the characterisation of a novel protease produced by the marine derived bacterium, *K. palustris*. The initial screen, using skim milk agar and an azocasein assay, show that *K. palustris* secrets an EDTA sensitive, E-64 inhibited extracellular protease, with a molecular weight of 22 kDa.

CONCLUSIONS

The implications of this work will lead to a further understanding of the importance of protease production by bacteria. By targeting the proteases responsible for virulence, through the use of protease inhibitors, it may be possible to reduce bacterial resistance to present day antibiotics by interfering with biofilm formation.[2] This may lead to novel therapies for the treatment of bacterial infection, as well as contributing to a significant decrease in patient morbidity and mortality.

REFERENCES

[1] Abdi-Ali A; Mohammadi-Mehr M; Agha Alaei Y. Bactericidal activity of various antibiotics against biofilm-producing *Pseudomonas aeruginosa*, *International Jounral Antimicrobial Agents* 2005; 27.196–200.
[2] Cathcart G. R; Gilmore B. F; Greer B; Harriott P; Walker B. Inhibitor profiling of the *Pseudomonas aeruginosa* virulence factor LasB using *N*-alpha mercaptoamide template-based inhibitors. *Bioorganic and Medicinal Chemirstry Letters*. 2009;19(21), Pages 6230–6232.
[3] Sanclement J.A; Webster P; Thomas J; Ramadan H.H. Bacterial biofilms in surgical specimens of patients with chronic rhinosinusitis. *The Laryngoscope*. 2005;115(4):578–82.
[4] Supuran C.T; Scozzafava A; Clare B.W. Bacterial Protease Inhibitors. *Medical Reseach Reviews*. 2002; 22(4).329–372.

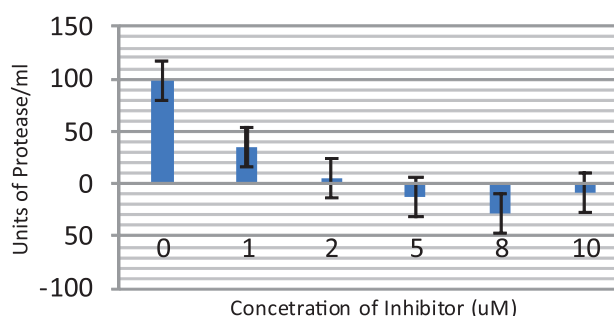**Figure 1.** Caseinolytic activity of *K. palustris* on skim milk agar

Figure 2. The enzymatic degradation of azocasein by *K. palustris* protease, gradually inhibited by increasing concentration of the cysteine protease inhibition E-64.

Marine-derived Bacteria; a Source of Quorum Sensing Inhibitors?

A. Busetti, B.F. Gilmore

School of Pharmacy, Queen's University, Belfast, UK.

Abstract – **Bacterial quorum sensing (QS), a cell-to-cell communication mechanism, influences the ability to form surface-associated, structured and cooperative consortia known as biofilms. Inhibiting QS represents a new crucial strategy for non-antibacterial antibiofilm therapy. Quorum sensing inhibitory (QSI) compounds isolated from several marine organisms [1] suggest that QSI represents a natural, widespread, "antimicrobial" strategy with significant impact on biofilm formation. 150 marine bacterial isolates were screened for QSI activity using indicator strains *C. violaceum* ATCC 12472, *S. marcescens* ATCC39006 and p48 NCIMB 11857. 6 strains displayed QSI activity in the overlay assays. Crude and extracted fractions of their supernatants are being used to perform biofilm formation assays on *P. aeruginosa* PAO1.**

INTRODUCTION

Microbial Biofilms, adherent structured communities of cells embedded in an EPS matrix, play an important role in bacterial pathogenesis and constitute a common cause of persistent infections [2]. Bacterial quorum sensing (QS) is the cell-to-cell signalling mechanism responsible for the pathogenic expression of genes for virulence factors, gene products required for bacteria-host interactions and regulating the ability to form biofilms. Inhibiting QS is unlikely to constitute a selective pressure for the acquisition of resistance, representing a new crucial strategy for non-antibacterial antibiofilm indwelling medical devices. QSI marine compounds have been shown to degrade AHL signals, compete with QS signals, act as antagonists of or mimic AHLs and affect QS regulators [3]. The aim of this research is to screen marine microorganisms for the production of quorum sensing inhibitors (QSI) and to evaluate their effects on biofilm formation and maturation of the opportunistic human pathogen *P. aeruginsosa* PAO1.

MATERIALS AND METHODS

150 marine bacterial isolates purified from marine samples collected in the Strangford Lough's intertidal zone were stored using the Microbank system at −80°C. 110 isolates were identified based on 16S rRNA sequence analysis following DNA extraction, 16S rRNA gene amplification and sequencing. The 150 isolates were screened for QSI activity using the overlay method [4] (Fig. 1), for the inhibition of quorum-sensing regulated pigment production in the indicator strains *C. violaceum* ATCC 12472, *S. marcescens* p48 NCIMB 11857 and ATCC 39006.

Crude filtered (0.22 μm) supernatants of positive QSI isolates were used in PAO1 biofilm formation crystal violet and MBEC assays.

Fig. 1. *C. violaceum* ATCC 12472 overlay on marine Isolate LL53 showing QSI.

Strains LL67 and KS6 were grown in large 2-L seeded 7 day tray cultures and compounds were extracted using ethyl acetate in the ratio 1:1 (v/v).

RESULTS AND DISCUSSION

6 isolates; KS6, KS8, ISO5, ISO9, LL53 and LL67 showed strong QSI in the overlay assays. Disc diffusion overlay assays with *C. violaceum* ATCC 12472 using the re-suspended LL67 organic extract, identified both an antimicrobial and a QSI effect present in the extract. The organic fraction was separated further using silica column MPLC.

CONCLUSIONS

Ongoing studies using HPLC, ^{1}H NMR, ^{13}C NMR, and Gas chromatography are necessary to identify and characterise the bioactive molecules involved.

REFERENCES

[1] Hentzer, M., Riedel, K., Rasmussen, T.B., Heydorn, A., Andersen, J.B., Parsek, M.R., Rice, S.A., Eberl, L., Molin, S., Hoiby, N., Kjelleberg, S. and Givskov, M., 2002. Inhibition of quorum sensing in Pseudomonas aeruginosa biofilm bacteria by a halogenated

furanone compound. *Microbiology (Reading, England),* **148**(Pt 1), pp. 87–102.

[2] Danese, P.N., 2002. Antibiofilm approaches: prevention of catheter colonisation. *Chemistry & biology,* **9**(8), pp. 873–880.

[3] Dobretsov, Sergey, Teplitski, Max andPaul, Valerie(2009) 'Mini-review: quorum sensing in the marine environment and its relation-ship to biofouling', Biofouling, 25: 5, 413 — 427, First published on: 19 March 2009 (iFirst)

[4] McLean, R.J., Pierson, L.S.,3RD and Fuqua, C., 2004b. A simple screening protocol for the identification of quorum signal antago-nists. *Journal of microbiological methods,* **58**(3), pp. 351–360.

New Vaccines for Infectious Diseases

A. Pathak[1], P. Fischer[1] and D.I. Pritchard[1]

[1]School of Pharmacy, University of Nottingham, Nottingham, UK.

Abstract **– New therapeutic agents are needed to treat *Pseudomonas aeruginosa* infections. Partial inhibition of the quorum sensing system (QSS) has shown to reduce pathogenicity of *Pseudomonas*. This study focuses on complete inhibition of the QSS by designing a vaccine against the quorum sensing signal molecules (QSSM). Synthetic routes have been established to produce the haptens of these QSSM. It is believed that a vaccine can be produced that targets most, if not all, Gram-negative bacteria.**

INTRODUCTION

Treating *Pseudomonas aeruginosa* has become a difficult challenge. With emerging multi-resistant drug strains, new effective therapeutics are needed to curb further resistance and treat this particularly virulent Gram-negative pathogen.

The quorum sensing system (QSS) controls the virulence of *Pseudomonas aeruginosa*. Inhibition of the QSS causes reduced pathogenicity without affecting the bacterial growth [1, 2], effectively minimising resistance.

Vaccines can be designed to inhibit the QSS by targeting the quorum sensing signal molecules (QSSM) of *Pseudomonas aeruginosa* (Figure 1). The QSSM can be derivatised (Figure 2) and haptenated to immunogenic carriers such as bovine serum albumin (BSA) and keyhole limpet haemocyanin (KLH) in order to increase the immunogenic character of these otherwise non-immunogenic molecules.

Haptenated derivatives of **1** have resulted in significant inhibition of the QSS [1, 3–5]. However, without the complete inhibition of the QSS, which has yet to be demonstrated, it is possible that bacteria can adapt and develop compensatory mechanisms.

This study attempts to address this issue by producing haptenised versions of QSSM. It is believed that complete inhibition of the QSS can be achieved by targetting these QSSM.

MATERIALS AND METHODS

The synthesis of **4** followed an adapted method by Kauffman et al [5]. An adapted synthetic route outlined by Hradil et al [6] was used to obtain **5**. Activated *N*-hydroxysuccinimide
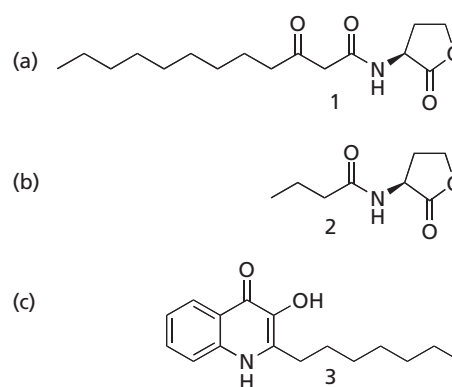

Fig. 1 The QSSM of *Pseudomonas aeruginosa.* a) *N*-3-oxododecanoyl-L-homoserine lactone, (OdDHL, $3OC_{12}$-HSL) b) *N*-butyryl-L-homoserine lactone, (BHL, C_4-HSL) c) 2-heptyl-3-hydroxy-4-quinolone, (*Pseudomonas* Quinolone Signal, PQS)

esters of **4** and **5** were used to haptenise BSA and KLH. Characterisation was performed by MALDI-TOF. Mice were immunised through standard protocols with the KLH conjugates. The polyclonal antibodies (pAB) were characterised using standard ELISA techniques against BSA conjugates.

RESULTS AND DISCUSSION

Synthetic routes have been established for **4** and **5** but need further optimisation. Haptenation resulted in 13 to 18 haptens per BSA carrier protein. The resulting immunisation with the KLH-**4** conjugate led to high titres whilst immunisation with the KLH-**5** conjugate has started. No cross-reaction was seen between pAbs against KLH-**4** and unconjugated BSA (Figure 3).

CONCLUSIONS

The haptens of this study have been carefully chosen in the view of achieving complete inhbition of the QSS. Further tests are needed to analyse the possible inhibitory action of the pAbs raised in this study.
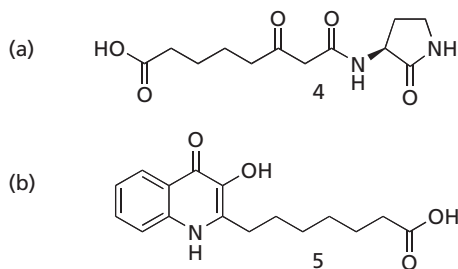
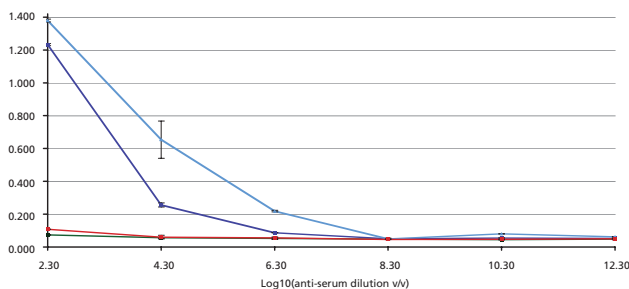Fig. 2 Haptens a) AHL derivative, **4** b) PQS derivative, **5**

Fig. 3. The specificity of the pAbs against BSA-**4** (blue), unconjugated KLH (purple), PBS (red) and unconjugate BSA (green).

It is belived that these haptens will be applicable for other Gram-negative pathogens, and a vaccine can be designed to vaccinate against most, if not all, of the Gram-negative bacteria.

ACKNOWLEDGMENTS

REFERENCES

1. Miyairi, S. 2006. Immunisation with 3-oxododecanoyl-L-homoserine lactone-protein conjugate protects mice from lethal Pseudomonas aeruginosa lung infection. *Journal of Medical Microbiology* 55:1381–1387.
2. Rumbaugh, K. P., J. A. Griswold, and A. N. Hamood. 2000. The role of quorum sensing in the in vivo virulence of Pseudomonas aeruginosa. *Microbes and Infection* 2:1721–1731.
3. De Lamo Marin, S., Y. Xu, M. M. Meijler, and K. D. Janda. 2007. Antibody catalysed hydrolysis of a quorum sensing signal found in Gram-negative bacteria. *Bioorganic and Medicinal Chemistry Letters* 17:1549–1552.
4. Charlton, K., A. Porter, L. Thornthwaite, K. A. Charlton, and A. J. R. Porter. 2006. Preventing biofilm formation by population of bacteria e.g. Bordetella pertussis and Pseudomonas aeruginosa, involves administering antibody to lactone/lactone-derived signal molecule secreted by bacteria. Haptogen Ltd.
5. Kaufmann, G. F., R. Sartorio, S. H. Lee, J. M. Mee, L. J. Altobell, D. P. Kujawa, E. Jeffries, B. Clapham, M. M. Meijler, and K. D. Janda. 2006. Antibody interference with N-acyl homoserine lactone-mediated bacterial quorum sensing. *Journal of the American Chemical Society* 128:2802–2803.
6. Hradil, P., M. Grepl, J. Hlavac, and A. Lycka. 2007. The study of cyclisation of N-acylphenacyl anthranilates with ammonium salts under various conditions. *Heterocycles* 71:269–280.

The Role of Functional Amyloid in Bacterial Biofilm Formation and Antimicrobial Susceptibility

Currie, K.W.J., Gorman, S., Walker, B., Gilmore, B.F.

School of Pharmacy, Queen's University, Belfast BT9 7BL

Abstract – **Bacterial resistance to conventional antibiotics is a ubiquitous phenomenon which threatens mankind's long-term ability to fight infectious diseases. Consequently, there is an unprecedented urgency in search for new antibiotics agents and new approaches to fight infections and particularly for combating biofilm-mediated infection which may account for up to 80% of chronic human infections.**

The discovery of functional amyloid adhesion proteins in some bacteria which confer strong affinity for a range of surfaces including host cells makes them an attractive target for anti-biofilm based therapeutics. The *E.coli* strains PHL 818, PHL 1087 and PHL 1137 have been screened for quantitative comparison of aggregative fimbriae production to investigate how this relates to biofilm adhesion.

INTRODUCTION

Targetting bacterial virulence factors represents an alternative approach to the development of new a anti-infective therapeutics that can disarm pathogens and modulate the host-pathogen interaction. Fimbriae are proteinaceous appendages involved in the early stages of adhesion and attachment to surfaces in biofilm formation. As a result, they represent an attractive target for anti-virulence therapeutics.

Recently the existence of fimbriae possessing an 'amyloid like' structure (AF) composed of cross β- pleated sheets has been a subject of interest. These highly aggregated proteins have been shown to be present in Gram negative bacteria such as *E.coli* and *Salmonella* spp. where they play a key role in

biofilm formation and adhesion to a range of host proteins as well as inert surfaces [1].

MATERIALS AND METHODS

Bacterial cultures of PHL 818, PHL 1087 and PHL 1137 were grown in sterile 96 well plates at 28 °C under static conditions in CFA broth for 72 hours. Crystal violet biomass assays were performed to analyse biofilm adhesion in relation to AF expression. Bacteria were screened for AF and cellulose production using CFA agar (10 g casamino acids, 1 g yeast extract, 10 g agar, 10 mg congo red) and calcofluor plates (LBA containing 200 µg/ml of Fluorescent brighter 28).

RESULTS AND DISCUSSION

Aggregative fimbriae production within bacteria confers greater adhesion to polystyrene surfaces. PHL 818 formed biofilms with a higher biomass than those observed for the other strains. PHL 1087 produced a slightly higher biomass than the AF negative strain, PHL 1087. This suggests that AF production within bacteria confers greater adhesion properties, and consequently higher biofilm biomass. In this work, the role of AF in biofilm susceptibility to antimicrobial challenge will also be discussed.

CONCLUSIONS

Aggregative fimbriae are now recognised as playing a key role in biofilm adhesion within a number of bacteria. These fibres not only allow greater adhesion to surfaces, but have been proposed to play a role in immune system evasion and cellular internalisation. However, the presence and characteri-
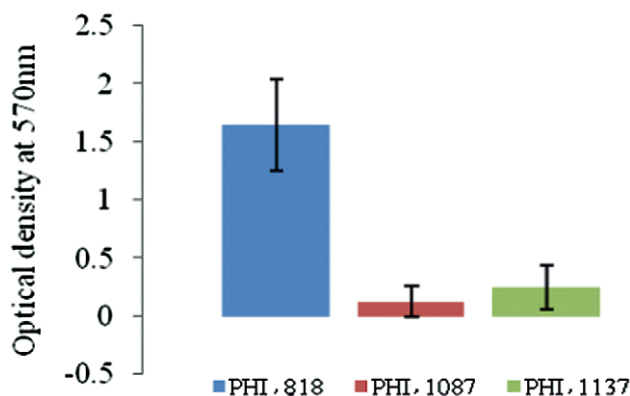

Fig 1: *Biofilm biomass of E.coli strains*
Strains differ in their quantities of AF production. PHL 818 produces vast quantities of AF '++'. PHL 1087 is negative for AF expression '−'. PHL 1137 produces small quantities of AF '+'. PHL 818 versus PHL 1087, $P = < 0.0001$.

sation of AF in other bacteria, particularly Gram positives have yet to be thoroughly explored. Screening of both marine derived and device associated pathogenic bacteria will be carried out using CFA and calcofluor agar, antimicrobial susceptibility profiling and techniques that employ the use of antibodies that are conformationally specific to AF.

REFERENCE

[1] Olsén, A., Wick, M. J., Mörgelin, M., & Björck, L. (1998). Curli, fibrous surface proteins of Escherichia coli, interact with major histocompatibility complex class I molecules. *Infection and immunity*, *66*(3), 944–9.

ZapA, a metalloprotease and virulence factor of *Proteus mirabilis*, disarms Protease Activated Receptors (PARs), altering host innate defences

L. Carson[1], H. Ceri[2], S.P. Gorman[1], and B.F. Gilmore[1]

[1]School of Pharmacy, Queen's University of Belfast, 97 Lisburn Road, Belfast BT9 7BL
[2]Department of Biological Sciences, University of Calgary, 2500 University Drive N.W., Calgary, Alberta, Canada T2N 1N4

INTRODUCTION

ZapA, a bacterial metalloprotease of the Serralysin family and secreted by the opportunistic pathogen *P. mirabilis*, is reported to degrade a number of host immune proteins, including Immunoglobulin A [1], and also play an important role in the establishment of chronic infection [2].

Protease Activated Receptors (PARs) are a unique family of G protein-coupled receptors, activated by the proteolytic cleavage of the receptor *N*-terminus, which in turn acts as a tethered ligand. PARs, of which there are four receptor subtypes (numbered 1 to 4), are commonly activated by regulatory serine proteases such as thrombin (PAR1) and trypsin

(PAR2), and among their wide range of physiological roles they are important mediators of innate immunity. Recently, focus has been placed upon the actions of bacterial proteases at PARs which may represent novel pathogenic mechanisms [3]. This study investigates the activity of ZapA at PARs in order to further understand the mechanism by which this protease exerts virulence.

MATERIALS AND METHODS

Cell culture – The human prostate cell lines RWPE-1 and DU-145 were cultured in Keratinocyte-SFM (supplemented

with bovine pituitary extract and epidermal growth factor), and RPMI 1640 media (supplemented with 10% FCS) respectively.

PAR activation assays – PAR activation was monitored through the measurement of intracellular Ca^{2+} mobilisation using the Fluo-4 Direct™ Calcium Assay Kit (Molecular Probes). RWPE-1 cells were stimulated with trypsin or thrombin (5 U/ml), the synthetic PAR activating peptides (PAR-APs) TFLLR-NH_2 and SLIGRL-NH_2 (100 μM), or ZapA (50 nM), and monitored for response.

Measurement of Interleukin-8 release – DU-145 cells were seeded at 3×10^5 cells/well and cultured until confluence, then starved of serum for 24 hours. Cells were treated with 100 nM ZapA in serum-free media, or media alone for 10 minutes at 37°C. Cells were next incubated with thrombin (1.0 U/ml), TFLLR-NH_2 (200 μM) or serum-free media alone for 18 hours. Cell conditioned media was collected and processed for measurement of IL-8 production by ELISA (R&D Systems, Abingdon, UK).

RESULTS AND DISCUSSION

Results obtained in PAR activation assays indicate that ZapA does not activate PARs, rather disarms them, preventing their subsequent activation by effector proteases (Fig. 1). ZapA, however, did not prevent PAR activation by the synthetic PAR-APs, peptides which mimic the sequence of the PAR tethered ligand. This indicates that while ZapA destroys or removes the N-terminus tethered ligand preventing proteo-lytic activation, the ligand binding domain is preserved, allowing for activation with PAR-APs.

The disarming of PARs by ZapA may play a role in patho-genesis through perturbation of the host immune response. In fact, this study has illustrated the ability of ZapA to inhibit thrombin-induced IL-8 production in vitro (Fig. 2).

CONCLUSIONS

It is well documented in the existing literature that P.mirabilis ZapA possesses the ability to degrade a range of host defence proteins, contributing to the virulence of this pathogen [1]. This study has highlighted a novel mechanism by which P.mirabilis may alter host defence mechanisms through the disarmament of PARs, which in turn may contribute to the pathogenic activities of this organism.

REFERENCES

[1] R. Belas, J. Manos, R. Suvanasuthi "Proteus mirabilis ZapA Metalloprotease Degrades a Broad Spectrum of Substrates, Including Antimicrobial Peptides" Infect. Immun.**72** (2004) 5159–5167
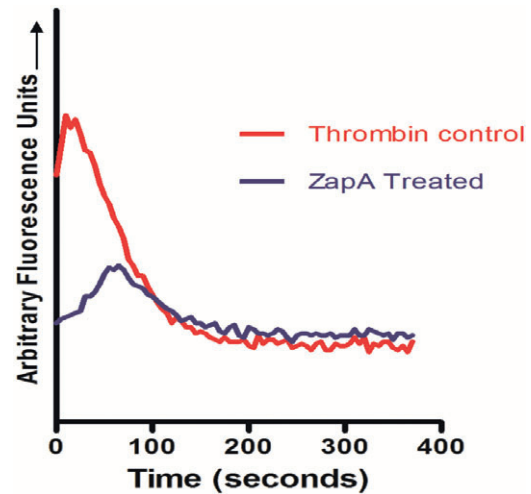

Fig. 1. Intracellular Ca^{2+} mobilisation shows ZapA disarms the PAR1 receptor and prevents normal activation by thrombin. These results are representative of three different experiments.
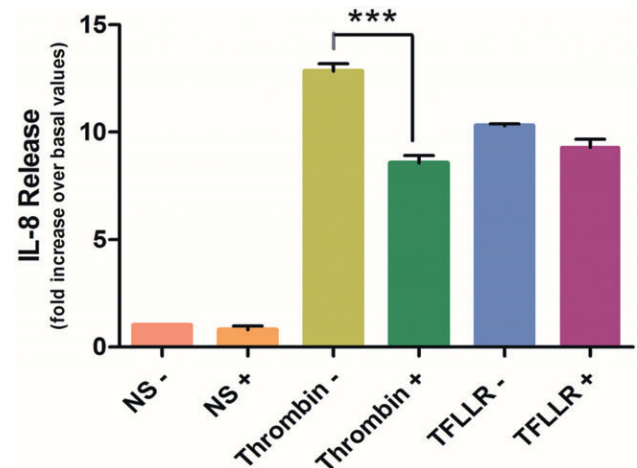

Fig. 2. PAR1-mediated IL-8 production by DU-145 cells following stimulation by thrombin or the PAR-AP, TFLLR. (NS, non-stimulated. +/-indicates ZapA pre-treatment, or non-treatment respectively) Data are means ± SEM of three to six experiments. ***$P > 0.05$

[2] V. Phan, R. Belas, B. F. Gilmore, H. Ceri "ZapA, a Virulence Factor in a Rat Model of Proteus mirabilis-Induced Acute and Chronic Prostatitis" Infect. Immun. **76** (2008) 4859–4864

[3] S. Dulon et. al. "Pseudomonas aeruginosa Elastase Disables Proteinase-Activated Receptor 2 in Respiratory Epithelial Cells" Am. J. Respir. Cell Mol. Biol. **32** (2005) 411–419

A Low-Energy Method for Preparing Stable Nanocrystals of Drug Molecules

Shahzeb Khan[1,2], Marcel de Matas[1] and Jamshed Anwar[1]

[1]Institute of Pharmaceutical Innovation, University of Bradford, Bradford, West Yorkshire, BD7 1DP, UK
[2]Department of Pharmacy, University of Malakand Chakdara, Lower Dir, N.W.F.P, Pakistan
Shahzeb_333@hotmail.com

INTRODUCTION

A major problem affecting the likelihood of a new drug reaching the market is low aqueous solubility. Recent publications suggest that more than 40% of drugs identified through high throughput screening are poorly water soluble (Lipinski, 2002). Amongst various formulation approaches employed to address this key issue, nanoparticles are rapidly becoming a platform solution. In principle, methods for nanoparticle production can be categorised as top down and bottom-up approaches (Liversidge and Cundy, 1995, Rabinow, 2004). The key issues with these methods however include high energy input, long processing times and uncontrolled particle growth. We report here a low energy bottom-up method that has been applied to generate stable nanocrystals with a uniform size distribution for the poorly soluble oral hypoglycemic drug glibenclamide.

MATERIALS AND METHODS

Nanocrystals were fabricated by infusing 2.7 ml of stabiliser solution comprising (1% w/v) of HPMC (15 cp) and PVP K-30 into 0.3 ml of 15 mg/ml drug solution in PEG-400. The solution was stirred in a 10 ml vial by a magnetic stirrer at 1200 rpm at a mixing temperature of 25°C. Particle size determination was carried out using dynamic light scattering (DLS) and transmission electron microscopy (TEM). The crystallinity of the processed and un-processed glibenclamide particles was assessed by powder x-ray diffraction (PXRD) and differential scanning calorimetery (DSC). Particle size measurements of a reconstituted suspension prepared from the recovered powder were also undertaken, using DLS. Stability studies of the nanosuspensions were carried out for one month at three different temperatures (4°C, 25°C and 40°C). The dissolution rate of the glibenclamide nanoparticles was compared with established marketed products including 5 mg glibenclamide tablets and 1.5 mg/ml glibenclamide microsuspension.

RESULTS AND DISCUSSION

The low energy nanocrystallisation method produced glibenclamide nanoparticles with average particle size and polydispersity (PI) values of approximately 298 nm and 0.15 respectively (see Figure 1). The initial particle size of glibenclamide determined by scanning electron microscopy was approximately 70 μm (see Figure 1). PXRD and DSC analy-
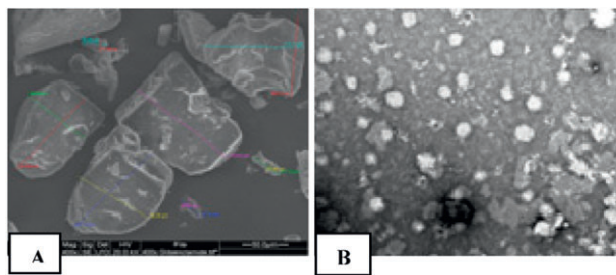

Fig. 1. SEM and TEM images of unprocessed (A) and processed (B) glibenclamide particles.
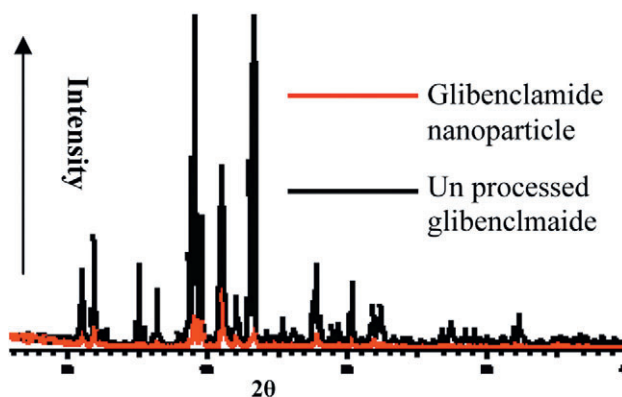

Fig. 2. PXRD patterns for processed and un-processed glibenclamide samples.

sis of the engineered nanoparticles showed that the drug had maintained its crystallinity following nanoprecipitation (see Figure 2). Stability studies showed that the particles were stable at 4°C and room temperature (25°C ± 2.5) compared to the samples stored at 40°C and no noticeable agglomeration had occurred. Average particle size of the reconstituted suspension determined by DLS was below 400 nm. Dissolution studies showed a faster dissolution rate for the nanoparticles compared to the conventional marketed products.

CONCLUSIONS

Low energy nanoprecipitation can yield stable nanocrystals of glibenclamide, eliminating the need for high energy methods and their associated problems. The nanoparticles

generated are stable for one month and yield rapid dissolution rates that are significantly higher than marketed products. The nanoparticles can be dried and reconstituted without marked changes in both particle size and dissolution rate and hence can be employed for fast dissolving solid dosage forms.

REFERENCES

[1] Lipinski, C. (2002) Poor aqueous solubility–an industry wide problem in drug discovery. Am. Pharm. Rev, 5 (3).

[2] Liversidge G. G. and Cundy, K. C. (1995) particle size reduction for improvement of oral bioavailability of hydrophobic drugs. International Journal of Pharmaceutics, 125 (1), 91–97.

[3] Rabinow, B.E. (2004) Nanosuspension in drug delivery. Nature reviews Drug Discovery, 3 (9), 785–796

A Novel Formulation for Oral Delivery of Probiotics

K.T. Mahbubani[a], A.D. Edwards[a,b], N.K.H. Slater[a]

[a]Department of Chemical Engineering and Biotechnology, University of Cambridge, U.K.
[b]Current address: Reading School of Pharmacy, Whiteknights, PO Box 224, Reading, UK.

Abstract **– Our focus is on the delivery of live probiotic bacteria to the intestine. There is a gauntlet of traps in the digestive system that need to be overcome for effective delivery of these beneficial bacteria.**

Our hypothesis was that a bile adsorbing resin (BAR) could be used with room temperature stable bacteria preparations to protect it from the deleterious effects of bile. We found up to 38% more live cells were released when BAR was present in the formulation.

INTRODUCTION

Probiotics are non-pathogenic, live microbial supplements that benefit the host through several mechanisms, by forming a natural barrier to pathogenic bacteria by adhering to the intestinal wall and out-competing potentially harmful microbes. However, when they are dried, some strains are highly sensitive to stomach acids and bile acids in the small intestine [1]. This increased sensitivity reduces the effective payload at the delivery site.

Enteric-coated capsules protect the dried bacteria from stomach acids but releases dried cells into varying concentrations of bile acids in the intestine. Through the use of bile adsorbing resin (BAR), there is an opportunity to allow bile tolerance to recover before complete exposure to bile [2].

BAR is a safe orally administered anion-exchange resin which has been used clinically for over 40 years to block intestinal bile re-absorption in order to lower cholesterol levels [3].

MATERIALS AND METHODS

Initial experiments determined the effect of drying on the bile sensitivity of various preparations and strains of probiotic bacteria. One commonly used probiotic strain, *L. casei*, was found to have 8000-fold loss of viable cells in bile compared to the same preparation rehydrated in water for 30 minutes. Capsules of *L. casei* with and without presence of the protective BAR were then tested for live cell release in a series of bile solutions.
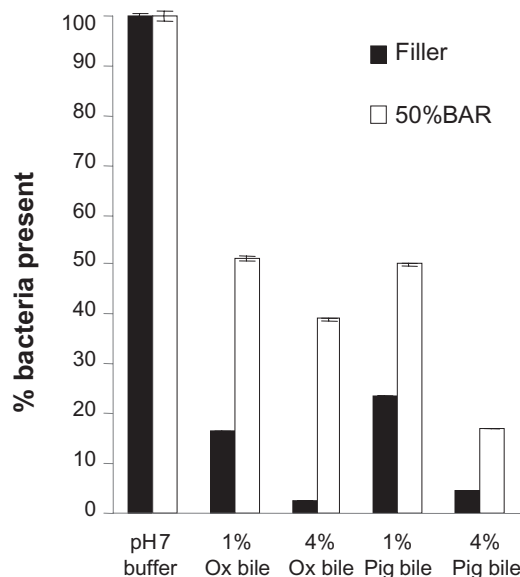

Figure 1. Protective effect of BAR against bile for dried *L. casei*

RESULTS AND DISCUSSION

Control capsules contained a mixture of filler and dried bacteria. The BAR capsules contained a mixture of bacteria along with BAR and filler at a 50:50 ratio. With control capsules, a clear dose response to bile is seen along with a 50-fold reduction in cell survival at high bile concentrations. A clear protection from this toxicity is seen when BAR was added (Figure 1).

CONCLUSIONS

We concluded that there is improved protection of dried probiotic bacteria when exposed to bile acids by simply adding BAR to the powdered dried bacteria.

ACKNOWLEDGEMENTS

REFERENCES

[1] A. D. Edwards and N. K. H. Slater, "Formulation of a live bacterial vaccine for stable room temperature storage results in loss of acid, bile and bile salt resistance" Vaccine, **26** (2008) 5675–5678.

[2] A. D. Edwards and N. K. H. Slater, "Protection of live bacteria from bile acid toxicity using bile acid adsorbing resins" Vaccine **29** (2009) 3897–3903.

[3] K.T. Mahbubani, A.D. Edwards and N.K.H. Slater, "Raising the BAR" TCE, **824** (2010) 28–31.

A Novel Immediate Release Active Film Coat Formulation for use with an Extended Release Gel Matrix Tablet Core

S.T. Charlton, S.J. Nicholson

Bristol-Myers Squibb, Biopharmaceutics R&D, Moreton, CH46 1QW, UK.

INTRODUCTION

The aim was to develop a fixed dose combination (FDC) tablet comprising a low dose of muraglitazar (1.25 mg) combined with a high dose (750 mg) of extended release metformin suitable for once daily dosing to treat type 2 diabetes. An active film coating strategy was selected whereby a film coat containing muraglitazar was applied to Glucophage XR 750 mg tablets; thus overcoming the challenge of combining a low dose drug with the relatively large extended release matrix tablet. To achieve comparable in vivo pharmacokinetic properties, it was required that the drug release profiles for metformin and muraglitazar from the FDC were comparable to the corresponding single entity tablet formulations. This work resulted in the development of a novel formulation comprising of crospovidone within the active film coat to enhance drug release.

Fig. 1. Muraglitazar dissolution profiles. Phosphate buffer pH 6.8; paddles at 50 rpm; n = 6, error bars ± SD.

MATERIALS AND METHODS

Opadry 85F, 00B, 33G, 417/118 and Surelease were supplied by Colorcon. Sodium starch glycolate (Explotab) was supplied by JRS Pharma and crospovidone (Polyplasdone XL) was supplied by ISP. Film coating was performed using an O'Hara Labcoat II-X. Dissolution testing was performed using standard USP apparatus with pH 6.8 phosphate buffer.

RESULTS AND DISCUSSION

Application of an Opadry 85F film coat incorporating muraglitazar 1.25 mg onto Glucophage XR tablets to achieve up to 9% weight gain did not significantly affect metformin dissolution from the ER matrix; however, muraglitazar dissolution was 40% at 30 minutes, which was lower than the target of 80%. The Glucophage XR formulation rapidly hydrates, swells and forms a gel in solution: it was hypothesised that the muraglita-zar was entrapped within the gel matrix, resulting in slower release and dissolution. An insoluble ethylcellulose coat (Surelease®) was utilised to separate the core tablet and the Opadry top coat containing muraglitazar, thereby reducing muraglitazar entrapment within the gel matrix. Applying Surelease to Glucophage XR tablets to achieve a 1% weight gain resulted in a negligible decrease in metformin dissolution and provided increased dissolution of muraglitazar (72% at 30 minutes). A thicker coat of Surelease was found to further increase muraglitazar dissolution at the expense of lower metformin dissolution. Finally, alternative Opadry top coat formulations were investigated, including incorporation of super-disintegrant, to increase the rate of muraglitazar release and dissolution. Only one formulation, Opadry 85F + 0.5% crospovidone, met target requirements (Fig. 1).
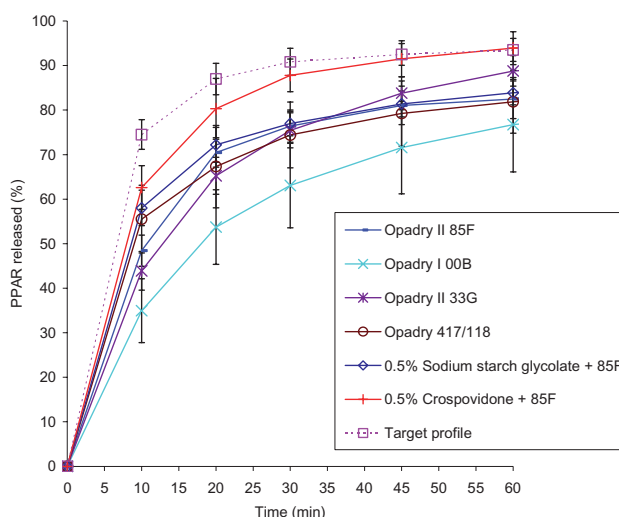
CONCLUSIONS

Formulating a FDC tablet comprising an immediate release active film coat on a gel matrix core is challenging because the film coat may become entrapped by the gel matrix during the hydration process. Use of a semi-permeable coat (Surelease) to separate the outer film coat from the core has been found to improve dissolution of the active coat; however, care must be taken not to diminish drug release from the core.

Furthermore, the novel approach of adding the superdisintegrant, crospovidone, to the active film coat layer has resulted in further enhanced drug release.

ACKNOWLEDGMENTS

A Preliminary Study on a Novel Gastroretentive Drug Delivery System

Ching Sieu Tay[1], Han Wen Ching[2], Colin Melia[2], Wu Lin[1], Peter Scholes[1]

[1]Pharmaceutical Sciences, Quotient Clinical, Nottingham, UK.
[2]Formulation Insights, School of Pharmacy, University of Nottingham, Nottingham, UK.

Abstract – **A novel formulation, with a combination of an expandable core tablet and an elastic film coating, has been designed for gastroretentive applications. Different core tablets were coated with different ratios of Kollicoat® SR30D/IR (KSR/KIR) and characterised by swelling and drug dissolution. Promising results were obtained with croscarmellose sodium based tablets coated with a 7:3 ratio of KSD/KIR.**

INTRODUCTION

For orally administered drugs demonstrating an absorption window in the upper small intestine, a gastroretentive drug delivery system (GRDDS) is required to achieve once daily dosing. Development of such technology has proven challenging with a variety of approaches evaluated to date [1].

An effective expandable GRDDS should ideally swell rapidly and possess sufficient rigidity to withstand the peristalsis and contractility of the stomach [2]. However, fast swelling materials normally cannot maintain the required size and rigidity due to the erosion after swelling. In the current preliminary study, a novel approach was assessed, in which tablets with different swelling agents were prepared in order to achieve rapid size expansion, and KSR was used as an elastic coating polymer to maintain the sufficient mechanical strength of the swollen tablets.

MATERIALS AND METHODS

Matrix core tablets were prepared from mixtures of either 40% sodium bicarbonate (NaHCO3) or croscarmellose sodium (swelling agents), a model drug (caffeine), HPMC K100LV and a lubricant (magnesium stearate). Powder blends were directly compressed into 12 mm × 16 mm oval, biconvex tablets. These cores were coated with aqueous coating solutions containing different ratios of Kollidon KSR/KIR (7:3 and 6:4) in different coat thicknesses (3–8 mg/cm^2).
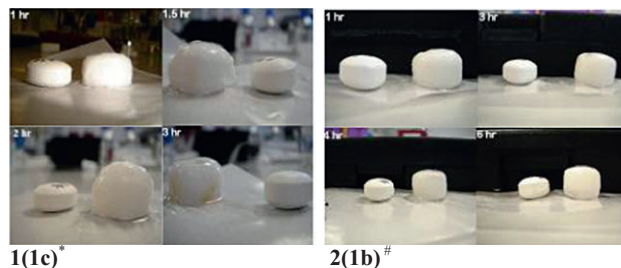

Figure 1. Comparison of tablets pre and post swelling test
* Sodium bicarbonate/KSR : KIR 7 : 3/8.00 mg/cm^2
# Corscarmellose sodium/KSR : KIR 7 : 3/5.77 mg/cm^2

Swelling tests measured the size and weight gain of each tablet as a function of time. Formulations which exhibited potential as a GRDDS were selected for dissolution testing. Dissolution tests were undertaken in USP Apparatus II in 900 mL Simulated Gastric Fluid (SGF) at 50 rpm, 37°C with UV quantification of caffeine at $\lambda = 273$ nm.

RESULTS AND DISCUSSION

Swelling tests showed that both NaHCO3 and croscarmellose based core tablets coated with a 7:3 ratio of KSR/KIR, demonstrated rapid swelling. Tablet sizes increased by 150% and 200% respectively (Figure 1). The weight of these two tablets doubled in 2 hours.

Figure 2 shows the behaviour of the optimal and other typical formulations from this study. All coated tablets with NaHCO3 based cores, ruptured after 2 hours, most likely from being unable to withstand the extensive carbon dioxide gas generation in the presence of SGF. Coated tablets with a croscarmellose sodium based core remained intact for a prolonged time and extended release was observed (Figure 2). Drug release was found to be modulated by the weight of film coating applied.
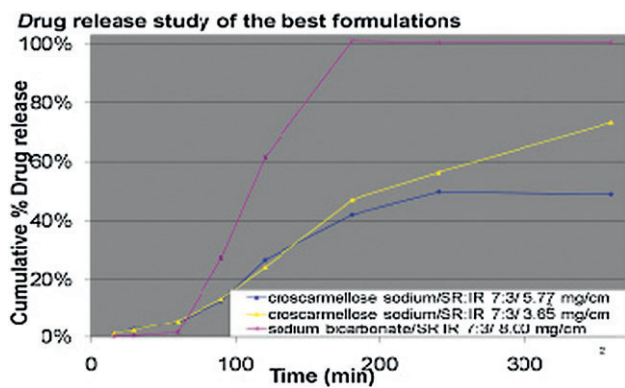
Figure 2. Dissolution profiles of the coated sodium bicarbonate and croscaremellose sodium tablets cores at optional coating levels

CONCLUSIONS

A novel formulation with combination of an expandable core tablet and an elastic film coating has been designed for gastroretentive application. Croscarmellose sodium based core tablets coated with KSD/KIR at 7:3 ratio showed promising results.

REFERENCES

[1] Davis SS (2005) *Drug Discovery Today* 10:249–257
[2] Klausner E, Lavy E, Friedman M & Hoffman A (2003) *J. Control. Release*, 90, 143–162

A simple test to predict and understand the impact of unit operations on powder flow

Bridgeen McCarron[1,2], Barry Crean[2], James Kraunsoe[2], Delroy Brooks[2] and Bindhu Gururajan[2]

[1]Department of Chemical Engineering, Queens University, Belfast, UK.
[2]Pharmaceutical Development, AstraZeneca R&D Charnwood, Loughborough, UK.

Abstract – **The aim of this study was to evaluate particulate flow properties using the novel powder adhesion and cohesion (PAC) classification of particulate flowability during various secondary manufacture processes. It was found that this simple small-scale method could (i) successfully discriminate particulate flowability between products processed by wet granulation, roller compaction or direct compression and (ii) predict the manufacturability of a given product at development and commercial scales.**

INTRODUCTION

A novel powder adhesion and cohesion (PAC) classification for interpretation of particulate flow properties has been developed previously and the practical benefits of this approach have been demonstrated during tablet development [1]. The simple PAC map, where particulate friction ($90-\varphi_w$; φ_w denotes wall friction angle) is plotted against flow function coefficient (FFc), provides an overview of the complex factors that influence particulate flow.

The aim of this study was to apply the PAC approach to measure and evaluate particulate flow properties of various drug products in late stage development and commercialisation which are processed using wet granulation, roller compaction and direct compression.

MATERIALS AND METHODS

Particulate flow properties were measured at various stages of wet granulation, roller compaction and direct compression manufacturing processes using a ring shear tester. The PAC approach was then used to track the flowability of particulates throughout secondary manufacture i.e., from drug substance through to lubricated granules/blends. The processing performance of the particulates was correlated against the PAC map.

RESULTS AND DISCUSSION

A PAC map showing the flow properties of examples of drug products processed by wet granulation, roller compaction or direct compression is shown in Fig. 1. Particulate flowability was discriminated throughout secondary manufacture and between different process types by dividing the PAC map into three regions: particulates are deemed to exhibit poor flow properties when $90-\varphi_w$ is <60° and FFc is <4 (Region 1); particulates exhibit marginal flow properties when $90-\varphi_w$ is 60–70° and FFc is 4–10 (Region 2) and particulates exhibit optimal flow properties when $90-\varphi_w$ is >70° and FFc is >10 (Region 3). Manufacturing experience was in turn correlated to these three regions of the PAC map in terms of flow problems (during storage, transport and charging) and ease of compression to specified quality limits at high speeds. Significant processability issues are prevalent in Region 1, potential manufacturing issues may manifest in Region 2 and minimal issues are present in Region 3.

CONCLUSIONS

A simple small-scale characterisation method has been developed that can predict when a secondary manufacturing
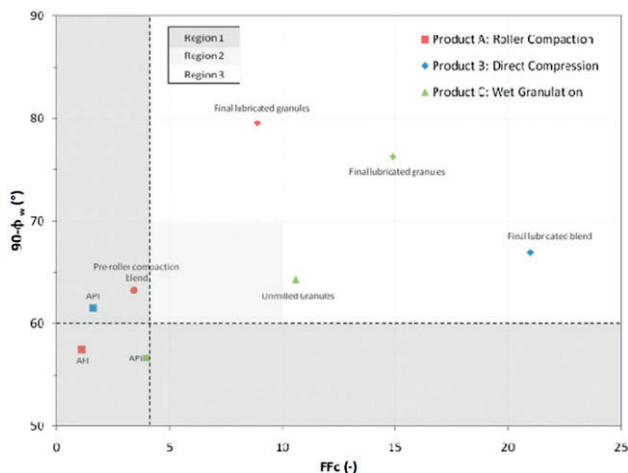
Fig 1. PAC map for particulates processed at various stages of secondary manufacturing processes.

process has been sufficiently optimised to ensure the absence of particulate processability issues.

The PAC map may be applied during late stage development as a powerful tool to understand and predict the impact of various unit operations on particulate flowability and to anticipate any potential particulate processability issues during routine commercial manufacture.

REFERENCE

[1] S. Tagestam, N. Sewell and B. Gururajan, "Powder adhesion & cohesion classification: A new approach to visualise powder flow properties" *World Congress on Particle Technology*, Germany, 2010.

A study of drug-polymer miscibility using dynamic mechanical thermal analysis

M.A. Williams[1], D.S. Jones[1] G.P. Andrews[1]

[1]School of Pharmacy, Queen's University, Belfast, Belfast, UK

ABSTRACT

Due to the high molecular mobility of amorphous drugs, the advantage of this form in terms of improved dissolution rate and hence improved bioavailability is usually eroded over time due to recrystallisation. Techniques which improve the stability of the amorphous forms are being explored as more and more newly developed drugs tend to possess low aqueous solubility. One such technique is the dispersion of the drug in a polymer. The ability of polymers to delay crystallisation has been demonstrated in numerous studies.

Intimate blending of the drug and polymer is necessary for stabilising the amorphous form and therefore they must be miscible. Analytical methods are therefore conducted on small quantities of drug and polymer to determine their miscibility. Differential scanning calorimetry (DSC) is a common technique used to determine miscibility as the presence of one glass transition of intermediate value of the glass transitions of the pure components indicates miscibility. With the advent of the powder pocket for use in the dynamic mechanical thermal analyser (DMTA), it may now be possible to utilise the DMTA in conducting miscibility studies. This will be of importance in cases where the glass transition is not easily detected on the DSC. Glass transitions are more easily detected on the DMTA.

AIMS

(1) To evaluate the usefulness of the dynamic mechanical analyser and the powder pockets for assessing miscibility.

(2) To determine the effect of polymer molecular weight, and hence viscosity on miscibility.

METHODOLOGY

Physical mixtures of drug and polymer were prepared at different drug loadings, with three different molecular weight PVPs. The mixtures as well as pure drug and pure polymer were analysed on a TA Differential Scanning Calorimeter (DSC) and a Tritec 2000 Dynamic Mechanical Analyser (Triton Technology Ltd., Nottinghamshire, UK) with the aid of a metal powder pocket.

RESULTS

The results obtained from the DMTA concurred with that obtained from the DSC. The presence of a single glass transition temperature (Tg) between the Tg value of both components was indicative of a miscible system. This was observed in all drug loadings with PVPK15 and PVPK30. However, higher drug loadings displayed two glass transitions temperatures when mixed with PVPK90.

CONCLUSION

The dynamic mechanical thermal analyzer is useful in the prediction of miscibility of drug and polymer for the manufacture of solid dispersions. Polymer molecular weight is an important factor in drug-polymer miscibility.

A Versatile Approach to Production ff Nano-Particles

Smitha Plakkot[1], Marcel de Matas[2], Peter York[2], B. Sulaiman[3]

[1]Lena Nanoceutics Ltd., Institute of Pharmaceutical Innovation, Bradford, West Yorkshire, BD7 1DP, UK
[2]Institute of Pharmaceutical Innovation, University of Bradford, Bradford, West Yorkshire, BD7 1DP, UK
[3]Dena Technology Ltd, Kastandene, Leeds, West Yorkshire, LS27 0JP, UK.
smitha@lenanano.com

ABSTRACT SUMMARY

The ability to produce nano-particles of medicinal compounds is markedly dependent on material mechanical properties. Particle size reduction of a range of compounds was therefore undertaken using a new comminution technology which resulted in production of crystalline particles with typical size <1 μm for all materials studied. Propensity for size reduction was influenced by the mechanical properties of the starting materials.

INTRODUCTION

The comminution of coarse particles down to sub-micron levels is widespread in industry [1]. This includes methods such as media milling, high pressure homogenisation and micro-fluidisation. Problems associated with these techniques include dealing with materials having extreme mechanical properties such as hard-abrasive substances. Table 1 gives the mechanical property indices of range of compounds.

This study describes the use of a versatile system which is able to reduce effectively the particle size of a range of materials with different mechanical properties down to sub-micron levels.

EXPERIMENTAL METHODS

Nano-particles of the range of compounds in Table 1 were produced by recirculation of suspensions through the DM-100 (Dena Technology Ltd, UK) [2]. This system comprises a size reduction chamber, in which grinding media sit within a narrow gap between a conical rotor and conical polymeric sleeve. The high energy and shear forces associated with impaction of milling media causes size reduction to nano-particulate levels. Compounds were processed at solids loads of 2%w/w to 15%w/w for 60 minutes in aqueous suspension. At-line measurements of particle size were undertaken using dynamic light scattering (DLS). Starting materials and processed samples were characterised by x-ray powder diffraction (XRPD), differential scanning calorimetry (DSC), transmission electron microscopy (TEM) and scanning electron microscopy (SEM).

RESULTS AND DISCUSSION

The results indicate that all compounds were rapidly reduced to sub-micron levels in periods less than 60 minutes. Figure

Table 1. Mechanical property indices of compound

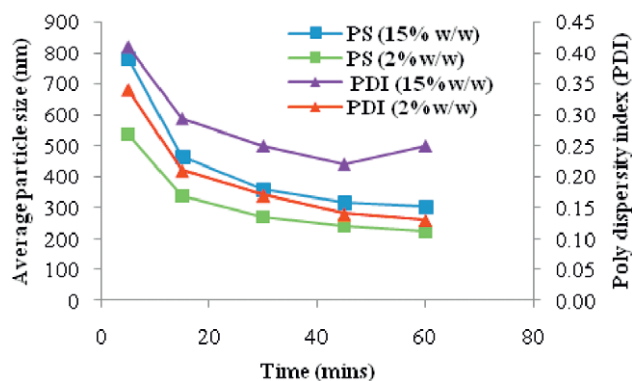| Compounds	Melting point (deg)	Yield stress (MPa)	Hardness (MPa)	Brittleness indices ($\mu m^{-1/2}$)
Asprin	136°	73	87	0.56
Adipic acid	152°	NA	123	0.88
Paracetamol	170°	102	421	3.65
Glibenclamide	172°	NA	NA	NA
Emcompress	Dehydrates at 100°	252	752	NA

Figure 1. Particle Size distribution by Dynamic light Scattering for particle produced after 60 minutes of processing

1 shows the reduction in average particle size (PS) and poly-dispersity index (PDI) versus time for glibenclamide.

Figures 2a and 2b show the respective SEM and TEM images of the particle size of glibenclamide for the raw material and size reduced glibenclamide after comminution.

Some differences in the rate of size reduction were observed between different materials with both hardness and brittleness index having an influence on comminution. XRPD and DSC showed that the crystal form of samples was typically maintained, although some of the samples were subject to reductions in the degree of crystallinity.

CONCLUSION

The studies have shown that sub-micron sized crystalline particles of compounds with a range of mechanical properties can be produced using a new comminution technology.
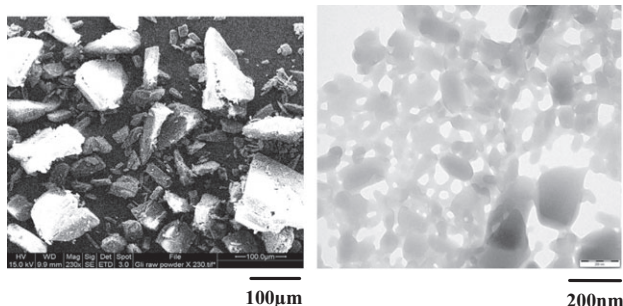
100μm

200nm

Fig. 2a SEM images glibenclamide before comminution   **Fig. 2b** TEM images glibenclamide after comminution

REFERENCES

[1] R. Bawa. NanoBiotech 2008: Exploring global advances in nanomedicine. Nanomedicine: nanotechnology, biology and medicine. 5(1) (2009) 5–7. [2] "The Milling System", Sulaiman, Brian, Patent no.:WO/2007/020407.

An observational study on the sticking propensity of a dicalcium phosphate based roller compaction formulation

E.L. McConnell, M.J. Pollitt

Formulation Development, MSD, Hertford Road, Hoddesdon, UK, EN11 9BU

Abstract **– Punch sticking, and hence tablet picking, can be problematic in producing elegant tablets. Sticking is usually attributed to the API, but here we demonstrate the tendency of a placebo roller compacted dicalcium phosphate based formulation to cause sticking and punch scratching. The results demonstrate there is a balance between the cohesion and adhesion of the material and punches.**

INTRODUCTION

Sticking can occur during tablet compression when a portion of a blend or granulation adheres to tablet tooling surface. Often sticking propensity is not picked up during development due to short runs and low compression speeds. A small scale sticking test was developed by Holstine and colleagues [1]. This qualitative test involves the use of embossed punches and optical imaging. The method is simple, straightforward and has been validated against large-scale manufacturing. An investigational compound demonstrated sticking and hazing at 20 % drug loading using a roller compacted (RC) granule. This was despite the abrasive nature of dicalcium phosphate. In this study we examined the potential of the placebo granule to be implicated in the sticking process.

MATERIALS AND METHODS

A blend was prepared using 60% microcrystalline cellulose (Avicel PH102), 36% dicalcium phosphate anhydrous (A-Tab), 3% sodium croscarmellose (Ac-Di-Sol) and lubricated using 0.5% magnesium stearate. It was roller compacted then split prior to milling. One portion was passed though 2.0 and 1.0 mm Conidur screens (for coarse granules) and the remainder through 1.0 and 0.5 mm screens (fine granules). Each RC lot was then lubricated (0.25% magnesium stearate). For comparison a direct compression (DC) blend was prepared with the same final composition. 250×200 mg

Table 1. Tablet tensile strength at 360 MPa compaction pressure

DC blend	(8.3 ± 0.1) MPa
RC coarse	(3.9 ± 0.6) MPa
RC fine	(7.5 ± 0.1) MPa

tablets were compressed using a Korsch XP-1 tablet press at 360 or 200 MPa. Photographs of the punches were taken under consistent lighting.

RESULTS AND DISCUSSION

The photographs of punches are shown in Figure 1 and tensile strength in Table 1. Sticking can be seen clearly in the lettering. Punch scratching (seen as a hazed surface) was also worse with the coarse granules. No sticking or scratching was observed with a DC blend.

The observation of sticking with the placebo formulation was a surprising result as sticking was anticipated to be mainly a function of the active material. It was expected to see more sticking with the fine granules due to lower lubricant per surface area of granule and the increased surface area interacting with the punch. However, Figure 1 shows more sticking with the coarse RC granules. Given finer granules produced stronger tablets (Table 1), this study is consistent with the adhesion-cohesion balance hypothesis [1]. The extra cohesion from fine granules (as measured by tensile strength) is more significant than the extra adhesion to tablet punches from lower relative lubrication. The direct compression formulation has low sticking propensity because of higher cohesion (Table 1) and possibly higher relative lubrication as all of the magnesium stearate is available rather than being compressed into granules. Furthermore this study demonstrates the abrasiveness of a dicalcium phosphate RC formulation, as observed by hazing / scratching of the tooling. As expected, smaller particles are less abrasive than large ones.
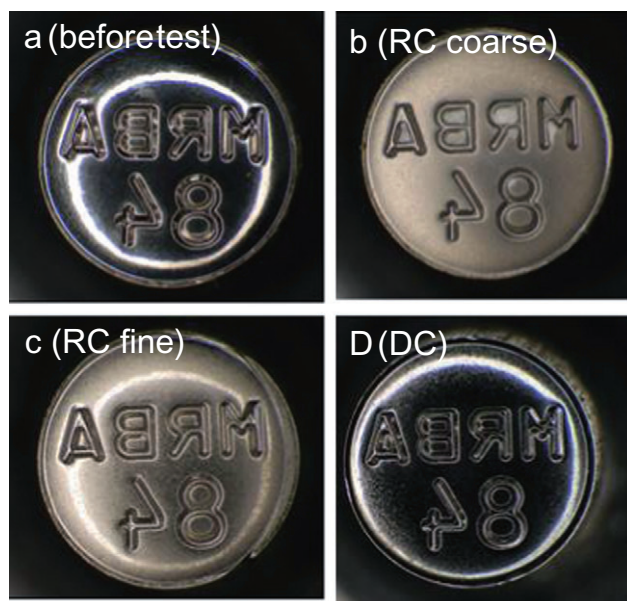
Fig. 1. Images of the tablet punches

CONCLUSIONS

Sticking represents a complex balance between adhesion, cohesion, abrasion and particle size. These results demonstrate the use of an imaging technique to assess sticking propensity, and also highlight that the issue is not as simple as a "sticky" active material; the placebo formulation, when roller compacted, may also demonstrate sticking to the punches and could contribute to the problem.

ACKNOWLEDGMENTS

REFERENCE

[1] Holstine B., Givand J., Smith, E., Sander S., Younan K., Rosen L., Zega J. Small scale evaluation of sticking propensity. The AAPS Journal 2005

Analytical solutions for roll compaction of pharmaceutical powders

James Andrews[1], Shen Yu[1], Bindhu Gururajan[2], Gavin Reynolds[3], Ron Roberts[3], Chuan-Yu Wu[1], Mike Adams[1]

[1]School of Chemical Engineering, University of Birmingham, Edgbaston, Birmingham, B15 2TT
[2]Pharmaceutical Development, AstraZeneca, Charnwood Bakewell Road, Loughborough, LE11 5RH
[3]Pharmaceutical Development, AstraZeneca, Macclesfield, Cheshire, SK10 2NA

Abstract – **Models for roll compaction of dry pharmaceutical powders can optimise production of tablets. Analytical methods provide insight but require significant simplification. The boundary condition at the rolls is largely unknown; an analytical approach has been pursued to investigate the possible effect of the boundary condition. One boundary condition appears to predict experimental results well.**

INTRODUCTION

There is a growing interest in the use of roll compaction in dry granulation within the pharmaceutical industry [1]. Analytical modelling of roll compaction was first derived and solved for small angles around the rolls at closest approach by von Karman [2]. Pharmaceutical powders may contain significant elastic components rather than the assumed rigid plastic component of von Karman's. Shield [3] derived a model for elastic powders in a general setting and observes that for uniaxial compaction the elastic component can often be ignored.

MATERIALS AND METHODS

Two commonly used pharmaceutical excipients: microcrystalline cellulose, MCC (Avicel PH102) and di-calcium phosphate dehydrate, DCPD (Calipharm D) were considered. The flow functions (ff_c) of these powders measured using a ring shear cell indicates that MCC is easy flowing (i.e. $4 < ff_c < 10$) while DCPD is cohesive (i.e. $2 < ff_c < 4$). The powders were roll-compacted using a lab-scale instrumented roll compactor. In this study, the minimum roll gap was fixed at 1.0 mm and a roll speed of 1 rpm. The pressure distributions were recorded with a pressure sensor, from which the maximum compression pressure and nip angle were determined. Comparisons were made with the derived analytical solutions to determine viable boundary conditions.

RESULTS AND DISCUSSION

The von Karman equations are solved analytically for a variety of boundary conditions without the small angle assumption. This enables the appropriate form of the bound-
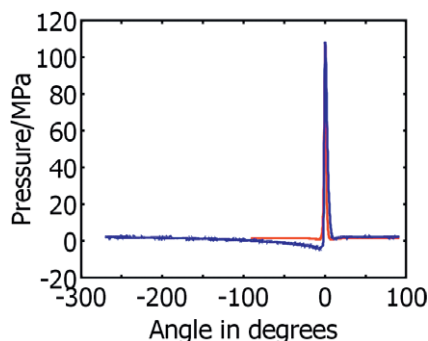
Fig. 1. Comparison of experimental and theoretical results for MCC. Experimental in blue and theoretical in red.
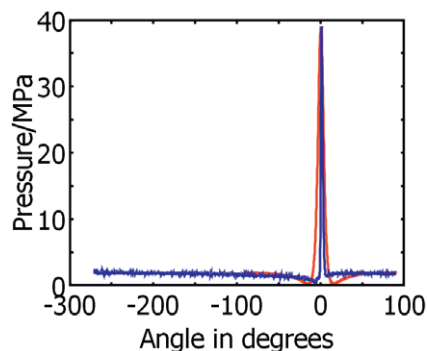

Fig. 2. Comparison of experimental and theoretical results for DCPD. Experimental in blue and theoretical in red.

ary condition to be examined. The only boundary condition which produced sensible model parameters for MCC and DCPD was $F = kW^m$, where F is the frictional force, W is the normal load and m is the power index. Fig. 1 and Fig. 2 compare the theoretical and the experimental over the full range of angles scanned.

CONCLUSIONS

The role of friction in roll compaction between the rolls and a powder has been considered, by solving von Karman's equations for roll compaction. It has been demonstrated that only one mathematical form of the boundary condition can satisfactorily explain the experimental results. The influence this boundary condition has on the nip region and the location of maximum pressure can be determined simply from material properties.

REFERENCES

[1] Y. Funakoshi, T. Asogaw and E. Satake, "Use of novel roller compactor with concave-convex roller pair to obtain uniform compacting pressure," Drug Dev. Ind. Pharm. **3** (1977) 55–573.

[2] Th. von Karman, "On the theory of rolling" Math. Mech., **5** (1925) 139.

[3] A. W. Jenike and R.T. Shield, "On the plastic flow of Coulomb solids beyond original failure," J. Appl. Mech-T ASME, **26** (1959) 599–602.

Assessing the Microbial Stability of Extemporaneously Prepared Oral Liquids – September 2010

H. Pearce[1], C. Newcomb[1], J. Ryan[1], J. Rogers[2], I. Formesyn[2], A. Lee[2]

[1]Pharmaceutical Sciences, Pfizer Pharmatherapeutics, Pfizer Ltd, [2]Pfizer Clinical Research Unit

Abstract **– Extemporaneous preparation (EP) of clinical doses is an option to Phase I dose preparation at Pfizer. In the absence of microbial quality assessment the maximum refrigerated shelf-life that has been assigned to oral EP liquids is 72 hours. This poster outlines the risk assessment and validation work undertaken to support extending the shelf-life to up to 14 days.**

INTRODUCTION

Preparation of doses at the clinical research units (CRU) increases speed, decreases cost and adds flexibility to the design and execution of early clinical trials. The pharmaceutical quality and accuracy of these doses are ensured during development by testing the key quality attributes of the development formulation; identity, potency and purity. In the past the microbial quality of these preparations has not been assessed and as such these preparations have been assigned a conservative maximum cold storage shelf-life of 72 hours. USP <795> provides guidelines for the compounding of non-sterile preparations and states that in the absence of stability information the recommended maximum cold storage shelf-life for water containing preparations should be 14 days [1]. To assess the microbial stability of EP liquids the factors contributing to microbial contamination must be fully recognised. The main sources of contamination are the formulation components [2], the manufacturing process [3, 4] and personnel facilitating the preparation [5]. In order to assess the impact of the above risks a study was conducted at three

CRUs with a formulation and process designed to represent a "worse case scenario" within assigned boundaries. The microbial quality of the test formulation was then assessed to determine its acceptability for oral administration.

MATERIALS AND METHODS

The components of the test formulation were elected by conducting a risk assessment on 29 pharmaceutical excipients, commonly employed in oral liquids, and assigning each a microbial risk based on bioburden and nutrient potential. Of these a suspending agent, wetting agent, solubilising agent, colouring agent and texturising agent categorised as a high microbial risk were chosen for inclusion in the test formulation. The preparation procedure was designed according to set boundaries (such as total preparation time and volume) with multiple manipulations to represent a complex preparation.

The test formulation was prepared in triplicate at three Pfizer CRUs by different personnel, dispensed into two container types, and stored at 2 to 8°C. After 7 and 14 days storage the test formulations were assessed at Wickham laboratories, UK, according to the Harmonised Pharmacopoeial criteria for the microbial quality of non-sterile dosage forms [6].

RESULTS AND DISCUSSION

At all time points (initial, t = 7 and t = 14 days) the microbial content (TAMC and TYMC) of all samples was undetectable (<1 × 10¹ cfu/mL). Therefore all the samples conformed to the Harmonised Pharmacopoeial Criteria after 14 days storage at 2 to 8°C (Table 1).

CONCLUSIONS

The successful outcome of this study demonstrates that EP solutions and suspensions, which remain within the boundaries of this study design, can be prepared on three different continents and stored in either standard dosing container type, for up to 14 days at 2 to 8°C, and will possess a microbial quality appropriate for oral administration. This study there-

Table 1: Compliance of the test formulations, prepared at three Pfizer CRUs, with the Harmonised Pharmacopoeial Criteria after a period of storage at 2 to 8°C

Location of CRU	Container type	Compliance with Pharmacopoeial Criteria		
		initial	7 days	14 days
US	Dosing Bottles (n = 3)	✓	✓	✓
	Oral syringes (n = 3)	✓	✓	✓
Singapore	Dosing Bottles (n = 3)	✓	✓	✓
	Oral syringes (n = 3)	✓	✓	✓
Belgium	Dosing Bottles (n = 3)	✓	✓	✓
	Oral syringes (n = 3)	✓	✓	✓

fore supports the extension of the maximum cold storage shelf-life from 72 hours to 14 days.

The principles of this study design can be applied to assess the microbial risk of any extemporaneous process providing the boundaries of the formulation and methodology are well-defined.

REFERENCES

[1] United States Pharmacopoeia, Chapter <795> "Pharmaceutical Compounding – Non sterile Preparations"., USP 32-NF 27, US Pharmacopoeial Convention Rockville, MD, (2009) www.USP.org

[2] M. C. de la Rosa, M. Rosario Medina and C. Vivar "Microbial quality of pharmaceutical raw materials" *Pharmaceutica Acta Helvetiae.,* **70** (1995) 227–232.

[3] A. Clegg and B. F. Perry "Control of microbial contamination during manufacture" *Microbial quality assurance in cosmetics, toiletries and non-sterile pharmaceuticals.* R. M Baird and S. F. Bloomfield. London, Taylor and Francis Ltd (1996) 49–68

[4] F. Negretti "Findings on the microbiological characteristics of pharmaceutical containers" *Bollettino Chimico Farmaceutico.,* **120** (1981) 193–201

[5] S. F. Bloomfield, Chapter 2 "Microbial contamination: spoilage and hazard." *Guide to microbial control in pharmaceuticals.* S. Denyer and R. M. Baird. Chichester, Ellis Horwood Ltd (1990) 29–52

[6] European Pharmacopeia, Chapter 5.1.4 "Microbiological Quality of Pharmaceutical Preparations: B: Harmonised method" EP 6.1, Strasbourg: Directorate for the Quality of Medicines, Council of Europe (2008) 529–530

Assessment of sub-dividable, extemporaneously prepared suspensions to support early phase clinical trials

P. Lumley-Wood[1], H. Pearce[1], C. Newcomb[1], J. Porreca[1], S. Morgan[2]

[1]Pharmaceutical Sciences, Pfizer Ltd. [2]Global Manufacturing, Pfizer Ltd.

Abstract **– Optimising the rapid and flexible delivery of clinical doses, Pfizer employ Extemporaneous Preparation (EP) as a standard approach to Phase I dose preparation. This abstract describes the analysis of suspension homogeneity as an example of EP process improvement.**

INTRODUCTION

The EP process delivers a wide variety of formulation types including; solutions (oral, sublingual, intranasal), oral suspensions, creams and gels, powders for inhalation, capsules and tablets (IR and MR).

Preparation of doses at the clinical trials pharmacy offers advantages of increased speed, decreased API demands and added flexibility to the design and execution of early clinical trials. A toolkit combining formulation technologies, Quality by Design[1], the EP process and the appropriate quality systems ensures that Pfizer delivers accurate preparation of individual subject doses of a quality appropriate to the early stage of development. Demonstrating the robustness and reproducibility of the formulation at the design phase assures the quality of both the product and process. A technology transfer to the clinical pharmacy completes the formulation design process.

Key to the success of this process as a platform for early clinical dose supply is an evaluation of the scope of key formulation parameters in a variety of dosage forms. For example, the development of robust criteria for homogeneity assessment and a framework within which to deliver sub-dividable suspensions (described below) has enabled clinical trials pharmacists to increase the speed of dose preparation.

MATERIALS AND METHODS

Statistically coherent acceptance criteria were devised based on USP Content Uniformity criteria[2] with the principle that a suspension is homogenous if there is 90% confidence that 90% of the subdivided doses will be between 85–115% of intent. The model was used to evaluate the test formulations in the experiments described in this abstract.

Sub-dividable suspensions combine API with a pre prepared suspending vehicle, commonly 0.5% (w/v) Methocel and 1.5% (w/v) Avicel RC581. The wetting agent Polysorbate 80 may be added in the range of 0.1 to 1% (v/v). Once the critical mixing parameters were established, 24 APIs were formulated into test suspensions, mixed with either high shear (UltraTurrax®) or low shear (Thinky mixer), then analysed for homogeneity using the newly developed criteria. Particle size, LogD, cLogP, pKa, melting point and true density were documented for each API and a statistical correlation between these parameters and suspension homogeneity was investigated.

RESULTS AND DISCUSSION

Mixing time and suspending agent were found to be influential factors in suspension homogeneity (Table 1) and a recom-

Table 1. Statistical impact of key mixing parameters

Factor Investigated	Range	Statistical impact on homogeneity
Mixing Time	1–5 min	Yes
Vessel Volume	130–250 mL	No
Mixing Volume	10–250 mL	No
Polysorbate 80	0.1%–1.0% v/v	No
Vehicle	Methocel / Avicel RC581	Yes
Pre-Mix	Y / N	No
API Conc	1–100 mg/mL	No

mendation of a minimum of 4 mins mix time was made for future formulations. Both Avicel RC581 and Methocel were taken into further experiments.

No simple relationship was found between API characteristics and suspension homogeneity however 22 out of 24 APIs were formulated into acceptable suspensions for subdivision. 79% of Avicel RC581 formulations met the homogeneity criteria with a 54% success rate in Methocel, thus identifying Avicel RC581 as the suspending agent of choice and delivering confidence that in almost 80% of cases suspension formulations can be prepared as a stock to be sub-divided.

CONCLUSION

Sub-division of suspension formulations significantly increases the capacity of the clinical trials pharmacy to prepare multiple doses in one session. This use of a QbD approach to formulation development has enhanced the design space available enabling a fast response to emerging clinical data utilising standard compounding pharmacy practice in a research environment with the quality oversight appropriate to the stage of development.

REFERENCES

[1] L. X. Yu. "Pharmaceutical Quality by Design: Product and Process Development, Understanding, and Control" *Pharmaceutical Research* **25** (2007) 781–791

[2] United States Pharmacopoeia, Chapter <905> "Uniformity of Dosage Units", USP 30-NF 25, US Pharmacopoeial Cnvention Rockville, MD. www.USP.org

Better aerosolisation performance of salbutamol formulated with lactose crystallised from binary mixtures of ethanol/butanol

A. Nokhodchi[1], M. D. Ticehurst[2], M.A. Mohammad[3,4], M.N. Momin, G.P. Martin[5], W. Kaialy[1]

[1]Medway School of Pharmacy, Universities of Kent and Greenwich, Kent, UK, [2]Pfizer, Sandwich, UK. [3]Department of Pharmacy, University of Damascus, Syria. [4]Faculty of Pharmacy, International University for Science and Technology, Syria, [5]King's College London, Pharmaceutical Sciences Research Group, London

Abstract – **Application of anti-solvent crystallisation resulted in lactose agglomerates and particles with corrugated surfaces. Solid state characterisation showed that commercial lactose was the α polymorph while crystallised lactose samples were mixtures of the α and β forms. All engineered lactose particles showed similar true density and flow properties compared to commercial lactose particles, but lower bulk and tap densities. Formulation blends containing crystallised lactose showed better aerosolisation performance compared to commercial lactose. The highest FPF of 37% was obtained for engineered lactose samples where FPF value for commercial lactose was 19%.**

INTRODUCTION

Dry powder inhalers (DPIs), are often formulated with excipient carrier particles. However, one of the major drawbacks of drug-carrier based formulations is the inadequate detachment of drug from carrier due to high drug-carrier adhesive forces which leads to poor drug deposition efficiency in drug-carrier DPI formulations [1]. There are a few approaches reported in the literature to overcome the poor detachment of drug from carrier [2]. In this research the authors provide an assessment on the effect of using different combinations of binary anti-solvents on the physicochemical properties of lactose and the aerosolisation efficiency of formulation blends containing those lactoses.

MATERIALS AND METHODS

1) *Crystallisation procedure*: Lactose was crystallised from different combinations of anti solvents, ethanol: butanol (80:0, 60:20, 40:40, 20:60, and 0:80 ml) at room temperature. The crystallised lactose particles were filtered and dried for 24 h in an oven at 70 °C.
2) *Micromeritic anlysis*: Particle size, true density, flow, elongation ratio and roundness of all crystallised samples and commercial lactose were determined.
3) *Solid state studies*: Solid state analysis of engineered lactose was investigated using FT-IR and DSC. The surface morphology of the crystals was also investigated using SEM.
4) *Deposition studies*: Deposition studies of all formulation blends were studied using MSLI at an operation flow rate of 92 L/min using Aeroliser device. Emitted dose (ED), recovered dose (RD), fine particle fraction (FPF) and impaction loss was calculated for all formulation blends.
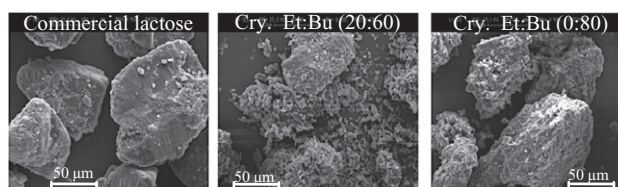

Fig. 1. SEM of various lactose crystals.

Table 1. The results of deposition studies for different formulation blends containing lactose crystallised from ethanol : buthanol

LS[1]	RD (µg)	ED (µg)	Impaction loss (%)	FPF (%)
CL[2]	317 ± 5	299 ± 6	67 ± 4.7	19 ± 2
80 : 0	400 ± 4	380 ± 5	55 ± 6.4	29 ± 5
60 : 20	423 ± 13	408 ± 13	49 ± 3.0	33 ± 3
40 : 40	391 ± 14	377 ± 14	53 ± 4.5	29 ± 3
20 : 60	416 ± 46	292 ± 50	40 ± 4.5	37 ± 1
0 : 80	391 ± 55	372 ± 56	47 ± 0.3	37 ± 0

[1]lactose sample; [2]commercial lactose

RESULTS AND DISCUSSION

The results showed that the morphology and surface properties (roughness) of lactose crystals can easily be modified by changing the ratio of ethanol to butanol (Fig. 1). The result showed that specific surface volume value increased as more butanol was added to the crystallisation medium.

DSC and FT-IR results proved that commercial lactose was α polymorph while crystallised lactose samples were mixtures of α/β form. Although all crystallised lactose samples showed similar true density and flow properties, formulation blends containing engineered lactose showed higher FPF values than commercial product (Table 1). Crystallised lactose formulations also showed lower impaction losses (P < 0.05) compared to commercial lactose formulation blend (Table 1) indicating the better aerosolisation performance. The enhanced aerosolisation performance could be attributed to an easier drug-carrier re-dispersion (detachment) for corrugated crystallised lactose carrier particles and/or the impact of the lactose fines. It was found that the higher the carrier bulk density and carrier tap density the better the DPI aerosolisation performance.

CONCLUSIONS

This study demonstrated that the use of different ratios of binary mixtures of anti-solvents in crystallisation of lactose can be employed as a potential particle engineering technique for preparing crystals with higher roughness, tap and bulk densities which are suitable for pulmonary delivery of salbutamol sulphate.

REFERENCES

[1] M. J Telko, A.J. Hickey. Dry powder inhaler formulation. *Respir. Care* **50** (2005) 1209–1227.

[2] T. Srichana, G.P. Martin, C. Marriott, Dry powder inhalers: The influence of device resistance and powder formulation on drug and lactose deposition in vitro. *Eur. J. Pharm. Sci.* **7** (1998) 73–80.

Colloidal, Relative Toxicity and Biodistribution of Liposome-Intercalated Amphotericin B Prepared from Distigmasterylhemisuccinoyl-glycero-phosphocholine

Maryam Iman[1], Mahmoud R. Jaafari[1], Zhaohua Huang[2], and Francis C. Szoka, Jr.[2]

[1]Nanotechnology Research Center, Biotechnology Research Center, School of Pharmacy, Mashhad University of Medical Sciences, Mashhad, Iran
[2]Departments of Pharmaceutical Chemistry and Biopharmaceutical Sciences, School of Pharmacy, University of California at San Francisco, San Francisco, USA

Abstract **– In this paper, we describe the preparation of 32 different 1, 2-Distigmasterylhemisuccinoyl-sn-glycero-3-phosphocholine (DSHemsPC)-AmB liposome formulations, their colloidal, red blood cell potassium release (RBCPR) properties, maximum tolerated dose (MTD) and biodistribution in BALB/c mice. The results showed that DSHemsPC provides a novel, stable matrix for solubilising and delivering AmB in liposomes.**

INTRODUCTION

The amphotericin B (AmB) is the most effective antibiotic for the treatment of most systemic and visceral fungal infections and leishmaniasis in humans. Its usefulness is limited by acute and chronic toxicities. AmB has been incorporated into various phospholipid and sterol complexes in an attempt to produce dosage forms that retain the pharmacologic spectrum but have an improved safety profile. DSHemsPC is a new lipid in which two molecules of stigmasteryl hemisuccinate (plant sterol) covalently linked to the sn-1 and sn-2 positions of glycerophosphocholin [1]. DSHemsPC provides liposomes with a greater stability in biological fluids because stigmasterol in DSHemsPC does not transfer from the liposome into lipoproteins and biomembranes. Since AmB interacts with sterols, we postulated that DSHemsPC might improve AmB liposome formulations [2].

MATERIALS AND METHODS

DShemsPC-AmB liposomes were prepared by thin lipid film hydration followed by sonication. In this study we examined the relative toxicity of these formulations as measured by RBCPR in order to determine the intrinsic toxicity of the formulation itself. Healthy female BALB/c mice were injected i.v. with the DSHemsPC-AmB formulations diluted in 5% dextrose. The dose was adjusted for each animal on the basis of body weight. Serum and tissue distribution of DSHemsPC-AmB formulations were determined after i.v. injection at 10 mg/kg AmB in 5% dextrose. Blood was collected from the mice 1 h, 6 h, and 12 h after dosing. After 24 h, the mice were sacrificed, the blood sample was removed via heart puncture and the kidneys, heart, liver, spleen, and lungs were removed, weighed, homogenised and extracted by a methanolic solution. AmB concentration was then determined using an HPLC method.

RESULTS AND DISCUSSION

Most of the DSHemsPC-AmB formulations had a particle size of around 100 nm. The RBCPR has an indirect relationship with AmB toxicity. The IC50 for RBCPR for some formulations was more than 100 µg/ml which is comparable with commercial liposomal AmB (AmBisome™). Based on vesicle characteristics and IC50, some formulations were chosen for the determination of MTD in mice. All the DSHemsPC-AmB formulations were clearly less toxic than Fungizone™. MTD of most of the formulations was less than 10 mg/kg, for two formulations was 20 mg/kg and one 60 mg/kg. The formulation which had MTD of 60 mg/kg had very good colloidal properties, and low IC50 for RBCPR was chosen for biodistribution study. The results showed that the concentration of AmB in different tissues for AmBisome™ and DSHemsPC-AmB were comparable.

CONCLUSIONS

In summary, DSHemsPC provides a novel, stable matrix for solubilising and delivering AmB in liposomes.

ACKNOWLEDGMENTS

REFERENCES

[1] Huang, Z., and F. C. Szoka, *Sterol-modified phospholipids: cholesterol and phospholipid chimeras with improved biomembrane properties.* J. Am. Chem. Soc, 2008. **130**: p. 15702–15712.

[2] Huang, Z., M.R. Jaafari, and F.C. Szoka, Jr., *Disterolphospholipids: nonexchangeable lipids and their application to liposomal drug delivery.* Angew Chem Int Ed Engl, 2009. **48**(23): p. 4146–9.

Comparative study of freeze-dried disaccharides by dielectric spectroscopy with respect to molecular mobility and stability

I. Ermolina, A. Pandya, G. Smith

School of Pharmacy, De Montfort University, Leicester. LE1 9BH, UK.

INTRODUCTION

Lyophilisation is invariably used to preserve moisture labile drugs over an extended shelf life. A variety of excipients (including disaccharides) are used routinely in lyophilised product formulation, to provide a moisture buffering environment and thereby sustain shelf life. The drug is frequently co-freeze-dried with excipients to produce an amorphous state which is more stable than the liquid form and has much better solubility than the crystalline form. The residual water or water absorbed during storage can significantly affect the chemical stability of drug (e.g. through hydrolysis). Therefore the study of the influence of water on the drug/matrix lyophile remains an important area for understanding the stability of the freeze-dried pharmaceuticals.

In this contribution we present a dielectric spectroscopy study of freeze-dried disaccharides (lactose, trehalose, sucrose and maltose) at various moisture contents. The premise of this study was based on the assumption of the correlation between molecular dynamics of disaccharide and the chemical stability of the drug.

MATERIALS AND METHODS

Lactose, trehalose, sucrose and maltose were individually freeze-dried to moisture contents in the region of 1–7%, and measured using a Solartron 1296/1255 dielectric analyser in the frequency range from 0.1 Hz to 1 MHz and temperature range from −100°C to +80°C. Routinely, ~0.3 g of disaccharide was weighed accurately and placed in a measuring cell, which is the plate capacitor of 25 mm diameter and 1 mm thickness [1].

RESULTS AND DISCUSSION

All four disaccharides revealed two (γ and β) sub-T_g relaxation processes. The faster γ-process (the rotation of the pendant hydroxyl-methyl groups [1]) was singled out for further analysis by fitting the Havrialiak-Negami (HN) function to each spectrum. The temperature dependency of the fit
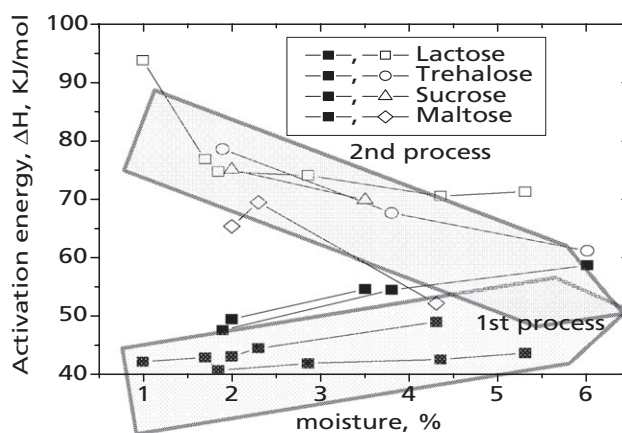

Figure 1. Activation energy of the sub-Tg relaxation processes for four disaccharides.

parameters ($\Delta\varepsilon$, ε_∞, τ) were used to calculate values for the Fröhlich parameter B(T), and activation energy ΔH. Previously [2] we suggested that the temperature dependency of the Fröhlich parameter B(T) is a key parameter to understanding the degree of molecular mobility of the sugar. Here we examine, in further detail, the impact of moisture on the Fröhlich parameter and speculate on the importance of the sub-T_g molecular dynamics to the moisture buffering capacity of these disaccharides.

Moisture content influences the sub-T_g processes exhibited by nearly dry disaccharides (both the relaxation time and activation energy increase with the moisture content for the γ process, but decrease for the β process (Fig. 1) [3]. Analysis of the Fröhlich parameter, B(T), for the γ process was performed at sub-Tg temperatures and the values extrapolated to 20°C (Fig. 2). Three of the four sugars demonstrate an increase in the B(T) parameter with increased moisture content which indicates a generalised increase in degrees of freedom. We expect these degrees of freedom to underpin (to a certain extent) the diffusion rate of the trace amounts of water within the material and thereby define a relative moisture buffering capability of a range of excipients.
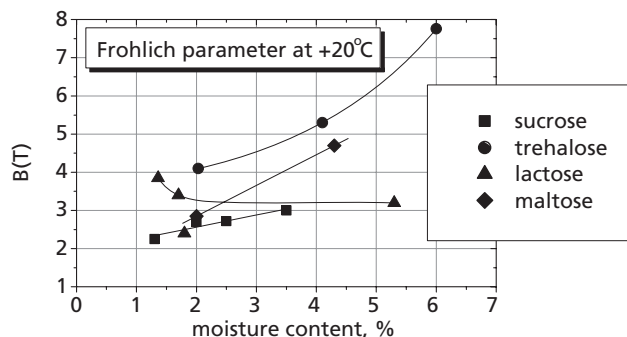
Figure 2. Fröhlich parameter as a function of moisture content.

CONCLUSIONS

This work supports the argument that moisture sensitive drugs will be more stable when freeze-dried with lactose, followed by sucrose/maltose and finally trehalose (with sucrose being more effective than maltose at the higher moisture contents). Further work will include an analysis of correlation between the chemical stability of the active ingredient co-freeze-dried with different disaccharides and the molecular mobility of the excipient.

REFERENCES

[1] I. Ermolina, et al, J. Non-Cryst. Solids, **353** (2007) 4485–4491.
[2] G. Smith, I. Ermolina, J. Pharm Pharmacol, **Suppl. 1**, (2008) A-61.
[3] I. Ermolina, G. Smith, J. Non-Cryst. Solids (2010) submitted.

Controlled Polymerisations for Preparation of Enhanced Protein-Polymer Conjugates

J.P. Magnusson[1], S. Bersani[2], S. Salmaso[2], P. Caliceti[2] and C. Alexander[1]*

[1]School of Pharmacy, University of Nottingham, University Park, Nottingham NG7 2RD, U.K.
[2]Department of Pharmaceutical Sciences, University of Padua – Via F. Marzolo 5, 35131, Padova, Italy

Abstract – **The application of atom transfer radical polymerisation (ATRP) for preparation of a novel class of protein-poly(ethylene glycol) methyl ether methacrylate (PEGMA) bioconjugates is described. The polymerisations were carried out at low temperature in solely aqueous conditions and were easily adoptable to a host of proteins. The effect of the polymerisation on proteins activity and structure were validated by the synthesis of a recombinant human growth hormone (rh-GH) PEGMA hybrid. PEGMA product exhibited properties consistent with the presence of attached hydrophilic polymer chains, namely, high stability to denaturation and proteolysis. In vivo the biological activity of the polymerised hormone was retained, when administered at high doses it surpassed the efficacy of the native protein.**

INTRODUCTION

Proteins are of increasing interest in medicine [1] and the emerging field of bionanotechnology [2]. However, the potential for applying proteins in clinical and technological settings has been limited since they are prone to denaturation and aggregation in vitro [3], while in vivo proteins administered by standard routes exhibit poor pharmacokinetic properties [4]. In efforts to circumvent these problems proteins have been conjugated to polymers, the attachment of poly(ethylene glycol) (PEG) polymers (PEGylation) has been most extensively studied [5] and has already created numerous successful products for the clinic which improve the treatment efficacy and patients compliance [6].

The alternative option to the "grafting on" approach is to grow a polymer from a protein such that no free polymer in solution is formed. The "growing from" approach facilitates the purification of the protein polymer conjugate and offer routes to new materials which can improve its stability and specificity. A system was developed where multiple proteins could be polymerised under very mild generic conditions, the extent of modification could be controlled by varying the linker chemistry and pH of the conjugation.

MATERIALS AND METHODS

Proteins were used as received from Sigma, recombinant human growth hormone (rh-GH) was a kind gift of Bio-Ker srl (Pula, Italy). Synthesises of ATRP initiator was carried from a common tetraethylene(TEG) precursor which was subsequently functionalised with a variety of amine and thiol reactive moieties. Polymerisations of the proteins were carried under solely aqueous conditions at 4°C. Protein polymer conjugates were analysed by SDS-PAGE, SEC and MALDI-TOF. Stability of the hybrids was tested in solution and in the presence of protease.

RESULTS AND DISCUSSION

Polymer created from the surface of the proteins exhibited narrow polydispersity and tuneable polymer architectures.

Modified polymer protein conjugates showed improved stability. rh-GH PEGMA hybrid exhibited enhanced efficacy
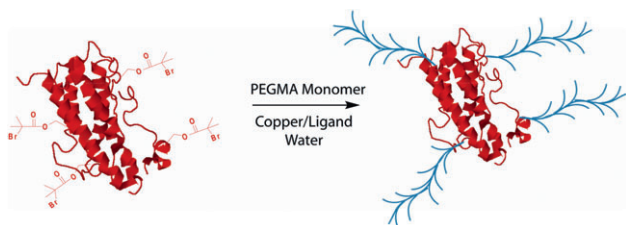
Figure 1. Schematic presentation of protein functionalisation using the growing from approach.

in vivo in comparison to the native protein. Animals receiving the modified protein demonstrated further increase in weight when compared to animals receiving native protein.

CONCLUSIONS

We have demonstrated that "grafting from" polymerisation methodologies can be successfully exploited to produce new protein-polymer bioconjugates with improved stability in vitro and efficacy in vivo. This approach opens new perspectives in optimisation of protein bioconjugates for pharmaceutical applications. The aqueous ATRP polymerisation method offers great versatility for controlling the polymer topology and creates materials with well-defined properties and customisable functionalities which are potential alternatives to "PEGylation" chemistries.

REFERENCES

[1] Pavlou, A. K., and Reichert, J. M. (2004) Recombinant protein therapeutics – success rates, market trends and values to 2010. Nature Biotechnology 22, 1513–1519.

[2] Sarikaya, M., Tamerler, C., Jen, A. K. Y., Schulten, K., and Baneyx, F. (2003) Molecular biomimetics: nanotechnology through biology. Nature Materials 2, 577–585.

[3] Kiefhaber, T., Rudolph, R., Kohler, H.-H., and Buchner, J. (1991) Protein Aggregation in vitro and in vivo: A Quantitative Model of the Kinetic Competition between Folding and Aggregation. Nat Biotech 9, 825–829.

[4] Veronese, F. M., and Pasut, G. (2005) PEGylation, successful approach to drug delivery. Drug Discovery Today 10, 1451–1458.

[5] Webster, R., Didier, E., Harris, P., Siegel, N., Stadler, J., Tilbury, L., and Smith, D. (2007) PEGylated Proteins: Evaluation of Their Safety in the Absence of Definitive Metabolism Studies. Drug Metabolism and Disposition 35, 9–16.

[6] Harris, J. M., and Veronese, F. M. (2003) Peptide and protein pegylation II – clinical evaluation. Advanced Drug Delivery Reviews 55, 1259–1260.

Correlation between erosion and hydrating gel strength

M. Qadir[1], H.N.E. Stevens[1], P. Gellert[2], M. Wikberg[3], F. McInnes[1]

[1]Strathclyde Institute of Pharmacy and Biomedical Sciences, University of Strathclyde, Glasgow, UK, [2]Astra Zeneca R&D Macclesfield, U.K; [3]Astra Zeneca, R&D, Mölndal, Sweden.

INTRODUCTION

An essential characteristic of rate controlling polymers, like hydroxypropylmethyl cellulose (HPMC) is to hydrate quickly and form a cohesive gel layer. A Texture Analyser (TA) method has already been developed to quantify the changing thickness and gel strength with hydration time [1]. The objective of this work was to gravimetrically quantify erosion rates of candidate polymers, and quantify any correlation between rate of erosion and gel strength in order to design a barrier layer formulation for colon targetting which will gradually erode in the small intestine over 3–4 hours.

MATERIALS AND METHODS

Erosion: Tablets were prepared by compressing 200 mg powder of various E and K grades of HPMC (alone or in combination), manually with a 7.9 mm flat faced punch and die (hardness 4–6 kp). Tablets were weighed and immersed in a USP type II dissolution apparatus containing 900 ml of distilled water (100 rpm, $37 \pm 0.5°C$) for 30, 60, 90, 120, 150, 180, 240 and 300 minutes, dried (80°C for 18 hrs) and weighed again to calculate percent polymer eroded using the following equation:

$$\% \text{ Polymer Eroded} = \frac{(\text{Wt}_{\text{initial}} - \text{Wt}_{\text{remaining}}) \times 100}{\text{Wt}_{\text{initial}}}$$

where $\text{Wt}_{\text{initial}}$ is the initial polymer weight and $\text{Wt}_{\text{remaining}}$ is the weight remaining after drying at each time point.

Texture Analysis: A Texture Analyser (TA-XT2) from Stable Micro Systems was used in "measure force in compression" mode, with a Ø 2 mm needle probe. Following exposure to the dissolution conditions described above, the force required to penetrate the hydrating gel layer at a speed of 0.1 mm/sec was recorded, until contact was made with the dry tablet core (detection a 5N force).

RESULTS AND DISCUSSION

The erosion profiles of matrices comprised of different molecular weight HPMC polymers, were linear suggesting that rate controlling mechanism of erosion predominates. A non-linear correlation between the molecular weight of the HPMC E grade polymers and percentage erosion was established, and it was found that higher molecular weight polymers show less erosion and vice versa as shown in Figure 1.

The maximum force at the gel layer diffusion front at 240 minutes, quantified by the TA method was taken as the maximum strength of the hydrated gel layer, and was correlated with percentage erosion, at the same time point. Low viscosity grade polymers show more erosion and have weaker gel strength as shown in Figure 2, however a combination of low and high viscosity grades provided gel strength values of 1.5–2.0N which would be suitable to withstand intestinal mechanical forces of 1.2N [2].

CONCLUSIONS

Correlation between erosion and gel strength was observed, showing that this methodology can be used to quantify polymer performance as a rate controlling barrier layer. A suitable polymer formulation will be selected from this study which will provide a progressively weakening cohesive gel layer with affordability to erode in 3–4 hours in the small intestine.

REFERENCES

[1] M.Qadir, H.N.E. Stevens, P. Gellert, M. Wikberg, F. McInnes. Probing hydrating gel layers using the texture analyser. 36th Annual meeting and exposition of the controlled release society, 379 (2009)

[2] Masaharu Kamba, Yasuo Seta, Akira Kusai and Kenji Nishimura. Comparison of the mechanical destructive force in the small intestine of dog and human. International journal of pharmaceutics,*237,2002, 139–149.*
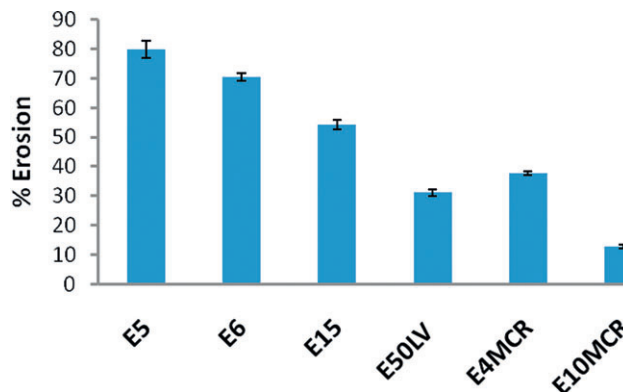
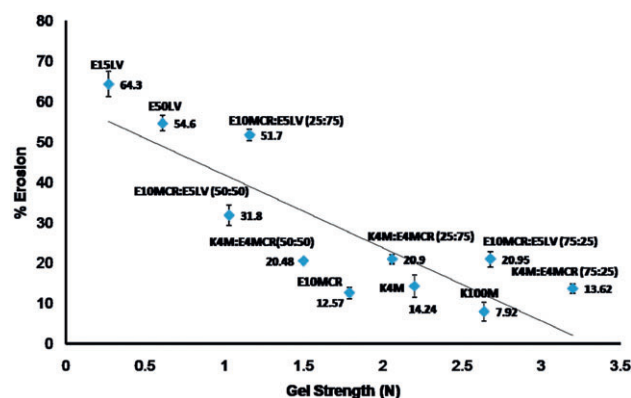**Figure 1:** Percentage erosion versus molecular weight (n = 6).

Figure 2: Correlation between percentage erosion versus gel strength at diffusion front (n = 6).

Crystallisation of APIs from Ionic Liquids

K.B. Smith[2], R.H. Bridson[1], G.A. Leeke[1]

[1]School of Chemical Engineering, University of Birmingham, Edgbaston, B15 2TT, UK.
[2]GlaxoSmithKline, NFSP, Third Avenue, Harlow, CM19 5AW, UK

Abstract **– Ionic liquids (ILs) are exciting new media for crystallisation. Composed entirely of ions the large number of possible combinations of anion and cation present a huge potential for altering functionality. The purpose of this work is to evaluate the largely unexplored application of using ionic liquids to influence crystallisation habits of organic materials. Work to date has focussed on developing methods required to understand the crystallisation mechanisms. Preliminary crystallisation work has shown that the use of ILs to carry out controlled recrystallisations looks promising.**

INTRODUCTION

Unlike conventional solvents ILs are liquids that are composed entirely of ions rather than molecules. Like molten salts they contain at least one cation and one anion; however the term IL is generally used to describe ionic substances that have a melting point below 100°C. The low melting point of ILs is achieved by having an asymmetrical cation which inhibits packing and hence crystallisation.

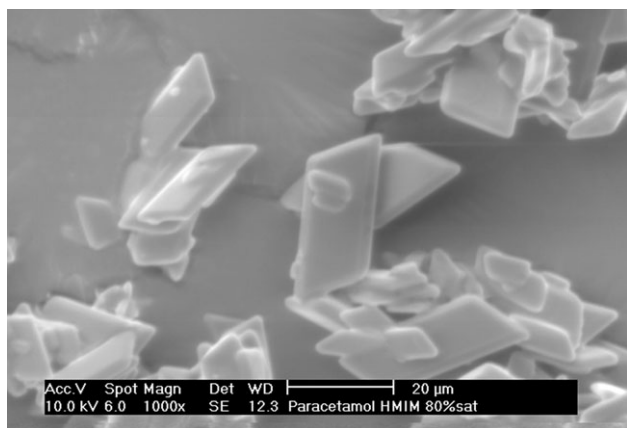It is proposed that ILs offer new opportunities as novel media for processing Active Pharmaceutical Ingredients

Fig. 1. SEM of Paracetamol crystallised from [hmim][PF$_6$]

(APIs), particularly with respect to habit control. It is likely that due to the high functional nature of these materials that they will offer a new route to manipulation of physical form during particle formation and growth. It is this hypothesis which the project aims to test.

The successful development and commercialisation of an API requires adequate processability, stability and bioavailability to be achieved. However APIs with the desired biological activities rarely exhibit adequate physical properties and so it is often necessary to explore ways to manipulate such properties.

Starting first with well characterised ILs and APIs, precipitations and crystallisations have been performed to establish whether the additional molecular functionality of ILs as solvents can be exploited to modify physical form and beyond that whether a rationale can be developed to describe in quali-

tative or quantitative terms the underlying mechanisms for crystal growth.

MATERIALS AND METHODS

Methods have been developed using two of the most common and structurally similar ILs 1-butyl-3-methylimidazolium hexaflourophosphate [bmim][PF$_6$] and 1-hexyl-3-methylimidazolium hexafluorophosphate [hmim][PF$_6$]. The two APIs used in conjunction for these initial studies were ibuprofen and paracetamol.

Methods to determine the solubility of APIs in ILs have been developed and used to determine the solubility profiles of the two APIs in each of the ILs across the temperature range 25°C to 65°C. Combining this data with the metastable zone width for the mixtures will allow the crystallisation of these materials from ILs to be explored.

RESULTS AND DISCUSSION

Initial cooling crystallisation studies have been completed with crystals of paracetamol formed from the two ILs. The precipitation was seen to form well ordered angular shaped crystals.

As ILs exhibit negligible vapour pressure this presents some significant challenges during the crystallisation process, in particular the separation of precipitate from the liquor will need to be carefully considered.

CONCLUSIONS

Initial work has demonstrated that ionic liquids offer an exciting opportunity as a novel media for crystallisation.

Design of experiment to study the effect of spray dryer operating variables on sugar powders intended for inhalation

M.I. Amaro, L. Tajber, O.I. Corrigan, A.M. Healy

School of Pharmacy and Pharmaceutical Sciences, Trinity College Dublin, Dublin 2, Ireland.

INTRODUCTION

Spray drying is a complex process involving multiple variables. Design of experiments (DOE) is a statistical method for identifying important parameters in a process and optimising the parameters with respect to certain specifications [1]. The present study aims to investigate the effect of operating variables of a laboratory spray dryer, in order to optimise the production of sugar powders, intended to be used as carriers of biomolecules for inhalation.

MATERIALS AND METHODS

Raffinose pentahydrate and trehalose dihydrate were purchased from Sigma, Ireland. n-butyl acetate and methanol were obtained from Merck (UK) and Lab Scan (Ireland), respectively. The sugars were spray dried as solutions from 80% methanol/20% n-butyl acetate (v/v) using a Büchi Mini Spray dryer B-290. A 2^4 factorial design was undertaken with repeats for statistical analysis. Process parameters studied were inlet temperature, gas flow rate, pump rate and feed
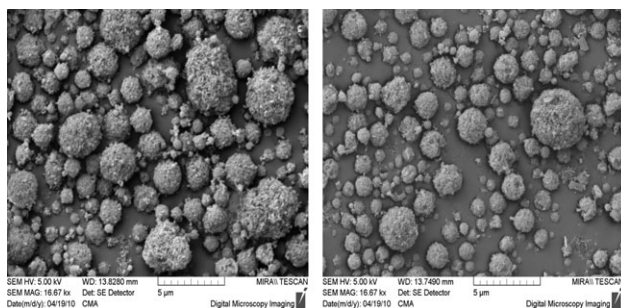
Fig. 1. SEM micrographs of spray dried raffinose (left) and spray dried trehalose (right) (x10 k).

concentration. Resulting powders where characterised in terms of yield, particle size (by laser diffraction), thermogravimetric analysis and specific surface area (by BET gas adsorption). Spray dryer outlet temperature was also examined.

RESULTS AND DISCUSSION

The powder yields of spray dried raffinose and trehalose varied between 33 and 69%. In studies of both materials the yield increased with a decrease in gas flow rate. A direct relation between yield and particle size was observed: as particle size increased, yield also increased.

Spray dried raffinose and trehalose powders were composed of small spherical and porous particles as shown by SEM (Fig. 1). The median particle size for raffinose or trehalose was in the range 1.4–4.2 μm. ANOVA indicated the main effect gas flow rate and feed concentration were the most important. Particle size increased when gas flow rate decreased and feed concentration increased.

The outlet temperature ranged from 48 to 99°C for raffinose and from 48 to 103°C for trehalose, mainly affected by the inlet gas temperature and pump setting, shown to be significant at $p < 0.05$. Residual solvent content ranged from 1.3 to 4.7% for raffinose powders and from 1.0 to 4.5% for trehalose powders.

ANOVA showed that spray drying parameters only affected residual solvent content for trehalose and not raffinose powder.

Specific surface area (SSA) values ranged from 27.61 to 68.61 m²/g for raffinose particles and from 27.21 to 57.75 m²/g for trehalose particles. This response was mainly affected by the gas flow rate in both studies with an increase of SSA observed with a decrease in gas flow rate.

CONCLUSIONS

The DOE conducted revealed that the most significant factors affecting raffinose and trehalose powders are: yield – gas flow and pump setting; particle size and specific surface area – gas flow rate; residual solvent and outlet temperature – inlet temperature.

ACKNOWLEDGMENTS

REFERENCE

[1] M.J. Maltesen et al. Quality by design – spray drying of insulin intended for inhalation. *Eur. J. Pharm. Biopharm.*, 70 (2008), 828–838.

Determination of particle size distribution from refractive index measurement

T.A. Salaoru, G. Nagy, and M. Li

School of Pharmacy, De Montfort University, Leicester, UK.

Abstract **– In this paper a novel method is described to determine the particle size distribution in suspensions by measuring the refractive index at multiple wavelengths.**

INTRODUCTION

The pharmaceutical and fine chemicals industries are strongly concerned with the manufacture of high value-added specialty products, often in solid form. On-line measurement of solid particle size is vital for reliable control of product properties. Many established techniques, such as laser diffraction or spectral extinction, require dilution of the process suspension when measuring from typical manufacturing streams because of their high concentration, such as crystallisation, which can result in changes of both size and form of particles. Light scattering by particles in a suspension can give information such as particle size and shape by causing a change of phase which affects the real component of the suspension's refractive index. Measuring suspension refractive index brings some significant advantages over alternative non-invasive methods of particle characterisation such as spectral extinction or laser diffraction: (1) It has been shown that the relationship between effective refractive index n' and volume fraction v_2 is linear for volumetric concentrations from 0 to 50%; (2) Mie scattering theory is appropriate for calculating

the effective refractive index even of highly concentrated suspensions; (3) Refractive index can be determined from critical angle measurement by total internal reflection so light is not required to pass through the turbid suspension; (4) Suspension effective refractive index is sensitive to the form of the particle size probability distribution. For this purpose a simple device has been designed to measure the refractive index of the suspension at multiple wavelengths and an inversion optimisation method has been developed to obtain particle size information, i.e. mean and standard deviation.

METHOD

The device was designed based on total internal reflection, a consequence of the well-known classical law of reflection and refraction. The measured refractive indexes are used to retrieve the mean and standard deviation of particle size distribution based on Mie's scattering theory [1,2] and iterative optimal search method. In this work the refractive indices at six wavelengths (400, 460, 520, 580, 640 and 700 nm) are used to determine particle size distribution. In the optimisation method, the starting search point is determined by an initial global search. The whole range of expected particle size and standard deviation is divided in 20 by 20 points evenly distributed on a log normal scale and the sum of squares of differences between calculated and measured refractive indices for each wavelength is calculated at each point. Initial values of the particle mean and standard deviation are set as the point with the minimum sum of differences. Variable steps are used for both the particle mean and standard deviation, which are set as the initial values of 3% of the searching ranges of particle mean and standard deviation. The optimisation method starts with increasing the particle mean by its searching step and keeps the standard deviation constant. The particle mean is updated with the new value if the sum of squares of differences decreases. Otherwise the particle mean is decreased by one searching step and is updated with the new value if the sum of squares of differences decreases. And then the same calculation is used to update the particle standard deviation by keeping the particle mean constant. If the differences do not decrease for both cases, the search steps of the particle mean and standard deviation will be reduced by 10% of their initial values and the same process will be repeated until the error is less than a pre-set small constant.

Table 1: The comparison of particle sizes

Original size (um)	Retrieved mean (um)	Retrieved st. dev
0.1	0.199	1.0719
0.3	0.522	1.0680
0.4	0.768	1.0581
0.8	1.297	1.0001
1.1	0.980	1.0181

RESULTS AND DISCUSSION

Experiments have been conducted to validate the proposed method using different standard reference polystyrene samples with diameters of a high accuracy and a small spread in diameter. Table 1 shows some of the comparison results of particle size distributions obtained using the proposed optimisation method. From the results it shows that the retrieved particle sizes are comparable with those originals

CONCLUSIONS

The study has shown that the proposed method using measured refractive indices of a suspension at multiple wavelengths can be used to determine the particle size distribution. More aspects have to be investigated including improving the accuracy of the optimisation method and mathematical modelling of non-spherical anisotropic particles in a suspension.

ACKNOWLEDGMENTS

REFERENCES

[1] Van de Hulst, C. Light scattering by small particles. John Wiley, New York, 1957.

[2] Champion, J.C., Meeten, G. H., and Senior, M., "Refraction by spherical colloid particles", J. Colloid Interface Sci, 72, 471–482, 1979.

Development of a fluidised bed method for assessing fine/coarse particle interactions in inhalation-grade lactose

John Willetts[1*], Phil Robbins[1], Rachel Bridson[1], Michael Bowley[2], Trevor Roche[3],

[1]Centre for Formulation Engineering, School of Chemical Engineering, University of Birmingham, U.K., B15 2TT
[2]GlaxoSmithKline, Global Manufacturing and Supply, Priory Street, Ware, Hertfordshire, U.K. SG12 0DJ
[3]GlaxoSmithKline, Research and Development, Inhaled Product Development, Park Road, Ware, Hertfordshire, U.K. SG12 0DP
* Email: jpw281@bham.ac.uk

INTRODUCTION

While fluidised beds are commonly used in the pharmaceutical industry for applications such as coating, granulation and drying, it is uncommon for them to be used for the deliberate separation of fine particles from coarse particles; indeed, particle elutriation from fluidised beds is often considered a problem. In this work, the elutriation of lactose particles from a classic fluidised bed system has been exploited to explore the behaviour of lactose particles that have been exposed to different high shear blending conditions. While the fluidisation conditions employed do not attempt to mimic those of an inhalatory event, the behaviour of particles under varying fluidisation regimes will provide a fundamental insight into particle-particle interactions and the effects that blending has on these. This abstract describes the fluidised bed system and comparisons between the fluidisation and elutriation behaviour of blended and unblended materials.

MATERIALS AND METHODS

A small-scale vibrational fluidised bed was designed to enable analysis of both unprocessed and high shear blended inhalation grade lactose (approx 20 g). Key design features included apparatus for the humidification of the air stream and for the effective collection of elutriated fines. Control of humidification allowed balance of electrostatic and capillary forces encountered within the fluidised bed [1]. In addition, the apparatus was designed to enable collection of various sized fractions of elutriated material, based on the superficial gas velocity of fluidising air.

Particle characterisation was performed using: dry laser diffraction (Sympatec HELOS/RODOS), wet laser diffraction (Malvern Mastersizer 2000) with propan-2-ol as dispersant [2], water sorption characteristics and BET surface area analysis with octane as the probe molecule [3] (DVS Advantage II, Surface Measurement Systems, UK). In addition, scanning electron microscope (SEM) images of the surface morphology and uniformity of material were obtained. Blending was performed using a high shear blender, as described in previous work. [4], [5].

RESULTS AND DISCUSSION

Both blended and unblended lactose were difficult to fluidise; no measurable differences were seen between the fluidisation curves (*pressure drop vs. flow rate*) of blended and unblended lactose. In addition, there were no statistically significant differences in the mass of material elutriated over a fixed periods of time and flow rates. However, there were measurable and consistent differences between particle size distributions of the elutriated fractions when comparing unblended and blended lactose. This provided information on how blending affected the distribution of different-sized lactose particles.

CONCLUSIONS

A vibrational fluidised bed has been used to assess the bulk behaviour of dry powder inhaler grade lactose, and in assessing DPI performance, the elutriated fraction is likely to be important. Experimentation here has shown that measurement of this elutriated fraction can be related to the effects of high shear blending. This method could prove important in assessing the behaviour of DPI formulations.

ACKNOWLEDGMENTS

REFERENCES

[1] Li, J., and Kato, K. (2001). Effect of electrostatic and capillary forces on the elutriation of fine particles from a fluidized bed. Advanced Powder Technology. 12, 2, 287–205.

[2] Adi, H., Larson, I., Stewart, P. (2007). Laser diffraction particle sizing of cohesive lactose powders. Powder Technology 179, 90–94.

[3] Brunauer, S., Emmett P. H., and Teller, E. (1938). Adsorption of gases in multimolecular layers. Journal of the American Chemical Society. 60, 309.

[4] Bridson, R. H., Robbins, P. T., Chen, Y., Westerman, W., Gillham, C. R., Roche, T. C., Seville, J. P. K. (2007). The effects of high shear blending on α-lactose monohydrate. International Journal of Pharmaceutics. 339, 84–90.

[5] Knight, P. C., Seville, J. P. K., Wellm, A. B., Instone, T. (2001). Prediction of impeller torque in high shear powder mixers. Chemical Engineering Science. 56, 4457–4471.

Development of Gastro-Retentive Systems for the Eradication of H-Pylori Infections in the Treatment of Pepetic Ulcer

A.O. Adebisi, B.R. Conway

School of Life and Health Sciences, Aston University, Birmingham, UK

INTRODUCTION

Helicobacter pylori has been implicated in the aetiology of gastro-duodenal diseases such as acute chronic gastritis, gastric lymphomas and peptic ulcers [1]. Obstacles to the successful eradication of these bacterial infections include: presence of antibiotic resistant bacteria; therapy requiring multiple drugs with complicated dosing schedules and bacterial residence in an environment where high drug concentrations are difficult to achieve [2]. Conventional oral formulations have a short gastric residence time thus limiting the duration of exposure to the bacteria. Gastro-retentive formulations such as floating systems can prolong the residence time of the formulation in the stomach and also maintain a controlled release of drug.

The purpose of this study is to characterise drug-loaded alginate beads and to evaluate drug release in different media.

MATERIALS AND METHODS

Metronidazole, clarithromycin, sodium alginate, calcium chloride and chitosan (low and medium molecular weight) (Sigma UK). Olive oil and Folins- Ciocalteu reagent (Fluka).

The drug-loaded beads were prepared by ionotropic gelation using 3%w/w sodium alginate solution and 1%w/v calcium chloride solution as the gelling medium. Beads were cured for 15 minutes, washed with water; snap frozen in liquid nitrogen and freeze dried. The beads were assessed based on diameter, weight, moisture content, density, floating properties, drug loading and drug entrapment efficiencies. Samples of the beads produced were modified in order to improve their floating characteristics and to modify their release profile by the addition of olive oil and chitosan in the bead structure. Also, drug release profiles and kinetics were studied.

RESULTS AND DISCUSSION

The unmodified drug-loaded beads were larger and heavier than unloaded beads with high entrapment efficiencies at 5% and 10%w/w drug loadings. Diameters ranged from 2–3 mm with densities of 0.92–1.69 g/cm^3. However, the unmodified beads failed the buoyancy tests and released most of the drug within 180 to 240 minutes.

Addition of olive oil in the bead formulation reduced drug loading and release rate of the drug extending release to over 240 minutes (metronidazole). Olive oil concentrations over 5%w/w resulted in 100% buoyancy, while those with less than 5% w/w olive oil failed the buoyancy test.
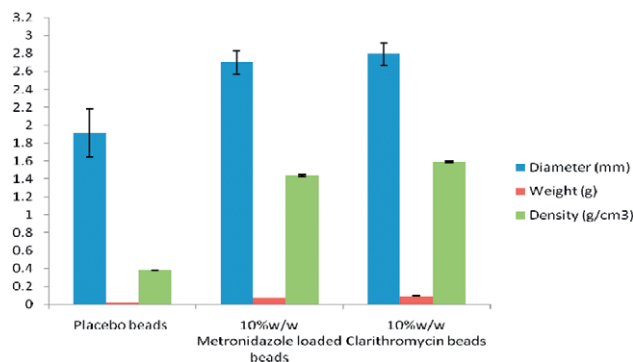

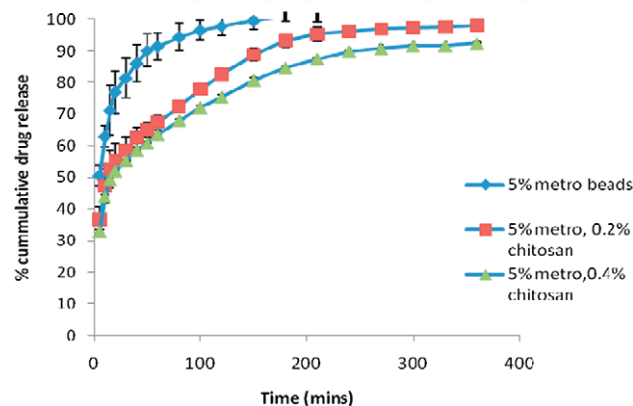Fig 1: Characterisation of calcium alginate beads

Fig 2: Release profile of coated and uncoated metronidazole loaded beads in 0.1 M Hcl (pH 1.2)

Chitosan coatings (0.2%w/w and 0.4%w/w) reduced the drug release rate and increased the duration of drug release to more than 360 minutes for both metronidazole and clarithromycin. Release from the alginate beads in acidic media correlated well with Higuchi kinetics.

CONCLUSIONS

Calcium alginate beads are useful gastro-retentive floating systems with high drug entrapment efficiencies and, with modification of the bead structure, can be useful sustained release delivery systems for antibiotics in the eradication of *Helicobacter pylori*.

REFERENCES

[1] BR Conway, "Drug Delivery Strategies for the Treatment of Helicobacter pylori Infections" *Frontiers in Medicinal Chemistry,* 4 (2009), 463–490

[2] SH Shah and NV Patel, "Gastro retentive floating drug delivery systems with potential herbal drugs for Helicobacter- pylori eradication – a review" *Journal of Chinese Integrative Medicine,* (2009) Oct:7 (10):976–82

Development of solvent free continuous cocrystallisation (SFCC) technique

R.S. Dhumal, A.L. Kelly, A.R. Paradkar

[1]Centre for Pharmaceutical Engineering, University of Bradford, Bradford, UK.

Abstract – **Cocrystallisation is now recognised as an important method to achieve enhanced material properties and is of particular interest in the pharmaceutical field. Cocrystals have already been proven useful in improving the stability, solubility, dissolution rate, bioavailability, and mechanical properties of APIs. Here we report application of hot melt extrusion (HME) for development of novel solvent free continuous cocrystallisation (SFCC) technique with simultaneous agglomeration.**

Figure 1: Scanning electron microphographs of Ibuprofen-Nicotinamide (1:1) co-crystal agglomerates at 1100x and its surface at 1800x

INTRODUCTION

Slow evaporation and grinding are the two most common techniques used to promote cocrystal growth. However, these approaches possess inherent scale-up limitations and are better suited to small scale screening operations [1]. Relatively few reports describe attempts to develop scalable cocrystallisation techniques; these have included the use of supercritical fluid [2] and ultrasound [3]. A more suitable approach is required to make cocrystallisation feasible on a manufacturing scale. We have invented a scalable HME technology to produce pharmaceutical cocrystals [4] using a combination of controlled heat and shear deformation.

HME is a widely used processing technology in the polymer and food industries and has been recently demonstrated to be a viable method to prepare several types of dosage forms and drug delivery systems [5]. Since its introduction into the pharmaceutical industry, use of HME has grown steadily due to advantages such as being a continuous, single step, solvent free and readily scalable process. Here we describe the application of this process for cocrystallisation using ibuprofen and nicotinamide as a model cocrystal pairing previously reported from solution and hot stage microscopy.

MATERIALS AND METHODS

Cocrystals of ibuprofen and nicotinamide in 1:1 ratio were produced using HME (Pharmalab HME16, Thermo Scientific, UK) at different barrel temperature profiles, screw speeds, and screw configurations. The product was characterised for crystallinity by XRPD and DSC, while the morphology was determined by SEM. Dissolution rate and tabletting properties of the product were compared with ibuprofen.
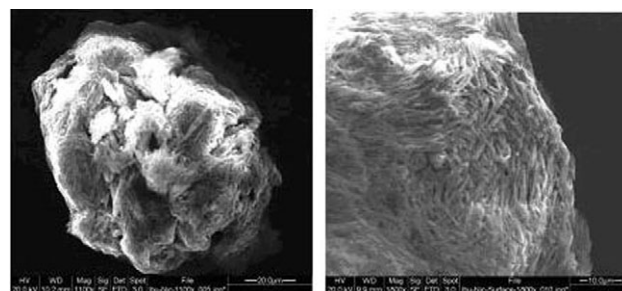
RESULTS AND DISCUSSION

Cocrystal purity was found to improve drastically by processing above the eutectic temperature of the blend. Screw geometry was found to have the most significant effect on the rate and extent of cocrystallisation when processed above eutectic temperature. Cocrystal purity was found to increase with set temperature and decrease with screw speed. Material extruded at lowest screw speed, highest shear screw configuration and higher temperature yielded the highest purity cocrystals. The product was in the form of spherical agglomerates of cocrystals (Figure 1) with directly compressible nature. This marks an important advantage over the conventional processes, as it negates the need for further size modification steps. The product showed enhanced dissolution rate compared to the ibuprofen.

CONCLUSIONS

A single step, scalable, solvent-free, continuous cocrystallisation (SFCC) technology was developed using HME offering flexibility for tailoring the cocrystal purity with simultaneous agglomeration. HME is an established technology which addresses the regulatory demand of quality by design (QbD) and process analytical technology (PAT) making SFCC highly potential technology for pharmaceutical cocrystallisation.

ACKNOWLEDGMENTS

REFERENCES

[1] N. Schultheissand A. Newman, "Pharmaceutical Cocrystals and Their Physicochemical Properties" *Crystal Growth & Design* **9** (2009) 2950–2967.

[2] H. Mazenand G. Townend. "Method of creating crystalline substances". *US 2008 0280858 A1*, (2008).

[3] S.L. Childs and P. Mougin, "Screening for solid forms by ultrasound crystallisation and cocrystallisation using ultrasound" *WO 2005 089375 A2*, (2005).

[4] A.R. Paradkar, A.L. Kelly, P.D. Coates, and P. York, "Method and product" *WO 2010013035 A1*, 2010.

[5] M.A. Repka, S.K. Battu, S.B. Upadhye, S. Thumma, M.M. Crowley, F. Zhang, C. Martin, and J.W. McGinity, "Pharmaceutical applications of hot-melt extrusion: Part II" *Drug Dev Ind Pharm*, **33** (2007) 1043–57.

Diluent Effects on Drug Release from Sustained-Release Compritol® 888 ATO Tablets

G. Treanor[1], M. Roberts[1], S. Mostafa[2], C. Miolane[3]

[1]School of Pharmacy and Biomolecular Science, Liverpool John Moores University, Liverpool, UK.
[2]Gattefossé (UK) Ltd, Bracknell, UK
[3]Gattefossé SA, St Priest, France

INTRODUCTION

Glyceryl behenate (Compritol® 888 ATO) is commonly used in formulating sustained-release lipid matrices [1]. When compressed, Compritol® 888 ATO forms an insoluble network structure, allowing water to penetrate and subsequent drug release to occur through diffusion. The aim was to assess the effects of various diluents on drug release from Compritol® 888 ATO matrices produced via direct compression under simulated production conditions using a Stylcam® 100R rotary press simulator.

MATERIALS AND METHODS

Formulations comprised; 16.7 %w/w anhydrous theophylline, 15 %w/w Compritol® 888 ATO, 3 %w/w, magnesium alumino silicate (Neusilin® US2), 1 %w/w magnesium stearate and 64.3 %w/w diluents (either; Microcrystalline cellulose (MCC, Avicel® PH101), Lactose (Lactopress® spray dried), dibasic calcium phosphate anhydrous (DCPA, Fujicalin®) or DCPA and lactose (2:1). Materials were blended for 2 mins (46 rpm) and subsequently for 1 min (96 rpm) with lubricant (2C turbula mixer, WAB, Switzerland). Tablets (600 mg, 12 mm) were produced using a Stylcam® 100R rotary press simulator (Medel'Pharm, France) at 12, 20 or 30 kN and 30 rpm (equivalent to rotary press production rate of ~120,000 tablets per hour). Tablet strength was measured (6D tablet tester, Schleuniger, Germany) and 12 h drug release profiles obtained (USP apparatus 2, phosphate buffer pH 4.5, 37°C) using a Sotax AT7 dissolution bath and an Agilent 8453 DAD Spectrophotometer at 271 nm. Data were analysed for statistical significance ($P < 0.05$) using the Minitab™ software package.

RESULTS AND DISCUSSION

Robust tablets were obtained from all formulations at each compaction force. Tablet strength was significantly higher
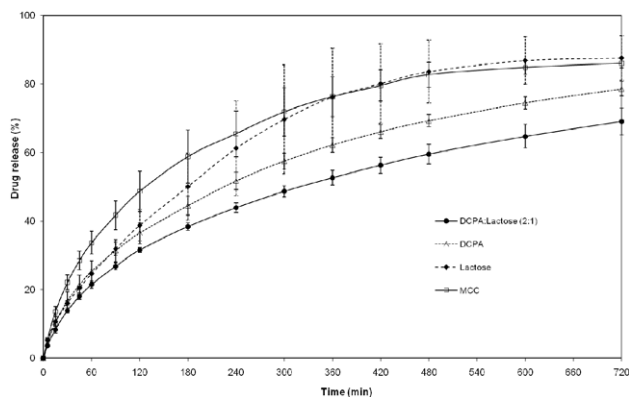

Fig. 1. Theophylline release from Compritol® 888 ATO tablets comprising various diluents produced at 12 kN (mean ± SD, n = 6)

with MCC (12–16 kP) in comparison with all other diluents(s) due to the compressibility of MCC. Tablets comprising lactose were weakest (4–6 kP), whilst those with DCPA alone and in combination lactose were comparable (5–9 kP).

Figure 1 shows release profiles from tablets produced at 12 kN. Initial drug release was rapid due to dissolution of drug particles on the surface of the matrix and release profiles were analogous to the Higuchi diffusion model. Drug release was sustained over 12 h from the tablets comprising DCPA: Lactose (2:1) and DCPA alone as the diluents(s). Faster and less consistent release was achieved from the tablets comprising MCC and the structures were observed to swell and split laterally during dissolution testing, which was ascribed to the nature of MCC promoting disintegration. A three-phase release profile (0–2, 2–6 and 6–12 h) was evident for the tablets comprising lactose, possibly due to the solubility of the diluent increasing solvent penetration into the matrix. Increasing compaction force decreased the release rate from all tablets and resulted in more consistent release profiles for tablets comprising MCC. The three-phase release profile for

tablets with lactose was less evident at higher compaction forces.

CONCLUSIONS

Robust tablets, able to sustain drug release over 12 h using Compritol® 888 ATO as the lipid matrix were successfully manufactured at conditions analogous to rotary tablet press production. The type of diluent and compaction force used in producing lipid based matrices via direct compression has a significant impact on the drug release profiles obtained.

REFERENCE

[1] A.A. Obaidat and R.M. Obaidat, "Controlled release of tramadol hydrochloride from matrices prepared using glyceryl behenate" *Eur. J. Pharm. and Biopharm.* **52** (2001) 231–235

Dissolution retardation from drug in capsule formulations due to gelling

A. Mistry[1], R.A. Storey[1], M. Ling[1], N. Stainforth[1], A. Desai[2]

[1]AstraZeneca Pharmaceuticals, Alderley Park, Cheshire, UK
[2]School of Pharmacy, Nottingham University, Nottingham, UK

Abstract – **Assessing the performance of formulations requires an understanding of the available surface area for dissolution. This study reports observations made for basic compounds when dissolved in acidic media. Due to a complex gel formation, dissolution has been effectively retarded from a drug in capsule presentation of a compound with a high solubility in acidic media.**

INTRODUCTION

Dissolution is a key process to ensure absorption of an active pharmaceutical ingredient. The process is heavily dependant on available surface area for interaction with the dissolution media as described by Noyes-Whitney equation[1]. Any changes in the formulation which effectively reduces the available surface for dissolution can have an effect on the performance of the formulation.

In the early phases of development, due to high attrition rates, simple formulations are preferable. These usually consist of solution (if solubility permits), suspension and drug in capsule (DiC). The DiC option offers great benefits for ease of dosing and also there is no need to perform further drug product stability trials. However, due to the lack of any dispersants the technology is not suitable for all compounds and early screening to investigate suitability is preferential.

MATERIALS AND METHODS

Capsules containing two crystalline basic APIs of similar pKa (within 1 pKa unit) were manufactured manually into size 0 HPMC capsules. Solubility measurements were performed by slurrying the compounds in their powder form for 24 hours at 37°C in Simulated Gastric fluid (SGF) followed by HPLC analysis. Results are summarised in Table 1.

Dissolution was performed in SGF pH 1.2 at 37°C at using USP2 setup at 50 rpm with HPLC finish. To investigate differences in the dissolution processes, studies were performed using a flow through dissolution apparatus linked to either a microscope or a magnetic resonance imaging (MRI) apparatus.

Table 1. Solubility data

Compound	Solubility (SGF*) (mg/ml)	Dose (mg)
A	5	80
B	0.123	10

*6.6 mls of 1M HCL, 0.2 g of NaCL, Water to 100 mls

RESULTS AND DISCUSSION

From the solubility data in Table 1 these compounds would be deemed acceptable for drug in capsule as they have reasonable solubility in relation to their dose in SGF. To investigate performance on dosing further dissolution testing was performed on these capsules.

Observations shown in Figure 1 during the dissolution of Compound A indicates the presence of the capsule has an effect on the dissolution compared to the API alone. MRI analysis of the drug in capsule indicates during dissolution a gel layer is set up due to the high solubility of the API in acidic media from which the drug slowly erodes. The effective surface area for interaction with the dissolution media is reduced thus retarding dissolution. Post dissolution analysis by powder X-ray diffraction and microscopy of the material remaining indicates an amorphous, non-birefringent gel layer of API at the surface with a crystalline core comparable to the starting material.

In contrast, results from Compound B indicate that although agglomeration is a factor during dissolution from a DiC and agitation easily overcomes this issue.

CONCLUSIONS

Even though DiC offers improvements for manufacture and investments for early formulations, careful assessment is
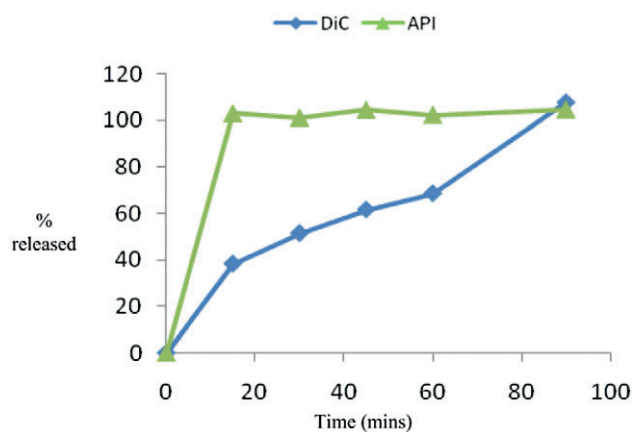
Fig. 1. Dissolution of API and DiC formulations for Compound A

the capsule, in combination with the high solubility in SGF (common for basic compounds), are providing an environment where a hydrated gel layer can be formed which reduces the effective surface area for dissolution.

ACKNOWLEDGEMENTS

REFERENCE

[1] Noyes: Sept. 13, 1866-June 3, Vol. 31, Columbia University Press, New York, 1958, pp. 322–346

required to understand the release profile from the capsule. Due to the lack of dispersants in these dosage forms simple solubility measurements are insufficient to assess the performance of these formulations. The physical constraints of

Effect of ageing on release of diltiazem hydrochloride from polyethylene oxide matrix tablets prepared by direct compression

S. Shojaee, A. Nokhodchi, K.I. Cumming

Medway School of Pharmacy, Universities of Kent and Greenwich, Kent, UK.

INTRODUCTION

Polyethylene oxide (PEO) is one of the hydrophilic polymers that has been extensively used to prepare sustained and modified release dosage forms. PEO is semi-crystalline, available in a wide range of molecular weights and miscible with water [1, 2]. The objectives of the present study were to investigate the effect of storage conditions on drug release behaviour of diltiazem HCl from matrix tablets containing different molecular weights of PEO.

MATERIALS AND METHODS

The diltiazem hydrochloride powder was obtained from Elan Drug Technologies. PEO grades 750, 1105, 301 and 303, produced by Dow chemical and distributed by Colorcon, Kent, England were used. Diltiazem HCl:PEO with a ratio of (1:1) was prepared and mixed in a turbula blender for a period of 10 min. Matrix tablets were prepared by the compression of the above mixtures using a hydraulic press at a compression force of 1500 psi (diameter of die was 8 mm). The tablets were stored at 40 °C and at different time intervals (2, 4 and 8 weeks) the release rate of the aged tablets was determined from dissolution testing.

In another series of experiments, 10 grams of each pure polymer was stored at 40 °C. At different time intervals (2, 4 and 8 weeks) polymer was taken out of oven and mixed with drug. The mixture was compressed at the same conditions as described above. Dissolution testing was performed for these aged tablets and non-aged polymer control tablets.

In order to investigate changes in solid state of drug and polymers subjected to 40 °C, DSC was performed and compared to the fresh samples. Other properties such as changes in true density and hardness of tablets were also investigated.

RESULTS AND DISCUSSION

As expected the results demonstrated that the release rate of diltiazem HCl was dependent on molecular weight of the polymer (Figure 1). The effect of storage conditions showed that the release rate of drug was significantly increased from tablets that were stored at 40 °C. Comparing the different molecular weights of PEO used in the present study showed that the higher molecular weights were more sensitive to the temperature than lower molecular weights of PEO. The effect of storage time on drug release showed that the drug release is faster at longer storage time (4 weeks) compared to fresh
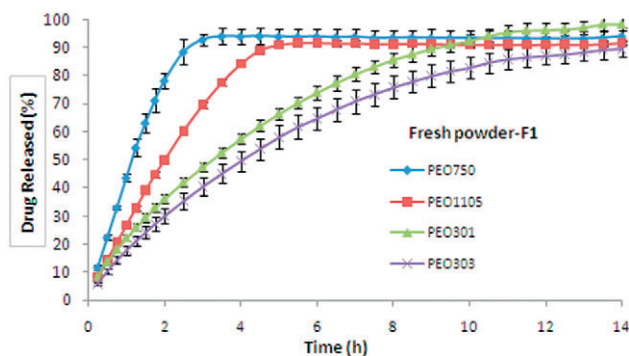
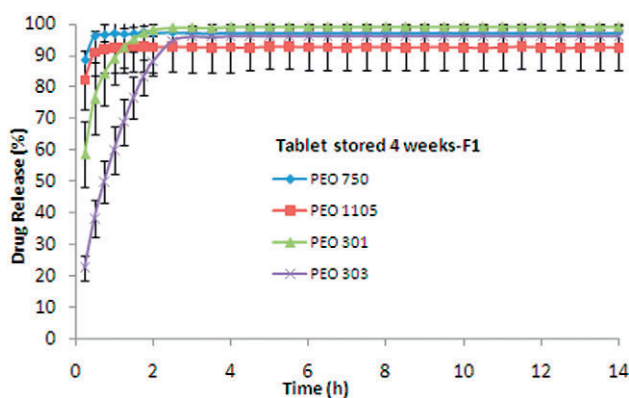**Fig. 1.** Effect of molecular weight of PEO on drug release (ratio of drug : PEO is 1 : 1)

Fig. 2. Effect of ageing on drug release from PEO matrix tablets (ratio of drug : PEO is 1 : 1)

samples (compare Figs 1 and 2). The increase in drug release is expected to be due to oxidative degradation primarily in the amorphous region of the polymer[3] and further work is underway to investigate this.

CONCLUSIONS

The impact of high temperature storage on increasing dissolution release rate was different across the range of polymers tested. The results revealed that there was no considerable difference between drug release rate from aged tablets and those tablets made from aged PEO powder. The results indicated that there was significant degradation of the polymer at elevated storage temperature.

ACKNOWLEDGMENTS

REFERENCES

[1] C.J. Kim, "Drug release from compressed hydrophilic POLYOX WSR tablets" J. Pharm. Sci, 84(3) 1995, 303–306.
[2] A. Moroni and I. Ghebre-Sellassie, "Application of polyethylene homopolymers in sustained release solid formulation" Drug. Dev. & Ind. Pharm. 21 (12) 1995, 1411–1428.
[3] M.M. Crowley, F. Zhang, J.J Koleng, and J.W. McGinity, "Stability of polyethylene oxide in matrix tablets prepared by hot melt extrusion" Biomaterials 23 (2002), 4241–4248.

Effect of excipient co-povidone prepared by in-situ lyophilisation and spray drying on nifedipine dissolution

M.F. Crum, A.A. Elkordy

Department of Pharmacy, Health and Well-Being, University of Sunderland, United Kingdom

The aims of this research were to use two process techniques: (i) a novel method which is in-situ lyophilisation in hard gelatin capsule shells and (ii) spray drying, to enhance the dissolution of nifedipine (a hydrophobic drug) in the presence of co-povidone, an enhancement excipient (to the best of our knowledge this excipient has not been previously used with nifedipine in a lyophilised form).

INTRODUCTION

Poorly water-soluble drugs present a challenge for the pharmaceutical industry due to agglomeration, poor dissolution, poor aqueous solubility and hence poor bioavailability of these drugs. Drugs administered via oral route are the preferred form of administration for patients, practitioners and manufacturers [1]. The Noyes-Whitney equation suggests ways of improving dissolution of hydrophobic drugs, allowing delivery via the oral route [2].

MATERIALS AND METHODS

Nifedipine (0.2%w/v) and co-povidone (Poly (1-vinylpyrrolidone-co-vinyl acetate)), in a range of concentrations of 1, 5 and 10%w/v were dissolved in a co-solvent system of tert-butyl alcohol/water (40%v/v) mixture. These solutions were either lypohilised or spray dried. In-situ lyophilisation (Figure 1) was performed by liquid filling of solutions into bodies of

size 000 hard gelatin capsule shells, and capsules were freeze dried.

Prepared formulations were stored in brown glass bottles (to protect the drug from light) at ambient temperature until analysis. Pure drug and all formulations were characterised by solubility, in-vitro dissolution (in capsule form) and wetting studies. Conformational integrity and thermal characteristics of nifedipine formulations were investigated using FT-IR spectroscopy and differential scanning calorimetry (DSC), respectively.

RESULTS AND DISCUSSION

The in-situ lyophilised formulations in the presence of 1%(w/v) co-povidone, increased nifedipine solubility by two-fold, whilst co-povidone at concentrations of 5% and 10%(w/v) increased drug solubility by about five-fold. For example, solubility of pure drug was 6.9 μg/mL compared to 12.3 and 33.5 μg/mL for nifedipine/1%(w/v) co-povidone and nifedipine/10%(w/v) co-povidone, respectively. The 10%(w/v) co-povidone prepared by spray drying increased drug solubility by two-fold (14.7 μg/mL).

In-situ lyophilised preparations significantly enhanced (p < 0.05) drug dissolution – the results of percentage drug released after 25 minutes were 74.7% versus only 28.3% from in-situ lyophilised 10%(w/v) co-povidone preparation and pure drug, respectively. Spray dried drug/10%(w/v) co-povidone after 25 mins had a percentage drug release of 78.5%.

To explain the results of drug dissolution, the surface tension properties were determined for different formulations and an example of results are: 48.3 and 65.4 mN/m from drug/10%(w/v) co-povidone prepared by in-situ lyophilisation and spray drying, respectively. Therefore, co-povidone prepared by in-situ lyophilisation and spray drying improved nifedipine wetting properties i.e. they increased the available surface area of drug particles in contact with dissolution medium and hence increased nifedipine dissolution (Noyes-Whitney equation).
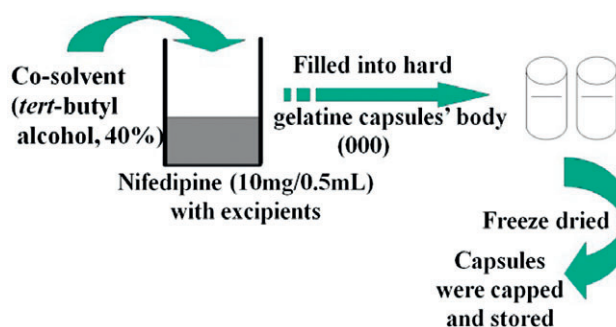

Fig. 1. Schematic representation for in-situ lyophilised nifedipine capsule formulations

Comparing the two drying processes, the in-situ lypohilisation produced 100% drug yield and the liquid capsule filling was found to be less tedious than powder filling (after spray drying). DSC thermograms showed that the in-situ lyophilised drug with 10%(w/v) co-povidone led to the disappearance of drug melting peak at 173°C, suggesting solubilisation or amorphousness of nifedipine. FT-IR confirmed DSC data.

CONCLUSIONS

These initial results for in-situ lyophilisation of nifedipine in hard gelatin capsules with co-povidone looks a promising technique not only in improvement of hydrophobic drug dissolution but also in enhancement of the final drug yield.

REFERENCES

[1] Gomez-Orellana, I. (2005). Strategies to improve oral drug bioavailability. Expert Opinion Drug Delivery 2, 419–433.
[2] Leuner, C., Dressman, J. (2000). Improving drug solubility for oral delivery using solid dispersions. Eur. J. Pharm. Biopharm 50, 47–60.

Effect of Systematic Change in Agitation on Drug Release from HPMC Matrices in Different pH Media (Fasted and Fed Conditions)

Kofi Asare-Addo[1], Marina Levina[2], Ali Rajabi-Siahboomi[2], Ali Nokhodchi[1]

[1]Medway School of Pharmacy, Universities of Kent and Greenwich, Kent, UK
[2]Colorcon ltd, Dartford, UK

Abstract – **The effect of systematic change in agitation on drug release from HPMC matrices were the objectives of this study. These were evaluated in a range of pHs: 1.2–7.5. Agitation had profound effects on drug releases from the low viscosity grade HPMC K100LV matrices, whereas, HPMC K4M and K100M matrices were more resilient to the effects of agitation. However the descending order of agitation also showed dissimilarity occurring for both K4M and K100M matrices. Use of systematic change of agitation method may indicate potential fed and fasted effects on drug release from hydrophilic matrices.**

INTRODUCTION

Hypromellose is a hydrophilic polymer carrier and this property is a determinant factor in its dominant use in the preparation of oral extended release (ER) drug delivery systems [1].
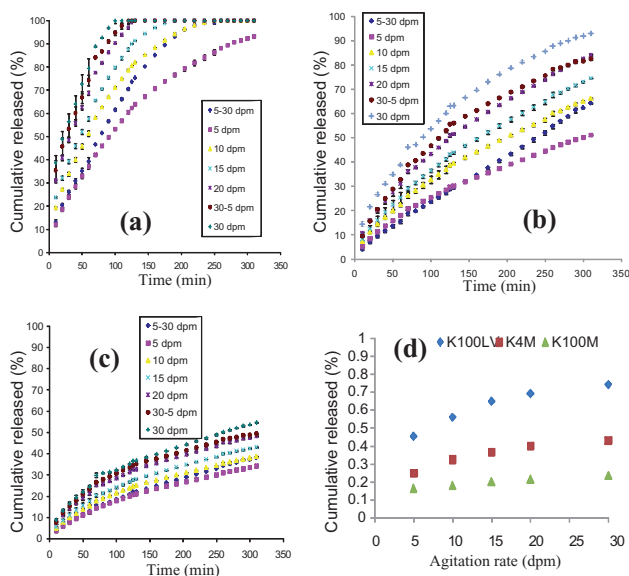
Fig. 1. The effect of rate and order of agitation on drug release from HPMC a) K100LV b) K4M c) K100M d) Release rate changes for K series.

It has been reported that food administration may affect the bioavailability of oral dosage forms [2]. There is no systematic study showing the effect of order of agitation (ascending and descending orders) on drug release at different pH values, on these ER systems. This study investigated the effect of agitation (dip rate) on the release of theophylline *in-vitro* and also the physiological characteristics of the different pH ranges in the GI tract on theophylline tablets.

MATERIALS AND METHODS

METHOCEL™ K100LV, K4M and K100M were used as the hydrophilic matrix former. Tablets with target weights of 250 mg were prepared by mixing theophylline with HPMC in the ratio of 4:1 and compressed at 6 kN (22 MPa).

The automated USP type III Bio-Dis was used for the dissolution tests. The dip rates ranged from 5 to 30 dpm. Vessels contained 250 ml of the appropriate media (pH 1.2–7.5) at $37.0 \pm 0.5°C$. The theophylline release was measured using a UV/Visible spectrophotometer at 271 nm.

RESULTS AND DISCUSSION

Robust matrix tablets with the breaking force values ranging from of $61 + 3.1$ to $69.70 + 1.5$ N were produced for all formulations used in the study. Figure 1 (a-d) shows the influence of agitation on drug release from tablets made using different HPMC polymer grades. The type and composition of a meal is vital to the extent of food interactions on tablet behaviour and may be mimicked by agitation rate.

Fig 1d showed low molecular weight K100LV to be more sensitive to effects of higher agitation intensity. Stronger gels produced by K4M and K100M had slower release when agitation intensity was increased.

CONCLUSIONS

Ascending and descending agitations resulted in a significant difference in theophylline releases for all systems. The resilient nature and the release mechanisms of the K4M and K100 M tablet matrices suggest that they might be the best candidates that will facilitate a zero-order release. Combination of polymer viscosity grade and level should be carefully considered when formulating hydrophilic polymers.

ACKNOWLEDGMENTS

REFERENCES

[1] P. Colombo, "Swelling-controlled release in hydrogel matrices for oral route". *Adv Drug Deliv Rev* **11** (1993) 37–57.

[2] B. Abrahamsson, K. Roos and J. Sjogren, "Investigation of prandial effects on hydrophilic matrix tablets *Drug Dev Ind Pharm* **25** (1999) 765–771.

Effect of the surfactant activity of ibuprofen on the structural stability of creams

T. Rokib, K. Dodou

Sunderland Pharmacy School, University of Sunderland, Sunderland, UK.

Abstract – **The effect of ibuprofen on cream structure was studied using two non-ionic cream formulations: low (A) and high (B) initial viscosity. The saturated concentration of ibuprofen in each formula was established and drug loaded creams were prepared over unsaturated and saturated concentrations. Rheological measurements of formula A showed a concentration-dependent decrease (p < 0.05) in cream viscosity and strength that plateaued at supersaturated concentrations. Formula B was resilient (p > 0.05) following ibuprofen addition.**

INTRODUCTION

The effect of ibuprofen on emulsion stability has been previously reported [1]. Preliminary studies showed the addition of ibuprofen in creams at unsaturated concentrations caused

a decrease in their viscosity [2]. The aim was to further investigate this finding.

MATERIALS AND METHODS

Preparation of creams: 50 g of formula A (50% Isopropyl myristate, 20% Span 80/Tween 80 at HLB = 11, 30% water) and formula B (30% emulsifying ointment, 70% water) were prepared (n = 3) at ibuprofen concentrations 0–12%w/w & 0–5% w/w respectively. The pH of each cream was determined in triplicate.

Polarised microscopy: Saturation concentration of ibuprofen in each formula was determined using an Olympus BH2 microscope fitted with a camera (AxioCam MRc-Zeiss, UK) and AxioVision vs4.4 software.

Rheological measurements: Viscometry, oscillatory rheometry and creep testing were performed at 32°C to characterise the viscoelastic properties of the creams, using a sunblasted stainless steel cone-plate (4°/40 mm) with 150 µm gap size.

RESULTS AND DISCUSSION

The saturation concentration of ibuprofen was between 7–10%w/w & 0.5–1%w/w in formulae A and B respectively. Unsaturated creams showed a significant concentration-dependent decrease in pH reaching a plateau at saturated concentrations. Model fit analysis of viscometry data from both cream formulations at all ibuprofen compositions demonstrated Herschel-Bulkley flow ($r^2 = 0.997–0.999$ for A & $r^2 = 0.712–0.997$ for B) with shear thinning behaviour (power index $n < 1$). Formula A creams showed a significant concentration-dependent decrease in viscosity (Fig. 1) and complex modulus (G^*), and an increase in creep compliance up to saturation point.

Rheological measurements did not detect any significant differences among formula B compositions (Fig. 2) aside from a small increase in strength at saturated ibuprofen concentrations.

CONCLUSIONS

Formula A was more sensitive to ibuprofen-induced structural changes than formula B, as demonstrated by rheological
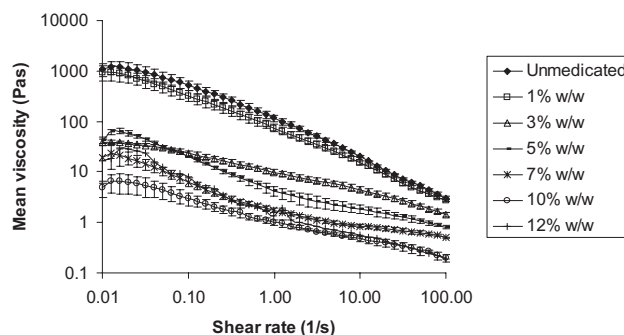

Fig. 1. Mean viscosity versus shear rate for formula A creams over a range of ibuprofen concentrations (%w/w).
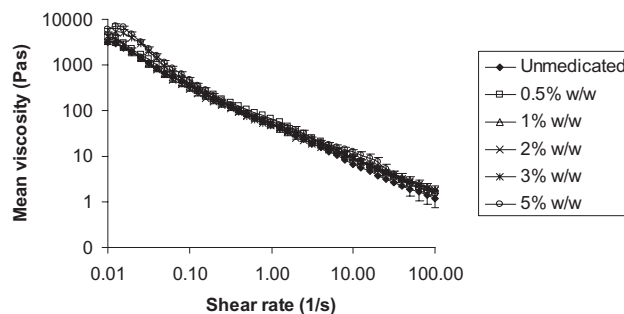

Fig. 2. Mean viscosity versus shear rate for formula B creams over a range of ibuprofen concentrations (%w/w).

measurements. This was due to the higher solubility of ibuprofen in formula A. Structural changes can be attributed to interaction of dissolved ibuprofen with the cream emulsifiers, resulting in HLB changes and instability; confirming the surfactant effect of ibuprofen.

REFERENCES

[1] F.R. Formiga, I.A.A Fonseca, K.B. Souza, A.K.A. Silva, J.P.F. Macedo, I.B. Araujo, L.A.L. Soares, E.S.T. Egito, "Influence of a lipophilic drug on the stability of emulsions: An important approach on the development of lipidic carriers" *Int. J. Pharm.*, **344** (2007) 158–160.

[2] S. Mavridou, "Preparation and testing of creams", Final year project 2008/9 (supervisor: Dr Kalliopi Dodou) unpublished.

Effects of formulation processing on physical properties of insulin-containing palmitin/palmitic acid nanoparticles

L.M Thong[1], N.Billa[1], C.R. Roberts[2] and J.C. Burley[2]

[1]School of Pharmacy, University of Nottingham, Malaysia Campus, Malaysia
[2]School of Pharmacy, University of Nottingham, UK

Abstract – **Insulin-containing NLC were formulated using palmitin/palmitic acid lipid composites. Z-average and crystallinity of the NLC were affected by the composite ratio. On one end, low z-average and polydispersity index was obtained when the liquid lipid content was low. Yet, these are necessary for high drug load. Therefore, it is necessary to study a range of concentrations in order to determine the threshold.**

Fig. 1. Scanning electron microscopy image of insulin crystals (left) and insulin-containing NLC (right).

INTRODUCTION

Nanostructured lipid crystals or NLCs have gained popularity over their older cousins, solid lipid nanoparticles (SLN). This being the result of several advantages associated with the former, such as high drug loading due to the presence of liquid domains, which distorts the crystallinity of the NLC. The physical characteristics of formed NLC depend on the composition of the lipids utilised, as well as the formulation processes. In the present study, palmitin and palmitic acid are used as solid and liquid components in formulating NLCs using insulin as model drug.

MATERIALS AND METHODS

NLCs were formulated by double emulsion cum solvent diffusion using poloxamer 188 and lecithin as surfactants according to the table below:

FORMULATION	LIPIDS (mg)	
	Tripalmitin	Palmitic acid
F1	100	–
F2	–	100
F3	75	25
F4	50	50
F5	25	75

RESULTS AND DISCUSSION

F1 registered the lowest z-average and polydispersity index (PDI). There was no apparent difference between the zeta potentials. As the v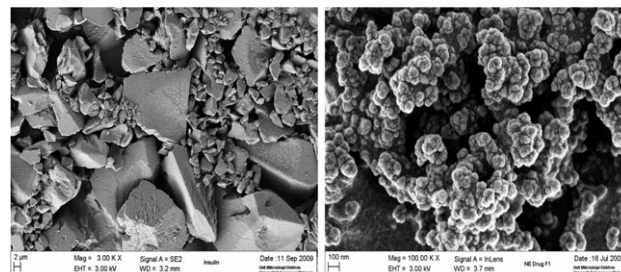olume of the same amount of surfactant-containing external phase was increased, the z-average decreased. At excessive dilutions, the z-average begun to increase. The largest z-average and highest PDI were recorded from F5. Calculated change in entropies (ΔS) indicate that as tripalmitin content is increased, so too does the value of ΔS. Thus, F1 is most crystalline and F2, the least. From a stability point, we would pursue F1 further, however as mentioned earlier, it is necessary to incorporate liquid lipids in NLC in order to perturb the crystalline structure [1]. Therefore a cut-off liquid lipid content should be sought, which in the present case is 25 mg palmitic acid (F3). Comparative EDX mapping based on di-sulphur bridges in insulin suggest that insulin is present within the NLC as a drug-enriched core.

Encapsulation efficiency and insulin release from the NLC are currently being run.

CONCLUSIONS

Although it is necessary to include solid lipids into NLC, the physical characteristics of the former are compromised. Therefore, it is necessary to study the crystallinity of the NLC, encapsulation efficiency as a function of increasing amounts of the liquid lipid.

REFERENCE

[1] A.G Mangoni, S.E., Mcgauley, 2003, Relationship between crystallisation behaviour and structure in Cocoa butter. *Crystal growth & design*.**3**, (2003) 95–108

Effects of speciation on the freeze drying properties of lyophiles

R.A. Storey[1], J. Norris[1], L. Salmela[1], K. Nurzyńska[2]

[1]AstraZeneca Pharmaceuticals, Macclesfield, Cheshire, UK
[2]School of Pharmacy, Nottingham University, Nottingham, UK

Abstract – **In the design of a formulation for a freeze dried product an understanding of the speciation of the components can provide opportunities to shorten the lyophilisation process. These effects have been investigated for two pharmaceutical compounds.**

INTRODUCTION

Freeze drying provides a simple method of producing stable and rapidly reconstituting pharmaceutical formulations. During the formulation stages, consideration of the speciation and proportion of different components is required as these will have an effect on the physical properties of the frozen solution. To achieve a sufficient drug loading it is frequently required to adjust the pH of the solution and the use of counterions such as citric acid is frequently adopted.

To permit rapid reconstitution we require the formulation to have a highly porous structure and the components in a highly soluble (normally amorphous) state. The lyophilisation process should ensure that, during the primary drying stage, the product temperature should not exceed its collapse temperature (T_c)[1] to maintain porosity and prevent changes in physical state. Following the freezing of aqueous solutions any components in the amorphous phase will contribute to the collapse temperature of the cake. Above this temperature, movement of the amorphous material may occur resulting in loss of porosity and potentially crystallisation of amorphous components (see Figure 1).

This study investigates how the speciation and content of counter-ion can affect physical properties of frozen solutions.

MATERIALS AND METHODS

Solutions of two pharmaceutical compounds, one with a single basic pKa and the other with multiple basic pKa's were made up using a range of API:citric acid molar ratios. The glass transition temperature of a maximally concentrated solution (T_g') produced by freezing solutions was measured using a TA instruments DSC. The correlation of the collapse temperature with T_g' was also measured using a freeze drying microscope.

Physical properties of the resultant lyophiles produced at freeze drying temperatures below the measured T_g' were also obtained.

RESULTS AND DISCUSSION

The measured T_g' for compounds A and B with different molar quantities of citric acid are shown in Figure 2. For
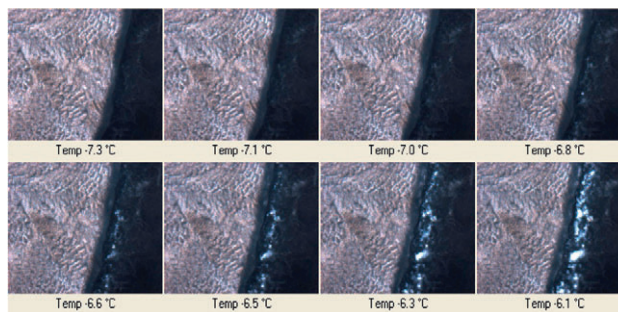

Figure 1. Collapse of frozen solution on heating by freeze drying microscopy
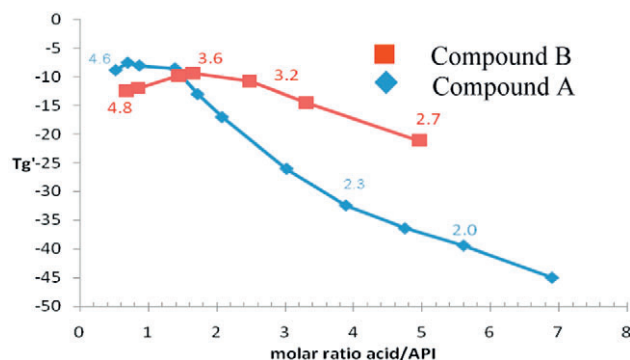

Fig. 2. T_g' measurements for different molar ratios of citric acid:API and resultant pH's of solutions

compound A (single pKa) the T_g' of the solution at approximately 1:1 ratio of acid:API is at a maximal value. Any deviation from this value produces a reduction in the value of T_g' as there are mixed species present. When there is an excess of API, i.e. where acid:API ratio < 1 (limited data in this area due to limited solubility of API at high pH's), or when there is an excess of acid (ratio > 1) the T_g' is suppressed. This has been reported[2] to be linked to the presence of the associated species similar to a salt form at relevant ratios of acid:API. This has the effect of "increasing effective molecular weights" similar to many nonionic molecules (*e.g.*, polyols, saccharides) having raised T_g' and Tg at higher molecular weights. The formation of ion-pairs in solution and in the freeze concentrated phase effectively increases the T_g' and the resultant T_c allowing a higher and hence more aggressive shelf temperature during freeze drying.

In comparison, compound B, with multiple pKa's shows a much shallower change in the T_g' with different proportions of acid. This is linked to the different species present over the

pH range and the ability to form different stoichiometry salts with the acid.

CONCLUSIONS

In the production of freeze dried formulations controlling the species present in solution provides an opportunity to increase the T_c of the formulation allowing processes to be optimised and drying times reduced.

REFERENCES

[1] Michael J. Pikal and Saroj Shah "The collapse temperature in freeze drying: Dependence on measurement methodology and rate" *International Journal of Pharmaceutics, 62 (1990) 165–186*

[2] Saori Kadoya, et. al. "Glass-State Amorphous Salt Solids Formed by Freeze-Drying of Amines and Hydroxy Carboxylic Acids: Effect of Hydrogen-Bonding and Electrostatic Interactions" *Chem. Pharm. Bull.* 56(6) 821—826 (2008)

Effects of substituting Fructose by Mannitol in a pharmaceutical formulation

E Schmidt, N Dooley, S Ford, M Elliot, G Halbert

Cancer Research UK Formulation Unit, Strathclyde Institute of Pharmacy and Biomedical Sciences, Strathclyde University, Glasgow, UK.

Abstract – **Pharmaceutical formulations can increase the solubility and stability of drug molecules. L-p-[10]Boronphenylalanine (BPA) has previously been formulated with Fructose. Here we present a novel BPA formulation with Mannitol resulting in improved kinetic solubility along with the removal of possible Fructose related intolerance reactions.**

INTRODUCTION

L-p-Boronphenylalanine is commonly used in Boron Neutron Capture Therapy (BNCT), treating malignant brain tumours such as glioblastoma multiforme. BPA has previously been formulated with Fructose (BPA 30 mg/mL, Fructose 28 mg/mL), whereby the formation of a BPA-Fructose complex [1, 2] prevents the precipitation of BPA upon administration and subsequent dilution in vivo. Fructose is no longer recommended as an ingredient for infusion fluids due to hereditary Fructose intolerance. In this abstract we investigate and compare the physico-chemical properties of the existing Fructose formulation to a novel Mannitol formulation. The ability of Fructose and Mannitol to complex BPA may therefore be applied to produce a pharmaceutical formulation with enhanced solubility of BPA at physiological pH.

MATERIALS AND METHODS

pKa and solubility measurements were performed using the Sirius T3 apparatus. Potentiometric pKa titrations were performed in ion strength adjusted water (0.15 M KCl) titrating with 0.5 M KOH and 0.5 N HCl, respectively. Triplicate titrations covered the pH range from pH 1.8–11 with an initial concentration of BPA of 3.6 mM (0.71 mg/mL). Solubility measurements were carried out using the CheqSol method [3]. Titrations were performed under the conditions described above. Initial concentration of BPA were 77 mM (16.0 mg/mL) and titrations performed from high to low pH. UV VIS data were collected during titrations using a MMS UV-VIS

Table 1: Average pKa values of BPA in the absence or presence of equimolar ratio of Mannitol and Fructose.

Sample (pKa pH-metric)	pKa 1	pKa 2	pKa3
BPA powder	2.06	8.36	9.61
BPA Mannitol	2.39	7.71	9.75
BPA Fructose	2.41	7.57	9.78

spectrometer with a Hellma ultra-mini immersion probe. Reference spectra were collected at the start pH of the titration.

RESULTS AND DISCUSSION

Both Fructose and Mannitol formed a sugar-BPA complex seen as a change in relative absorbance at 233.6, 237.9, 264.1 and 274.9 nm. As previously reported this change in absorbance is due to the change in electronic environment from the mainly trigonal boronic acid centre to a tetrahedral BPA-sugar cis-diol complex [1, 2, 4, 5]. This also results in a large pKa shift of the boronic acid group to lower values and only minor influence on the amine and carboxylic acid pKa (Table 1). Solubility assays showed BPA-Mannitol remained in solution over a wider pH range than BPA-Fructose (Fig. 1). Kinetic solubility of BPA-Mannitol was 1.6-fold higher than in presence of Fructose.

CONCLUSIONS

The presentation of BPA (100 mg/mL) in combination with an equimolar ratio of Mannitol (110 mg/mL) shows similar behaviour to the Fructose formulation regarding the sugar complex formation. However, the kinetic solubility of the Mannitol complex was superior to Fructose. Since Mannitol does not produce lactic acidosis and has the ability to disrupt the blood brain barrier, a BPA-Mannitol formulation provides
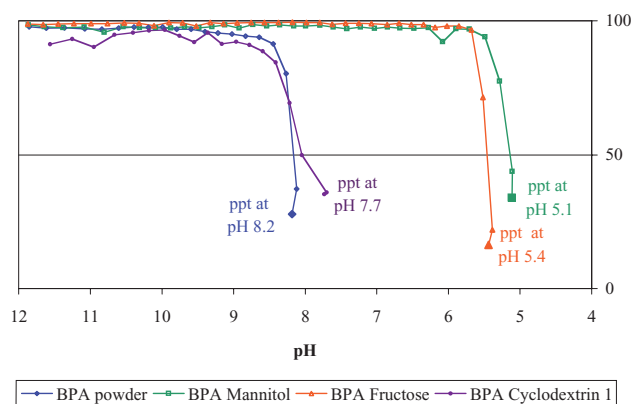
Fig. 1. pH-dependant precipitation (ppt) of BPA, BPA-Fructose and BPA-Mannitol.

improved pharmaceutical characteristics for BNCT glioma treatment compared to the Fructose formulation.

ACKNOWLEDGMENTS

REFERENCES

[1] Y. Mori, A. Suzuki, K. Yoshino, H. Kakihana "Complex-Formation of P-Boronophenylalanine with Some Monosaccharides" *Pigment. Cell Research,* **2** (1989) 273–277.

[2] K. Yoshino, et al., "Improvement of solubility of p-boronophenyla-lanine by complex formation with monosaccharides" *Strahlenther. Onkol.* **165** (1989) 127–129.

[3] K. Box, J.E. Comer, T. Gravestock, M. Stuart, "New ideas about the solubility of drugs" *Chem. Biodivers.,* **6** (2009) 1767–1788.

[4] B.K. Shull, et al., "Studies on the structure of the complex of the boron neutron capture therapy drug, L-p-boronophenylalanine, with fructose and related carbohydrates: chemical and 13C NMR evidence for the beta-D-fructofuranose 2,3,6-(p-phenylalanylorthoboronate) structure" *J. Pharm. Sci.,* **89** (2000) 215–222.

[5] M. Matsumoto, K. Ueba, K. Kondo, "Separation of sugar by solvent extraction with phenylboronic acid and trioctylmethylammonium chloride" *Separation and Purification Technology.* **43** (2005) 269–274.

Elucidation of the potential of starch-based multiparticulates for use as a platform in novel drug delivery systems

Y. Dawood, V. Pillay*, Y.E. Choonara, L.C. du Toit

University of the Witwatersrand, Department of Pharmacy and Pharmacology, 7 York Road, Parktown, 2193, Johannesburg, South Africa
Correspondence: viness.pillay@wits.ac.za

INTRODUCTION

Starch is a widely available and inexpensive natural food source which is used within the pharmaceutical industry as simple excipients [1]. The study is therefore aimed at expanding the use of commercial starch products by employing them as the actual core of drug delivery systems thus eliminating the cost and process required to formulate a core.

MATERIALS AND METHODS

1) *Determination of drug entrapment efficiency*: 5 g samples of starch-based multiparticulates (SBM) were accurately weighed out and placed into 15 mL diphenhydramine (DPH) solution (100 mg/mL). The SBM were allowed to hydrate at a temperature of 50ºC for 1 hour. The SBM were then removed, placed on petri dishes, weighed and allowed to dry at a temperature of 25ºC until constant mass was achieved. The SBM were weighed and 1 g samples of the drug-loaded SBM were homogenised in 10 mL deionised water for 120 seconds. The homogenised suspension was then made up to 500 mL with water maintained at 100°C, stirred and allowed to cool. Three 10 mL samples from the cooled suspension were then centrifuged for 90 minutes after which they were filtered through a 0.45 µm filter. The filtered samples were then analysed using UV spectroscopy at a wavelength (λ max) of 254 nm to determine the drug content within the SBM.

2) *Preparation of tablets*: 12 tablet formulations each having a mass of 1000 mg were prepared as depicted in Table 1. In formulations 1–4 260 mg of drug-loaded SBM represents the equivalent of 50 mg DPH. In formulations 5–8 granules were formed from the tablet substituents prior to tabletting and in formulations 9–12 direct compression of powder blends was performed.

3) *Fourier transform infrared spectroscopy (FTIR) analysis:* FTIR was carried out to elucidate the mechanism of drug entrapment within the SBM.

4) *In vitro drug release studies*: These were performed on the tablets using the USP dissolution apparatus II (paddle method) in 900 mL pH 6.8 phosphate buffer solution

Table 1. Preparation of tablets

	1	2	3	4	5	6	7	8	9	10	11	12
Drug loaded SBM	260	260	260	260								
DPH					50	50	50	50	50	50	50	50
Starch	740			370	950			475	950			475
Ethylcelluose		740		370		950		475		950		475
Chitosan			740				950				950	
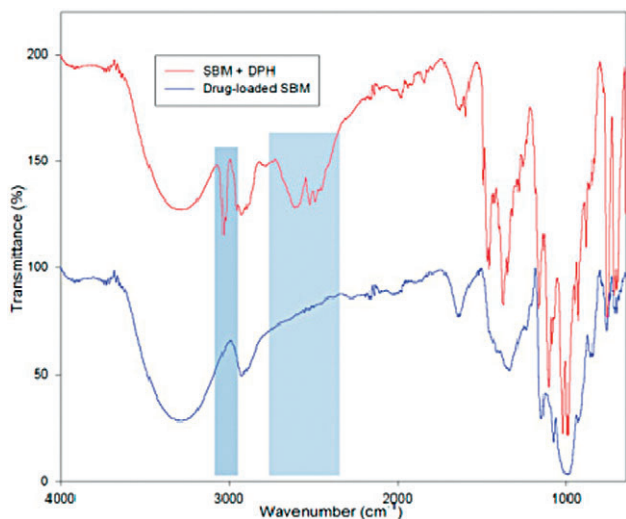
Figure 1. FTIR spectra depicting drug-loaded SBM and composite multiparticulates and DPH

Figure 2. Drug release profiles of tablet formulations

(PBS), at $37+0.1^0$C and rotated at 50 rpm. Samples (5 mL) were withdrawn every 30 minutes over a 12 hour period and replenished with fresh buffer to maintain sink conditions. The absorbance values were measured using UV spectroscopy at a wavelength of 254 nm (λ max) and drug release was calculated using a predefined calibration curve.

RESULTS AND DISCUSSION

The drug entrapment efficiency was calculated as 52+1.1 % with FTIR illustrating possible bond formation between the drug and the SBM at a wavenumber 3012 and in the region between wavenumber 2040 and 2070.
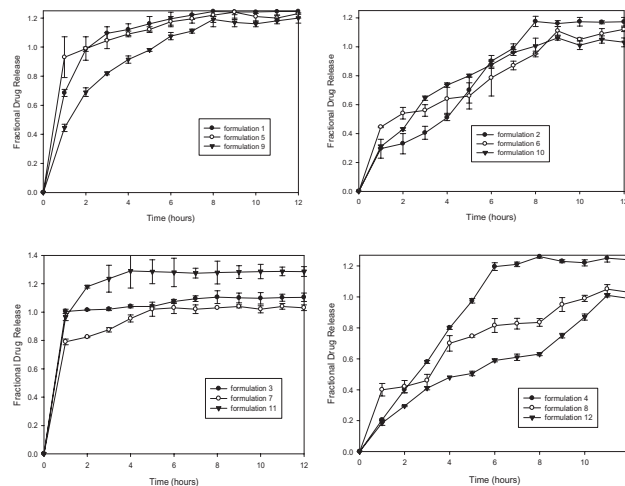
Drug release profiles show that the SBM/polymer formulations (1–4) control release to the greatest extent over the first 8 hours compared to the granulated or powder blend formulations. The SBM/Ethylcellulose formulation (2) displayed the most favourable drug release kinetics.

CONCLUSIONS

Starch based multiparticulates demonstrate satisfactory entrapment efficiency and serves as a functional platform for controlled release drug delivery systems.

REFERENCE

[1] S. Galland, T. Ruiz and M. Delalonde, "Twin product/process approach for pellet preparation by extrusion/spheronisation Part I: Hydro-textural aspects", *Int. J. Pharm.* 337 (2007) 239–245.

Encapsulation, release, bioactivity and cytotoxicity of lysozyme loaded poly(glycerol adipte-co-ω-pentadecalactone) microparticles

H. M. Tawfeek[1,2], S.H. Khidr[2], E.M. Samy[2], S.M. Ahmed[2], A. Evans[1], E.E. Gaskell[1], G.A. Hutcheon[1]

[1]School of Pharmacy and Biomolecular Sciences, Liverpool John Moores University, Liverpool, UK.
[2]Department of Industrial Pharmacy, Assiut University, Assiut, Egypt.

INTRODUCTION

A novel polyester, poly(glycerol adipate-co-ω-pentadecalactone), PGA-co-PDL, was synthesised, characterised and evaluated for α-chymotrypsin delivery [1,2]. The aim of this work was to evaluate the use of PGA-co-PDL for encapsulation and release of lysozyme, (LS) as well as to assess the bioactivity and cytotoxicity of the formed microparticles. The effect of altering the polymer chemistry and making the material more hydrophobic was studied by testing the related polymer poly(1.3-propandiol adipate-co-ω-pentadecalactone), PPA-co-PDL.

MATERIALS AND METHODS

1) *Microparticles preparation*: PGA-co-PDL Mw: 26.0 KDa and PPA-co-PDL Mw: 22.0 KDa were used to prepare microparticles by using the double emulsion solvent evaporation technique as previously reported [2].

2) *Microparticles characterisation*: The produced microparticles were evaluated for their encapsulation efficiency (EE) and enzyme loading, from their wash solutions, by measuring the amount of non-encapsulated protein. The particles morphology and size were determined using scanning electron microscopy (SEM) and laser diffraction particle size analysis.

3) *In-vitro release and bioactivity*: Release of LS from microparticles into phosphate buffer saline (PBS) was measured in three different batches over 24 hr. Samples were taken at each time point, centrifuged at 13500 rpm and analysed UV (282 nm). The bioactivity of LS was measured fluorometrically [3] and expressed as a bioactive fraction of the released enzyme [4].

4) *Cytotoxicity*: The cytotoxicity of different concentrations of blank microparticles was evaluated in human bronchial epithelium cell lines 16HBE14o using the MTT assay. Treatments were carried out for 24 hr and the results obtained from two different occasions.

RESULTS AND DISCUSSION

PPA-co-PDL gave a slightly higher encapsulation, loading and particle size compared to PGA-co-PDL loaded microparticles, see Table 1. SEM images showed regular, spherical particles with a rough surface in case of PGA-co-PDL or smooth surface with PPA-co-PDL, see Fig 1. This morphology was previously reported [5].

Table 1. Encapsulation efficiency, loading and mean median particle size of lysozyme loaded PGA-co-PDL and PPA-co-PDL microparticles

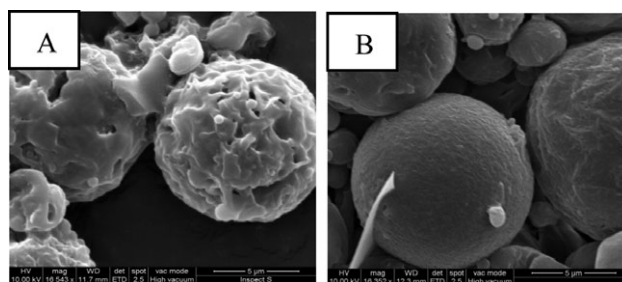| Polymer	EE (%)	Enzyme loading (µg/mg particle)	Mean median p.s. (µm)
PGA-co-PDL Mw:26.0 KDa	32.62 ± 0.5	107.50 ± 2.1	12.23 ± 0.9
PPA-co-PDL Mw:22.0 KDa	36.40 ± 2.8	121.33 ± 11.6	14.47 ± 1.5

Fig.1. SEM images of LS loaded PGA-co-PDL (A) and PPA-co-PDL (B) microparticles.
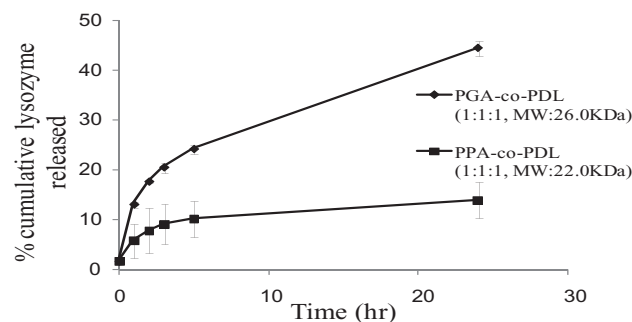

Fig.2. Percentage cumulative LS released from PGA-co-PDL and PPA-co-PDL microparticles in PBS buffer at 37°C.

It was clear from the release patterns that using a more hydrophobic polymer (PPA-co-PDL) decreased the initial burst and the continuous release, see Fig 2. The bioactive fraction of the released LS after 24 h was found to be 64% and 25% for the PGA-co-PDL and PPA-co-PDL particles respectively.

The cytotoxicity studies showed 86.7% and 93.5% cell viability was obtained after the cells were treated with 10 mg/

ml of blank (non-LS loaded) PGA-co-PDL and PPA-co-PDL microparticles respectively.

CONCLUSIONS

PGA-co-PDL and PPA-co-PDL polymers have proven to be safe and promising carriers for LS delivery. There is no significant difference in the EE and enzyme loading between the two polymers however, the release profiles are affected by the chemistry of the polymer

REFERENCES

[1] P. Kallinteri, *et al.*, "Novel functionalised biodegradable polymers for nanoparticle drug delivery systems" *Biomacromolecules* **6** (2005) 1885–1894.

[2] E.E. Gaskell, G. Hobbs, C. Rostron, G.A. Hutcheon, "Encapsulation and release of alpha-chymotrypsin from poly(glycerol adipate-co-omega-pentadecalactone) microparticles" *J. Microencapsul.*, **25** (2008) 187–195.

[3] H. Fukuda, et al., "Enhancement of the sensitivity of a fluorometric lysozyme assay system by adding beta-N-acetylhexosaminidase" *Chem. Pharm. Bull.*, **33** (1985) 3375–3380.

[4] C. Srinivasan et al., Effect of additives on encapsulation efficiency, stability and bioactivity of entrapped lysozyme from biodegradable polymer particles, J. Microencapsul. 22 (2005) 127–138

[5] C.J. Thompson *et al.*, "Evaluation of ibuprofen-loaded microspheres prepared from novel copolyesters", *Int. J. Pharm.*, **329** (2007) 53–61.

Engineered mannitol as potential carrier for enhanced DPI performance

Waseem Kaialy[1,4], Gary P. Martin[2], Martyn D. Ticehurst[3], Mohammed N. Momin[1], Ali Nokhodchi[1]

[1]Medway School of Pharmacy, University of Kent, ME4 4TB, Kent, UK; [2]King's College London, Pharmaceutical Sciences Research Group, Stamford St., Franklin-Wilkins Building, London, UK; [3]Pfizer Global R & D, Pharmaceutical Sciences, Sandwich, Kent; [4]Pharmaceutics and Pharmaceutical Technology Department, University of Damascus, Syria

Abstract – **Crystallised mannitol carriers from different binary mixtures of acetone/water were prepared and investigated. Crystallised mannitol particles were more elongated, with different polymorphic form, poorer flowability, and considerably better aerosolisation performance than that of the commercial mannitol formulation blends. It was shown that, generally, carriers having a high tapped density and high fraction of fine mannitol particles produced a high FPF. Abbreviations – API: Active pharmaceutical ingredient, CI: Carr's Index, CV: Coefficient of variation, DPI: Dry powder inhaler, DSC: Different scanning calorimetry, FPF: Fine particle fraction, FT-IR: Fourier Transform infra red, SEM: Scanning electron microscope. S_v: volume specific surface area, ρ_{true}: true density, ρ_{bulk}: bulk density, ρ_{tap}: tap density.**

INTRODUCTION

DPI formulations usually incorporate a carrier (usually lactose) to facilitate aerosolisation of the API. However, the use of lactose has some disadvantages. Therefore, other excipients such as mannitol have been suggested [1]. However, the effects of engineered mannitol crystallised from binary mixtures of solvent as carrier on DPI performance has to date not been investigated systematically. In this study, mannitol particles were crystallised using different binary combinations of acetone/water and their physicochemical properties were characterised to investigate the suitability of engineered mannitol for inclusion as DPI excipient.

MATERIALS AND METHODS

1. *Preparation of crystallised mannitol powder*
   A series of binary combinations of anti-solvents with different ratios of acetone:water (100:0, 95:5, 92.5:7.5, 90:10, 85:15, 80:20 and 75:25 ml) were employed to prepare crystallised mannitol samples.
2. *Micromeritic, flow, and solid state properties*
   Bulk density, tap density, Carr's Index, Hausner ratio, true density, roundness, elongation ratio, and particle size were determined for all mannitol samples studied. SEM was also employed to investigate the particle morphology. DSC and FT-IR were employed to detect any changes in mannitol polymorphic form.
3. *In vitro formulation assessment*
   MSLI was employed to assess the aerosolisation behaviour of crystallised mannitol formulations in comparison with commercial mannitol operating at 92 L/min flow rate and actuated from Aeroliser®.

RESULTS AND DISCUSSION

The results showed that crystallised mannitol samples had lower ρ_{bulk} (0.11–0.26 g/cm^3) and ρ_{tap} (0.17–0.40 g/cm^3), less flowability (CI: 25.67–38.00 %), higher span values (0.71–2.06), higher amounts of fines (0.00–29.17%), higher S_v (0.07–0.69 m^2/cm^3) compared to commercial mannitol (ρ_{bulk} = 0.54 g/cm^3, ρ_{tap} = 0.63 g/cm^3, CI = 14.17 %, span = 0.77, fines = 0.00%, S_v = 0.06 m^2/cm^3). Lower carrier bulk density,

Fig. 1. SEM images for (a) commercial mannitol (b) mannitol crystallised from acetone: water (100:0 ml) and (c) from acetone: water (97.5, 2.5).

Table 1. CV (%) and deposition parameters obtained from commercial and crystallised mannitol formulations.

Man.[a]	CV (%)	Recovery (%)	Emission (%)	FPF (%)
Com[b].	1.76	79.3 ± 1.7	96.3 ± 0.2	15.4 ± 1.1
100/0[c]	6.25	88.7 ± 5.3	92.9 ± 1.6	41.5 ± 2.6
97.5/2.5	10.56	91.3 ± 7.1	93.3 ± 0.9	43.2 ± 0.7
95/5	3.39	95.4 ± 15.4	94.5 ± 0.6	44.0 ± 2.6
92.5/7.5	6.43	87.8 ± 14.7	94.7 ± 0.9	42.9 ± 1.3
90/10	7.67	94.7 ± 6.8	94.9 ± 1.1	41.6 ± 7.9
85/15	5.33	82.2 ± 19.8	93.9 ± 3.3	34.0 ± 5.3
80/20	6.39	91.8 ± 4.3	93.9 ± 0.7	41.0 ± 0.5
75/25	17.40	83.2 ± 8.5	93.6 ± 2.7	33.1 ± 3.7

[a]Mannitol; [b]Commercial; [c]Anti-solvent mixture (Acetone/Water)

tap density and higher carrier fines and surface area may be responsible for their enhanced inhalation performance. SEM showed that all engineered mannitol crystals were more elongated than the commercial mannitol (Figure 1). Carriers with higher elongation ratios were proved to produce better drug aerosolisation properties (Table 1).

Crystallised mannitol formulations produced lower content uniformity, but higher recovery, emission, and FPF indicating better performance for crsytallised samples (Table 1).

CONCLUSIONS

All crystallised mannitol samples were in different physico-chemical properties and improved deposition behaviour. Carriers with higher ρ_{true}, amounts of fines, S_v produced higher FPF.

REFERENCE

[1] Steckel, H., Bolzen, N., 2004. Alternative sugars as potential carriers for dry powder inhalations. Int. J. Pharm. 270,297–306.

Experiences of melt fill production of Fenretinide/Lym-X-Sorb™ hard gelatin capsules for Phase I clinical trial

M.A. Elliott, E. Schmidt, S.J. Ford and G.W. Halbert

Cancer Research UK Formulation Unit, Strathclyde Institute for Pharmacy and Biomedical Sciences, University of Strathclyde, Glasgow, G4 0NR, UK.

Abstract – **Fenretinide is a pro-apoptotic, cytotoxic, synthetic Vitamin A analogue with application in the treatment of Ewing's sarcoma. For paediatric study, a 'cookie dough' formulation had been developed, improving upon an existing corn oil formulation. We report on a simplified capsular formulation of fenretinide with the novel solubility and bioavailability enhancing lipid matrix, Lym-X-Sorb™.**

INTRODUCTION

4-HPR [N-(4-Hydroxyphenyl) retinamide, Fenretinide] in corn oil capsules can give poor dosing consistency and wide patient-to-patient variation. In children's cancer studies, consumption of large numbers of capsules and big capsule size has lead to poor patient compliance. To overcome these issues, a formulation was developed using Lym-X-Sorb™ (LXS), an organised lipid matrix designed to enhance solubility and bioavailability. When blended with sugar and wheat flour, a 'cookie dough' of 4-HPR and LXS was produced for mixing in food or liquids [1].

For UK Phase I trial, a simplified capsular formulation was sought for ease of GMP production, and to regulate and escalate doses given.

MATERIALS AND METHODS

4-HPR was provided by the National Cancer Institute (NCI), Maryland, USA. Avanti Polar Lipids Inc., Alabama and BioMolecular Products Inc., Massachusetts, USA gifted the LXS. Size 0 hard gelatin Licaps® were used on a CFS1000 capsule-filling machine (Capsugel, Belgium). Other materials were of laboratory grade or better from the Sigma-Aldrich Company Limited, Dorset, UK. 'Fed' buffer dissolution was according to the method of Dressman and Reppas [2].

RESULTS AND DISCUSSION

LXS has a 'buttery' consistency at room temperature and can be melted by heating to around 30°C. A maximum of 11% w/w 4-HPR was incorporated into LXS by blending into the molten base. Hand filled size 0 capsules gave 'fed' buffer dissolution profiles indicative of slow release when compared with 11% 4-HPR in corn oil, and with poor release from a 4-HPR powder only capsule (Figure 1).

Using the 11% w/w 4-HPR in LXS formulation on the CFS1000 machine resulted in a 'bridging' phenomenon [3] during the fill. Specifically, the capsule fill was not clean, producing a melt 'trail' over the capsules and dosing stations. This was potentially attributable to melt viscosity and assumed thixotropic behaviour.

Bridging during the fill was overcome with alterations to hopper filling temperature, rate of melt stirring and machine fill speed. Capsules produced were analysed by UV for drug content, and for uniformity of mass.

CONCLUSIONS

4-HPR in LXS capsules for oral dosing can be consistently made. Full-scale analytical and stability studies would be required on the proposed formulation before entering clinical trial.

ACKNOWLEDGMENTS

Cancer Research UK sponsored this work. The authors acknowledge the invaluable assistance of Dr. Rao Vishnuvajjala (NCI), Dr. Walter Shaw (Avanti Polar Lipids) and Dr. Nigel Westwood (Cancer Research UK). Lym-X-Sorb™ was invented by David W. Yesair, is proprietary to
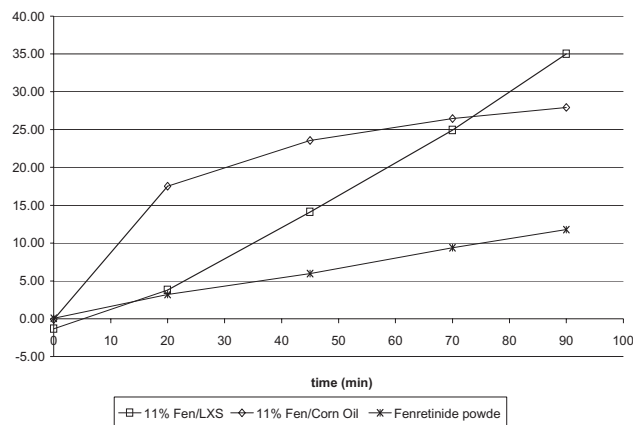

Fig. 1. 'Fed' buffer capsule dissolution for 4-HPR powder only, 11%w/w 4-HPR in LXS and in corn oil.

BioMolecular Products Inc., and manufactured under license by Avanti Polar Lipids Inc.

REFERENCES

[1] B. J. Maurer, O. Kalous, D. W. Yesair, X. Wu, AV. Maldondo, V. Khankaldyyan *et al*, "Improved oral delivery of *N*-(4-Hydroxyphenyl) Retinamide with a novel LYM-X-SORB organised lipid complex" *Clin. Cancer Res.*, **13(10)** (2007) 3079–3086.

[2] J. B. Dressman and C. Reppas, "In vitro-in vivo correlations for lipophilic, poorly water soluble drugs" *Eur. J. Pharm. Sci.*, **11** Suppl 2 (2000) S73-S80.

[3] A. Kattige and G. Rowley, "Influence of rheological behaviour of particulate/polymer dispersions on liquid-filling characteristics for hard gelatin capsules" *Int. J. Pharm.*, **316** (2006) 74–85

Exploring roll compaction of two commonly used pharmaceutical powders

Shen Yu[1], Bindhu Gururajan[2], Gavin Reynolds[3], Ron Roberts[3], Chuan-Yu Wu[1], Mike Adams[1]

[1]School of Chemical Engineering, University of Birmingham, Edgbaston, Birmingham, B15 2TT
[2]Pharmaceutical Development, AstraZeneca, Charnwood Bakewell Road, Loughborough, LE11 5RH
[3]Pharmaceutical Development, AstraZeneca, Macclesfield, Cheshire, SK10 2NA

Abstract – **The effect of powder flow properties on roll compaction behaviour of microcrystalline cellulose (MCC) and di-calcium phosphate dihydrate (DCPD), which have distinctive flow properties, was experimentally investigated. A robust approach for determining the nip angle that defines the compaction region was also developed. It was found that powder flow properties play a significant role in roll compaction.**

INTRODUCTION

Roll compaction is widely used as a dry granulation process in the pharmaceutical industry. The densification of the feed powder is primarily described by two parameters: the maximum pressure and the nip angle. The process behaviour depends on system layouts, processing conditions and feed powder properties.

MATERIALS AND METHODS

Two commonly used pharmaceutical excipients: MCC (Avicel PH102) and DCPD (Calipharm D) were considered. The flow functions (ff_c) of these powders measured using a ring shear cell indicates that MCC is easy flowing (i.e. $4 < ff_c < 10$) while DCPD is cohesive (i.e. $2 < ff_c < 4$). The powders were roll-compacted using a lab-scale instrumented roll com-

pactor. In this study, the minimum roll gap was fixed at 1.0 mm and the roll speed was varied from 0.5 to 5 rpm. The pressure distributions were recorded with a pressure sensor, from which the maximum compression pressure and nip angle were determined. A robust method was developed to accurately determine the nip angle by multivariate fitting the pressure gradient with the Johanson equations [1].

RESULTS AND DISCUSSION

The maximum pressures for MCC and DCPD at different roll speeds are shown in Fig. 1. And the corresponding nip angles determined from various approaches are shown in Fig. 2. It can be seen that the maximum pressure and nip angle for DCPD decrease sharply as the roll speed increases. However, the maximum pressure and nip angle are relatively independent of the roll speed for MCC. The nip angles determined using the present approach are comparable with those obtained using the method employed in ref. [2]. Nevertheless, the present approach is based on the intrinsic features of slip and no-slip interactions during the process without resourcing to independent measurements of wall friction.

CONCLUSIONS

Roll compaction behaviour of two common pharmaceutical powders with distinctive flow properties was investigated. A robust method with the advantage in determining the nip angle directly from roll compaction experiments was developed. It was found that the flow properties of powders play a significant role and the maximum pressure and nip angle depends strongly on the material flow properties

REFERENCES

[1] J.R. Johanson, "A rolling theory for granular solids" *J. Appl. Mech.*, **32** (1965) 842–848.
[2] G. Bindhumadhavan, J.P.K. Seville, M.J. Adams, R.W. Greenwood, S. Fitrzpatrick, "Roll compaction of a pharmaceutical excipient: Experimental validation of rolling theory for granular solids" *Chem. Eng. Sci.*, **60** (2005) 3891–3897.

Fig. 1. Maximum pressure for MCC and DCPD at various roll speeds.
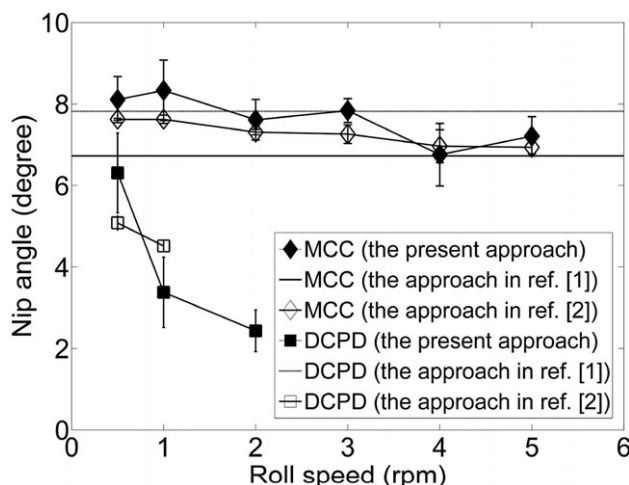
Fig. 2. The variation of nip angle with roll speed.

Feasibility study to investigate the application of Mechanofusion to improve flow properties of a cohesive API

Ravi Paw, Paul Goggin, Gurjit Bajwa

Global Research and Development, Pfizer Inc, Ramsgate Road, Sandwich, Kent CT13 9NJ, UK

INTRODUCTION

Mechanofusion (MF) is a dry coating process where a thin coating of excipient is applied onto the surface of an active pharmaceutical ingredi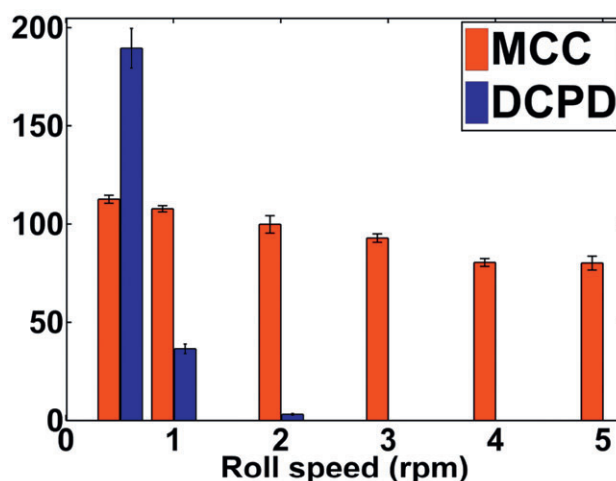ent (API) using high shear forces. The aim of this feasibility study was to investigate if MF could be used to improve the flow properties of 'Compound X'. Compound X is a cohesive drug and has a mean particle size of ~80 μm. A range of techniques were used to determine the flow properties of the processed blends. In addition, the effect on dissolution was also investigated.

MATERIALS AND METHODS

Twenty blends containing API were processed using a Hosokawa AMS-Mini Mechanofusion processor with the following excipients: Magnesium Stearate (MgSt), Fumed Silica, Sodium Stearyl Fumerate, L-leucine, Microcrystalline Cellulose (Avicel PH 101) and Polyvinylpyrrolidone (PVP). The following experimental parameters were considered: concentration of excipients (1, 5 and 20 %w/w), time (3, 5, 15 and 20 minutes), speed (1000 and 2000 rpm) and two different processing heads (Nobilta or Nonocular). For comparison, turbula blending was also investigated using the same excipients. Processed samples were characterised using the following flow tests: Carr's Index, Schulze ring shear cell (RST-XS) and Freeman Technology Rheometer (FT-4). Dissolution testing was carried out using USP II apparatus.

RESULTS AND DISCUSSION

Flow data showed that the Nobilta processing head with the following excipients and experimental parameters exhibited the largest improvement in flow; Sodium Stearyl Fumerate, MgSt and Fumed Silica using 5 %w/w concentration, processed at 2000 rpm for 5 minutes (higher energy). The results from the ring shear tester showed that the Flow Function Coefficient (FFC) increased from 4.4 (unprocessed API) to 7.3, 8.9, and 6.7 respectively (Table 1). Also, 1 %w/w MgSt at 1000 rpm for 20 minutes (lower energy) demonstrated a good improvement in flow, FFC 6.6. One-way ANOVA was used to compare FFC between batches and there are statistically significant batch differences ($p < 0.05$). The Carr's Index and FT-4 flow results for the different blends were in good agreement with the ring shear tester results above.

Dissolution testing was undertaken on processed blends which exhibited good flow. An effect on dissolution was observed, unprocessed API showed a rapid release (80% release within 2 minutes). Time taken for 80% release for API processed using the Nobilta head with 1 %w/w MgSt at 1000 rpm for 20 minutes increased to 6 minutes. A similar change in dissolution was observed for blends processed using the Nobilta head with 5 %w/w MgSt, Fumed Silica and Sodium Stearyl Fumerate (Fig. 1) at 2000 rpm for 5 minutes, the time taken for 80% release increased to 6, 4, and 6 minutes, respectively.

Table 1: FFC determined by Schulze ring shear cell

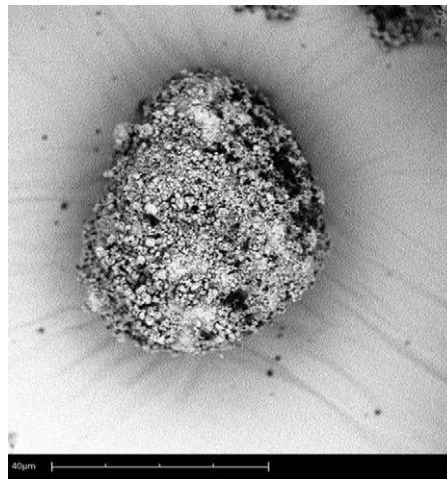| Powder flow behaviour	Flow Function Coefficient (FFC)
Severe Deficiency	<3.5
Deficiency	3.5–5.0
Marginal	5.0–8.0
Attribute	>8.0

Fig. 1 SEM image of API coated with Sodium Stearyl Fumerate.

CONCLUSIONS

This study has demonstrated that MF can be used to improve the flow properties of the cohesive API investigated. The different flow tests used showed good reproducibility and the results were in good agreement. Furthermore, we have also seen that MF can affect dissolution by slowing down the release. The addition of disintegrants may offset any changes in dissolution observed.

ACKNOWLEDGMENTS

Development of Fly Model for Anti-Cancer Drug Screen

Anjali Bajpai[1], Sumbul Jawed Khan[1], Subhabrata Pal[1], Mohammad Atif Alam[1], Ram Prakash Gupta[1], Sneh Harsh[1], Arati Mishra[1], Poulam Patel[2] and Pradip Sinha[1]

[1]Department of Biological Science and Bioengineering, Indian Institute of Technology Kanpur, Kanpur, India
[2]School of Molecular Medical Sciences, Division of Clinical Oncology, University of Nottingham

INTRODUCTION

The model organism fruit fly, *Drosophila,* displays strong conservation of human disease-linked genes, cancers in particular [1, 2]. It has thus emerged as an excellent model organism to explore basic cellular mechanisms linked to carcinogenesis and also for anti-cancer drug screen [3]. We are exploring this model organism to uncover the signalling path-

ways linked to cancer, their cellular roles during carcinogenesis and develop *in vivo* anti-cancer drug screening strategies.

MATERIALS AND METHODS

The strategy of tumour induction entailed generation of somatic clones [4], mutant for tumour suppressor genes, such as *lgl* and *scrib,* in larval epithelial sheets, called imaginal discs, which give rise to future adult organs. These somatic clones, therefore, are equivalent to surgical transplants of initiated tumours in a host. The mosaic epithelium is then examined during larval development for cellular phenotypes, expressions of individual genes and also gene expression profiles in transcriptomes. Tumours were clonally initiated using three strategies: (a) in *M* mutant host genetic background that eliminated intercellular surveillance by the surrounding healthy cells to permit unbridled growth of the initiated clone; (b) in a host genetic background that compromises apoptosis, (c) finally, by co-activating any one of the misregulated pathways to drive tumour progression. Clonal progression of tumour was examined after growing the host larvae in medium containing selected anti-cancer agents.

RESULTS AND DISCUSSION

Here we report development of multiple *in vivo* models for tumour progression and its utility in anti-cancer drug screen. Genome-wide transcriptional profiling of these tumours revealed activation of multiple cooperating partners during tumour progression, including N, WNT, TGF-beta, HIPPO, TOR, MYC and RAS. Further, in functional tests, upregulation of any one of these cooperating partners resulted in metastasis of *lgl* or *scrib* mutant somatic clones. We also show that these pathways drive tumour progression by arresting apoptosis, induced by the neighbouring healthy cells.

Finally, we also show that all the three models of clonal progression of tumour reported here are amenable to *in vivo* anti-cancer drug screen.

CONCLUSIONS

Our results provide a comprehensive catalogue of the multiple signalling pathways that partner during tumour progression besides uncovering the contributions of the intercellular surveillance mechanisms and regulation of apoptosis during tumour progression. The models of tumour progression reported here are therefore suitable for anti-cancer drug screens, particularly those targetted against specific signalling pathways.

ACKNOWLEDGMENTS

REFERENCES

[1] M.E. Fortini, M.P. Skupski, M.S. Boguski, I.K. and I.K. Hariharan, "A survey of human disease gene counterparts in the Drosophila genome" J. Cell Biol., **150** (2000) F23–30.

[2] I.K. Hariharan, D. Bilder, "Regulation of imaginal disc growth by tumour-suppressor genes in Drosophila" Annu. Rev. Genet, **40** (2006) 335–361

[3] M. Vidal, R.L. Cagan, "Drosophila models for cancer research" Curr. Opin. Genet Dev., **16** (2006) 10–16

[4] T. Xu, G.M. Rubin, "Analysis of genetic mosaics in developing and adult Drosophila tissues" Development **117** (1993) 1223–1237.

Gluconolactone as a Potential Carrier to Improve Dissolution Rate of Carbamazepine from Physical Mixtures and Solid Dispersion Formulations

Hiba Al-Hamidi[1], Alison A. Edwards[1], Mohammad A. Mohammad[2,3], Ali Nokhodchi[1]

[1]Medway School of Pharmacy, Universities of Kent and Greenwich, Central Avenue, Kent ME4 4TB, UK
[2]Department of Pharmaceutics and Pharmaceutical Technology, Damascus University, Syria
[3]Faculty of Pharmacy, International University for Science and Technology, Syria

Abstract – **Gluconolactone was used as a hydrophilic carrier to enhance the dissolution of carbamazepine (CBZ) from its solid dispersion and physical blend formulations. The results showed that the type of solvent used in the preparation of solid dispersion had a significant effect on CBZ dissolution. Solid dispersions made from binary mixtures of ethanol/water or acetone/water showed a significant enhancement in the dissolution rate of CBZ. Characterisation of the solid state of the solid dispersions showed the complete absence of crystallinity for samples that showed the highest dissolution rate.**

INTRODUCTION

The most effective method for improving the dissolution rate of poorly water-soluble drugs is the solid dispersion technique, but this is reliant on a suitable carrier and solvent

[1, 2]. The aim of the present work is to explore D-gluconolactone as a potential hydrophilic carrier to improve the dissolution rate of a poorly water-soluble drug, carbamazepine, from physical mixtures and solid dispersion formulations. The effect of solvent used, for the preparation of solid dispersion, on the dissolution rate of carbamazepine-carrier dispersion formulations was also investigated.

MATERIALS AND METHODS

Solid dispersions of the carbamazepine (Sigma, USA) and D-gluconolactone (Sigma, USA) were prepared using different ratios by the conventional solvent evaporation method. Different solvents (ethanol, acetone and water) were used in the preparation of solid dispersions. Carbamazepine and carrier (gluconolactone) were dissolved in a single or binary solvent mixture. The solvents were then removed at 40 °C for 24 hours under stirring conditions. The resultant solid dispersions were collected, pulverised using a mortar and pestle, and stored in desiccators for further analysis. Corresponding physical mixtures of carbamazepine and gluconolactone were prepared for comparison purposes. The properties of all solid dispersions and physical mixtures were studied using a dissolution tester, FTIR, SEM and DSC.

RESULTS AND DISCUSSION

The results showed that the presence of gluconolactone can increase the dissolution rate of CBZ compared to unprocessed CBZ (Table 1). However, all solid dispersions of CBZ-gluconolactone prepared from single solvent (acetone or ethanol) and the physical mixtures showed a considerably high dissolution rate for CBZ when the percentage of the drug was high (drug:carrier ratio was 2:1 for physical mixture and 1:2 for solid dispersions prepared from single solvent). Solid dispersions (1:4) prepared from binary solvents (acetone/water or ethanol/water) showed a higher dissolution rate for CBZ compared to a single solvent (Figure 1) due to the complete absence of crystallinity. The dissolution efficiency of solid dispersions prepared with different solvents can be ranked as follows acetone/water > ethanol/water > acetone > ethanol.

CONCLUSIONS

The use of D-gluconolactone in both solid dispersion formulations and physical mixtures enhanced the dissolution rate of a poorly water-soluble drug (carbamazepine). The method of

Table 1. Effect of solvent type on the dissolution parameters of solid dispersion formulations and physical mixtures

CBZ : carrier	Solvent	DE$_{120min}$	MDT	MDR
Pure CBZ	–	13.66 ± 2.5	7.76 ± 1.6	0.09 ± 0.02
2 : 1	PM	65 ± 4.6	28.2 ± 2.3	1.2 ± 0.05
2 : 1	Acetone	21.3 ± 4.3	46.5 ± 20	0.36 ± 0.04
1 : 2	Acetone	58.3 ± 2.9	34.4 ± 3.2	1.1 ± 0.03
2 : 1	Ethanol	8.4 ± 4.5	80.4 ± 1.9	0.31 ± 0.1
1 : 2	Ethanol	51.3 ± 4.9	39.7 ± 7.7	0.9 ± 0.13
2 : 1	A/W	39.3 ± 13	41.9 ± 35	0.6 ± 0.1
1 : 4	A/W	66.3 ± 2.0	27.0 ± 3.9	1.1 ± 0.03
2 : 1	E/W	36.8 ± 7.3	44.5 ± 2.0	0.66 ± 0.15
1 : 4	E/W	63.1 ± 0.5	23.4 ± 0.7	1.02 ± 0.01

DE = dissolution efficiency; MDT = mean dissolution time; MDR = mean dissolution rate; PM = physical mixture; A = acetone; E = ethanol; W = water
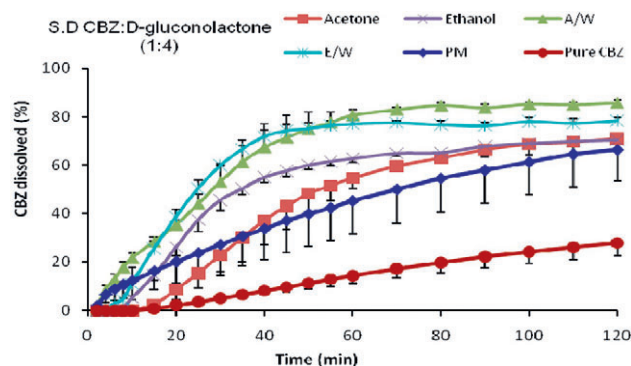

Figure 1. Dissolution profiles of CBZ from physical mixtures with different ratios of CBZ: gluconolactone.

preparation played a major role in the dissolution enhancement of CBZ and the ratio of drug:carrier caused the highest impact on the dissolution rate of CBZ containing gluconolactone.

REFERENCES

[1] J.L Ford, The Current Status of Solid Dispersions, *Pharm Acta Helv*., **61** (1986) 69.

[2] H. Al-Hamidi, M.M. Amin, A.A. Edwards, A. Nokhodchi. To enhance dissolution rate of poorly water-soluble drugs: Glucosamine hydrochloride as a potential carrier in solid dispersion formulations. *Colloids and Surface B-Biointerfaces*, **76** (2010) 170–178.

Growth mechanisms during fluidised hot melt granulation (FHMG): effects of binder / filler properties

H. Zhai[1], S. Li[1], D. S. Jones[1], G. Walker[2], G. P. Andrews[1]*

[1]School of Pharmacy, Queen's University of Belfast, Belfast, UK.
[2]School of Chemistry and Chemical Engineering, Queen's University of Belfast, Belfast, UK.

INTRODUCTION

Fluidised hot melt granulation (FHMG) is a novel granulation technique for processing pharmaceutical powders. Various process variables have been investigated and several parameters have been considered to influence the granulation process significantly [1]. The aim of our study is to investigate the effects of the binder and filler properties on the agglomerate growth mechanisms during fluidised hot melt granulation.

MATERIALS AND METHODS

Low-melting point co-polymers of polyoxyethylene- polyoxypropylene, Lutrol® F68 and Lutrol® F127 were used as meltable binders, whereas hydrophilic and hydrophobic ballotini beads were used as model fillers.

A laboratory fluid bed dryer was used for the FHMG process. The binder content for each experiment was fixed at 6% w/w, which has been determined as a suitable value for ballotini-Lutrol® system in previously published work [2]. The size distribution of granules was determined using standard sieve analysis and optical microscopy was used to investigate binder distribution within formed granules.

RESULTS AND DISCUSSION

Increasing binder particle size and rendering the filler surface more hydrophobic delayed the onset of granulation. A higher viscosity binder and a larger binder particle size prolonged the time required to achieve constant granule mass due to the increased resistance of the binder to deformation (function of viscosity) and thus the reduced immersion of the filler in the large binder droplets. Additionally, breakage of the formed granules was promoted using a smaller binder particle size, lower binder viscosity and a more hydrophilic surface on the filler.

As shown in Fig. 1, when using a smaller binder size, agglomerate growth via a distribution mechanism was found to dominate. Increasing the binder particle resulted in a shift on growth mechanism from distribution to immersion. The
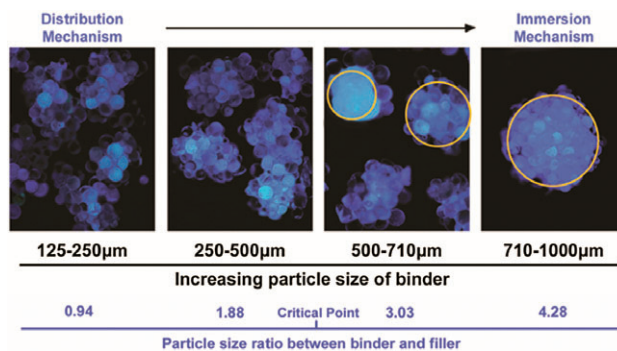

Fig. 1. Microscopic images of granules produced by binders of different particles size. In all cases, the filler had a particle size of 200 ± 50 μm

ratio between the particle size of the binder and filler has been shown to be informative for prediction of the granulation growth process.

CONCLUSIONS

Agglomerate growth mechanisms during FHMG were investigated in this study using simple glass beads and model fillers in combination with low melting point binders. Binder particle size, viscosity and the surface hydrophilicity of the filler were determined to affect the size distribution, onset time of granulation and the breakage characteristics of granules. Fluorescence microscopy was successfully used as an effective tool to investigate the agglomerate growth mechanisms during the FHMG process.

REFERENCES

[1] G. Walker, S. Bell, M. Vann, H. Zhai, D. Jones, G. Andrews, "Pharmaceutically engineering powders using FHMG: the effects of process parameters and formulation variables" *Chem Eng. Res. Des.* **85(A7)** (2007), 981–986.

[2] H. Zhai, S. Li, G. Andrews, D. Jones, S. Bell, G. Walker, "Nucleation and growth in fluidised hot melt granulation" *Powder Technology* **189(2)** (2009), 230–237.

HPMC solution properties and extended release performance of HPMC matrices containing a homologous series of alkyl sulphate surfactants

J. Mongkolpiyawat , C.D. Melia

Formulation Insights, School of Pharmacy, University of Nottingham, Nottingham, NG7 2RD, UK.

Abstract – **HPMC solution properties showed a dependence on alkyl chain length and evidence of polymer solubilisation at micellar concentrations. Extended release kinetics of HPMC matrices were similarly influenced but this dependency was reduced when Starch1500 was used as a tablet diluent.**

INTRODUCTION

Sodium dodecyl sulphate is thought to alter the hydrophobic/hydrophilic balance of hydroxypropyl methylcellulose (HPMC) through micellar solubilisation of hydrophobic domains [1]. This work explores (i) the effects of surfactant chain length (ii) if this influences drug release from HPMC matrices, and (iii) whether the use of a less soluble tablet diluent obviates surfactant effects.

MATERIALS AND METHODS

The homologous series was sodium hexyl sulphate (C6), sodium octyl sulphate (C8), sodium decyl sulphate (C10) and sodium dodecyl sulphate (C12). HPMC was Methocel™E4M CR. Surface tensiometry (Sinterface tensiometer PAT1, Berlin, Germany) was undertaken on 0.1%w/v HPMC solutions containing surfactant. Sol-gel transition temperatures (SGTT) were determined on 1%w/v HPMC solutions by turbidimetry (CPA-QMC, Nottingham, UK). Matrix tablets (flat-faced, round, 8 mm, 250 mg) containing 30% HPMC, 10% Caffeine anhydrous, 10% surfactant and 50% dextrose or Starch1500 (Colorcon, UK) were direct compressed at 280 MPa using a Manesty F3 press (Liverpool, UK). Drug release studies were undertaken using USP apparatus 1, 100 rpm, 900 ml water, $37 \pm 0.5°C$ (n = 3).

RESULTS AND DISCUSSION

The effect of surfactants on HPMC solutions: Tensiometry showed that all surfactants exhibited critical aggregation concentrations (CAC) in solution with HPMC. Pre-micellar concentrations of surfactants also lowered the SGTT of HPMC solutions but progressively raised this temperature at post-micellar concentrations. There was a direct correlation (r = 0.997) between the inflexion in the SGTT curve and CAC, and the rate of SGTT elevation at post-micellar concentrations, correlated directly with the carbon chain length of the surfactant.

The lowering of SGTT suggests these ionic surfactants exert a Hofmeister effect at pre-micellar concentrations, in which there is ionic depletion of the polymer water sheath

Table 1. Dependence of HPMC solution and matrix drug release properties on alkylsulphonate chain length.

	Concentration of surfactant (mM)		Drug release dextrose (T80%) mins
	CAC	SGTT	
C6	500	300	167
C8	130	100	162
C10	30	22	195
C12	4	6	222

around the hydrophobic, methoxyl-rich, regions of HPMC. When micellar concentrations are reached the tensiometry suggests polymer:surfactant associations intervene, resulting in an increase in polymer molecular hydration through solubilisation of the hydrophobic regions. The relationship between different chain length surfactants, their ability to solubilise HPMC and to raise SGTT, reflects their increasing ampiphile nature as carbon chain length is increased.

The effect of surfactants on HPMC matrices: In matrices containing a soluble diluent (dextrose) surfactant chain length had a rank order effect on drug release kinetics (Table 1). C6 and C8 accelerated release, whereas C12 retarded drug release in comparison with a dextrose control. This suggests polymer-surfactant interactions may influence the diffusion barrier properties of the matrix gel layer. Matrices containing Starch1500 showed no difference in release profile with surfactant chain length.

CONCLUSIONS

These results suggest that micellar association between alkyl sulphate surfactants and HPMC is strongly influenced by surfactant chain length. This may also influence the extended release performance of HPMC matrices containing soluble diluents but not those containing Starch1500.

ACKNOWLEDGMENTS

REFERENCE

[1] S. Nilsson, "Interactions between Water-Soluble Cellulose Derivatives and Surfactants. 1. The HPMC/SDS/Water System" *Macromolecules*, **28** (1995) 7837–7844.

Hydrocortisone Mini-Tablets for Pediatric Delivery

F. Mohamed[1], R. Saleem[1], M. Roberts[1], U.U. Shah[2], L. Seton[1], J.L. Ford[1]

[1]School of Pharmacy and Biomolecular Science, Liverpool John Moores University, Liverpool, UK.
[2]Medicines for Children Research Network, Alder Hey Children's NHS Foundation Trust, Liverpool, UK.

INTRODUCTION

Hydrocortisone, a steroid used as replacement therapy in adrenocortical deficiency state, is available as 10 mg tablets which are routinely quartered in an attempt to deliver the recommended 2.5 mg dose to paediatric patients. Previous work has shown the inaccuracy of dosing via this method and highlighted the need for appropriate paediatric formulations of hydrocortisone [1]. Mini-tablets are compact dosage forms, typically 2–3 mm in diameter, and a recent study demonstrated that they are a suitable formulation for 2–6 year-old children [2]. The aim of this work was to investigate the feasibility of developing hydrocortisone mini-tablets for accurate paediatric dosing under simulated rotary press production conditions. The weight and dose uniformity of mini-tablets was compared with quartered tablets.

Fig. 1. Hydrocortisone release from mini-tablets and quartered tablets (mean ± SD, n = 6)

MATERIALS AND METHODS

Hydrocortisone 10 mg tablets (Auden Mckenzie Ltd, UK) were quartered using a standard tablet cutter. A model formulation for mini-tablet production was developed, comprising; 16.67% w/w hydrocortisone (Courtin & Warner Ltd, UK), 72.33% w/w lactose (Tablettose® 80, Meggle, Germany), 0.5% w/w Aerosil® 200 (Evonik, Germany) and 0.5% w/w magnesium stearate (BDH, UK). Materials were initially blended for 5 min at 42 rpm using a turbula mixer (Type 2C, WAB, Switzerland) prior to sieving (500 μm aperture, Endecotts, UK) and subsequent blending for 2 min with magnesium stearate. Hydrocortisone mini-tablets, 3 mm in diameter, were manufactured by direct compression using a Stylcam® 100R rotary press simulator (Medel'Pharm, France) at a compression force of 2–3 kN and speed of 20 rpm (equivalent to a rotary tablet press production rate of ~80,000 tablet per hour). The weight uniformity of mini-tablets and quartered tablets was calculated and the strength of the mini-tablets determined (6D tablet tester, Schleuniger, Germany). Drug release from quartered tablets and mini-tablets was evaluated (USP apparatus 2, 50 rpm, 900 ml water at 37°C) over a period of 30 min using a Varian VK 7000 dissolution tester and Cary 50 UV spectrophotometer at 248 nm. Data were analysed for statistical significance ($P < 0.05$) using the Minitab™ software package.

RESULTS AND DISCUSSION

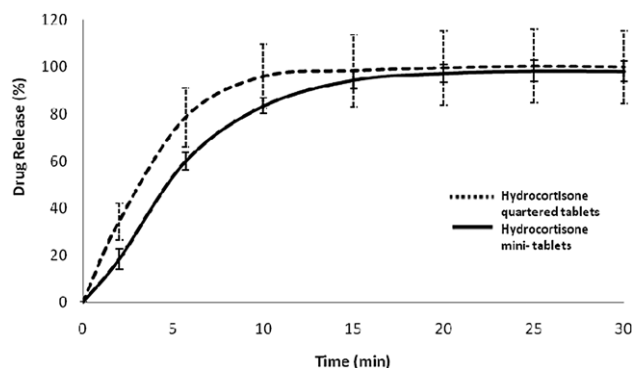Robust mini-tablets with a mean strength of 1.73 (±0.54) MPa were successfully manufactured under simulated rotary press production conditions using a model hydrocortisone formulation. Mini-tablets displayed significantly better weight uniformity (mean = 16.1 mg, CV = 4.29%) when compared to quartered tablets (mean = 58.9 mg, CV = 13.6%). Although rapid and complete dissolution was achieved from both mini-tablets and quartered tablets (Fig. 1), a high variation in the intended dose of 2.5 mg (83.5–115.5%) was observed with quartered tablets, whilst a significantly lower dose variation was achieved with mini-tablets (95.1–105.7%).

CONCLUSIONS

This research has illustrated the improved weight and dose uniformity achieved through a hydrocortisone mini-tablet formulation, which could improve the accuracy of paediatric dosing over the current practice of manipulating adult dosage forms via quartering tablets. The feasibility of industrial scale production of hydrocortisone mini-tablets has been demonstrated.

REFERENCES

[1] K. Heames, P. Riby, U.U. Shah, J. Blair and J.L. Ford. "Risk of inaccurate hydrocortisone dosing from quartered tablets", 37th Meeting of the British Society for Paediatric Endocrinology and Diabetes (2009), Reading, UK.

[2] S.A. Thomson, C. Tuleu, I.C.K. Wong, S Keady, K. Pitt and A. Sutcliff. "Assessing the acceptability of mini-tablets for use in children aged 2–6 years old", *Pediatrics* **123** (2009) 235–238

In situ characterisation of pharmaceutical crystallisation using Vis spectroscopy

G. Nagy, T.A. Salaoru, M. Li

School of Pharmacy, De Montfort University, Leicester, UK.

Abstract **– In this paper, a Vis spectrometer equipped with transmission and reflection probes has been used to monitor a pharmaceutical crystallisation process *in situ*. The experimental results during a batch crystallisation of glycine have shown that the information obtained by the two probes can be used to characterise the dynamics of the process, such as onset of crystallisation, meta-stable zone width (MSZW), crystal size/size distribution, and crystal growth rate.**

INTRODUCTION

Crystallisation is an important unit operation in the pharmaceutical, food and fine chemical industries. In-process measurement and control of the process parameters, such as crystal size distribution, solid and solution concentrations, and onset of crystallisation, are important to understand the process and for close control of high value-added product quality [1]. Many online process analytical techniques, such as NIR, IR, Raman, FBRM (Focused Beam Reflectance Measurement), video microscopy and UV-Vis spectroscopy, have been used for *in situ* monitoring and control of crystallisation processes. In early studies [2, 3], it has been shown that the particle size and concentration in a suspension can be determined accurately using simple techniques based on optical transmission measurements. They have, however, limited applicability in practical applications as they are usually accurate for suspensions with a low concentration of solid particles. In this work, a combination of reflection and transmission measurements of Vis spectroscopy has been investigated to monitor the process parameters during the crystallisation of glycine from aqueous solutions.

MATERIALS AND METHODS

The cooling crystallisation of glycine (Sigma-Aldrich, <99% purity) from water was performed in a 0.5 L jacketed vessel. Experiments on the crystallisation of glycine were carried out by cooling an aqueous solution of 27.6% by mass [4] from 45°C to 10°C using a linear cooling rate of 0.2°C /minute. The temperature was then kept constant at 10°C for 300 minutes. The *in-situ* transmittance and reflection spectral measurements were carried out using an Avantes2048 dual channel spectrometer equipped with a transmission dip probe with variable path length and a reflection probe. The spectral data from 400–900 nm were collected every 6 minutes. Integration time of 6000 ms and an average of 20 spectra were used for each of the recorded spectra.

RESULTS AND DISCUSSION

Figure 1 shows the variation of reflectance and transmittance spectra with time at five different wavelengths during the crystallisation process.
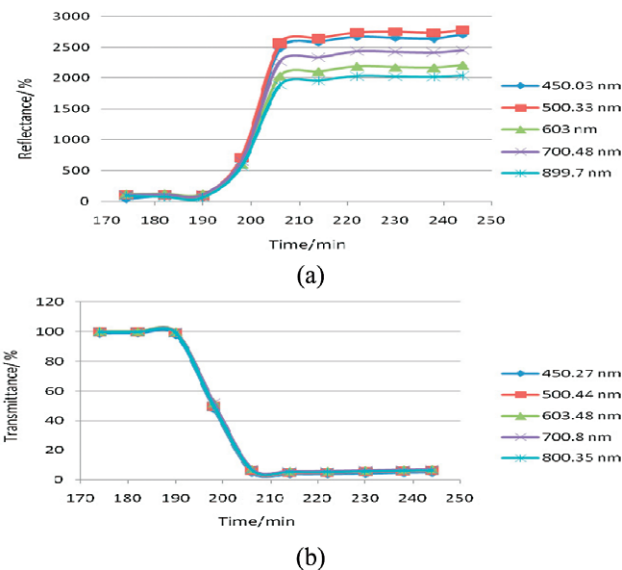

Fig. 1. Variation of reflectance (a) and transmittance (b) with time at different wavelengths during cooling crystallisation of glycine.

Figure 1a shows the reflectance during the process, which increases dramatically at 198 minutes, indicating the onset of crystallisation of the glycine. The same information is shown in Figure 1b in the transmission spectra. Before 198 minutes the transmittance is stable at 100%, after which it falls to 0. The sudden change in reflectance and transmission spectra is associated with the primary nucleation of glycine. Compared with the transmittance spectra which stays constant at 0 after 198 minutes, the reflectance spectra continue to increase steadily with the progress of the crystallisation shown in Figure 1a, indicting the growth of the glycine crystals. Therefore, the reflectance spectral data can be correlated with the crystal size/size distribution and their growth rate.

CONCLUSIONS

Our preliminary study shows that the Vis spectroscopy employed with transmission and reflection probes can be used to monitor the dynamic changes during the crystallisation processes, from which valuable information on important parameters can be characterised, such as onset of crystallisation, MSZW, crystal size distribution, and crystal growth rate.

REFERENCES

[1] R. Davey, and J. Garside, '*From Molecules to Crystallisers (An Introduction to Crystallisation)*, Oxford University Press, 2000

[2] M. Li, D. Wilkinson, "Particle Size Distribution Determination from Spectral Extinction using Evolutionary Programming', *Chem. Eng. Sci.*, **56** (2001), 3045

[3] M. Li, M., D. Wilkinson, "Particle Size Distribution Determination from Spectral Extinction using Neural Networks', *Industrial and Eng. Chemistry Res.*, **40**, (2001), 2275

[4] J.B. Dalton, C.L.A. Schmidt, 'The solubilities of certain amino acids in water, the densities of their solutions at 25 degrees and the calculated heats of solution and the partial molar volumes', Journal of Biological Chemistry, 103, (1933), 549–578

In-situ Phase Screening of Kofler Melt by Confocal Raman Mapping

Aalae Alkhalil[1], Jagadeesh B. Nanubolu[1], Clive J. Roberts[1&2], Jonathan W. Aylott[1&2], Jonathan C. Burley[1&2]

[1]Laboratory of Biophysics and Surface Analysis, School of Pharmacy, University of Nottingham, UK
[2]Nottingham Nanotechnology and Nanoscience Centre, Nottingham, UK

INTRODUCTION

Pharmaceutical co-crystals have been studied as a means to modify the properties of single-component materials, which is a matter of importance in drug development and delivery [1]. We report here the first application of spectroscopic mapping for screening Kofler melt preparations. Raman spectroscopy provides information on the inter-molecular vibrations by employing the lower energy phonon-mode bands (10–400 cm^{-1}) which proved to be far more sensitive to crystalline packing than traditional intra-molecular bands [2]. Thereby, such a screening was used to investigate the phases present in Kofler melt preparations.

MATERIALS AND METHODS

A Kofler melt preparation was carried out by placing a small amount of nicotinamide (NCT) on a glass microscopic slide under a coverslip which was heated until melting occurred, then allowed to solidify. Flurbiprofen (FBP) was then placed at the opposite edge of the coverslip and melted. Once melted, it was drawn by capillary action under the coverslip dissolving the juxtaposed part of the NCT. The whole preparation was then allowed to cool, a process through which components are then recrystallised. Afterwards, Raman mapping of 4030 spectra for the FBP-NCT Kofler system was performed using confocal Raman microscopy. Principal Component Analysis (PCA) of the Raman data in the phonon-spectral regions was undertaken. The first three principal components (PCs) were selected in this study having statistically significant values accounting for >93% of variances.

Raman spectra of the starting materials NCT and FBP form I, FBP form II, and co-crystal at the zone of mixing were acquired and used for assigning principal components' loadings to their original components.

RESULTS AND DISCUSSION

Raman mapping of the NCT-FBP Kofler melt preparation was conducted and the data was analysed by means of PCA. The first three principal components selected for this study, showed heavily loadings for the present compounds in the
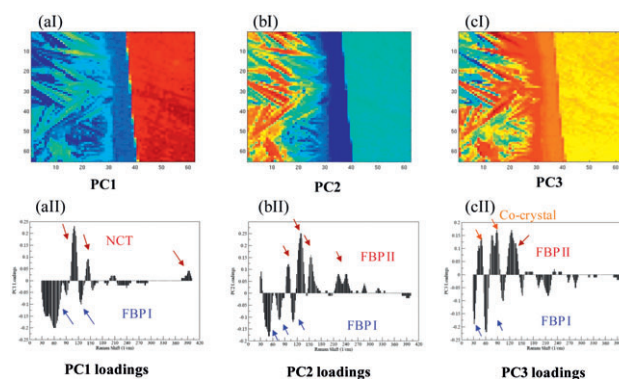

Fig. 1. PCA analysis results. The first three PCs' scores are shown in aI, bI, and cI; their corresponding loadings in aII, bII, and cII.

three optically different regions (figure 1 aI-cI). They displayed a homogeneous distribution of pure composition in the higher melting region (NCT), which forms a very distinct boundary once reaching the zone of mixing. In contrast, they highlighted the non-uniformity in components' distribution in the lowest melting region (FBP). The homogeneous composition at the higher melting region was clearly confirmed by studying the first principal component (PC1). PC1 was positively weighted by only NCT (figure 1aII). Alternatively, the lower melting region displayed heterogeneity in components' composition. Such an issue was proven by investigating PCs' loadings. Figures 1bII-cII show that components' weight on PC2 and PC3 refer to both FBP and co-crystal. They also exhibit some positive loadings, specifically on PC2, which don't match with any of the reference spectral bands. This highlighted the existence of another chemical form apart from the expected ones.

CONCLUSIONS

The work presented outlines the first use of confocal Raman microscopy to characterise Kofler melt preparations. This was shown to be valuable in generating detailed information on the investigated phases. It provided qualitative information about the new phases (co-crystal and component's poly-

morphs). From this work, we know that coupling the hot-stage with Raman microscopy provides new insight into the use of the Kofler method to screen co-crystal formation.

ACKNOWLEDGMENTS

REFERENCES

[1] A. V. Trask, et al. "Pharmaceutical Cocrystallisation: Engineering a Remedy for Caffeine Hydration", Crystal Growth & Design, 2005, **5**, 1013–1021.

[2] S. Al-Dulaimi, et al. "Rapid polymorph screening on milligram quantities of pharmaceutical material using phonon-mode Raman spectroscopy", Cryst. Eng. Comm, 2010, **12**, 1038–1040.

Investigating the Potential of a Reconstituted Oral Paediatric Hydrocortisone Formulation with Hydroxypropyl-B-Cyclodextrin

M. Orlu-Gul[1,2], G. Fisco[1,3], C. Tuleu[1]

[1]Department of Pharmaceutics and Centre for Paediatric Pharmacy Research, The School of Pharmacy, University of London, London, UK.
[2]NIHR, Medicines for Children Research Network, London and South East Local Research Network, London, UK.
[3]Department of Pharmaceutical Chemistry and Technology, Faculty of Pharmacy, University of Palermo, Palermo, Italy.

INTRODUCTION

Hydrocortisone (HC) is commonly used in children for the treatment of adrenal insufficiency as a life-long replacement therapy. Due to its frequent unlicensed use in practice [1] and great deal of concern regarding HC administration to paediatric patients, there is a need for development of age-appropriate formulation, especially for the age group 0–2 years. The pH range of maximum stability of HC is 3.5 to 4.5 [2]. The low aqueous solubility and bitter taste of HC represent a limiting step in the development of its paediatric formulation which could be overcome by cyclodextrins (CyDs). CyDs are potential child-friendly excipients for oral formulations and they act as solubility enhancer and taste masking agent by incorporating the drug molecule into their cavity and shielding it from the exterior. Based on the superior physicochemical enhancements of CyD, derivates over the natural CyDs, hydroxypropyl-β-CyD (HP-β-CyD) was selected to increase the solubility of HC in this study. As the antimicrobial efficacy of preservatives could reduce due to the complexation with CyD, various preservative combinations were tested. The form of powder for reconstitution provides a dry alternative to liquid by carrying the advantage of dosing flexibility as well as eliminating the longer term shelf-life stability issues related to liquid forms. The aim of this work was to formulate a reconstitutable oral paediatric HC formulation and study its chemical and microbiological in-use stability.

MATERIALS AND METHODS

HC (Fagron, UK) formulation (5 mg/ml) was optimised by screening excipients depending on their aqueous solubility, compatibility, non-toxicity and stability at the same pH range of the drug. It was pH stabilised by citric acid (Sigma Aldrich, UK) buffer pH 4.2, solubilised by the inclusion in HP-β-CyD (Sigma Aldrich, UK) at different drug:CyD molar ratios, flavoured by orange tangerine (Givaudan, Switzerland), sweetened by neotame (Nutra Sweet Company, US) and preserved by methyl paraben sodium salt (MP) (Sigma Aldrich, UK) and potassium sorbate (PS) (Sigma Aldrich, UK) at different concentrations. Four formulations were tested differing in their preservative concentration with a MP:PS of 0.15%:0.05% for F1, 0.1%:0.1% for F2, 0.05%:0.15% for F3 and no preservative in F4 which was a control. The stability test was conducted on samples kept either in tightly closed bottles or in bottles sampled each day to mimic parent/caregiver administration conditions, both at room temperature and in the fridge. A stability indicating HPLC method (mobile phase: acetonitrile: water+1% acetic acid (30:70), gradually to (60:40); stationary phase: 5 μm, C18 silica; flow rate: 1.0 ml/min; injection volume: 30 μl; wavelength: 247 nm) was developed and validated. The microbiological stability was tested by means of 'efficacy of antimicrobial preservation', 'total viable aerobic count' and 'absence of *Escherichia coli*' tests described in European Pharmacopeia [3].

RESULTS AND DISCUSSION

The HC: HP-β-CyD inclusion complex at a ratio of 1:6 allowed the complete solubilisation of the drug following reconstitution within 1 minute of handshake. All tested formulations were found to be chemically stable with a HC recovery of >95% after a month. The microbiological assessment proved that the selected preservative combination (F2) was efficient at room temperature and showed that tested formulations including preservative met the recommended acceptance criteria for microbiological quality after reconstitution with or without repetitive sampling.

CONCLUSIONS

The developed reconstituted oral paediatric HC formulation stable for 1 month has the potential to facilitate availability, affordability and acceptability. Future studies on taste assessment and long term stability are required with respect to patient adherence and safety.

REFERENCES

[1] A.R. Lowey and M.N. Jackson. "A survey of extemporaneous preparation in NHS trusts in Yorkshire, the north-east and London" *Hospital Pharmacist* **15** (2008) 217–219

[2] L.A. Trissel. 'Trissel's stability of compounded formulations' American Pharmacists Association, 2005 Washington, US.

[3] Pharmacopeia European, 6th edition, 2008, Strasbourg, France.

Investigation into tablet picking and sticking using an Instrumented Adhesion Punch

B. Ager, A.J. Mills, A.C. Bentham

Formulation Design and Development, Pharmaceutical Development, Pfizer Ltd., Sandwich, Kent, UK.

INTRODUCTION

Picking and sticking is a common problem encountered during tablet compression. It occurs when powder accumulates on the surface of the tablet punch, causing punch filming and picking on the tablet surface. Various quantitative techniques have previously been investigated to assess punch adhesion. Toyoshama *et al.* showed that evaluation of punch surface roughness can quantify the problem [1]. Roberts *et al.* identified punch surface roughness, compaction force and blend composition as main contributory factors [2]. Waimer *et al.* studied the adhesion force when an instrumented punch is removed from a tablet surface, suggesting that similar factors were the cause [3]. These conclusions emphasise the complexity of the problem, and this subsequently makes it difficult to design a holistic method to predict punch picking and sticking.

The aim of this study was to evaluate the utility of a compaction simulator equipped with an instrumented adhesion punch as a laboratory scale tool for prediction of picking and sticking at manufacturing scale. Test articles included single excipients (with/without external lubricant), and an internally-lubricated drug-excipient blend (with/without external lubricant) for which picking had previously been observed.

MATERIALS AND METHODS

Excipients examined were mannitol (Pearlitol 50 C, Roquette) and microcrystalline cellulose (MCC) (Avicel PH102, FMC Biopolymer). The internally-lubricated drug-excipient blend contained Drug A (Pfizer), MCC (Avicel PH102, FMC Biopolymer), lactose monohydrate (Fast Flo 316, Foremost Farms), sodium starch glycolate (Explotab, JRS Pharma) and magnesium stearate (vegetable-sourced, Mallinckrodt). This blend was prepared at 100 g scale to a standard 'blend-screen-blend' manufacturing process, with magnesium stearate added as lubricant prior to compression.

Tablets were compressed to a target weight of 300 mg and a target solid fraction of 0.7 using a 10 mm diameter flat-face instrumented adhesion punch (Phoenix Calibration and Services Ltd.) on a single-station compaction simulator (EHS
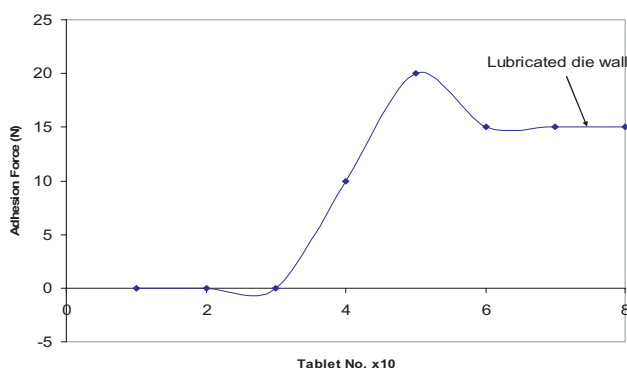

Fig. 1. Adhesion force response from instrumented punch with drug-excipient blend (internally lubricated), with/without external lubrication.

Ltd.). A single-sided compression profile for the punch was utilised, with a compression dwell time of 100 ms. Multiple compression events were run, with adhesion being detected by an amplified voltage response which was converted to an adhesion force (Newton) via a signal transducer.

RESULTS AND DISCUSSION

A progressively larger adhesion force was observed with mannitol, consistent with the known adhesion behaviour of this hygroscopic material. However, following external lubrication of the die, no adhesion force was subsequently detected, indicating die wall friction as the main contributory factor to the measured adhesion response. Conversely, no adhesion force was detected with 'non-sticking' microcrystalline cellulose.

For the drug-excipient blend, an adhesion force was first detected after 30 consecutive compression events (see Figure 1). External lubrication of the die wall after 75 compression events had no effect on the signal, suggesting adhesion to the punch surface is causing the dominant response. A repeat of this experiment failed to replicate the initial results, with no adhesion response detected. This indicates that further under-

standing of the critical test parameters that influence the adhesion response is required, to define an appropriate test regime.

CONCLUSIONS

The Phoenix instrumented adhesion punch has been developed for the quantitative assessment of adhesion forces between upper punch and tablet during compression using a compaction simulator. Initial experimental results are encouraging, although further work is necessary to define robust test regimes that ensure predictive reliability, including 'benchmarking' versus controls (manufactured drug products) with known adhesion character.

ACKNOWLEDGMENTS

REFERENCES

[1] K. Toyoshima, M. Yasumara, N. Ohnishi and Y. Ueda, "Quantitative evaluation of tablet sticking by surface roughness measurement" *Int. J. Pharm.,* **46** (1988) 211–215.

[2] M. Roberts, J.L. Ford, G.S. MacLeod, J.T. Fell, G.W. Smith and P.H. Rowe, "Effects of surface roughness and chrome-plating of punch tips on the sticking tendencies of model ibuprofen formulations" *J. Pharm. Pharmacol.*, **55** (2003) 1223–1228.

[3] F. Waimer, M. Krumme, P. Danz, U. Tenter, and P.C. Schmidt, "A novel method for the detection of sticking of tablets" *Pharm. Dev. Tech.*, **4** (1999) 359–367.

Investigation of hydrate formation using small scale wet granulation

J.C. Hooton, P. Lee, S.R. Holland, D.J. Murphy, T. Harris, S.C. Brown.

Pharmaceutical Development, AstraZeneca, Macclesfield, UK.

Abstract **– In order to investigate the formation of hydrate during wet granulation, small scale manufacturing trials were performed. The addition of small amounts of hydrate were found to seed the formation of hydrate in the granules produced. In addition it was also possible to get spontaneous formation of the hydrate in the absence of seed.**

INTRODUCTION

During the development of a novel, anhydrous compound (Compound A), solid state analysis showed that a hydrate form existed. Subsequent slurrying work indicated that small amounts of the hydrate could seed conversion of the anhydrous form of Compound A into hydrate at room temperatures in minutes. In order to understand if the rapid kinetics of conversion observed in the laboratory experiments were applicable to the wet granulation manufacturing process used to manufacture tablets, a small scale investigation was performed.

MATERIALS AND METHODS

Small scale granulations were performed using a Mi-Pro high shear mixer granulator (Pro-C-epT, Zelzate, Belgium). The current tablet formulation was used, and processing parameters used were scaled down from the current manufacturing process.

To investigate the potential for conversion to hydrate during the manufacturing process, a series of experiments

Table 1. Amount of hydrate formed during experiments.

	Material	Immediate dry	24 hour hold
Pure Compound A	Run 1	0%	0%
	Run 2	7%	–
2% Hydrate Seed		17%	74%
4% Hydrate Seed		30%	70%
100% Hydrate		100%	–

were undertaken using different amounts of hydrate as a percentage of the total API amount in the formulation. Manufactures with 0, 2, 4 and 100% hydrate present were performed. Material was either dried immediately or held wet for 24 hours prior to drying.

Granules were analysed using a Raman method to quantify the levels of the hydrate produced during the manufacturing process.

RESULTS AND DISCUSSION

The amounts of hydrate found in each experiment are shown in Table 1. It is seen that the amount of hydrate produced after immediate drying post-granulation is proportional to the amount added. However when dried after 24 hours the level is independent of the amount of hydrate initially added.

The formation of hydrate in the second run of the pure anhydrous API was unexpected. This suggests that hydrate formation may also occur by a self nucleation process.

In addition to this, tablets were made using the 100% hydrate and dissolution work was performed (data not shown). This data indicated that the presence of hydrate could impact upon the bioavailability of the API.

CONCLUSIONS

This work shows that small scale wet granulation may be used to investigate the formation of hydrate during processing. The small scale work showed that small amounts of hydrate may behave as seeds for the subsequent formation of hydrate in the product. In addition, the work has also shown that hydrate may also form by self nucleation during the wet granulation process.

ACKNOWLEDGMENTS

Investigation of the Effects of Sodium Lauryl Sulphate on the Roller Compaction of Spray Dried Dispersions

M.P. Thompson[1], W.C. Pantin[1], M. Vernon[1], S.T. Charlton[1], A.B. Dennis[1], P. Timmins[1]

[1]Bristol-Myers Squibb, Biopharmaceutics R&D, Moreton, CH46 1QW, UK.

INTRODUCTION

Spray drying of an API with a polymer to form a spray dried dispersion (SDD) is a technique of increasing importance to the pharmaceutical industry [1]. Spray drying can improve bioavailability by presenting the amorphous form in a stabilised state and creating a dispersion product that is suitable for manufacture [2, 3].

Hydroxypropyl methylcellulose acetate succinate (HPMC-AS) has been shown to form stable amorphous spray dried dispersions with a variety of different pharmaceutical compounds [2]. The study aim was to compare the processing properties of formulations containing spray dried HPMC-AS with or without the surfactant sodium lauryl sulphate (SLS), commonly used to facilitate drug release from tablet formulations.

MATERIALS AND METHODS

Tablet formulations contained 8.6 to 49.9% w/w of microcrystalline cellulose (Avicel PH 102) and mannitol SD200, and 0.3% w/w magnesium stearate (quantities adjusted for level of SDD and SLS). Each formulation contained 0, 10 or 80% w/w spray dried HPMC-AS, with and without SLS (2.5%w/w) included in the overall formulation.

Batches manufactured were split into sub-lots A or B (0 and 2.5% w/w SLS respectively). Blending was performed using a Turbula blender and roller compaction using a Freund Vector TF-Mini. Parameters were established using sub-lot A for each batch. B sub-lots were then processed using the same parameters. Ribbons were milled using a Frewitt MF-Lab. A Stylcam® tablet press replicator was used to produce 400 mg compacts with 0.85 solid fraction (SF).

True density of lubricated blends and granules were determined using helium pycnometry. Tensile strength of 400 mg compacts with 0.85 SF (obtained via a true density calculation) produced from blend and granule were calculated from

Table 1: Ribbon tensile strengths at the midpoint of the roller compaction process for formulations containing 0 or 10% SDD with 0 or 2.5% SLS. n = 5

Average Ribbon Tensile Strength (N mm^{-2}) n = 5	Percentage SDD in the formulation	Percentage SLS in the formulation
2.3	0.0	0.0
1.7	0.0	2.5
2.1	10.0	0.0
1.2	10.0	2.5

data generated using the Stylcam® and a tablet hardness tester. Granule surface area was determined using a nitrogen absorption method. Ribbon porosity was determined using a GeoPyc 1360. Fracture force and tensile strength of ribbon were determined using a texture analyser fitted with a 2 mm diameter cylinder probe.

RESULTS AND DISCUSSION

The inclusion of SLS resulted in different processing properties for the formulations investigated. Ribbon thickness was found to be generally lower, whereas roller compaction through-put time and ribbon porosity increased (23 and 30% porosity with 0 and 2.5%w/w SLS respectively) with reductions in ribbon tensile strength, *c.f.* 2.4–2.1 & 1.7–1.0 N mm^{-2} for sub-lots A & B; respectively (*Table 1*). Paradoxically, the compressibility of the granulations was found to be markedly reduced (tablet hardness at 2500 dN of 25 and 10SCU with 0 and 2.5%w/w SLS respectively). Historically in the pharmaceutical industry, tablet hardness is expressed in terms of Strong-Cobb Units or SCU, an *ad hoc* unit of force. It is generally believed that 1.4 Strong-Cobb Units represents approximately 1 Kg F. Hence, each strong-cobb unit is equiv-

alent to 0.7 Kg F or *circa* 7 Newtons. Further investigations were completed to elucidate a mechanistic understanding of the effect of SLS upon the ribbon, granule and tabletting characteristics.

CONCLUSIONS

SLS in formulations undergoing roller compaction was shown to alter the granule, ribbon and tabletting properties. SLS may have influenced particle-particle compaction and flow properties possibly by surface association. Increasing the level of SDD in the formulation appears to magnify the effects of the SLS. The spherical nature of the SDD particles may allow the

SLS to exert a greater surface effect and further decrease interparticulate cohesion and frictional forces.

REFERENCES

[1] C.A. Lipinski, "Poor Aqueous Solubility – An Industry Wide Problem in Drug Discovery" *Am. Pharm. Rev.*, **5** (2002) 82–85.
[2] T. Vasconcelos, B. Sarmento and P. Costa, "Solid dispersions as strategy to improve oral bioavailability of poor water soluble drugs" *Drug Discov. Today*, **12** (2007) 1068–75.
[3] C. Leuner and J. Dressman, "Improving Drug Solubility for Oral Delivery using Solid Dispersions" *Eur. J. Pharm. Biopharm.*, **50** (2000) 47–60.

Lyosense™ Lyophilisation Process Control

G. Smith[1], E. Polygalov[1], T. Page[2]

[1]School of Pharmacy, De Montfort University, Leicester, LE1 9BH, UK
[2]GEA Pharma Systems, School Lane, Chandlers Ford, Eastleigh, SO53 4DG

INTRODUCTION

State-of-the-art freeze-drying process control is limited to: the measurement of pressure (to monitor the duration of primary drying in which ice is removed directly to vapour); the control of the shelf coolant temperature; and the occasional in-vial temperature measurement (to measure the onset of ice formation) [1]. However, pressure measurements provide only the average drying time of the whole batch and individual vial data is inaccessible. Moreover, the inclusion of the "in-vial" sensor impacts both the on-set temperature (one is trying to measure) and the structure of ice (which in turn impacts the drying time). More recent attempts to develop on-invasive methods for measuring individual vial drying times have been proposed. However, these necessitate the application of a mathematical function to the measurement of some in-line physical parameter (e.g. external vial temperature), a process which is non-trivial [2].

The aim of this work is to develop an individual vial monitoring system (Lyosense™) for characterising lyophile product characteristics and process end points to establish and control lyophilisation regimes.

Lyosense™ is a process analytical technology based on dielectric analysis of the lyophilisation process. The system measures the pseudo-relaxation process associated with the interfacial polarisation of the glass wall, through the resistance of the sample. This process undergoes characteristic changes in amplitude and peak frequency, such that the progress of freeze-drying and condition of the sample can be controlled.

MATERIALS AND METHODS

Lyosense™ comprises a modified glass freeze-drying vial, with an electrode system deposited on the external surface, coupled to a high precision impedance analyser via miniature
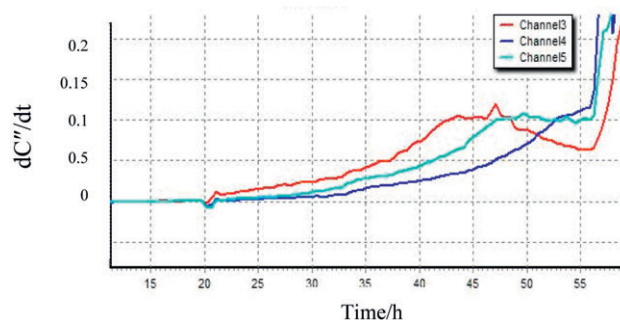

Fig. 1 Peak frequency and peak amplitude measurements throughout a typical freeze-drying cycle. Stages A to C are the freezing stage, primary drying, and secondary drying respectively.

coaxial connectors, which are surface mounted at the neck of the vial. The thermal mass of the vial-electrode-connector-system is <0.5% of the mass of the vial/product. Frequency scans of the system impedance were recorded during a range of freeze-drying cycles and placebo formulations. By varying the salt loading it was possible to simulate the impact of drug loading on the electrical conductivity of lyophile products. This is a critical parameter in the function of the Lyosense™ system, as it defines the limiting values of the peak frequency (from the high frequency limit in the non-frozen state to the low frequency limit in the frozen state).

RESULTS AND DISCUSSION

Changes in phase (e.g. ice formation) and completion of freezing, the onset of micro-collapse, and the end-points of primary and secondary drying are all detected by this method through changes in the measured impedance of the vial-electrode assembly.

These transitions are more easily determined if the impedance is displayed as a complex capacitance or dielectric permittivity, where the cell constant is presumed to equal 1.

The imaginary capacitance (C'', dielectric loss) is characterised by a peak in the frequency spectrum, which arises from the composite capacitor of the product in series with the glass vial. It has been demonstrated, in general, that the frequency of the peak is strongly coupled to the temperature of the product (through the interdependency of product temperature and/or phase on the electrical resistance of the product) whereas the height of the peak is dependent on the amount of ice remaining (in primary drying) and the residual surface moisture (in secondary drying).

As the cycle progresses the peak height decreases, with a characteristic sigmoid time-dependence (Figure 1) such that the derivative of the time-profile can be used to define the end of the primary drying.

CONCLUSIONS

In-process control may be established using the Lyosense™ system, through the definition of set-points (i.e. the product temperature during primary drying, to drive the process at a high temperature while avoiding collapse) and end points (to establish the moisture content of the product).

REFERENCES

[1] T.A. Jennings. Lyophilisation, 1999, InterPharm Press, Denver; p. 615–617

[2] A.A. Barresi et al. "In-line control of the lyophilisation process. Gentle PAT approach using software sensors" *Int. J. Refridgeration* **32** (2009) 1003–1014

Melt Granulation using a Twin-Screw Extruder

H.R. Allsop, M. Aurangzeb, N. Bhatti, G.E. Kaye

Department of Pharmacy, University of Bradford, Bradford, UK

AIMS

A literature review will be undertaken to determine various processes of granulation and melt granulation, and to verify if research supports the use of a twin-screw extruder for the process of melt granulation. Granules will be produced using a twin screw extruder at different levels of variables.

The granules will undergo tests to measure; particle size distribution, angle of repose, Carr's Index, Hausner Ratio, Heckel Plot and crushing strength so their flow properties may be determined.

METHODOLOGY

Using a Thermo Scientific Pharma HME 16 twin screw extruder, a mixture of Lactose and PEG 4000 was granulated to produce five batches with differing variables of screw speed and binder fraction.

Following extrusion, granules were observed when hot and cold. Properties in terms of their size shape and size distribution were noted. A Retsch AS 200 sieve shaker was used to determine particle size distribution through the use of 12 sieves arranged in descending aperture size. In another test, granules were poured by hand through a fixed funnel where they formed a heap below. The circumference of the

Figure 1 – Twin Screw Extruder:

heap was measured so the diameter (D) could be obtained. The height (h) of the heap was measured using a ruler. These values were used to calculate the Angle of Repose.

Measuring Carr's Index and the Hausner ratio was a simple process whereby a known amount of granules were poured into a measuring cylinder and the volume they occupied recorded (bulk density). The granules were tapped manu-
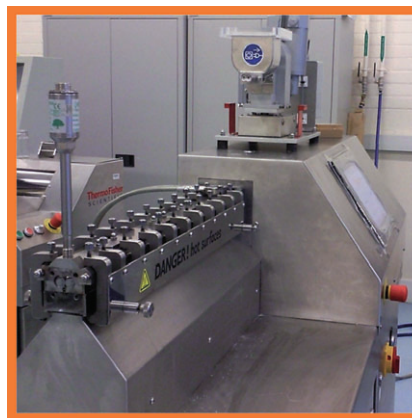
Table 1: Experiment parameters

Batch	Lactose (g)	PEG 4000 (g)	Binder Fraction (%)	Screw Speed (rpm)
1	50	5	10	100
2	50	5	10	50
3	30	6	20	50
4	30	7.5	25	50
5	30	7.5	25	100

ally until there was no more change in volume to give a value for tapped density. These figures were used in the following equations;

Equation 1 – Angle of Repose:

$$\text{Tan}\theta = \frac{2h}{D}$$

Equation 2 – Hausner Ratio:

$$\text{Hausner Ratio} = \frac{\text{Tapped Density}}{\text{Bulk Density}}$$

Equation 3 – Carr's Index:

$$\text{Carr's Index}\,(\%) = \frac{\text{Tapped Density} - \text{Bulk Density}}{\text{Tapped Density}} \times 100$$

Tablets were made in a compaction press and a Heckel plot produced; another test to determine compressibility. Each tablet was then placed into the Schleuniger 4M (Copley) so its crushing strength could be measured.

RESULTS

Although different batches of granules displayed better properties in some tests over others, trends of results were identified. The first variable of screw speed appeared to have little effect upon the granules, and significant effect was shown with the change in binder fraction; the larger the amount of binder the better the compaction properties of the granules. It was found however that too much binder could be detrimental to the flow properties of granules.

CONCLUSIONS

Melt granulation using a twin-screw extruder is a viable, continuous, solvent free, cost efficient and easily scalable method of granulation.

Initial observations showed that batches 3 and 4 appeared to be the most granular. It was found that batch 4 had the narrowest particle size distribution and the lowest angle of repose, suggesting this was the batch with the best overall flow characteristics. Compressibility tests were inconclusive as all batches yielded the same or very similar results. Various limitations were identified as to why this was the case.

ACKNOWLEDGMENTS

Modelling of the flow of cohesive powders during pharmaceutical tabletting

Chuan-Yu Wu, Yu Guo

School of Chemical Engineering, University of Birmingham, Birmingham, B15 2TT. (C.Y.Wu@bham.ac.uk)

Abstract **– Flow of cohesive powders during the die filling stage of pharmaceutical tabletting was analysed using a coupled discrete element method and computational fluid dynamics (DEM/CFD), in which a two-way air-particle interaction coupling mechanism was established for modelling the effect of the presence of air and the JKR theory was incorporated to simulate the interaction between cohesive particles. It has been found that for cohesive powders intermittent flow occurs, in which powder flows as chunks of agglomerates. In addition, make-up of vessel walls, arching and air entrapment can be induced.**

INTRODUCTION

Most pharmaceutical tablet manufacturing is conducted in the presence of air. Depending on the powder properties, the interaction between powder and air can be significant. Furthermore, for fine powders, the Van der Waals force acting between particles will become dominant, which will affect powder flow behaviour dramatically. Therefore, it is important to understand how the presence of air affects the flow behaviour of cohesive powders. For this purpose, we employed a coupled DEM/CFD method to analyse the flow of cohesive powder in air.

DEM/CFD

The DEM/CFD treats a powder as an assembly of solid spherical particles which interact with each other and the interaction is modelled with classical contact mechanics. The air is treated as a continuous fluid phase governed by the continuity and momentum equations. A fluid-particle interaction scheme
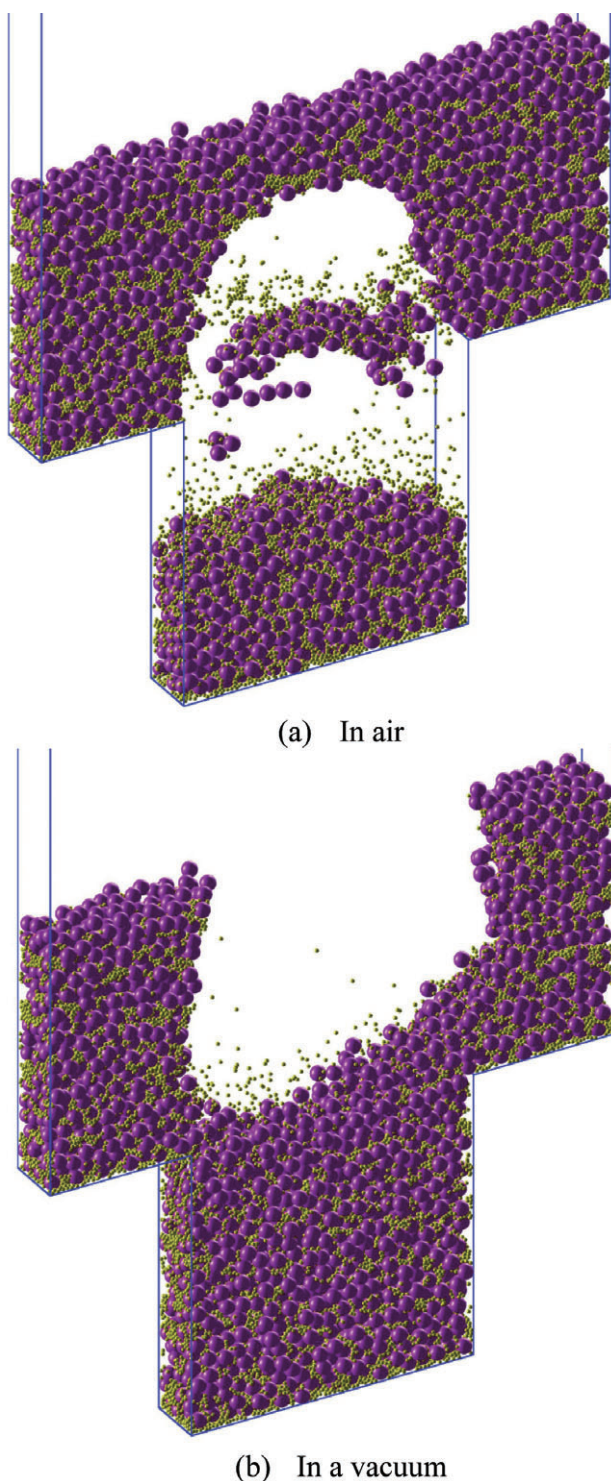
is introduced to model the two-way coupling between the two phases. It has been demonstrated that this method is capable of simulating the flow of powders in air [1–3].

RESULTS AND DISCUSSION

By introducing interface energy in particle contacts, the flow of cohesive powders in air and in a vacuum was investigated, as shown in Fig.1. It was found that agglomerates of particles are formed due to the effect of cohesion and the particles are deposited into the container chunk by chunk. An intermittent powder flow process is hence induced. In addition, the particles are too 'sticky' so that they can either stick with the walls or form a stable arch, demonstrating that both cohesion and the presence of air can significantly affect the powder flow behaviour.

CONCLUSIONS

A coupled DEM/CFD method was employed to model the flow of cohesive powder in air. It has been shown that the presence of air and cohesion can significantly affect the powder flow behaviour. It has been found that for cohesive powders intermittent flow occurs with the make-up of vessel walls, arching and air entrapment being induced.

ACKNOWLEDGMENTS

REFERENCES

[1] Y. Guo, K.D. Kafui, C.-Y. Wu, C. Thornton, J.P.K. Seville, "A coupled DEM/CFD analysis of the effect of air on powder flow during die filling". AIChE J., 55 (2009) 49–62.

[2] Y. Guo, C.-Y. Wu, K.D. Kafui, C. Thornton, "Numerical analysis of density-induced segregation during die filling". Powder Technology 197 (2009) 111–119.

[3] S. Yu, Y. Guo, C.-Y. Wu, DEM/CFD modelling of the deposition of dilute granular systems in a vertical container, Chinese Science Bulletin. 54 (2009), 4318–4326.

(a) In air

(b) In a vacuum

Fig. 1. Final patterns during the flow of cohesive binary mixtures

Mucosa-mimetic hydrogels for evaluating mucoadhesive properties of dosage forms

D.J. Hall, O. Khutoryanskaya, V. Khutoryanskiy

Reading School of Pharmacy, University of Reading, Whiteknights, Reading, UK.

INTRODUCTION

Mucoadhesive polymers have received considerable attention as platforms for controlled delivery due to their ability to prolong residence time on mucosal surfaces and enhance drug bioavailability. One of the commonly used approaches to evaluate the performance of mucoadhesives is the determination of the force required to detach a dosage form from animal mucosal tissue (F_{det}) and calculation of the work of adhesion (W_{ad}). In most *in vitro* studies evaluating mucoadhesives, animal tissues were typically used. The objective of the present work was to develop hydrogels that can mimic animal mucosal tissues and be used as substrates for testing mucoadhesives.

MATERIALS AND METHODS

Model mucoadhesive tablets were prepared based on Carbopol-934P and hydroxypropylmethylcellulose (HPMC) by compressing the powder mixtures at different ratios. The adhesion of tablets towards mucosal tissues and hydrogel was studied using a TA XT.plus Texture Analyser (Stable Microsystems, UK). Porcine buccal and gastric mucosal tissues were used for assessment of mucoadhesion. Polymeric hydrogels were synthesised by three-dimensional copolymerisation of 2-hydroxy-ethylmethacrylate (HEMA) with 2-hydroxyethylacrylate [1], *N*-vinyl pyrrolidone, sorbitol methacrylate and N-acryloyl glucosamine (AGA) and were purified by extracting unreacted monomers with deionised water.

RESULTS AND DISCUSSION

Previously [2], we have used ultrathin hydrogel multilayers covalently-attached to glass surfaces as substrates to evaluate adhesion of Carbopol-934P tablets. It was established that these hydrogels can potentially mimic the W_{ad} values observed for detachment of tablets from porcine buccal mucosa but fail to exhibit identical detachment profiles.

In this study we used three-dimensional copolymerisation of 2-hydroxyethylmethacrylate (HEMA) with 2-hydroxyethylacrylate, *N*-vinyl pyrrolidone, sorbitol methacrylate, N-acryloyl glucosamine (AGA) to synthesise hydrogels and evaluated their applicability as potential mucosal mimics.

The structure and properties of the hydrogels were found to be dependent on the monomer ratios in the feed mixtures. Higher content of HEMA in the monomer mixtures resulted
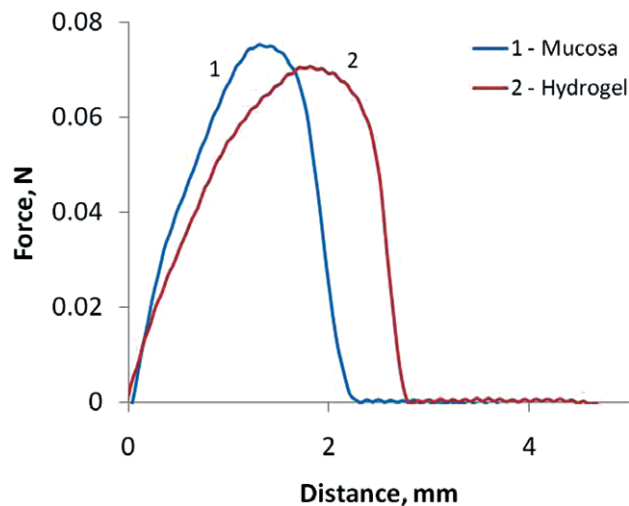

Figure 1. Detachment profile of Carbopol-934P tablet from porcine buccal mucosa (1) and HEMA-AGA hydrogel (2).

in less transparent hydrogels, having smaller pore sizes, higher elastic moduli and lower swelling capacity.

More than 60 hydrogels have been tested as potential substrates for evaluating mucoadhesive properties of Carbopol-934P / HPMC tablets. It was established that the HEMA-AGA hydrogel demonstrates excellent potential to mimic animal mucosa. The values of F_{det} and W_{ad} as well as the detachment profiles observed for this hydrogel are nearly identical to the parameters recorded for detaching mucoadhesive tablets from animal tissues (Figure 1).

The excellent mimicking characteristics of HEMA-AGA are likely related to its chemical structure (combination of functional groups) and physicochemical properties (hydration degree, elasticity and porosity).

CONCLUSIONS

It is hoped that the synthetic hydrogel developed in this work can offer a suitable substitute to animal tissues for experiments with mucoadhesives.

ACKNOWLEDGMENTS

REFERENCES

[1] Khutoryanskaya O.V., Mayeva Z.A., Mun G.A., Khutoryanskiy V.V., "Designing temperature-responsive biocompatible copolymers and hydrogels based on 2-hydroxyethyl(meth)acrylates" *Biomacromolecules* **9** (2008), 3353–3361.

[2] Khutoryanskaya O.V., Potgieter M., Khutoryanskiy V.V., "Multilayered hydrogel coatings covalently-linked to glass surfaces showing a potential to mimic mucosal tissues" *Soft Matter* **6** (2010), 551–557.

Niosomes with Span 65 and Pluronic F-127 as a novel delivery system for lysozyme

R.R. Haj-Ahmad, C.S. Chaw and A.A. Elkordy

Department of Pharmacy, Health and Well-Being, University of Sunderland, Sunderland, SR1 3SD

INTRODUCTION

Proteins have been termed the "servants of life" [1] as they are crucial for many biological processes in the body. The oral administration of protein pharmaceuticals to the systemic circulation has numerous barriers, including, sharp pH gradients, proteolytic enzymes and low epithelial permeability. Trying to overcome these barriers, researches had invented several techniques such as: intestinal patches, liposomes, enteric-coated capsules, mucoadhesive tablets and non-ionic surfactant vesicles [2]. Niosomes are non-ionic surfactant vesicles obtained on hydration of synthetic nonionic surfactants, with or without incorporation of cholesterol. The encapsulation of proteins in niosomes can increase protein absorption and stability by restricting its action to target cells.

MATERIALS AND METHODS

In the present study niosomal formulations of lysozyme (from egg white) were successfully prepared via film hydration method using span 65 (which has not been studied before to prepare niosomes), cholesterol and pluronic F-127. Also CremophorELP and Solutol HS-15 were used in the preparation of niosomes. Table 1 shows the formulations.

Unentrapped drug was separated by ultracentrifugation ($60000 \times g$ for 1 hour at 4 C°). Morphology and vesicular sizes of the prepared niosomes were investigated by optical microscope and dynamic light scattering (ZetaPlus), respectively. The entrapment efficiency of lysozyme in niosomes (Equation 1) was determined by complete vesicle disruption using 50:50 isopropanol:water, followed by analysis of the resulted solutions by UV spectrophotometry at 280 nm.

Entrapment efficiency (EF) = (Amount entrapped of lysozyme/total amount of lysozyme)×100

Thermal behaviour of the formulated niosomes was investigated using differential scanning calometry (DSC).

RESULTS AND DISCUSSION

It was found that there was no noisome formation by using span 65 and cholesterol in the absence of a co-surfactant

Table 1: protein niosomal formulations

Sample	Span65	Cholesterol	Pluronic F-127	Cremophor ELP	Solutol HS 15
1	50	50	0	0	0
2	48.5	48.5	3	0	0
3	64.7	32.3	3	0	0
4	32.3	64.7	3	0	0
5	45	45	0	10	0
6	45	45	0	0	10
7	0	22	56	22	0

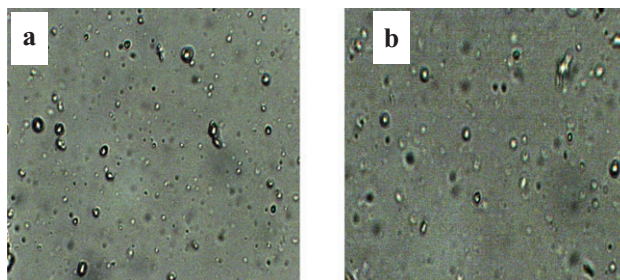**Figure 1.** Microscopic examination of lysozyme noisomes. a) sample no.3 and b) sample no.4 (magnification was ×400), see Table 1 for sample no.

(pluronic F-127). However, the inclusion of pluronic F-127 helped in forming niosomes (Figure 1) with entrapped lysozyme; using different concentrations of span65 and cholesterol (Table 1) has an effect on the amount of encapsulated protein; the results of encapsulation efficiency were: 62.1%, 46.4% and 36.1% for samples 2, 3 and 4, respectively. From the other hand, using of CremophorELP and Solutol HS-15 as co-surfactants resulted in niosome formation but without any entrapped lysozyme. The particle size of the prepared niosomes was 127.7 ± 3.9 nm, 235.7 ± 120 nm and 305.4 ± 54.3 nm for samples 2, 3 and 4, respectively. This means that sample 2 showed the narrowest particle size distribution.

The DSC data showed that all formulated niosomes (samples 1–6) had only one peak at about 50°C, for sample no 7 there were two peaks at 50 and 150°C, suggesting incompatibility of this formulation.

CONCLUSIONS

The results of this study show that span 65, cholesterol and pluronic F-127 type of non-ionic surfactants were successfully used in preparation of nisomes containing lysozyme. The ratio of 1:1 for span 65 to cholesterol produced the highest encapsulation efficiency with the smallest particle size.

REFERENCES

[1] Franks, F. (1988). In characterisation of proteins (Franks, F., Ed) Humana Press, Clifton, New Jersey, pp. V–vi.
[2] Uchegbu IF and Vyas SP. 1998. Non-ionic surfactant based vesicles (niosomes) in drug delivery. *Int.j.Pharm.*172: 33–70.
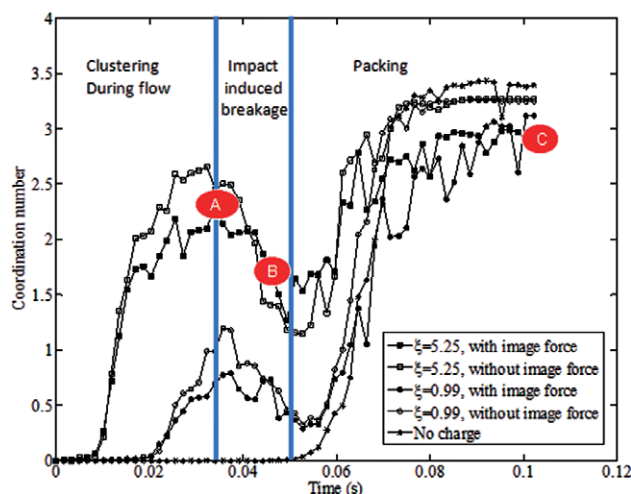
Numerical analysis of electrostatic effects during powder deposition using DEM/CFD

Chunlei Pei[1], Chuan-Yu Wu[1], Stephen Byard[2], David England[3]

[1]School of Chemical Engineering, University of Birmingham, Birmingham, B15 2TT. (C.Y.Wu@bham.ac.uk)
[2]Sanofi-Aventis, Northumberland, NE66 2JH, UK
[3]Sanofi-Aventis Deutschland GmbH, Frankfurt, Germany

Abstract – **Electrostatic interaction can play a significant role in pharmaceutical powder processing. In this study, a coupled discrete element method and computational fluid dynamics (DEM/CFD) model was developed with an implementation of electrostatic interactions. Using the developed DEM/CFD, deposition processes of monodisperse particles with and without electric charges were simulated. It was found that the electrostatics significantly affects the deposition behaviour of particles. In particular, it was revealed that for charged particles three distinctive processes were identified during deposition: 1) clustering; 2) impact fragmentation; and 3) packing. It was also observed that charged particles could stick with the vessel walls due to the presence of electrostatics.**

Fig. 1 Coordination number for various cases considered.

INTRODUCTION

In various pharmaceutical powder handling operations, particles can inevitably get electrically charged, which can significantly influence the particulate processes. The electrostatic interaction can induce cohesion of particles and adhesion of particles to walls, especially for fine particle systems. This phenomenon is usually detrimental to pharmaceutical powder processing, as it affects powder flow and reduces fill and dose uniformity. Therefore, understanding the mechanisms of electrostatic interactions is of fundamental importance in pharmaceutical research. A numerical investigation of the effect of electrostatics on powder deposition is then performed and reported here.

RESULTS AND DISCUSSION

Electrostatic models are developed and implemented to the DEM/CFD code [1] and the effect of electrostatics on deposition behaviour of charged particles is then explored. Figure 1 shows the evolution of coordination number (CN), which defines as the average number of contact for each particles and reflects the microstructure of a particle system, for various cases considered. It can be seen that for the particle system without charge the CN only starts to increase once particles begin to pack in the container. While for charged particle systems, the deposition process can be divided into three distinctive stages: clustering, impact breakage and packing. At the beginning of the deposition, particles can agglomerate due to the long-range electrostatic forces, as shown in Fig. 2a and the highly charged particles have a larger amount of contacts due to the larger attractive force. When particles reach the bottom of the container, fragmentation of clusters is observed as a result of collision with the base (Fig.2b). Re-clustering and packing take place thereafter (Fig.2c) and consequently the CN increases. It is also clear from Fig.2 that some particles stick with the walls due to the strong attractive forces.

CONCLUSIONS

A coupled DEM/CFD method was developed to explore the effect of electrostatics on pharmaceutical powder processing.

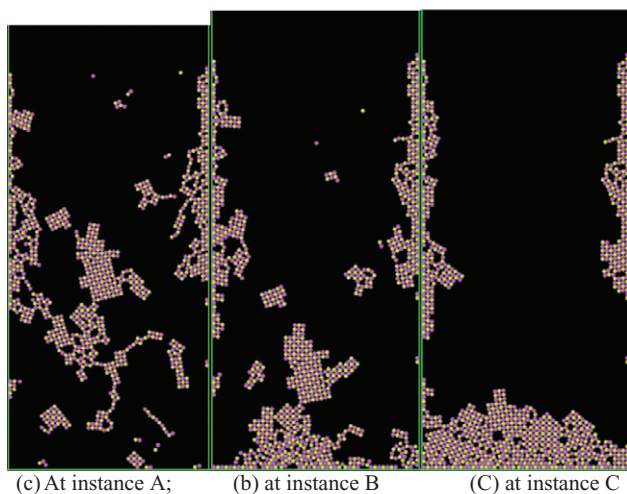(c) At instance A;   (b) at instance B   (C) at instance C

Fig. 2. Particle packing patterns for the instances marked in Fig.1.

Deposition of charged particles was simulated. It has been found that three distinctive stages, i.e., clustering; impact fragmentation and packing, exists for charged particles systems and charged particle can stick with the vessel walls due to electrostatics.

ACKNOWLEDGMENTS

REFERENCE

[1] Y. Guo, K.D. Kafui, C.-Y. Wu, C. Thornton, J.P.K. Seville, "A coupled DEM/CFD analysis of the effect of air on powder flow during die filling". AIChE J., 55 (2009) 49–62.

Online measurement of residence time distribution in hot melt extrusion

R.S. Dhumal[1], A.L. Kelly[1], E.L. Burton[2], A.R. Paradkar[1]

[1]Centre for Pharmaceutical Engineering, University of Bradford, Bradford, BD7 1DP, UK
[2]Interdisciplinary Research centre in Polymer Engineering, University of Bradford, BD7 1DP, UK

Abstract – **The aim was to study the effect of processing variables on the residence time distribution (RTD) of Kollidon SR during hot melt extrusion (HME). The residence time was monitored by measuring the UV absorbance of the tracer by the probe mounted on the die of the extruder. The feed rate and the screw geometry were found to influence the RTD prominently. This study indicates the significance of processing variables during HME and its utility in optimising the new process and improving the established processes.**

INTRODUCTION

Hot-melt extrusion is a widely applied processing technique with early applications in the plastics and rubber industries [1]. For pharmaceutical systems, several research groups have recently demonstrated that melt processing of pharmaceutical polymers is a viable method to prepare SDs, sustained release tablets, transdermal drug delivery systems and implants [2]. Apart from being solvent free, extrusion is a continuous, single-step, easily controlled and readily scalable technique. Continuous and closed process units prevent cross-contamination and readily address the regulatory demand for QbD (Quality by Design) and PAT (Process Analytical Technology). High mixing efficiency and short processing time make extrusion suitable for pharmaceuticals. Residence time of drug polymer mixture in the extruder determines the stability of drugs and polymers and hence determines the utility of technology [3]. In this work, the effect of processing variables on the residence time distribution (RTD) of a pharmaceutical polymer Kollidon SR was studied.

MATERIALS AND METHODS

Extrusion was carried out using 16 mm co-rotating twin screw extruder (Pharmalab, Thermo Scientific, UK). The UV probe was mounted on die for online UV spectroscopic measurements after introducing the tracer into the inlet of the extruder. The effect of different temperatures, screw configurations (low, medium and high shear) consisting of forward feeding elements, a mixing section and a discharge section, feed rates (200, 700 and 900 gm/hr) at different screw speeds (200, 300 and 400 rpm) and plasticiser (TEC) levels were studied. Uvitex OB was mixed with Kollidon SR and masterbatch was extruded using Minilab to give a tracer.

RESULTS AND DISCUSSION

The mean residence time (MRT) was influenced very effectively with the residence time shifting dramatically to lower values of time when the feed rate was increased. As the screw speed at the given feed rate increased the residence time curves shifted to lower time values.

MRT was found to reduce with increase in temperature. This might be due to an increase in polymer flow due to reduction in viscosity at higher temperatures, which could be confirmed from the reduced values of torque. The incorpora-
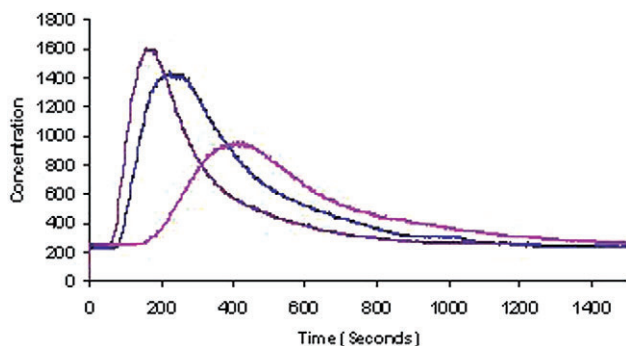
Fig. 1. Representative residence time distribution patterns for different batches extruded.

tion of plasticiser was not found to influence the MRT significantly, though a small delay was observed with increase in the plasticiser. The MRT was found to decrease from low shear to medium and high shear configurations i.e. with increase in the number of mixing elements added in the screw configuration. When the reversing elements are added in screw configuration it significantly increases the residence time.

CONCLUSIONS

The online measurement of residence time distribution was successfully performed using UV spectroscopic probe. Though MRT was found to be influenced by all the variables studied, feed rate and the screw geometry were found to have a prominent effect. Increase in feed rate was found to decrease the MRT, while increase in the mixing elements and their staggering angle was found to increase the MRT. Addition of reversing element was found to have the most significant effect with dramatically reduced MRT. This study indicates the significance of processing variables during hot melt extrusion of polymeric systems. This is particularly important for pharmaceuticals, where the material is sensitive and stringent regulatory constrains of the impurities generated due to degradation.

REFERENCES

[1] I. Ghebre-Sellassie, C. Martin, "Pharmaceutical extrusion technology". Informa Healhcare USA, New York.

[2] M.A. Repka, S.K. Battu, S.B. Upadhye, S. Thumma, M.M. Crowley, F. Zhang, C. Martin, J.W. McGinity. "Pharmaceutical applications of hot-melt extrusion: Part II" *Drug Dev Ind Pharm*. **33** (2007) 1043–57.

[3] T.J.A. Melo. "An optical device to measure in-line residence time distribution curves during extrusion" *Polymer Engineering and Science* **42** (2002) 170–181.

On-line Moisture Measurement during Granule Drying Using a Near-Infrared Sensor: An Evaluation of Equipment Setup Variables

Graham Holland, Peter Ferrie, John F. Gamble, Andrew Dennis, Stuart T. Charlton

Bristol-Myers Squibb, Biopharmaceutics R&D, Moreton, UK.

INTRODUCTION

The use of near-infrared (NIR) for moisture determination is a widely accepted process analytical technology (PAT). PAT is often an important part of ensuring process control and is inextricably linked to Quality by Design (QbD). To enable earlier process understanding, such monitoring is now required at much smaller scales of unit operation. The aim of this work was to determine measurement robustness with respect to NIR probe angle, focal distance, and probe height for a lab-scale fluid-bed drier.

MATERIALS AND METHODS

Placebo granules were produced by wet granulation using a Diosna P1–6 high shear mixer (1 kg batch size). The Pro-CepT Mini Airpro and NDC MM710 NIR probe were calibrated in conjunction with data generated using loss on drying (LOD). A model was developed to predict the moisture content in the granules from the absorbance value measured by the probe. Model values were subsequently compared to experimental values to determine accuracy.

NIR probe angle, the distance between the NIR probe and the drying vessel, and the height on the drying vessel at which the NIR probe was focussed were investigated. The prediction model was then applied to the data sets and analysed using principal component analysis (PCA) against the calibration data set to determine the influence exerted by each variable.

RESULTS AND DISCUSSION

Calibration. Calibration of the NIR probe showed a strong linear relationship linking NIR absorbance and granule moisture content (Fig. 1). Mean span (calibration curve gradient) and trim (calibration curve y-axis intercept) values were 1.26 and 6.14, respectively. A linear relationship between NIR absorbance and predicted moisture content was demonstrated.

Angle. It was hypothesised that a shallower angle may result in attenuation of the signal because specular reflection from
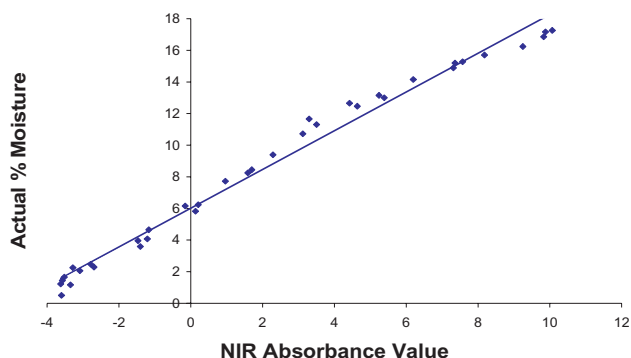
Fig. 1. Calibration curve of the NIR probe, $R^2 = 0.9853$

the drier surface may enter the probe; whereas a steeper angle may cause the signal to be lost as the collection efficiency decreases. Changing the probe angle altered the position of the focal point within the sample bed, subsequently the product density within the focal point of the

sensor may be different due to differences in the degree of fluidisation. However, analysis of the data using PCA indicated that angle did not exert a significant influence on the prediction model at the selected probe height.

Height. Changing the height changes the position of the focal point within the sample bed. PCA indicated that probe height did not affect accuracy of the readings.

Distance. The sensor has a fixed focal distance and it is recommended that the sensor be 20 cm from the sample. However, increasing the distance of the sensor from the dryer by up to 40 cm did not affect the model.

CONCLUSIONS

Analysis by PCA showed that the model had a univariate response, that being moisture content. None of the variables investigated affected probe performance. It is concluded that the sensor tolerance was sufficiently robust to allow for variability in probe setup within the parameters of this study and supports use of NIR for on-line monitoring of drying kinetics during manufacture of lab-scale batches.

Pharmaceutical Nanomaterials: The preparation of solid core drug delivery systems (SCDDS)

John Mitchell, Vivek Trivedi

Medway Sciences, University of Greenwich, UK.

Abstract – **In this study a solid core drug delivery system is prepared with silica as a model core, fatty acid as a shell material and supercritical fluid technology as the process. Solid core drug delivery systems (SCDDS) can be developed as targeted delivery systems or as sustained/controlled release platforms. SCDDS are coated with fatty acids using supercritical fluid technology (SCFT), allowing the creation of nano-particulate and micro-particulate delivery systems. The operating conditions of low temperature and pressure used to formulate these systems make it attractive for pharmaceutical research, especially for thermo-labile or sensitive bio-materials.**

INTRODUCTION

As the size and the sensitive nature of bio-molecules prohibit the preparation of traditional non-invasive delivery systems (i.e. oral, transdermal, pulmonary), the development of new protein based drugs is impeded by the lack of an appropriate delivery method. [1,2] Recently, we have been expanding our range of delivery vehicles through investigation of the preparation and microencapsulation of protein particles absorbed/adsorbed on solid cores.

MATERIALS AND METHODS

The solubility or phase change of lauric, myristic, palmitic and stearic fatty acids were determined in liquid and supercritical (SC) carbon dioxide. Scanning electron microscopy, differential scanning calorimetry and X-ray diffraction results showed that no morphological changes occurred due to the processing of fatty acids in liquid or SC CO_2. For the preparation of a SCDDS, silica was used as the core and bovine serum albumin (BSA) as a model drug. SCDDS preparation was carried out in two stages which included adsorption of BSA on silica (BSA-Si) [3] followed by coating of the BSA-Si particles with fatty acid via SC processing.

RESULTS AND DISCUSSION

Both, 0.5 µm and 1.0 µm silica particles were used as a model core material. In order to determine the best system to achieve maximum adsorption of BSA, isotherms were obtained in water, 0.15 M NaCl solution and a citrate/phosphate buffer at pH 4.0, 4.7, 5.0, and 7.0. Adsorption isotherms were obtained for silica particles with a specific surface area of 2.2 m²/g (1.0 µm) and 4.4 m²/g (0.5 µm). Results showed an increase
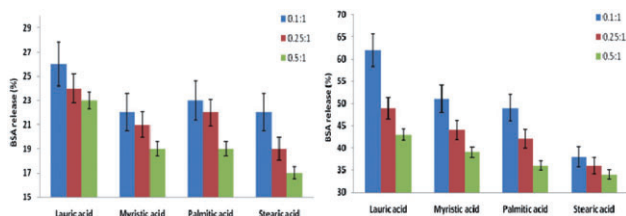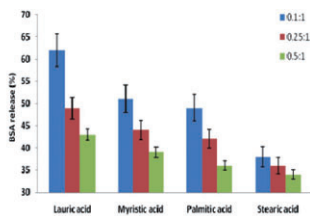
Fig. 1. Comparison of 24 hour BSA release from SCDDS prepared with 1.0 μm silica.

Fig. 2. Comparison of 24 hour BSA release from SCDDS prepared with 0.5 μm silica.

acid was found to be fastest and highest whilst stearic acid formulations showed the slowest release amongst all systems.

CONCLUSIONS

A SCDDS was prepared by the immobilisation of BSA on silica particles and a subsequent coating with fatty acid via supercritical processing. SCDDS prepared with lauric acid showed highest and fastest BSA release from the formulations studied followed by myristic, palmitic and stearic acid. BSA release was also related to the ratio of fatty acid in the formulation. Formulations with higher ratios of fatty acid provided the slowest release rate. A relationship between particle size/specific surface area to the release of adsorbed protein was also observed as BSA release from SCDDS prepared with 0.5 μm silica (4.4 m^2/g) was higher than 1.0 μm, 2.2 SA silica (2.2 m^2/g) formulations.

REFERENCES

[1] Luppi, B., Bigucci, F., Cerchiara, T., Mandrioli, R., Di Pietra, A.M., Zecchi, V., "New environmental sensitive system for colon-specific delivery of peptidic drug*s." International Journal of Pharmaceutics,* 2008. **358** (1–2): p. 44–49.

[2] Davies, O.R., Lewis, A. L., Whitaker, M. J., Tai, H., Shakesheff, K. M., Howdle, S.M., "Applications of supercritical CO2 in the fabrication of polymer systems for drug delivery and tissue engineering". *Advanced Drug Delivery Reviews,* 2008. **60**(3): p. 373–387.

[3] Yeung, K.M., Lu, Z. J., Cheung, N. H., "Adsorption of bovine serum albumin on fused silica: Elucidation of protein-protein interactions by single-molecule fluorescence microscopy". *Colloids and Surfaces B: Biointerfaces,* 2009. **69**(2): p. 246–250.

in the amount of BSA adsorbed, observed with the increasing specific surface area of silica particles. Isotherms demonstrated that maximum adsorption of BSA can be achieved at or close to the iso-electric point (IEP) of the protein. A SCDDS was prepared by adsorbing BSA on silica at pH 5.0 in citrate/phosphate buffer and then using SCFT to coat these particles with fatty acid in the ratio (fatty acid:silica) of 0.1:1, 0.25:1 and 0.5:1. Release studies were conducted in phosphate buffer saline at pH 7.4 over 24 hours using a continuously stirred micro-dissolution apparatus with UV monitoring. The release of BSA was found to be highest from SCDDS prepared using 0.5 μm silica with a specific surface area of 4.4 m^2/g. (Fig 1) SCDDS prepared using 1.0 μm silica with a specific surface area of 2.2 m^2/g provided lowest BSA release. BSA release from the SCDDS was also dependent on the chain length of fatty acid used and its ratio in the formulation. The release of BSA from SCDDS prepared with lauric

---

Phototoxicity of curcumin loaded alginate foams to *Enterococcus faecalis* and *Escherichia coli in vitro*

Anne Bee Hegge[1], T. Andersen[2], J.E. Melvik[2], E. Bruzell[3], S. Kristensen[1], H.H. Tønnesen[1]

[1]School of Pharmacy, University of Oslo, Oslo, Norway
[2]NovaMatrix/FMC BioPolymer AS, Sandvika, Norway
[3]Nordic Institute of Dental Materials (NIOMas), Haslum, Norway

INTRODUCTION

Curcumin is a potential photosensitiser (PS) with low water solubility. The present study presents curcumin loaded alginate foams intended for use in antimicrobial photodynamic therapy (aPDT) of infected wounds. aPDT is a treatment modality to inactivate bacteria including strains resistant to conventional antibiotics. Most PS, including curcumin, are hydrophobic compounds which aggregate in aqueous environments, resulting in photochemical and thus pharmacological inactivation [1]. Gelled alginate foams have been loaded with hydrophobic curcumin, using selected solubilisers i.e. cyclodextrins (CDs) and polyethylene glycol 400 (PEG 400). The phototoxicity of the curcumin loaded foams to

Enterococcus faecalis (E. faecalis) and *Escherichia coli (E.coli) in vitro* has been investigated.

MATERIALS AND METHODS

Foams were prepared by [2]: 1) Solubilisation of curcumin in CDs or PEG. 2) Followed by addition of alginate, plasticiser, foaming agent, salt with gelling ion (CaCO$_3$) and buffer before initialisation of alginate gelling and simultaneous incorporation of air by high shear mixing. 3) Initiation of gelling by adding glucono-δ-lactone (GDL) which slowly reduced the pH of the blend and resulted in Ca^{2+} release from CaCO$_3$. 4) Moulding and drying of the blend resulted in the finished foams (Fig. 1).
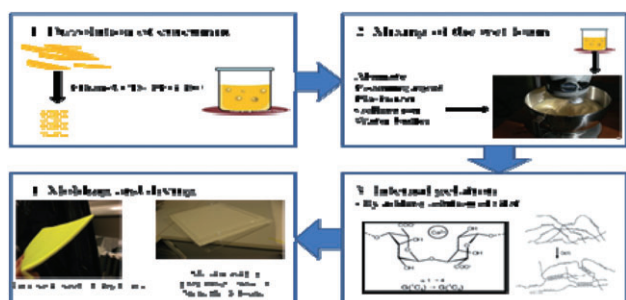
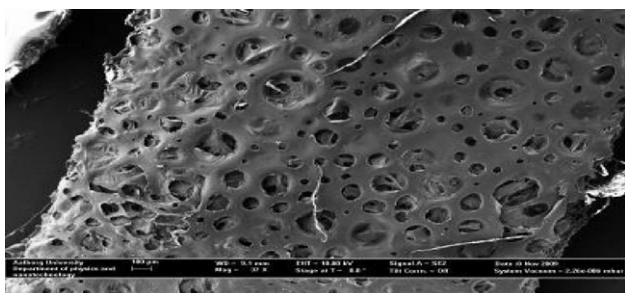**Fig. 1:** The main steps in the preparation of curcumin loaded alginate foams.

Fig. 2: SEM of a dried curcumin loaded alginate foam.

Foam phototoxicity on bacteria [2]: Gram positive *E. faecalis* and gram negative *E. coli* were exposed to curcumin loaded foams for 1 h prior to irradiation with blue light (emission maximum 450 nm). Radiant exposure of ~30 J/cm^2 was used for *E. coli* and ~10 J/cm^2 for *E. faecalis*, prior to incubation for 1 h. Aliquots of the bacterial suspensions were plated on TSB agar plates for determination of colony forming ability. The detected CFU/ml was compared to controls.

RESULTS AND DISCUSSION

Curcumin (0.18%, w/w) was loaded into the hydrophilic alginate matrix. Hydroxypropyl-γ-CD, hydroxypropyl-β-CD and PEG 400 were selected as solubilisers of curcumin (Table. 1). The resulting foams were porous with a wide pore size distribution (Fig. 2). All the foams were demonstrated to hydrate within 1 min in a model physiological fluid, and curcumin was released into the aqueous environment (results not shown).

Table 1 shows the effects of the selected solubilisers on the phototoxicity of curcumin loaded foams. Exposure by

Table 1: The selected solubilisers of curcumin in the alginate foams and the phototoxicity of selected curcumin loaded foams on *E. faecalis* (gram positive) and *E. coli* (gram negative) *in vitro*

Selected solubilizer of curcumin	Inactivation of *E. faecalis*	Inactivation of *E. coli*
PEG 400	100%*	81%*
HPβCD + PEG 400	100%	Non
HPγCD	100%	Non

* Compared to control samples (<10^6 CFU/ml)

foams containing PEG 400 as the solubiliser resulted in complete inactivation of the viable gram positive bacterial cells (CFU/ml) however only a small (81%) reduction of the viable gram negative bacteria compared to the control samples. The curcumin foams containing CDs were highly phototoxic towards *E. faecalis*, however, no significant phototoxic effect was found on *E. coli*.

CONCLUSIONS

Curcumin loaded alginate foams containing CDs and/or PEG 400 as solubilisers were highly phototoxic to gram positive *E. faecalis in vitro*. The selected solubilisers were, however, different with respect to curcumin phototoxicity towards gram negative bacteria (*E. coli)* as only the foam containing PEG 400 showed a significant phototoxic effect.

ACKNOWLEDGMENTS

REFERENCES

[1] Konan, Y.N., R. Gurny, and E. Allemann, *State of the art in the delivery of photosensitisers for photodynamic therapy.* Journal of Photochemistry and Photobiology B-Biology, 2002. **66** (2): p. 89–106.

[2] Hegge, A.B., et al., *Formulation and bacterial phototoxicity of curcumin loaded alginate foams for wound treatment applications Studies on curcumin and curcuminoides XLII.* Journal of Pharmaceutical Sciences, 2010: In progress.

Physical Stability of Extemporaneously Prepared Oral Hydrocortisone Suspensions

A. Rogerson[1], S. Hiom[2], J.C. Smith[2], B.R. Conway[1]

[1]School of Pharmacy, Life and Health Sciences, Aston University. [2]Cardiff and Vale University Health Board, SMPU

Abstract **– The aim of this investigation is to establish and compare the physical stability of extemporaneous suspensions of hydrocortisone acetate prepared using the viscosity modifiers Orasweet/Oraplus<®>, xanthan gum and methylcellulose. Licensed oral suspensions of hydrocortisone acetate are not available in the UK and as a consequence, hospital pharmacies prepare unlicensed formulations extemporaneously.**

INTRODUCTION

Oral formulations of hydrocortisone are used as replacement therapy in primary and secondary adrenocortical insufficiency and current oral formulations in the UK are limited to 10 mg and 20 mg hydrocortisone acetate tablets (BNF 58, 2009). Oral liquid preparations of hydrocortisone would be a useful alternative, being the 13th most common extemporaneous formulation, for administration to children (Lowey and Jackson, 2008). Current practice involves extemporaneous production from hydrocortisone acetate tablets and dispersal in a suitable aqueous medium, typically the commercially available, taste-masking suspension Orasweet/Oraplus®. Currently there is a lack of data regarding the influence viscosity modifiers may have on the physical stability of these suspensions.

MATERIALS AND METHODS

The suspensions were prepared using manually ground or milled (Pulverisette 7, Fritsch) hydrocortisone acetate 20 mg tablets (Auden McKenzie Pharma Division Ltd) and Orasweet/Oraplus® or vehicles containing xanthan gum and methylcellulose (Sigma, UK). Each suspension was formulated at an equivalent viscosity, (determined using a Brookfield DV-1 viscometer) and maintained under ambient conditions undisturbed for 15 days or agitated regularly to simulate storage and usage conditions respectively. The concentration of hydrocortisone in suspension (UV, 241 nm), particle size and zeta potential were used to monitor physical stability over the experimental period.

RESULTS AND DISCUSSION

Under the described conditions of storage, hydrocortisone concentrations in the undisturbed upper portion of the suspensions fell below therapeutic levels after 9, 4 and 3 days for xanthan gum, Orasweet/Oraplus® and methylcellulose formulations respectively. Significant differences were found between hydrocortisone concentrations for the xanthan gum and methylcellulose formulations by day 6 (Mann Whitney, $p < 0.05$).

All suspensions re-dispersed to therapeutic concentrations following agitation after 15 days of storage, although more efficiently in the xanthan gum suspensions than in the methylcellulose suspensions (Mann-Whitney, $p = 0.001$)

Therapeutic concentrations were maintained over the duration of the experiment for suspensions that were in regular use and frequent shaking was maintained. There were no significant differences between formulations (Kruskal-Wallis $p = 0.646$).

Further research was carried out to investigate differences in physical stability between manually ground and milled hydrocortisone tablets suspended in Orasweet/Oraplus®. Sedimentation rate under storage conditions was faster in the manually prepared suspension, however statistical differences did not occur until day 15 (Mann-Whitney, $p < 0.001$). In all other studied respects the suspensions were similar.

CONCLUSIONS

Hydrocortisone suspensions formulated with methylcellulose are the least stable of those studied. Ostwald ripening and low zeta potentials contributed to poor stability and increased sedimentation rate. Suspensions prepared with anionic viscosity modifiers, such as xanthan gum are more stable and may be suitable for use as alternatives to Orasweet/Oraplus®. In particular, the formulation containing xanthan gum had the slowest sedimentation rate, an efficient particle re-dispersal following agitation and most consistent concentrations during sampling.

REFERENCES

[1] British National Formulary (2009), BNF 58, RPSGB.
[2] Lowey A and Jackson M, (2008). A survey of extemporaneous preparation in NHS trusts in Yorkshire, the North-East and London. *Pharmaceutical Journal,* 15, 217–219

Polymer-surfactant mixtures for production of griseofulvin nanoparticles by wet-bead milling

L.J. Tirop[1], J.M. Butler[2], M.J. Lawrence[1]

[1]Pharmaceutical Science Division, King's College London, London, SE1 9NH, UK.
[2]GlaxoSmithKline, New Frontiers Science Park, Harlow, Essex CM91 5AW, UK.

Abstract **– The advent of wet-bead milling, in which drug is milled in presence of stabilisers such as polymers and surfactant, has enabled the successful formulation of poorly water-soluble drugs as nanoparticles. Despite the success of wet-bead milling, an understanding of the mechanism behind the polymer/surfactant stabilisation of nanoparticles is lacking. Using griseofulvin (BCS class II), the effect of surfactants and/or polymers on nanoparticle production/stabilisation has been investigated. Griseofulvin nanoparticles could only be produced in presence of anionic stabilisers, which are sub-optimal for formulation purposes. Consequently, the potential of anionic surfactant/polymer co-stabilisation using the non-ionic polymer hydroxypropylmethylcellulose (HPMC) was investigated. The presence of HPMC reduced the amount of anionic surfactant required to stabilise the griseofulvin nanoparticles.**

INTRODUCTION

Wet-bead milling achieves particle size reduction of drug to within the nanometer size range using a high impact bead mill to fracture drug particles dispersed in a crude concentration suspension. The presence of polymer and/or surfactant is required during the milling process to ensure the stabilisation of the resulting nanoparticles against agglomeration. The polymer and/or surfactant adsorbs to the freshly formed drug crystal surfaces during milling, to provide either a steric and/or ionic barrier around the drug nanoparticles. Unfortunately, however, the use of an ionic surfactant to stabilise drug nanoparticles can lead to a range of challenges with the formulation, for example the risk of incompatibility with charged molecules, membrane irritation and toxicity.

MATERIALS AND METHODS

Griseofulvin, a poorly water-soluble antifungal, was selected as the model drug. A range of ionic and non ionic polymers and surfactants were screened for their ability to produce griseofulvin nanoparticles. Wet-bead milling was carried out using a Retsch MM 200 mill as reported in [1]. Dynamic light scattering was used to determine particle size. Surfactant adsorption isotherms were obtained using the colorimetric 'stains all' assay [2].

Table 1. Size and surfactant adsorption of griseofulvin nanoparticles stabilised by anionic surfactant and non ionic polymer

Surfactant/polymer combinations (wt %)	Weight ratio of drug: stabiliser	Particle size (nm) after 6 h milling	Total amount of surfactant adsorbed (mg/m^2)
SDS			
0.5% SDS	50:1	269.2 ± 4.3	0.986 ± 0.08
0.25% SDS	100:1	304.3 ± 4.2	0.627 ± 0.02
0.1% SDS	125:1	<1000	N/D
AOT			
0.5% AOT	50:1	254.4 ± 3.3	0.874 ± 0.06
0.25% AOT	100:1	290.5 ± 2.6	0.692 ± 0.04
0.1% AOT	125:1	<1000	N/D
SDS/HPMC			
1.88% HPMC + 0.5%SDS	11:1	250.4 ± 2.3	0.687 ± 0.02
1.88% HPMC + 0.25%SDS	12:1	306.1 ± 4.7	0.656 ± 0.03
1.88% HPMC + 0.1%SDS	13:1	321.4 ± 4.3	0.379 ± 0.02
1.88% HPMC + 0.05%SDS	13:1	330.5 ± 3.6	0.197 ± 0.01
1.88% HPMC + 0.025%SDS	13:1	<1000	N/D
AOT/HPMC			
1.88% HPMC + 0.5% AOT	11:1	274.1 ± 4.8	0.694 ± 0.13
1.88% HPMC + 0.25% AOT	12:1	301.9 ± 3.3	0.643 ± 0.03
1.88% HPMC + 0.1% AOT	13:1	335.8 ± 3.2	0.396 ± 0.03
1.88% HPMC + 0.05% AOT	13:1	<1000	N/D

RESULTS AND DISCUSSION

Griseofulvin nanoparticles could only be stabilised by anionic surfactants and polymers: HPMCAS (hydroxypropylmethyl-cellulose acetate succinate), SDS (sodium dodecyl sulphate) and AOT (sodium dioctyl sulfosuccinate). Nanoparticles were achieved even outside the "optimal" drug to stabiliser weight ratio of 20:1 and 2:1 reported by Merisko-Liversidge [3]. The non-ionic polymer, HPMC 8000 (fixed concentration of 1.88 wt%) was selected for use in combination with anionic surfactant for nanoparticle stabilisation. Note that

HPMC 8000 was not able to stabilise griseofulvin nano-particles when used alone. Inclusion of HPMC 8000 in the stabilising mixture allowed a reduction in the amount of sur-factant required for nanoparticle stabilisation – a ten and five fold reduction in the amount of SDS and AOT respectively. Anionic surfactant adsorption isotherms confirmed a reduc-tion in the amount of anionic surfactant absorbed in the pres-ence of HPMC 8000 (Table 1), suggesting that HPMC 8000 was absorbed onto the griseofulvin nanoparticles in the pres-ence of anionic surfactant

CONCLUSIONS

Anionic surfactant or a combination of anionic surfactant with non ionic polymer can be successfully employed to produce griseofulvin nanoparticles.

ACKNOWLEDGEMENTS

REFERENCES

[1] Sepassi-Ashtiani, S., "Polymer stabilised drug nanoparticles" *PhD Thesis* (2003), University of London.
[2] Rusconi F., Valton E., Nguyen R., Dufourc E., "Quantification of sodium dodecyl sulfate in microliter-volume biochemical samples by visible light spectroscopy" *Anal. Biochem.* **295**, (2001) 31–37.
[3] Merisko-Liversidge E., Liversidge G.G., Cooper E.R., "Nanosizing: a formulation for approach for poorly water soluble compounds" *Eur. J. Pharm. Sci.* **18**, (2003) 113–120.

Predicting Compaction Parameters for Producing Inhalation Powder Compacts for Use in the Wright's Dust Feeders

Richard Burrell, Elaine Harrop

AstraZeneca Pharmaceutical Development, Charnwood, Loughborough

INTRODUCTION

Inhalation compounds are delivered as dry clouds by dust feeder in early safety studies. The dust feeder requires micronised powder to be compressed into a cake, which is then scraped to release compound for aerosolisation. Having the correct cake characteristics is essential for the generation of a good particle cloud to give the desired inhalation expo-sure required.

Historically, powder compacts were produced in a manual press using a stainless steel canister and plunger by trial and error. If the compact is over-compressed, it would render the compact unsuitable for use. If the compact is under-com-pressed, it will collapse when incised. In this early stage development, drug substance is in short supply and timings are tight. A more predictable process was desired.

A method has been developed whereby the compression properties of the material can be modelled and used to predict the optimum punch pressure required to give good delivery.

EXPERIMENTAL

The Compaction Simulator uses less than 400 mg of material to measure the compaction properties of a powder. The two parameters chosen to assess compaction properties from the compaction simulator data were the yield pressure and the ejection force.

Yield pressure, which relates the relative density to com-paction pressure, was determined using the Heckel equation [1].

Three model materials, compounds R, E and L, covering a range of hardness and stickiness were used to gather information about how the compaction pressure affects the performance of the cake. From this a suitable working range of compaction was determined for each model material.

RESULTS AND DISCUSSION

A chart of yield pressure versus compaction pressure used to produce the cake was plotted for the model materials – see Figure 1. This shaded area on the chart shows the range of compaction pressures over which a good cake can be pro-duced for a new compound whose yield pressure has been measured on the compaction simulator. For softer materials the range is narrower making suitable selection more critical, e.g. compound R.

A high ejection force shows compounds are sticky and when compressed close to the predicted optimum pressure they tend to stick to the punch and perform poorly in the dust feeder. These sticky compounds therefore require a slightly lower pressure to allow for this effect and are compressed close to the bottom of the range on the chart.
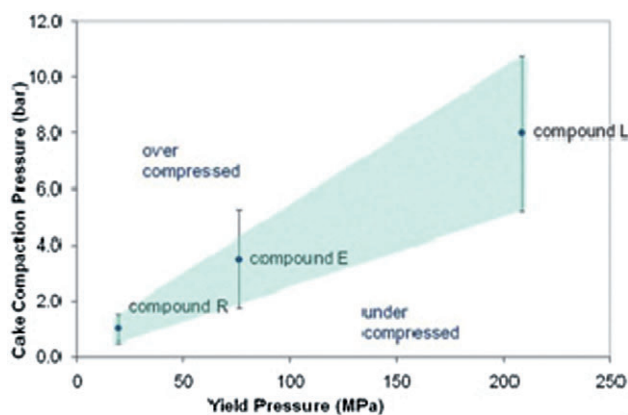
Figure 1: Plot of Compaction Pressure used versus Yield Pressure derived from the Compaction Simulator

CONCLUSIONS

The yield pressure obtained can be used to predict the compaction pressure required to produce the ideal inhalation cake.

This new prediction method has been used successfully for several inhalation compounds. All successfully delivered a good particle cloud to achieve the desired inhalation exposure.

REFERENCE

[1] R.W. Heckel, Trans. Metall. Soc. AIME 221, 1001–1008 (1961)

Preparation and optimisation of PMAA-Chitosan-PEG nanoparticles for oral drug delivery

H. Pawar[1], D. Douroumis[1], J.S. Boateng[1].

[1]University of Greenwich, School of Science, Chatham Maritime, ME4 4TB, UK

INTRODUCTION

In the current study pH sensitive polymethacrylic acid – chitosan–polyethyleneglycol (PCP) nanoparticles, were developed through a free radical polymerisation process [1]. Metoprolol was used as a model active substance and the obtained PCP nanoparticles presented excellent drug loading (20–30%) and bioadhesion properties.

MATERIALS AND METHOD

Nanoparticles were prepared from a combination of methacrylic acid (MAA), polyethylene glycol (PEG) and chitosan (CS). The polymerisation process took place under continuous mixing of the above excipients in various combinations. In a typical process, the excipients were dissolved in 300 ml of distilled water with constant stirring at 60°C for 6 hrs. The nanoparticles were evaluated by using SEM, DSC, XRD and dissolution studies.

RESULT AND DISCUSSION

The development of pH sensitive PCP nanoparticles was carried out by using inter-ionic complexation between PMAA-CS. In brief, the amino group of CS interacts with carboxylic acid of MAA, and serves as a counter ion leading to the spontaneous generation of particles during the polymerisation process. In addition, PEG interacts with the PMAA's carboxylic groups to induce bioadhesive properties by forming interpolymer complex. By adjusting the excipi-
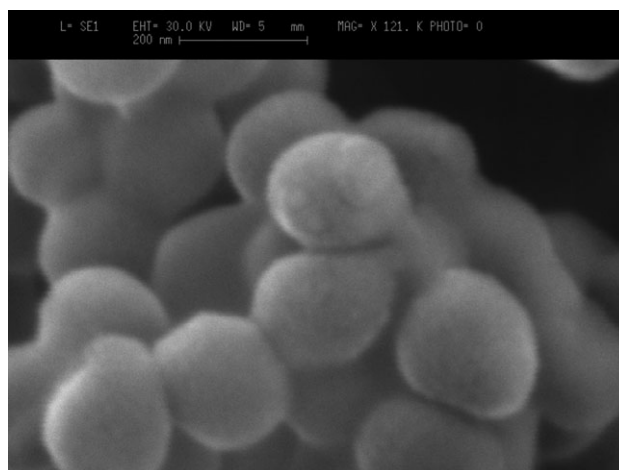
Fig. 1. SEM image of PCP nanoparticles

ents' ratio it was possible to tune the particle size. PCP empty nanoparticles with an average particle size of 200 nm were prepared as shown in Fig. 1. The particles were uniform with a smooth surface and spherical shape.

Metoprolol incorporation of 20.68% and 29.30% (drug loading, DL) was achieved by varying the initial drug amounts added during the polymerisation process. The XRPD diffractograms of two formulations (F1, F2) with different drug loading showed that metoprolol was in amorphous state as shown in Fig.2. These results were also confirmed by DSC studies by the absence of the metoprolol's endothermic peak at 45°C.
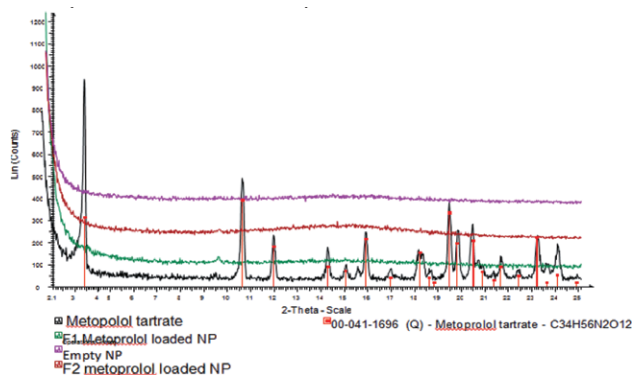
Fig. 2. X-ray powder diffractograms of pure metoprolol and PCP loaded nanoparticles
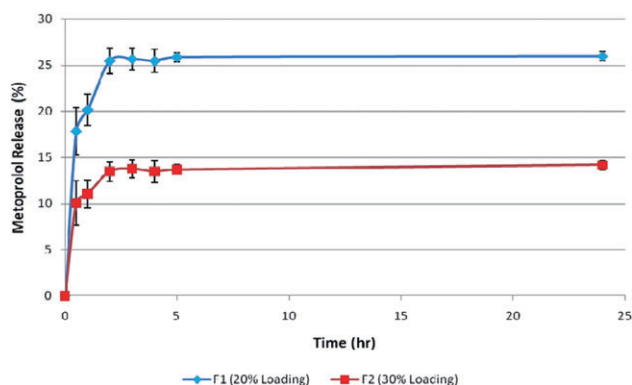

Fig. 3. Drug release profiles of PCP nanoparticles.

Dissolution studies were carried out in acidic (2 hrs, pH 1.2) and basic (pH 6.8) medium for 24 hrs. As can be seen in Fig. 3, metoprolol's release was observed only for the first two hours. At pH 6.8 drug release was negligible indicating that PCP synthesised nanoparticles dissolve in acidic pH (1.2) to allow the release of drug (25 and 14%) in the first 2 hours. Due to polycationic nature, amino groups in CS will get ionised at pH less than its pKa (pH ~6.5) and this causes the network to swell in acidic solution.

CONCLUSIONS

PCP synthesised nanoparticles can be efficiently used as pH sensitive drug delivery system with high drug loading capacities.

ACKNOWLEDGEMENTS

The authors would like to thank Dr Ian Slipper for his help with SEM and XRD experiments.

REFERENCE

[1] Sajeesh S, Sharma CP. Novel pH responsive polymethacrylic acid-chitosan-polyethylene glycol nanoparticles for oral peptide delivery. J Biomed Mater Res B Appl Biomater. 2006, 76:298–305

Production of Calcium Pectinate Microspheres for Oral Colonic Drug Delivery: Exploring Process Parameters

P. McCarry, R.W. Greenwood, A.M. Smith, R.H. Bridson

School of Chemical Engineering, University of Birmingham, Birmingham, UK.

INTRODUCTION

Pectin is a biopolymer that can be cross linked with Ca^{2+} to produce calcium pectinate which is an attractive material for the controlled release of drug molecules. In particular, pectin has potential for drug delivery to the colon since it is naturally degraded by the colonic flora.

The overall aim of this work is to produce a drug delivery system composed of a calcium pectinate/drug core coated in a pH responsive polymer layer. The outer coating protects the drug core from the conditions of the upper GI tract. Drug release is triggered upon the cores' entry to the colon by swelling and degradation.

This abstract focuses on one part of this work – understanding the effects that process parameters have on the shape, size and swellability of the calcium pectinate microspheres.

MATERIALS AND METHODS

Microspheres were produced by a water in oil emulsion method [1]. Pectin solution (2% w/v) was dispersed in isooctane with span 85 as a surfactant. After the droplets had been produced calcium chloride solution was added to cross link the spheres. The microspheres were filtered and dried.
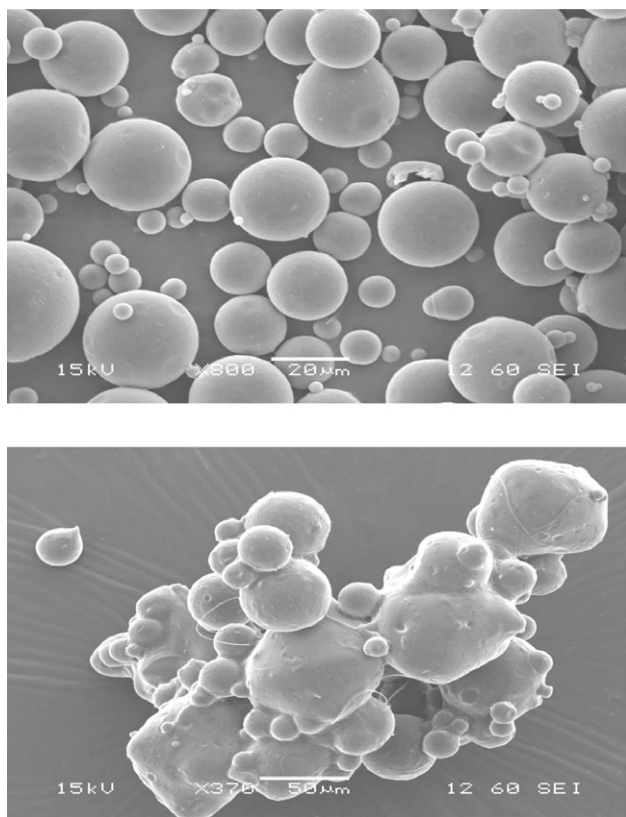
Figure 1 – Particles made at 1000 RPM with 30% CaCl$_2$ with (top) 5% span and (bottom) 2% span at 1000 rpm.

A detailed study into the effects of stirring rate (500–1500 rpm) and the relative concentrations of surfactant (2–5% w/v) and calcium chloride (10, 20, 30% w/v in the solutions added) was carried out. The resultant size, shape and swellability of the particles were investigated using SEM, laser diffraction particle sizing and light microscopy.

RESULTS AND DISCUSSION

Particles produced using the chosen method ranged in size from around 10 to 50 microns. As expected, increasing the stirring rate during emulsion formation generally led to smaller particles. The quality (shape and definition) of the particles was dependent on surfactant concentration. Higher concentrations of span 85 were needed to stabilise the emulsions formed at the higher stirring rates. Lower concentrations of surfactant could not support the formation of discrete particles resulting in the formation of lumps of gelled pectin (Figure 1). The concentration of the calcium chloride used for cross linking had a significant effect on the swellability of the particles and their permeability. Calculated 'swelling ratios' decreased from 0.75 to 0.4 when increasing calcium chloride concentration from 10 to 30%.

CONCLUSION

The investigated parameters saw that successful particle formation was dependent on achieving satisfactory emulsions and the concentration of surfactant was particularly important. The strength of calcium chloride affected particle swelling and the effects that this has on drug release are now being explored along with design of the outer polymer coats including using blends of different polymers.

REFERENCE

[1] T.W. Wong, H.Y. Lee, L.W. Chan, P.W.S. Heng, 2001. Drug release properties of pectinate microspheres prepared by emulsification method. Int. J. Pharm. 242, 233–237.

Relationship between ATP hydrolysis and molecular dynamics in co-freeze-dried sugar-ATP mixtures

A. Pandya[1], I. Ermolina[1], R Storey[2], G. Smith[1]

[1]School of Pharmacy, De Montfort University, UK. [2]AstraZeneca UK Ltd, Macclesfield, UK.

INTRODUCTION

Predicting the shelf-life of freeze dried formulations continues to present a challenge to both academic and industrial scientists. Our approach is based on an understanding of the relationship between the molecular dynamics of the freeze-dried matrix and the stability of a co-freeze-dried moisture labile model-drug substance, adenosine tri-phosphate (ATP). The molecular dynamics of co-freeze-dried sugar-ATP mixtures were studied using broadband dielectric spectroscopy (BDS) and the degradation of ATP (to ADP and AMP) was studied using high pressure liquid chromatography (HPLC).

MATERIALS AND METHODS

3 mL aliquots of solutions of 1% w/w ATP with 10% w/w sugar (either trehalose, maltose, or lactose) were freeze-dried

Table 1: % ADP + AMP detected on storage of ATP at 40°C (n = 9)

Day	Lactose		Maltose		Trehalose	
	ADP + AMP	Error +/−	ADP + AMP	Error +/−	ADP + AMP	Error +/−
0	0.00	0.00	0.00	0.00	0.00	0.00
2	0.91	0.29	0.85	0.36	1.47	0.47
4	0.98	0.10	1.62	0.15	2.04	0.10
6	1.91	0.06	2.00	0.16	2.94	0.12
8	3.00	0.41	2.35	0.11	4.40	0.54
10	3.45	0.04	3.62	0.14	5.08	0.06
15	4.45	0.45	4.45	0.09	6.50	0.18
30	6.20	0.13	6.40	0.15	10.77	0.15

in 20 mL glass vials according to the following protocol: freezing at −40°C for 2 h; primary drying at −30°C for 60 h; and secondary drying at 20°C for 10 h. Moisture contents of the freeze-dried mixtures (~1.5%) were determined by TGA. HPLC and BDS analysis were also performed before storing the batch of the vials at 40°C for 30 days.

An ion pair reverse phase HPLC method was used [1] with an Agilent Eclipse C_{18} column (length 150 mm × 46 mm) and a two component mobile phase (phosphate buffer, pH 6, and methanol) with the detector set at wavelength 260 nm. For identifying initial concentration of ATP at day zero, three freeze-dried vials were reconstituted with water to its original solution weight and 250 µl of this solution was added to 750 µl of phosphate buffer. HPLC analysis was repeated at day 4, 8, 15 and 30 days for each co-freeze-dried sugar-ATP formulation.

Isothermal broad band dielectric spectra were recorded between 0.1 Hz and 1 MHz by placing ~300 mg freeze-dried sample between two gold-coated electrodes of 25 mm diameter and 1 mm separation, at day 0.

RESULTS AND DISCUSSION

Degradation of ATP was assessed from the area under the curve of the degradation products adenosine diphosphate (ADP) and adenosine monophosphate (AMP). ATP was equally stable in maltose and lactose whereas in trehalose the degradation was almost twice that of the other two sugars (**Table 1**).

Molecular dynamics were assessed in terms of the dielectric relaxation time (τ) and Fröhlich parameter B(T) for the sub-Tg γ-process. Of these two parameters it was the magnitude of B(T) for relaxation process of freeze-dried sugars at day 0 that followed the trend trehalose > maltose ~ lactose (**Figure 1**).

Notwithstanding the fact that estimates for B(T) of sugar-ATP matrix were measured at sub-zero temperatures, and the degradation of ATP was assessed at elevated temperatures, there is a correlation between the trends observed for the three sugars investigated. The high magnitude B(T) observed for trehalose suggests greater degrees of rotational freedom of hydroxymethyl pendant group [2] which in turn might reflect
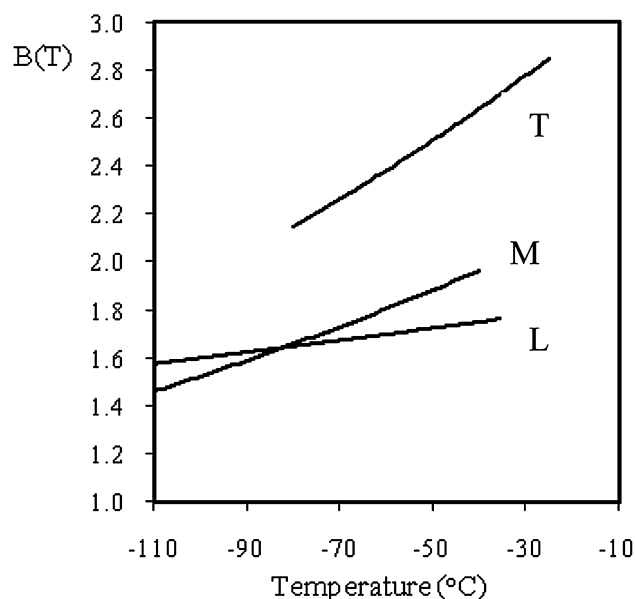

Figure 1: Fröhlich parameter B (T) for dielectric relaxation of lactose (L), maltose (M) and trehalose (T) measured at a range of temperatures.

more generalized degrees of freedom for water diffusion in the matrix.

CONCLUSION

The apparent correlation between the rank order of the sugars from the molecular relaxation study and the rank order of the sugars from the ATP stability study is pre-supposed to arise from the fact that the micro-scale relaxation phenomena are at the same scale for water diffusion through the matrix, which is in turn defines the stability of a moisture labile chemical such as ATP.

ACKNOWLEDGMENTS

REFERENCES

[1] S. Giannattasio, S. Gagliardi, M. Samaja, E. Marra, *Brain Res Protocols* **10**: 168–174

[2] I. Ermolina, E. Polygalov, C. Bland, G. Smith, *J. Pharm. Pharmacol, suppl* **1** (2007) A1–42

Rheology and differential scanning calorimetry used for the detection of drug crystallisation in drug-in-adhesive layers

F. Readman, K. Dodou

Sunderland Pharmacy School, University of Sunderland, Sunderland, UK.

Abstract **– The saturation concentration of ibuprofen in acrylic adhesive layers was established using microscopy, differential scanning calorimetry (DSC) and rheometry, 21 days after preparation. DSC predicted a saturation solubility of 14.84%w/w similar to the microscopic examination showing the presence of crystal nuclei at 14.8%w/w after 21 days. Rheological measurements predicted a saturation concentration of between 19.5–21.5%w/w, similar to the macroscopic appearance of the layers.**

INTRODUCTION

The aim was to examine whether DSC and rheological measurements can predict drug crystallisation and saturation in adhesive layers.

MATERIALS AND METHODS

Preparation of the drug-in-adhesive layers: Drug-in-adhesive layers containing 100 mg ibuprofen (Knoll Pharmaceuticals, Nottingham) in acrylic adhesive (DUROTAK 87–4287, Henkel, Slough) were prepared at concentrations between 10–33% w/w. The layers were stored at room conditions for 21 days and then examined in the following sequence:

Polarised microscopy: The presence of ibuprofen crystals in the layers was established using an Olympus BH2 microscope with an Olympus 10× lens fitted with a camera (AxioCam MRc-Zeiss, UK) and AxioVision vs4.4 image analyser software.

Differential Scanning Calorimetry: Enthalpy of fusion (ΔHf) values (n = 3) were recorded in hermetic pans using a standard DSC (Q1000, TA Instruments, USA) ramp test from 0°–100°C at 10°C/min. Precalibration was via an indium standard.

Rheological measurements: An amplitude sweep test over a shear stress range of 0.1–30,000 Pa at a constant frequency of 1 Hz at 32°C was used. The complex modulus (G*) within the linear viscoelastic region was recorded.

RESULTS AND DISCUSSION

After 21 days' storage, microscopic examination showed isolated ibuprofen crystal nuclei at 14.8%w/w. Macroscopic appearance showed visible crystal formation at 19.5%w/w
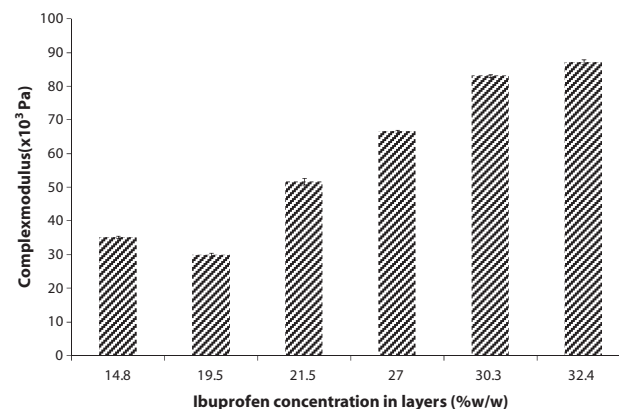

Fig. 1. Mean (n = 3) complex modulus G* versus ibuprofen concentration.
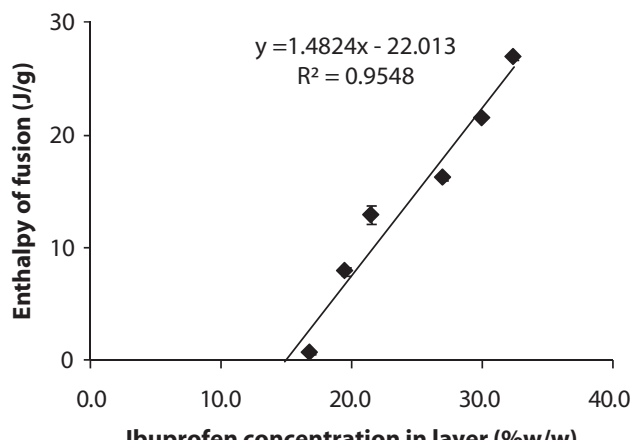

Fig. 2. Mean (n = 3) enthalpy of fusion ΔHf versus ibuprofen concentration.

ibuprofen concentration. Rheological studies showed a simultaneous increase in G* and ibuprofen concentration in supersaturated layers, similar to previous findings [1]. The saturation solubility was determined from the onset of this increasing trend, within the range 19.5–21.5% w/w (Fig.1).

Saturation solubility using DSC [2] was estimated at 14.84%w/w ibuprofen concentration (Fig.2).

CONCLUSIONS

Enthalpy of fusion measurements showed similar sensitivity to microscopy in the detection of ibuprofen crystals in the adhesive layers. The saturation concentration of ibuprofen in the acrylic layer, as predicted using the rheological complex moduli, was in agreement with macroscopically evident crystallisation levels.

ACKNOWLEDGMENTS

Dr Dodou would like to thank Henkel for the kind provision of DUROTAK 87–4287.

REFERENCES

[1] K.Y. Ho and K. Dodou, "Rheological studies on pressure-sensitive silicone adhesives and drug-in-adhesive layers as a means to characterise adhesive performance" *Int. J. Pharm.*, **333** (2007) 24–33.

[2] G.S. Oladiran and H.K Batchelor, "Determination of ibuprofen solubility in wax: A comparison of microscopic, thermal and release rate techniques" *Eur. J. Pharm. Biopharm.*, **67** (2007) 106–111.

Rotational Rheometry for Characterising Formulations for Melt Extrusion

S.A. Roberts[1], P. Hodder[2]

[1]MS&T, Abbott Laboratories, Queenborough, Kent, ME11 5EL, UK.
[2]TA Instruments, Crawley, RH10 9NB, UK.

Abstract **– Rheological properties are central to a successful hot melt extrusion process. An understanding of these properties for the candidate formulation helps in the optimisation of the extrusion process. Eudragit E and Plasdone S630 were chosen as model polymers suitable for melt extrusion and binary mixtures were prepared with either Paracetamol or Ibuprofen as a model drug, at drug loadings of 0, 5, 10 and 20 wt.%. The rheological properties were recorded over a temperature range of 110–150°C for the Eudragit E blends, and 130–170°C for the Plasdone S630 blends. Increasing temperature reduces the resistance to flow of the formulation, potentially reducing the required processing torque and die pressure. Increasing drug loading within the polymer matrix can result in either an increase or a decrease in the resistance to flow. Through our study of these model systems we demonstrate how simple rheological measurements can help to determine the effect of drug loading on the rheological properties.**

INTRODUCTION

Hot melt extrusion is widely used in the plastic, rubber and food industries. It is being increasingly used in the pharmaceutical industry to produce a wide variety of dosage forms. Rheological properties are central to a successful hot melt extrusion process. Rotational rheometry can be successfully used in the development of suitable formulations, in addition to providing an understanding of potential processing conditions. This can help to minimise the use of potentially costly and time consuming development trials.

MATERIALS AND METHODS

Binary mixtures of polymer and drug were prepared with drug loadings of 0, 5, 10 and 20 wt. %. The polymer phase was formed from either Eudragit E (Evonik, Germany) or Plasdone S630 (ISP, UK). Paracetamol (Rhodia, France) or Ibuprofen (BASF, Germany) was used as the model drug component.

Rheological characterisation was performed using an AR-G2 rheometer (TA Instruments) fitted with an Environmental Test Chamber and a 25 mm parallel plate. Mechanical spectra were recorded over a temperature range of 110–150°C for the Eudragit E blends and 130–170°C for the Plasdone S630 blends.

RESULTS AND DISCUSSION

The rheological properties of all the blends studied decreased as temperature increased. The incorporation of Paracetamol in the Eudragit E polymer matrix resulted in an increase in the values of G′, G″ and η* at temperatures below 130°C due to the drug particles acting as filler particles. At higher temperatures the drug becomes miscible with the polymer and the measured rheological properties drop below those of the polymer. In the case of the lower melting Ibuprofen, the values of G′, G″ and η* decreased with increasing API content at each temperature.

Binary mixtures of Paracetamol and Plasdone S630 demonstrated similar behaviour to those of Eudragit E and Ibuprofen, with G′, G″ and η* decreasing with increasing API content, illustrating the miscibility of the APIs with the respective polymers. The binary mixtures of Ibuprofen and
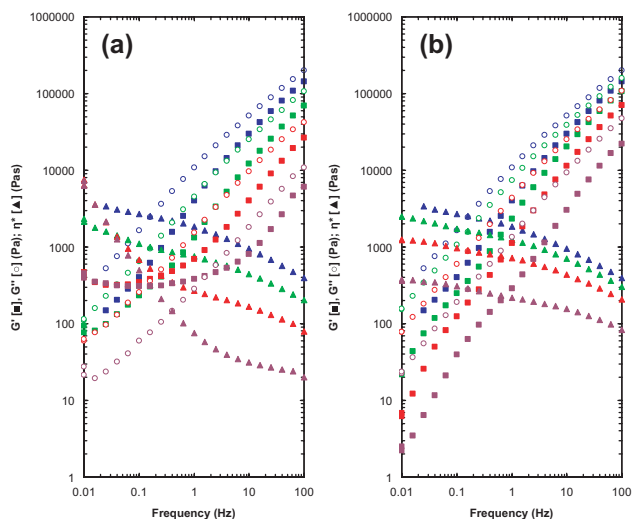
Fig. 1. Frequency dependence at 170°C of (a) Plasdone S630/Ibuprofen binary mixtures and (b) Plasdone S630/Paracetamol binary mixtures at 0, 5, 10 and 20% drug loading.

Plasdone S630 showed a deviation from this behaviour at high drug loadings above 150°C, with the data showing a change from terminal zone behaviour to rubbery behaviour at low frequency (see Fig. 1). In this case the molten Ibuprofen is not completely miscible with the polymer, resulting in the API imparting a higher viscosity on the polymer at low frequency.

CONCLUSIONS

Rotational rheometry has been successfully used to characterise a number of model formulations for hot melt extrusion. Paracetamol was shown to be miscible with Eudragit E and Plasdone S630, whereas Ibuprofen was shown to be miscible with Eudragit E, but not fully miscible with Plasdone S630. The differences in behaviour observed on heating of the Plasdone S630/Ibuprofen formulation could result in difficulties during the extrusion process. This may also lead to instabilities in the resultant drug product.

The rheological data generated can be utilised in the development of large scale melt extrusion processes, providing a valuable insight into the selection of critical processing parameters to ensure successful manufacturing.

Semi-empirical approach for scaling up wet granulation process

Andzrej Gallas[1,2], Bindhu Gururajan[1], Barry Crean[1], James Kraunsoe[1] and Gavin Reynolds[1]

[1]Pharmaceutical Development, AstraZeneca R&D, U.K.
[2]School of Pharmacy, University of Nottingham, U.K.

Abstract – **Wet granulation is often used to produce agglomerates from primary particles. The goal of scale-up is to obtain similar granule and tablet attributes in both micro and macro scale granulation. It is typical in the pharmaceutical industry to use a constant tip speed approach for scaling up this process. The aim of this work was to evaluate the suitability of using impellor power measurement for successfully scaling up the high shear granulation process.**

INTRODUCTION

A measurable process parameter, such as power draw in a wet granulator, is often used to determine the desired process residence time (e.g., endpoint in a batch granulator). There are numerous references on the use of power draw, torque or other similar indicator for endpoint control and scale-up of granulation processes in the literature [1,2]. In this work an attempt is made to validate the use of dimensionless power number for scaling up wet granulation process.

$$\text{Dimensionless Power Number, } N'_p = \frac{\Delta P}{N^3 R^2 M}$$

Where N is the impeller speed (s^{-1}), ΔP is the overall variation of power draw: $P_{max} - P_{baseline}$ (W), R is the bowl radius (m), M is the powder mass (kg).

MATERIALS AND METHODS

Granulation trials were performed using 10 L and 65 L granulators with a batch size of 2 kg and 12 kg, respectively. Formulation containing drug, lactose, microcrystalline cellulose, sodium starch glycolate, hydroxy propoyl cellulose and magnesium stearate was used for this investigation. Experimental investigation was carried out using a Design of Experiments at the 10 L scale, to understand the impact of granulation process parameters on the granule properties. Using the dimensionless power number approach, process conditions for 65 L scale granulation were defined. Two confirmatory batches were run at the defined conditions to validate the approach.

RESULTS AND DISCUSSION

The data generated at 10 L scale were evaluated using Design Expert and SIMCA P$^+$ multivariate analysis software. The
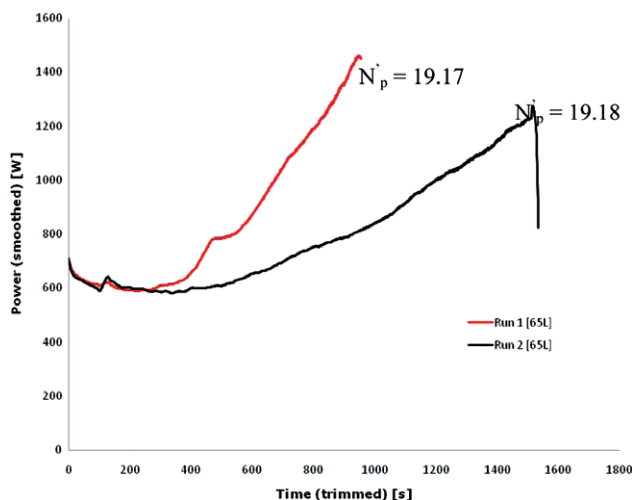
Fig. 1. Impeller power profile from 65 L granulation trials

dimensionless power number was calculated using the 10 L granulation impellor power profile. Using SIMCA P$^+$, the power number was found to be suitable for predicting the effect of granulation parameters on the granule size distribu-tion and flowability. Two batches were run using constant power number approach. Figure 1 shows the impellor power profile for 65 L granulation process run using two different process conditions with constant power number.

The properties of the granules and tablets produced were comparable with the 10 L product data.

CONCLUSIONS

Dimensionless numbers, namely the power number, was successfully used to define process parameters for scale-up of the wet granulation process. The granules and tablets produced at 10 L met the desired product quality and correlated well with those produced at the 65 L scale.

REFERENCES

[1] P Mort, "Scale up of high shear binder agglomeration processes" in Granulation, A.D.Salman, M.J. Hounslow and J.P.K. Seville, Elsevier publications, Amsterdam, ch. 19, 2007, pp. 854–896.

[2] F Bayard, B Gururajan, G Reynolds, B Crean and J Kraunsoe, "Scale independent approach for scale up of wet granulation" J. Pharm. Pharmacol., 2009, pp. 102–138 (37).

Sonocrystallisation Particle Engineering for Inhalable Medicines

G. Ruecroft, D. Parikh

Prosonix Ltd, The Magdalen Centre, Robert Robinson Avenue, Oxford Science Park, Oxford, OX4 4GA, UK

Abstract – **Ultrasound Mediated Amorphous to Crystalline transition (UMAX®) and Solution Atomisation and Crystallisation with Ultrasound (SAX™) can be used for the manufacture of optimal particles for asthma and COPD drug products. Fluticasone propionate (FP) can be prepared for both Dry Powder Inhalation (DPI) and Metered Dose Inhalation (MDI) whereby the respiratory and fine particle fraction (FPF) can be significantly improved over mechanically micronised material.**

INTRODUCTION

Sonocrystallisation [1] can be used to manufacture corticosteroid particles for inhaled medicines, in turn characterised as crystalline products with superior *in vitro* performance when compared with micronised material. UMAX can be used to obtain optimal performance attributes including size, shape, surface rugosity / free energy, crystallinity and stability, and can deliver both spheroidal and more regular shaped FP particles for DPI and MDI. In all cases respiratory doses and fine particle fraction (FPF) can be significantly improved over mechanically micronised material.

PROCESS METHODS

SAX is reported elsewhere [2]. UMAX (Fig. 1) [3] comprises the steps of (i) spray drying of an API solution, (ii) collecting the spray dried particles in a non-solvent, and (iii) applying power ultrasound to the unstable amorphous particles to effect crystallisation. The product can then be harvested by, for example, spray-drying.

RESULTS AND DISCUSSION

In vitro impactor (Next Generation Impactor –NGI; Anderson Cascade Impactor – ACI to measure FPF) and stability studies reveal that UMAX particles have outstanding performance when compared with conventionally manufactured products. Importantly, the process of aerosolisation from inhalers and deposition of particles in the lung is dependent on the particle surface interfacial properties, which will ultimately govern the performance and efficacy.

The FP particles in the DPI and MDI formulation must aerosolise appropriately so that they can be transported to the lung. Due to their small contact area and the potential large
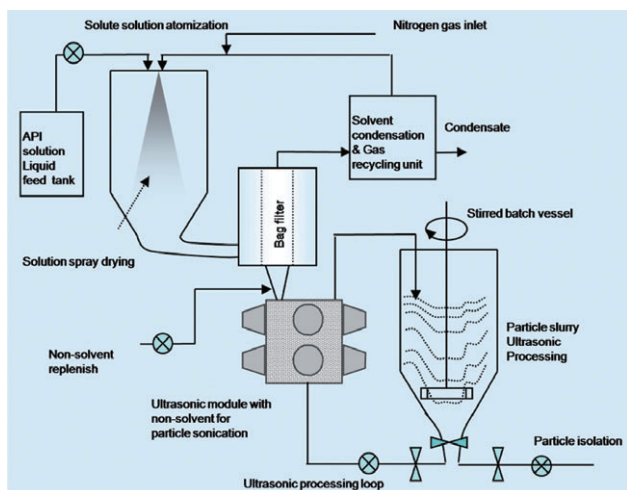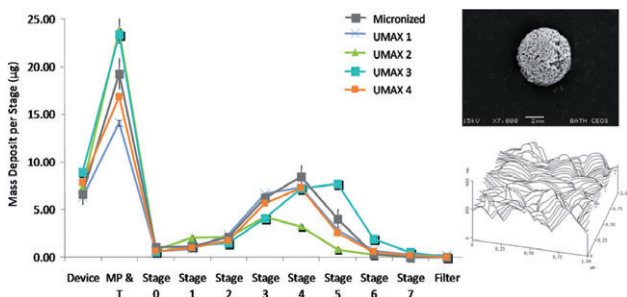
values of 1, being ideal for optimal FPF. UMAX particles have superior dispersion properties in both DPI and MDI due to irregular surface morphology as shown in Fig. 2. The aerosolisation efficiency of UMAX particles (sample 3) was significantly greater than that of micronised steroid.

Importantly, the optimal UMAX particles showed excellent stability over a 6 month period. Flixotide® 50 derived micronised FP has been compared with UMAX samples (Fig. 2). The study showed that the ACI distribution profile could be matched to that of Flixotide® 50 (using a proprietary MDI device). UMAX samples could be prepared to over-perform (UMAX 3) and under-perform (UMAX 2) the commercial micronised formulated test sample until optimal conditions were found (UMAX 1 and 4).

CONCLUSIONS

Particle engineering techniques, such as UMAX, involving the use of ultrasound can be used to engineer microcrystalline single and dual component particles for both DPI and pMDI, in turn yielding structured drug products that can out-perform the existing commercial products. In addition to superior *in vitro* performance the products and particles show greater medium to long term stability over micronised material.

REFERENCES

[1] G. Ruecroft, *et al*; "Sonocrystallisation: The Use of Ultrasound for Improved Industrial Crystallisation," *Org. Process Res. Dev*., **9** (2005) 9, 923–932.

[2] R. Price, J.S. Kaerger, WO 2005/073827; "Processing of spherical crystalline particles via SAXS technique," *J. Pharm. Res*., (2004) **21** (2), 372–381.

[3] G. Ruecroft, D. Parikh, D. Hipkiss, WO 2010/007447 and WO 2010/007447.

[4] R. Price, *et al*, "An investigation into the relationship between carrier-based dry powder inhalation performance and formulation cohesive-adhesive force balances," *Eur. J. Pharma. Biopharma*., **69**, (2008), 496–507.

Fig. 1. The UMAX process

Fig. 2. ACI studies for UMAX particles – UMAX 3 SEM is shown

separation distance between particles (decreased attachment forces and improved powder re-dispersion), spherical particles with high surface rugosity would have ideal attributes for aerosolisation. UMAX particles with increased surface rugosity are characterised by cohesive-adhesive balance (CAB) [4]

Spatial Map of Freeze-Drier Shelf Temperature Variations Using Product Collapse as a Surrogate Temperature Probe

K. Nazari, G. Smith, I. Ermolina

School of Pharmacy, De Montfort University, Leicester, UK

INTRODUCTION

In any freeze-drying process, the product temperature during primary drying must not exceed a critical temperature (T_c) in order to avoid the collapse of the product. This parameter is material dependent and can be determined by cryomicroscopy [1]. In the case of primary drying above the collapse temperature, a loss of structure in the dried region may be observed leading to unacceptable product quality. Therefore an accurate determination of T_c is essential in order to define an optimal freeze-drying process with an acceptable drying time [2]. The optimisation of process parameters (e.g. shelf temperature distribution) and formulation attributes are pre-requisites to the development of optimal freeze-drying cycles. The aim of this study is to use the phenomenon of product collapse (in simple freeze-dried sucrose formulations) as a surrogate temperature probe to identify problematic locations across the freeze-drier shelves.

Table 1. Parameters of the freeze-drying cycle

Batch	Number of vials	Freezing		Primary drying		Secondary drying	
		Tem (°C)	Time (h)	Tem (°C)	Time (h)	Tem (°C)	Time (h)
1	154	−37	9.5	−33	35	+30	12.5
2	154	−37	9.5	−33	72	+30	12.5
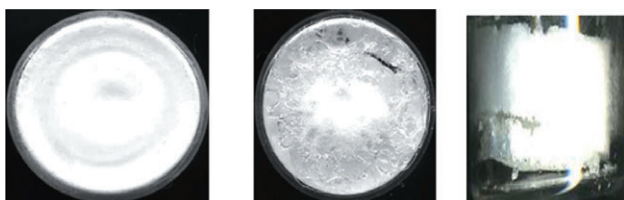
Fig. 1. Scanning image from base of vials of good product (left) and collapsed product (middle) and a photo of the side of vial for a collapsed product (right)

MATERIALS AND METHODS

The collapse temperatures of a range of sucrose solutions (2.5, 5, 7.5, 10, 12.5, 15% w/v) were determined by cryomicroscopy (JVC TK-C1380). Approximately 20 µl of each solution was placed on a glass cover slip, cooled to −40°C (5°C/min) and then reheated at 1°C/min. A video of each cycle were recorded at 0.02 frames/s then analysed using software (ArcSoft ShowBiz DVD 2) to give the collapse temperature.

3 ml aliquots sucrose solution (5% w/v) were freeze dried in 10 ml vials (Table 1). Freeze-drying runs were preformed in a 4-shelf HETO FD8 freeze-drier. Vials were located on the surface of the 2nd shelf from the bottom and arranged in clusters of hexagonal arrays.

The product appearance in each vial, from the two batches, was evaluated visually. Images taken from the base and side of each vial were used to identify regions of micro-collapse and cake morphology (Fig. 1).

RESULTS AND DISCUSSION

The collapse temperature of sucrose was found to be independent of concentration, across the range studied, and had a mean value of −31 °C (in agreement with the literature value of −31°C) [3]. In order to identify any hot spots on the shelf (which may lead to product failure) the nominal primary drying temperature of the shelves was set just below the T_c of sucrose (-33°C). Any vials experiencing local temperatures corresponding to the nominal shelf temperature would not collapse, whereas those experiencing local temperatures higher than the nominal set temperature would have a greater probability of collapse.

Visual inspection of each vial showed there was considerable variation in product quality, in batch 1, depending on the position of individual vials on the freeze-drier shelf. In general, those vials at the edge of the shelf gave better quality product characteristics. Vials located near the centre of the shelf were collapsed in batch 1 but not in batch 2. It is likely that batch 1, which had a relatively short primary drying phase, still contained residual ice at the end of primary drying, which then melted on raising the temperature in secondary drying. It follows therefore that product collapse was not because of hot spots on the shelf but instead more likely to be due to cold spots and less heat transfer in certain region so the shelf.

This observation indicates that the vials located in the center of the shelf received the least amount of heat, resulting in slow rates of sublimation and therefore the residual ice which causes the product to collapse when switching to secondary drying. From the observation that the second batch did not collapse at all, it may be infered that no regions of the shelf were in fact at temperatures higher than the nominal set temperature. In addition, because the second batch was permitted a longer primary drying phase, one can presume that all the ice was removed prior to the start of secondary drying.

CONCLUSIONS

Although further work is required, the study shows the potential for mapping of shelf temperature distributions, using surrogate temperature measurements inferred from product collapse phenomenon. More importantly, such studies can be used to validate new in-process measurement technologies that enable the process to be driven as the highest primary drying temperature achievable (without product collapse) and thereby minimise the time and cost required to complete the cycle.

REFERENCES

[1] M. J. Pikal, and S. Shah. *Int. J. Pharm.* **62** (1990) 165–186.
[2] W. Y. Kuu, L. M. Hardwick and J. M. Akers. *Int. J. Pharm.* **313** (2006) 99–113.
[3] W. Wang. *Int. J. Pharm.* **203** (2000) 1–60

Sticky Web, a Novel Powder Dispensing Technology

H.W. Biddle, R.A. Haines, F.C.R. Williamson

42 Technology, St. Ives, Cambridgeshire, UK.

Abstract – **Accurate active powder dosing in milligram and sub-milligram quantities for drug manufacturing is a challenge for pharmaceutical companies. Usually this is overcome by bulking out active pharmaceutical ingredients (APIs) with excipients and then volumetrically dosing. However, this process requires extensive formulation and stability studies to ensure that there are no adverse reactions between actives and the excipient.**

"Sticky Web" is a powder dosing technology developed to avoid the need for excipients with significant benefits in terms of accuracy of dosing, dissolution rate and manufacturability.

INTRODUCTION

Sticky Web exploits the simple but newly-discovered phenomenon that the mass of powder which adheres to a pressure sensitive adhesive is directly proportional to the area. The dosing technology involves coating active powder over a predetermined masked area of adhesive tape and then removing the excess.

This paper presents the current state of development of the Sticky Web powder dosing technology.

MATERIALS AND METHODS

Powder dosing accuracy testing

1) A pre-weighed section of adhesive tape was placed over a machined aperture in the powder coating drum.
2) The powder coating drum was then rotated through a single revolution to provide the adhesive tape with a dose of powder.
3) The section of adhesive tape was then removed from the drum and re-weighed to determine the mass of the dosed powder.

Sticky Web dissolution testing

1) Two replicate Sticky Web samples were prepared using edible adhesive tape and a commercially-available API. The powder had poor flow and compression properties that is typical of many such pure APIs and normally requires them to be blended with additional excipients in order to be handled successfully in regular oral solid dose processing equipment.
2) The Sticky Web samples were placed inside standard capsules. Two "control" capsules were also filled with the same quantity of pure API (without Sticky Web).
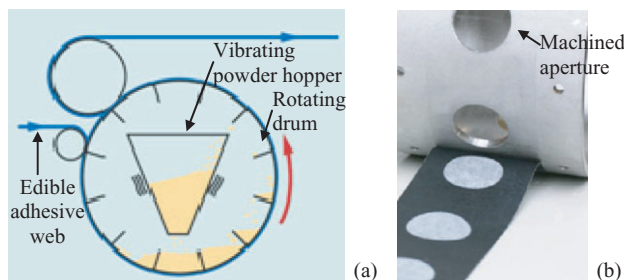3) Dissolution tests were then performed on each of the Sticky Web samples.

Fig. 1. (a) Schematic showing a continuous Sticky Web dosing process, (b) Powder coating drum and adhesive tape with dosed powder areas
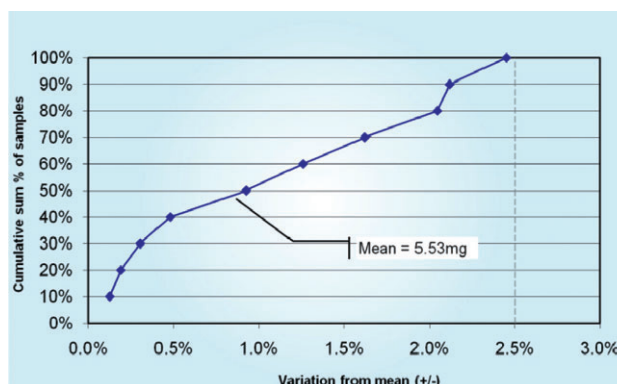

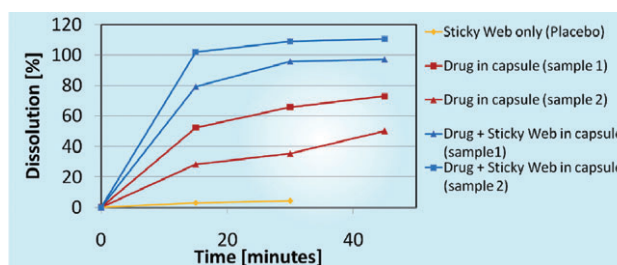**Fig. 2.** Graph of percentage of samples and their variation from the mean powder mass.

Fig. 3. Dissolution profiles for API samples dosed using Sticky Web versus bulk powder in capsules

RESULTS AND DISCUSSION

Powder dosing accuracy testing

The powder dosing tests show that all of the samples tested were within 2.5% of the mean powder mass. Figure 2 below shows the variation of the samples from the mean powder mass.

Dissolution testing

Dissolution test results shown in Figure 3 show that the API samples dosed using Sticky Web technology dissolve at nearly twice the rate of the bulk powder in capsule samples.

CONCLUSIONS

Initial testing of the Sticky Web powder dosing technology has shown that its dosing accuracy is excellent, outper-

forming current sub-milligram pharmaceutical manufacturing methods.

The method of manufacture of the Sticky Web doses is highly scalable for high speed production. At production speeds it is anticipated that a 16 lane version would be able to exceed 500,000 doses/hour.

Study the influence of film coating formulation on the mechanical and thermal properties

A.M. Abrahem, M. De Matas, I. Grimsey

Institute of Pharmaceutical Innovation, University of Bradford, UK
E-mail: a.m.a.benhadia@bradford.ac.uk

INTRODUCTION

The formulation of drugs into Multiple Unit Pelletised System (MUPS) has gained popularity over recent years due to the advantages of this dosage form. Tabletting of these systems is however challenging, particularly for coated pellets because of the potential for rupture of the release controlling membrane. It is therefore necessary to predict the mechanical properties of the film coating to ensure that release characteristics are adequate. Film coat characteristics are typically dependent upon composition alongside the attributes of the film coat components. The aim of this study was therefore to develop a sensitive analytical method with potential for detecting the impact of inter-batch variations in formulation composition and polymer characteristics on film quality attributes. Initial work has primarily focussed on the effects of film composition.

MATERIALS AND METHODS

Free cast films were prepared from solutions of ethyl cellulose containing the plasticiser polyethylene glycol (PEG 400) and Triethyl citrate (TEC) at levels of 0, 5, 10, 20, and 30 w/w. 50 ml of the polymeric solution was poured onto a glass plate of 14 cm in diameter. The films were dried at 40°C for 48 h and peeled off the mould using a spatula and surgeon's knife. Free film samples were characterised by thermogravimetric analysis (TGA), differential scanning calorimetry (DSC), and dynamic mechanical analysis (DMA).

RESULTS AND DISCUSSION

DSC was unable to detect any changes in thermal properties of the film; however, DMA demonstrated that by increasing the level of the plasticiser (0, 5, 10, 20 and 30%w/w PEG400) the Tg decreased from 131.88 to 108.55 C° (see Figure 1).

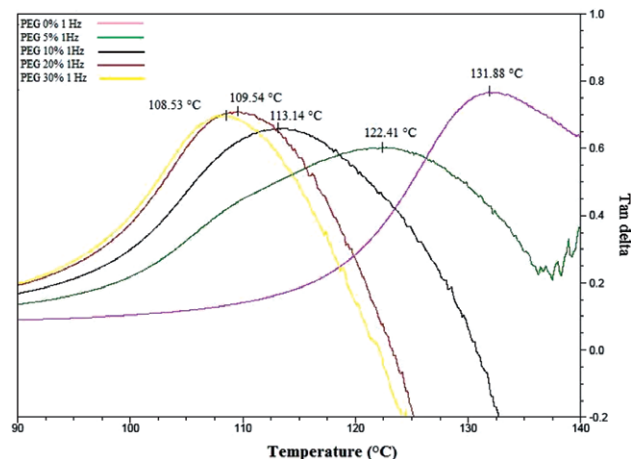The Tg for the EC film measured by DMA was markedly dependent on the rate of frequency applied during measure-

Figure 1. The influence of plasticiser level on the Tg.

ments. Greater discrimination between films of different composition was observed when changing the frequency rate from 1 HZ to 100 Hz. Other measurements which enabled discrimination between different coating formulations included storage and loss modulus.

CONCLUSIONS

The thermal and mechanical properties of polymers films are markedly dependent on composition. DMA has been shown to be a more applicable tool for detecting the effects of changes in polymer composition than DSC.

Using this method, discrimination between formulations can be improved through manipulation of testing conditions. Future work will therefore be focused on optimisation of the method and evaluation of its use in detecting the impact of inter-batch variation in the characteristics of raw materials.

Suppression of ibuprofen crystallisation in drug-in-adhesive acrylic layers at low temperature storage

K. Dodou, F. Readman

Sunderland Pharmacy School, University of Sunderland, Sunderland, UK.

Abstract – **Drug-in-adhesive acrylic layers containing ibuprofen were prepared at unsaturated (10% w/w, 15% w/w) and saturated (20% w/w, 25% w/w) concentrations and stored at three different conditions: ambient (RT), high relative humidity (HH) and low temperature (LT). X-ray analysis confirmed the presence of the same ibuprofen polymorph in layers stored at all conditions despite subtle morphological differences. Enthalpy of fusion measurements on the layers after 76 days' storage indicated suppression of ibuprofen crystallisation at low temperature.**

INTRODUCTION

Previous microscopic studies on 10% w/w ibuprofen-in-acrylic layers stored at RT, HH & LT conditions showed differences in ibuprofen morphology [1]. The aim was to further investigate this finding and to quantify the extent of crystallisation using Differential Scanning Calorimetry (DSC).

MATERIALS AND METHODS

Preparation of the drug-in-adhesive layers: Drug-in-adhesive layers containing 100 mg ibuprofen (Knoll Pharmaceuticals, Nottingham) in acrylic adhesive (DUROTAK 87–4287, Henkel, Slough) were prepared at concentrations of 10%, 15%, 20% and 25% w/w. The layers were then stored at ambient RT (20.1 ± 1.4°C, 34% RH), high humidity HH (20.1 ± 1.4°C, 62% RH) and low temperature LT (3.2 ± 1.7°C, 33% RH) conditions (n = 3 at each storage condition).

Polarised microscopy: Onset of crystallisation and crystal morphology in the layers was examined weekly using an Olympus BH2 microscope fitted with a camera (AxioCam MRc-Zeiss, UK) and AxioVision vs4.4 image analyser software.

Differential Scanning Calorimetry: Enthalpy of fusion (ΔHf) values of ibuprofen crystals in acrylic layers were recorded in hermetic pans using a standard DSC (Q1000, TA Instruments, USA) ramp test from 0°–100°C at 10°C/min, after 76 days' storage. Precalibration was via an indium standard.

RESULTS AND DISCUSSION

Microscopic analysis of layers stored at all storage conditions showed mostly plate/columnar ibuprofen crystals with sharp, angular corners (Fig. 1a) and also crystal clusters (Fig. 1b). X-ray analysis confirmed that these crystals belonged to the same polymorph of ibuprofen.
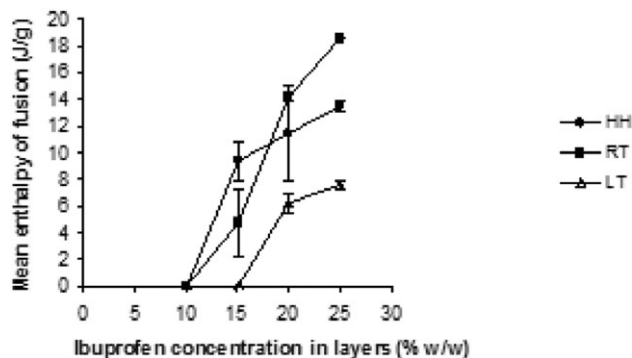

Fig. 1. Ibuprofen crystals in 15% w/w layers at RT (a); Ibuprofen crystal clusters in 15% w/w layers at HH (b)

Fig. 2. Mean enthalpy of fusion (n = 3) values versus ibuprofen concentration in layers after 76 days' storage.

Thermal analysis of the layers after 76 days' storage showed significantly lower enthalpy of fusion values for layers stored at LT compared to layers stored at RT & HH (Fig. 2). Layers stored at LT had no detectable crystalline content at 15% w/w drug loading in contrast to layers stored at RT and HH.

This finding agrees with recent guidelines on the storage of transdermal patches at low temperatures as a means to delay crystallisation [2].

CONCLUSIONS

An identical ibuprofen polymorph in the acrylic layers formed at all three storage conditions. Storage at low temperature suppressed ibuprofen crystallisation.

ACKNOWLEDGMENTS

REFERENCES

[1] N. Martin, Z. Ali, K. Dodou, "Effect of environmental conditions on the crystallisation patterns and in vitro release of ibuprofen from drug-in-adhesive acrylic layers" *J. Pharm. Pharmacol.* **60** (2008) A-55.

[2] UCB Pharma Inc., "UCB to implement full cold-chain for Neupro®" (2008). Accessed from www.ucb.com.

Tadalafil–Soluplus Solid Dispersion using Melt Extrusion for Improved Dissolution

Olajide Onike[1,2], Ravindra Dhumal[12], Adrian Kelly[1, 2], and Anant Paradkar[1,2 3].

[1]Centre for Pharmaceutical Engineering, University of Bradford, Bradford, UK,
[2]Intedisciplinary Research Centre in Polymer Engineering, University of Bradford, Bradford, UK.
[3]Institute of Pharmaceutical Innovation, University of Bradford, Bradford, UK.

Abstract **– The aim of this study was to improve the dissolution rate of tadalafil via solid dispersion (SD) with a novel polymer, soluplus. SDs containing different drug: soluplus ratios were prepared using hot melt extruder (HME). SDs were characterised for in vitro drug release and for crystallinity by powder X-ray diffraction (PXRD). Characteristic peaks for crystalline tadalafil were suppressed with an increase in polymer ratio indicating amorphisation of drug. Rate and extent of dissolution also increased with polymer ratio indicating suitability of soluplus for enhancing the solubility of tadalafil.**

INTRODUCTION

Tadalafil is a selective phosphodiesterase-5 inhibitor (PDE5) indicated for treating erectile dysfunction [1]. Poor aqueous solubility of tadalafil results in highly variable blood levels leading to therapeutic failure [1]. As a result it is essential to identify effective means of improving dissolution rate of tadalafil to obtain better predictability of its bioavailability [1]. Preparing solid dispersions using HME is an established processing technology for improving solubility of poorly soluble drugs [2]. HME was employed in this study using a novel polymer soluplus. Soluplus is a novel polymer designed for enhancing solubility of poorly soluble drugs and can be easily processed using HME.

MATERIALS AND METHODS

SDs of tadalafil and soluplus were prepared in varying ratios using a hot melt twin screw extruder. Processing temperature of extruder was stabilised at 200°C prior to extrusion. The SDs were characterised for crystallinity by powder X-ray diffraction patterns. Dissolution of 10 mg samples was performed using USP dissolution test apparatus II (Copley Scientific, UK) in 900 ml of 0.1N HCl with paddle speed 100 rpm at 37°C $\pm$ 0.5°C. Samples (5 mL) were withdrawn at predetermined time intervals and analysed spectrophotometrically at 280 nm after filtration.
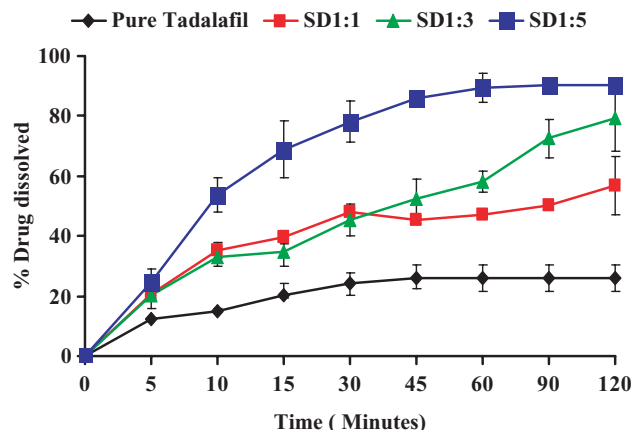

Figure 1 Dissolution profiles of pure tadafil and hot melt extruded SDs with soluplus in different ratios (1:1, 1.3, 1:5)

RESULTS AND DISCUSSION

The PXRD patterns of tadalafil showed characteristic peaks at $2\theta = 7.8°$, $10.2°$, $12.2°$, $14.5°$, $18.2°$, $22.2°$ and $24.5°$. SDs displayed a halo PXRD pattern and suppression of the characteristic peaks with increasing ratio of polymer indicating generation of amorphous SD. It was interesting to note that the melting point of tadalafil is 300°C and SD 1:5 processed at 200°C showed complete amorphisation indicating good miscibility of drug in molten soluplus. However, the lower polymer ratios were insufficient to dissolve the total drug in molten polymer and hence maintained traces of crystalline tadalafil as indicated by peaks in their PXRD. The dissolution rate and extent was also found to improve with increasing polymer ratio. At 45 min, 45% of drug dissolved from SD1:1, 52% from SD1:3 and approximately 90% from SD 1:5 in comparison to only 25% from pure tadalafil indicating the feasibility of SD with soluplus for enhance tadalafil dissolution rate.

CONCLUSIONS

Amorphous SD of tadalafil and soluplus was successfully prepared by hot melt extrusion. SD showed an increase in dissolution rate with increasing polymer concentration. Over 90% drug dissolved at 120 min from SD (1:5). This indicates the suitability of soluplus for HME and solubility enhancement. As part of further work, spectroscopic studies are being investigated for analysis of possible hydrogen boding interactions and mechanism of dissolution rate enhancement.

ACKNOWLEDGMENTS

REFERENCES

[1] S.M.Badr-Eldin, S.A.Elkeshen, M.M.Ghorab. Inclusion complexes of Tadalafil with natural and chemically modified β-cyclodextrins. Preparation and in-vitro evaluation. *Eur. J. Pharm. Biopharm*. **70** (2008) 819–827

[2] Repka MA, Majumdar S, Kumar Battu S, Srirangam R, Upadhye SB. Applications of hot-melt extrusion for drug delivery *Expert Opin. Drug Deliv.* (2008) **5** 1357–76.

Terahertz Pulsed Spectroscopy Study of Amino Acids and Gelatin

J. Darkwah, G. Smith, I. Ermolina

School of Pharmacy, De Montfort University, Leicester LE1 9BH, UK.

INTRODUCTION

Previously, Rapid Disintegrating Tablets (RDTs) have been formulated with gelatin and sugars e.g. mannitol to enhance the porosity and amorphous character of the RDT matrix. More recently, research has focused on the use of amino acids as a replacement component for polyols and sugars. The benefit is that lower concentrations of amino acids, up to 10% of the total solid material, are required [1]. However, there is an intrinsic stability issue with both types of RDTs. The conversion from amorphous to crystalline (devitrification) impacts the solubility and hence dissolution time. Understanding this devitrification process and ability to measure it is very important to the RDT formulations.

Terahertz Pulsed Spectroscopy (TPS) is a new tool that can be used to quantify any morphological changes associated with devitrification and recrystallisation, as a function of moisture content, composition/formulation, and storage conditions. Amino acids show distinct phonon resonances when probed with terahertz radiation. This study identifies these characteristic peaks and uses their existence to quantify recrystallisation of amino acids in gelatin loaded films and pellets.

MATERIALS AND METHODS

The amino acids used were serine (Ser), alanine (Ala) and lysine (Lys). These amino acids and gelatin (Gel) were obtained from Sigma Aldrich UK.

Polyethylene (PE) was used as the diluent in preparing 400 mg (±0.005%) pellets. The mixtures of PE and amino acid (up to 10%) were compressed into pellets with a Carver hydraulic press (compression force 2 tons for 2 mins). Pellets are used as the standard formulation for TPS measurements and for the calibration curves.

Films of thickness 0.3 ± 0.07 mm were prepared by casting 10% aqueous gelatin loaded with: Ser (5%); Lys (10%); Ala (10, 5 and 2%). This was followed by evaporation of water overnight. The concentration of amino acids in dry films was 50%, 33% and 17%, respectively. The thickness of each sample was measured at six different points with a micrometer and the average was taken.

Formulations were measured using TPS 3000 (Teraview Cambridge, UK). The sample compartment was purged with dry nitrogen for 10 minutes prior to measurements. The reference used was 400 mg PE pellet compressed for 2 minutes with 2 tonnes of force.

RESULTS AND DISCUSSION

The aqueous solubility of these amino acids follows in the order of Ala < Ser < Lys [2]. During sample preparation, it was observed whilst Ser and Lys had a limit of up to 10% solubility in the aqueous Gel films, Ala had a limit of 15%. This may be attributed to hydrophobic interactions between the methyl side groups within the gelatin. Thus, in our experiment the concentration of amino acid in solution was below 10%.

The frequencies of the principle absorption peak for Serine and Lysine were independent of sample preparation (i.e. pellet or film) as shown in Fig. 1A and B. However the amplitude of the peak and area under the peak is dependent on concentration of amino acid, method of preparation and thickness of sample.

For pellets the peak area (PA) is linearly proportional to concentration of amino acid for all three samples (see for example Fig. 1A). For films the PA increases with concentration of amino acid, but demonstrates non-linear dependence. To compare the results for film and pellets, the peak area was normalised per thickness of sample and concentration of
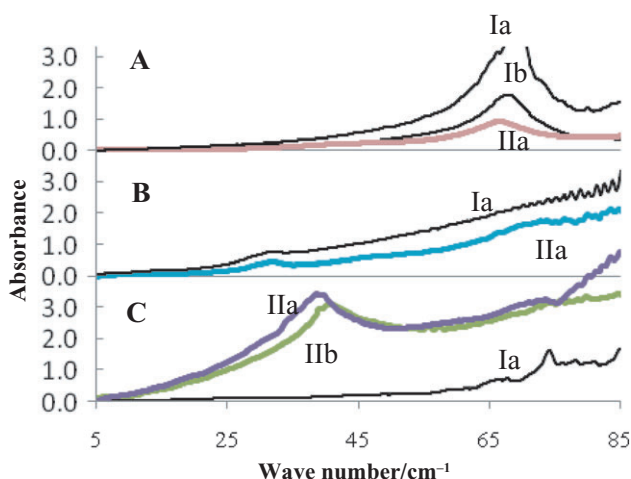
Fig. 1. Spectra of PE/amino-acid pellets and Gel/amino-acid films: (A) Ser, (B) Lys, and (C) Ala; (I) – Pellets, (II) – Films; (a) – 10%, (b) – 5%, (c) – 2%.

amino acid. The analysis has shown that amino acid in film is not a fully crystalline state.

CONCLUSIONS

TPS has been shown to provide quantitative measurements from the unique spectral profiles of different amino acids. There is evident potential for estimating the amount of crystalline amino acid in complex films and RDTs, which has relevance to dissolution rates and bioavailability.

REFERENCES

[1] F. Alhusban, Y. Perrie, A.R. Mohammed, "Formulation and characterisation of lyophilised rapid disintegrating tablets using amino acids as matrix forming agents" *Eur. J. Pharm. Biopharm.*, in press

[2] The Merck Index, Merck & Co., Inc., Whitehouse Station, NJ 12, (1996).

The Application of QbD to Pharmaceutical Powder Processing

Tim Freeman[1]

[1]Freeman Technology, Castlemorton Common, Malvern, UK.

Abstract **– The majority of delivery systems in the pharmaceutical industry are either based around a powdered formulation or utilise a powder in one or more manufacturing stages. To achieve the goals set out in recent ICH guidelines it is necessary to understand the behaviour of powders at all stages of manufacturing – formulation, process development, and manufacturing. This presentation reviews how powder characteristics and processing environments can be evaluated to generate the 'Design Space' necessary for the implementation of Quality by Design.**

INTRODUCTION

The Quality by Design (QbD) concept [1] was developed to reduce compliance costs and to improve product quality. The emphasis is for manufacturers to demonstrate that they are aware of what factors influence product variability and how their processes can be managed in order to mitigate such factors – the 'design space'. As a high proportion of feedstocks are powders, then it is incumbent on manufacturers to understand powder behaviour.

Powders are, however, complex systems, and there is no comprehensive understanding of their behaviour. Many factors can influence the way a powder can be behave – particle size and shape, stress, moisture and electrostatics are a small selection. Single number approaches to powder characterisation are unlikely to capture their multifaceted nature.

MATERIALS AND METHODS

In order to better understand the relationship between powder properties and process behaviour, modern instrumental methods – such as powder rheometry and shear cell testing – have been employed to provide data on powder behaviour over a wide range of stress conditions. Correlating this data with observed process behaviour allows for the quantification of the 'design space'.

RESULTS AND DISCUSSION

A specific example of this methodology applied to tablet compression is shown. There are several sub-processes within this particular operation; in this instance achieving consistent flow from the hopper is considered (Figure 1). Shear and wall friction are the obvious properties which impact powder flowing from the hopper, but permeability and compressibility are also important. Compressibility is required for bin design, and poor permeability can result in a "pulsating" flow rate or air-locking which can lead to significant tablet weight variability.

If the processability of three formulations is considered, then their relative performance can be judged, as shown in Figure 2.

Then, following measurement of the most relevant properties for that process, a series of boundaries can be defined representing the 'design space'. New materials can be formulated with confidence.
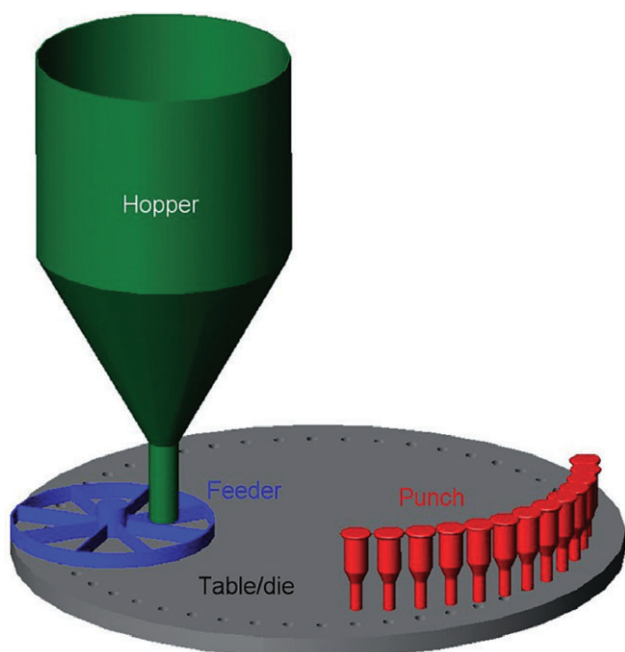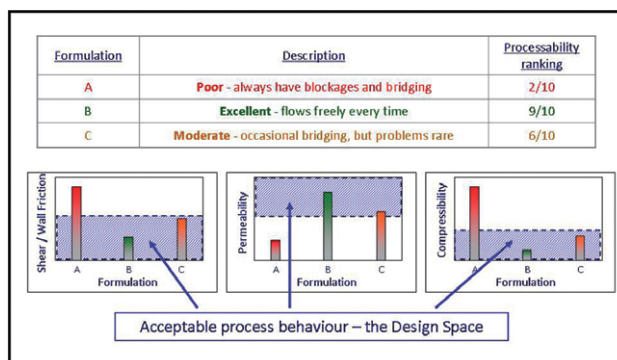
Figure 1: Tablet Press Schematic

Figure 2: Developing the Design Space concept

identified. This correlation must be achieved for every step in the process – including the interaction with the delivery system and patient. New formulations should be engineered to fall within the design space for each of the parameters identified as important in every process step. Reduced time to market, cost efficient processing, high quality product and the possibility of real time release are all potential benefits of adopting this methodology, the basis of which is a clear understanding of powder characteristics.

CONCLUSIONS

Correlation of process and delivery system ranking with measured flow properties enables the 'design space' to be

REFERENCE

[1] International Conference On Harmonisation Of Technical Requirements For Registration Of Pharmaceuticals For Human Use 2008, *Pharmaceutical Development Q8(R1).*

The Effects of High-Shear Blending on Interactive Mixtures For DPIs – Blending Kinetics & Scale-Up

J.M. Takher-Smith

Inhalation & Devices Centre of Emphasis, Pfizer Ltd, Sandwich, UK.

Abstract **– The product performance of a passive pre-metered dry powder inhaler (DPI) using an interactive mixture formulation approach was investigated at three blend batch sizes ranging from lab to commercial scale. Process factors of impeller rotational speed, blend time and bowl mass fill were summarised as a specific blend energy input (kJ/kg). Good relationships between specific blend energy input and aerosol performance criteria such as fine particle fraction (% FPF) and mass median aerodynamic diameter (MMAD) were observed both within and between scales.**

INTRODUCTION

Interactive / ordered mixtures [1] remain a standard methodology for manufacturing powder for inhalation within industry. Most typically the formulation contains a lactose monohydrate carrier with respirable sized active ingredient(s) adhered onto the carrier surface. Vertical axis 'high-shear' mixers are commonly employed for blending of these components due to their ability to rapidly deagglomerate the active substance and disperse it amongst the carrier lactose. Akin to a stirred liquid tank, the power transferred to the powder during this process can be measured via a variety of techniques [2].

This work intended to investigate the applicability of the findings by Bridson et al [3] with extension to a typical drug containing product and to also evaluate the use of a specific blend energy input as a key criterion during batch size scale-up.

MATERIALS AND METHODS

Lactose monohydrate carrier and micronised active pharmaceutical ingredient (mAPI) were mixed at three differing

impeller rotational speeds using a lab scale high-shear mixer. During each of the runs the process was interrupted and samples taken at six logarithmically spaced time intervals to allow the powder to be filled into a proprietary DPI. For each sample generated the aerodynamic performance from the DPI was assessed using the Next Generation Impactor (NGI) (n = 4 for each sample). This process was repeated at two increased scales using geometrically similar equipment (4× lab scale and 10× lab scale). The specific blend energy input was calculated from electrical impeller motor power readings using a factory installed wattmeter. Fine particle fraction is defined as the % of the emitted dose <4.46 μm aerodynamically. MMAD was calculated using a probit-log transformation of the cumulative % undersize vs. effective cut-off diameter (ECD) plot and hence a linear regression to determine the 50th percentile value.

RESULTS AND DISCUSSION

Similar to the findings by Bridson et al [3], the power regime under which the active product is made appears to be secondary in importance to the total blend energy input, especially under conditions which are likely to give broadly similar flow profiles within the bowl during blending. A characteristic kinetics curve was observed at each scale in relation to the device output aerosol size (MMAD) and aerosol efficiency (% FPF). Total emitted dose ex-device remained broadly constant through all sample points after unit-dose homogeneity was achieved.

A distinct robust plateau region was observed for the product where further blending caused little product change, although evidence for detrimental over-blending was apparent at excessive blend energy inputs. This robust region is likely due to an ordered mixture structure which approaches a steady-state style particulate / agglomerate arrangement.

CONCLUSIONS

A specific blend energy input appears a useful summarising descriptor of typical process parameters used during high-shear blending of interactive mixtures for inhalation. This measure also appears a useful criterion to monitor during batch size scale-up. The evolution of a typical mixture also shows a clear trend with respect to aerosol performance characteristics which may allow correlation with mAPI physical properties.

ACKNOWLEDGMENTS

REFERENCES

[1] J.A. Hersey, "Ordered mixing: a new concept in powder mixing practice" *Powder Technology*, **11** (1975) 41–44.

[2] G. Ascanio, B. Castro and E. Galindo, "Measurement of Power Consumption in Stirred Vessels – A Review" *Chemical Engineering Research and Design*, **82** (2004) 1282–1290.

[3] R.H. Bridson et al., "The effects of high shear blending on α-lactose monohydrate" *International Journal of Pharmaceutics*, **339** (2007) 84–90.

The Influence of Dissolution Method on In-Vitro Drug Release from Polyethylene Oxide Extended Release Matrix Tablets

D. Palmer, M. Levina, A. Nokhodchi[1] and A.R. Rajabi-Siahboomi

Colorcon Ltd, Dartford, UK
[1]Medway School of Pharmacy, University of Kent, UK

Abstract – **The aim of this study was to investigate the effect of dissolution method, agitation speed and media type on the release of drugs with different aqueous solubility (ibuprofen, <1 mg/mL; theophylline, 8 mg/mL and propranolol HCl, 360 mg/mL) from polyethylene oxide extended release matrices. USP II method with sinkers produced slightly faster dissolution than USP I. Drug release was slightly slower at 50 rpm compared to 100 and 150 rpm. Different dissolution results were produced in various media (water, buffers with pH 1.2, 6.8 and 7.2), i.e. faster release of freely soluble propranolol HCl was obtained in water.**

INTRODUCTION

Hydrophilic matrices are popular and a widely used strategy for oral extended release (ER) drug delivery. Hypromellose [hydroxypropyl methylcellulose (HPMC)] is the polymer of choice as the rate-controlling carrier [1]. In addition to HPMC, polyethylene oxide (PEO) has recently been studied as a matrix-forming polymer [2]. It has been reported that the type and composition of food may affect drug release from hydrophilic matrices resulting in a significant change in API bioavailability [3]. Some authors proposed that the influence of food may be mimicked by using different media agitation

in-vitro [3]. Here the influences of dissolution method, agitation speed and media pH on in-vitro release of APIs with different aqueous solubility has been studied.

MATERIALS AND METHODS

Model formulations containing 49.75%w/w drug, 49.75%w/w PEO (POLYOX™ WSR 1105 or Coagulant, Dow Chemical Company) and 0.5%w/w magnesium stearate were prepared. Low molecular weight (MW) PEO (1105; 900,000 Da) was used with ibuprofen and theophylline and high MW PEO (Coagulant; 5,000,000 Da) in the propranolol HCl formulation. The choice of the polymer viscosity grade was dependent on drug solubility. 10 mm flat-faced tablets with a target weight of 320 mg were produced on a semi-automated handpress (T8, Specac) at 20 kN. Dissolution tests were conducted in a Sotax, AT7 dissolution bath using either Apparatus I (baskets) or Apparatus II (paddles) with 15×31 mm sinkers (Sotax); in 900 mL of various media (water, buffers with pH 1.2, 6.8 and 7.2) at 50, 100 and 150 rpm. Absorbance was measured using UV/Vis spectrophotometer (PerkinElmer) at 222, 272 and 319 nm for ibuprofen, theophylline and propranolol HCl, respectively.

RESULTS AND DISCUSSION

Robust matrix tablets with the breaking force values of 10–14 kp were produced for all studied formulations. Figures 1 and 2 show the influence of dissolution method, agitation rate and media on ibuprofen and propranolol HCl release, respectively. For all tested formulations, USP II produced slightly but not significantly faster release than USP I that could be explained by the fact that a tightly woven mesh of the basket can potentially interfere with the erosion process of the matrix gel layer. That difference however was more pronounced with a very slightly soluble ibuprofen ($f2 = 52$) compared to theophylline ($f2 = 68$) and propranolol HCl ($f2 = 71$). For all tested formulations, the release obtained at 50 rpm was slower compared to 100 and 150 rpm. This difference was particularly obvious for ibuprofen ($f2 = 47, 56$). Dissolution medium had no significant effect on the release of the neutral drug, theophylline ($f2 = 84, 93$) and some effect on dissolution of the ionic drug propranolol HCl ($f2 = 62, 64$) which has pH-dependant solubility. For ionic drug ibuprofen, sink conditions were only achieved in pH 7.2 buffer.
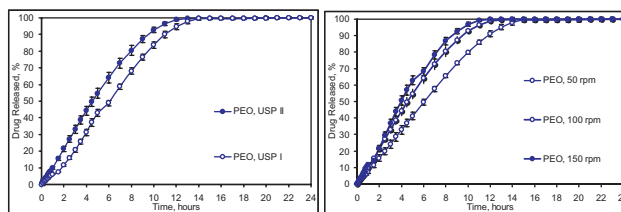

Fig. 1. Effect of (a) dissolution method (USP I or USP II with sinkers; pH 7.2, 100 rpm) and (b) agitation (USP II with sinkers; 50, 100 & 150 rpm; pH 7.2) on ibuprofen release
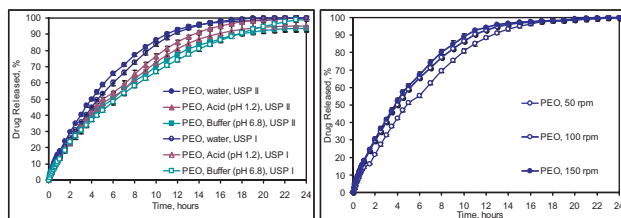

Fig. 2. Effect of (a) dissolution method (USP I or USP II with sinkers, 100 rpm) and media (100 rpm) and (b) agitation (USP II with sinkers; 50, 100 & 150 rpm; water) on propranolol HCl release

CONCLUSIONS

Robust PEO ER matrices were produced for all the formulations. A choice of the dissolution method and agitation rate had a more pronounced effect on a very slightly soluble drug ibuprofen compared to theophylline and propranolol HCl. Dissolution medium had a stronger influence on propranolol HCl and ibuprofen release due to their pH-dependant solubility.

REFERENCES

[1] Rajabi-Siahboomi A. and Jordan M.P., Slow release HPMC matrix systems, *Eur. Pharm. Rev.,* 5 (2005), 21–23.
[2] Choi S.U., Lee J., Choi Y.W. Development of a directly compressible poly(ethylene oxide) matrix for the sustained-release of dihydrocodeine bitartrate. *Drug Dev. Ind. Pharm.*, 29 (2003) 1045–1052.
[3] B. Abrahamsson, K. Roos and J. Sjogren, "Investigation of prandial effects on hydrophilic matrix tablets". *Drug Dev Ind Pharm.,* **25** (1999) 765–771.

The Influence of Hydrophilic Pore Formers on Metoprolol Succinate Release from Mini-tabs Coated with Aqueous Ethylcellulose Dispersion

H. Vuong, Marina Levina, Tom Farrell and Ali R. Rajabi-Siahboomi

Colorcon Limited, Dartford, UK

This study investigated the influence of incorporating a water-soluble pore former (based on polyvinyl alcohol; PVA) into aqueous ethylcellulose dispersion (Surelease®) film coating on *in vitro* release of a model drug, metoprolol succinate, from mini-tabs.

INTRODUCTION

Mini-tabs combine the advantages of MP dosage forms with the established manufacturing techniques of tabletting and have fewer constraints compared to extrusion-spheronisation. Additionally, mini-tabs produced via direct compression (DC) are an attractive alternative to pellets, since the use of liquids is avoided. Like other MP technologies, mini-tabs are filled into hard capsules, which may be used as whole or opened and mixed with food for easy administration to the elderly and children. Additional benefits of mini-tabs include excellent size uniformity, regular shape and a smooth surface, offering an ideal substrate to coat with polymeric membranes for MR purposes.

MATERIALS AND METHODS

Mini-tabs used in this study contained 10% w/w metoprolol succinate (S & D Chemicals Ltd), 85.5% w/w lactose (FastFlo®, Kerry Bio-Science), 0.5% w/w fumed silica (Aerosil® 200, Evonik), 2% w/w stearic acid (Meade King Robinson) and 2% w/w magnesium stearate (Peter Greven). The mini-tabs were manufactured by DC on a modified, instrumented, 10-station rotary press (Piccola, Riva) fitted with 2 mm double radius 16-tip tooling (B & D Italia); at 12 kN compression force and 30 rpm to a target weight of 8.0 mg.

Mini-tabs (0.6 kg batch size) were seal-coated with a 20% w/w aqueous solution of a PVA-based Opadry® II Clear (Colorcon) to 5% weight gain (WG), followed by a 15% w/w aqueous EC dispersion (Surelease®, Colorcon) with pore former (the same Opadry II Clear) at two different ratios (85:15 and 80:20) up to 16% WG. The trials were conducted in a GPCG 1.1 fluid-bed coater (Glatt) using bottom spray (Würster column) set up.

RESULTS AND DISCUSSION

The coated mini-tabs exhibited good appearance, showing no visual defects. Their mechanical strength improved significantly after the application of a seal-coat. Breaking force increased from 2.1 kp (uncoated) to 3.0 kp (seal-coated) and friability was reduced from 0.46% to less than 0.01% respec-
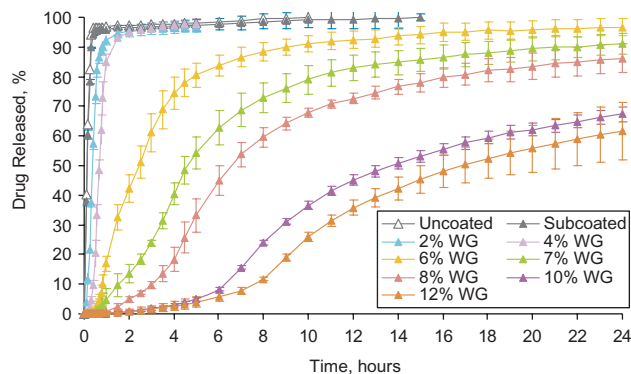

Fig. 1. Metoprolol succinate release from mini-tabs coated with Surelease/pore former (85:15)
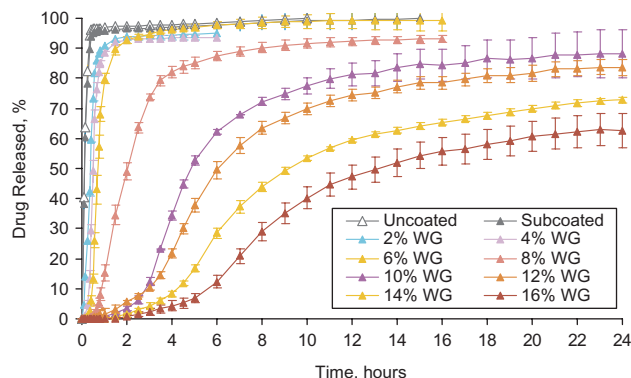

Fig. 2. Metoprolol succinate release from mini-tabs coated with Surelease®/Pore former (80:20).

tively. Disintegration time of seal-coated tablets was less than 10 minutes.

Figures 1 and 2 show that for both pore former concentrations, immediate release of drug was produced for low coating WGs, 2–4% and 2–6% respectively. With an increase in coating levels up to 16%, metoprolol succinate release rate decreased significantly. All profiles demonstrated consistent release with low variability as indicated by standard deviation values.

Slower release rates were produced for mini-tabs containing lower pore former concentration. For example, at 10% WG only 62% of the drug was released from 85:15 coating compared to 86% metoprolol succinate dissolved from 80:20 system, after 24 hours. This significant difference in the amount of drug release can be explained by the increased permeability of the film when more pore former was used.

Additionally, a lag time developed which increased with increasing coating weight gain.

CONCLUSIONS

Robust metoprolol succinate mini-tabs were manufactured using multi-tip tooling and their mechanical strength was significantly improved by the application of 5% WG of an Opadry II seal-coat.

Drug release rate from mini-tabs coated with ethylcellulose coating was modulated by varying the amount of hydrophilic pore former and/or the level of film coating applied. Mini-tabs offer a reliable alternative to conventional multiparticulate systems with consistent substrate from which drug release is effectively modulated.

The use of near infrared spectroscopy to provide mechanistic insights into gel layer development in HPMC hydrophilic matrices

P. Avalle, A. Midwinter, N. Gower and S.R. Pygall

Development Laboratories, MSD, Hoddesdon, Hertfordshire, UK

INTRODUCTION

Novel spectroscopic and microscopic techniques provide surface and internal chemical imaging and observations of the whole dosage form or of individual components on a macro-, micro- or nanoscale. Such spectroscopic methods offer the advantages of characterisation on the molecular level coupled with non-invasive, non-destructive component imaging of ingredients and behaviour [1].

The present work aims to explore the feasibility and potential application of NIR imaging to hydrating solid oral controlled release dosage forms, thus mapping the drug release as a function of both time and position within the tablet matrix and providing novel mechanistic insights into the drug liberation phenomena.

MATERIALS AND METHODS

To validate the robustness of the NIR experimental set-up, compound A was formulated in "slow" and "fast" drug releasing formulations with high (56% w/w) and low (18% w/w) levels of HPMC K100M respectively. NIR microscopy was subsequently used to (i) define the extent of HPMC pseudo-gel swelling, (ii) elucidate the polymer swelling front movement during dissolution and (iii) track movement of drug through the gel layer. A bespoke tablet hydration cell enabled the facile acquisition of NIR data from the hydrating matrix tablet (Figure 1).

The tablet holder was placed in an open-topped plastic container which was filled with hydrating medium. The hydrating medium (deionised water) was allowed to flow between the two stainless steel plates and hydrated the tablet.

USP II dissolution testing of each formulation allowed correlation of dissolution mechanistic details ascertained using NIR with the rate and extent of drug release.

RESULTS AND DISCUSSION

The hydration experiments were carried out in triplicate and the API and HPMC profiles were obtained. A profile of signal
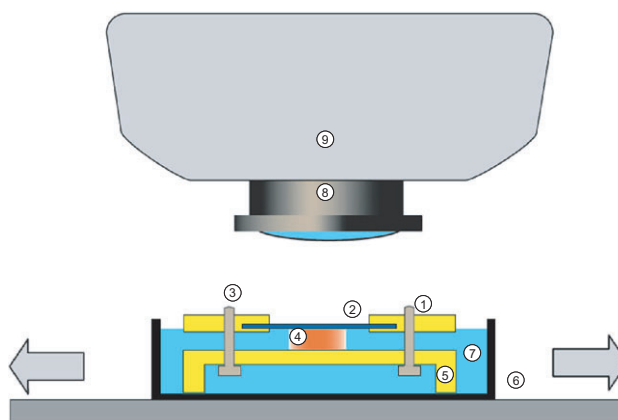

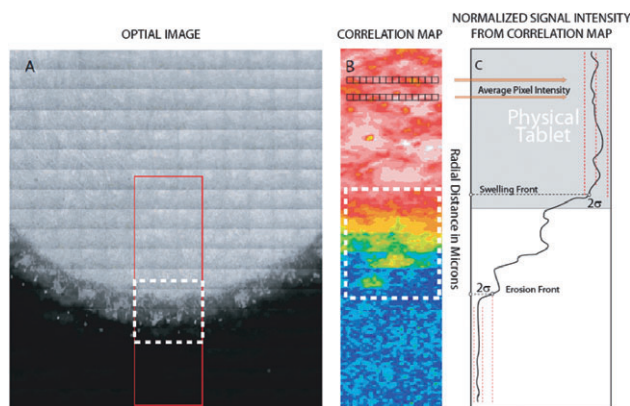**Figure 1.** Schematic diagram of the tablet hydration cell.

Figure 2. A: Optical image of a hydrating tablet recorded using the NIR microscope and (B) a full spectral image also recorded using the NIR microscope, then transformed into a correlation map (C). The top plate (1), with glass slide (2) clamped in place is fixed by two bolts (3) over the tablet (4) onto the base plate (5). The holder is placed in a plastic container (7) and filled with hydrating medium. The whole apparatus is placed on the NIR microscope moveable stage (6) and manipulated under the microscope lens and body (8, 9).

intensity as a function of the radial position was obtained, with the X-axis distance normalised to zero at the point of the dry tablet boundary.

The profiles exhibited several trends: (i) an apparent high intensity plateau, corresponding to a uniform distribution of HPMC across the dry tablet core, (ii) a sloped region indicative of a decreasing HPMC or drug concentration across the pseudo-gel layer and (iii) a plateau of low intensity arising from the bulk of the hydration medium.

In the "fast" formulation, HPMC swelling front movement occurred at a slower rate and to a lesser extent compared with the release of drug, suggesting an inadequate gel layer formation and a partial loss of extended release characteristics. In contrast, the "slow" formulation exhibited a similar rate of HPMC swelling front movement compared to API release, suggesting a drug release mechanism controlled by polymer erosion, supported by an apparent zero order API dissolution curve in USP I.

CONCLUSIONS

The data suggests that NIR can be applied to monitor the hydration time course of controlled release formulations, providing molecular level characterisation in a non-invasive and non-destructive manner.

REFERENCE

[1] Chan KLA, Kazarian SG. Applied Spectroscopy 2003; 57(4):381–389.

Triple-layered Solid Matrix Tablet Configurations for Constant Multiple Drug Delivery

K. Moodley[1], V. Pillay*[1], Y.E. Choonara[1], L.C. Du Toit[1]

[1]University of the Witwatersrand, Department of Pharmacy and Pharmacology, 7 York Road, Parktown, 2193, Johannesburg, South Africa, University of the Witwatersrand.
*Correspondence: viness.pillay@wits.ac.za

INTRODUCTION

The purpose of the study was to establish an optimal triple-layered tablet formulation that is capable of providing zero-order release of three different water soluble drugs. Drug release profiles were compared to those depicted by commercial drug products SLEEPEZE-PM® containing diphenhydramine (DPH), Ranihexal® containing ranitidine (RDH) and Phenergan® containing promethazine (PMZ).

MATERIALS AND METHODS

1) *Experimental design:* A Box-Behnken experimental design template comprising 17 formulations was generated using Minitab® V15 software after obtaining formulation variables during preformulation.
2) *Preparation of formulations*: Drug-loaded triple-layered tablet (TLT) matrices were prepared by direct compression according to the design template with varying polymer and salt quantities. Polymers employed were polyamide 6,10 (PA6,10), PEO WSR 301 and salted-out PLGA (s-PLGA). Sodium sulphate (SS) was combined with PA6,10. Model drugs loaded into the TLT formulations were DPH, PMZ and RDH.
3) *In vitro dissolution testing:* Formulations were subjected to *in vitro* dissolution testing using a USP 25 rotating paddle method in a dissolution apparatus (Caleva Dissolution Apparatus, model 7ST; G.B. Caleva Ltd., Dorset, UK) at 50 rpm with 900 mL simulated gastric fluid (SGF) (pH 1.2; 37°C) and 900 mL phosphate-buffer solution (PBS) (pH 6.8; 37°C High performance liquid chromatography (HPLC) was employed to analyse *in vitro* dissolution samples.
4) *Textural profile analysis:* A calibrated TA.*XTplus* Texture Analyser (Stable Microsystems, UK) was used to determine the Brinell Hardness Number (BHN) of various formulations.
5) *Morphological characterisation:* Scanning electron microscopy (SEM) was utilised to ascertain the surface morphology of the matrices after compression.

RESULTS

In vitro dissolution results revealed a capability to provide zero-order drug release of all three drugs from certain TLT formulations. Drug release profiles from these formulations illustrated linear release of DPH, PMZ and RDH over 24 hours. A trend was observed that showed a higher PA6, 10 to SS ratio presented with a more linear release of DPH and higher BHN values, which may be explained by a higher mechanical stability [1] due to a more efficient compact matrix allowing for adequate retardation of drug release, while a lower s-PLGA to PEO ratio presented with a more linear release of RDH from the outer layer and higher BHN values, the s-PLGA may control the swelling of PEO resulting in uniform drug release. The formulations containing PA6,10 within the range of 200–350 mg and s-PLGA within the range of 50–100 mg illustrated more desirable linear release profiles. The middle (second) layer was kept constant at 350 mg of PEO. The optimised formulation profile depicted a significant superior release of DPH, PMZ and RDH as

compared to the respective commercial products. The disintegration times of SLEEPEZE-PM® tablets, Ranihexal® tablets and Phenergan® tablets were approximately 1 hour and 1 hour and 30 minutes respectively. SEM showed irregular surfaces with minimal pores.

CONCLUSIONS

This study has provided evidence that the TLT formulations are capable of providing improved uniform release of three different water soluble drugs which may be greatly beneficial for further application in combination therapy for various disease states.

REFERENCE

[1] R. Patel, V. Pillay, Y.E. Choonara and T. Govender, "A Novel Cellulose-Based Hydrophilic Wafer Matrix for Rapid Bioactive Delivery" *Journal of Bioactive and Compatible Polymers,* **22** (2007) 119–142.

Use of terahertz time-domain spectroscopy to correlate refractive index and hardness for Avicel PH-101 tablets

L.A. Wall,[1] I. Ermolina,[1] M.J. Gamlen,[2] G. Smith[1]

[1]Leicester School of Pharmacy, De Montfort University, Leicester. LE1 9BH, UK.
[2]PAS, Beckenham, London. BR3 4UF, UK.

INTRODUCTION

We present a study to apply terahertz time-domain spectroscopy (THz-TDS) for the rapid and non-destructive determination of refractive indices (RI) of compacted Avicel® PH-101 tablets. A Precision Compaction Tester (PCT tablet press) was used to produce fixed weight tablets under various compression forces and another set under fixed compression forces with variable masses. Following RI determination using THz-TDS, tablet thickness and geometric densities were deduced and used to correlate hardness and density with RI. The study aims to demonstrate RI as a surrogate measurement for hardness and, consequently the potential relevance of THz-TDS in the QbD domain as an in-line process control method e.g. during roller compaction/dry-granulation.

MATERIALS AND METHODS

Samples of Avicel® PH-101 (FMC BioPolymer, Belgium) were weighed, sufficiently tapped and compacted into 10 mm diameter tablets at a rate of 20 mm/min. Set 1 (9 samples) were compressed at a force of 417 kg (±2 kg) on a PCT (PAS, Beckenham, UK), giving tablets with a weight range of 200–450 mg. Set 2 tablets (8 samples) of 295 mg (±5 mg) were compacted with compression forces ranging from 209 kg–427 kg. All tablets were weighed and the thickness determined using a slide gauge 48 hours post-compaction.

Following compaction, THz-TDS scans were made of the Avicel tablets with a TPS-3000 (TeraView, Cambridge, UK), and RI read at a wave number of 25 cm^{-1} from RI spectra calculated by batch software (TeraView). Finally, tablet hardness measurements were made with use of a PharmaTest PTB 311E.

RESULTS AND DISCUSSION

Given a greater compression force the resultant displacement of intra-particulate-voids resulted in a more densely packed structure within tablets of Figure 1, Set 2. At a constant force, density is expected to remain equal, yet the slight reduction of density with increased thickness in Set 1 indicates a resistive response to pressure as the powder mass becomes more massive.

The sensitivity of RI measurements to material density is illustrated in Figure 2, whereby an increasing RI corresponds with an increasing density in an apparent linear relationship [1]. As discussed, tablet density represents the material/air fraction within the packing structure and regression analysis of Set 2 tablets ($R^2 < 0.99$) predicts an RI approaching 1 (R.I. air ≈ 1) when density is equal to zero. In previous work, the effect of compaction force on RI closely resembles the effect of density on RI and is also described by Palermo *et. al.* [2]

For any given compression force, the mechanisms/degree of internal cohesion forces are likely to remain similar. With reference to Figure 2 and tablets of Set 1, the increased hardness will result from the greater stress required to shear tablets of increasing thickness. Yet with Set 2, as fill weights are equal, these mechanisms of internal cohesive forces vary with void fraction along with RI.

CONCLUSION

As a controlled operating parameter during the roller-compaction process, roll gap greatly influences the thickness of the resultant ribbon. Coupling RI to the inferred thickness in-situ leads to a surrogate measurement for hardness and a
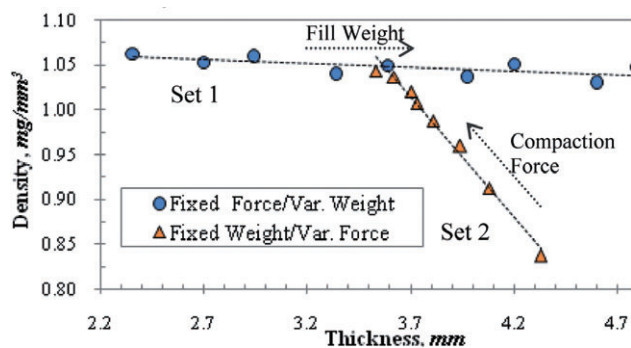
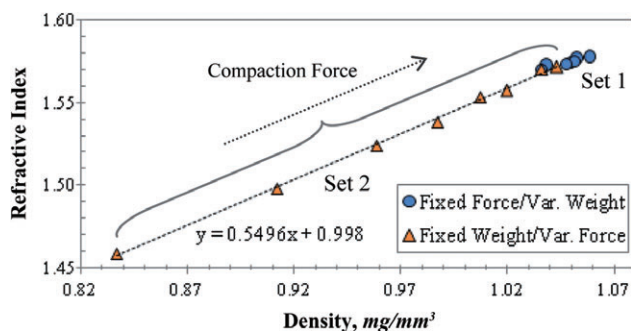**Figure 1:** Profile of tablet density and thickness.

Figure 2: The effect of tablet density post-compaction on RI.
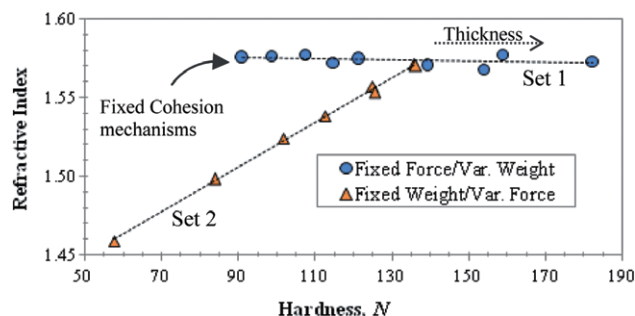

Figure 3: The effect of tablet hardness post-compaction on RI.

platform for downstream QbD principles concerning hardness effects i.e. granule size/fines fraction/milling energy.

REFERENCES

[1] M. Pore, J.A. Zeitler, S. Ngai, P.F. Taday, and C. Cooney, "Application of terahertz pulsed spectroscopy for evaluation of properties of pharmaceutical tablets" in: *Pittcon, The Pittsburgh Conference*. (2007) Chicago, USA.

[2] R. Palermo, R. Cogdill, S.M. Short, J.K. Drennen III and P.F. Taday, "Density mapping and chemical component calibration development of four-component compacts via terahertz pulsed imaging" *J. Pharm. BioMed. Anal.* **46** (2008) 36–44.

Effects of *Tulsi* (*Ocimum sanctum* Linn) on immune parameters of healthy volunteers

S. Mondal[1], V.D. Bamola[1], S.Varma[2], S. N. Naik[3], B.R. Mirdha[4], N. Mehta[1], M.M. Padhi[5], S.C. Mahapatra[1]*

Departments of [1]Physiology and [4]Microbiology, All India Institute of Medical Sciences, New Delhi – 110029
[2]Institute of Pathology, Indian Council of Medical Research, Safdarjung Hospital Campus, New Delhi – 110029
[3]Center for Rural Development and Technology, Indian Institute of Technology Delhi, New Delhi – 110016
[5]Central Council for Research in Ayurveda and Siddha, Department of Ayurveda, Yoga & Naturopathy, Unani and Sidhha (AYUSH), Janakpuri, New Delhi-110065. *Corresponding author email: scmahapatra@gmail.com

INTRODUCTION

Tulsi (*Ocimum sanctum* Linn) is considered as a sacred plant in the Indian subcontinent. Its medicinal properties have been described in ancient medical literatures like *Ayurveda* [1]. Traditionally, this plant is used in the treatment of upper respiratory infections, digestive disorders, skin infections, and so on, and it is also supported by the findings of the modern researches [2]. There is a general belief among the people that taking *Tulsi* on an empty stomach increases immunity.

MATERIALS AND METHODS

The study was conducted through a double-blinded randomised controlled clinical trial on 24 healthy volunteers in a cross-over format. Inclusion criteria were apparently healthy subjects, not on medication for at least one month prior to the study, age between 18–60, either sex. Pregnant/lactating women, persons undergone surgery in past year, persons taking any medication or having allergies/immune disorders or major systemic illnesses/diseases, were excluded from the study. Three hundred milligrams of 70% Tulsi extract or

placebo capsules were administered once daily on an empty stomach for 4 weeks followed by a 3 week washout period and then after a cross-over, the study continued for another 4 weeks. T-helper and T-cytotoxic cells, B-cells and NK-cells were monitored using Flowcytometry. Results of 22 subjects were analysed. Two-way ANOVA for crossover design was applied and $p < 0.05$ was considered significant.

RESULTS AND DISCUSSION

A statistically significant increase in T-helper cells and NK-cells was observed in the intervention group compared to the placebo group (Figures 1 & 2). Significant increases in the secreted levels of IFN-γ and IL-4 in whole blood culture were observed (data not shown) following stimulus with LPS and PHA. This was supported by the increased percentages of T-helper cells and NK-cells. We have not studied the mechanism of action, however bioactive principle of leaf extract of *O. sanctum*, like ursolic acid, oleanolic acid and salrigenin are proposed chemicals responsible for immuno-modulatory effects [3].

CONCLUSIONS

Consumption of *Tulsi* extract increased general preparedness of immune response in the study population.

ACKNOWLEDGMENTS

REFERENCES

[1] S.K. Gupta, J. Prakash, S. Srivastava, "Validation of traditional claim of Tulsi , *Ocimum sanctum* Linn. as a medicinal plant". *Ind. J. Exp. Biol.* **40** (2002) 765–773.

[2] S. Mondal, B.R. Mirdha, S.C. Mahapatra, "The science behind sacredness of Tulsi (*Ocimum sanctum* Linn.)". *Ind. J .Physiol. Pharmacol.* **53** (2009) 291–306.
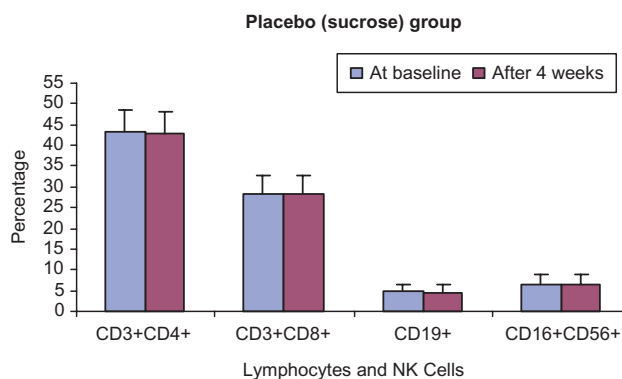

Figure 1: Intervention effects of placebo (sucrose) capsules on T-Lymphocytes, B-Lymphocytes and NK-cells after 4 weeks (n = 22). All values in mean ± SD. There was no significant increase in T-helper cells (CD3+CD4+) or NK-Cells (CD16+CD56+).
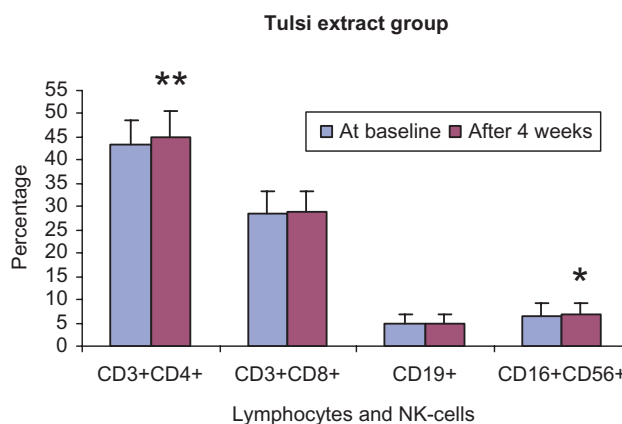

Figure 2: Intervention effects of *Tulsi* extract capsules on T-Lymphocytes, B-Lymphocytes and NK-cells after 4 weeks (n = 22). All values in mean ± SD. There was a signific2ant increase in T-helper cells (CD3+CD4+) (**p = 0.001) and NK-Cells (CD16+CD56+) (*p = 0.017) after 4 weeks of intervention.

[3] R. Mukherjee, P.K. Dash, G.C. Ram "Immunotherapeutic potential of *Ocimum sanctum* (L) in bovine sub clinical mastitis". *Res. Vet. Sci.* **79** (2005) 37–43.

Investigation of the anti breast cancer activity of five traditionally used Sudanese medicinal plants

Ashraf N. Abdalla, Peter M. Fischer and Tracey D. Bradshaw

Centre for Biomolecular Sciences and School of Pharmacy, University of Nottingham, NG7 2RD Nottingham, U K ashraf_abdalla@hotmail.com

INTRODUCTION

Five Sudanese medicinal plants: *Kigelia africana* (Bignoniaceae), *Hygrophila auriculata* (Acanthaceae), *Aerva javanica* (Amaranthaceae), *Indigofera astragalina* (Fabaceae) *and Boscia senegalensis* (Capparidaceae); were selected after examining local reports of traditional herbal treatment of breast cancer [1, 2].

MATERIALS AND METHODS

Plants were authenticated and extracted with methanol. Growth inhibitory properties of extracts were then examined by MTT assay against 4 breast carcinoma, 1 pancreatic carcinoma, a normal non-transformed fibroblast and normal endothelial cell line. Two extracts (6 and 7 from *Indigofera astragalina*) demonstrated the highest anticancer activity. Viable cell counts were performed after treatment of MDA468 cells with extract 6 and cell cycle perturbations examined. Cells undergoing early apoptosis were detected by flow cytometry (annexin V); simultaneous cell cycle/annexin V staining revealed from which phase apoptotic populations emerged [3]; detection of cleaved PARP by Western blot corroborated apoptosis. Extract 6 was then fractioned by liquid extraction [4], flash chromatography and HPLC; and MTT assays conducted to validate the activity of the fractions. Acid hydrolysis performed to main compound.

RESULTS AND DISCUSSION

Extract 6 results with MTT showed selective activity against cells (GI_{50}: 12–69 µg/ml). It decreased the number of viable MDA468 cells in a dose- and time-dependent manner; and increased total $preG_1$ and G_2/M cell cycle events (4–9% and 35–42% respectively) after 48 h 50–100 µg/ml treatment. Annexin V staining/PI exclusion revealed early apoptotic cells (40–46%) after 24 h treatment. Simultaneous cell cycle/ apoptosis treatment with extract 6 exposed apoptotic populations emerging from each cell cycle compartment. The intensity of cleaved PARP proteins detected after treatment

(50–100 µg/ml; 24 h, 48 h) with the same extract increased in a dose- and time-dependent manner. Extract 6 was fractionated into water, hexane and ethylacetate/chloroform. The hexane fraction was inactive against MDA468, the aqueous fraction showed weak activity, whereas the ethylacetate/chloroform fraction showed the highest activity (GI_{50}: 23 µg/ml). The latter gave 16 sub-fractions by normal phase silica gel flash chromatography, of which fractions 9, 10, 12 and 13 demonstrated the highest growth inhibitory activity (GI_{50}: 5, 9, 10 and 7 µg/ ml respectively) against MDA 468 cells. Fraction 9 (yield = 0.066% of original methanol extract) was less potent against fibroblast cells (32 µg/ml). Analytical RP-HPLC fractionation of fraction 9 resulted in 3 main components, of which one was acid hydrolysed and extracted with ethylacetate giving pure glycone and aglycone.

CONCLUSIONS

Extract 6 possesses growth inhibitory and pro-apoptotic properties against human MDA468 breast cancer cells. To date no investigations of the pharmacological activity of *I. astragalina* have been reported. Identification of active compounds are underway.

ACKNOWLEDGMENTS

REFERENCES

[1] Andrews, F.W. "The Flowering Plants of the Anglo-Egyptian Sudan", Vol. **II** (1952).
[2] Brown, A.F. and Massy, R.E. "Flora of the Sudan" (1929).
[3] Deding Tao *et al*. "New method for the analysis of cell cycle-specific apoptosis". *Cytometry* part A, **57A** (2004) 70–74.
[4] Maria a. De Moraes E Souza *et al*. "Arylbenzofurans from *I. microcarpa*". *Phytochemistry*. **27** (1988) 1817–1819.

LC-MS & DFT Investigations of *Cryptolepis Sanginolenta* Root Extracts

F.M.D. Ismail[1], A. H. Cox[1], N. M. Dempster[1], J. L. Ford[1], M.J. Dascombe[2], M.G.B. Drew[3]

[1]School of Pharmacy and Biomolecular Sciences, Liverpool John Moores University, Liverpool, UK.
[2]Faculty of Life Sciences, Manchester University, Manchester, UK. [3]Department of Chemistry, Reading, UK.

Abstract – **The roots of *Crytolepis sanguinolenta*, a medicinally important ethanobotanical source of the antimalarial cryptolepine, were soxhlet extracted in anaerobic conditions, using hexane then ethanol. Samples of each extract were fractioned using flash chromatography and preparative TLC and compound identity was established using gradient HPLC-positive ion electrospray mass spectrometry. The use of argon depressed the formation of quindoline and hydroxycrytolepine. In addition to known compounds such as cryptolepine, several as yet unidentified compounds remain to be characterised in this root extract.**

INTRODUCTION

In West Africa the roots of *Cryptolepis sanguinolenta* are traditionally used to treat malaria and upper respiratory tract infections by making an aqueous decoction of the roots to drink [1]. However, to our knowledge, details of the exact methodology for analysis of *Cryptolepis* extracts, by HPLC-MS, have not been published. In this study, the roots of the plant were extracted and chromatographic methods employed to isolate known compounds e.g. cryptolepine.

MATERIALS AND METHODS

A number of systems were investigated from which chloroform: methanol: ammonia 90:10:1 (v/v/v) was chosen for medium pressure (N_2 gas) flash chromatography on silica gel. Analysis and combination of 160 fractions, using UV excitation at 254 and 366 nm (fluorescent indicator), gave 32 fractions that were analysed on preparative TLC. Spots on the baseline were further separated by switching the solvent composition from chloroform: methanol: ammonia 90:10:1 to 70:30:1 (v/v/v). A C18 X Bridge HPLC column (2.1 × 50 mm, particle size of 3.5 µm) was used in conjunction with a Waters 2695 separation Module and masses were detected in positive ion mode at high resolution (HRPIESMS), using a Waters 486 tunable absorbance detector and a Waters Micromass LCT Classic. Density functional theory (DFT) calculations were performed using published methodology [2]. Purified cryptolepine was incubated with hemin chlorine in methanol water at various apparent pH values and analysed with HRPIESMS.

RESULTS AND DISCUSSION

On comparing the four soxhlet extracts, the masses corresponding to cryptolepine and, its isomers, were present in a
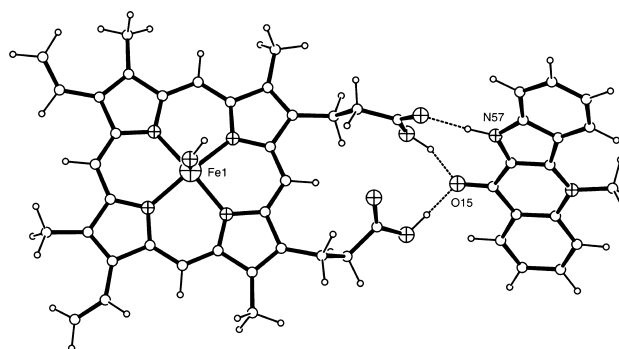

Fig. 1. An optimised structure of hematin-hydroxycryptolepine complex (keto tautomer) in edge binding mode. Hydrogen bonds shown as dotted lines are 1.761, 1.570, 1.570 Å reading from top to bottom. HRPIESMS, e.g. pH 14, $C_{50}H_{44}FeN_6O_5^+$; predicted: 864.2717; Found: 864.2710 Da.

higher % abundance in ethanol extracts (fresh and one year old) than in hexane extracts. In contrast, the masses relating to quindoline, hydroxycryptolepine (and its tautomer), cryptoheptine, 11-isopropylcryptolepine and cryptolepicarboline each showed lower % abundances in ethanol extracts. The remaining compounds, cryptomisrine and its isomer, cryptoquindoline as well as cryptospirolepine each showed similar % abundance within the four extracts.

Incubation of purified cryptolepine with hemin chloride at apparent pH 14, pH 7 and pH 2 (methanol/water, HCl, O_2) indicated conversion of cryptolepine (7 h) to hydroxycryptolepine in solution (HRPIESMS). DFT experiments revealed that edge binding to hematin (as opposed to above or below face) structural motifs previously considered important for the bisquinoline metaquine [3] (molecular mechanics study) [4], was enhanced by hydroxylation of cryptolepine (Fig. 1), suggesting that cryptolepine acts as an antiplasmodial prodrug, undergoing conversion to hydroxycryptolepine, both in the host liver and within *Plasmodium falciparum* food vacuoles. Poor solubility of these drug receptor complexes at low pH has, until now, excluded investigations at acidic apparent pH values close to those found in parasite food vacuoles.

CONCLUSIONS

A novel flash chromatography/preparative TLC method has been developed to isolate compounds from *Cryptolepis sanginolenta*. Cryptolepine isolated from freshly ground root interacts with hematin in air and produces hydroxycryptolepine, suggesting prodrug action within parasite vacuoles; a process that can be readily detected using HRPIESMS.

REFERENCES

[1] F.M.D. Ismail, N.M. Dempster, J. L. Ford. *J. Pharm. Pharmacol.* **461** (2009) A9-A-10.

[2] M.G.B. Drew, J. Metcalfe, F.M.D. Ismail. *J. Mol. Struct.-Theochem* **756** (2005) 87–95.

[3] F.M.D. Ismail, M.J. Dascombe, P. Carr, S.A. M. Merette, P. Rouault. *J. Pharm. Pharmacol.* **50** (1998) 483–492.

[4] M. J. Dascombe *et al. J. Med. Chem.*, **48** (2005) 5423–5436.

Antihyperlipedemic Effect of the Seabuckthorn Berry Extract, a Comparative In Vivo Study in Rabbits

M. Zeeshan Danish[1], M. Jamshaid, A. Bashir, N.I. Bukhari, F.Z. Khan, K. Hussain, I. Aslam

University College of Pharmacy, University of the Punjab, Lahore 54000, Pakistan

INTRODUCTION

Seabuckthorn (*Hippophae rhamnoides, Elaeagnaceae*) is a naturally grown bush which is widely distributed in the mountain regions of Asia and Europe [1]. Several studies have been carried out on different parts of the plant [2], particularly on its berries. The berries have been reported as an effective adjunctive to the cancer treatment [3], to help improving cardiovascular risk factors [4], beneficial for gastrointestinal ulcers and for variety of skin disorders [5–6] and liver cirrhosis.

MATERIALS AND METHOD

Seabuckthorn berries were dried, pulverised and extracted from alcohol after a three day maceration process. Rabbits were made hyperlipidemic with oral administration of 250 mg/kg BW cholesterol filled in hard gelatin capsules for 7 days. The induction of hyperlipidemia was confirmed with the measurement of serum cholesterol, triglyceride (TG), low density lipoproteins (LDL) and high density lipoproteins (HDL) levels using randox and human kit method. The hyperlipidemia was maintained in animals by continued administration of 250 mg/kg BW cholesterol for the entire study period. After 7 days, the rabbits were randomly divided into groups I to V, each having 6 animals.

Total serum cholesterol, TG, LDL, and HDL levels were measured after different treatments on day 0 to day 35 with intervals of 7 days. An emulsion containing 100 mg/ml of extract in distilled water was prepared by dry gum method. The emulsion was administered orally at a dose of 500 mg/kg BW of the animal in group I. Vitamin C (30 mg/kg BW), vitamin E (30 mg/kg BW), atorvastatin (3 mg/kg BW) and sample vehicle (control) as empty hard gelatin capsule shells were administered to group II, group III, group IV and V, respectively. Change in base line values of the above hyperlipidemic markers after all treatments were compared using *post hoc* Tukey's test using SPSS version 13 (Evaluation version). A *p* value <0.05 was considered as significant difference.

RESULTS AND DISCUSSION

There was a marked decrease of 72 ± 4% in serum cholesterol at day 28 by atorvastatin. The extract, vitamin C and vitamin E, demonstrated a reduction in cholesterol as 69 ± 4.04%, 52 ± 7.21%, and 58 ± 4.7%, respectively. In the case of serum LDL levels, atorvastatin exhibited the highest percentage reduction (65 ± 4.2%), followed by 56 ± 5.7%) reduction with SBT extract, 50 ± 6.5% by vitamin E, 48 ± 11.3% by vitamin C and 33 ± 4.6% by the control. Similarly, a marked decrease in TG was observed as 70 ± 3.5% by atorvastatin, followed by 57 ± 8.1% with the extract, 51 ± 3.8% by vitamin E, 47 ± 11.2% by vitamin C, and 29 ± 7% by control. On the contrary, vitamin C was considered to increase the HDL levels with the highest value of 51 ± 5.1%. Serum HDL levels gradually increased significantly with the treatment of extract (49 ± 19.8%) as compared to 45 ± 4.7% with vitamin C, 19 ± 5.9% with atorvastatin and 5 ± 1.6% with control respectively from day 7 to day 28, until the end of the total period of study.

CONCLUSION

The findings of the present study indicated that the extract had remarkably decreased the levels of total cholesterol, LDL, and TG as compared to the well known antioxidant vitamins such as vitamin E and vitamin C. The extract may be of value in lowering the cardiovascular risk factors in human related to hyperlipidimia.

KEY WORDS

Sea buckthorn, Low density lipoprotein, High density lipoprotein, Triglyceride.

REFERENCES

[1] Rousi, A. The genus Hippophae L. a taxonomic study, *Ann. Bot. Fenn,* (1971), 8: pp.177–227.

[2] Baoru Yang and Heikki Kalli, Composition and physiological effects of sea buckthorn (Hippophaë), *Trends in Food Science & Technology, Volume 13, Issue 5*, May 2002, Pages 160–16.

[3] Zhang, P. Z., Ding, X. F., Mao, L. N., Li, D. X. & Li, L. P. Anti-cancer effects of sea buckthorn juice and seed oil and their effects on immune function. *In Proceedings of International Symposium on Sea Buckthorn (H. rhamnoides L.)*, 1989, pp. 373–381. Xi'an, China.

[4] C. Eccleston, B. Yang, R. Tahvonen, H. Kallio, G. Rimbach and A. Minihane , Effects of an antioxidant-rich juice (sea buckthorn) on risk factors for coronary heart disease in humans. *Journal of Nutritional Biochemistry 13*, 2002, pp. 346–354.

[5] Xing J, Yang B, Dong Y, Wang B, Wang J, Kallio HP. Effects of sea buckthorn (Hippophae rhamnoides L.) seed and pulp oils on experimental models of gastric ulcer in rats. *Fitoterapia.* 2002;73:644–650.

[6] H. Kallio, B.Yang, P. Peippo, R. Tahvonen and R. Pan, Triacylglycerols, glycerophospholipids, tocopherols and tocotrienols in seabuckthorn (Hippophaë rhamnoides L). ssp. sinensis and ssp. mongolica berries and seeds. *Journal of Agricultural and Food Chemistry 50*, 2002, pp. 3004–3009.

Blood, Sweat and Tregs; Immunological Regulation in the Tumour Environment

H.K. Angell[1], D.G. Blount[1], S.A. Watson[2], R.W. Wilkinson[3], D.I. Pritchard[1]

[1]Immune Modulation Research Group, School of Pharmacy, University of Nottingham, Nottingham, UK.
[2]Division of Pre-Clinical Oncology, School of Medical and Surgical Sciences, University of Nottingham, Nottingham, UK.
[3]Cancer Infection Research Area, AstraZeneca Pharmaceuticals, Alderley Park, UK.

Regulatory T cells may support tumour growth by suppressing the anti-tumour immune response, resulting in tumour progression. Here, we address the relationship between regulatory T cells in peripheral blood of colorectal cancer patients and those found *in situ* within the tumour.

INTRODUCTION

Immunological regimes have been intensely studied in colorectal cancer (CRC). However the prognostic significance of infiltrating FOXP3^{+} regulatory T cells (Tregs) in CRC tumour tissue remains unclear [1, 2].

The aim of our study was to analyse the level of Tregs in peripheral blood of CRC patients and to investigate any correlation between this and infiltrating FOXP3^{+} Tregs *in situ*.

MATERIALS AND METHODS

1) *Peripheral Blood (PB) Treg analysis*: PB was incubated with anti-CD4, anti-CD3 and anti-CD25 antibodies for 30 min. Red blood cells were lysed using Optilyse then cells were fixed and permeabilised before being stained with an anti-FOXP3 antibody. Cell counting beads were added prior to running on a Beckman Coulter FC 500. Flow cytometric data was analysed using an unpaired Student's t-test.

2) *Immunohistochemistry (IHC)*: Formalin-fixed tissues were deparaffinised and heat-induced epitope retrieval was performed using a microwave. After blocking peroxidise activity, slides were incubated with a biotin conjugated anti-human FOXP3 antibody (clone PCH101, eBioscience). Sections were incubated with Avidin Biotin Complex (ABC, Dako) followed by liquid DAB (Dako) before counter-staining with Haemalum (Mayers' aqueous).
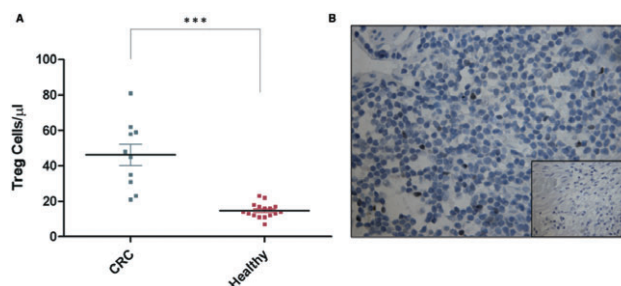

Fig. 1. A) Whole blood FACS analysis of Treg cells/µl in colorectal cancer patients compared to healthy volunteers. B) IHC staining of FOXP3+ Tregs in tissue-matched CRC patient material, with a non-specific antibody negative control (inset).

3) *Treg Functionality Assay:* Purified PBMC were separated into CD4^{+}CD25^{+} Treg fractions using magnetic beads (Miltenyi) and co-cultured with varying ratios of CD4^{+}CD25^{-} PHA activated effector cells. Treg suppression of effector cell proliferation was measured by ^{3}H-Thymidine incorporation.

RESULTS AND DISCUSSION

Eleven CRC patients and seventeen healthy volunteers were analysed, consisting of 6 males and 5 females of varying tumour stage with a mean age of 68.5. Treg cells/µl of PB were significantly higher ($p < 0.0001$) in CRC patients compared to healthy volunteers (Fig. 1A).

FOXP3 IHC staining of corresponding CRC patient tumour tissue was used to investigate correlations between elevated Tregs in PB and Treg numbers found at the tumour site. Preliminary data revealed that elevated Tregs in PB correlated with increased Treg presence in CRC tissue (example image Fig. 1B).

The suppressive ability of Tregs isolated from CRC patient PB was also demonstrated. Here, increased numbers of Tregs correlated with increased suppression of effector cell proliferation, measured by ^{3}H-Thymidine incorporation.

CONCLUSIONS

Our study adds new data to the ongoing discussion on the role of Tregs in malignant diseases. We demonstrate an increase in PB Tregs in CRC compared to healthy donors, which correlates with matched *in situ* tumour tissue analysis.

It is becoming increasingly acknowledged that the inhibition of Treg function in cancer patients could contribute to the success of existing standards-of-care and lead to potential novel treatments. It is suggested that Tregs co-exist with tumour cells, suppressing the anti-tumour immune response, resulting in tumour progression.

REFERENCES

[1] P. Salama, M. Phillips, F. Grieu, M. Morris, N. Zeps, D. Joseph, *et al.* "Tumour-infiltrating FOXP3$^+$ T regulatory cells show strong prognostic significance in colorectal cancer" *J. Clin. Oncol.,* **27** (2009) 186–192.

[2] H. Suzuki, N Chikazawa, T. Taska, J. Wada, A. Yamasaki, Y. Kitaura, *et al.* "Intratumoural CD8T/FOXP3 cell ratio is a predictive marker for survival in patients with colorectal cancer" *Cancer Immunol. Immunother.,* **59** (2010) 653–661.

Taking off the tumour immunity 'handbrake'

A.R. Khan[1, 2], S.A. Watson[3], R.W. Wilkinson[4], D.I. Pritchard[2]

[1]Doctoral Training Centre for Targeted Therapeutics, School of Pharmacy, University of Nottingham, UK
[2]Division of Molecular and Cellular Sciences, School of Pharmacy, University of Nottingham, UK
[3]Division of Pre-Clinical Oncology, School of Medical and Surgical Sciences, University of Nottingham, UK
[4]Cancer Infection Research Area, AstraZeneca Pharmaceuticals, Alderley Park, UK

Abstract – **The immune system can play a vital role in not only tumour growth and development, but also tumour clearance. Here, we aim to demonstrate the pharmacological inhibition of the migration and activity of regulatory T cells which could be conducive to the propagation of tumour immunity.**

INTRODUCTION

Increasing clinical and preclinical evidence supports the relationship between elevated numbers of regulatory T cells (Treg) in solid and haematological cancer with both disease progression and severity [1, 2]. Restricting the impact of these cells within the tumour microenvironment could lead to an induction of a more effective anti-tumour immune response. This project aims to modulate the suppressive and tumour-infiltrating capacity of Treg through targetting toll-like receptors [3] and the CCR4-CCL22 chemokine axis, as a means to repolarise the immune-suppressive milieu (a characteristic in malignant disease) and potentiate anti-tumour efficacy.

MATERIALS AND METHODS

Treg were isolated via magnetic separation from peripheral blood mononuclear cells of healthy donors (Invitrogen). Due to the small numbers of Treg obtained on isolation, an in-house expansion protocol was developed by culturing isolated cells in the presence of IL2 and anti-CD28 superagonist. These cells were phenotyped by flow cytometry for key Treg markers with their suppressive activity demonstrated *in-vitro*. Treg migration was also monitored in response to the migratory chemokines CCL17 and CCL22 (Peprotech) using a classical Boyden migration chamber. The suppressive and migratory activity of Treg were challenged using a TLR 7/8 agonist, Imiquimod (Merck) and a CCR4 antagonist (AstraZeneca) respectively.

RESULTS AND DISCUSSION

Here, we discuss the development of an in-house expansion protocol for Treg which provides us with quantities of cells suitable for *in-vitro* assays. These cells have a 'natural' Treg phenotype (CD4$^+$CD25$^+$Foxp3$^+$) and retain their suppressive properties. We go on to demonstrate the migration of Treg *in-vitro* (Figure 1a). CCL17 and CCL22 are migratory chemokines that are produced by ovarian tumours. These chemokines cause the migration of Treg (via the chemokine receptor CCR4) to the tumour, thus enhancing the immune suppressive milieu. The suppressive effects of Treg were abrogated using Imiquimod (Figure 1b), suggesting that Treg suppression can be affected. Pharmacological inhibition of Treg migration was also successful (data withheld).
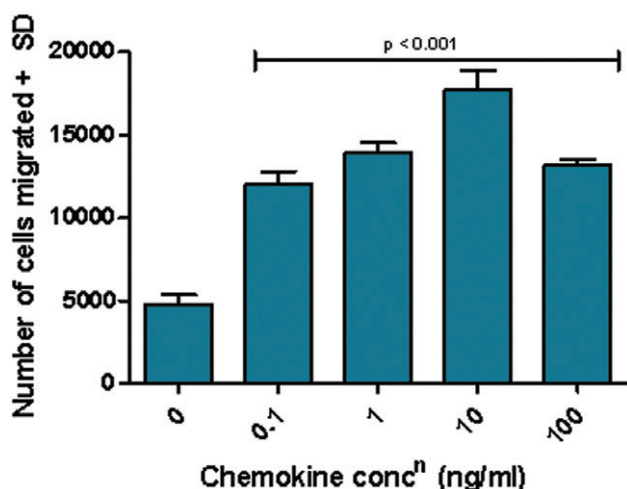
Figure 1a – Treg migration profile in response to CCL22. Mean and SD $n = 4$. $p < 0.001$
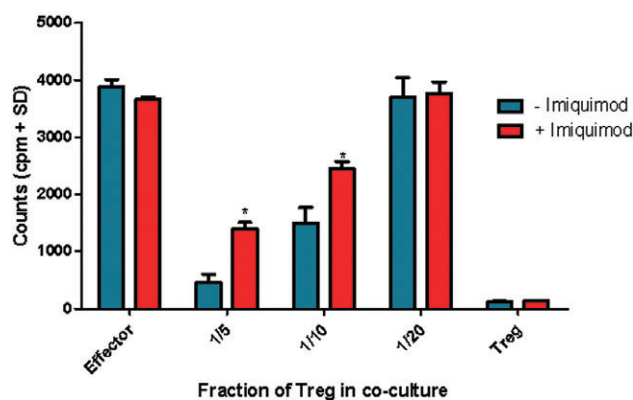

Figure 1b – Treg suppression of $CD4^+CD25^-$ effector cells abrogated by 3 μM of TLR7/8 agonist Imiquimod. Mean and SD, $n = 2$. * = $p < 0.05$ compared to DMSO controls

CONCLUSIONS

In summary, we have been able to demonstrate that the migratory and suppressive properties of Treg can be altered *in vitro*. Although there are many different suppressive mechanisms occurring within a tumour, it is hoped that selective targeting of Treg will lead to a repolarisation of the immune suppressive environment of a tumour.

ACKNOWLEDGMENTS

REFERENCES

[1] T.J. Curiel, G. Coukos, L.H. Zou, X. Alvarez, P. Cheng, P. Mottram, M. Evdemon-Hogan, J.R. Conejo-Garcia, L. Zhang, M. Burow, Y. Zhu, S. Wei, I. Kryczek, B. Daniel, A. Gordon, L. Myers, A. Lackner, M.L. Disis, K.L. Knutson, L.P. Chen, and W.P. Zou, Specific recruitment of regulatory T cells in ovarian carcinoma fosters immune privilege and predicts reduced survival. Nature Medicine 10 (2004) 942–949.

[2] E. Sato, S.H. Olson, J. Ahn, B. Bundy, H. Nishikawa, F. Qian, A.A. Jungbluth, D. Frosina, S. Gnjatic, C. Ambrosone, J. Kepner, T. Odunsi, G. Ritter, S. Lele, Y.T. Chen, H. Ohtani, L.J. Old, and K. Odunsi, Intraepithelial CD8+ tumour-infiltrating lymphocytes and a high CD8+/regulatory T cell ratio are associated with favourable prognosis in ovarian cancer. Proc Natl Acad Sci U S A 102 (2005) 18538–43.

[3] R.P. Sutmuller, M.E. Morgan, M.G. Netea, O. Grauer, and G.J. Adema, Toll-like receptors on regulatory T cells: expanding immune regulation. Trends Immunol 27 (2006) 387–93.

The Tumour Immunology 'Tube Map'

A.R. Khan[1, 2], S.A. Watson[3], R.W. Wilkinson[4], D.I. Pritchard[2]

[1]Doctoral Training Centre for Targeted Therapeutics, School of Pharmacy, University of Nottingham, UK
[2]Division of Molecular and Cellular Sciences, School of Pharmacy, University of Nottingham, UK
[3]Division of Pre-Clinical Oncology, School of Medical and Surgical Sciences, University of Nottingham, UK
[4]Cancer Infection Research Area, AstraZeneca Pharmaceuticals, Alderley Park, UK

Abstract – **Here, we present the first incarnation of the tumour immunology 'tube map'. This is an illustration of some of the key cellular components and mechanisms that co-exist within an immunogenic tumour. The schematic incorporates chemokines, cytotoxic CD8$^+$ T cells, helper T cells, tumour-associated macrophages, dendritic cells, natural killer cells and tumour cells. The rationale behind the 'tube map' is to identify key interactions within the tumour and thus gain a greater understanding of the complexity of the environment. It is anticipated that the map could be used as a means for identifying potential strategies for immunotherapy**

INTRODUCTION

A growing body of preclinical and clinical evidence suggests that tumours in certain settings can be immunogenic [1, 2]. Novel immunotherapeutic approaches that aim to exploit and enhance this immunogenicity have had mixed success [3]. It

is clear that whilst many tumours express tumour-associated antigens they do not stimulate durable and effective immune responses *in-vivo*. This may reflect the fact that tumours develop a network of escape mechanisms to circumvent tumour-specific immunity.

Discussion

Tumour immunity refers to the success or failure, respectively, of the immune system to reject a tumour. The tumour microenvironment, which is composed of tumour cells, immune cells, stromal cells and the extracellular matrix, is the principal hub of interaction during tumour development, favouring proliferation, survival and migration of tumour cells. Not only can tumours survive and disseminate to distant sites, they can, more importantly, utilise some of the signalling pathways of the immune system to propagate conditions that favour immune tolerance. The induction of this anergic state is the result of imbalances in the tumour microenvironment, including changes in antigen-presenting-cell types, co-stimulatory and co-inhibitory molecule alterations and altered ratios of effector T cells and regulatory T cells.

Gaining further understanding of this environment is key to developing effective therapies. The 'Tube Map' aims to provide an overview of the key immunological interactions within a tumour.

CONCLUSIONS

Improving the tumour-associated immune response can be achieved by either boosting components of the immune system that produce an effective immune response or by inhibiting suppressive factors. The complex and redundant milieu in the tumour microenvironment means that selective targetting of a particular cell type or receptor can be either circumvented by the tumour or lead to adverse systemic effects on the patient. The 'tube map' has the capacity to highlight areas which may provide avenues for improved immunotherapy.
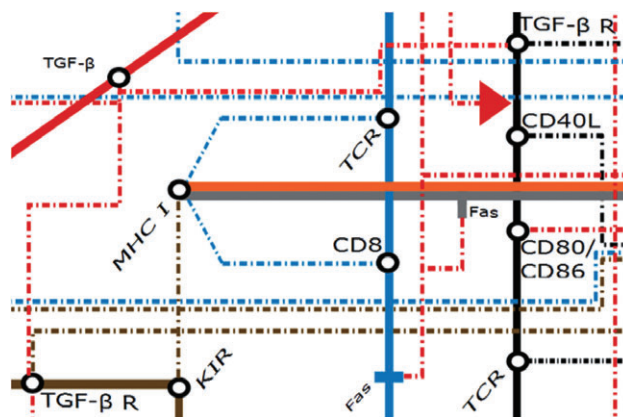

Fig. 1. Snapshot of the tumour immunology 'tube map'.

REFERENCES

[1] T.J. Curiel, G. Coukos, L.H. Zou, X. Alvarez, P. Cheng, P. Mottram, M. Evdemon-Hogan, J.R. Conejo-Garcia, L. Zhang, M. Burow, Y. Zhu, S. Wei, I. Kryczek, B. Daniel, A. Gordon, L. Myers, A. Lackner, M.L. Disis, K.L. Knutson, L.P. Chen, and W.P. Zou, Specific recruitment of regulatory T cells in ovarian carcinoma fosters immune privilege and predicts reduced survival. Nature Medicine 10 (2004) 942–949.
[2] N. Leffers, M.J. Gooden, R.A. de Jong, B.N. Hoogeboom, K.A. ten Hoor, H. Hollema, H.M. Boezen, A.G. van der Zee, T. Daemen, and H.W. Nijman, Prognostic significance of tumour-infiltrating T-lymphocytes in primary and metastatic lesions of advanced stage ovarian cancer. Cancer Immunol Immunother 58 (2009) 449–59.
[3] H. Borghaei, M.R. Smith, and K.S. Campbell, Immunotherapy of cancer. Eur J Pharmacol 625 (2009) 41–54.

Tissue Engineering in Hostile Environments: The Effect of Proinflammatory Cytokines on Embryonic Stem Cells and Primary Bone Cells

L. E. Sidney[1], D. Walsh[2], L. D. K. Buttery[1]

[1]School of Pharmacy, University of Nottingham, Nottingham, UK.
[2]Academic Rheumatology, University of Nottingham, Nottingham City Hospital, Nottingham, UK.

INTRODUCTION

Little work has been performed showing the effect of proinflammatory cytokines, on the activity of stem cells, particularly embryonic stem cells. The reaction of cells being placed within a damaged, diseased and inflammatory environment could have an effect on their use in tissue engineering applications.

In the bone microenvironment there is a delicate balance of bone resorption and formation. Proinflammatory cytokines such as interleukin-1β (IL-1β) and tumour necrosis factor-α (TNF-α) are associated with the innate inflammatory response

during tissue healing and are also critical for control of bone tissue remodelling [1].

This study aims to compare the *in vitro* effect of inflammatory cytokines on osteogenically differentiated embryonic stem cells and primary bone cells.

MATERIALS AND METHODS

Mouse embryonic stem cells (mESCs) were cultured on a feeder layer of mitotically inactivated mouse fibroblasts in basal media containing leukaemia inhibitory factor (LIF). Differentiation was induced by spontaneous formation of embryoid bodies (EBs) by mass suspension. EBs were cultured for 3 days before dissociation to single cell solution. Primary bone cells were extracted from 1–3 day old CD1 mouse calvariae by trypsin and collagenase enzyme digestion.

Both cell types were seeded at 50,000 cells/mL on gelatin-coated plates, in osteogenic media containing the supplements ascorbate-2-phosphate and β-Glycerophosphate.

IL-1β and TNF-α were added on day 7 and culture medium was collected after 48 hours for use in nitrite and prostaglandin E_2 (PGE_2) assays.

RESULTS AND DISCUSSION

Nitrite concentration in the supernatant was measured as an estimate of nitric oxide (NO) release (Fig. 1A). NO is released in the inflammatory response in response to cytokines [2]. Prostaglandins have been strongly implicated as mediators of proinflammatory cytokines on bone [3], thus concentration of PGE_2 released into the media was measured (Fig 1B). Nitrite and PGE_2 release for both cell types was low when stimulated by IL-1β and TNF-α alone and for both cell types there was an innate nitrite release. In combination, IL-1β and TNF-α caused a large nitrite and PGE_2 release in the bone cells, but not in the mESCs, suggesting a difference in the inflammation pathway.

CONCLUSIONS

Early results show differences in mESCs and primary bone reaction to proinflammatory cytokines, suggesting that mESCs may have more tolerance to the presence of inflammatory molecules.
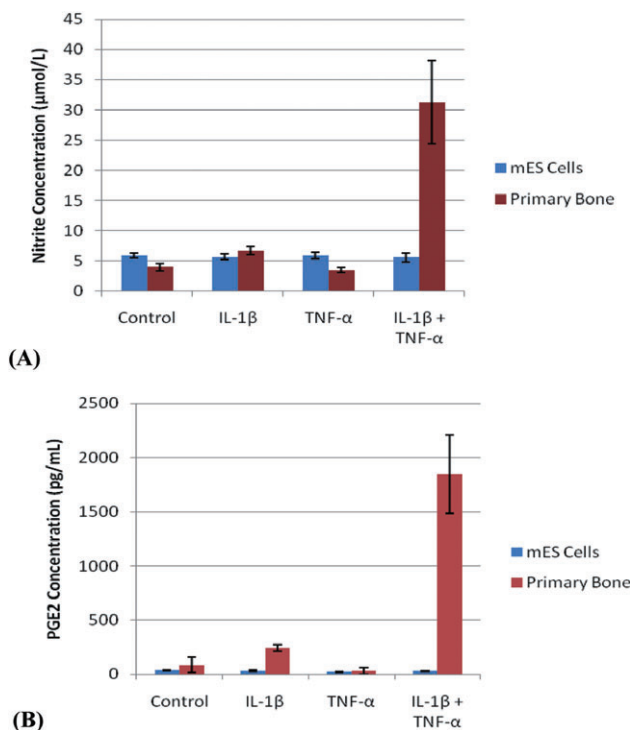

Fig. 1. (**A**) Nitrite and (**B**) PGE_2 release in response to proinflammatory cytokines

REFERENCES

[1] F. J. Hughes et al., "Cytokine-induced prostaglandin E-2 synthesis and cyclooxygenase-2 activity are regulated both by a nitric oxide-dependent and -independent mechanism in rat osteoblasts in vitro" *J. Biol. Chem.* **274** (1999) 1776–1782.

[2] S.H Ralston, D. Todd, M. Helfrich, N. Benjamin, P.S.Grabowski, "Human osteoblast-like cells produce nitric oxide and express inducible nitric oxide synthase. *Endocrinology* **135** (1994) 330–336.

[3] Akatsu, T., *et al.* "Role Of Prostaglandins In Interleukin-1-Induced Bone-Resorption In Mice In Vitro." *J. Bone Miner. Res.* **6**, (1991) 183–190.

Tumour Cell Adhesion of Endothelial Cell Monolayer

Abdullah, A., Arrigoni, F. and Freestone, N.S.

School of Pharmacy and Chemistry, Kingston University London, UK.

INTRODUCTION

Cancer is the second leading cause of death in the modern world. Tumour cell metastasis is one of the most important factors in the prognosis of cancer patients. Metastasis is a complex multistep process that involves the detachment of tumour cells from the primary tumour, migration through tumour-derived vessels into blood stream, survival in blood circulation, extravasation (migration through vascular endothelium to target organs), and finally establishment of secondary tumours. All these steps are dependent upon adhesions between the endothelial cells that line the circulatory system vessels and the tumour cells themselves.

Certain inflammatory cytokines, for example, tumour necrosis factor-α (TNF-α) may play an important role in cancer metastasis through their ability to induce expression of adhesion molecules on the surface of endothelial cells, thus presenting suitable sites for tumour cell adherence. A protein kinase C activator, 12-O-tetradeconylphorbol-1, 3-acetate (TPA) has also been reported to stimulate cell adhesion.

The purpose of the present study is to investigate the effect of TNF-α and phorbol ester on tumour cell adhesion to the surface of endothelial cells. This study also investigates the effect of different anti-tumour agents to reduce the tumour cell adhesion by these two molecules.

MATERIALS AND METHODS

Human vascular endothelial (HUVEC) cells were seeded in a 96 well plate and incubated for 48–72 hours to form a monolayer. The endothelial cells were then activated by treating them with a different concentration of TNF-α (0.03–300 ng/mL) and phorbol ester (0.1–1000 ng/mL) for one hour. Human breast cancer cells (MCF7) and Prostate cancer cells (PC3 and DU-145) were labelled with cell tracker green dye. Fluorescent labelled tumour cells were then added to the HUVEC monolayer in a concentration of 20,000, 40,000 and 80,000 tumour cells/well. After incubation of one hour, the tumour-endothelial co-culture was washed with PBS. Phase contrast and fluorescent microscopy was done to observe tumour adhesion onto the endothelial surface.

The plates were then read using a fluorescent plate reader with wavelength (excitation) set at 485 nm and (emission) set at 538 nm. Results are shown as mean ± SEM of three experiments.

RESULTS

Following activation of the human endothelial cell line (HUVEC), with phorbol ester TPA and subsequent co-culture with labelled MCF7, PC3 and DU-145 cells, tumour cell attachment was observed to increase in a dose dependent
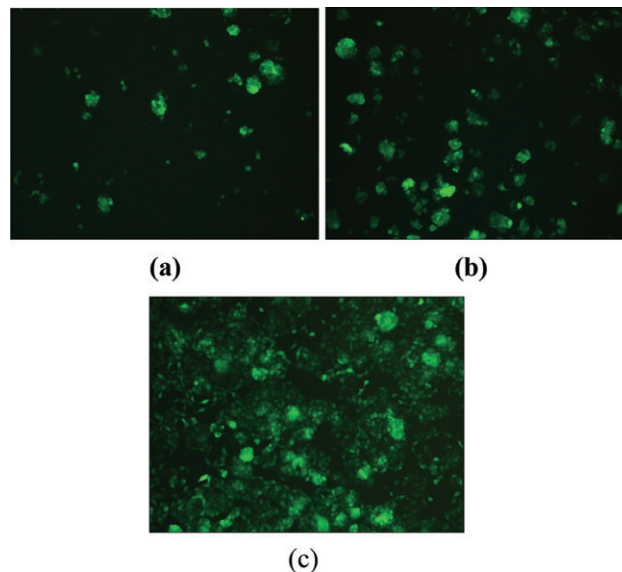
Fluorescence labelled MCF7 cells attached to the HUVEC monolayer (a) in the absence of TNF-α and phorbol ester (b) with 0.1 ng/mL of TNF-α (c) with 30 ng/mL of phorbol ester.
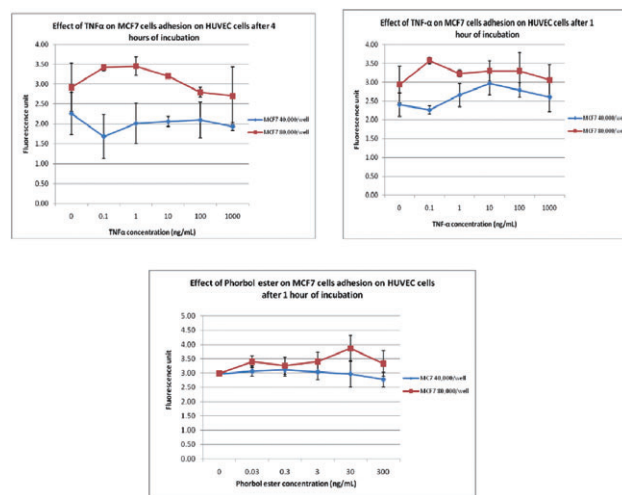
manner with a maximum effect seen with 30 ng/mL. The stimulatory effect on cell attachment by TNF-α was shown with an endothelial cell pre-treatment time of 4 hrs. The maximum activity of TNF-α was seen with concentration of 0.1 mg/mL.

CONCLUSION

We can conclude that both phorbol ester and TNF-α have a positive effect on tumour cell attachment to endothelial cells.

Phorbol ester is a protein kinase C activator thus tumour metastasis could potentially be treated via elements in the kinase cascade. Further investigation into the role of TNF-α and phorbol ester in tumour cell adherence could be undertaken by using inhibitors of these two molecules and also other anti-tumour agents.

'Smart Culture' of Mouse Embryonic Stem Cells

Sabrina Dey[1], Morgan Alexander[2], Barrie Kellam[3], Cameron Alexander[1], and Felicity RAJ Rose[1]

Division of Drug Delivery and Tissue Engineering, Division of Medicinal Chemistry and Structural Biology[2], Laboratory of Biophysics and Surface Analysis[3], School of Pharmacy, The University of Nottingham, Nottingham, NG7 2RD, UK

INTRODUCTION

Current culture methods for mammalian cells use trypsin as means to detach them from the culture surface. This inflicts damage to cell membrane receptors (mainly integrins) which can be detrimental for further adhesion to a new substrate[1]. In addition, using trypsin may contaminate cell cultures destined for clinical applications. Therefore, an alternative, affordable, and scalable method of passaging is a new and active area of research. Stimuli responsive polymers can be used to avoid the deleterious effects of trypsin/EDTA as the cells detach from the culture substrate upon a stimulus (temperature[2], pH and light). Application of thermo-responsive polymers to mammalian cell culture, and ultimately for use with embryonic stem cells, is the focus of this research project.

METHODS

poly (MEO2MA-co-OEGMA) grafting of thermo-responsive polymers: Grafting of MEO_2MA and OEGMA monomers onto poly (allyl-alcohol) plasma coated glass cover slips was achieved using Atomic Transfer Radical Polymerisation (ATRP).

Surface characterisation: Surface characterisation included X-ray photoelectron spectroscopy (XPS), water contact angle (WCA) measurements, and Atomic force microscopy (AFM).

Cell response on the thermo-responsive surfaces: 3T3 mouse fibroblasts were cultured on these surfaces in DMEM supplemented with 10% FCS. Prior to feeder free mouse embryonic stem cell (mES; E14Tg2A) culture in DMEM supplemented with 15% FCS and 100 µL/ml LIF, the surfaces were incubated with 5 µg/ml fibronectin at 37°C overnight. Cell response (attachment and detachment) was observed using optical microscopy.

RESULTS

WCA and adhesion force-curve measurements using AFM below and above the lower critical solution temperatures (LCST) indicated that the copolymer, poly(MEO2MA-co-OEGMA) grafted brushes had a reversible temperature switching behaviour from hydrophobic at 37°C to hydrophilic

Fig. 1: Adhesion force-curve of the surface studied at different temperatures (Above and below LCST).

Fig. 2: 3T3 fibroblast and Feeder free mouse embryonic stem cell response on the surfaces: **1** and **3**, 3T3 fibroblasts and mESC attachment at 37°C respectively. **2** and **4** 3T3 fibroblast and mESC detachment from poly(MEO2MA-co-OEGMA) grafted surfaces following a temperature drop below the LCST.

at 20°C. In addition, this switching was found to be reversible (Fig. 1).

3T3 fibroblasts adhered, spread, proliferated, and reached confluency on thermo-responsive surfaces in the same manner as seen on control surfaces (Tissue Culture
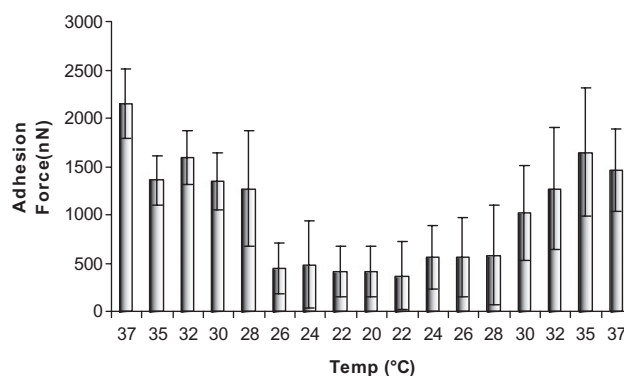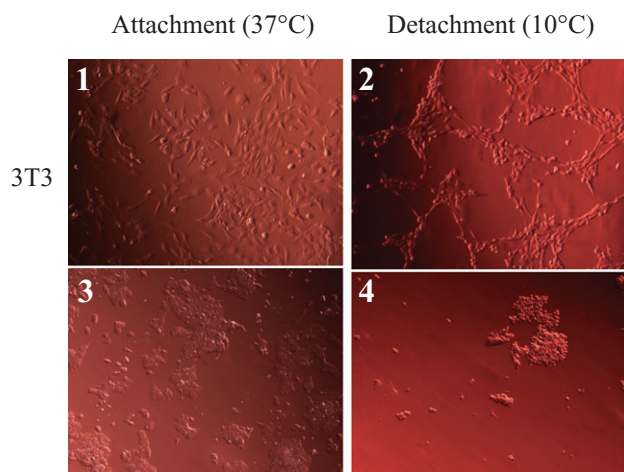
Polystyrene; TCP). Detachment studies were performed at 20°C for 2 hrs and full recovery of cells was observed.

mES cells cultured on fibronectin coated surfaces at 37°C were observed to adopt a similar morphology as seen on gelatine coated TCP (control). Cells detached from the thermo-responsive grafted surfaces when the temperature was lowered to 10°C (Fig 2). This was achieved over 2 passages with maintenance of the stem cell phenotype.

CONCLUSIONS

We have shown that poly(MEO$_2$MA-co-OEGMA) was grafted successfully from a glass surface and that a switchable response to temperature achieved. 3T3 fibroblasts adhered, spread and proliferated at 37°C and detached when the temperature was lowered to 10°C. A similar effect was observed with mES cells and no differentiation was observed following two passage cycles.

REFERENCES

[1] Waymouth, C. To disaggregate or not to disaggregate injury and cell disaggregation, transient or permanent? *In vitro*. **10** (1974) 97–111.
[2] Okano T. *et al*. Mechanism of cell detachment from temperature-modulated, hydrophilic-hydrophobic polymer surfaces. *Makromol. Chem., Rapid Commun.* **11** (1990) 571–576.
[3] Lutz, J.F. *et al*. Point by Point Comparison of Two Thermosensitive Polymers Exhibiting a Similar LCST: Is the Age of Poly(NIPAM) Over? J. Am. Chem. Soc. **128** (**2006**) 13046–13047.

An Injectable Scaffold for Cell and Growth Factor Delivery

L.G. Hamilton, R.A. Quirk[1] and K.M. Shakesheff.

Wolfson Centre for Stem Cells, Tissue Engineering and Modeling (STEM), CBS, School of Pharmacy, University of Nottingham, UK .
[1]RegenTec Ltd.

Abstract – **Bioabsorbable engineered scaffolds are temporary structures that preserve tissue dimensions, providing anchorage and guidance to cells during regeneration and repair. Successful translation and exploitation of cell therapy requires both cell survival and prolonged growth factor release to promote proliferation and differentiation activities[1]. We have developed a biodegradable and injectable particulate transporter system for cells and therapeutic actives.**

INTRODUCTION

Injectable polymer particulates that form macroporous scaffolds can act as delivery systems for cells with the differentiation fate being directed by the growth factor released. Bone healing requires a combination of mechanical stability, osteoconductive surface, growth factors and osteogenic cells. Our goal was to develop a biodegradable, injectable paste to support new bone formation using a two-component poly(α-hydroxy acid) based scaffold.

MATERIALS AND METHODS

A particles of PLGA (DL-lactide 50:50 glycolide Low I.V. 0.5–0.65 dL/g, Lakeshore Biomaterials) were produced using an emulsification and solvent evaporation method, employing the solvent dichloromethane and 0.3% poly(vinyl alcohol) 13000–23000 molecular weight (Mw) as stabiliser. For protein loaded Type 1 particles, 0.01% BSA fraction V was lyophilised with rhBMP-2 and added to the polymer prior to emulsification. Type 2 particles were produced by blending up to 15 wt% PEG (Mw 400, Fluka 81172) and PLGA (lactide-co- glycolide 85:15 High I.V. 0.6–0.8 dL/g). The ratio of adhesive to carrier particle was 3:1. A suspension of 5×10^5 C2C12 cells in HBSS buffer was mixed with particles in the barrel of a 1 ml syringe (in situ seeding) forming a paste that was placed in a 37°C incubator for 30 minutes before being ejected as a cylindrical cast into media. There were three experimental conditions: (a) scaffold with an empty carrier in media; (b) scaffold with an empty carrier in media supplemented with 100 ng/ml rhBMP-2 and (c) scaffold with a carrier loaded with rhBMP-2. Scaffolds were examined at day 5, 18 and 28 for cell viability and alkaline phosphatase activity. At day 18 the rhBMP-2 growth factor was withdrawn from the supplemented media condition.

RESULTS AND DISCUSSION

Scaffold porosity could be controlled from 35–65%. Within 15 minutes of injection in HBSS scaffold strength increased from 0.045–2 MPa at 37°C. Over the duration of the BMP-2 release experiment, there was sustained cell proliferation up to day 28.

At day 5 there was no significant difference in alkaline phosphatase production between the treatments and control. A very significant difference ($p < 0.01$) in alkaline phosphatase activity was detected at day 18 between the untreated control and C2C12 cells exposed to rhBMP-2 supplemented media and growth factor loaded carrier. There was no significant difference in alkaline phosphatase levels detected between supplemented media and controlled release of rhBMP-2 from particles. No significant difference in cell proliferation was detected between the groups up to day 18. At day 18 the 100 ng/ml supplement of rhBMP-2 to the media was withdrawn. The level of alkaline phosphatase activity in

the withdrawn supplement group was very significantly (p < 0.01) reduced in comparison to the controlled release group at day 28 despite having very significantly (p < 0.001) more cells present on the scaffolds.

CONCLUSIONS

We have demonstrated wet formation of a scaffold structure from a two-component injectable paste, cell adhesion, proliferation and the controlled release of rhBMP-2 to direct the differentiation of myogenic C2C12 to an osteoblastic phenotype. The scaffold was designed to sinter at body temperature, forming a macroporous self-supporting structure. The duration of the experiment and proliferation results demonstrate the benign nature of the solidification process. The scaffold system therefore shows potential as a delivery system for both cells and growth factors.

ACKNOWLEDGMENTS

REFERENCE

[1] D.J. Mooney, H. Vandenburgh Cell delivery mechanisms for tissue repair. *Cell stem cell,* 2008. 2(3): p. 205–13

An Injectable Scaffold with sustained release of rhBMP2 for bone regeneration

A. Boussahel[1], C. Rahman[1] F.R.A.J. Rose[1] & K. M. Shakesheff[1]

[1]Wolfson Centre for Stem Cells, Tissue Engineering and Modeling (STEM), School of Pharmacy, University of Nottingham, UK

INTRODUCTION

Musculoskeletal conditions pose a huge burden on health services especially with an increasing aging population [1]. The limitations of available treatments raise the need for novel tissue engineering alternatives. Applying osteoinductive growth factors with tissue-engineering scaffolds is currently a promising strategy for reconstructing bone defects. In particular, recombinant human bone morphogenetic protein 2 (rhBMP2) has been extensively investigated for this purpose [2]. However, with a short half-life and potential toxicity at systematic levels, a drug delivery system is imperative to achieve a therapeutic response [3]. We aim to develop an injectable *in situ* solidifying polymer scaffold that provides a delivery system for rhBMP2 and promotes bone regeneration.

MATERIALS AND METHODS

The *in situ* solidifying scaffold was prepared from melt blended poly(lactic-*co*-glycolic) acid/poly(ethylene glycol) (PLGA/PEG) particles. Encapsulation of model proteins (Human serum albumin (HSA), Bovine serum albumin (BSA), Horseradish peroxidase (HRP) and Lysozyme) into PLGA microspheres was compared using passive adsorption, double emulsion (W/O/W) and single emulsion (S/O/W) methods. The latter method was then used to encapsulate rhBMP2 into PLGA microsphere using HSA as a carrier protein. The rhBMP2 was first micronised with HSA at different ratios and then encapsulated maintaining the amount of HSA constant and varying the rhBMP2 amount allowed for dose alteration. The activity of micronised rhBMP2 was confirmed using both an ELISA and a C2C12 cell/Alkaline Phosphatase (ALP) biological activity assay.

RESULTS AND DISCUSSION

An injectable formulation of PLGA/PEG and PLGA microparticles has been developed. The melt blended PLGA/PEG particles are thermosensitive with a glass transition temperature of 37°C. The particles are mixed with a solution at room temperature forming an injectable paste; at 37°C it solidifies at the site of injection forming a scaffold. PLGA microspheres were used as a protein carrier. The incorporation of proteins was compared using the above three methods. The adsorption method was found to be dependent on particle structure and composition. For the W/O/W, encapsulation efficiency (EE%) improved by varying the Polyvinyl alcohol (PVA) concentration, loading weight and additives. The S/O/W dispersion method on the other hand was mainly controlled by the micronisation step, where the proteins were micronised to particles 500 nm-2 μm in diameter (Figure 1a & b) through phase separation induced by freeze condensation. We found this step to be dependent on the PEG molecular weight, the PEG:protein ratio, and the freezing rate. An ELISA confirmed the preservation of micronised rhBMP2 activity at all HSA/rhBMP2 ratios, and when compared to a positive control (rhBMP2 alone), it also stimulated C2C12 cell differentiation towards a bone cell-like lineage (Figure 1c). The micronised HSA/rhBMP2 was then encapsulated into PLGA microspheres with an EE of between 60–80%. Initial results suggest that a sustained release of rhBMP2 from these particles can be achieved.

CONCLUSIONS

We optimised protein incorporation into the developed injectable scaffold formulation using three methods. A novel improved approach of rhBMP2 micronisation has been dem-
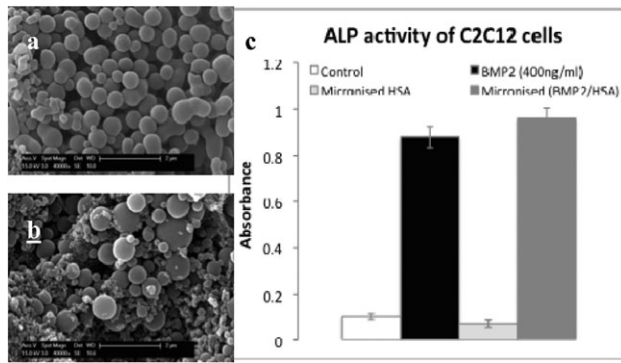
Fig. 1. Representative SEM images of micronised BSA(a & b), ALP activity of C2C12 cells following stimulation with micronised rhBMP2 (c)

onstrated, along with enhanced protein encapsulation within microparticles using the S/O/W technique. Future studies will focus on studying the release kinetics and determining the biological activity of released rhBMP2 through *in-vitro* cell differentiation studies. The ultimate aim is to develop an injectable scaffold for bone regeneration using a mixture of rhBMP2 containing microparticles and cells.

ACKNOWLEDGMENTS

REFERENCES

[1] S.L. Weinstein, "The Bone and Joint Decade" *J Bone Joint Surg Am* **82** (2000) 1–3.

[2] M.F. Termaat, F.C. Den Boer, F.C. Bakker, P. Patka and H. J. Haarman "Bone morphogenetic proteins. Development and clinical efficacy in the treatment of fractures and bone defects" *J Bone Joint Surg* **87** (2005) 1367–78.

[3] J.E Babensee, L.V. McIntire, and A.G. Mikos "Growth factor delivery for tissue engineering" *Pharm Res* **17** (2000). 497–504.

Bone Morphogenetic Proteins (*Bmps*) are essential for normal adult physiology and survival

Abhishek L. Narayanan, Paritosh Parashar, Aditi Nag and Amitabha Bandyopadhyay

Department of Biological Sciences and Bioengineering
Indian Institute of Technology Kanpur, India

Abstract – **The roles of many of the signalling molecules in development are well characterised but in adult life they are yet to be explored systematically. Here, using an inducible knock out system [1], we look beyond development stages, focussing on the roles of BMP2 and BMP4 in maintenance of normal adult physiology. Our preliminary data suggests that BMP2 and BMP4 are essential for the survival of adult mice.**

INTRODUCTION

Bone Morphogenetic proteins are members of the Transforming Growth Factor-β (TGF-β) superfamily. There are at least 15 known *Bmp*s[2]. There are considerable evidences to show that they are essential for normal development – from early embryonic stage to the development of various organ systems [3]. We hypothesised that BMPs may play important role(s) in maintaining these organ systems in adult life.

MATERIALS AND METHODS

The mice used for this study have LoxP sites flanking the protein coding region of the Bmp2 and Bmp4 genes [4][5][6]. This strain was crossed with a tamoxifen inducible deleter strain.

The second generation progeny mice used are $Bmp2^{c/c}$;$Bmp4^{c/c}$ $Gt(ROSA)26Sor^{tm1}Cre/Esr1)$Nat/$Gt(ROSA)26Sor^{tm1}Cre/Esr1)$ Nat. These mice are phenotypically wild type but when induced with tamoxifen, Cre-recombinase acts causing depletion of *Bmp2* and *Bmp4* activity.

Six week old mice and their litter mate controls are injected intraperitoneally with tamoxifen for five consecutive days using a previously described protocol to induce Cre-recombination and *Bmp* depletion [7]. Phenotypic assessment as well as histopathological examination of all major organs is underway. Recombination efficiency in various organs is being characterised by PCR amplification, in situ hybridisation and RT PCR. Biochemical parameters of the mice are also being assessed.

RESULTS AND DISCUSSION

We find that the mice do not survive beyond 7 days from the first day of tamoxifen injection. They consistently show rapid, significant weight loss in addition to other phenotypic abnormalities. Sudden rapid deterioration in health suggests involvement of multiple major organ systems. Detailed phenotypic analysis is currently underway. In order to investigate whether both *Bmp2* and *Bmp4* are individually essential in adult life, we are generating single conditional mutant strains.

CONCLUSIONS

To our knowledge this is the first attempt at evaluating role(s) of *Bmp* ligands in any adult organism. Previous studies show that many disorders ranging from pulmonary hypertension, brain infarction to renal disease and colonic polyposis may result due to defective *Bmp* signalling[9][10]. We demonstrate, for the first time, that *Bmp* signalling is essential for an adult mouse. Our approach is likely to reveal roles of *Bmp* signalling in various aspects of adult physiology providing a framework for directed search for human geneticists in unravelling the molecular basis for certain genetic diseases.

REFERENCES

[1] Branda, C. S. & Dymecki, S. M. Talking about a revolution: The impact of site-specific recombinases on genetic analyses in mice. Dev Cell 6, 7–28 (2004).

[2] Massague, J. TGFbeta signaling: receptors, transducers, and Mad proteins. Cell 85, 947–50 (1996).

[3] Bone morphogenetic proteins: multifunctional regulators of vertebrate development. B L Hogan Genes Dev. 1996 10: 1580–1594

[4] Genetic analysis of the roles of BMP2, BMP4, and BMP7 in limb patterning and skeletogenesis. Bandyopadhyay A, Tsuji K, Cox K, Harfe BD, Rosen V, Tabin CJ. PLoS Genet. 2006 Dec;2(12):e216. Epub 2006 Nov 6.

[5] Liu, W. et al. Bmp4 signalling is required for outflow-tract septation and branchial-arch artery remodeling. Proc Natl Acad Sci U S A 101, 4489–94 (2004).

[6] Selever, J., Liu, W., Lu, M. F., Behringer, R. R. & Martin, J. F. Bmp4 in limb bud mesoderm regulates digit pattern by controlling AER development. Dev Biol 276, 268–79 (2004).

[7] Efficient recombination in diverse tissues by a tamoxifen-inducible form of Cre: a tool for temporally regulated gene activation/inactivation in the mouse. Hayashi S McMahon AP 2002 Dev Biol.Apr 15;244(2):305–18.

[8] Bmp2 and Bmp4 genetically interact to support multiple aspects of mouse development including functional heart development. Uchimura T, Komatsu Y, Tanaka M, McCann KL, Mishina Y Genesis: 2009 Jun;47(6):374–84.

[9] BMP signaling inhibits intestinal stem cell self-renewal through suppression of Wnt-beta-catenin signalling. He XC, Zhang J, Tong WG et al. Nat Genet. 2004 Oct;36(10):1117–21. Epub 2004 Sep 19

[10] Increased susceptibility to pulmonary hypertension in heterozygous BMP2R mutant mice Song Y, Jones JE, Beppu H, Keaney JF Jr, Loscalzo J, Zhang YY.Circulation: 2005 Jul 26;112(4):553–62. Epub 2005 Jul 18.

Characterisation of collagen I coated polyacrylamide gels intended for direction of embryonic stem cell differentiation

S. N. Patankar[1,2], S. Allen[1], P. M. Williams[1], L. D. Buttery[2], M. R. Alexander[1]

[1]Laboratory of Biophysics & Surface Analysis, Boots Science Building, School of Pharmacy, University of Nottingham, Nottingham, NG7 2RD, United Kingdom.
[2]STEM, Centre for Biomolecular Sciences, School of Pharmacy, University of Nottingham, Nottingham, NG7 2RD, U.K.

Regenerative medicine offers the prospect of forming replacement tissue derived from cells of the injured host. Embryonic stem cells are able to differentiate into all cells of the mammalian body, and consequently are of interest for application in regenerative medicine. Recent work has shown that the mechanical characteristics of the stem cells' local environment can influence the type of cells that result from differentiation [1]. Much of the work in this area has been carried out on polyacrylamide gel substrates utilising mesenchymal stem cells. Here we present a full and detailed characterisation of polyacrylamide gel surface chemistry, topography, and modulus. This is carried out using time of flight mass spectrometry (ToF-SIMS), x-ray photoelectron spectroscopy, sessile drop water contact angle goniometry, atomic force microscopy and environmental scanning electron microscopy. Uniform collagen I coverage was determined by ToF-SIMS, using a preparation procedure based upon the literature [2]. This work goes on to explore how these fully characterised coated gels influence embryonic stem cell differentiation as a function of stiffness, with PCR data and fluorescence microscopy, comparing the differentiation outcomes from mesenchymal stem cell culture.

INTRODUCTION

This work details the surface characterisation of collagen I coated polyacrylamide gels, with varying surface stiffness, suitable for stem cell differentiation.

MATERIALS AND METHODS

Surface chemistry: ToF-SIMS was carried out on a SIMS IV time-of flight instrument (ION-TOF GmbH, Münster, Germany), sputtering Bi^{3+} ions at 25 KeV. XPS spectra were acquired on a Kratos Axis Ultra (Kratos, UK) with a monochromated Al kα source (1486.6 eV). Sessile drop water contact angle goniometry was measured using a CAM200 instrument (KSV Instruments, Finland). Surface stiffness/morphology: Atomic force microscopy was carried out on a Molecular Force Probe (Asylum Research, California, USA) using a Veeco DNP cantilever. Environmental scanning electron microscopy was carried out on a FEI/Philips XL30 FEG-SEM (Eindhoven, Netherlands). Surface chemistry data was analysed using the principal component analysis technique. This was carried out using Matlab R2009a (Natick, MA, USA), with the PLS Toolbox add-on module (Eigenvector Research, WA, USA).

Fig. 1. PCA Scores plot showing different groupings of data after each chemical treatment.

RESULTS AND DISCUSSION

Principal component analysis of the ToF-SIMS data suggests that there are distinct surface chemistry differences at each chemical step. The scores plot (Fig.1) from the PCA shows changes in surface chemistry before and after collagen I treatment, despite their gluteraldehyde, polyacrylamide, sulfo-SANPAH, and type I collagen all being organic structures difficult to distinguish.

CONCLUSIONS

Polyacrylamide gels of varying surface stiffness and controlled surface chemistry have been used extensively for the investigation of effects on mesenchymal stem cells [1, 2]. This work shows that these polyacrylamide gels do hav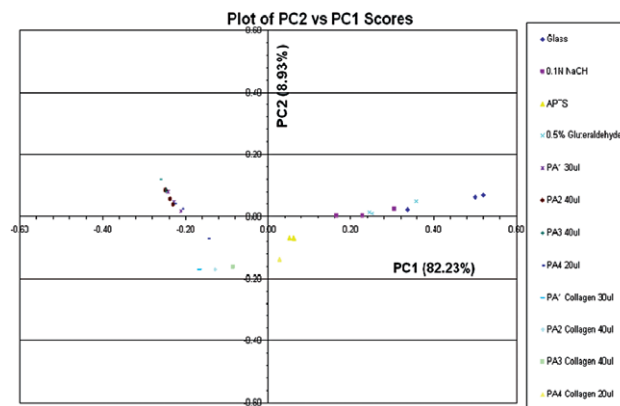e specific surface chemistry, uniform coverage of type I collagen, and are effective for the measurement of differentiation of murine embryonic stem cells as a function of surface stiffness.

REFERENCES

[1] A.J. Engler, S. Sen, H.L. Sweeney, D.E. Discher, "Matrix elasticity directs stem cell lineage specification" *Cell*, **126** (2006) 677–689.
[2] R.J. Pelham and Y.L. Wang, "Cell locomotion and focal adhesions are regulated by substrate flexibility" *PNAS (USA)*, **94** (1997) 13661–13665.

Characterisation of Viability and Proliferation of 3t3 Fibroblasts Encapsulated in Alginate-chitosan-hyaluronate Capsules

Paulina Cygan[1], Snow Stolnik[1], Anna Grabowska[1], Steve Wedge[2], Paul Elvin[2], Sue Watson[1]

[1]School of Pharmacy, University of Nottingham
[2]AstraZeneca, Macclesfield, UK

INTRODUCTION

For successful application of tissue engineering to 3D culture, cell viability and proliferation in the polymeric matrix must be taken into account because biomaterials may affect the viability of encapsulated cells. Although histological and colorimetric methods are widely used to measure cell proliferation in 2D culture, they still present problems when applied to 3D cultures. Dyes, such as formazan, the product of cellular metabolic activity, may interact with biopolymers of the matrix and be difficult to dissolve and to analyse due to slow release from the matrix [1–3]. Methods, such as the trypan blue exclusion assay, used for cell viability assessment *in situ*, often produce results difficult to interpret due to the cell growth throughout the whole depth of the matrix [2, 4].

The objective of this study was to optimise MTT and trypan blue tests and use them, together with live-dead cell staining, to characterise 3T3 fibroblasts, as model cells, encapsulated in alginate-chitosan-hyaluronate capsules.

MATERIALS AND METHODS

Murine 3T3 fibroblasts were cultured in DMEM (Sigma) medium with 10% of foetal bovine serum (FBS). The cells were encapsulated by passing through a 21G needle. Recovery of cells from complex polymer network was achieved using an optimised 'disruption buffer'. Liberated cells were stained with 0.04% trypan blue solution and counted using a Neubauer haemocytometer. Metabolic activity was assessed by (3-(4,5-Dimethylthiazol-2-yl)-2,5-diphenyltetrazolium bromide (MTT) reduction assay. The same 'disruption buffer' was employed to liberate formazan crystals formed by living cells inside beads, for spectrophotometric analysis. For live-dead staining calcein acetoxymethylester (CaAM) and ethidium homodimer-1 (EthD-1) were used together with Hoechst stain for DNA labelling.

The absorbance of dissolved formazan crystals was measured with MRX microplate reader, using Dynex Revelation 4.21 software (Dynex Technologies). Light and fluorescent images were captured on Leica DM IRB microscope with camera fast 1394, analysed with QCapture Pro software and merged using GNU Image Manipulation Program (GIMP) 2.6 (http://www.gimp.org).

RESULTS

Disruption methods routinely used for non-modified alginate capsules did not give satisfactory results for our system, leaving cells entrapped in matrix fragments. An optimised composition of new 'disruption buffer' is based on the breakdown of non-covalent bonds between polymer components. This buffer enabled reliable analysis of 3T3 fibroblasts cultured for 20 days in matrix. The cells showed an initial increase in metabolic activity followed by a decrease on day 15. Cell number increased continuously despite a decrease in metabolic activity. This decrease may have resulted from overpopulation of capsules and development of hypoxia. Live-dead staining confirmed that the culture was mostly composed of live cells, although with time an increasing number of dead or dying cells was observed.

CONCLUSIONS

Our optimised MTT and trypan blue methods give accurate and rapid and easy-to-interpret results and together with live-dead cell staining allow characterisation of various cell types encapsulated in our alginate-based system and assessment of cell growth *in vitro*.

3T3 fibroblasts were successfully cultured for 20 days in alginate-chitosan-hyaluronate capsules and analysed with optimised MTT, trypan blue and live-dead staining methods. The cells increased in number throughout the 20-day culture period but their metabolic activity decreased at the end-stage.

REFERENCES

[1] Khattak SF, Spatara M, Roberts L, Roberts SC: Application of colorimetric assays to assess viability, growth and metabolism of hydrogel-encapsulated cells. *Biotechnology Letters*. 2006; **28**: 1361–1370.

[2] Bünger CM, Jahnke A, Stange J, de Vos P, Hopt UT: MTS Colorimetric Assay in Combination with a Live-Dead Assay for Testing Encapsulated L929 Fibroblasts in Alginate Poly-l-Lysine Microcapsules In Vitro. *Artificial Organs*. 2002; **26**: 111–116.

[3] Baruch L, Machluf M: Alginate-chitosan complex coacervation for cell encapsulation: effect on mechanical properties and on long-term viability. *Biopolymers*. 2006; **82**: 570–579.

[4] Krol S, del Guerra S, Grupillo M, Diaspro A, Gliozzi A, Marchetti P: Multilayer nanoencapsulation. New approach for immune protection of human pancreatic islets. *Nano Letters*. 2006; **6**: 1933–1939.

Controlling the morphology and mechanical properties of supercritical fluid foamed scaffolds

L.J. White[1], V. Hutter[1], S.M. Howdle[2], K.M. Shakesheff[1]

[1]School of Pharmacy, University of Nottingham, Nottingham, UK.
[2]School of Chemistry, University of Nottingham, Nottingham, UK.

Abstract – **Whilst supercritical fluid foamed scaffolds have found significant utility in tissue engineering, these scaffolds may possess divergent pore architecture. This study shows that the morphology and mechanical integrity of supercritical CO_2 scaffolds can be tailored by manipulation of process parameters.**

INTRODUCTION

Supercritical CO_2 scaffold formation is a solvent free, low temperature process which produces open cell, interconnected foamed structures. Drug molecules and proteins can be encapsulated within these scaffolds as protein structure and activity are retained during processing. Successful applications of this technique include the controlled release of proteins [1], promotion of bone formation *in vitro* and *in vivo* [2] and the induction of angiogenesis *in vitro* [3].

Supercritical CO_2 scaffold fabrication can produce scaffolds of divergent pore size and structure. Hence, this study sought to elucidate the effects of processing conditions on the porosity, pore size distribution and mechanical properties of the scaffolds.

MATERIALS AND METHODS

Three molecular weights of poly(D,L-lactic acid) ($P_{DL}LA$) (15 kDa, 24 kDa and 57 kDa) were used to form scaffolds under different depressurisation rates. The porous scaffolds fabricated had diameters of approximately 10 mm and were 5–10 mm in height; a non-porous skin surrounded each scaffold.

The morphology, including pore size, strut size and porosity, of the resultant scaffolds was characterised by micro x-ray computed tomography (µCT) (Skyscan 1174, Skyscan, Aartselaar, Belgium). Mechanical properties were tested using a TA.HD plus Texture Analyser (Stable Micro Systems Ltd., Surrey, UK). Scaffolds were cut into uniform cubes with width, length and height of 5 ± 0.5 mm prior to µCT scanning and mechanical testing.

RESULTS AND DISCUSSION

Scaffolds created from different molecular weights showed varying morphologies (Fig. 1). Vent time had a pronounced effect upon scaffold architecture – this was particularly observed with 15 kDa scaffolds. The porosity of all scaffolds significantly increased with decreased depressurisation rates (increased vent times).

Upon mechanical testing, 57 kDa $P_{DL}LA$ scaffolds displayed a typical stress-strain curve for elastomeric open cell foams, comprising a linear elastic region, a collapse plateau and densification.

The elastic collapse stress, Young's modulus and ultimate stress were considerably increased by using shorter vent times in scaffold fabrication; the ultimate stress ranged from 5.1 MPa using a 10 minute vent to 2.8 MPa for a 45 minute vent for 57 kDa $P_{DL}LA$ scaffolds.

The compressive behaviour of 24 and 15 kDa scaffolds did not follow an elastomeric open cell foam stress-strain curve but rather indicated brittle behaviour [4]. A fault line generally propagated through the structure to cause the brittle fracture.

CONCLUSIONS

This study conclusively shows that the architecture and mechanical properties of $P_{DL}LA$ scaffolds can be tailored by
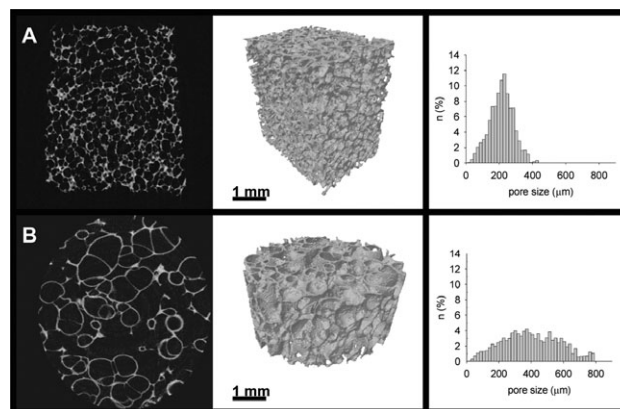

Fig. 1. Effect of molecular weight and depressurisation rate on the morphology of $P_{DL}LA$ scaffolds, with A: $M_w = 57$ kDa and B: $M_w = 15$ kDa with two dimensional slices perpendicular to the direction of foaming (first column), three dimensional µCT reconstructions (second column) and pore size distributions (third column). Scaffolds were created with a vent time of 30 minutes. Scale bar = 1 mm.

adjusting the processing conditions and the molecular weight of the polymer.

REFERENCES

[1] Howdle, S.M., M.S. Watson, M.J. Whitaker, V.K. Popov, M.C. Davies, F.S. Mandel, et al., "Supercritical fluid mixing: preparation of thermally sensitive polymer composites containing bioactive materials" *Chem. Common.*, (2001) 109–110.

[2] Yang, X.B.B., M.J. Whitaker, W. Sebald, N. Clarke, S.M. Howdle, K.M. Shakesheff, et al., "Human osteoprogenitor bone formation using encapsulated bone morphogenetic protein 2 in porous polymer scaffolds" *Tissue Eng.*, **10** (2004) 1037–1045.

[3] Kanczler, J.M., J. Barry, P. Ginty, S.M. Howdle, K.M. Shakesheff and R.O.C. Oreffo, "Supercritical carbon dioxide generated vascular endothelial growth factor encapsulated poly(dl-lactic acid) scaffolds induce angiogenesis *in vitro*". *Biochem. Biophys. Res. Commun.*, **352** (2007) 135–141.

[4] Gibson, L.J., "Biomechanics of cellular solids". *J. Biomech.*, **38** (2005) 377–399.

Development of an Immunocompetent and Self-reporting 3D Human Respiratory Model

P.A. Cato[1,3]*, H.C. Harrington[1,2]*, J.W. Aylott[2], F.R.A.J. Rose[3], A. Ghaemmaghami[1]

[1]Allergy Research Group, School of Molecular Medical Sciences, University of Nottingham, UK. [2]Laboratory of Biophysics and Surface Analysis, School of Pharmacy, University of Nottingham, UK. [3]Division of Drug Delivery and Tissue Engineering, Centre for Biomolecular Sciences, University of Nottingham, UK. *authors contributed equally

Abstract – **Polymeric electrospun scaffolds incorporating analyte responsive, optical nanosensors have been prepared to produce novel self-reporting scaffolds. Furthermore the scaffold surface has been modified using post-production techniques to enhance epithelial and fibroblast cell line attachment and viability in cell culture. These self-reporting biocompatible scaffolds will be used in the development of a perfusable and immunocompetent self-reporting 3D human upper respiratory model.**

INTRODUCTION

Current research tools modelling human disease are either reliant on animal models of limited physiological relevance or 2D cell-based *in vitro* assays which lack complexity. We aim to develop a perfusable and immunocompetent self-reporting 3D human upper respiratory model; a tri-culture of human epithelial, fibroblast and dendritic cells each supported on a multilayered biocompatible polymer scaffold that mimics the extracellular matrix. A shortfall of existing 3D models is the lack of appropriate means for non-invasive, real-time monitoring of the microenvironment and cellular response. By incorporating ratiometric optical nanosensors to produce novel self-reporting scaffolds and also intracellular delivery of nanosensors to cells cultured upon the scaffold we can address this shortfall.

MATERIALS AND METHODS

PLGA 85:15, 70:30, 50:50, and PLA polymers were dissolved in dichloromethane at varying concentrations (5–20%w/w) and electrospun under a steady flow rate and set voltage. The electrospun scaffold fibres accumulated on a grounded collector plate set at a distance of 20 cm from the syringe tip. Nanosensors were incorporated into the scaffold at the time of electrospinning. The morphology and nanosensor incorporation of the electrospun scaffold was assessed using SEM and confocal microscopy (CLSM). The epithelial cell line, BEAS-2B (2×10^5 cells/scaffold) was seeded onto pre-sterilised and protein treated (FBS/fibronectin) scaffolds and imaged by light microscopy.

RESULTS AND DISCUSSION

Nanosensors have been immobilised in PLGA scaffolds (Fig. 1a,b,c) and have also been delivered to fibroblasts cultured upon PLGA scaffolds (Fig. 1d). The nanosensors remain
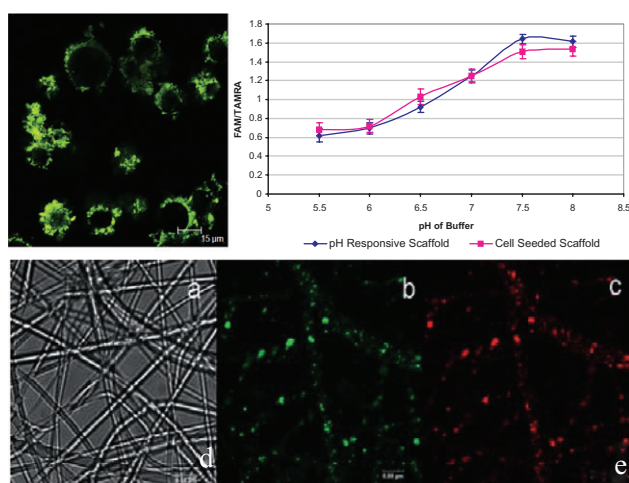

Fig. 1: *CLSM images of self-reporting PLGA scaffold (a) Transmission (b) FAM pH responsive dye (c) TAMRA reference dye (d) Co-localisation of FAM and TAMRA from nanosensors transfected into fibroblasts cultured upon PLGA scaffolds (e) Calibration of pH responsive scaffolds with and without cells cultured upon the scaffold.*
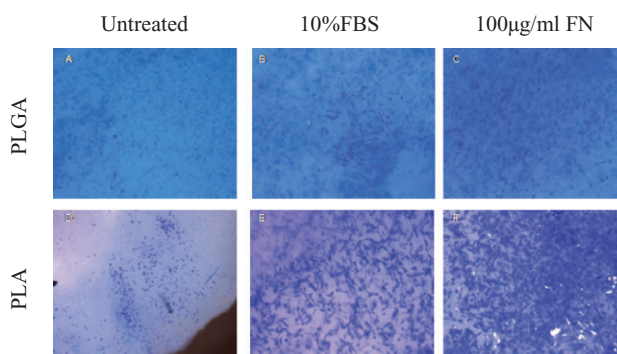

Fig. 2. Light microscopy images of BEAS-2B seeded onto PLGA 85 : 15 and PLA scaffolds for 24 h. Samples stained with May-Grunwald and Giemsa.

optically active and responsive to changes in pH enabling real-time measurements of the analyte of interest (Fig. 1e).

A greater degree of BEAS-2B cell attachment was achieved on scaffolds pre-treated with protein rich solutions (media +FBS / fibronectin); pre-treated PLA indicated greater biocompatibility compared with PLGA 85:15 (Figure 2).

CONCLUSION

The developed 3D model will provide a structural and cellular representation of the lung tissue and be amenable to in-situ monitoring therefore providing an invaluable tool for lung biology, disease modelling and drug discovery.

Directed Differentiation of Human Embryonic Stem Cells to Functional Cardiomyocytes by Defined Factors

James E. Dixon, Emily Dick, Maria D. Barbadillo-Munoz, David Anderson, Chris Denning[§], Kevin M. Shakesheff[§]

Wolfson Centre for Stem Cells, Tissue Engineering and Modelling (STEM), University of Nottingham, NG7 2RD, UK.
[§]To whom correspondence should be addressed:
Kevin.Shakesheff@nottingham.ac.uk or Chris.Denning@nottingham.ac.uk

Lineage commitment and differentiation are considered permanent cellular processes, however recent work has impressively demonstrated reprogramming of differentiation potential to pluripotency (induced pluripotent stem cells; iPSCs)[1] or conversion of lineages (induced neuronal cells; iNs)[2] by the ectopic activity of specific transcription factors (TFs).

As damaged or diseased hearts cannot regenerate direct generation of new cardiomyocytes (CMs) would be beneficial to cell therapy strategies. We tested whether a combination of cardiac-specific TFs could directly produce induced CMs (iCMs) from pluripotent human embryonic stem cells (hESCs)[3]. A HUES7 hESC cell-line (MYH6-mRFP) was created which expresses mRFP (monomeric red fluorescent protein) under the control of the mouse *MYH6* promoter and was used for detecting CM differentiation. Furthermore, CM differentiation was assayed by live TMRM staining, QPCR and immunofluorescence.

We employed a pool of fifteen genes and identified a combination of four that rapidly and efficiently induce the differentiation of hESCs into functional beating CMs *in vitro* (Figure 1). Time course experiments show that iCM differentiation events mirror normal differentiation with beating iCM clusters (10–200 cells) readily identified 15 days post infection. These cells (when dissociated with collagenase B) exhibit normal electrical activity (patch clamp and MEA analyses) and pharmacology. The number of iCMs produced demonstrates a >1000-fold enhancement of cardiac differentiation over embryoid body methods.

This study demonstrates a potentially important method for controlling cardiac differentiation and programming of large populations of iCMs for regenerative and drug screening purposes. We are now beginning testing of these factors for activity to directly convert human somatic lineages to iCMs. The generation of large numbers of functional iCMs is
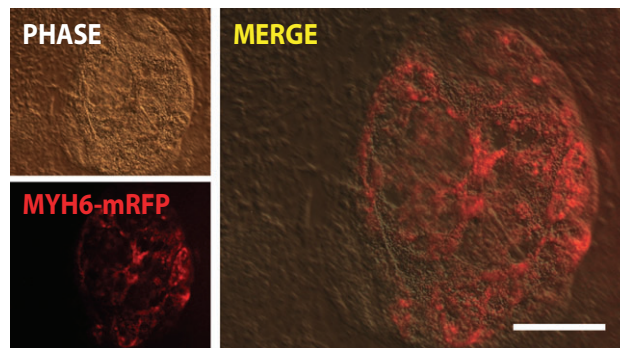

Figure 1. iCM by defined factors. *MYH6-mRFP expressing iCM cluster 15 days post-infection. Bar = 400 µm*

important for large-scale cardiac tissue engineering projects, and these cells will be employed to generate functional tissue constructs. Furthermore we will employ human iPSCs to create large quantities of patient-matched iCMs. These experiments will have important implications for cardiac disease modelling, aid cell therapy approaches and validate drug screening in more physiological patient-specific contexts.

REFERENCES

[1]K. Takahashi, et al. (2006) *Cell*, 126: 663–76. [2]T. Vierbuchen, et al. (2010) *Nature*, 463: 1035–1041. [3]J. Yu, et al. (2007) *Science* 318: 1917–1920.

Effects of Dynamic Compression on Fibrous PLGA Scaffolds Seeded with Rodent Foetal Chondrocytes

C.M. Rogers,[1] T.S. Woolley,[2] S.C. Cruwys,[2] L.D.K. Buttery,[1] F.R.A.J Rose,[1] K.M. Shakesheff[1]

[1]University of Nottingham, Nottingham, NG7 2RD, UK, [2]AstraZeneca, Loughborough, LE11 5RH, UK.

INTRODUCTION

Cartilage defects result in disability for millions worldwide. Such defects can lead to the development of osteoarthritis (OA) for which presently there is no cure [1]. Tissue engineering (TE) holds great promise for generating high-fidelity *in vitro* models to simulate both healthy and defective tissues. The ultimate aim of this study is to engineer cartilage *in vitro* to mimic the histology and anatomy of healthy rat tissues. In future studies, this engineered cartilage will be subjected to damage to generate a model of OA for use in drug development. As the maintenance of native cartilage structure and integrity critically depends on mechanical forces [2], the impact of compressive loads on *in vitro* cell proliferation, differentiation and extracellular matrix (ECM) production by rodent foetal chondrocytes cultured in fibrous PLGA constructs was investigated.

MATERIALS AND METHODS

Primary rodent foetal chondrocytes were isolated and expanded before being seeded (4×10^5 cells/ml) on fibrous poly(lactic-co-glycolyic acid) scaffolds and cultured statically (plate) or in a rotary cell culture system (RCCS™, Cellon). At day-56 of culture, constructs were transferred to a Flexcell 3000C™ (Flexercell®) bioreactor and subjected to 1 of 3 regimes: 0, 7 or 10 kPa at a frequency of 0.5 Hertz (Hz) for 2 hours, twice a week, for 4 weeks. These compressive forces were based on previous cell monolayer and pellet studies [3–4]. Cell proliferation, differentiation and ECM production was assessed using PCR, immunohistochemistry, total collagen (Hydroxyproline) and DNA (Hoechst 33258) assays.

RESULTS AND DISCUSSION

After 4 weeks of culture under dynamic compression, changes in chondrocyte number, ECM production and scaffold structure were seen for the cell-seeded constructs. Mechanical stimulation was seen to have a negative impact on expression of collagen type II, cell number and scaffold integrity, and total collagen content (Fig 1.) present within the constructs decreased as load increased (Fig 2.). After culture under 10 kPa, constructs originally cultured in the RCCS were too damaged to image.
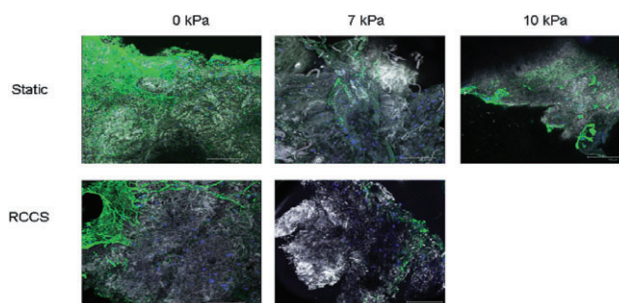

Fig. 1. Representative immunohistochemistry images showing collagen type II expression (FITC) and cell number (DAPI).
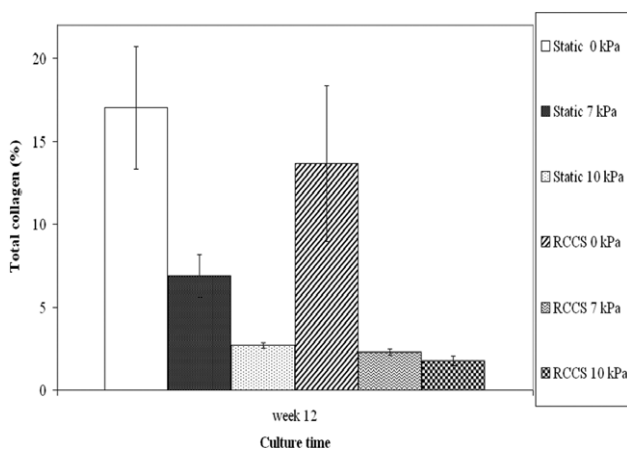

Fig. 2. Total collagen (dry weight %) of constructs cultured either statically or in the RCCS and under different dynamic compression regimes. Error bars represent SEM; n = 3.

pression regimes used had a negative impact on cell growth and ECM production. This is in line with previous *in vitro* work which has shown that compression can lead to a reduction in collagen type II gene expression [5]. However, as mechanical stimulation is known to have a critical role in maintaining the delicate balance between chondrocyte/ECM anabolism/catabolism to maintain healthy cartilage, fine-tuning of loading regimes may be required to enhance matrix production *in vitro*. Further investigation into suitable compression regimes to aid *in vitro* cartilage tissue engineering is currently underway.

CONCLUSIONS

Initial investigations into the effect of mechanical forces on chondrocyte-PLGA constructs found that the dynamic com-

ACKNOWLEDGMENTS

REFERENCES

[1] M. Ochi, Y. Uchio, M. Tobita and M. Kuriwaka. "Current Concepts in Tissue Engineering Technique for Repair of Cartilage Defect" *Artificial Organ*, **25**, 3 (2001):172–9.

[2] S.J. Millward-Sadler and D.M. Salter. "Integrin-Dependent Signal Cascades in Chondrocyte Mechanotransduction". *Annals of Biomedical Engineering*, **32**, 3 (2004):435–46.

[3] C.Y. Lee and Z.P. Luo. "Metabolism of Chondrocytes is Regulated Differently by Compression and Tension". *52nd Annual Meeting of the Orthopaedic Research Society*, **Paper 1341**.

[4] R.D. Graff, E.R. Lazarowski, A.J. Baines and G.M. Lee. "ATP Release by Mechanically Loaded Porcine Chondrons in Pellet Culture". *Arthritis & Rheumatism*, **43**, 7 (2000):1571–9.

[5] R.L. Mauck, B.A. Byers, X. Yuan and R.S. Tuan. "Regulation of cartilaginous ECM gene transcription by chondrocytes and MSCs in 3D culture in response to dynamic loading". *Biomechan Model Mechanobiol*, **6**, (2007):113–25.

Injectable Scaffold for Bone Tissue Engineering Applications

C.V.Rahman[1], H.C.Cox[2], L.G.Hamilton[1], R.A.Quirk[2], F.R.A.J.Rose[1], K.M.Shakesheff[1]

[1]School of Pharmacy, University of Nottingham, Nottingham, UK.
[2]RegenTec Ltd, Nottingham, UK.

Abstract – **We describe here a new injectable scaffold formed by liquid sintering of temperature-sensitive polymer microparticles. The scaffold is injectable at room temperature and hardens over time at body temperature. The scaffold can be used to deliver growth factors and/or cells for bone tissue engineering applications.**

INTRODUCTION

Scaffolds can be used to deliver a high density of cells and controlled dose of growth factors to a site of tissue damage. A major limitation for applications of scaffolds is the surgical difficulty of locating the material at the intended site of regeneration. Therefore, an important enabling technology for regenerative medicine is an injectable scaffold that can be delivered via a syringe to fill a 3D space.

We previously reported the development of an injectable scaffold formed by liquid sintering of poly (lactic co-glycolic acid) (PLGA)/poly (ethylene glycol) (PEG) microparticles [1]. Liquid sintering describes a process in which the polymer particles lose a plasticiser and hence experience an increase in their glass transition temperature over time. Here we describe further development of the scaffold formulation.

MATERIALS AND METHODS

PLGA/PEG particles were fabricated by high temperature blending of PLGA (85:15 53 kDa) and PEG 400 polymers. The polymer pieces were ground into particles in a bench-top mill and sieved to obtain the 100–200 μm size fraction. Scaffolds were prepared in PTFE moulds. Each mould produced cylindrical scaffolds of 12 mm length and 6 mm diameter.

Compressive strength of composite scaffolds was tested using a TA.HD+ texture analyser (Stable Microsystems). The Young's Modulus of Elasticity was computed by determining the slope of the stress-strain curve along the elastic portion of deformation.
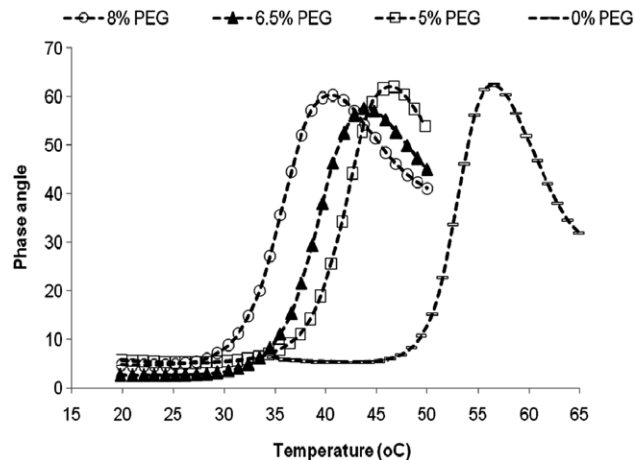

Fig. 1. Reduction of glass transition temperature of poly(lactic co-glycolic) acid caused by the addition of polyethylene glycol

The structural morphology of the scaffolds was examined using a scanning electron microscope (SEM) (JEOL JSM-6060LV) and micro-computed tomography (Skyscan 1174).

RESULTS AND DISCUSSION

The PLGA/PEG formulation has a maximum compressive strength at fracture point of between 4 and 5 MPa (unconstrained), with a Young's Modulus of Elasticity close to 80 MPa. These values exceed those achieved by many non-injectable scaffolds in clinical use. The material has porosities of between 40% and 50% and pore diameters between 50 and 100 microns.

By manipulating certain variables in the formulation we have fabricated scaffolds with suitable rheological properties for use in an injectable formulation (Fig. 1). Furthermore, the plasticisation of the polymer has been enhanced to within 25–37°C.

Following injection, the scaffold begins to harden in less than 15 minutes, with full strength developing over 24 hours. The scaffold formation mechanism is independent of the composition of the aqueous carrier and we have formed the scaffold containing MSCs. Viability and proliferation of MSCs within the scaffold has also been demonstrated.

CONCLUSIONS

PLGA/PEG injectable particulate scaffolds that harden at body temperature have been developed. The PLGA/PEG scaffolds are porous and have unconstrained compressive strength in the region of cancellous bone. Viability and proliferation of cells grown on the scaffolds has been demonstrated. Future work will assess bone regeneration in *in vivo* models.

REFERENCE

[1] L. Hamilton, R.M. France and K.M. Shakesheff, "Development of an injectable scaffold for application in regenerative medicine to deliver stem cells and growth factors" *J. Pharm. Pharmacol.*, **58** (2006) A52-A53.

Interconnectivity of Tissue Engineering Scaffolds

Y. Reinwald[1], G. Lemon[2], C. Rahman[1], K.M. Shakesheff[1]

[1]Division of Drug Delivery and Tissue Engineering, School of Pharmacy, University of Nottingham, University Park, Nottingham, NG7 2RD, UK
[2]Division of Applied Mathematics and Theoretical Mathematics, School of Mathematical Sciences, University of Nottingham, University Park, Nottingham, NG7 2RD, UK

INTRODUCTION

Supercritical fluid technology was utilised to produce biodegradable tissue engineering scaffolds. The effect of polymer properties and processing conditions on the scaffold architecture were investigated and led to the possibility to tailor scaffold characteristics for tissue engineering applications [1]. Pore interconnectivity (IC) is an important measure for the characterisation of scaffolds as it influences the circulation of extracellular material [2], nutrient diffusion [3] and ingrowth of blood vessels and bone tissue [4, 5]. To date, IC has mainly been determined qualitatively [2]. This study presents an approach to quantify IC in 3D applying a novel computer algorithm and to determine correlation between interconnectivity, pore size, porosity and permeability. Moreover, it aims to investigate the effect of IC on cell distribution throughout the scaffold.

MATERIALS AND METHODS

Scaffolds were fabricated from supercritical carbon dioxide ($scCO_2$) using poly (lactic-*co*-glycolic acid) (PLGA). Micro computed tomography (MicroCT) and scanning electron microscopy (SEM) were then utilised to obtain pore size, porosity and window size. To investigate IC an algorithm was applied to image datasets obtained from MicroCT. Scaffold permeability was determined from pressure measurements across the scaffolds and further calculations applying Darcy's Law. Human mesenchymal stem cells (hMSC) were seeded onto $scCO_2$-foamed scaffolds. Their distribution throughout the scaffolds was determined by MicroCT analysis.
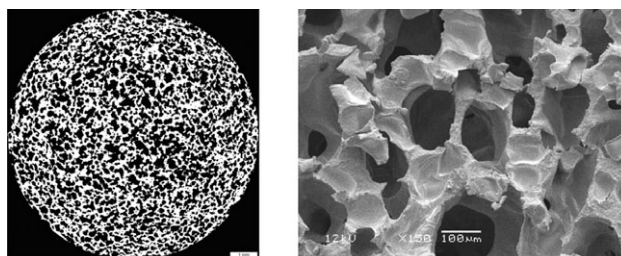

Figure 1: Representative images illustrating the structure of $scCO_2$-foamed PLGA scaffolds. MicroCT image (left) and SEM micrograph (right).

RESULTS AND DISCUSSION

Scaffolds were fabricated from 37, 53 and 109 kDa PLGA (85:15; Figure 1). Higher polymer Mw resulted in lower porosities and average pore sizes as shown in Table 1. IC was defined as the ratio of pore volume accessible by a sphere of known diameter from the scaffold exterior, to the total pore volume.

Increase in sphere diameter and Mw resulted in a decrease in IC, e.g. at a sphere diameter of 102 µm the interconnectivities (IC_{102}) were 40%, 17% and 5% for 37, 53, and 109 kDa respectively.

CONCLUSIONS

Physical properties of $scCO_2$-foamed scaffolds were influenced by the polymer molecular weight [1], including pore

Table 1: Average pore sizes, porosities and interconnectivities of scCO$_2$-foamed scaffolds.

Mw [kDa]	Pore size [μm]	Porosity [%]	IC$_{102}$ [%]
37	142 (±3)	53 (±9)	40
53	127 (±4)	49 (±3)	17
109	98 (±4)	39 (±4)	5

interconnectivity and permeability. Further investigations are necessary to examine the effect of process conditions on scaffold interconnectivity.

ACKNOWLEDGMENTS

REFERENCES

[1] Tai, H. European Cells & Materials 2007, 14: 76–77.
[2] Gross, K. A.; Rodriguez-Lorenzo, L. M. Biomaterials 2004, 25, 4955–4962.
[3] Hui, P. W. Journal of Biomechanics 1996, 29, 123–132
[4] Kuboki, Y.; Takita, H.; Kobayashi, D.; Tsuruga, E.; Inoue, M.; Murata, M.; Nagai, N.; Dohi, Y.; Ohgushi, H. Journal of Biomedical Materials Research 1998, 39, 190–199.
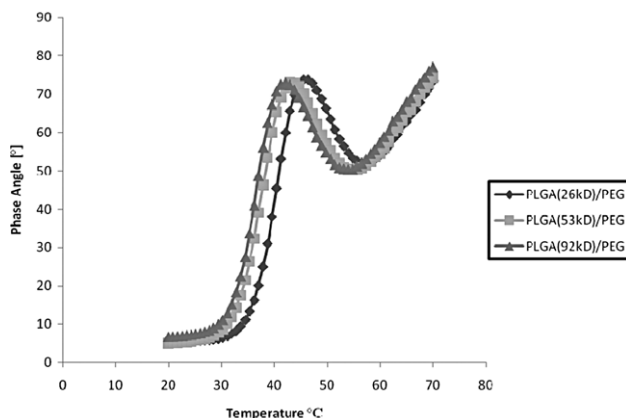[5] Otsuki, B.; Takemoto, M.; Fujibayashi, S.; Neo, M.; Kokubo, T.; Nakamura, T. Biomaterials 2006, 27, 5892–5900.

Physical and Biological Characterisation of a Novel Injectable Scaffold Formulation

A. Dhillon[1], C. Rahman[2], L.J. White[2], B.E. Scammell[1], K.M. Shakesheff[2]

[1]Division of Orthopaedic and Accident Surgery, University of Nottingham, Queen's Medical Centre, NG7 2UH
[2]School of Pharmacy, University of Nottingham, NG7 2RD

Abstract – **In the UK, the calculated fracture incidence is 3.6 fractures per 100 people per year[1]. The prevalence of osteoporosis and incidence of fragility fractures is exceeding ahead of predictions due to rapidly changing population demographics. The level of morbidity associated with such fractures combined with the limitations of current therapies is high with inimical effects on the quality of life. Hence, there is a clinical need for the development of a sythetic bone graft substitute with the potential to deliver cells and bioactive molecules through minimally invasive techniques. This project has developed and tested an existing novel injectable scaffold that self-assembles *in situ* to form a biodegradable porous osteoconductive material. Thus, it has been possible to deliver osteogenic components within a scaffold that shares similar physical properties to cancellous bone.**

Fig. 1. Rheology Profiles of the most mechanically competent PLGA (26 kDa, 53 kDa and 92 kDa)/PEG formulations that self-assemble at 37°C.

INTRODUCTION

Injectable scaffolds which also deliver cells and bioactive molecules to augment bone healing may overcome many of the limitations associated with current bone graft substitutes[2]. The aim of this study was to develop and test a novel injectable scaffold that self-assembles isothermically *in situ* to form a biodegradable porous osteoconductive material. In addition, an assessment of the viability of human mesenchymal stem cells (hMSC) seeded onto the scaffold was made.

METHODS

Rheological assessment was performed on three different molecular weights (Mw) of poly(lactic-co-glycolic acid) (PLGA) (26 kDa, 53 kDa and 92 kDa) combined with differing ratios of polyethylene glycol (PEG) to control the temperature required for scaffold self-assembly. The strength (MPa) and stiffness (Young's Modulus) patterns of the scaffolds were assessed in compression. The cell viability, prolif-

eration and distribution patterns of hMSCs seeded within the scaffold microparticle mixture prior to injection and self assembly were assessed using Alamar Blue®, confocal microscopy and micro x-ray computed tomography (µCT).

RESULTS

Rheological assessment identified a stepwise control of the trigger-temperature (37°C) required for scaffold self-assembly through adjustment of PLGA Mw and PLGA/PEG ratios. Mechanical analysis of the most competent scaffolds after 2 hours at 37°C revealed compressive strengths (1–2 MPa) and stiffness (Young's Modulus of 3.5–5.5 MPa) similar to that of cancellous bone. Confocal microscopy analysis of LIVE/DEAD® assays conducted on cell-seeded scaffolds demonstrated the scaffold's biocompatibility post-injection/assembly. This is further complemented by subsequent cell proliferation assays of the viable hMSCs present. µCT analysis of cell seeded scaffolds further indicated the scaffold's potential to provide a supporting osteoconductive environment for bone formation and deposition.

DISCUSSION AND CONCLUSIONS

This study has confirmed specific injectable scaffold formulations that self-assemble at physiologically relevant temperatures and possess compressive and stiffness strengths in the range of cancellous bone. It is possible to tailor the architecture/mechanical/biodegradable properties of the scaffold through manipulation of PLGA Mw and PEG ratios. This injectable scaffold system provides a 'potential' means of delivery for hMSCs (and growth factors or antibiotics) and is an architecturally suitable 3D scaffold that has the potential to not only be osteoconductive, but also osteoinductive and osteogenic.

ACKNOWLEDGEMENTS

REFERENCES

1 L J Donaldson, I P Reckless, S Scholes, J S Mindell and N J Shelton (2008) *J. Epidemiol. Community Health* 62:174–180
2 Q. Hou, P.A. De Bank, K.M. Shakesheff (2004) J. *Mater. Chem.* 14:1915–1923

Slow Release Model of Simvastatin Loaded Poly (lactide-co-glycolide) Microparticles for Osteogenesis

O. Qutachi[1], K.M. Shakesheff, L.D. Buttery

Wolfson Centre for Stem Cells Tissue Engineering and Modelling, Centre of Biomolecular Sciences, School of Pharmacy, University of Nottingham, Nottingham, U.K.

Abstract – **Simvastatin has been found to exert bone anabolic effects and could have applications in bone tissue engineering. Our aim is to design a slow release model from PLGA microparticles (MP) loaded with simvastatin and apply this to controlling osteogenic differentiation within aggregates of embryonic stem cells. The MPs were fabricated using the single emulsion method. The particle size distribution was assessed by coulter counter and detection and quantification of simvastatin was achieved using HPLC. The mean diameter of the MPs was 10 µm with 80% of the MP population range between 5 to 18 µm. The encapsulation efficiency for simvastatin was 79%, and the release profile of simvastatin was gradual with 10% of the drug released at day 1 and continuing for 3 weeks where 60% release was achieved. In conclusion the size range of the MPs together with the encapsulation efficiency and the release profile render the model useful for osteogenic differentiation using embryoid bodies.**

INTRODUCTION

Simvastatin is a pro-drug that inhibits the hepatic enzyme, 3-hydroxy-3-methylglutaryl-coenzymeA reductase which is the rate limiting step in cholesterol synthesis. Simvastatin also has anabolic effects on bone and could aid applications for bone repair [1]. Our aim is to design a slow release model from PLGA microparticle (MP) loaded with simvastatin to be used for inducing osteogenic differentiation within aggregates of stem cells.

MATERIALS AND METHODS

PLGA MPs loaded with simvastatin were fabricated using single emulsion method. 1 g PLGA (42 kDa) and 5 mg simvastatin were dissolved in 6 ml DCM then homogenised in 0.3% PVA at 19000 RPM. The created MPs are vortexed

overnight, then centrifugation, washed with distilled water and freeze dried before storing at −20°C [2]. The size distribution was checked using coulter counter. Simvastatin detection and quantification for encapsulation and release was achieved by HPLC. The detection wave length was 238 nm, the column C18, hypersil, ODS (5 µm–4.6 ml width −100 mm length) and mobile phase was 15% of 1 mM Ammonium acetate in PH 4.4 and MeOH 85%.

RESULTS AND DISCUSSION

Up to 80% of the fabricated PLGA MPs ranged from 5 to 18 µm diameters with a mean of 10 µm. This size range is suitable for drug delivery purposes within cell aggregates being neither too small to be engulfed by the cells nor too big to interfere with cell/MPs aggregation process. The encapsulation efficiency for simvastatin was 79%. The release profile for simvastatin was controlled. There was no burst release with 10% released at day 1 reaching 40% by day 10 and continuing until day 21 where around 60% of the encapsulated drug was released. Simvastatin was found to have osteogenic potential at low concentrations [3]. This release profile is interesting where smooth release over a 3 week period will avoid the toxic concentrations and enhance osteogenesis.

CONCLUSIONS

This study was successful in fabricating simvastatin loaded PLGA MPs. The size range of these MPs was desirable for tissue engineering purposes where it can be used within aggregates of stem cells. Upon releasing the factor of interest, it will help to direct differentiation at early stages which will end with more homogeneous differentiation. In addition the release profile of simvastatin has been tested and it is particularly promising for *in vitro* osteogensis. This model could be
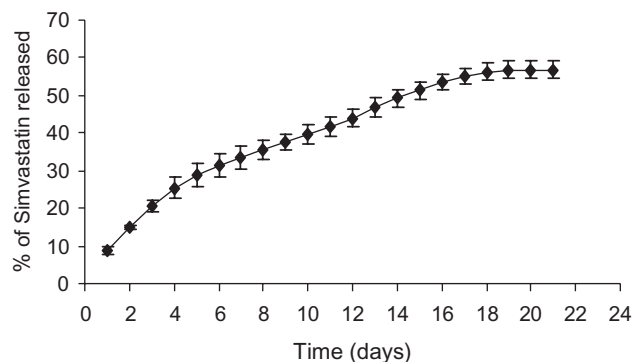

Fig. 1. Cumulative percentage of simvastatin released from PLGA microspheres.

used in the future for enhancing osteogenic differentiation of stem cells.

ACKNOWLEDGMENTS

REFERENCES

[1] Mundy, G., et al., *Stimulation of bone formation in vitro and in rodents by statins.* Science, 1999. **286**(5446): p. 1946–9.

[2] ODonnell PB, McGinity JW. Preparation of microspheres by the solvent evaporation technique. Advanced Drug Delivery Reviews 1997; 28: 25–42.

[3] Whang, K.M., et al., *A novel osteotropic biomaterial OG-PLG: In vitro efficacy.* Journal of Biomedical Materials Research Part A, 2005. **74A**(2): p. 247–253.

Surface modification of an elastomeric membrane for cardiac tissue engineering

Isha Paik[1], James E. Dixon[1], Peter Rivett[2], Kevin M. Shakesheff,[1,§]

[1]Wolfson Centre for Stem Cells, Tissue Engineering and Modelling (STEM), School of Pharmacy, University of Nottingham, NG7 2RD, UK.,
[2]Tannlin Ltd. Irvine, Ayrshire, KA11 4HP, UK.
[§]To whom correspondence should be addressed: Kevin.Shakesheff@nottingham.ac.uk

INTRODUCTION

Cardiovascular disease is the leading cause of death and disability worldwide. Current therapies including cardiac myoplasty and donor transplantation provide outcomes with limited success [1]. Cardiac tissue engineering (CTE) using mechanically compatible materials to include elastomers may provide cells with a physical support *in vivo* and improve clinical outcomes. Recently, significant findings were published where 'muscular thin films,' consisting of micro-patterned polydimethylsiloxane (PDMS) were manufactured, cultured with synchronously contracting neonatal rat cardiomyocytes (CMs) and used to produce fully active CM-driven devices [2]. Below we describe two separate techniques, plasma polymer deposition and micropatterning with fibronectin to encourage cell attachment. The long term aim being to develop an *in vitro* pump that is driven by human embryonic stem cell (hESC)-derived CMs which will efficiently deform PDMS tubes to produce fluid flow.

MATERIALS AND METHODS

PDMS (Sylguard 184, Dow Corning, Midlands) was spin coated on to glass slides, using a 400 Lite Spinner (Laurell Technologies, North Wales) at 2000 rpm. PDMS membranes were oxygen etched and plasma coated with allylamine monomer, this method has been previously described [3]. Seven different surface types were investigated, (see Figure 1). Static water contact angle (WCA) was measured with a CAM 200 Optical Contact Angle Metre (KSV Instruments LTD) to investigate surface wettability over 15 days.

PDMS membranes were micro-patterned by airbrushing labelled fibronectin, (Alexa Fluor 488, Invitrogen, UK) through a micro-stencil (Tannlin, Irvine, UK) at 20 psi. The fibronectin band width was 25 µm, with a 90 µm gap between each band. A total of 0.5×10^6 GFP-labelled 3T3 cells were seeded. Images were taken using the Nikon Eclipse TS100 Microscope at ×10 magnification.

RESULTS AND DISCUSSION

PDMS shows consistent hydrophobic behaviour (<90°), (see Figure 1). Oxygen etched and allylamine treated surfaces are initially hydrophilic (approximately 71°), but regain their hydrophobicity over time. Thicker allylamine depositions appear most stable (78/92 nm thickness). Clearly defined fibronectin bands were visible on the PDMS surface following airbrushing through micro-stencils (Figure 2a), with successful attachment of 3T3 cells to these regions, (Figure 2b).

DISCUSSION & CONCLUSIONS

PDMS surfaces treated with plasma polymerised allylamine may prove unstable over long periods of time, and therefore were not taken forward for cell attachment experiments. Controlled cell growth through fibronectin micropatterning was more promising with respect to 3T3 cell attachment. Future studies will investigate hESC derived CMs attachment to these modified membranes and whether they exhibit synchronous contraction on these membranes.

Figure 1. WCA of plasma coated surfaces as a function of time post plasma treatment. Note: Each thickness in (nm) represents the allylamine deposition thickness.
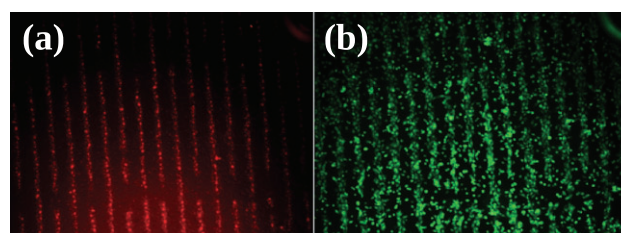
Figure 2. (a) Fibronectin micro- patterned (red) PDMS and (b) adhered 3T3 cells (green).

ACKNOWLEDGEMENTS

REFERENCES

[1] L.A. Hidalgo-Bastida, et al., "Cell adhesion and mechanical properties of a flexible scaffold for cardiac tissue engineering" *J Act Bio,* **3** (2007) 457–467.

[2] A.W. Feinberg, et al., "Muscular Thin Films for Building Actuators and Powering Devices" *Science,* **317** (2007) 1366–1370.

[3] M. Zelzer, et al., "Investigation of cell–surface interactions using chemical gradients formed from plasma polymers" *Biomat,* **29** (2008) 172–184.

Contract Research: Indian Pharmaceutical Perspective – September 2010

A.Gupta[1], S.Drabu[2]

[1,2]Maharaja Surajmal Institute of Pharmacy, affiliated to Guru Gobind Singh Indraprastha University, New Delhi, India.

Abstract – **The pharmaceutical sector is one of the fastest growing sectors of the Indian economy and has made rapid strides in the past few decades in clinical research industry in the world. Having proved its mettle in the international market, India is now on the helm of taking up the challenge of proving its efficiency as the capital for global clinical trials. After India became a member of World Trade Organisation in 1995 and agreed to adhere 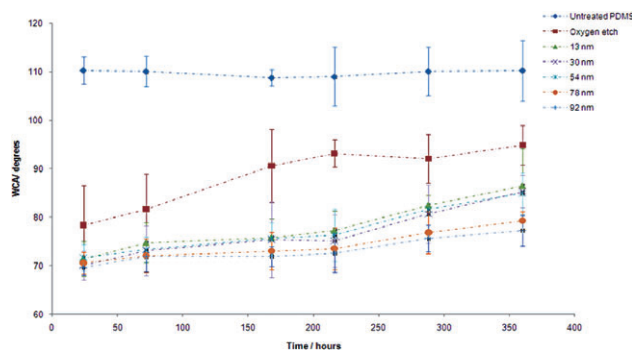to the patent regime by 2005, it has become a favourable destination for conducting clinical trials as it provides opportunity in terms of high patient population, low-cost services, a well educated specialised workforce, favourable intellectual property environment and round the clock services. The proposed presentation will highlight how the Indian pharmaceutical industry in symbiotic collaboration with government and regulatory agencies is well positioned to emerge as the global CRO market destination in the future.**

INTRODUCTION

With pharma majors facing increased pressure on profit margins, spiraling R&D costs and major drugs going off patent, outsourcing of clinical research and manufacturing services comes as a relief as they save 40–60 per cent of overall cost in drug development. India is fast emerging as the global hub for contract research and manufacturing services. Leading players in contract research industry provide services like product development; manufacturing services; clinical trial management; safety monitoring; data management; biostatistics; medical writing services; regulatory affairs support and many other complementary services. The global contract research opportunity was pegged at USD 14 billion in 2006 and is expected to reach USD 24 billion by this year end. The CRO segment has grown and is expected to flourish in coming years in India and across the globe.

SUMMARY

Contract Research Organisations (CROs) are becoming important strategic partners for pharmaceutical companies as they help pharmaceutical companies to transition new drugs from concept stage to FDA marketing approval without the pharmaceutical company having to invest time, money and people for these services. Indian companies are providing an excellent platform for contract research services to local and global pharmaceutical companies due to a large and diverse patient pool, low costs of research for conducting clinical trials, IT skills and infrastructure, intellectual talent pool in biosciences, favourable intellectual property right environment and advanced medical fraternity and healthcare practices. India has a huge population base of more than 1 billion (Indians represent about 15% of the global population). It is home to a wide variety of diseases ranging from tropical infections to degenerative diseases. The biggest advantage is that the large and diverse Indian population is willing to undergo clinical trials. Indian CROs do not see any near-term impact of recession as large pharma customers such as

AstraZeneca and Glaxo continue to send more work to India. With many bio-pharmaceutical companies' clinical trials already in the pipeline, and with patent expiry dates remaining constant, Indian CROs working for clinical research projects are somewhat insulated from any slump so far in the economy. So let's not be myopic and conclude by looking at the current recession that the growth in contract research industry is over. Business cycles are inevitable and recessions and booms will always come. In the long run, we should continue to invest in the development of infrastructure, people and the regulatory framework, so we emerge out of the current recession in a much stronger position.

CONCLUSION

The concept of outsourcing for the development and global studies on new drugs has become widely accepted in the pharmaceutical industry and the Indian pharmaceutical industry with its rich scientific talent, research capabilities and intellectual property protection regime is well positioned to emerge as a global CRO market destination in the future. But still 'miles to go' to fulfill the pre-requisites to ensure India's success. In spite of all the pitfalls, India provides a lucrative environment to attract multinational companies to outsource their clinical research.

REFERENCES

[1] Borfitz D. Lifting India's barriers to clinical trials. *Center Watch* 2003; 10(8): 1–9.
[2] Bhatt AD. Clinical trials and regulatory tribulations. Express Pharma Pulse 2002; Nov 21:32–3.
[3] Fenn CG, Wong E, Zambrano D. The contemporary situation for the conduct of clinical trials in Asia. International Journal of Pharmaceutical Medicine 2001; 15: 169–73.
[4] Nichol FR. Contract clinical research: value to in-house drug development, in Clinical Drug Trials and Tribulations, Cato, A., Sutton, L., and Cato III, A., Eds., Marcel Dekker, New York, 2002, chap. 21.

Online pharmacies: Global Regulatory Perspective – September 2010

A. Gupta[1], S. Drabu[2], A. S. Lather[3]

[1,2]Maharaja Surajmal Institute of Pharmacy, affiliated to Guru Gobind Singh Indraprastha University, New Delhi, India, [3]School of Management Studies, Guru Gobind Singh Indraprastha University, New Delhi, India.

Abstract – **In the light of growth potential for e-pharmacies/online pharmacies/cyber pharmacies due to the advent of Internet Technology in particular and Information Communication Technology in general; developed nations and the developing countries like India should be able to exploit it to its full extent. The era of e-commerce has paved the way for an upward trend in global online pharmaceutical advertising. The websites are devising and designing innova-tive advertisements to attract potential customers – physicians, pharmacists and patients. Web Direct to Customer pharmaceutical advertising has become a strong medium, thanks to its low cost and high speed of communication, which can be used to reach out to anybody, anytime and anywhere in the world. *This presentation will critically deal with regulatory considerations involved in pharmaceutical promotion on the web and assess future potential.***

INTRODUCTION

Many countries regulate the advertisement of drugs, which are promoted to customers by pharmaceutical manufacturers. Enforcement of the legislation and the code of conduct to guide promotional practices is vital in ensuring that advertising promotes the appropriate use of medicine. The World Health Organisation advocates "Ethical criteria for Medicinal Drug promotion" as a model guideline for promotional practice which is consistent with the national health policy and support rational use of drugs. Regulatory authorities should follow strict vigilance to curb pseudo educational campaigns by pharmaceutical companies.

Discussion: To enforce Internet advertising regulation, the following measures should be given due consideration:

a. Prescription medicine should be promoted to physicians with appropriate clinical guidelines
b. Promotion of OTC (over the counter) medicines should be subject to as strict controls as prescription only drugs
c. The information in advertisements should be presented in a balanced manner, bringing attention equally to claims about benefits and warnings about risks
d. All promotional claims about health effects must include validated up to date scientific evidence to support the claims
e. All advertising should include legibly presented information in everyday language for consumers to understand and include explanatory graphics where appropriate; namely, name and amount of active ingredient, brand name, approved therapeutic use, dosage form, dosage regimen, side effects, precautions, contraindications, warnings, major interactions, documentary evidence related to placebo controlled clinical trial studies, name and address of manufacturer.
f. Manufacturers should not promote their product for indications that are not listed in approved product information
g. The word 'safe' should not be used in online promotion unless substantiated
h. Unsolicited reprint of journal articles must be consistent with product information

To implement a Universal Code of ethics for web drug advertisements there is an utmost need to constitute a Global Ethical Committee comprising of members of different nations which will monitor legal aspects of pharmaceutical online promotion. Monitoring requirements include fair balance, accuracy, avoidance of false or misleading statements or promotion of unapproved uses, an adequate discussion of risks as well as benefits and prescreening etc. This Global Ethical Committee in coordination with committees of different countries should collect complaints and other information regarding unethical promotion through National Drug Control Authorities. To enforce strict regulation further in the context of online pharmaceutical promotion, the government should frame broader policies and take special measures. The government in every nation must be prepared to play an active role where a code of ethics appears to be failing and provide necessary resources to strengthen regulatory machinery.

CONCLUSION

Using the internet as one of the advertising media to promote drugs can be of great use if proper security and other issues in every country are taken care of. Such measures will help maximise use of the Internet by physicians/patients/pharmacists/manufacturers and influence efficiency of Internet communication and pharmaceutical promotion in a global health care system.

REFERENCES

[1] Kendra L; Schwartz MD, Family medicine Patients' use of the internet for health Information, Journal of American board of family Medicine,19: 39–45 (2006).
[2] US Department of Health and Human Services, FDA, Draft guidance for industry: Consumer directed ads, federal register, Aug12,62(155): 171–3 (1997).

Primary Care Physicians Opinion on Insulin Initiation in Type 2 Diabetes Patients

D. Sreedhar, Virendra S. Ligade, Manthan D. Janodia, Ajay G. Pise and N. Udupa

Department of Pharmacy Management, Manipal University, Manipal – 576 104

Abstract – **Type 2 Diabetes is the most common type of diabetes and prevalent in both developed and developing nations. Treatment guidelines by various diabetic associations recommend the use of insulin in patients with type 2 Diabetes. Present study was carried out to know the opinion of primary care physicians about initiating insulin therapy in type 2 Diabetic patients. Although the use of insulin initiation is recommended by diabetic associations, there is a reluctance of insulin initiation by most of primary care physicians in the study.**

INTRODUCTION

Diabetes is a syndrome of disordered metabolism, usually due to a combination of hereditary and environmental causes,

resulting in abnormally high blood sugar levels. Type 2 Diabetes is the most common type in which either the body does not produce enough insulin or the cells ignore the insulin [1]. Type 2 Diabetes is a progressive disease and often diagnosed late. Patients who are put on multiple oral anti-diabetic agents also don't achieve target glycemic control [2]. Insulin initiation therapy not only helps in achieving target glucose levels but also provides health and cost related benefits. Treatment guidelines by various diabetic associations recommend the use of insulin in type 2 Diabetic patients [3]. However, there is unwillingness among the patients and physicians to initiate insulin therapy [4].

MATERIALS AND METHODS

This study consists of both primary and secondary data.

A questionnaire based survey was conducted among the primary care physicians treating patients with type 2 Diabetes. Final sample size was 60. Questionnaire consisted of structured closed ended questions. Questionnaire was pre-tested. Responses were tabulated, analysed and interpreted.

Literature was searched for the evidence of recommended use of insulin initiation in type 2 Diabetes patients.

RESULTS AND DISCUSSION

Average duration of practice of primary care physicians included in the study was 17.8 years. 53% of the physicians see more than 80 patients with type 2 Diabetes in a month. Non-pharmacological treatment (Diet control and exercise) is preferred by most of the physicians (85%) over oral anti-Diabetic drugs and insulin. Referrals, complexity of treatment regimen, weight gain and fear of hypoglycaemia were some of the reasons behind reluctance of prescribing insulin. Referrals and complexity of treatment regimen were major

barriers to initiate insulin therapy. Premix insulin was preferred over basal insulin among the physicians who were prescribing insulin.

CONCLUSIONS

Most of the primary care physicians are hesitant to initiate insulin in patients with type 2 Diabetes due to various reasons. There is an urgent need to conduct awareness programmes to drive away misconceptions about initiating insulin therapy. Awareness should basically focus on advantages of insulin initiation therapy and the tools available for accurate use of insulin.

ACKNOWLEDGMENTS

REFERENCES

[1] American Diabetic Association, Diabetes Basics, Type 2. Available from http://www.diabetes.org/diabetes-basics/type-2/.

[2] T. M. Wallace, D. R. Matthews. Poor glycaemic control in type 2 diabetes: a conspiracy of disease, suboptimal therapy and attitude. QJM, 2000; 93: 369–74,

[3] D. M. Nathan, J. B. Buse et al. Management of hyperglycemia in type 2 diabetes: a consensus algorithm for the initiation and adjustment of therapy. A consensus statement from the American Diabetes Association and the European Association for the Study of Diabetes. Diabetes Care, 2006; 29: 1963–72.

[4] M. Peyrot, R. R. Rubin et al. The International DAWN Advisory Panel. Resistance to insulin therapy among patients and providers: results of the cross-national Diabetes Attitudes, Wishes, and Needs (DAWN) study. Diabetes Care, 2005; 28: 2673–9.